UNIVERSITÄT ZU LÜBECK

From the Lübeck Institute of Experimental Dermatology
of the University of Lübeck
Director: Prof. Dr. Ralf Ludwig

"Screening for wound healing promotors using a human wound healing organ culture model"

Dissertation
for Fulfillment of
Requirements
for the Doctoral Degree
of the University of Lübeck

from the Department of Natural Sciences

Submitted by

Caren Jacobi
From Hamburg, Germany

Lübeck 2023

First referee:	Prof. Dr. med. vet. Jennifer Hundt
Second referee:	Prof. Dr. rer. nat. Lars Redecke
Date of oral examination:	Lübeck, 1st October 2024
Approved for printing.	Lübeck, 2nd October 2024

For my parents

Table of content

1 Summary

Human skin wound healing is a complex dynamic, and highly regulated process. It consists of four overlapping, but distinct phases: homeostasis, inflammation, proliferation, and remodeling. Under physiological conditions wound healing is an automated process that requires little support or treatment to run smoothly and with satisfactory outcome. However, if the healing process is somehow disrupted, non-healing chronic wounds can occur. These wounds get stuck in one of the healing phases and cannot process further on their own. Mostly they stay in the inflammation phase and are thus characterized by an exuberant immune response, many pro-inflammatory signaling molecules and little signs of actual healing or skin cell proliferation and migration. Treatment of chronic wounds is extremely expensive and the quality of life of those affected is severely diminished. Current treatment options are not satisfactory. Often underlying diseases such as type 2 diabetes mellitus are the reason that wounds become chronic. As these diseases become more frequent with age and our society is getting older, finding new treatment strategies to aid wound healing becomes a more and more pressing research demand. This study aims to do so.

Therefore, the wound healing organ culture (WHOC) model out of human full-thickness skin was established in our working group. The WHOC was performed as a punch-in-a-punch model: 4 mm skin punches with a 2 mm wound in the center were taken out of skin donations from elective surgeries. All three layers of the skin were kept intact. Wound depth was about 500 µm and standardized with the help of a spacer. The skin punches were placed in specifically designed retainers and placed in 24 well plates filled with culture medium. The retainers kept the skin upright, thus ensuring that the epidermis is always kept at the air-liquid interface.

At first, the WHOC model was characterized in a time-course experiment, which revealed that the wounds healed nicely over the course of 7 days.

To avoid contaminations the non-alcoholic disinfectant Octenisept® was tested and found to have a detrimental effect on *ex vivo* wound healing.

The core piece of this work was the screening of the 136 substances of the Highly Selective Inhibitor Library L3500 der Firma Selleck Chemicals. As these substances were dissolved in dimethyl sulfoxide (DMSO), different DMSO concentrations were tested in the WHOC regarding their skin toxicity. 0.1 % DMSO were found to be well tolerated by the skin and thus chosen as vehicle control. 10 µM sodium gualenate (SG) seemed to aid top-view wound closure enough to be a sufficient positive control. Parameters evaluated during the screening were the relative top-view wound area, relative top-view wound perimeter, and relative wound volume obtained by optical coherence tomography. Due to the limited amount of retainers and skin available, the substances were divided in substances that already were in clinical trials and those that were not. Both groups were further divided into several sub-screenings. The clinical trials screening revealed eight promising and the non-clinical trials screening two promising substances, which might aid wound healing. These substances were further validated to see if the findings were reproducible. In the end three substances were chosen to be further evaluated: S2891, S2149, and S1180 – especially S1180 was found to have a strong positive effect on wound healing.

So far, all substances had only been tested in a concentration of 1 µM. Now different concentrations and repetitive treatment were investigated. Moreover, more parameters were studied: microscopic wound area and diameter, area and length of the epithelial tongues, cytokeratin 6 expression, and CD31 expression. S2891 was beneficial in most parameters but different concentrations performed best for different parameters, which made evaluation challenging. Treatment with 1 µM S2149 seemed to have a small positive effect onto wound healing – which would be highly interesting, as this drug is in clinical trials as treatment against type 2 diabetes mellitus. 1 µM S1180 and 10 µM

S1180 showed a strong, wound healing aiding effect on many parameters. This inhibitor was found to be the most successful one of the entire screening.
Interestingly, repetitive treatment with the three substances was not found more effective than one time treatment at day 1.
Skin donations are almost exclusively female. As one male skin was available, a pilot study was performed on male skin. Here, the three substances performed differently than on female skin. 1 µM S2891 aided wound healing strongly in this patient.
S1130 was the substance that performed worst in the entire screening. In a test of principle, where it was again tested, this finding could be replicated.
In the last step, the most successful substance, S1180, was tested in a pathological model. This model was developed by Post *et al.* and should mimic a chronic wound by withdrawal of insulin, addition of glucose and hydrogen peroxide while inducing hypoxia in a hypoxic incubator. However, in this work the pathological conditions were too harsh to study wound healing. Instead, the skin degraded.

To summarize: the WHOC is a powerful tool to study human wound healing and find possible treatment options. The screening revealed S1180 as a potential drug to aid wound healing. More research on the most efficient concentration and the exact mode of action are needed. Also, the pathological model should be adjusted to less harsh conditions to test S1180 in a mimicked chronic wound.

1.1 Zusammenfassung

Humane Wundheilung ist ein komplexer, dynamischer und streng regulierter Prozess. Er besteht aus vier überlappenden, aber eindeutige Phasen: Hämostase, Entzündung, Proliferation und Gewebeumbau. Unter physiologischen Bedingungen ist Wundheilung ein automatischer Prozess und benötigt wenig Unterstützung oder Behandlung, um reibungslos mit zufriedenstellendem Ergebnis abzulaufen. Aber wenn der Heilungsprozess irgendwie unterbrochen wird, können nicht heilende, chronische Wunden entstehen. Diese Wunden bleiben in einer der Heilungsphasen stecken, statt im Heilungsprozess voranzuschreiten. Meisten bleiben chronische Wunden in der Entzündungsphase und sind deshalb durch eine überschießende Immunantwort und charakterisiert. Heilung ist kaum sichtbar, genauso wenig wie Hautzellproliferation und -migration. Die Behandlung von chronischen Wunden ist sehr teuer und die Lebensqualität der Betroffenen ist stark beeinträchtigt. Die derzeitigen Behandlungsmöglichkeiten sind nicht zufriedenstellend. Oft sind Grunderkrankungen wie Diabetes mellitus Typ 2 der Grund dafür, dass Wunden chronisch werden. Da diese Krankheiten mit zunehmendem Alter häufiger werden und unsere Gesellschaft immer älter wird, wird die Suche nach neuen Behandlungsstrategien zur Unterstützung der Wundheilung zu einem immer dringenderen Forschungsbedarf. Diese Arbeit zielt darauf ab, Wundheilung besser zu verstehen und neue Medikamentenkandidaten zu finden.

Dafür wurde das Wundheilungsorgankultur (WHOK) Model aus humaner Vollhaut in unserem Labor etabliert. Die WHOK ist ein „*punch-in-a-punch*" Model: 4 mm Hautbiopsien mit einer 2 mm Wunde in der Mitte wurden von Hautspenden nach elektiven chirurgischen Eingriffen genommen. Dabei wurden alle drei Schichten der Haut erhalten. Die Tiefe der Wunde war ca. 500 µm tief und wurde mit Hilfe eines Abstandhalters standardisiert. Die Hautbiopsien wurden in extra entwickelten Hauthaltern platziert und dann in einer 24 *well* Platte mit Kulturmedium kultiviert. Die Hauthalter sorgten dafür, dass die Haut aufrecht blieb und somit die Epidermis immer an der Luft-Flüssigkeitsgrenzfläche blieb.

Als erstes wurde das WHOK-Model im Zeitverlauf charakterisiert. Dieses zeigte, dass die Wunden gut über die sieben Tage Kultur heilten.

Um Kontaminationen zu vermeiden, wurde das nicht alkoholische Desinfektionsmittel Octenisept® in der WHOK getestet und es wurde herausgefunden, dass dieses einen vernichtenden Effekt auf die *ex vivo* Wundheilung hatte.

Das Herzstück dieser Arbeit war das Screening der 136 Substanzen der *Highly Selective Inhibitor* Bibliothek L3500 der Firma *Selleck Chemicals*. Da diese Substanzen in Dimethylsulfoxid (DMSO) gelöst waren, wurden verschiedene DMSO-Konzentrationen in der WHOK getestet, um deren Toxizität an Haut zu testen. 0,1 % DMSO wurden von der Haut gut vertragen und wurden entsprechend als Vehikel-Kontrolle gewählt. 10 µM Sodiumgualenat schien den Aufsicht-Wundverschluss genug zu unterstützen um als Positivkontrolle zu dienen. Die Parameter, die während des Screenings evaluiert wurden, waren die relative Aufsicht-Wundfläche, der relativer Aufsicht-Wundperimeter und das relative Wundvolumen (durch optische Kohärenztomografie bestimmt). Auf Grund der begrenzten Anzahl an Hauthaltern und vorhandenen Haut, wurden die Substanzen in solche aufgeteilt, die bereits in klinischen Studien waren und denen die es nicht waren. Beide gruppen wurden weiterhin in mehrere Unter-Screenings eingeteilt. Das Screening der Substanzen aus den klinischen Studien zeigte acht und das aus den nicht-klinischen Studien zwei erfolgsversprechende Substanzen, die die Wundheilung unterstützen könnten. Diese Substanzen wurden weiter validiert, um zu untersuchen, ob die Ergebnisse reproduzierbar waren. Letztlich wurden drei Substanzen für weitere Untersuchungen ausgesucht: S2891, S2149 und S1180 – insbesondere S1180 unterstützte die *ex vivo* Wundheilung deutlich.

Bisher wurden alle Substanzen in einer Konzentration von 1 µM getestet. Nun wurden unterschiedliche Konzentrationen und wiederholte Behandlung untersucht. Außerdem wurden weitere Parameter ausgewertet: mikroskopische Wundfläche und -durchmesser, Fläche und Länge der Epithelzungen, Zytokeratin 6 Expression und CD31 Expression. S2891 wirkte sich auf die meisten Parameter positiv aus, aber bei unterschiedlichen Parametern waren andere Konzentrationen am besten, was die Bewertung erschwerte. Behandlung mit 1 µM S2149 schien einen leicht positiven Effekt auf die Wundheilung zu haben. Dies wäre sehr interessant, da sich S2149 in klinischen Studien gegen Typ 2 Diabetes mellitus befindet. 1 µM S1180 und 10 µM S1180 zeigten einen starken, die Wundheilung unterstützenden Effekt auf viele der untersuchten Parameter. Dieser Inhibitor war der erfolgreichste des ganzen Screenings.
Interessanterweise brachte eine wiederholte Behandlung mit den Substanzen keinen Vorteil gegen über einmaliger Behandlung an Tag 1 der Kultur.
Die Hautspenden waren beinahe ausschließlich weiblich. Da eine männliche Haut verfügbar war, wurde eine Pilotstudie an männlicher Haut durchgeführt. Die drei Substanzen verhielten sich anders als auf weiblicher Haut. 1 µM S2891 unterstütze die Wundheilung deutlich bei diesem Patienten.
S1130 war die Substanz, die am schlechtesten im gesamten Screening wirkte. In einem Grundsatztest, in dem S1130 erneut getestet wurde, konnte dieses Ergebnis reproduziert werden.
Als letztes wurde die erfolgreichste Substanz, S1180, in einem pathologischen Model getestet. Dieses Model wurde von Post *et al.* getestet und soll eine chronische Wunde eine chronische Wunde durch den Entzug von Insulin, die Zugabe von Glukose und Wasserstoffperoxid bei gleichzeitiger Induktion von Hypoxie in einem hypoxischen Inkubator imitieren. In dieser Arbeit waren die pathologischen Bedingungen jedoch zu hart, um die Wundheilung zu untersuchen. Stattdessen zersetzte sich die Haut.

Zusammenfassend lässt sich sagen, dass die WHOK eine sehr nützliche Methode ist, menschliche Wundheilung zu erforschen und mögliche Behandlungsstrategien zu testen. Das Screening zeigte, dass S1180 ein potenzielles Medikament sein könnte, um Wundheilung zu unterstützen. Weitere Forschungen bezüglich der effizientesten Konzentration und dem Wirkmechanismus sind nötig.
Außerdem sollte das pathologische Modell so angepasst werden, dass die Bedingungen weniger hart sind. Anschließend kann S1180 in diesem Modell getestet werden, um zu untersuchen, ob es die chronische Wundheilung ebenfalls unterstützt.

2 Introduction

This chapter introduces the reader to the function and structure of the human skin, as well as the human skin wound healing. The different phases of the wound healing are described. Moreover, the problem of chronic wounds and their treatment is illustrated. Finally, different models to study human wound healing are discussed.

2.1 The human skin

The human skin is a large organ with an area of about 2 m^2. It serves as a barrier between the "inside" (the human body) and the "outside" (the environment). Next to its predominant task of separating the body from the outside, the human skin is also essential for perceiving the outside world. For example, our sense of touch is transmitted by mechanoreceptors in the skin. Moreover, the human skin plays an important role in thermoregulation and containing the bodies liquid and prevents the body from drying up. As a barrier to the outside, the skin is also the first line of defense against harmful environmental influences as well as various pathogens, thus making the skin a crucial part of the immune system (Chambers & Vukmanovic-Stejic, 2020; Fritsch & Schwarz, 2018; Röcken *et al.*, 2010; Sterry *et al.*, 2011; Tsuruta *et al.*, 2002).

The human skin is about 1.5-4 mm thick (without the subcutis), depending on the anatomical location. As **Figure 2.1** shows, the skin consists of three layers: epidermis, dermis, and subcutis (Fritsch & Schwarz, 2018; Gonzales & Fuchs, 2017). These layers will be further discussed in the following:

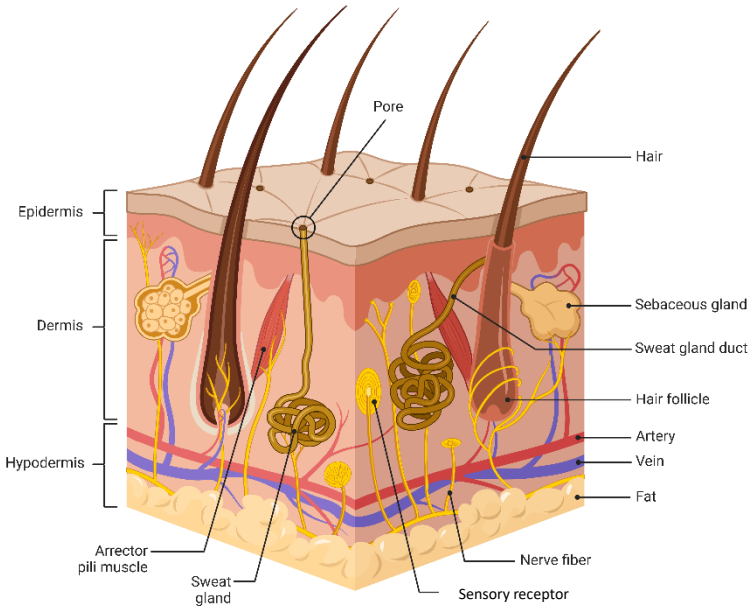

Figure 2.1: Structure of human skin
The human skin has three layers: the epidermis, the dermis and the subcutis. The epidermis is the outermost layer and protects the body. The dermis is innervated and perfused and nurtures the epidermis. Moreover, skin appendages such as hair follicles and sweat glands can be found here. The subcutis mainly consists out of fatty tissue. Illustrated with BioRender.

2.2.1 The epidermis

The epidermis is the outer layer of the human skin. It is about 100 µm thick and a keratinized squamous epithelium. It consists predominantly out of keratinocytes, which give it structure (Baroni *et al.*, 2012; Chambers & Vukmanovic-Stejic, 2020; Sterry *et al.*, 2011). The epidermis is ordered in the following layers, which can also be seen in **Figure 2.2**:

- *Stratum basale*: The *stratum basale* is the innermost layer of the epidermis. It consists of a single layer of cylindrical keratinocytes. They are anchored in the basal membrane, which separates the epidermis from the dermis. In the *stratum basale* the stem cells of the epidermis are found, making it an important region in case of wound healing and regeneration (Fritsch & Schwarz, 2018; Sterry *et al.*, 2011).
- *Stratum spinosum*: The *stratum spinosum* consists out of several layers of large, cubic cells, which are connected via desmosomes. The cornification of keratinocytes already begins here (Fritsch & Schwarz, 2018; Sterry et al., 2011).
- *Stratum granulosum*: The *stratum granulosum* is made of fewer layers of keratinocytes than the *stratum spinosum*. The cells have a more flattened shape and contain granules, in which important structural proteins of the *stratum corneum* are produced. They are connected by tight junctions, sealing the skin against the environment more effectively. Within this layer the keratinocytes begin to consist more and more of keratohyalin granules and less of organelles (Fritsch & Schwarz, 2018; Sterry *et al.*, 2011).
- *Stratum corneum*: The *stratum corneum* is the outermost layer of the epidermis. It consists of corneocytes, dead squamous keratinocytes without nuclei or organelles, but with a lot of keratin, which is a sufficient barrier against the environment. The *stratum corneum* serves as mechanical protection of the skin and is important for protection against water loss. Depending on the location and mechanical stress the skin must endure at that position, the *stratum corneum* can up to 20 layers deep. The *stratum corneum* is thickest at the palms and foot soles (Fritsch & Schwarz, 2018; Menon *et al.*, 2012; Tsuruta et al., 2002).

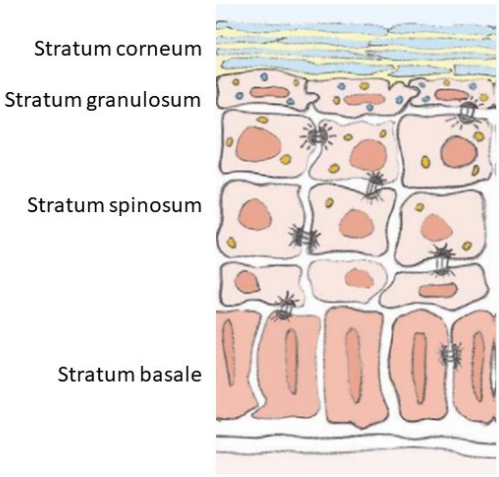

Figure 2.2: Layers of the human epidermis
The keratinocytes move from the *stratum basale* up to the *stratum corneum* and differentiate along the way, until they are dead corneocytes without nuclei. The black structures between the cells depict desmosomes, which are important for cell-cell contact. Figure modified from Baroni *et al.* (Baroni *et al.*, 2012).

From the stem cells in the *stratum basale*, the basal layer, the keratinocytes differentiate along the layers of the epidermis to the *stratum corneum*, where they are discarded as corneocytes. This process of differentiation takes 4 to 6 weeks (Fritsch & Schwarz, 2018; Röcken *et al.*, 2010).

While the keratinocytes make up the majority of cells in the epidermis, there are more sorts of cells present:

- Melanocytes (compare **Figure 2.3**): The melanocytes sit in the basal layer of the epidermis and can also be found in the hair follicle. They make up about 5-10 % of the basal layer cells and synthesize the pigment melanin. After synthesis, melanin is transported into the keratinocytes in the *stratum spinosum*, *stratum granulosum* and *stratum corneum*. Within the keratinocytes melanin is deposited around the nucleus, where it absorbs the harmful UV light. Thus, by producing melanin the melanocytes protect the skin from UV damage and the resulting cancer (Fritsch & Schwarz, 2018; Lin & Fisher, 2007).

Figure 2.3: Schematic drawing of a melanocyte
Created with BioRender.

- Langerhans cells (compare **Figure 2.4**): Langerhans cells are situated in the *stratum spinosum*. They are the most important immune cells in the epidermis. As dendritic cells they can phagocytose antigens, which e.g. get into the skin via a wound. Upon phagocytosis the Langerhans cells differentiate and travel to the next lymph node as antigen presenting cells. In this way, they alert the circulating immune cells to potential threads in the epidermis before pathogens can penetrate deeper into the human body (Clayton et al., 2017; Fritsch & Schwarz, 2018).

Figure 2.4: Schematic drawing of a Langerhans cell
Created with BioRender.

- Merkel cells (compare **Figure 2.5**): The Merkel cells can be found in the basal layer of the epidermis. They are amongst the most sensitive mechanoreceptors of the human skin (Fritsch & Schwarz, 2018).

Figure 2.5: Schematic drawing of a Merkel cell fiber
Created with BioRender.

The epidermis is neither innervated nor perfused. It is nurtured by the underlying dermis (Sterry *et al.*, 2011).

2.1.2 The dermis

The dermis is the connective tissue directly below the epidermis. It is connected to the basal membrane of the epidermis by anchoring fibrils and about 3-4 mm thick. The dermis is innervated and perfused, so it can supply the epidermis with nutrients (Chambers & Vukmanovic-Stejic, 2020; Röcken *et al.*, 2010).
Like the epidermis, the dermis consists out of different layers, though in the case of the dermis there are only two layers, as **Figure 2.6** shows:

- *Stratum papillare*: The *stratum papillare* is the upper layer of the dermis, which is directly below the epidermis and connected to it in the dermal-epidermal junction. It is relatively thin. The *stratum papillare* consists out of collagen-rich connective tissue, that forms a rather loose but fine network and is also rich in elastin. It contains comparatively many cells, as well as blood- and lymph vessels (Sterry *et al*., 2011; Woodley, 2017).
- *Stratum reticulare*: The *stratum reticulare* is the lower, much thicker layer of the dermis. Its connective tissue network is denser and coarser. Though fewer cells in total, there are more fibroblasts present among those cells. Hair follicles, sebaceous glands and sweat glands are situated here (Sterry *et al.*, 2011; Woodley, 2017).

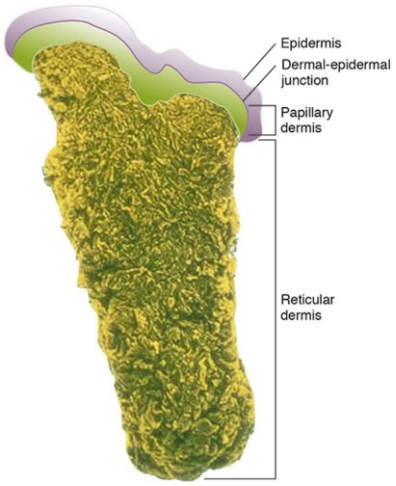

Figure 2.6: Ratio of epidermis and the dermal layers
The epidermis is the uppermost layer of the human skin. Below it lays the dermis, which is separated into two layers. The papillary dermis is roughly as thick as the epidermis while the reticular dermis is much thicker. Figure from Woodley. (Woodley, 2017).

Unlike the epidermis, which basically consists only out of cells, the dermis is mainly made of connective tissue and only a few cells "scattered" between. The main component of the connective tissue is collagen (mostly collagen type I), it makes up 70 % of the dry weight of the dermis. Next to collagen fibers, the dermis also consists out of elastin fibers and proteoglycans (Fritsch & Schwarz, 2018; Oikarinen, 1994).

Multiple types of cells can be found in the dermis:

- Fibroblasts (compare **Figure 2.7**): Fibroblasts are spindle-shaped and the most common cells in the dermis. They synthesize and rearrange the collagen fibers, proteoglycans, and elastic fibers of the extra cellular matrix of the dermis (Sterry *et al.*, 2011; Woodley, 2017).

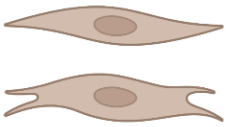

Figure 2.7: Schematic drawing of a resting (above) and activated (below) fibroblast
Created with BioRender.

- Tissue resident macrophages (compare **Figure 2.8**): Under healthy, physiological conditions tissue resident macrophages are the most abundant hematopoietic cells in the skin. They are important to ensure skin integrity and functions. They are crucial in sensing invading pathogens and injury to the skin and attract other immune cells to the site of injury or pathogen invasion. Tissue resident macrophages are the first line defense against pathogens, but also have homeostatic functions and functions in wound healing (more see **Chapter 2.2**) (Tay *et al.*, 2013).

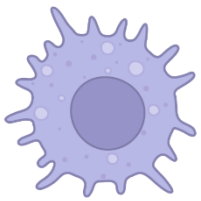

Figure 2.8: Schematic drawing of a macrophage
Created with BioRender.

- Mast cells (compare **Figure 2.9**): Mast cells are positioned close to blood vessels in the dermis. They are important effectors of the immune response and can have pro- and anti-inflammatory roles. They might participate in pathogen defense, contact hypersensitivity, allergic reactions, and wound healing (Tay *et al.*, 2013).

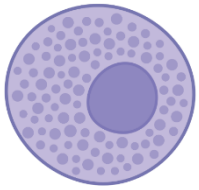

Figure 2.9: Schematic drawing of a mast cell filled with granules
Created with BioRender.

- Lymphocytes (compare **Figure 2.10**): Here, especially skin resident T memory cells are worth mentioning. These T cells do not circulate but instead are stationary in the skin. They play an essential role in immune surveillance and initiating a sufficient immune response after infection (Chambers & Vukmanovic-Stejic, 2020; Tay *et al.*, 2013).

Figure 2.10: schematic drawing of a T cell
Created with BioRender.

Next to the cells and the connective tissue, the following structures are present in the dermis:

- Blood vessels (compare **Figure 2.11**): The blood vessels of the dermis (and subcutis) provide the skin with oxygen and nutrients, while removing metabolic waste products and thus keeping the skin healthy and alive (Gunin *et al.*, 2014).

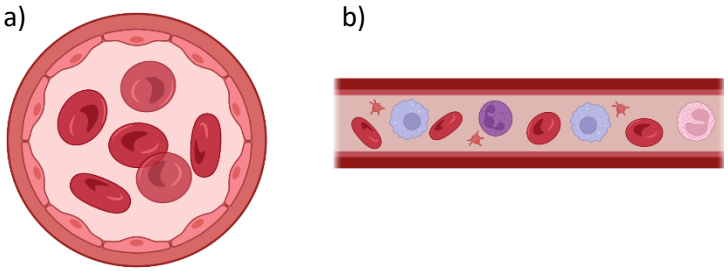

Figure 2.11: Schematic drawing of blood vessels
a) Cross section of a vessel filled with erythrocytes, b) longitudinal section of a vessel filled with erythrocytes, platelets, and immune cells. Created with BioRender.

- Lymphatic vessels (compare **Figure 2.12**): Lymphatic vessels in the dermis (and subcutis) are crucial for the immune response. They allow antigen presenting cells, e.g. Langerhans cells to travel to the next lymph node. Here they can present their antigen to the lymphocytes in the lymph node and thus help triggering an optimal immune response in case of infections (Lukas *et al.*, 1996). Moreover, lymphatic vessels and the fluid within them, the lymph, have an important role in maintaining the fluid balance in the body (Albertin *et al.*, 2023).

Figure 2.12: Schematic drawing of lymphatic vessels with lymph nodes
Created with BioRender.

- Sweat glands (compare **Figure 2.13**): The main role of sweat glands is the production of sweat, so they have an important role in the thermoregulation of the human body. There are different types of sweat glands, the most prominent ones are apocrine and eccrine sweat glands. The almost omnipresent eccrine sweat glands might also play a role in wound healing (Groscurth, 2002; Rittié *et al.*, 2013).

Figure 2.13: Schematic drawing of a sweat gland
Created with BioRender.

- Sebaceous glands (compare **Figure 2.14**): The sebaceous glands can be mostly found combined with the hair follicle in the pilosebaceous units of the dermis. Exception to this are a few regions with no to little hair growth, where sebaceous glands are situated alone, for example the eye lids or oral mucosa. The main task of the sebaceous glands is the production of sebum, which protects the skin from water loss and might also have antibacterial properties (Niemann & Horsley, 2012).
- Hair follicle (compare **Figure 2.14**): Hair follicles are present in the skin of all mammals. In humans the scalp hair is the most prominent, but most of our bodies are covered in finer, less dense hair. Hair helps keeping the body temperature stable and can protect the skin from mechanical stress (Buffoli *et al.*, 2013). The hair follicle is a source of stem cells and progenitor cells, that can help with the re-epithelialization in wound healing (Ansell *et al.*, 2011; Tiede *et al.*, 2007). The hair follicle is associated with the sebaceous gland and often the arrector pili muscle. This muscle can erect the hair when humans get cold and can stimulate sebum excretion (Pascalau & Kuruvilla, 2020; Poblet *et al.*, 2005).

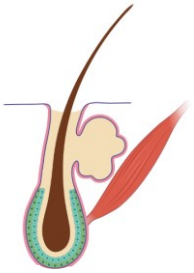

Figure 2.14: Schematic drawing of a hair follicle with adjacent sebaceous gland and arrector pili muscle
Created with BioRender.

- Nerves (compare **Figure 2.15**): The dermis is crisscrossed by fine nerve fibers and the sensory receptors are located here. This allows the transmission of sensory impressions, such as pain, temperature, pruritus, touch, and vibration, from skin to the central nervous system (Sterry *et al.*, 2011).

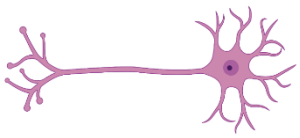

Figure 2.15: Schematic drawing of a neuron
Created with BioRender.

2.1.3 The subcutis:

The subcutis is the often overlooked, third layer of the human skin. It mainly consists out of adipocytes and connective tissue (compare **Figure 2.16**). The subcutis serves as isolation against cold and as mechanical protection. Adipocytes may also play a crucial role in the immune response. Next to the epidermis, the adipocytes of the subcutis produce antimicrobial peptides (Eming *et al.*, 2014; Fritsch & Schwarz, 2018; Guan *et al.*, 2023).
Moreover, adipose derived stem cells might aid wound healing (Ahmadi *et al.*, 2020; Kim *et al.*, 2017).

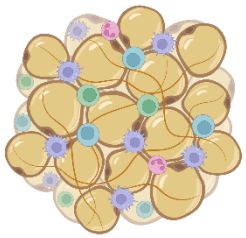

Figure 2.16: Schematic drawing of adipose tissue with connective fibers and different immune cells.
Created with BioRender.

2.2 Wound healing of the human skin

As the skin is the outer layer of the body and as such the barrier to the environment, skin defects or wounds are inevitable (Enoch & Leaper, 2005; Zomer & Trentin, 2018). An intact skin is, however, crucial for the homeostasis of the body. In fact, large wounds (e.g. after burns) are life threatening for the patient due to loss of fluid, cooling of the body and the high risk of infection. So, wounds need to heal quickly. The aim of wound healing is the restoration of the destroyed tissue. If the injury reaches the *stratum reticulare* of the dermis, the healing will leave a scar, as the originally complex, interwoven collagen fibers will be replaced by simple, dense, parallel collagen bundles. Moreover, destroyed skin appendages cannot be replaced in this case (Eming *et al.*, 2014; Fritsch & Schwarz, 2018; Monavarian *et al.*, 2019) .

Depending on the depth and size of the injury, wound can heal within 24 hours (in case of a clean cut and wound edges that are very close to each other), or take multiple weeks to heal (in the case of large, deep wounds, e.g. burns) (Enoch & Leaper, 2005; Fritsch & Schwarz, 2018).

Healing of acute wounds is an automated dynamic, very complex, highly regulated and coordinated process, in which many different tissues and cells take part in. For acute wounds this process can be divided into four overlapping phases. **Figure 2.17** shows the timely order of these phases (Goldberg & Diegelmann, 2017; Zomer & Trentin, 2018):

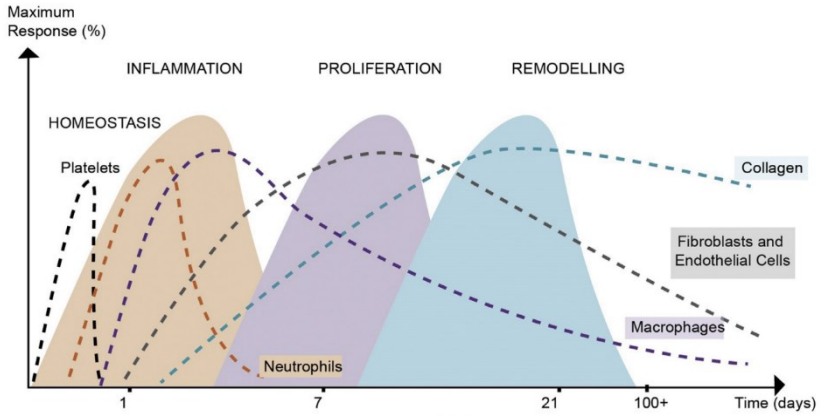

Figure 2.17: Timeline of the phases of wound healing
Shown here is the course and maximum of the four wound healing phases and important cellular players in human wound healing. Figure taken from Zomer and Trentin (Zomer & Trentin, 2018).

Before describing the phases of wound healing in more detail it should be noted that the literature is not unanimous regarding the division of the phases. Some authors combine homeostasis and inflammation in one phase and accordingly speak of three phases of acute wound healing (Baron *et al.*, 2020; Zomer & Trentin, 2018).

1. Homeostasis
(compare **Figure 2.18**):
The homeostasis occurs directly after wounding and takes less than a day. It is characterized by vasoconstriction and blood clotting (Frykberg & Banks, 2015). When the skin is wounded, the blood vessels in the dermis will be injured and bleed. The bleeding activates the coagulation cascade, which results in a clot formation. The clot is made of fibrin, fibronectin and vitronectin. It seals the blood vessels, which stops the blood loss. Moreover, this network of macromolecules severs as a provisory matrix for cell migration. The thrombocytes in the clot serve as a source of cytokines and growth factors (e.g. epidermal growth factors (EGF), platelet derived growth factor (PDGF), insulin-like growth factor 1 (IGF 1)), which activate fibroblasts, endothelial cells and macrophages. This starts the wound healing cascade (Diegelmann & Evans, 2004; Enoch & Leaper, 2005; Fritsch & Schwarz, 2018).

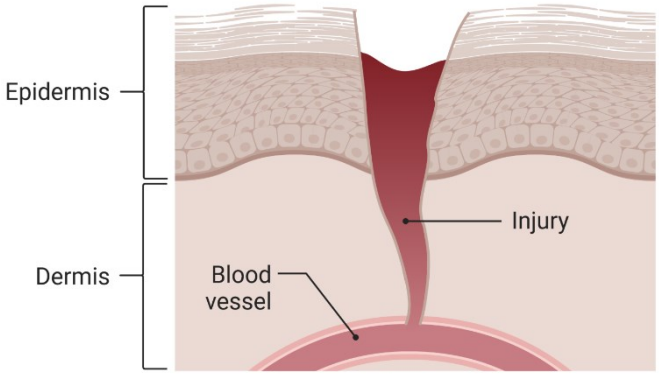

Figure 2.18: Phase 1 of wound healing: hemostasis
The wound is fresh, and healing has yet to start. Created with BioRender.

2. Inflammation (compare **Figure 2.19**):
The inflammation phase is the second phase of the wound healing. It starts with the coagulation and can last up to seven days. Here, immune cells are recruited to the wound site to clean the wound of pathogens and debris. At the end of the phase there should be no more pathogens or contamination present in the wound and the wound bed should thus be prepared for the formation of the ECM of the new dermis (Enoch & Leaper, 2005; Fritsch & Schwarz, 2018; Frykberg & Banks, 2015; Goldberg & Diegelmann, 2017).
After an injury, many substances present in the wound can serve as chemoattractant, for example growth factors, extra cellular matrix debris, and bacterial peptides. These molecules together with chemokines attract immune cells to the wound. Moreover, pathogens can be recognized via pathogen-associated-molecular-patterns (PAMPs) and damaged cells by the release of damage-associated-molecular-patterns (DAMPs) by immune cells via their toll-like receptors. This recognition also triggers an immune response (Eming *et al*., 2014; Fritsch & Schwarz, 2018; Mamilos *et al*., 2023).
To follow the chemokine gradient to the site of injury, the leukocytes must leave the blood vessels and migrate through the tissue to the wound. The extravasation of immune cells out of the vessel is called leukocyte diapedesis. To make the diapedesis possible, the adhesion molecules on the endothelial cells and on the leukocytes need to change (Enoch & Leaper, 2005; Fritsch & Schwarz, 2018).

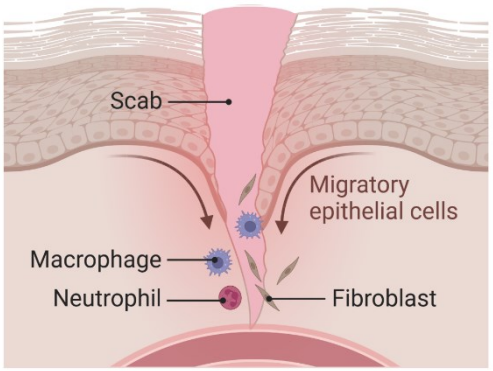

Figure 2.19: Phase 2 of wound healing: inflammation
A scab/blood clot closed the wound and serves as a provisory matrix for migrating cells. Immune cells are recruited to the wound. The healing cascade is activated. Created with BioRender.

In human skin healing two sorts of immune cells are most important: the neutrophil granulocytes in the early stages of inflammation and the macrophages in the later stages (Enoch & Leaper, 2005).

Neutrophil granulocytes are the first cells at the site of injury. They reach the wound within minutes after injury (Fritsch & Schwarz, 2018). Neutrophils phagocytose and kill pathogens among others by the release of reactive oxygen species (ROS) and proteases (Enoch & Leaper, 2005; Frykberg & Banks, 2015). They also remove other contamination and debris out of the wound, so that the wound bed is clean (Enoch & Leaper, 2005; Fritsch & Schwarz, 2018; Frykberg & Banks, 2015). Next to their phagocytotic role, neutrophils also produce and secrete proinflammatory cytokines, which activate fibroblasts and keratinocytes. For example, neutrophils have been found to secrete interleukin (IL) 6, which induces proliferation of keratinocytes and attracts more neutrophils to the wound in a murine study (Gallucci *et al*., 2004; Pastar *et al.*, 2014).

Usually, neutrophils are only active for a few days in the inflammation phase of wound healing. The remaining neutrophils are then flushed out of the wound or get phagocytosed by macrophages; which take over in the later stage of the inflammation phase (Enoch & Leaper, 2005; Fritsch & Schwarz, 2018).

Macrophages are crucial players in the inflammatory response. They are also crucial for wound healing. In case of an injury, next to the tissue resident macrophages, monocytes out of the blood circulation are attracted to the site of injury, extravasate into the tissue, migrate through the tissue and differentiate into macrophages (Goldberg & Diegelmann, 2017; Mamilos *et al.*, 2023; Tay *et al.*, 2013). At the wound site macrophages phagocytose remaining pathogens, debris, and neutrophils, thus cleaning the wound further. At least equally essential is the secretion of multiple, important growth factors, chemokines, and cytokines (Fritsch & Schwarz, 2018; Goldberg & Diegelmann, 2017). Some of these molecules are proinflammatory cytokines and chemokines, that attract specific sets of immune cells to the side of injury (e.g. dependent on the severity of infection) (Tay *et al*., 2013). These cytokines and growth factors serve as an additional, more potent activation for the cells involved in wound healing and inflammation (Fritsch & Schwarz, 2018). This proinflammatory phenotype is referred to as M1 macrophages. In the later stages of the inflammation phase of wound healing the macrophages switch from the M1 phenotype to the growth-promoting, less inflammatory M2 phenotype. The M2 macrophages secrete growth factors and cytokines which are, among others, important for recruitment of fibroblasts, keratinocytes and endothelial cells, ECM production by fibroblasts and induction of angiogenesis and are generally associated with tissue and regeneration (Frykberg & Banks, 2015; Goldberg & Diegelmann, 2017; Mamilos *et al.*, 2023; Tay *et al.*, 2013).

Macrophages are highly plastic and can inhibit or stimulate cell proliferation and tissue repair. This gives them a regulatory function (Mamilos *et al.*, 2023; Zomer & Trentin, 2018).

The crucial role of macrophages in wound healing has been confirmed by macrophage-depletion mouse models, which showed severe wound healing defects (Sim *et al.*, 2022).

Though neutrophil granulocytes and macrophages are key players of the inflammation phase, other cells of the complex human immune system play a role in wound healing. Regulatory T cells for example, are crucial in the switch from inflammation to proliferation phase. They might also directly aid wound healing via the epidermal growth factor receptor (Nosbaum *et al.*, 2016; Zaiss *et al.*, 2019).

Already in the inflammation phase an increase in the proliferation of the basal keratinocytes can be observed. Also, the migration of cells into the wound and the collagen synthesis starts. In this phase first collagen fibers at the wound edges become visible (Enoch & Leaper, 2005).

As a small side note I want to point out here: While the inflammation is crucial to clean the wound, fetal studies show that a scarless wound healing is only possible if no inflammation response is present (Eming et al., 2014).

3. Proliferation (compare **Figure 2.20**):
   The third phase of wound healing is characterized by epithelialization, tissue granulation and angiogenesis. It becomes noticeable about 3 days after injury and takes 2 – 4 weeks. The inflammation subsides during this phase and apoptosis of immune cells can be detected. By the end of this phase, the re-epithelialization is finished and the wound is covered by a thin layer of epithelium (Enoch & Leaper, 2005; Frykberg & Banks, 2015).
   Re-epithelialization means that the keratinocytes close a defect with a new epidermis and thus restore the epithelial barrier. This process is crucial for wound healing, as the wound is only really closed once the epidermis is intact again (Pastar *et al.*, 2014).

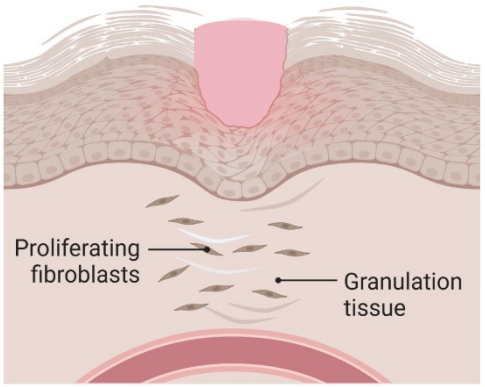

Figure 2.20: Phase 3 of wound healing: proliferation
Fibroblasts proliferate and synthesize new connective tissue, thus forming the granulation tissue. Also the keratinocytes proliferate and start to close the epidermal defect. The scab is slowly replaced by new tissue. Created with Biorender.

   If the skin is injured, epidermal cells are lost and they must be replaced. This is why an increase in proliferation of the basal keratinocytes is detectable during wound healing. These proliferating cells are located slightly behind the newly growing and migrating epithelium, the so called “epithelial tongues” (ETs). Though the proliferation phase only really starts at day 3, first basal and suprabasal epidermal cells migrate into the wound within hours after wounding (Fritsch & Schwarz, 2018; Pastar *et al*., 2014).
   The ETs grow along the border between the dermis and the fibrin clot. Therefore, certain factors are expressed on the cells of the “tip” of the ETs lyse the provisory matrix and make way for the migrating ETs. Especially important here are matrix metalloproteases (MMPs). For example, MMP1 helps keratinocytes to move on type 1 collagen. Additionally, the hemidesmosomes, anchoring the basal keratinocytes to the basal membrane need to be dissolved. Only then can the keratinocytes adhere to the provisory matrix or the wound dermis. This is achieved by a change in the expressed adhesion molecules. Then the cells can travel by contraction of their actomyosin cytoskeleton and by formation of lamellipodia, pseudopodia like protuberances. The changes in cytoskeleton and surface receptors of these activated, migrating keratinocytes are essential for the migration process. For example, the increased expression of cytokeratin (CK) 6, CK 16, and CK 17 might increase the viscoelasticity of migrating cells (Fritsch & Schwarz, 2018; Pastar *et al*., 2014).
   The migration of keratinocytes is triggered by the secretion of growth factors from several cell types: thrombocytes secrete EGF and transforming growth factor (TGF) α and β, macrophages secrete TGFα and β, and keratinocytes secrete TGFα. Especially important is the secretion of stimulating growth factors by already activated fibroblasts, e.g. keratinocyte growth factor (KGF), fibroblast growth factor (FGF), and IGF 1. An example of an important cytokine for the proliferation phase is IL 1. IL 1 induces keratinocyte migration and proliferation, as well as the expression of CK 6 and CK 16 in keratinocytes, that migrate through the wound. Furthermore, IL 1 activates nearby fibroblasts (Fritsch & Schwarz, 2018; Pastar *et al*., 2014).

As soon as the re-epithelialization is completed, meaning the wound area is completely covered with a new epidermis, the migration process stops. Now the synthesis of a new basal membrane and new hemidesmosomes begins. The keratinocytes switch from the activated, hyperproliferating and migrating state to the "normal" differentiation program of the epidermis. In the last step of the epidermal healing, the keratinocytes are fixated on the basal lamina by anchoring fibrils (Freedberg *et al.*, 2001; Fritsch & Schwarz, 2018).

Next to re-epithelialization by keratinocytes also a new dermis has to be built. Fibroblasts are attracted to the wound by different growth factors, chemokines and cytokines. They produce and deposit the connective tissue of the new dermis. The formation of the so called "granulation tissue" begins 3 – 4 days after wounding. It replaces the fibrin/fibronectin matrix provided by the blood clot in the 1st phase. This makes the migration of different cells into the provisory wound matrix easier. The granulation tissue is characterized by proliferating fibroblasts, a loose, collagen-rich ECM, and capillaries. The fibroblasts are activated by several different growth factors, e.g. PDGF and TGF β secreted by thrombocytes and macrophages and autocrine production of activin and connective tissue growth factor.
Just like keratinocytes fibroblasts also need different adhesion molecules to adhere to the provisory matrix and use fibronectin as "guide bar". For fibroblasts a switch from α2 integrins to α3, α5 integrins is detectable (Fritsch & Schwarz, 2018; Goldberg & Diegelmann, 2017; Pastar *et al.*, 2014).

Another crucial process during the proliferation phase is the angiogenesis, i.e. the formation of new vasculature into the new dermis (Fritsch & Schwarz, 2018; Grambow *et al.*, 2021). Endothelial cells are activated by multiple stimuli. Among those are proangiogenic cytokines and grow factors released by keratinocytes and fibroblasts (Pastar *et al.*, 2014). Moreover, platelets release the vascular endothelial growth factor (VEGF) upon hypoxia after wounding. VEGF is especially essential in promoting endothelial cell migration and proliferation (Pastar *et al*., 2014). M1 macrophages also secrete VEGFα and other proangiogenic factors. M2 macrophages secrete proteases like MMP9, which cleave the extracellular matrix (ECM) and thus form space for new vessel formation in the granulation tissue. They also phagocytose redundant vessels (Mamilos *et al.*, 2023).
The now activated skin endothelial cells migrate into the granulation tissue, proliferate and thus new, immature vasculature can form. As before the migration into the provisory matrix requires a switch in adhesion molecules (Pastar *et al.*, 2014).
Moreover, the injured endothelial cells support the growth of new vessels from the surrounding capillaries by secreting basic fibroblast growth factor (Fritsch & Schwarz, 2018).
In this phase also the regeneration of terminal nerves takes place. The exact mechanisms are not clear, though it is probably induced nerve growth factor (NGF), which is upregulated by TGF β (Fritsch & Schwarz, 2018).

About one week after injury, the fibrin clot is completely traversed by activated fibroblast and the collagen synthesis is in full swing. Induced by mechanical factors and TGFβ some of the fibroblasts become myofibroblasts. They now express smooth muscle actin. Contraction of the myofibroblasts brings the wound edges closer to each other, which aids healing. However, the contraction in human wound healing is highly variable depending on the anatomical region and much less pronounced than in e.g. mice. The essential key processes in human wound healing are re-epithelialization and granulation tissue formation not contraction (Fritsch & Schwarz, 2018; Zomer & Trentin, 2018).

As soon as the wound is closed, the growth factor receptors on fibroblasts are downregulated and they either undergo apoptosis (especially the myofibroblasts) or enter a "resting stage"(Fritsch & Schwarz, 2018).

4. Remodeling

The remodeling phase is the last phase of wound healing. It starts about one week after the injury once the wound has closed. It can last several weeks; in some cases, the remodeling process even takes up a few years (Enoch & Leaper, 2005; Frykberg & Banks, 2015).

This phase is characterized by a continuous production, degradation, and remodeling of collagen, so that in the end the provisory matrix is then structured into organized collagen bundles. Usually, a steady state is reached about 21 days after wounding. During the remodeling process, the density of macrophages and fibroblasts as well as the blood flow and metabolic activity decrease in the wound side (Frykberg & Banks, 2015).

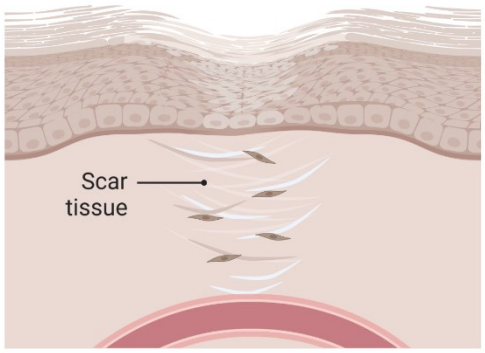

Figure 2.21: Phase 4 of wound healing: remodeling The wound is healed and scar tissue was formed. The new tissue is remodeled and further optimized. Created with BioRender.

The remodeling of the wound is orchestrated by a close interaction of MMPs and their regulators tissue inhibitors of MMPs (TIMPs) (Enoch & Leaper, 2005).

The skin can heal epidermal defects extremely well. However, if the dermis is hurt and granulation tissue was formed, it becomes scar tissue, as **Figure 2.21** shows. Scar tissue arises due to excessive deposition of extra cellular matrix (mainly collagen). This tissue consists mainly of inactive fibroblasts, dense collagen and other extra cellular matrix components (Eming *et al.*, 2014; Enoch & Leaper, 2005). Scarring can happen to a different degree. Relatively minor scarring is inevitable in case of deeper wounds. If the scar tissue proliferates out of the wound area due to enhanced collagen deposition and decreased degradation this severe scar is called a keloid. Scars can severely decrease the quality of life of those affected, as scaring can lead to physical deformations and psychological harm (Gantwerker & Hom, 2011; Monavarian *et al*., 2019).

During the continuing remodeling phase the scar tissue will mature. This includes also remodeling of collagen from type III to type I. During the proliferation phase mainly collagen type III is produced, while in unwounded skin type I collagen predominates (with a ratio of 4:1). Moreover, the fibronectin of the provisory matrix is degraded and the collagen bundles become thicker, stronger and more ordered. However, they will never reach the same tensile strength as the original tissue(Eming *et al.*, 2014; Fathke *et al.*, 2004; Frykberg & Banks, 2015; Gamelli & He, 2003; F. Wang *et al.*, 2018).

Not all details of the wound healing cascade are fully understood yet. At the end of it, the wound is closed and (most of) the tissue function is restored. This process usually runs automatically with a sufficient outcome. However, as soon as the complex wound healing cascade is disrupted of some sort, the wound healing can stagnate, and a chronic wound arises (Eming *et al.*, 2014; Enoch & Leaper, 2005).

2.2.1 Chronic wounds, current strategies to deal with them and why more research on this topic is needed

While physiological wounds usually heal well within 3 weeks, chronic wounds can take weeks up to years to heal. However, the exact point at which a wound is considered chronic, is not defined. The food and drug administration (FDA) of the United States of America defines a wound as chronic, "when it does not heal in a defined time period, despite intensive therapy". In this definition also an exact time point, when a wound is no longer considered acute but chronic is missing as well. In the clinics, a wound is considered chronic when it takes longer than 3 weeks up to 3 months to heal (Dissemond, 2006; Eming *et al.*, 2014; Enoch & Leaper, 2005).

Even if the time scape of chronic wounds is not sufficiently defined and might differ between chronic wounds, in all chronic wounds the healing process is disrupted. It no longer passes through all phases of wound healing smoothly and automatically. Instead, it becomes "trapped" in one of the phases. This is almost always the inflammation phase, rarely the granulation phase. So, chronic wounds are characterized by a prolonged, chronic inflammation within the wound, which prevents wound healing. In almost all cases of chronic wounds, there is an underlying condition, that impairs blood flow or damages the nerves. Vascular insufficiency, type 2 diabetes mellitus and local pressure effects are found as major causes of chronic wounds (Dissemond, 2006; Eming *et al.*, 2007, 2014; Frykberg & Banks, 2015; Lazarus et al., 1994).

The exact mechanisms, that transform an acute wound into a chronic wound are still unknown, but within all chronic wounds a hostile micromilieu can be found. This hostile micromilieu can be characterized by changes in secretion of growth factors and cytokines, as well as changed expression profiles and activity of different cells and differences in composition of the ECM. Chronic wounds are usually not re-epithelialized. Also, the microflora of the skin can differ from healthy skin. Moreover, edema, bacteria, ROS, pro-inflammatory mediators and proteases can be present (Eming *et al.*, 2007; Enoch & Leaper, 2005).

In chronic ulcers, increased proinflammatory infiltrates, especially increased numbers of macrophages and neutrophils, can be found, which delay the wound healing (Eming *et al*., 2007, 2014). **Figure 2.23** shows a schematic overview of a chronic inflammation. The reason for the increased number of immune cells could be that an increase of endothelial adhesion molecules. For example the intercellular adhesion molecule was found elevated in chronic wounds. This leads to more extravasation of immune cells and thus more neutrophils and macrophages in the wound. The many immune cells could be one reason for the main characteristic of chronic wounds: an increase in pro-inflammatory cytokines (Eming *et al.*, 2014; Mamilos *et al.*, 2023). Also, a dysregulation or an excess activation of macrophages can lead to proinflammatory conditions (Tay *et al.*, 2013).

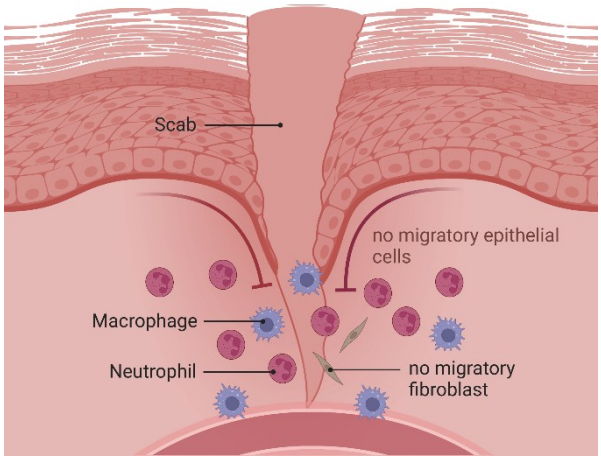

Figure 2.22: Schematic drawing of a persistent inflammation in a chronic wound
No migration of epithelial cells or fibroblasts is observed. Instead, an increase in extravasated macrophages and neutrophils can be seen. Created with BioRender.

Moreover, other immune cells next to macrophages and neutrophils can be found and an increase in ROS is observed (Eming *et al.*, 2014). Immune cells also produce ROS in acute wounds, but to a lesser extent. ROS are a powerful defense against microorganisms. In chronic wounds however the high concentration of ROS damages ECM proteins and cells. This too leads to an increase in protease activity and pro-inflammatory cytokines (Frykberg & Banks, 2015).
So, in chronic wounds the cytokine profile is completely changed towards inflammation (Goldberg & Diegelmann, 2017). This includes a de- and upregulation of key proinflammatory cytokines, e.g. IL 1β and TNF α. Upregulation of these two cytokines results in an increased activity of MMPs, which then degrade too much of the local ECM, which should be build up instead. Without a proper ECM, the cellular migration is impaired and thus no sufficient wound healing possible (Eming *et al*., 2014). In general, the proteases are deregulated in chronic wounds. An increase in protease activity (important here are MMPs, serin proteases and bacterial proteases), is associated with less extra cellular matrix remodeling and uncontrolled degradation of cytokines and structural proteins (Eming *et al*., 2007). For example, a degradation of fibronectin impairs migration and a breakdown of VEGFα will be detrimental for angiogenesis (Eming *et al.*, 2007; Krisp *et al.*, 2013).
Interestingly, if a chronic wound starts to heal, the pro-inflammatory cytokines are down-regulated again (Goldberg & Diegelmann, 2017).
Also, a severe infection of the wound or the presence of a biofilm can lead to more pro-inflammatory signals and thus impair wound healing. While all wounds are infected to a certain degree (a.o. due to the skin microbiome, which gets into the wound), in acute wound healing, the infection is contained in the inflammation phase and does not interfere with wound healing. In case of an infection the epidermis secretes and up-regulate antimicrobial peptides as a first line defense. These proteins are crucial for wound closure and their secretion is dysregulated in chronic wounds (Eming *et al.*, 2014; Pastar *et al.*, 2014).
Furthermore, the skin microbiome is important in wound healing. A change of the microbiome has been observed after wounding and in case of chronic wounds the diversity of the microbiome is significantly decreased compared to healthy skin (Gontcharova *et al.*, 2010; Pastar *et al.*, 2014).

As stated above, without re-epithelialization wound closure is impossible. Accordingly, this process is hindered in all chronic wounds. Keratinocytes at the edges of chronic wounds differ from keratinocytes in acute wounds. In acute wounds, only keratinocytes of the basal layers are proliferating, while in chronic wounds also cells of the proliferation in the suprabasal layers can be

found, sometimes nuclei are even present in the *stratum corneum*. Moreover, keratinocytes in chronic wounds show a change in expression profile, that impairs migration. For example, the transcription enhancer β-catenin was found in the nuclei of keratinocytes in chronic wounds was responsible for the nonmigratory, hyperproliferating phenotype of the keratinocytes. These changes impair the re-epithelialization and restoration of the skin barrier (Pastar *et al.*, 2014; Stojadinovic *et al.*, 2005).

In chronic wounds anti-angiogenic proteins, such as myeloperoxidase were found to be upregulated, while pro-angiogenic proteins were down regulated, resulting in less angiogenesis and thus more cell death instead of wound healing (Eming *et al.*, 2014; Krisp *et al.*, 2013).
Defects in local or systemic stem cells and progenitors will also impair wound healing. Furthermore, in long lasting chronic wounds the local stem cell populations can become depleted, aggravating the healing problem (Eming *et al.*, 2014).

Senescent cells, especially senescent fibroblasts, might also impair proper healing in pathological wounds, though the exact mechanism is not clear yet (Eming *et al.*, 2014; Wall *et al.*, 2008). Moreover, most patients with chronic wounds are old. This is partly due to the fact that aging attenuates wound healing, but also because systemic hormones such as estrogen are crucial for regulation of wound healing. Decreased amounts of estrogen might be a reason for impaired wound healing in old age (Eming *et al.*, 2014).

One of the most prominent underlying conditions of chronic wounds is type 2 diabetes mellitus. In chronic wounds associated with this disease, microvascular and neovascularization impairments were observed. This is probably due to a decreased response to hypoxia. One of the key players to resolve hypoxia in acute wound healing is the transcription factor of hypoxia inducible factor 1α (HIF-1α). It activates multiple pathways, that aid wound healing, among those angiogenic processes. For example, up-regulation of HIF-1α induces an increased secretion of VEGFα. In diabetic wounds the stabilizing cofactor p300 was found to be modified due to the high glucose levels, rendering HIF-1α less stable. Dallas *et al.* could show that by stabilizing HIF-1α wounds healed better in a diabetic mouse model (Dallas *et al.*, 2019).

Chronic wounds last usually about 12-13 months. They occur in 1-2 % of the population of western, industrialized nations. In people over 80, the incidence increases to 4-5 %. In the United States of America up to 4.5 million people suffer from chronic lower extremity ulcers alone. 25 % of diabetic patient have at least 1 foot ulcer in their lifetime. The recurrence rate is 66 % and in about 12 % of cases an amputation is necessary. Half of the amputated diabetic patients die within the next 5 years (Dallas *et al.*, 2019; Dissemond, 2006; Eming *et al.*, 2014; Frykberg & Banks, 2015).

The financial burden of chronic wounds on healthcare systems is immense. The care of nonhealing wounds costs the United States healthcare system 9-13 billion $ each year. Even more importantly the quality of life of patients is severely decreased (Dallas *et al.*, 2019; Eming *et al.*, 2014; Frykberg & Banks, 2015; Powers *et al.*, 2016). Chronic wounds can lead to loss of function of the tissue and social isolation. They can even result in an incapacity to work (Eming *et al.*, 2007; Frykberg & Banks, 2015). The social isolation can impair wound healing even more. Pyter *et al.* found that social isolation resulted in low cortisol levels in mice, which then led to a reduced secretion of KGF and VEGF, crucial mediators of a successful wound healing (Eming *et al.*, 2014; Pyter *et al.*, 2014).
To summarize, chronic wounds are associated with a decreased quality of life, a high morbidity, and high treatment costs. Moreover, the number of chronic wounds will probably increase in the coming

years, as to the aging population and therefore the increase of type 2 diabetes patients. All this clearly shows how urgent development of new treatment strategies and new wound healing aiding drugs is (Frykberg & Banks, 2015; Powers *et al.*, 2016).

As chronic wounds do not heal on their own and severely affect the lives of patients affected, they need to be treated. Currently the treatment strategies mostly focus on the chronic wound itself, not so much on the underlying disease (Eming *et al.*, 2014).
Local treatments include the disinfection of the wound and to ensure that it is clean without any infection or contamination. Preparation of the wound bed is essential in the treatment of chronic wound so that the wound can finally start to heal. Depending on the severity of the chronic wound, debridement, the removal of necrotic tissue, might be necessary (Eming *et al.*, 2007, 2014; Frykberg & Banks, 2015; Powers *et al.*, 2016).
It is crucial to assure the optimal wound climate. This is mostly achieved by specific wound dressings, which will protect the wound against the environment and keep it moist, while absorbing excess exudate. Furthermore, the wounds dressings can be antibacterial, able to reduce pain, attract circulating cells, stimulate local cells to migrate and proliferate, and support appropriate ECM deposition. Despite the vast number of different dressings available, they are not yet sufficient in aiding the healing of chronic wounds. Moreover, the data which of the many different dressings works best for each specific wound (Frykberg & Banks, 2015).
As chronic wounds often stagnate in an inflammatory state, modulation of inflammation could help to create a beneficial wound milieu, that allows healing to progress. Therefore, it could be useful to modulate specific pro-inflammatory signaling pathways, such as the IL 6 pathway, and find methods to remove the excess ROS. In fact, current treatment options like vacuum treatment probably aid healing in chronic wounds, because they remove the excess pro-inflammatory mediators. However, modulation of the wound exudate must be performed with care because there are also factors present in the exudate, that support wound healing (Eming *et al.*, 2007; Frykberg & Banks, 2015).
The delivery of local wound healing promoting growth factors to the wound, also called “biologically active therapies” has showed some positive effects. For example, administering fibroblast-growth-factor 2 resulted in better granulation tissue formation and epithelialization. However, the overall performance of local growth factors as treatment in chronic wounds is not yet satisfactory and always bears the risk of malignancy after treatment (Eming *et al.*, 2007).
In chronic wounds, the proteolytic equilibrium is disrupted, so introducing protease-resistant wound healing mediators into the wound or inhibiting the excess proteolytic activity might be useful. In case of the inhibition of proteases, a fine balance must be kept, as too much inhibition will stop the wounds from healing (Eming *et al.*, 2007).
For large wounds, tissue transplantations are used to aid wound healing, for example split skin for burn wounds. Skin replacements might help here in the future. Moreover, cellular therapies are currently developed and administering keratinocytes, fibroblasts or stem cells into the wound seems promising in first pre-clinical trial (Danner & Ciba, 2009; Eming *et al.*, 2007, 2014; Liao et al., 2019; Powers *et al.*, 2016).
To successfully treat chronic wounds the TIME concept can be helpful, which is illustrated in **Figure 2.24** (Frykberg & Banks, 2015).

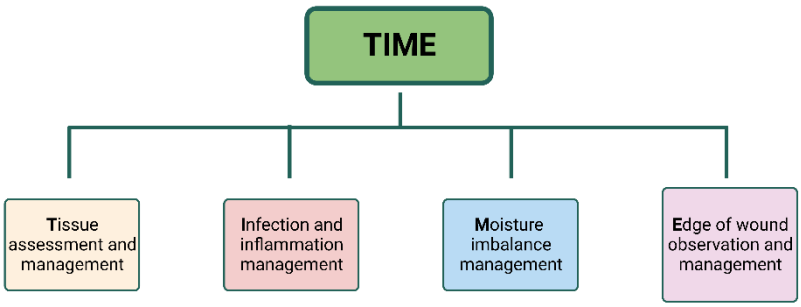

Figure 2.23: TIME concept for the treatment of chronic wounds
A successful treatment of chronic wounds relies on the four pillars tissue assessment and management, infection and inflammation management, moisture imbalance management, and edge of wound observation and management. Concept taken from Frykberg and Banks *(Frykberg & Banks, 2015)*. Created with BioRender.

Chronic wounds are a complex, multilayered problem. For successful treatment more than one strategy is necessary. A combination therapy supporting angiogenesis, correct extra cellular matrix deposition and growth of ETs early on will likely be key (Eming *et al.*, 2007, 2014; Frykberg & Banks, 2015; Powers *et al.*, 2016).
For a complete healing of a chronic wound, it is also necessary to treat the underlying cause, such as type 2 diabetes mellitus. Depending on the underlying disease, chronic wound differ in their pathologies and treatment needed. So, one kind of treatment will probably not fit all the diverse patients and a personalized medicine approach will be necessary to help all patients sufficiently (Eming *et al.*, 2014; Frykberg & Banks, 2015). Therefore, the diagnosis of what kind of chronic wound and which underlying pathology is present, is crucial. The current gold standard is a biopsy of the wound tissue for analysis. Development of quicker, noninvasive techniques would be desirable here. Also, the analyzation of the wound secrete could be helpful. In any case, better diagnostic and prognostic tools are necessary to learn more about the different chronic wounds (Eming *et al.*, 2007, 2014; Frykberg & Banks, 2015). However, the so direly needed clinical research is made difficult by the multimorbid patient populations, little research funding and little public awareness (Eming *et al.*, 2014).

To summarize: chronic wounds are an immense health threat, that despite many efforts and different treatment strategies cannot yet be sufficiently treated in all patients. To overcome this, more research is needed, as we currently only have a basic knowledge of the pathophysiological mechanisms of chronic wounds (Eming *et al.*, 2007; Frykberg & Banks, 2015).

2.3 Models to study wound healing

There are many different models to study wound healing. The following chapter will give a short overview over *in vitro*, *in vivo*, and *ex vivo* models and their advantages and disadvantages.

2.3.1 In vitro models

In vitro models allow the detailed studies of a specific cell population and their reaction to an injury or another sort of stimulus. The most prominent *in vitro* model for wound healing is probably the scratch assay, as depicted in **Figure 2.25**. Here, a scratch is set into a monolayer of cells, e.g. fibroblasts or keratinocytes, and it can be observed how the cells migrate and close the gap. This assay is relatively simple and fast to perform and brings first insights into wound healing processes. However, the scratch assay and *in vitro* models in general can never depict the complexity of the entire wound healing process or the crucial crosstalk between different cell types involved in wound healing. *In vivo* animal models are necessary for this (Martinotti & Ranzato, 2020; Pastar *et al.*, 2014; Stephens *et al.*, 2013; Zomer & Trentin, 2018).

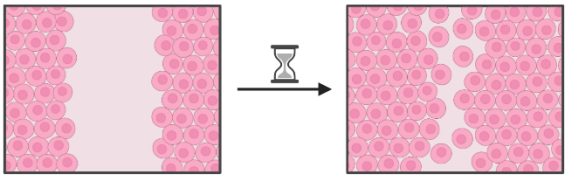

Figure 2.24: Schematic drawing of a scratch assay
A defect is set into a cellular monolayer and the closure of this defect is observed time. Created with BioRender.

2.3.2 In vivo models

In vivo models or animal models are much more complex than the *in vitro* models, as here an entire organism and its reaction to injury can be studied. Thus, these models are in principle well suited for preclinical experiments and are important test systems for e.g. the drug drug safety before clinical trials (Grambow *et al.*, 2021; Pastar *et al.*, 2014; Zomer & Trentin, 2018).

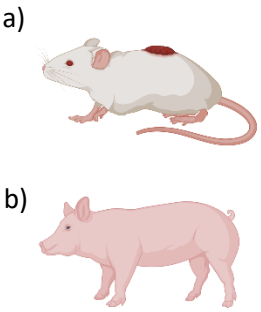

Figure 2.25: Schematic drawing of animals often used in wound healing studies a) a lab mouse with a skin defect, b) a pig. Created with BiorRender.

There are a lot of different animal models present, but few satisfactory in the research area of wound healing. Most known perhaps are murine models, as the mouse is the most commonly used lab animal in research. Mice studies have several advantages: mice are easy to handle even in large numbers, they have a fast reproduction cycle, are not too expensive, and there are many different genetically modified lineages available. Moreover, mice can be easily standardized regarding age, sex, and other factors. There are several models of pathological wound healing available, for example by artificially generating diabetes mellitus in mice. However, none of these models really depict all aspects of chronic wounds in humans (Eming *et al.*, 2014; Stephens *et al.*, 2013; Zomer & Trentin, 2018).
Human and murine wound healing are similar in some regards, as both species show the 4 phases of wound healing described in **Chapter 2.2**. Murine studies have helped gain important knowledge about wound healing, which can be transferred to human wound healing. For example, Dallas *et al* showed the important role of HIF-1α in wound healing in a mouse model. However, mice are much smaller than humans, only have a very short life span, and there are strong differences in the physiology of humans and mice, so not all human pathologies can be represented in mice. These differences are especially pronounced in wound healing. Murine skin has the panniculus carnosus muscle, which cannot be found in humans and will contract upon injury. That is why murine wound healing is 90 % due to contraction, while in humans migration and proliferation are the crucial process and contraction can almost be disregarded. This striking differences in biomechanics must be kept in mind when translating results from murine to human studies (Dallas *et al.*, 2019; Eming *et al.*, 2014; Pastar *et al.*, 2014; Zomer & Trentin, 2018).

Porcine models are a valuable alternative to mice in wound healing studies. Pigs are larger than mice and physiologically more like humans. These similarities are especially pronounced in the skin structure and in wound healing. Porcine skin also heals mainly by migration, as does human skin. With the help of porcine wound healing models Hachem *et al* discovered a new ointment to treat severely infected wounds. On the downside, pigs are much more expensive in handling and must be trained for thus. Their size makes it more difficult to handle large numbers necessary for reliable results. Moreover, pigs are more genetically heterogeneous and not as well characterized as mice. For porcine studies, often specific reagents (such as antibodies) are not available. (Debeer *et al.*, 2013; Hachem *et al.*, 2021; Zomer & Trentin, 2018)

Interesting lessons can also be learned from non-mammalian animal models. Some amphibians can grow entire new limbs and their wounds heal scarless. Studying these animals might give insides on how human skin regeneration can be possible (Meier *et al.*, 2013; Pastar *et al.*, 2014).

In *in vivo* experiments a lot of different wounding approaches can be used: wounds can be full thickness, or only partial. They can be made by incisions, punched, or burned, depending on the research question (Stephens *et al.*, 2013).

In general, *in vivo* models have the advantage that an entire organism and thus all influences on wound healing are studied, however the results may not always be transferable and must thus be considered with care (Grambow *et al.*, 2021; Pastar *et al.*, 2014; Zomer & Trentin, 2018).

2.3.3 Ex vivo models

Ex vivo models refer in the case of skin wound healing to studies performed on skin, not on the entire organism or just one cell layer. They are somewhat in between *in vitro* and *in vivo* models and thus provide more sound data than the simpler *in vitro* models. As *in vivo* wound studies on humans are difficult to perform due to ethical issues, *ex vivo* human skin studies allow unique insights into human wound healing and can help reducing the number of animal studies necessary (Pastar *et al.*, 2014; Stephens *et al.*, 2013). However, one must keep in mind that blood flow is disrupted in *ex vivo* models and not a whole organism but just an organ can be studied. Moreover, the culturing period of human skin before necrosis occurs is limited, meaning that *ex vivo* wound healing cannot be studied for months on end (Stephens *et al.*, 2013).
Still, for wound healing studies of the skin *ex vivo* models, such as depicted in **Figure 2.27** are a very valuable tool. Most of the models consist out of a punch biopsy of all skin layers or of just epidermis and dermis. Within this biopsy, a smaller biopsy might be set as a wound. The sizes of both punches and the depth of the inner wound may vary depending on the respective study. The so formed wound can then be kept in culture for multiple days and the healing process closely monitored (Gherardini *et al.*, 2020; Stephens *et al.*, 2013). Liao *et al.* and Sturmheit *et al.* studied the wound healing aiding function of sweat gland derived stem cells with the help of such a model (Liao *et al.*, 2019; Sturmheit *et al.*, n.d.). Post *et al* found that theroid hormone L-thyroxine can aid wound healing under pathological conditions, mimicking a chronic wound (Post *et al.*, 2021). This study is especially interesting, because there are so far no widely established models of chronic wounds (Pastar *et al.*, 2014). Meyer *et al.* showed that the hormone thyrotropin-releasing hormone can promote wound healing in *ex vivo* human and frog skin (Meier *et al.*, 2013). These examples show the versatile use of *ex vivo* organ cultures in the search for possible new treatment strategies to promote wound healing.

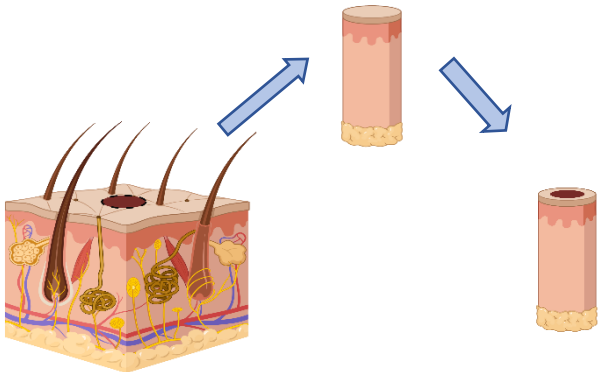

Figure 2.26: Schematic drawing of making an *ex vivo* wound
A biopsy punch is taken out of full human skin, obtained from elective surgeries. A smaller biopsy punch is set into the lager one, creating a skin wound. Created with BioRender.

Another advantage of *ex vivo* wound healing models of human skin is that they forego the administrative and ethic difficulties associated with *in vivo* experiments and lab animals.

2.4 Drug repurposing

In this work, an inhibitor library is screened to find new candidates that might aid wound healing. Partly this is "just" a regular drug screening process. However, some of the substances tested were already in clinical trials or even approved drugs, which makes testing these substances a sort of drug repurposing. Drug repurposing is defined as "studying the drugs that are already approved to treat one disease or condition to see if they are safe and effective for treating other diseases" by the National Centre for Advancing Translational Sciences, a part of the National Institute of Health of the United States. Drugs can be repurposed at any stage of their development (Hema Sree *et al.*, 2019).
The classical process of drug development is immensely time- and resources-consuming. Moreover, it can still not be predicted, if a new drug candidate can enter the market at the end of this process. By repurposing drugs, that already passed some or all steps of drug development, both time and resources can be saved. If a thorough literature research pre-faces the experimental phase, also the rate of successful market-entry should increase (Hema Sree *et al.*, 2019).
The most prominent example of drug-repurposing was an accidental found: Sildenafil was developed as a treatment against hypertension and was then found to be extremely useful against erectile dysfunction (Hema Sree *et al.*, 2019).

2.5 Signaling pathways important in this study

2.5.1 Tropomyosin receptor kinase A

The Tropomyosin receptor kinase A (TrkA) is a membrane bound kinase, which serves as receptor for neurotrophins, proteins that are among others. essential for survival and function of neurons. TrkA has an especially high affinity to the neurotrophin NGF. As **Figure 2.28** shows, after binding of the ligand NGF, TrkA dimerizes and activates important signaling pathways such as the mitogen activated protein kinase (MAPK) pathway through phosphorylation. These pathways then regulate transcription and translation of multiple, specific genes. In the case of NGF, activation results for example in neuronal differentiation and proliferation (Marlin & Li, 2015).
Regarding wound healing, NGF and TrkA are important for regeneration of nerves after wounding the dermis (Fritsch & Schwarz, 2018). Moreover, TrkA is also found on keratinocytes, especially epidermal stem cells. Together with its counterpart the low affinity receptor CD271, TrkA plays an important role

in the regulation of epidermal homeostasis (M. Zhang *et al*., 2018). Zhang *et al* hypothesize that a change in the ratio of TrkA and CD271 in favor of CD271 might improve wound healing (M. Zhang *et al.*, 2017).

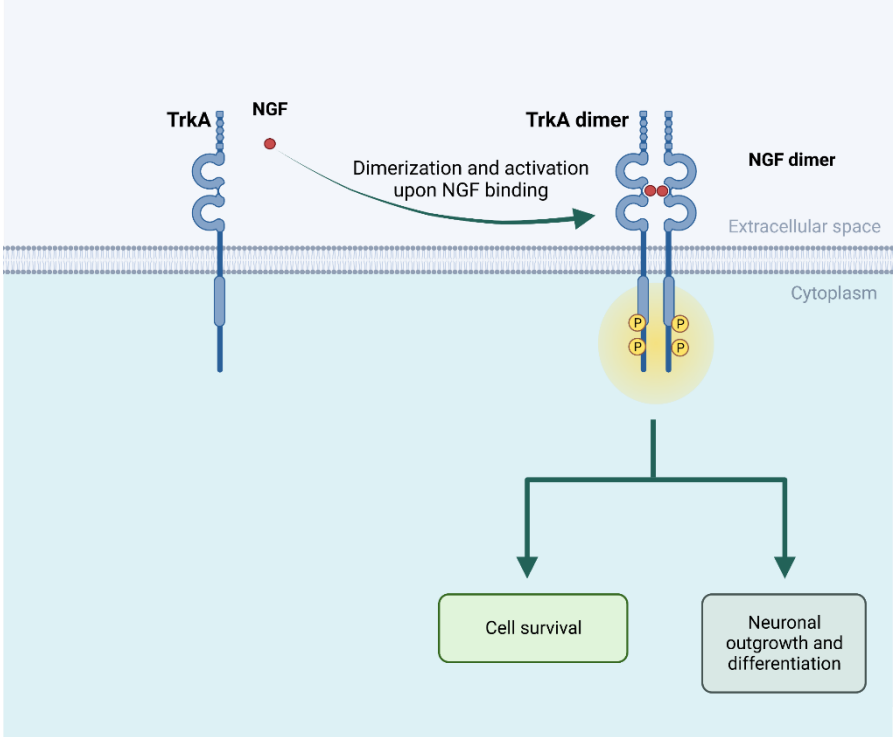

Figure 2.27: Mode of action of Tropomyosin kinase A (TrkA)
Upon binding of its ligand, neuronal growth factor (NGF), TrkA dimerizes and activates important signaling pathways via phosphorylation. The activated pathways lead to cell survival and neuronal outgrowth and differentiation. Created with BioRender.

2.5.2 G-protein coupled receptor

G-protein coupled receptors (GPCRs) are receptors, that are situated in the cell membrane. They have the distinct form of a helix, that has 7 trans-membrane domains. They are evolutionary conserved in eukaryotes and serve as cell surface receptor proteins. Upon binding of its extracellular ligand their conformation changes, which activates the intra cellularly bound G-protein. The G-protein then dissociates in its subunits and triggers thereby downstream signaling cascades. Which cascades are activated depends on the respective ligand, GPCR, and G-protein. **Figure 2.29** shows the principal mechanisms of how GPCRs are working (Trzaskowski *et al*., 2012; Weis & Kobilka, 2018; Wettschureck & Offermanns, 2005).

The GPCR-family is huge. There are many kinds of GPCRs, which are involved in a lot of different physiological processes, among them the sense of taste and smell but also the regulation and metabolism. Due to their omnipresence in signaling processes, GPCRs are also involved in many diseases, making them an attractive drug target. Currently about one third of the FDA approved drugs targets GPCRs (Hauser *et al.*, 2018; Weis & Kobilka, 2018; Wettschureck & Offermanns, 2005).

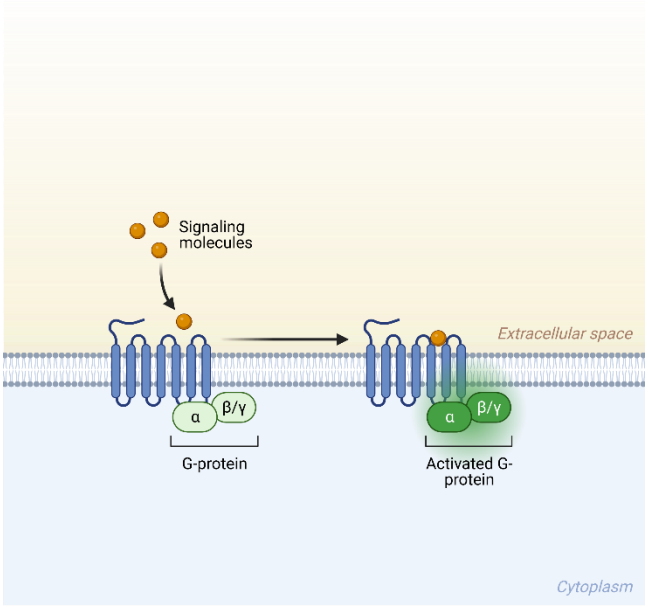

Figure 2.28: Mode of action of a G-protein coupled receptor
Upon binding of a specific signaling molecule, the transmembrane receptor undergoes a conformational change, which activates the bound G-protein. This G-protein then activates specific intracellular cascades. Created with BioRender.

The GPR119 is mainly expressed in the pancreas and gastrointestinal tract of rodents and humans. Due to its regulation of secretion of incretin and insulin hormone, it is important in the regulation of metabolic processes. Overton *et al.* could show, that the activation of GPR119 resulted in less food intake and a reduced weight gain in rats. These findings make GPR119 a promising target for the treatment of diabetes (Manaithiya *et al.*, 2021; Overton *et al.*, 2006).

2.5.3 Wnt/β-catenin pathway and tankyrase

Wnt signaling pathways are a group of pathways that allow the cell to react to outside stimuli. Those pathways are crucial for all cells and highly conserved among eukaryotes. Here, the focus will be on the canonical Wnt/β-catenin pathway, which allows the regulation of gene transcription. The relatively small glycoproteins of the Wnt family serve as extracellular ligands in this pathway. The word wnt is a combination of wingless and int. β-catenin supports and activates transcription of specific target genes, though the exact mechanisms of the β-catenin function are not yet known. (Cadigan & Nusse, 1992; Nusse & Varmust, 1992; Rao & Kühl, 2010)

If Wnt is not bound, several proteins, among them axin 1 and 2 form a β-catenin-destruction complex, which as the name indicates target β-catenin for degradation. Accordingly, no transcription of the target genes takes place. If Wnt binds its target, a cell surface receptor of the Frizzled family, the receptor and the intracellular Dishevelled protein will become activated. This leads to a degradation of axin 1 and 2. The β-catenin destruction complex degrades, and β-catenin can migrate into the nucleus to active transcription of target genes (Cadigan & Nusse, 1992; Nusse & Varmust, 1992; Rao & Kühl, 2010).

The enzyme tankyrase marks axin 1 and 2 for degradation and thus supports the activation of β-catenin. **Figure 2.30** illustrates the Wnt/ β-catenin pathway (W. Wang *et al.*, 2021; Y. Zhang *et al.*, 2010).

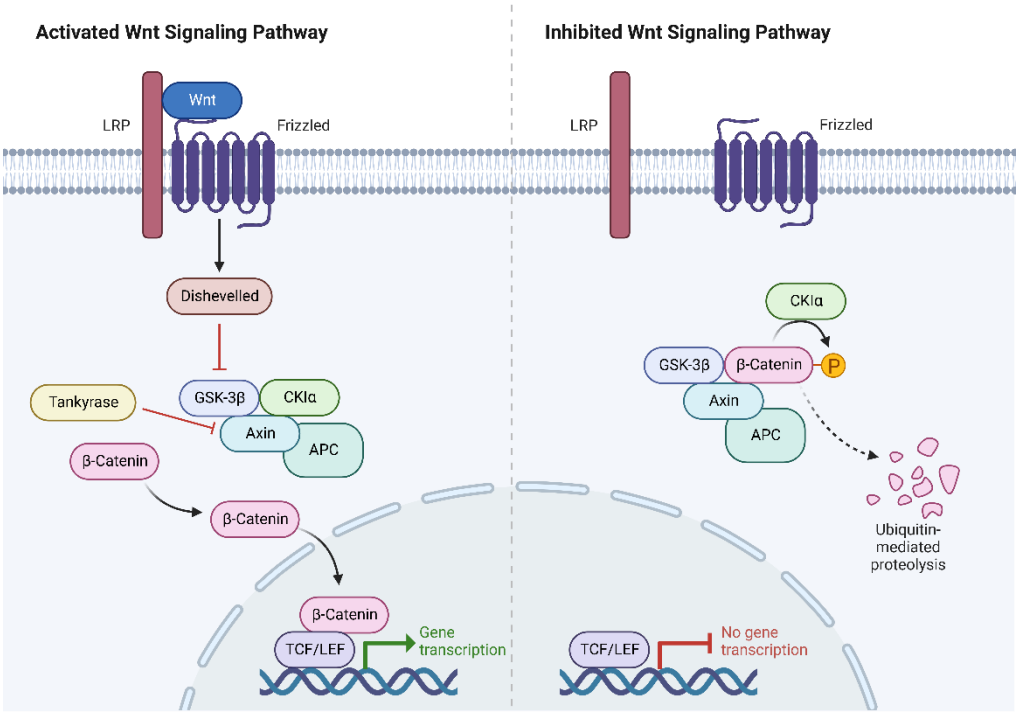

Figure 2.29: Canonical Wnt/β-catenin pathway
If Wnt is present, the β-catenin pathway is activated, meaning that β-catenin is not degraded and can enter the nucleus, where it helps translating specific genes. Without Wnt, β-catenin is marked for degradation by the β-catenin destruction complex, consisting of glycogen synthase kinase 3β (GSK-3β), axin, and adenomatous polyposis colo protein (APC). B-catenin then is degraded and the genes are not transcribed. TCF/LEF = T cell factor/lymphoid enhancer facor family, CKI*α* = casein kinase Iα, LRP = Low densitiy lipoprotein receptor-related protein. Created with BioRender.

The Wnt/β-catenin pathway is essential for the correct embryogenesis in eukaryotes. Moreover, the Wnt/β-catenin is also important in many cellular processes of adult individuals, for example in skin development and regeneration (Augustin, 2014; Cadigan & Nusse, 1992; Rao & Kühl, 2010).
Unregulated activation or mutation of the Wnt/β-catenin pathway can however result in cancer or other diseases (W. Wang *et al.*, 2021; Zhan *et al.*, 2017).

2.6 Aim of this study

As this chapter shows, there is a lot known about the complex process of wound healing in acute and chronic wounds. However, the exact mode of action is still not fully understood, and more research and new treatment strategies are crucially needed. This study aims to address these research questions:

- The WHOC model will be characterized in a time-course experiment to gain more insights in *ex vivo* human skin wound healing.
- To avoid contaminations the disinfectant Octenisept® will be tested in the WHOC.
- The Selleck Chemicals Highly Selective Inhibitor Library L3500 will be screened in the WHOC to find new drug candidates that might aid wound healing.
- These candidates will be further studied in different concentrations to find the most effective concentration.
- The most successful candidates will be tested in a pathological wound healing model that mimics a chronic wound.

3 Materials and methods

3.1 Materials

In this chapter all used materials area listed.

3.1.1 Devices

Table 3.1: List of all devices used in this work

Device	Company	Company headquarters
Bottle: *Laborflasche, rund* 50 mL, 100 mL, 250 mL, 500 mL	VWR International	Radnor, United States
Cooling plate *Histoblock Jung*	Leica Biosystems	Wetzlar, Germany
Cryostat CM 3050S with stamp	Leica Biosystems	Wetzlar, Germany
Drying cabinet	Binder GmbH	Tuttlingen, Germany
Embedding machine Leica CV5030	Leica Biosystems	Wetzlar, Germany
Fourier-domain-mode-locking-laser based home-built 3.3 MHz Optical coherence tomography system	Working group of Prof. Dr. rer. nat. Robert Huber, Institute of Biomedical Optics, University of Lübeck	Lübeck, Germany
Freezer, -20 °C	Liebherr	Bulle, Schweiz
Freezer, -80 °C (TXS series V-Drive)	Thermo Fisher Scientific	Waltham, United States
Fridge, 4°C	Ggmgastro	Ochtrup, Germany
GloMax Discover	Promega GmbH	Walldorf, Germany
Humid chamber for immunofluorescence	LabArt	Waldbüttelbrunn, Germany
Incubator	HeraCell/Thermo Fisher Scientific	Waltham, United States
Invivo$_2$ 400 Hypoxic Workstation	Baker Ruskinn	Sanford, United States
Keyence BZ 9000	Keyence Germany	Neu-Isenburg, Germany
Leica Autostainer XL	Leica Biosystems	Wetzlar, Germany
Light microscope, Leitz Biomed	Leica Biosystems	Wetzlar, Germany
Magnetic Heater and stirrer RSM-044	PHOENIX Instrument	Garbsen, Germany
Measuring cylinder 100 mL 1 L	 Vitlab VWR International	 Grossostheim, Germany Radnor, PA, United States
Microtome 1140/ Autocut	Reichert & Jung/Ametek	Depew, United States
Multichannel pipet, 200 µL	Eppendorf AG	Hamburg, Germany
pH meter pH7110	inoLab/VWR International	Radnor, United States
Pipetboy pipetus®	Hirschmann *Laborgeräte*	Eberstadt, Germany
Piston pipette: 100-1000 µL, 20-200 µL, 2-20 µL, 0.5-10 µL	Eppendorf AG	Hamburg, Germany
Sakura Tissue Tek® TEC Embedding Center	Sakura Finetek USA, Inc. 2022	Torrance, United States
Sterile work bench/ NUAIRE Biological Safety Cabinet Class I	NUAIRE	Plymouth, United States

Stereomicroscope Stemi-2000 with camera	ZEISS	Oberkochen, Germany
Stereomicroscope SZX 7 with camera	OLYMPUS	Hamburg, Germany
Surgical scissors	Karl Hammacher GmbH	Solingen, Germany
Surgical forceps	Karl Hammacher GmbH	Solingen, Germany
Systec™ Dx-65 table autoclave	Sytec™/Thermo Fisher Scientific	Waltham, United States
Racks for reaction tubes, TPP	Biochrom AG/ Merck KGaA	Darmstadt, Germany
Retainer, Freiburg	Dr. med. Andreas Thomsen, Department of Radiation Oncology, University Hospital Freiburg	Freiburg, Germany
Retainer, *Einrichtung für marine Biotechnologie* (EMB)	Fraunhofer Research Institution for Individualized and Cell-Based Medical Engineering	Lübeck, Germany
Tissue processor Leica ASP300S	Leica Biosystems	Wetzlar, Germany
Water bath type 1004 (for cell culture)	*Gesellschaft für Labortechnik mbH*	Burgwedel, Germany
Water bath type 25900 (for paraffin cutting)	Medax/Nagel GmbH	Kiel, Germany

3.1.2 Reagents

Table 3.2: List of all reagents used in this thesis
DAPI = 4',6-Diamidino-2-phenylindol, DMSO = Dimethyl sulfoxide

Reagent	**Article no**	**Company**	**Company headquarters**
Acetone, p.A.	2626.4000	Th Geyer GmbH & Co. KG	Hamburg, Germany
Acetic acid	1.00063.1000	Merck KGaA	Darmstadt, Germany
Ammonia water made out of Ammonia solution 25 % p.a.	2672.1011	LABSOLUTE by TH Geyer GmbH & Co. KG	Hamburg, Germany
Ampuwa *Spüllösung*	8230672	FRESENIUS KABI German headquarters	Bad Homburg, Germany
Cryomatrix™	6769006	Epredia/Thermo Fisher Scientific	Waltham, United States
DAPI Fluoromount-G medium	0100-20	Southern Biotech	Birmingham, United States
DMSO (Dimethylsulfoxid) z.A.	23.471.000	Th Geyer GmbH & Co. KG	Hamburg, Germany
Distilled water	From tap in house 32		
Ethanol, absolute, pure, 99.8%	2273.1000	Th Geyer GmbH & Co. KG	Hamburg, Germany
Ethanol, 99.8%, denatured	K928.4	Roth Industries GmbH & Co. KG	Dautphetal, Germany
Eosin, yellowish	1B-425	Waldeck GmbH & Co KG	Münster, Germany
Eukitt	03989	Sigma-Aldrich/Merck	Darmstadt,

		KGaA	Germany
Formaldehyde solution, min. 37 %	1.04003.2500	Merck KGaA	Darmstadt, Germany
Hematoxylin after Papanicoulos	1.09253.2500	Merck KGaA	Darmstadt, Germany
Hydrochloric acid	1.00316.1000	Merck KGaA	Darmstadt, Germany
L-thyroxine cell culture tested	T1775	Sigma Aldrich/Merkc KgaA	Darmstadt, Germany
Methylen blue	1.15943.0025	Th Geyer GmbH & Co. KG	Hamburg, Germany
Nitrogen, liquid	From tap house 32		
Octenisept® wound disinfectant	70002293	Schülke & Mayr GmbH	Norderstedt, Germany
Roti-Histofix, 4 %	P087.3	Roth Industries GmbH & Co. KG	Dautphetal, Germany
Surgipath Paraplast Plus	39602004	Leica Biosystems	Wetzlar, Germany
Xylol	360.2500	CHEMSOLUTE by TH Geyer GmbH & Co. KG	Hamburg, Germany

3.1.3 Consumables

Table 3.3: List of all consumables used in this thesis

Consumable	**Article no**	**Company**	**Company headquarters**
24-well plate for suspension cells	83.3922.500	Sarstedt	Nümbrecht, Germany
96-well plate, transparent with flat bottom for suspension	83.924.500	Sarstedt	Nümbrecht, Germany
Biopsy punch, 2 mm	48201	Pfm medical	Köln, Germany
Biopsy punch, 4 mm	48401	Pfm medical	Köln, Germany
Cryostat blades *Mikrotomklingen* Type 819 50 pieces	LE63065-LP	Leica Biosystems	Wetzlar, Germany
Disposable pipettes, 3 mL	11.313.03	TH Geyer GmbH & Co KG	Hamburg, Germany
Embedding cassettes Active Flo Routine I, loose, Aqua 1000	39LL-500-3	Leica Biosystems	Wetzlar, Germany
Fat pen marker	S2002	Agilent DAKO	Santa Clara, United States
Feather disposal scalpel 20x	02.001.03.010	Pfm medical	Köln, Germany
Filter paper	46-6200-00	Medite GmbH	Burgdorf, Germany
LLG-sample container	6.265.656	TH Geyer GmbH & Co KG	Hamburg, Germany
MoliCare premium Bed Mat	161061	Paul Hartmann AG	Heidenheim, Germany

Microtome blades, high profile	109209	TH Geyer GmbH & Co KG	Hamburg, Germany
Microscope Slides Cut frosted	AA00000112E01MNZ10	Epredia	Portsmouth, United States
Serological pipettes, sterile: 5 mL 10 mL 25 mL	 86.1253.001 86.1254.001 86.1685.001	Sarstedt	Nümbrecht, Germany
Petri dish, 92 mm x 16 mm	82.1472	Sarstedt	Nümbrecht, Germany
Petri dish, 145 x 20 mm	639102	Greiner BioOne	Frickenhausen, Germany
Pipette tips for… 50-1000 µL 2-200 µL 0.5-10 µL	 70.762 70.760-012 701.115	 Sarstedt Sarstedt Sarstedt	Nümbrecht, Germany
Reaction tube SafeSeal 0.5 mL 1.5 mL	 72.704.400 50.135.307	Sarstedt	Nümbrecht, Germany
Reaction tube 1.5 mL, RNase- and DNase-free	7696751	TH Geyer GmbH & Co KG	Hamburg, Germany
Reaction tube 2 mL	73.695.006	Sarstedt	Nümbrecht, Germany
Reaction tube, 15 mL	62.554.002	Sarstedt	Nümbrecht, Germany
Reaction tube, 50 mL	62.547.254	Sarstedt	Nümbrecht, Germany
Reservoir for multichannel pipet	REBP-3000	Diversified Biotech Inc	Dedham, United States
Superfrost™ plus adhesion microscope slides white tab	J1800AMNZ	Gerhard Menzel GmbH	Braunschweig, Germany
TissueTek IntermediateCryomold	4566	Sakura Finetek USA Inc	Torance, United States

3.1.4 Kits

Table 3.4: List of the kits used in this thesis and their use

Kit	**Article No**	**Company**	**Company headquarters**	**Used for…**
ApopTag® Fluorescein In situ apoptosis detection kit	S7110	Sigma-Aldrich/Merck KGaA	Darmstadt, Germany	KiTUNEL immunofluorescence staining
Cytotoxicity detection kit	11 644 793 001	Roche	Basel, Switzer Company headquarters	Lactate dehydrogenase-assay

3.1.5 Antibodies and sera

Table 3.5: List of the primary antibodies used in this thesis, the dilution in which they were used and the respective clone

Primary antibody	Dilution	Clone	Article number	Company	Company headquarters
Mouse anti-human cyto keratin 6	1:300	Ks6.KA12	61090	Progen	Heidelberg, Germany
Mouse anti-human cortactin	1:100	771716	MAB6096-SP	RnD Systems	Wiesbaden, Germany
Mouse anti-human PECAM-1/CD 31	1:100	JC70A	M0823	DAKO Agilent	Santa Clara, United States
Mouse anti-human Ki-67	1:20	MIB-1	M7140	DAKO Agilent	Santa Clara, United States

Table 3.6: List of the secondary antibodies used in this thesis, the dilution in which they were used and the respective clone

Secondary antibody	Dilution	Clone	Article number	Company	Company headquarters
Goat anti-mouse IgG (H+L) Alexa Fluor Plus 488	1:200	Polyclonal	A11029	Life Technologies/ Thermo Fisher Scientific	Darmstadt, Germany
Goat anti-mouse IgG (H+L) rhodamine red	1:200	Polyclonal	115-295-062	Jackson ImmunoResearch Europe LTD.	Ely, United Kingdom

Table 3.7: Serum used in this work

Serum	Article no	Company	Company headquarters
Normal goat serum	X0970	DAKO Agilent	Santa Clara, United States

3.1.6 Buffers

Table 3.8: List of buffers used in this thesis as well as their composition
NaCl = sodium chloride, Na_2HPO_4 =disodium phosphate, H_2O = water, NaH_2PO_4 = monosodium phosphate, TRIS = Tris(hydroxymethyl)aminomethan

Buffers	Composition	Article number	Company	Company headquarters
Phosphate Buffered Saline, pH 7.2 in 1 L distilled water	9 g NaCl 1.74 g Na_2HPO_4 x 2 H_2O 0.2034 g NaH_2PO_4x 2 H_2O	BP358-10 4984.1 1.06342.1000	Fisher BioReagent/ Thermo Fisher Scientific Roth Industries GmbH & Co. KG Merck KGaA	Waltham, United States Dautphetal, Germany Darmstadt, Germany
TRIS-buffered	8.8 g NaCl	BP358-10	Fisher BioReagent/	Waltham, United

Saline, pH 7.6 in 1 L aqua dest.	6.1 g Tris-Base	T1503-500	Thermo Fisher Scientific Sigma-Aldrich/Merck KGaA	States Darmstadt, Germany

3.1.7 Culture media and supplements

Table 3.9: Basic culture medium used for the wound healing organ culture model

Culture medium	Article number	Company	Company headquarters
Williams' Medium E	BS.F 1115	BIO&SELL	Feucht, Germany

Table 3.10: Supplements used for the culturing of the skin in the wound healing organ culture model

Supplements	Article number	Company	Company headquarters
L-glutamine	K0283	Biochrom Ltd.	Cambridge, United Kingdom
Penicillin/streptomycin	15140-122	Gibco/ Thermo Fisher Scientific	Waltham, United States
Hydrocortisone	H0135-1MG	Sigma-Aldrich/Merck KGaA	Darmstadt, Germany
Human insulin	i2643	Sigma-Aldrich/Merck KGaA	Darmstadt, Germany
Gentamicin/amphotericin B 500x	50-0640	Gibco/ Thermo Fisher Scientific	Waltham, United States

Table 3.11: Additional supplements for the pathological wound healing model

Supplements for pathological models	Article number	Company	Company headquarters
D-(+)-glucose solution	68644-100mL	Sigma-Aldrich/Merck KGaA	Darmstadt, Germany
Hydrogen peroxide	1009-100mL	Sigma-Aldrich/Merck KGaA	Darmstadt, Germany

Table 3.12: Composition of the different media used in this thesis
"Physiological" refers to the standard, non-pathological culturing conditions.
WEM = Williams' Medium E

Medium	Supplements
Physiological WEM	- 0.1 µg/mL hydrocortisone - 10 µg/mL insulin - 2 mM L-glutamine - Penicillin (10 mg/mL)/streptomycin (10 IU/mL)
Physiological WEM for day 0	- 0.1 µg/mL hydrocortisone - 10 µg/mL insulin - 2 mM L-glutamine - Penicillin (10 mg/mL)/streptomycin (10 IU/mL) - 1x Gentamicin/amphotericin B 500x

Pathological WEM	- 138.8 mM (2500 mg/dL) D-(+)-glucose - 0.1 µg/mL hydrocortisone - 10 mM hydrogen peroxide - 2 mM L-glutamine - Penicillin (10 mg/mL)/streptomycin (10 IU/mL)
Pathological WEM for day 0	- 138.8 mM (2500 mg/dL) D-(+)-glucose - 0.1 µg/mL hydrocortisone - 10 mM hydrogen peroxide - 2 mM L-glutamine - Penicillin (10 mg/mL)/streptomycin (10 IU/mL) - 1x Gentamicin/amphotericin B 500x

3.1.8 Selleck chemicals inhibitors

In this work an inhibitor library from the company Selleck Chemicals was screened, the Highly Selective Inhibitor Library L3500. **Table 3.13** lists all inhibitors tested, their article number, name, mode of action and in which screening they were tested. All information can be found at https://www.selleckchem.com/ (last time used December 27, 2022). The company headquarters of Selleck Chemicals LLC is in Houston, United States.

Table 3.13: List of all substances of the Selleck Chemicals company used in this thesis

c = clinical trials, nc = non-clinical tirals, MEK = Mitogen-activated protein kinase kinase, EGFR = epithelial growth factor receptor, ErbB2 = HER2 = v-erb-b erythroblastic leukemia viral oncogene homolog 2 = human epidermal growth factor receptor, Bcr = breakpoint cluster region, Abl =Abelson murine leukemia viral oncogene homolog 1, mTOR = mammalian target of rapamycin, VEGFR = vascular endothelial growth factor receptor, ROCK = regulator of cullins, PKC = protein kinse C, MDM 2 = mouse double minute 2 homolog, GSK = glycogen synthase kinase, Akt = protein kinase B, PARP = poly (adenosine phosphate-ribose) polymerase, IGF-1R = insulin-like growth factor-1 receptor, CYP = cytochrome P, HSP = heat shock protein, p110β = Phosphatidylinositol-4,5-bisphosphate 3-kinase catalytic subunit beta isoform, BET = bromodomain and extra-terminal motif, BRD = bromodomain-containing protein, HIF = hypoxia induced factor, COX = cyclooxygenase, PDK =pyruvate dehydrogenase kinase, GABAA = gamma-aminobutyric acid A, PLK = polo-like kinase, PI3K = Phosphoinositide 3-kinase, JNK = c-Jun N-terminal kinase, TGF = transforming growth factor, STAT = signal transducers and activators of transcription, , PDE = phosphodiesterase, FLT = feline McDonough sarcoma like tyrosine kinase, , mGlu receptor = metabotropic glutamate receptor, SIRT = sirtuin, CB = cannabinoid receptor, hSGLT = human selective sodium glucose cotransporter, ATM = ataxia-telangiectasia mutated kinase, CD = cluster of differentiation, Tie2 = angiopoietin-1 receptor, PKA = protein kinase A, HDAC = histone deacetylases, FAK = focal adhesion kinase, GRP = G-protein coupled receptor, HMG-CoA reductase = 3-hydroxy-3-methyl-glutaryl-coenzyme A reductase, FGFR = fibroblast growth factor receptor, P-CAB = potassium-competitive acid blocker, APC = Adenomatous-polyposis-coli, 5HT = 5-hydroxytryptamine receptor, FAAH = fatty acid amide hydrolase, HIV = human immunodeficiency virus, gp = glycoprotein, DNA-PK = deoxyribonucleic acid-dependent protein kinase, Chk1 = checkpoint kinase 1, Msp = membrane scaffold protein, JAK = janus kinase, IKK = IkappaB kinase, NOD = nucleotide-binding oligomerization domain, TRKA = tropomyosin kinase A, CXCR = cxc chemokine receptor, PPAR = peroxisome proliferator-activated receptor, CETP = Cholesteryl ester transfer protein, DPP-IV= Dipeptidylpeptidase IV, NF-KB = nuclear factor kappa-light-chain-enhancer, SMAC = *second mitochondria-derived activator of caspases, Smo = Smoothened, Pak =* p21-activated kinase, IDO = indolamin-2,3-dioxygenase, DUB = Deubiquitinating enzyme, Pim = Proto-oncogene serine/threonine-*protein* kinase, CSF-1R = colony stimulating factor 1 receptor

Article number	**Name**	**Function**	**Sub-screening number**
S1008	Selumetinib (AZD6244)	MEK inhibitor	c1
S1013	Bortezomib (PS-341)	20S Proteasome inhibitor	nc1
S1028	Lapatinib (GW-572016) ditosylate	EGFR and ErbB2 inhibitor	nc1
S1033	Nilotinib (AMN-107)	Bcr-Abl inhibitor	nc1
S1039	Rapamycin (Sirolimus)	mTOR inhibitor	nc1
S1046	Vandetanib (ZD6474)	VEGFR2 inhibitor	c1
S1049	Y-27632 2HCl	ROCK 1 inhibitor	nc1
S1055	Enzastaurin (LY317615)	PKCβ inhibitor	c3
S1061	Nutlin-3	MDM2 antagonist	nc1

S1070	PHA-665752	c-Met inhibitor	nc1
S1075	SB216763	GSK-3 inhibitor	nc1
S1078	MK-2206 2HCl	Akt 1/2/3 inhibitor	c3
S1079	PD153035 HCl	EGFR inhibitor	nc1
S1082	Vismodegib (GDC-0449)	hedgehog inhibitor	nc1
S1087	Iniparib (BSI-201)	PARP1 inhibitor	c2 and c5
S1091	Linsitinib (OSI-906)	IGF-1R inhibitor	c3
S1110	Varespladib (LY315920)	Human non-pancreatic secretory phospholipase A2 inhibitor	c2 and c5
S1115	Odanacatib (MK-0822)	Cathepsin K inhibitor	c2 and c5
S1123	Abiraterone	CYP17 inhibitor	nc1
S1130	YM155 (Sepantronium Bromide)	Survivin suppressant	c3
S1133	Alisertib (MLN8237)	Aurora A inhibitor	c3
S1139	ADL5859 HCl	λ-opioid-receptor agonist	c3
S1141	Tanespimycin (17-AAG)	HSP90 inhibitor	c2
S1147	Barasertib (AZD1152-HQPA, AZD2811)	Aurora B inhibitor	c2
S1158	MK-8245	Stearoyl-CoA desaturase inhibitor	c2 and c5
S1165	ABT-751 (E7010)	Inhibits polymerization of microtubules	c1
S1169	TGX-221	p110β-specific inhibitor	nc1
S1180	XAV-939	Tankyrase 1/2 inhibitor	nc1
S1186	BIBR 1532	Telomerase inhibitor	nc2
S1191	Fulvestrant	Estrogen receptor antagonist	nc1
S1200	Decitabine	DNA Methyltransferase Inhibitor (intra-S-Phase arrest)	nc1
S1202	Dutasteride	Dual 5-α teductase inhibitor	nc1
S1208	Doxorubicin (Adriamycin) HCl	Antibiotic agent, inhibits DNA topoisomerase II	c3
S1216	PFI-1 (PF-6405761)	BET inhibitor for BRD4	nc1
S1231	Topotecan HCl	Topoisomerase I inhibitor	nc1
S1233	2-Methoxyestradiol (2-MeOE2)	Depolymerizes microtubules and blocks HIF1-α	c3
S1235	Letrozole	Aromatase inhibitor	nc2
S1250	Entzalutamide (MDV3100)	Androgen-receptor antagonist	nc2
S1259	Ramelteon	Melatonin receptor agonist	nc2
S1261	Celecoxib	Selective COX-2 inhibitor	nc2
S1274	BX-795	Potent and specific PDK1 inhibitor	nc4
S1289	Camofur	Acid ceramidase inhibitor	nc2
S1324	Doxazosin Mesylate	Selectively antagonizes postsynaptic α1-adrenergic receptors	c3
S1329	Etomidate	GABAA receptor agonist	c3
S1362	Rigosertib (ON-01910)	PLK1 inhibitor	c3
S1410	AS-605240	PI3Kγ inhibitor	nc2
S1453	Tipifarnib (P11577)	Farnesyltransferase inhibitor	c2 and c5
S1456	Zibotentan (ZD4054)	Endothelin A antagonist	c3
S1460	SP600125	JNK inhibitor	nc2

S1476	SB525334	TGFβ receptor I inhibitor	nc2
S1491	Fludarabine	STAT1 activaition inhibitor	nc2
S1498	NVP-BEP800	HSP90β inhibitor	nc2
S1512	Tadalafil	PDE-5 inhibitor	nc2
S1525	Adavosertib (MK-1775)	Wee1 inhibitor	c3
S1526	Quizartinib (AC220)	FLT3 inhibitor	c3
S1531	BIX 02189	MEK5 inhibitor	nc2
S1536	JNJ-42153605	mGlu2 receptor positive allosteric modulator	nc2
S1541	Selisistat (EX 527)	SIRT1 inhibitor	c4
S1544	AM1241	CB2 receptor agonist	nc2
S1548	Dapagliflozin	hSGLT2 inhibitor	c5
S1549	Nebivolol HCl	β1-adrenoceptor inhibitor	nc2
S1550	Pimobendan	PDE3 inhibitor	nc2
S1570	KU-60019	ATM inhibitor	nc2
S1572	BS-181 HCl	CD57 inhibitor	nc2
S1574	Doramapimod (BIRB 796)	Pan-p38 MAPK inhibitor	c1
S1577	Tie2 kinase inhibitor	Tie2 inhibitor	nc2
S1578	Candesartan	Angiotensin II receptor antagonist	nc2
S1582	H 89 2 HCl	PKA inhibitor	nc4
S1630	Allopurinol	Xanthine oxidase inhibitor	nc3
S1657	Enalaprilat Dihydrate	Angiotensin-converting enzyme inhibitor	nc3
S1801	Ranitidine Hydrochloride	Histamine H2-receptor antagonist	c4
S1847	Clemastine Fumarate	Histamine H1 receptor antagonist	nc3
S2012	PCI-34051	HDAC8 inhibitor	nc3
S2013	PF-573228	FAK inhibitor	nc3
S2131	Roflumilast	PDE4 inhibitor	nc3
S2149	GSK1292263	GPR119 agonist	c2 and c5
S2163	PF-4708671	p70 ribosomal S6 kinase inhibitor	nc3
S2169	Rosuvastatin Calcium	HMG-CoA reductase inhibitor	nc3
S2182	SB743921	Kinesin spindle protein inhibitor	c5
S2183	BGJ398 (NVP-BGJ398, Infibratinib)	Inhibitor of FGFR1/2/3	c4
S2199	Aliskiren Hemifumarate	Renin inhibitor	c4
S2215	DAPT (GSI-IX)	γ-secretase inhibitor	c4
S2216	Mubritinib (TAK 165)	HER2/ErbB2 inhibitor	c4
S2220	SB590885	b-raf inhibitor	nc5
S2222	PF-3716566	p-CAB inhibitor	nc4
S2225	TAME	APC inhibitor	nc5
S2232	Ketanserin	5-HT 2A serotonin receptor antagonist	c4
S2459	Clozapine	5-HT antagonist	c4
S2497	Pancuronium dibromide	Nicotinic acetylcholine receptor antagonist	nc4
S2507	Salbutamol sulfate	β2-adrenergic receptor agonist	c4

S2516	Xylazine	α2-Adrenergic receptor agonist	nc5
S2550	Tolterodine tartrate	Muscarinic receptor antagonist	nc5
S2593	Tolvaptan	Vasopressin V2 receptor antagonist	c4
S2631	URB597	FAAH inhibitor	c5
S2632	BMS-378806	Inhibits the binding of HIV-1 gp120 to the CD4 receptor	nc4
S2636	A66	p110α inhibitor	c1
S2638	NU7441 (KU-57788)	DNA-PK inhibitor	nc4
S2683	CHIR-124	Chk1 inhibitor	nc4
S2690	ADX-47273	mGlu5 positive allosteric modulator	nc4
S2700	KX2-391	Src inhibitor	c2 and c5
S2720	ZM 336372	c-Raf inhibitor	nc5
S2722	JTC-801	Opioid receptor-like receptor antagonist	nc4
S2731	AZ 3146	Mps1 inhibitor	nc5
S2789	Tofacitinib (CP-690550, Tascocitinib)	JAK3 inhibitor	nc4
S2799	Daporinad (FK866, APO866)	Nicotinamide phophoribosyltransferase inhibitor	c4
S2806	CEP-33779	JAK2 inhibitor	nc4
S2818	Tacedinaline (CI994)	HDAC inhibitor	c4
S2823	Tideglusib	GSK-3β inhibitor	c5
S2824	TPCA-1	IKK-2 inhibitor	nc4
S2863	ML130 (Nodinitib-1)	NOD1 inhibitor	nc5
S2891	GW441756	TrkA inhibitor	c1
S2912	WZ811	CXCR4 antagonist	nc4
S2915	GW9662	PPARγ antagonist	nc4
S2925	Evacetrapib (LY2484595)	CETP inhibitor	c2 and c5
S2929	Pifithrin-α HBr	p53 inhibitor	c1
S3021	Rimonabant	CB1 antagonist	nc4
S3147	Entacapone	Catechol-O-methyltransferase inhibitor	nc4
S4002	Sitagliptin phosphate monohydrate	DPP-IV inhibitor	nc4
S4009	Mirabegron	β3-adrenoceptor agonist	nc5
S4073	Sodium 4-Aminosalicylate	Antibiotic used to treat tuberculosis via NF-kB inhibition	c2 and c5
S6003	Ataluren (PTC124)	Selectively induces ribosomal read-through	2 and 5
S7015	Birinapant	SMAC mimetic antagonist	c5
S7024	Stattic	STAT3 inhibitor	nc5
S7092	SANT-1	Inhibits Smo agonist effects	nc5
S7093	IPA-3	Pak1 inhibitor	nc5
S7111	NLG919, Navoximod	IDO pathway inhibitor	nc5
S7140	TCID	DUB inhibitor for ubiquitin C-terminal hydrolase L3	nc5
S7153	10058-F4	c-myc inhibitor	nc5

S8005	SMI-4a	Pim1 inhibitor	nc5
S8008	RGD (Arg-Gly-Asp) Peptides	Cell adhesion motive which can mimic cell adhesion proteins	c1
S8028	Tariquidar	P-glycoprotein inhibitor	c5
S8031	NSC 23766	Rac inhibitor	nc5
S8032	PRT062607 (P505-15, BIIB057) HCl	Syk inhibitor	nc5
S8038	UPF 1069	PARP2 inhibitor	nc5
S8042	GW2580	CSF-1R inhibitor for c-FMS	nc5
S8048	Venetoclax (ABT-199, GDC-0199)	Bcl-2 inhibitor	c5
S5322	Sodium gualenate	Anti-inflammatory substance.	Candidate for positive control
S5634	L-arginine	Necessary for protein biosynthesis, role in immune regulation	-

3.1.9 Software

Table 3.14: List of all software programs used in this thesis

Software	Company	Company headquarters
Axiovision	ZEISS	Oberkochen, Germany
BioRender Illustrator	BioRender	Toronto, Canada
BZ Analyer	Keyence Germany	Neu-Isenburg, Germany
BZ Viewer	Keyence Germany	Neu-Isenburg, Germany
cellSens Entry	Olympus	Hamburg, Germany
Fiji Image J	National Institute of Health	Bethesda, MD, United States
GloMax Discovery	Promega GmBH	Walldorf, Germany
Graphpad Prism 9.5.0	GraphPad Software Inc.	San Diego, CA, United States
Inkscape 1.2	The Inkscape Project	Boston, MA, United States
Microsoft Office 365	Microsoft Corporation	Redmond, WA, United States

3.2 Methods

3.2.1 Wound healing organ culture

Human skin was obtained from elective plastic surgery after patients gave their informed consent according to the declaration of Helsinki. This study was approved by the Ethics Committee of the University of Lübeck (compare **Appendix pages 258-259**). Most of the skin used in this thesis is abdominal skin. Breast, upper arm, and thigh skin were also used. Except for skin 20-004 and 22-023 donors were female. The mean year of birth is 1976. A detailed list of all skin used for this work can be found in **Table 3.15**.

Tabel 3.15: Human skin used in this thesis

SG = sodium gualente, DMSO = dimethyl sulfoxide, L-Arg = L-arginine, clinical scr = screening of the clinical trials substances, non-clinical scr = screening of the non-clinical trials substances, V = validation, 4 x 1 = continuous treatment with the inhibitors tested and their respective controls

[1] Dr. med Stephan Valina, *Holstentor Privatklink Plastisch-Ästhetische Chirurgie*, Lübeck; [2] Dr. med Hans-Leon, Nathrath, *Plastische Chirurgie Arabella Praxisklinik*, Munich,, [3] Dipl. oec med. Dr. med Marcus Schlichter, *Aestheticum Praxisklinik*, Bremen; [4] Prof. Dr. Mailänder, Plastic Surgery University hospital Schleswig-Holstein, campus Lübeck, Lübeck, [5] Dr. Reifenrath, *Plastisch Ästhetische Chirurgie*, Dortmund; [6] Dr. Akbari, Azarm Akbari *Plastische und Ästhetische Chirurgie*, Recklinghausen

Human skin number	Location	Sex	Year of Birth	Surgeon	Used for
20-002	Abdomen	Female	1966	Dr. Valina[1]	DMSO
20-004	Abdomen	Male	1967	Dr. Valina[1]	SG
20-005	Abdomen	Female	1982	Dr. Valina	SG, L-Arg
20-006	Abdomen	Female	1965	Dr. Nathrath[2]	DMSO
20-011	Abdomen	Female	1969	Dr. Valina	SG
20-012	Breast	Female	1960	Dr. Schlichter[3]	SG
20-016	Abdomen	Female	1972	Dr. Schlichter	L-Arg
20-018	Abdomen	Female	1980	Dr. Valina	Clinical scr 1, L-Arg
20-019	Abdomen	Female	1983	Dr. Schlichter	Clinical scr 2
20-022	Breast	Female	1967	Dr. Schlichter	Clinical scr 3
20-023	Abdomen	Female	1976	Dr. Valina	SG, clinical scr 4
20-026	Abdomen	Female	1982	Dr. Schlichter	Clinical scr 5
20-028	Abdomen	Female	1980	Dr. Valina	Clinical scr 6, SG
21-001	Abdomen	Female	1984	Dr. Valina	Non-clinical scr 1
21-005	Abdomen	Female	1951	Dr. Valina	Non-clinical scr 2
21-009	Upper arm	Female	1978	Dr. Valina	V1
21-010	Thigh	Female	1975	Dr. Valina	V1
21-011	Abdomen	Female	1991	Dr. Schlichter	Non-clinical scr 3
21-012	Breast	Female	1963	Plastic surgery unit of the UKSH campus Lübeck[4]	Non-clinical scr 4, V1
21-016	Abdomen	Female	1964	Dr. Nathrath	Non-clinical scr 5, V1
21-020	Abdomen	Female	1985	Dr. Valina	V1, V2, S2891
21-021	Breast	Female	1964	Dr. Reifenrath[5]	V2
21-022	Breast	Female	1969	Dr. Reifenrath	S2891
21-024	Breast	Female	1975	Dr. Reifenrath	S2891, V2
21-025	Breast	Female	1971	Dr. Reifenrath	S2891, V2
21-026	Abdomen	Female	1979	Dr. Reifenrath	S2891, V2
21-027	Abdomen	Female	1982	Dr. Schlichter	S2891, V2
21-031	Abdomen	Female	1978	Dr. Valina	S1180, S2149
21-032	Abdomen	Female	1988	Dr. Reifenrath	S1180, S2149

21-033	Abdomen	Female	1965	Dr. Reifenrath	S1180, S2149
21-036	Abdomen	Female	1980	Dr. Valina	S2149
21-038	Abdomen	Female	1975	Dr. Reifenrath	S2149
21-041	Abdomen	Female	1966	Dr. Reifenrath	S2149, S2891, PamGene
22-021	Abdomen	Female	1986	Dr. Valina	S1180, S2891, Octenisept
22-022	Abdomen	Female	1974	Dr. Reifenrath	S1180, S2891, Octenisept, PamGene
22-023	Abdomen	Male	1999	Dr. Reifenrath	Octenisept, male skin, pathological model
22-025	Abdomen	Female	1975	Dr. Schlichter	Pathological model, 4x1
22-026	Abdomen	Female	1980	Plastic surgery unit of the UKSH campus Lübeck	S2891
22-027	Abdomen	Female	1977	Dr. Reifenrath	S2891
22-028	Abdomen	Female	1990	Dr. Schlichter	S2891, pathological model, 4x1, DMSO
22-032	Abdomen	Female	1983	Dr. Valina	PamGene, 4x1 DMSO
22-033	Breast	Female	1993	Dr. Schlichter	4x1, DMSO
23-001	Abdomen	Female	1986	Dr. Akbari[6]	Exemplary pictures for the methods part of this thesis

Directly after the surgery the skin was placed in sterile Williams Medium E (WEM) and transferred to the laboratory in Lübeck within 24 hours. The skin was kept at 4°C for the entire transport.
Figure 3.1 shows a schematic flow chart of the wound healing organ culture (WHOC). The first step to establish the WHOC was to trim the excess amount of subcutaneous fat until only the uppermost layer of adipocytes (directly below the dermis) remained. Too much subcutaneous fat hinders the course of the experiment, but it is essential that some of the subcutis does remain. This is because the WHOC is a full human skin model, so all three layers need to be intact.

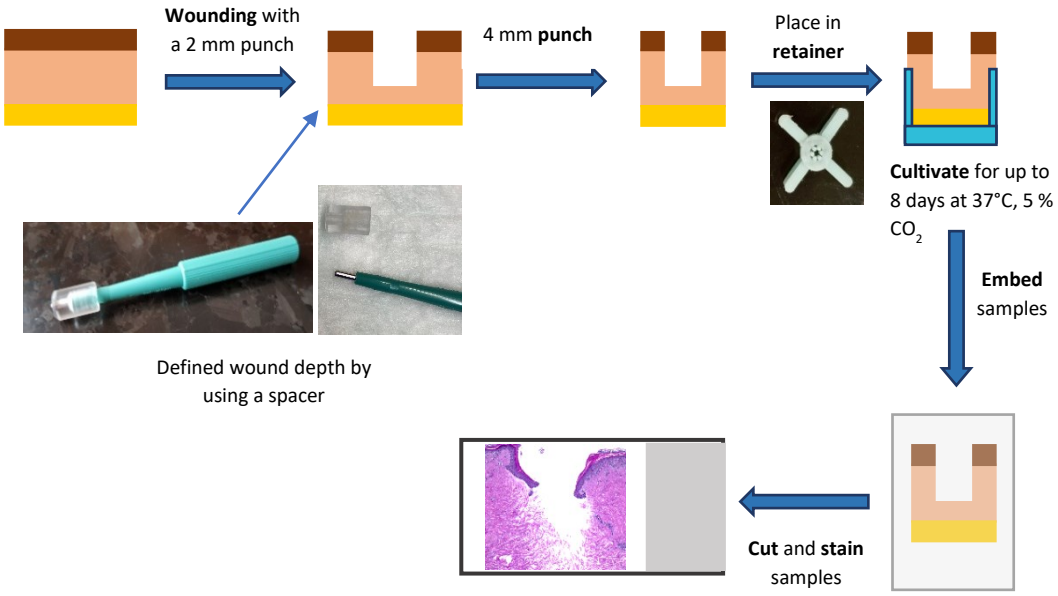

Figure 3.1: Flowchart of the wound healing organ culture
A wound is set into the skin by using a 2 mm biopsy punch. To define the wound depth a spacer is placed on top of the 2 mm biopsy punch, limiting the wounding depth. Then, a 4 mm biopsy punch is taken centered around the 2 mm wound. This wounded punch is placed in a retainer, that ensures its upright position and the air-liquid interface at the epidermis. The wounds are cultured for up to 8 days at 37 °C and 5 % carbon dioxide (CO_2) and then embedded, cut, and stained for further evaluation. Spacer and retainers were developed by Dr. Andreas Thomsen, University Hospital Freiburg.

After trimming the wounds were set. Because this model follows the punch-in-a-punch approach (as described by (Gherardini *et al.*, 2020; Liao *et al.*, 2019)) wounds were set using a 2 mm biopsy punch. To standardize wound depth the 2 mm biopsy punches were equipped with a spacer, which limited the punch depth (compare **Figure 3.1**). The half-punched biopsy was cut out using a surgical scissor, giving rise to wounds of roughly 500 µm depth. A 4 mm biopsy punch was placed centered over the wound, so that a 4 mm biopsy around a 2 mm wound was obtained. **Figure 3.2** shows exemplary pictures of how the process of trimming, wounding, and punching looks like in the laboratory.

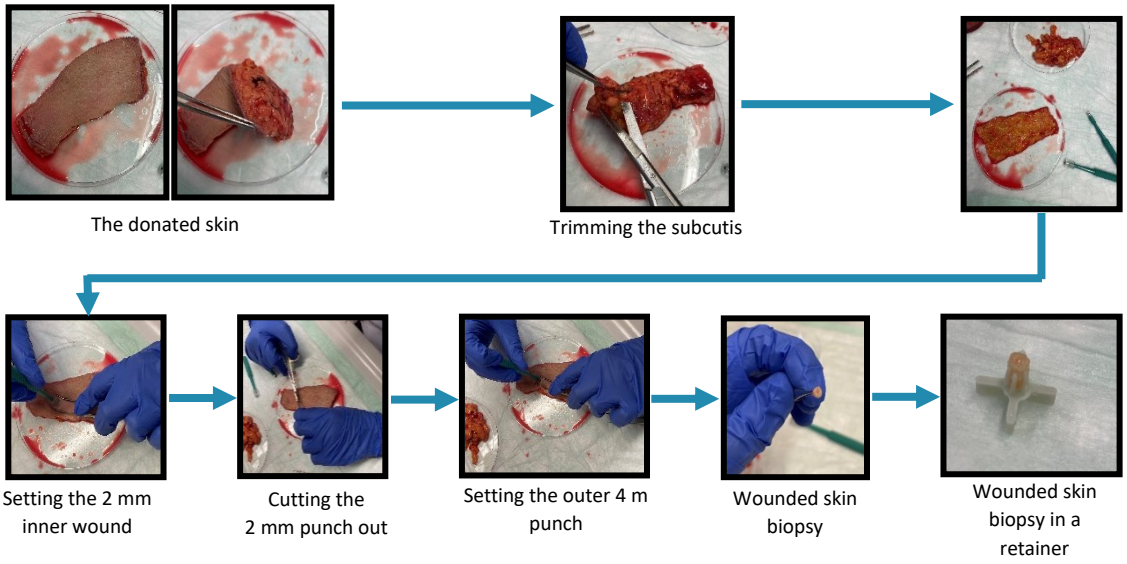

Figure 3.1: The process of the punch in a punch
The donated skin is placed in a petri dish and flipped around so that the subcutis is on the upside. The excessive fat of the subcutis is trimmed with the help of surgical scissors and forceps but a thin layer of fat is kept having all three skin layers intact. Next the skin is flipped over to have the epidermis up. With a 2 mm biopsy punch with a spacer on top a 2 mm wound is punched into the skin. Next, the wound is cut out. A 4 mm biopsy is punched out of the skin with the 2 mm wound in the middle, resulting in a wounded biopsy punch. This skin piece is placed in a specific retainer and is now ready for culturing.

This wounded biopsy punch was placed in specifically designed retainer, ensuring the air-liquid interface at the epidermis during the culturing period. In this work two different kind of retainers were used. The *Einrichtung für Marine Biotechnologie* (EMB)-retainers were already in use by our lab when this work started. As they were only available in very limited numbers and could not be autoclaved, the Freiburg-retainer was developed in cooperation with Dr. Andreas Thomsen from the University of Freiburg. **Figure 3.3** shows photos of the retainers.

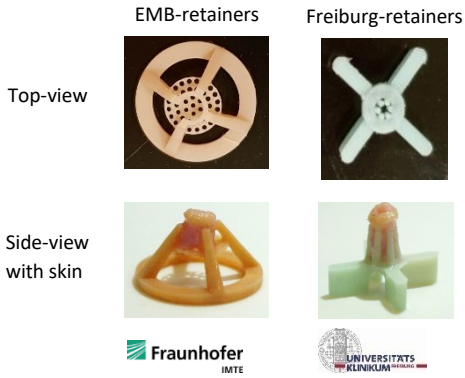

Figure 3.2: Different skin retainers used in this thesis
Shown here are the *Einrichtung für Marine Biotechnologie* (EMB)-retainer on the left, without skin (upper panel) and with skin (lower panel) and the Freiburg-retainer on the right, without skin (upper panel) and with skin (lower panel)

The skin in the retainer was placed into a well of a 24-well-plate. Depending on the respective experimental set up, between 2 and 4 punches were prepared per condition as technical replicates. The wells of the 24-well-plate were filled with 1.1 mL (EMB-retainer) or 1.25 mL (Freiburg-retainer) fresh WEM respectively.
The timeline of a standard WHOC is illustrated in **Figure 2.4**. After trimming and wounding, top-view microscopy pictures were taken. These allow to determine the top-view wound area and wound perimeter. If available, optical coherence tomography (OCT) was performed on the wounds for wound volume measurement (compare **Chapter 2.2.4**). Thereafter, the medium was exchanged once more. This time with preheated, supplemented WEM (compare **Table 2.12**). To prevent fungal infections, an antimycotic was added to the wells on this day only. Finally, the skin was placed in an incubator at 37 °C and 5 % carbon dioxide (CO_2) for 24 hours. The day of the start of the culture is referred to as day 0 in the following.

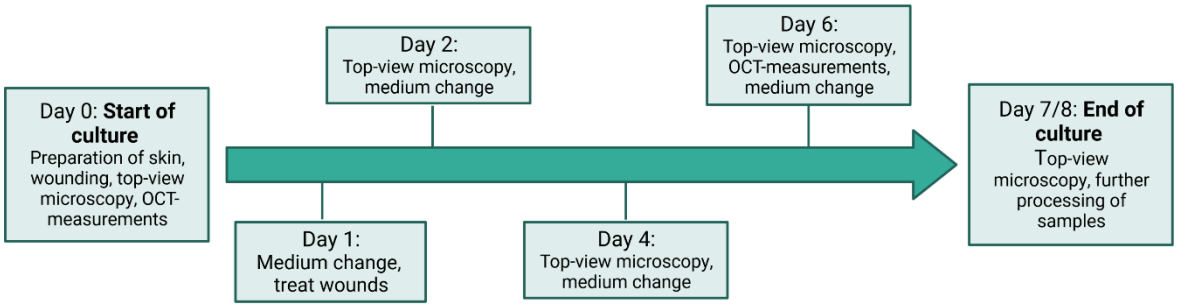

Figure 3.3: Timeline of the wound healing organ culture
The wound healing organ culture (WHOC) starts at day 0, on which the skin is trimmed (excess fatty tissue removed) and wounded. Top-view microscopy pictures are taken and if the optical coherence tomography (OCT) system is available, OCT measurements are performed for wound volume determination. At day 1, the medium is changed and the wounds are treated with the substance that is tested in the respective experiment. At day 2 (24 hours after day 1), the medium is changed and top-view microscopy is done. The same happens at day 4 and day 6. Here, if possible, OCT-measurements are performed again. At day 7 or 8 the WHOC is stopped. Top-view microscopy pictures are taken a last time and the wound specimens are further processed, e.g. snap frozen or embedded for microscopic evaluation. If desired, treatment can happen at any medium change. Created with BioRender.

The next day (day 1), the medium was exchanged for pre-heated, supplemented WEM that contained the substances tested in the respective WHOC. If not otherwise specified, the substance concentration in the well was 1 µM. The punches were incubated with the substance for 24 hours (unless stated otherwise) at 37 °C, 5 % CO_2. On day 2, top-view microscopy pictures were taken, and the medium containing inhibitor was exchanged for pre-heated, supplemented WEM. The punches were incubated for 48 hours at 37 °C, 5 % CO_2. Afterwards (day 4), top-view microscopy was done, and the medium was changed again. The punches were incubated for 48 hours at 37 °C, 5 % CO_2. On day 6, again top-view microscopy pictures were taken. If OCT measurements were done on day 0, the wound volume was measured once more via OCT, allowing a comparison between the volume of each wound at day 0 and day 6. Afterwards, the medium was changed, and the punches were incubated for another 24 or 48 hours. Thereafter top-view microscopy was performed one last time at day 7/8, for the top-view wound area and perimeter could be compared throughout the course of the culture. Processing of the samples at the end of the culture, tissue staining, microscopy and evaluation will be described on the following pages.

3.2.1.1 Pathological wound healing organ culture model

To mimic chronic wounds with their micro-environment that is harmful to wound healing, Post *et al*. established a pathological wound healing culture model (Post *et al.*, 2021) to study the effect of the thyroid hormone L-thyroxine (T4) on the ETs under normal and pathological conditions. Utilizing their model, the influence of different substances on the *ex vivo* wound healing was tested here under pathological conditions. Basically, the pathological WHOC started with trimming and making wounds as the “regular” WHOC. But the wounded punches were then cultivated in a specific incubator (Invivo$_2$) with only 5 % oxygen (O_2) in a specifically supplemented pathological WEM, containing high levels of glucose and no insulin to mimic a type 2 diabetes mellitus like environment and hydrogen peroxide to induce oxidative stress. **Table 3.12** shows the exact composition of the pathological culture medium. The low O_2 saturation led to hypoxia in the skin, which induced the expression of a specific set of hypoxia-genes, the most prominent being hypoxia-induced factor 1α (HIF1-α). As HIF1-α remains expressed only for a very short time under normoxic conditions (Lee *et al.*, 2004). For the

course of the culture the wounds had to remain in hypoxia. This means, that top-view microscopy pictures could only be taken at the start and the end of the culture. For the pathological model wounds were cultivated for either 3 days or 6 days. Corresponding to the "regular" WHOC model, the wounds were treated at day 1 for 24 hours in the pathological model also. Due to availability and accessibility of the Invivo$_2$ incubator medium change was performed on day 1, 2, and 5. The Invivo$_2$ workstation allowed the medium change under hypoxic conditions. To ensure continuous hypoxic conditions, the pathological medium was kept in hypoxia for at least 24 hours before medium change. As the pathological wound healing model differed from the "normal" WHOC, a control plate was always included, which was also cultured for 3 or 6 days with top-view microscopy at day 0 and day 3 or day 6 and medium changes at day 1 (treatment day), 2, and 5. This allowed a direct comparison between wound healing under physiological and pathological conditions.

3.2.2 Processing the skin specimens

Depending on the respective WHOC, the skin punches were processed differently: Embedding for paraffin sections, embedding for cryosections or snap-frozen for other analysis.

3.2.2.1 Paraffin embedding

For paraffin embedding the skin punches were removed from the retainer with the help of a surgical forceps and were placed into **paraffin** embedding cassettes as **Figure 3.5** shows. The cassettes were then stored in 4 % Roti-Histofix® for 3-10 days and embedded in the routine laboratory of the UKSH Dermatology on the campus Lübeck.

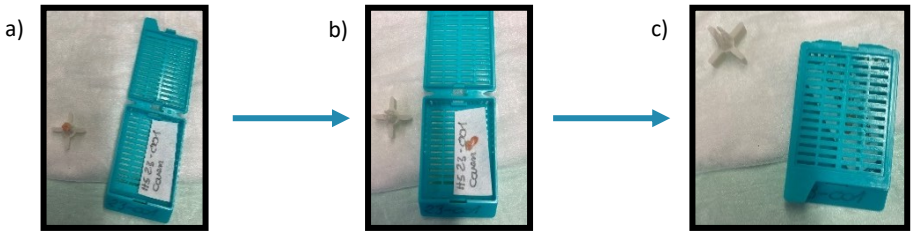

Figure 3.5: Preparation for paraffin embedding
a) At the end of the culture the embedding cassette was labeled and for further details a piece of filter paper was added. b) The biopsy punch was placed inside the cassette and c) the cassette was closed and could now be placed in 4 % Roti-Histofix® for fixation.

At this laboratory the tissue is dewatered and slowly transferred into paraffin wax by passing a series of ascending ethanol concentration and xylol incubation (compare **Table 3.16**).

Table 3.16: dewatering of the paraffin samples

Repetitions	Incubation time	Substance
1x	2 hours	Formaldehyde solution
1x	30 minutes	70 % Ethanol
1x	1 hour	80 % Ethanol
2x	1 hour	96 % Ethanol
1x	1 hour	100 % Ethanol
2x	1 hour 30 minutes	100 % Ethanol
2x	1 hour	Xylol
1x	1 hour	Xylol
4x	1 hour	Paraffin (at 60°C)

The process of dewatering will take about 16.5 hours and is done overnight. The next day the samples can be embedded into paraffin with the help of the embedding machine. **Figure 3.6** shows exemplary pictures of the paraffin embedding process. Briefly, 60 °C warm, liquid paraffin was filled into small metal mold. Those metal molds were then placed at room temperature (RT) and the skin punch was taken out of the cassette. It was quickly (before the paraffin became solid) placed horizontally into the metal mold, allowing for complete cross sections of the wound and all three skin layers when cutting later. The mold was then transferred a cooling plate set to -5 °C where the paraffin with the sample embedded inside became solid. The paraffin blocks were stored at RT.

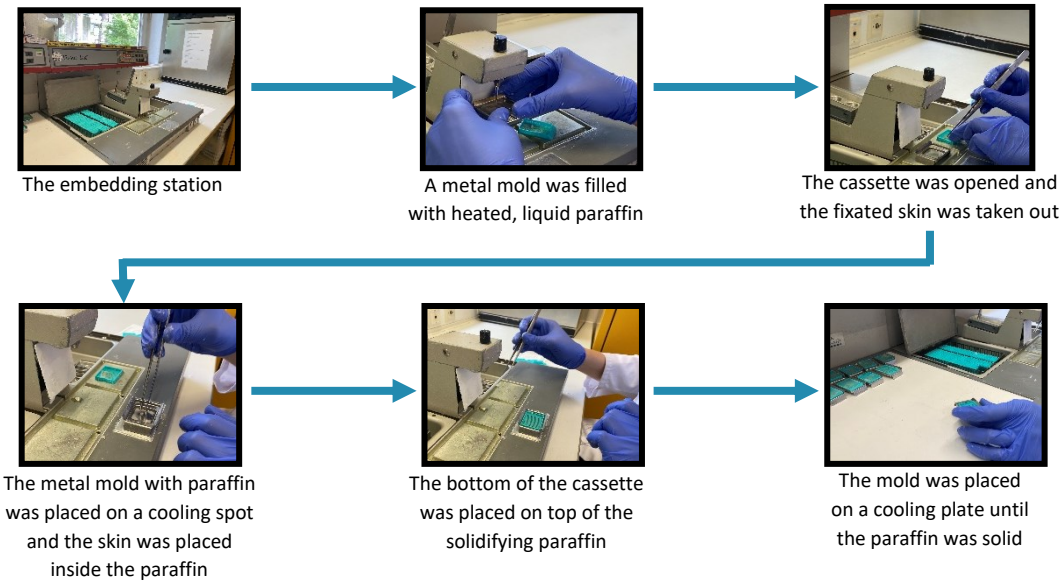

Figure 3.6: Paraffin embedding process
After fixation and dehydration of the skin samples, they were embedded in paraffin. The work was done at the embedding station. First, a metal mold was filled with pre-heated liquid paraffin. The paraffin embedding cassette was opened. The lid was discarded. The metal mold with the paraffin was placed on a cooling spot of the embedding station. The skin piece was taken with forceps and horizontally placed into the now rapidly solidifying paraffin, so that, when the samples were later cut, the cross sections contained all three skin layers. Next, the bottom of the paraffin cassette was placed on top of the mold, which then was placed on a cooling plate until the paraffin was completely solid.

3.2.2.2 Cryo-embedding

For cryo-embedding Tissue Tek®® was filled into cryomolds. The wounded skin samples were removed from the retainer with the help of surgical forceps' and were placed into the Tissue Tek® horizontally. When the samples were cut in the cryostat complete cross sections of the wound containing all three skin layers could be generated. The punches in the Tissue Tek® and cryomold are placed into the cryostat (at -20 °C) until fully frozen and are then transferred to -80 °C for long term storage. **Figure 3.7** shows the cryo-embedding process.

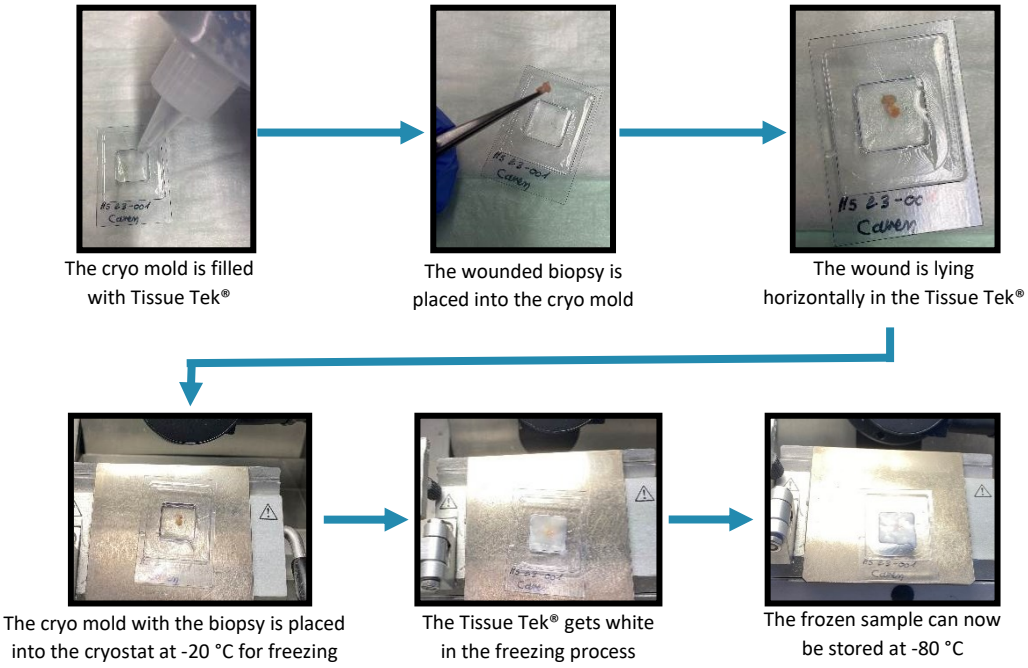

Figure 3.7: Cryo-embedding of skin samples
The cryo mold is filled with Tissue Tek® and the wounded skin biopsy is placed into the mold horizontally. When the samples are later cut the cross sections contain all three skin layers. The cryo mold with the biopsy is then placed into the cryostat at -20 °C for freezing. After the Tissue Tek® is completely frozen, the cryo samples are stored at -80 °C.

3.2.2.3 Preparation for PamGene analysis

For PamGene analysis, the skin punches were removed from the retainers with the help of a surgical forceps and placed in sterile reaction tubes. Those tubes were snap frozen in liquid nitrogen and then stored at -80 °C until further processing. As the salts in Tissue Tek® interfere with the PamGene analysis measurements later it is important to snap-freeze only the skin punches and to not have them embedded in anything.

3.2.3 Development of the screening/organization of the library

The core of this work was the screening of the Highly Selective Inhibitor Library L3500 provided by the company Selleck Chemicals (https://www.selleckchem.com/ last time used December 27, 2022). This library contained 136 compounds which bind and mostly inhibit cellular targets with a very high specificity. **Figure 3.8** shows the organization process of the library and the screening. First, the parameters to measure the *ex vivo* wound healing in the WHOC had to be defined. Due to time-constraints, only parameters were chosen that did not require elaborate preparation of stained tissue slides. Thus, the *ex vivo* wound healing was assessed based on the top-view wound area and perimeter as well as the wound volume obtained by OCT.
All substances were dissolved in dimethyl sulfoxide (DMSO). Before the screening could be carried out, the tolerable DMSO concentration had to be determined and a suitable positive control had to be found. For the latter the manufacturer recommended L-arginine (L-Arg) or sodium gualenate (SG). Especially in the beginning of the screening process, when the Freiburg-retainers were yet in the making, the amount of skin retainers accessible was very limited. Together with the varying amount of skin per donation and the time-consuming process of wounding and culturing the skin not all of

the 136 inhibitors could be tested in one screening. Hence the library was divided into two: those substances, which were in clinical trials according to the manufacturer and clinical trials.gov (https://clinicaltrials.gov/ last time used December 22, 2022) (further referred to as clinical trials substances) and those who were not (non-clinicals trial substances). In the first group the substances which have shown to have a positive effect onto the human skin organ culture model in our lab (Burmester *et al.*, 2019, 2020) were included too.

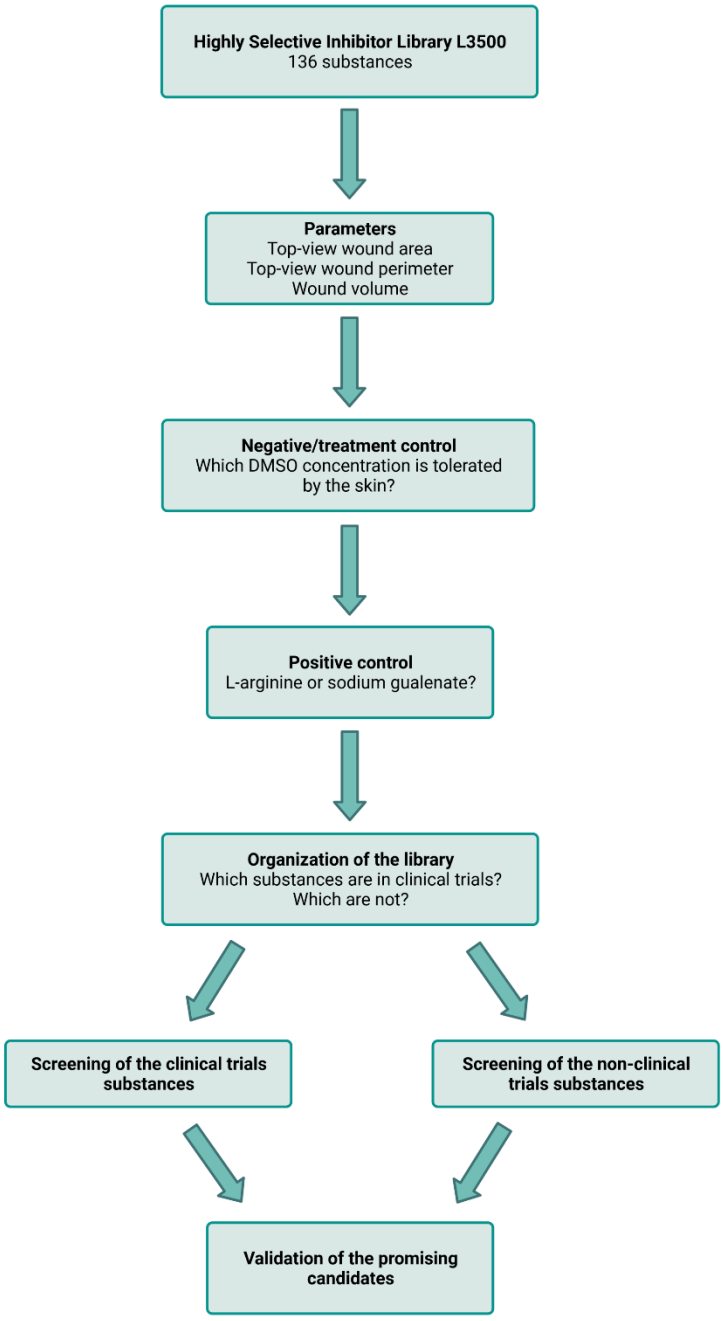

Figure 3.8: Flowchart of the screening process
The Highly Selective Inhibitor Library L3500 containing 136 different substances is screened for their effect on wound healing in the wound healing organ culture (WHOC) model. As the substances are dissolved in dimethyl sulfoxide (DMSO), first a tolerable DMSO concentration is determined. Next, a suitable positive control is chosen from L-arginine and sodium gualenate. Then, the library is divided into substances already in clinical trials and those which are not (non-clinical trials). Both parts are screened and candidates that are promising, i.e., showed a positive effect on the wound healing in the WHOC are further validated to ensure their effect.
Created with BioRender.

All inhibitors were screened at a 1 µM concentration and added for 24 hours at day 1 of the WHOC. Two punches were used per inhibitor tested. 0.1 % DMSO severed as vehicle control, 10 µM sodium gualenate as positive control.

The clinical trials substances were screened first. As those substances were in or had already passed the toxicity tests necessary for drug approval (Berdigaliyev & Aljofan, 2020; Williams, 2016), they could easily and with relatively little effort be repurposed as drugs for wound healing. These substances were tested with skin punches in the EMB-retainers as the Freiburg-retainers were yet in development.

After finishing the clinical trials substances, the non-clinicals trial substances were screened in the same manner as the clinical trials substances but using the Freiburg-retainers. For both screenings a certain number of "sub-screenings" were necessary due to handling and time reasons. **Table 3.17** shows which inhibitors have been tested in which (sub)screening.

Table 3.17: Overview of the sub-screenings and the different inhibitors tested in each. Inhibitors area listed with their article number. Some promising inhibitors were tested twice because the positive control did not work properly in Sub-screening II.

Clinical trials substances

Screening I	Screening II	Screening III	Screening IV	Screening V	Screening VI
S1008	S1087	S1055	S1541	S1087	S1115
S1046	S1110	S1078	S1801	S1110	S1453
S1574	S1115	S1091	S2183	S1158	S2182
S1165	S1141	S1130	S2216	S1548	S4073
S2636	S1147	S1133	S2232	S2149	
S2891	S1158	S1208	S2459	S2631	
S2929	S1453	S1233	S2507	S2700	
S8008	S2149	S1324	S2593	S2823	
	S2182	S1329	S2799	S2925	
	S2700	S1362	S2818	S6003	
	S2925	S1456		S7015	
	S4073	S1525		S8028	
	S6003	S1526		S8048	

Non-clinical trials substances

Screening VII	Screening VIII	Screening IX	Screening X	Screening XI
S1013	S1186	S1630	S1274	S2220
S1029	S1235	S1657	S1582	S2225
S1033	S1250	S1847	S2222	S2516
S1039	S1259	S2012	S2497	S2550
S1049	S1261	S2013	S2632	S2731
S1061	S1289	S2131	S2638	S2738
S1070	S1410	S2163	S2683	S2690
S1075	S1460	S2169	S2722	S2720
S1078	S1476	S2199	S2789	S2863
S1079	S1491	S2215	S2806	S4009
S1082	S1498		S2824	S7024
S1123	S1512		S2912	S7092
S1169	S1531		S2915	S7093
S1180	S1536		S3021	S7111

S1191	S1541		S3147	S7140
S1200	S1544		S4002	S7153
S1202	S1549			S8005
S1216	S1550			S8031
S1231	S1570			S8032
	S1572			S8038
	S1577			S8042
	S1578			

The clinical trials substances showing a positive effect on 2 out of the 3 parameters determined (top-view wound area, perimeter and wound volume) were defined as “promising” and were further validated. For the non-clinical trials substances promising candidates showed a positive effect on all 3 parameters.
To ensure maximal objectiveness, the evaluation of the screening was performed by one blinded person.

3.2.4 Optical coherence tomography for wound volume determination

OCT is an imaging technique that displays some similarity to ultrasound imaging, but it uses infrared laser light instead of sound waves. In both techniques, light or soundwaves are sent onto a biological sample, which reflects, scatters, or attenuates the waves depending on the samples properties. It then can be measured how fast and how intense the backscattered or reflected waves return and with which intensity. These measurements allow the construction of a 3D image of the inside of the sample. The properties of a wave, especially its wavelength, determine how deep the wave can penetrate the sample and how high the resolution of the constructed image will be. Generally, longer waves can penetrate a sample deeper but lead to a lower resolution, while short waves have limited penetration depth but can achieve a higher image resolution. For OCT with its infrared laser light, the penetration depth is around 2 mm but the resolution is in the micrometer area and 3-100 times higher than that of ultrasound (Ha & Hundt, 2019).
As light travels extremely fast, it is not feasible to measure the waves reflecting from a sample directly in the case of OCT. Instead, the so-called Michelson interferometry is used as shown in **Figure 3.9**.

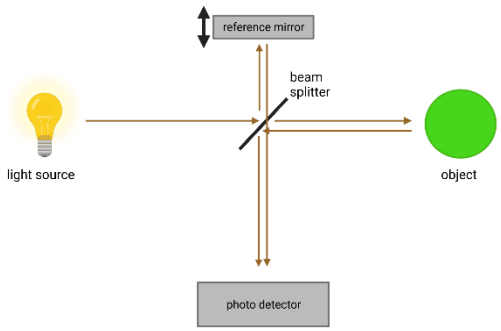

Figure 3.9: Principle of the Michelson interferometry in optical coherence tomography
Low coherence laser light is emitted from a light source. At the beam splitter the light beam is split into 2 beams. One beam goes on to the object, that is imaged and reflected by it depending on the objects properties. The other light beam is steered to a reference mirror and reflected from there. Both reflected light beams meet on the way to the photo detector. If the path between light source and reference mirror is equal to the path between the light source and the object, the light beams will interfere with each other. This can be detected by the photo detector. By adjusting the position of the reference mirror the distance between light source and object can be calculated indirectly.
Created with BioRender, simplified from Podoleanu (Podoleanu, 2012).

Briefly, the laser light beam is split into two parts with the help of a beam splitter. One part travels onto the sample, the other is directed down a reference path with a known length. Both beams reflect on the sample/surface at the end of the reference path and are directed together to a detector. On this way, the light beams will interfere with each other, but only if the sample path and the reference path have the same length. This interference pattern can then be detected. As the reference path length can be changed while scanning the sample, this allows for image construction (Podoleanu, 2012).

Unlike ultrasound OCT works contactless, due to different properties of sound and laser waves. Also, OCT is a non-invasive and extremely fast technique. Acquisition of the scans happens within seconds (Glinos *et al.*, 2017; Ha & Hundt, 2019; Podoleanu, 2012). This makes multiple measurements of the same samples on different days possible. For this project, OCT allows a “look into” the same wound on different days, without having to embed, to cut and to stain the sample.
Here, it was decided to measure the wound volume at day 0 and day 6, based on the work of Sturmheit *et al.* (Sturmheit *et al.*, n.d.).
All measurements were performed in cooperation with the Institute for Biomedical Optics (BMO) of the University of Lübeck on the OCT system build in the BMO. All measurements and wound assessments were performed by Madita Göb, M.Sc. . The measurements were performed as described by Sturmheit *et al.* (Sturmheit *et al.*, n.d.). The fourier domain mode locking (FDML)-laser based, home build 3.3 Mhz OCT system has a lateral resolution of 22 µm, an axial resolution of about 7 µm in tissue. The field of view is 6.4 mm x 6.8 mm x 5 mm (in air). It can scan a wound and construct a 3D video of the wound allowing for the volume determination (Huber *et al.*, 2006; Pfeiffer *et al.*, 2020; Sturmheit *et al.*, n.d.).
For the screening of the Selleck Chemicals Library many wounds had to be scanned. While the actual measurement is very fast (acquisition within seconds), placing each wound into the scanning area was very time-consuming. Therefore, a xyz-positioning unit was constructed, which could move the scanning-unit over the well plate automatically. This allows for automated scans of the plates. 24 wounds can be measured in less than 10 minutes.
The data obtained by the OCT measurements is a 3D scan, but exemplary pictures can be found in **Figure 3.10**. The green line here illustrates the segmentation algorithm, developed in the BMO, which automatically calculates the wound volume.
For this algorithm it is necessary to determine how much residual fluid is left in the wound. This is because the refraction index (i.e. how fast the light wave passes through a specific material) is ca. 1.32 in water but ca. 1 in air (for wavelength of 1300 nm) (Sturmheit *et al.*, n.d.). So, distances in aqueous fluids appear 1.32 times larger than they actually are. It is possible to correct for this by assessing how much fluid is in the wound and correcting the wound volume respectively, leading to precise wound volumes.

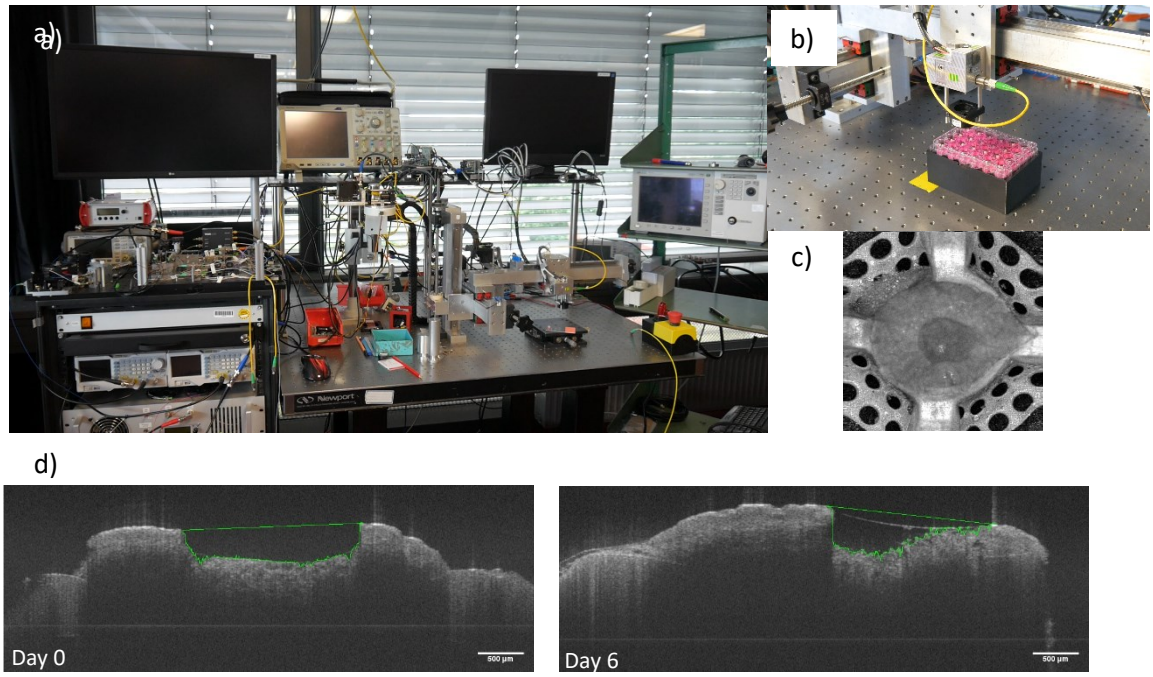

Figure 3.10: Optical coherence tomography in *ex vivo* wound healing
a) picture of the OCT system used for imaging the wounds and later calculating the wound volume b) picture of a 24-well-plate with *ex vivo* wounds beneath the stage, ready to be imaged c) exemplary top-view image reconstructed from the OCT-scans. c) exemplary cross sectional scans of the ex vivo wound at day 0 and 6. The green line is the segmentation algorithm, that calculates the wound volume. Scale bar = 500 µm. Pictures taken by Madita Göb, M.Sc..

3.2.5 Lactate dehydrogenase assay

The lactate dehydrogenase (LDH) assay allows the determination of LDH enzyme in the organ culture supernatant. As LDH is usually a cytosolic enzyme, a high LDH amount in the supernatant is a sign of damaged cells (Kabakov & Gabai, 2018).

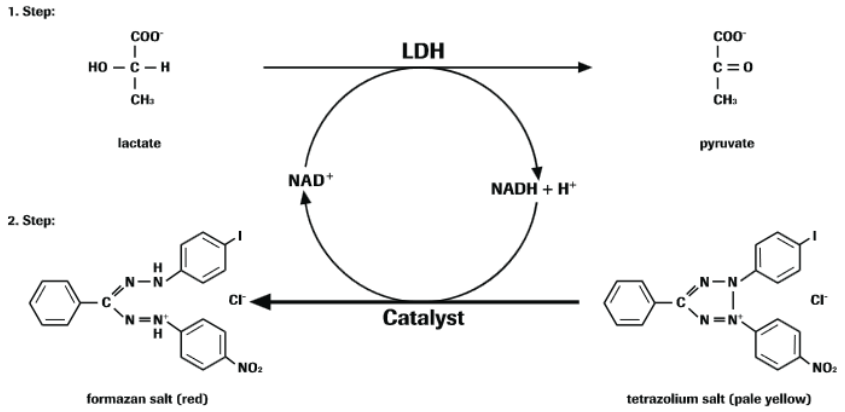

Figure 3.11: Principle of the lactate dehydrogenase assay
Damaged cells (also cells undergoing apoptosis) release lactate dehydrogenase (LDH), a cytosolic enzyme of all mammalian cells. LDH transforms lactate to pyruvate. During this process NAD^+ is reduced to NADH/ H^+. The generated proton is transferred by the catalysator to a tetrazolium salt which becomes formazan in the following process. While the tetrazolium salt is pale yellow, formazan is red.
Picture taken from:
https://www.sigmaaldrich.com/deepweb/assets/sigmaaldrich/product/documents/215/534/11644793001bul.pdf
(last time used December 29, 2022)

Figure 3.11 shows the basic principle of the LDH assay. For this assay, the Cytotoxicity detection kit from Roche was used. The assay was performed in a transparent 96-well-plate with a flat bottom. The LDH-release in the supernatant was measured in triplicates for all conditions tested. For the blank, 200 µL of culture medium were pipetted per well. 100 µL sample (supernatant) were pipetted into the respective wells. Next the reaction solution was prepared by mixing catalyst and dye solution in a 1:46 ratio. A 100 µL of the reaction solution was added to each sample well with the help of a multichannel pipette. Then, the plate was incubated for 30 minutes at room temperature (RT) protected from light, as the reaction solution is light sensitive. After incubation, the extinction was measured at 490 nm with the Glomax discovery plate reader. For evaluation, the mean of the triplicates was calculated. Then the mean of the blank was subtracted from the mean of the samples, thus obtaining the adjusted extinction. Those adjusted extinction values can now be compared among each other.

3.2.6 Cutting of paraffin embedded wounds

To obtain paraffin sections, the paraffin embedded samples needed to be cut with the help of a microtome. Therefore, the paraffin blocks must be cold. So, they were stored at -20 °C over night before cutting and on a -15 °C cooling plate during breaks in the cutting process. The paraffin block was placed into the holder of the microtome. By cranking the wheel, the holder with the sample will move down and sections get cut. First, the samples were trimmed at 20 µm until the edge of the wound was reached. To find the wound edge, sections were regularly checked with the help of a light microscope. At the wound edge, the microtome was adjusted to 4 µm cutting depth. A chain of sections was cut and transferred to a water bath at approximately 37 °C. Two sections each were transferred onto a microscope slide. Two microscope slides were taken at the wound edge (wound I). To get a better picture of how the wound healed, after the initial two slides, it was cut 60 µm deeper into the wound and two microscope slides were taken (wound II). This process was repeated twice more, so that in total 4 different wound depth (wound I-IV) could later be examined.
The microscope slides with the paraffin sections were dried over night at 37°C.

3.2.7 Cryosection cutting

The immunofluorescence (IF) stainings were performed on cryosections in humid chambers. To obtain cryosections, the skin punches embedded in Tissue Tek® were attached to a metal stamp, which was then fixed in the cryostat. The chamber temperature was set to -22 °C, the object table temperature to -20 °C. By cranking the wheel, the sample was trimmed (20 µm per section) until the wound edge was reached. As with paraffin cutting the sections were regularly checked by light microscopy if the wound edge was reached. At the wound edge 7 microscope slides with 2 6 µm thick sections each were taken (wound I). The block was trimmed 250 µm more, before another 7 slides with 2 sections each were taken (wound II). As more slides needed to be taken compared to paraffin, here slides were taken at only two wound sides, the edge and the middle (here wound II is taken at a similar depth as wound IV in paraffin cutting).
The cryosection cutting was done with the help of Sylva Bruhns.

3.2.8 Hematoxylin and eosin staining

The Hematoxylin and eosin (H&E) staining is a tissue overview staining and was performed on the cut and dried paraffin sections in the routine laboratory of the Dermatoloty of the University hospital Schleswig-Holstein campus Lübeck. After 20 minutes at 80 °C to drain excessive paraffin from the sections the slides were transferred into the Leica Autostainer XL, which performed the H&E staining

and embedding of the sections at RT automatically. Briefly, the slides were deparaffinated by incubation first in Xylol and then ethanol of decreasing concentration finishing in distilled water (compare **Table 3.18**).

Table 3.18: Descending alcohol series for hematoxylin and eosin staining

Chemicals	Staining duration
Xylol (1st cycle)	20 minutes
Xylol (2nd cycle)	Pivot briefly
Xylol (3rd cycle)	Pivot briefly
100 % Ethanol (1st cycle)	Until the sections are free of streaks
100 % Ethanol (2nd cycle)	Until the sections are free of streaks
96 % Ethanol	Until the sections are free of streaks
70 % Ethanol	Until the sections are free of streaks
Distilled water	Pivot briefly

The next step is the staining with hematoxylin by Papanicoulos for 5 minutes at RT. The sections were shortly washed with tap water to discard the staining solution. Next, the sections were briefly incubated in acetic acid/ethanol and then washed under running tap water until the foaming stopped. Thereafter, the sections were briefly incubated in ammonia water before they are thoroughly rinsed first under tap water and then using distilled water. Next, the sections were counterstained with eosin for 30-90 seconds (depending on the age of the staining solution). In the next step the slides were rehydrated by a row of increasing ethanol concentrations followed by xylol (compare **Table 2.19**).

Table 3.19: Ascending alcohol series for hematoxylin and eosin staining

Chemicals	Staining duration
96 % Ethanol	Until the sections are free of streaks
100 % Ethanol (1st cycle)	Until the sections are free of streaks
100 % Ethanol (2nd cycle)	Until the sections are free of streaks
Xylol (1st cycle)	1 minute
Xylol (2nd cycle)	1 minute
Xylol (3rd cycle)	1 minute

As a last step the slides are mounted and covered with the help of the covering machine.

3.2.9 Immunofluorescence staining

The basic principle of immunofluorescence applied here is as follows: the tissue cross section is first incubated with an antibody that is directed against a protein of interest and comes from a different species than the tissue that is stained, e.g. a mouse-antibody that recognizes a human target protein, this antibody is called the “primary antibody”. After the primary antibody bound its target protein, a so called “secondary antibody” is added. This antibody comes from a different species than the stained tissue and the primary antibody and recognizes the Fc-part of the primary antibody, e.g. a goat-anti mouse antibody. To the secondary antibody a fluorescent dye is attached, allowing to visualize the binding of the primary antibody and thus the expression of the protein of interest with a fluorescence microscope. To avoid unspecific binding of the secondary antibody to the stained tissue, it must be preincubated with serum from the species of the secondary antibody (normal goat serum in this case) before incubation with any antibody.

IF provides a deeper insight into the processes of wound healing. In this thesis, four IF stainings were performed against the following targets:

- Cytokeratin (CK) 6, a marker of hyperproliferative tissue and thereby wound healing. Uninjured, adult human skin does not express CK 6 (Freedberg *et al.*, 2001; Groh & Magin, 2023).
- Cluster of differentiation 31 (CD31) or platelet endothelial cell adhesion molecule-1 (PECAM-1), a protein expressed among others in endothelial cells thus allowing conclusions about angiogenesis during the WHOC (Xie & Muller, 1996).
- Cortactin, a cytoplasmic protein that upon activation promotes reorganization of the actin cytoskeleton and is important in migration of cells (Ammer & Weed, 2008).
- KiTUNEL: in this double staining Ki67 is a marker for proliferative cells and TUNEL (Terminal deoxynucleotidyl transferase dUTP nick end labeling) denotes an enzymatic staining visualizing apoptotic cells (Dmitrieva & Burg, 2007; Scholzen & Gerdes, 2000).

3.2.9.1 CK 6 immunofluorescence staining

For the CK 6 IF staining the slides were dried for 10 minutes at RT, fixed in acetone for 10 minutes at -20 °C and washed twice with phosphate buffered saline (PBS) for 5 minutes each at RT. After encircling the sections with a fat pen, they were preincubated with 10% normal goat serum (NGS) in PBS for 20 minutes. Next the sections were incubated with the mouse anti-human CK 6 antibody (clone Ks6.KA12) in a 1:300 dilution in PBS and 2 % NGS at 4 °C over night. For the control of unspecific binding of the secondary antibody one section per microscope slide was incubated with just 2 % NGS in PBS at 4 °C over night. The next day, the slides were washed three times with PBS for 5 minutes each bevor the sections were incubated with a goat anti-mouse immunoglobulin G (IgG) antibody coupled with Alexa Fluor Plus 488 at a 1:200 dilution in PBS and 2% NGS for 45 minutes at RT. The slides were washed three more times with PBS for 5 minutes each. Then, the sections were mounted with DAPI Fluoromount-G and covered with a cover slip. After an hour of drying at RT, the slides were stored at -20 °C until IF microscopy.

The CK 6 immunofluorescence staining was performed with the assistance of Luna Gao, Cand. B.Sc.

3.2.9.2 CD31/PECAM-1 Immunofluorescence staining

For the CD31-IF the slides were dried for 10 minutes at RT and fixed in acetone for 10 minutes at -20 °C. After letting the slides dry for another 10 minutes at RT the sections were circled with a fat pen. Next the slides were washed three times for 5 minutes each with Tris(hydroxymethyl)aminomethane (TRIS)-buffered saline (TBS). Then the slides were preincubated with 10% NGS in TBS for 20 min before they were incubated with the primary monoclonal mouse anti-human PECAM-1/ CD31 antibody (clone MO823) at a 1:00 dilution and 2 % NGS at 4 °C over night. For the control of unspecific binding of the secondary antibody one section per slide was incubated with just 2 % NGS in TBS. The next day the slides were washed three times with TBS 5 minutes each. Then, the sections were incubated with the secondary rhodamine red coupled goat anti-mouse IgG (H+L) antibody at a 1:200 dilution in TBS supplemented with 2 % NGS. After incubation with the secondary antibody, the slides were washed again three times with TBS each. Finally, the sections were mounted with DAPI Fluoromount-G, covered with a cover slip, dried for an hour at RT and then stored at -20 °C until immunofluorescence.

The CD31 immunofluorescence staining was performed with the assistance of Mareike Otto, M. Sc.

3.2.9.3 Cortactin immunofluorescence staining

For the cortactin IF, the slides were dried for 10 minutes at RT, before fixation in acetone for 10 minutes at -20 °C. After another drying step for 10 minutes at RT, the sections were encircled with a fat pen. Following, the slides were washed for three times for 5 minutes each with TBS. Next, the sections were preincubated with 10 % NGS in TBS for 20 minutes at RT. Then the sections were incubated with the primary monoclonal mouse anti-human cortactin antibody (clone 771716) at a 1:100 dilution supplemented with 2 % NGS in TBS at 4 °C over night. The control of unspecific binding of the secondary antibody was incubated just with 2% NGS in TBS at 4 °C over night. After the incubation, the slides were washed again three times 5 min each with TBS. Then, the sections were incubated with the secondary goat-anti mouse IgG (H+L) antibody at a 1:200 dilution in TBS supplemented with 2% NGS for 45°minutes at RT. Next, the slides were washed three more times for 5°minutes each with TBS before mounted with DAPI and covered with cover slips. After drying for an hour, the slides were stored at -20 °C until microscopy.

3.2.9.4 KiTUNEL immunofluorescence staining

The KiTUNEL IF is a double staining utilizing the ApopTag® Fluorescein in situ apoptosis detection kit and combines it with a Ki67 IF staining.

While the Ki67 IF staining is a “normal” IF staining as described above, the TUNEL staining is based on a different principle: Here, the terminal deoxynucleotidyl transferase (TdT)-enzyme and its ability to add nucleotides to the 3’ OH termini of DNA double strand breaks or otherwise damaged DNA with free 3’ OH ends. The TdT-enzyme is added to the tissue cross section together with digoxigenin-labeled nucleotides and incorporates those nucleotides onto free 3’ OH ends. In a second step, a fluorescence-labeled anti-digoxigenin antibody is added, enabling the visualization of DNA double strand breaks or other DNA damage under the fluorescence microscope and thus showing apoptotic or otherwise damaged cells (Dmitrieva & Burg, 2007).

The process of the KiTUNEL staining is explained in the following: First, the slides were dried at RT for 5 minutes, following fixation in 1% formaldehyde for 10 minutes at RT. After 3 washes of 5 minutes each with PBS, the sections were post-fixated in ethanol-acetic acid (in a 2:1 ratio). Next, the slides were washed 3 more times with PBS for 5 minutes each. Then the sections were encircled with a fat pen marker. After 5 minutes incubation with the equilibrium buffer at RT, the slides were incubated with the TdT-enzyme solution for 60 min at 37°C. The control sections of unspecific binding of the secondary antibody were incubated with reaction buffer only. The enzymatic reaction was stopped by putting the slides into the stop-buffer solution for 10 minutes at 37 °C. Next, the sections were washed 3 times with PBS for 5 minutes each, followed by preincubation with 10 % NGS for 20 minutes at RT. To detect the expression of Ki67+ cells, the sections were then incubated with the primary monoclonal mouse-anti human Ki67 antibody (clone MIB-1) in a 1:20 dilution in PBS supplemented with 2 % NGS at 4 °C overnight. The control sections of unspecific binding of the secondary antibody were incubated with just 2 % NGS in PBS. The next day the slides were washed 3 times for 5 minutes with PBS at RT. Following was the incubation with the first secondary antibody, which visualizes the TdT-enzyme reaction. This fluorescein-labelled anti-digoxigenin antibody solution consisted out of 48.7 % blocking solution and 51.3 % of the antibody solution. The sections were incubated for 30 min at RT. Then the slides were washed again 3 times for 5 minutes each at RT with PBS. Next the sections were incubated with the second secondary antibody visualizing Ki67: goat anti-mouse-IgG antibody coupled to Rhodamine Red. This antibody was used in a 1:200 dilution in PBS supplemented with 2 % NGS. The sections were incubated for 45 min at RT. The slides were washed 3 more times for 5 minutes each with PBS, before they were mounted with DAPI Fluoromount-G. After drying for an hour at RT the slides were stored at -20°C until immunofluorescence microscopy.

3.2.10 Microscopy of hematoxylin and eosin-stained wounds

H&E slides were imaged using the light microscope module of the Keyence BZ 9000. The cross sections of the respective wound were imaged at 100x magnification. If the wound was larger than one visual field (VF) at this magnification, more than one picture was taken without overlap so that the entire wound was depicted. For evaluation of the newly formed epithelial tongues (ETs), the inner and outer ETs were imaged at 200x magnification. The term “inner ETs” refers to the newly formed epidermis within the wound, while “outer ETs” means the ETs at the edges of the 4 mm biopsy punch, as illustrated in **Figure 3.12**. Again, for large ETs more than one picture had to be taken without overlap.

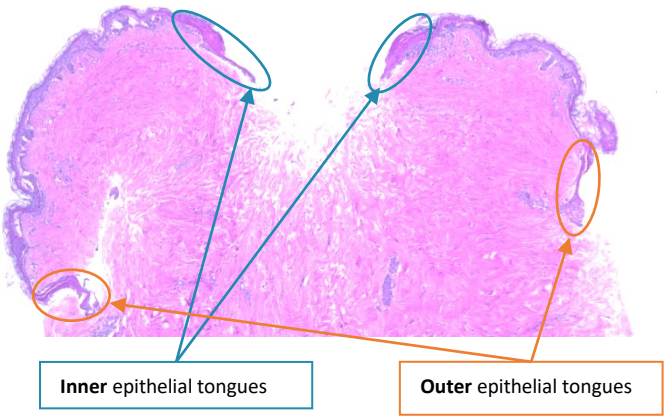

Figure 3.12: Epithelial tongues of a wounded skin biopsy
Picture of an exemplary H&E stained section to show where the inner and outer epithelial tongues are.

3.2.11 Microscopy of the immunofluorescence stainings

This chapter explains how the different IF stainings were imaged at the Keyence BZ 9000.

3.2.11.1 Microscopy of the cytokeratin 6 immunofluorescence staining

200x magnification pictures were taken of the outer and inner epithelial tongues.

3.2.11.2 Microscopy of the CD 31 immunofluorescence staining

As CD 31 is a marker of endothelial cells (Xie & Muller, 1996) and the epidermis is not perfused (Fritsch & Schwarz, 2018), for this IF staining the dermis was of special interest. Hence, four pictures of the dermis were taken: on the left side next to the wound, on the right side next to the wound, lower left side of the dermis and lower right side of the dermis. **Figure 3.13** illustrates this as well as shows examples of cross sections and vessel cuts. If the skin sample was too small, only three pictures were taken.

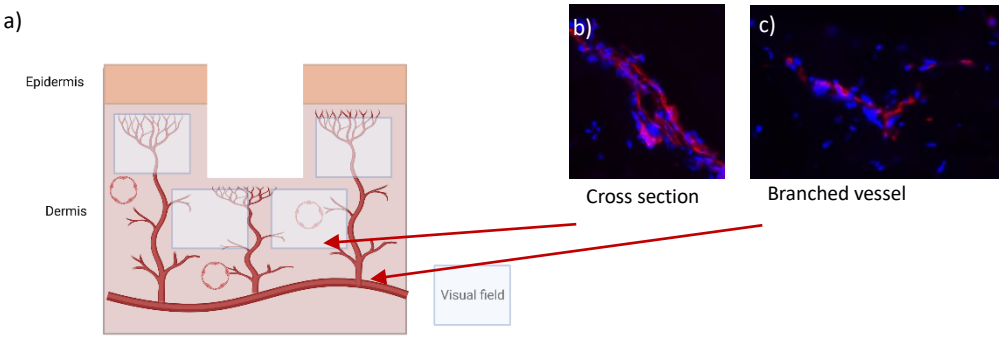

Figure 3.13: Evaluation of CD31 immunofluorescence staining
a) Schematic illustration (created with Biorender.com) of a wound cross section and where in the dermis pictures for further evaluation were taken. Exemplary picture of a CD31 stained b) cross section and c) branched vessels

3.2.11.3 Microscopy of the Cortactin immunofluorescence staining

Representative, qualitative pictures of the epithelial tongues were taken at 200x magnification.

3.2.11.4 Microscopy of the KiTUNEL immunofluorescence staining

Pictures of the inner and outer ETs were taken at 200x magnification.

3.2.12 Evaluation of the wound healing parameters of the wound healing organ culture

This chapter illustrates how the different microscopy pictures were evaluated.

3.2.12.1 Evaluation of the top-view wound area and top-view wound perimeter

During the course of the WHOC top-view pictures were taken of the wounds at day 0 (start of the culture), 2, 4, 6 and 7 or 8 (depending on when the culture was terminated). These pictures allow the measurement of the top-view wound area (compare **Figure 3.14a**) and perimeter (**Figure 3.14b**). Depending on the rigidity of the skin (e.g. breast skin is much softer than abdominal skin) the size of the wounds at day 0 could vary quite a bit. To adjust for this the relative top-view wound area and perimeter to day 0 were calculated respectively and compared among the cultures instead of using absolute values. During the culturing the skin loses some of its rigor and can become tilted or collapsed. Strongly tilted or collapsed samples were excluded from the evaluation process, because they would distort the results.

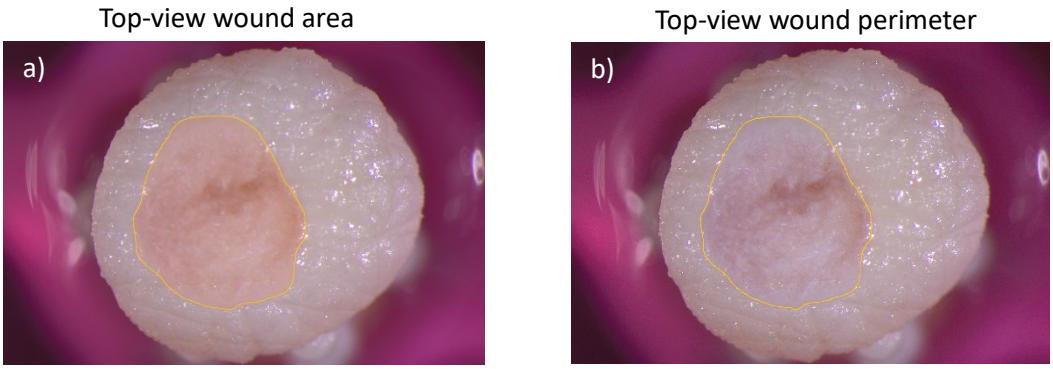

Figure 3.14: Top-view wound area and perimeter
Shown here is an exemplary top-view picture of a wound at day 0 (start of culture) to illustrate the a) top-view wound area (transparent orange area) and b) top-view wound perimeter (orange line circling the wound).

Next to the top-view wound area, seen when looking at the wounds from above, there is also wound area visible when cutting the wound open and looking at the cross section. **Figure 3.15** illustrates the difference between these two kinds of wound areas.

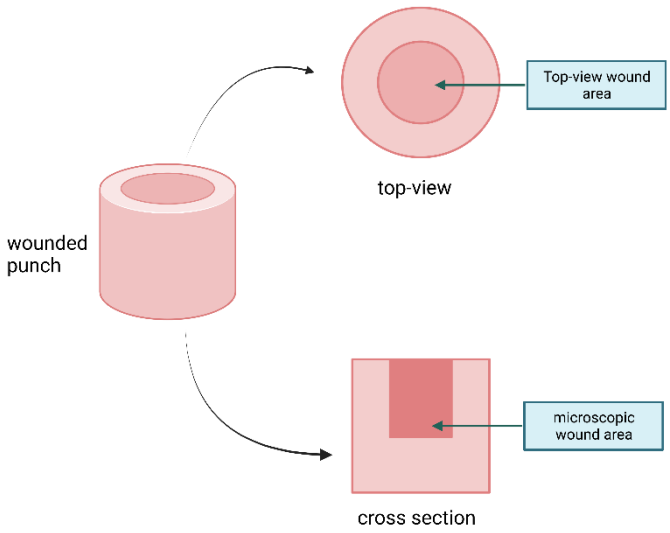

Figure 3.15: The difference between top-view and microscopic wound area
Shown here is a schematic drawing of a wounded biopsy punch. During the culture it is only possible to look onto the wound from above by top-view microscopy. The wound area visible in this way is referred to as top-view wound area. After the actual culture is over, the wounded biopsy punches can be embedded, cut, and stained. This allows the assessment of the cross section of wounds, the so called microscopic wound area.
Created with Biorender.

2.2.12.2 Evaluation of hematoxylin and eosin stained wounds

Evaluation was done using Fiji Image J. **Figure 3.16** shows the evaluated parameters of the H&E staining. The microscopic wound area was determined with the help of the polygon tool of Fiji Image J (**Figure 3.16a**). The wound diameter was defined as the distance of the beginning of the ETs on the top of the wound (**Figure 3.16b**). It was measured using the segmented line tool of Fiji Image J. ETs could easily be recognized by missing the upper most skin layer, the *Stratum corneum.* As the differentiation process of keratinocytes from the *Stratum basale* up to the *Stratum corneum* takes 4 weeks (Fritsch & Schwarz, 2018; Röcken *et al.*, 2010), the newly formed tissue in our one-week

WHOC could not yet have *Stratum corneum.* The end of the ETs was defined as a line perpendicular to the *Stratum corneum*. The area of the ETs was determined using the polygon tool of Fiji Image J (**Figure 3.16c**). The length of the ETs was measured with the segmented line tool of Fiji Image J along the basal membrane of the newly formed epidermis (**Figure 3.16d**).

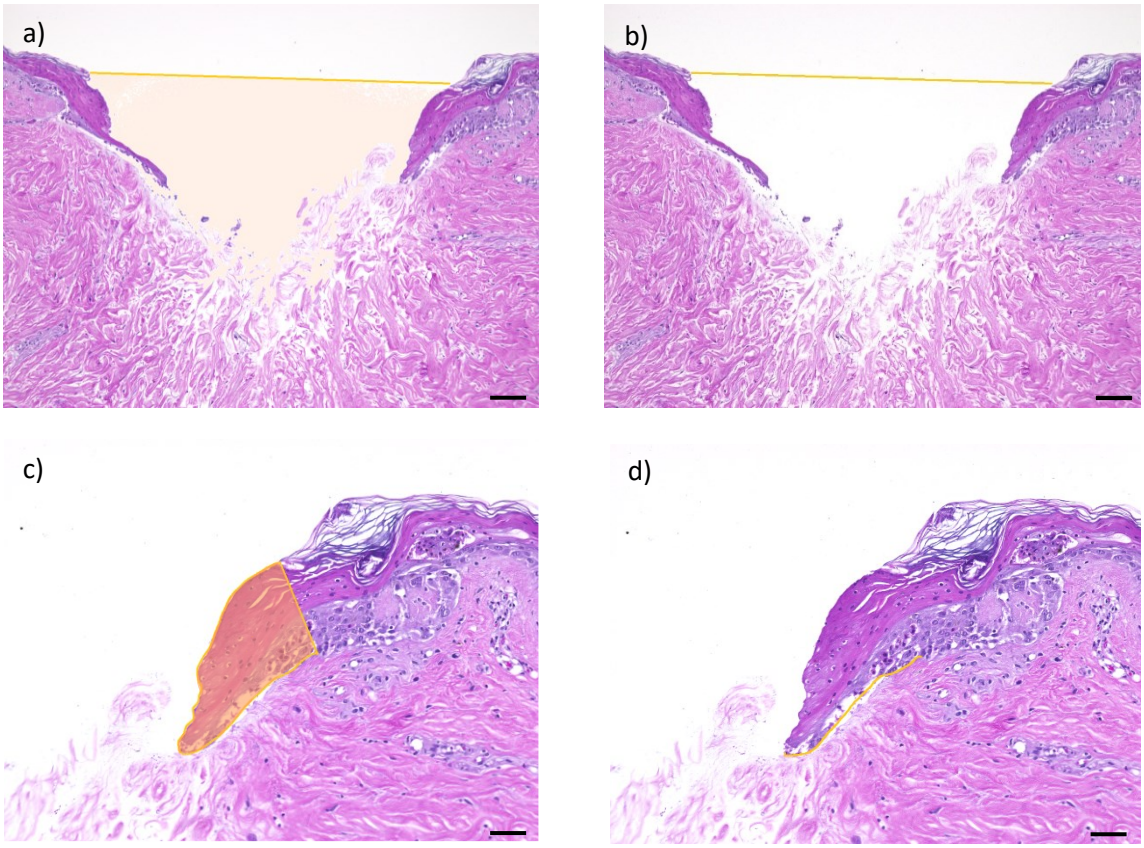

Figure 3.16: Evaluation of hematoxylin & eosin staining of wounds
Shown here are exemplary pictures of a hematoxylin & eosin stained wound (40x) and epithelial tongue (ET, 200x)) at day 7 (end of culture) and how different parameters are measured. a) microscopic wound area b) microscopic wound diameter, scale bar = 100 µm c) area of the epithelial tongue d) length of epithelial tongue, scale bar = 50 µm

3.2.12.3 Evaluation of the cytokeratin 6 expression

With the polygon tool of Fiji Image J the ETs were selected and their mean fluorescence intensity was measured in the green channel. **Figure 3.17** shows an exemplary picture of this.

As the intensity of an IF staining differs strongly between different repetitions, the intensity of each culture was normalized on the treatment control (0.1 % DMSO). This way the data of different WHOCs could be compared and summed up in one graph, allowing a statistical evaluation.

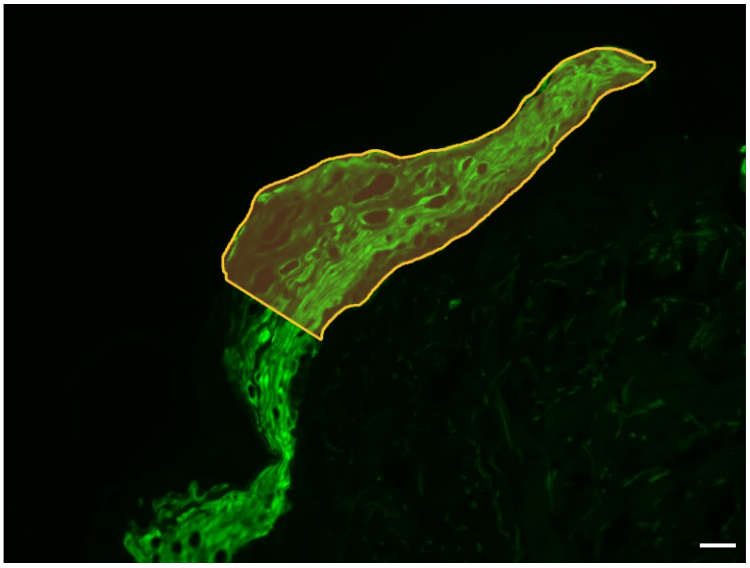

Figure 3.17: Illustration of the measurement of the cytokeratin 6 intensity in the epithelial tongues
The transparent orange area shows the area of the ET measured. Picture taken at 200x magnification. Scale bar = 50 µm

2.2.12.4 Evaluation of the CD31 expression

For CD31 evaluation four different parameters were measured with the help of Fiji Image J: the mean intensity, the number of CD31 positive cells, the number of CD31 positive cross sections and the numbers of CD31 positive branched vessels. **Figure 3.13** shows exemplary pictures of a cross section (b) and a branched vessel (c). For all pictures the mean intensity of the entire VF in the red channel was measured. Again, this data was normalized on the solvent control, allowing the comparison of different WHOCs. Then the number of CD31 positive cells was counted, as well as the number of positive cross sections and vessels. A cross section showed as circles of positive cells, while a branched vessel could be recognized by its Y-shaped form.

2.2.12.5 Evaluation of the KiTUNEL staining

With the help of Fiji Image J the number of Ki67 positive cells, TUNEL, and DAPI positive cells was counted in the inner and outer ETs. Then the percentage of Ki67 positive cells or TUNEL positive cells of all cells (= DAPI positive cells) was calculated.

2.2.14 Statistics

Statistics were performed using the GraphPad prism 9.5.0 software. Sample groups were tested for outliers by using the Grubbs' outlier test (https://www.graphpad.com/quickcalcs/grubbs1/, last time used July 23, 2023) and for normal (Gaussian) distribution using the Shapiro-Wilk test. Normal distributed data was analyzed by a one-way ANOVA followed by Turkey's multiple comparisons test for more than 2 groups or an unpaired t-test for two groups. Not normally distributed data was analyzed by a Kruskal-Wallis test followed by Dunn's multiple comparisons test for more than two groups or a Mann-Whitney test otherwise. Data was considered significant if the p-value was below 0.05.

* = $p < 0.05$, ** = $p < 0.01$, *** = $p < 0.001$, **** = $p < 0.0001$

4 Results

4.1 Characterization of the course of the wound healing organ culture model

In this chapter, *ex vivo* wound healing over the course of the WHOC model is characterized, to understand how the wounds heal over time and how the different parameters for evaluation change during the WHOC. Therefore, untreated wounds were cultured for 7 days and samples were taken for further analysis at day 0 (directly after wounding and before the culture began), 2, 4, 6 and 7 (end of the culture). This allowed the evaluation of the top-view and microscopic wound healing as well as the expression of different markers relevant for wound healing over the course of the entire WHOC.

4.1.1 The top-view wound area and top-view wound perimeter decrease significantly over the course of the wound healing organ culture

Figure 4.1 displays the evaluation of the top-view wound healing over the course of the culture. In the exemplary pictures (**Figure 4.1a**) it becomes clear that the wounds get smaller from day 0 to day 7, though at the end of the culture the difference between day 6 and day 7 is hard to distinguish by bare eye.

Measurement of the relative top-view wound area (**Figure 4.1b**) and perimeter (**Figure 4.1c**) confirmed this observation. Starting from day 2 all measured areas and perimeters were significantly smaller than those at day 0 and became smaller from measurement point to measurement point except for day 6 to day 7. Here, a small increase is detectable. At day 2, the relative top-view wound area was 68.42 %. It decreased significantly to 51.54 % at day 4 and further to 44.33 % at day 6, both with a significance level of $p < 0.0001$. The relative top-view wound area at day 7 was 46.40 % and thus slightly higher than the area at day 6, but still significantly lower than the relative top-view wound area at day 0 with a significance level of $p < 0.0001$. The relative top-view wound perimeter was 87.46 % at day 2 and decreased to 76.83 % at day 4 and 69.07 % at day 6, both with a significance level of $p < 0.0001$.
Just like the relative top-view wound area, the relative top-view wound perimeter is higher at day 7 with 71.03 % than at day 6, but still significantly smaller than the perimeter at day 0 ($p < 0.0001$). The small increase from day 6 to day 7 might be due to the relatively high variation between the samples from the different donors. The relative top-view wound perimeter of day 4, 6, and 7 were also significantly smaller than the area at day 2 with a significance level of $p < 0.001$ for day 4 and 7 and $p < 0.0001$ for day 6. The same is true for the relative top-view wound perimeter. The relative top-view wound perimeter at day 4 is significantly smaller than that of day 2 with a significance level of $p < 0.01$, the perimeter of day 6 is significantly smaller than that of day 2 with a significance level of 0.0001 and the difference between day 2 and day 7 is significant with a significance level of $p < 0.001$. So, clearly the wounds heal well over the course of the WHOC.
Unfortunately, the OCT system was not available for measurements.

a)

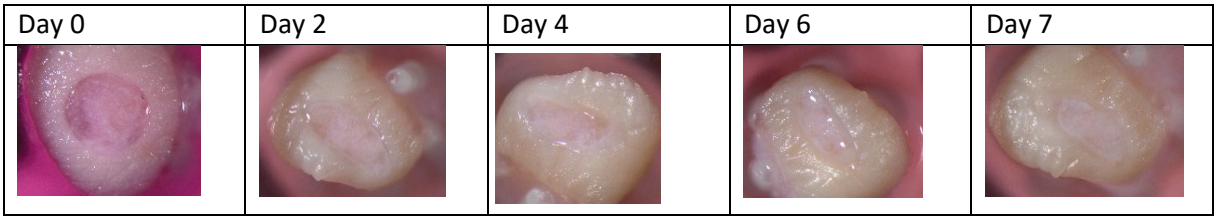

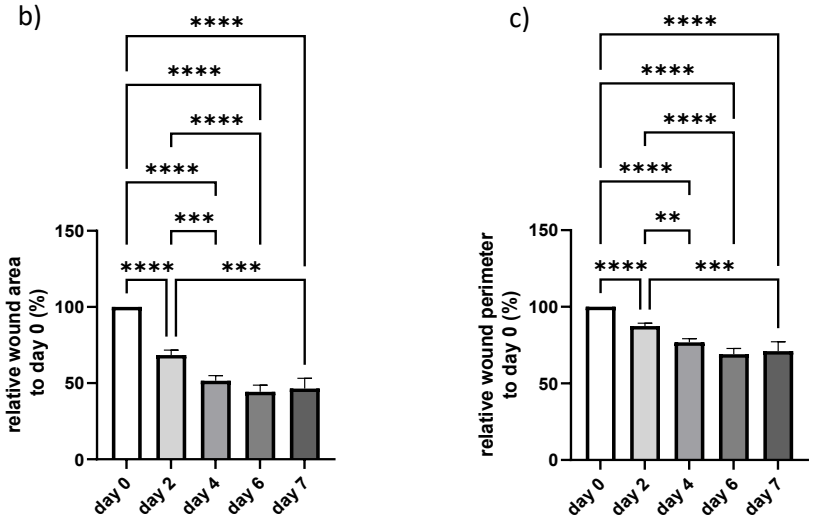

Figure 4.1: Top-view characterization of the wound healing process in the wound healing organ culture model
a) Exemplary top-view microscopic pictures during the wound healing organ culture. Relative top-view b) wound area and c) perimeter to day 0 throughout the wound healing organ culture. n = 4 (1-4 wounds/day). Data is depicted as mean + standard error of the mean. Significances were determined by one-way ANOVA followed by Turkey's multiple comparisons test.
** p < 0.01, *** p < 0.001, **** p < 0.0001

4.1.2 The microscopic wound area decreased significantly over the course of the wound healing organ culture while the area and length of the epithelial tongues increased significantly

Next to the top-view wound healing, also the microscopic wound healing was investigated. **Figure 4.2** shows the microscopic wound area and diameter as well as the area and length of the ETs. When examining the microscopic cross sections of the wounds in the exemplary pictures in **Figure 4.2a**, it is noticeable, that at day 0 the wounds still have a very sharp border, where the wound was punched and cut out. Over the course of the WHOC the new dermis begins to form as granulation tissue, a less dense, ragged looking dermal tissue. Moreover, at the beginning of the WHOC the epidermis ended sharply at the wound edge, not yet displaying any sort of newly formed epithelial tongues (ETs). Over the course of the culture, ETs grew continuously with the aim of closing the skin defect.

The microscopic wound area is shown in **Figure 4.2b**. The wounds started with a mean microscopic area of 570,976 µm^2 at day 0. The microscopic wound areas of day 4, 6, and 7 were significantly smaller than that at the beginning of the culture. At day 2 it was 371,649 µm^2 and further decreased to its minimum of 112,744 µm^2 at day 4. The difference between day 0 and day 4 was significant with a significance level of $p < 0.001$. The microscopic wound area at day 6 was 188,011 µm^2 and at day 7 it is 186,245 µm^2. Both areas were significantly smaller than that of day 0 ($p < 0.001$ for both days). While it was expected that the wounds become smaller over the course of the culture, it is surprising

that the microscopic wound area was smallest at day 4. It was significantly smaller than the area at day 2 with a significance level of $p < 0.05$ but also smaller than the microscopic wound area measured at day 6 and 7.
For the microscopic wound diameter, the picture was not as clear as it was for the top-view evaluation or the microscopic wound area (compare **Figure 4.2c**). All effects observed were not significant. The wound diameter was smallest at the beginning of the WHOC with a value of 1,287.11 µm. The wound diameter was largest at day 2 with 1,922.16 µm and decreased from day 4 (1,642.67 µm) to day 6 (1,385.1 µm), while an increase to 1,757.81 µm was observed at day 7.

Next, the area and length of the newly formed ETs was investigated. The results can be found in **Figure 4.2d-k**. **Figure 4.2a** shows exemplary pictures of the ETs. As expected, there were no ETs at day 0, because the skin was just wounded, and no formation of new epidermis could have taken place. Starting at day 2 the ETs were clearly visible. ETs are distinguishable from the rest of the skin because they do not yet have a *stratum corneum,* which appears as the dark purple, uppermost, cell-free layer in the H&E staining. The area and length of the ETs were measured and compared amongst each other. The ETs were further divided into different groups: the ETs growing in the actual wound, in this work referred to as "inner ETs", the "outer ETs" growing on the outside of the 4 mm biopsy punch and the inner and outer ETs combined to the "total ETs". Moreover, the area and length of the inner ETs were normalized on their respective wound diameter. This normalization was performed to correct for observed partly huge differences in the wound diameter between different samples. **Figures 4.2d-g** show the area of the ETs. The areas of all ETs investigated here show a very similar trend. They generally grow over the course of the culture.
Figure 4.2d shows the areas of the inner ETs. Over the course of the WHOC the area of the inner ETs grew steadily from 0 μm^2 at day 0 to 11,388.70 μm^2 at day 2, to 17,782.90 μm^2 at day 4, 32,230.00 μm^2 at day 6 and finally to 4,514.60 μm^2 at day 7. The difference between day 0 and all other days of the culture was significant. At day 2 the area of the inner ETs was significantly higher than that of day 0 with a significance level of $p < 0.001$, for day 4, 6, and 7 the significance level was $p < 0.0001$. The differences in inner ETs' area between day 2 and day 6 and day 2 and day 7 were also significant with a significance level of $p < 0.0001$ for day 6 and $p < 0.001$ for day 7 respectively. The difference in the inner ETs' area between day 4 and day 7 was also significant with a level of significance of $p < 0.01$.
As shown in **Figure 4.2g** normalization of the inner ETs' area did not change the trend described above. Normalized inner ETs show a steady increase from 0 µm at day 0 over the course of the culture to finally 28.25 µm at day 7. The difference between day 0 and all other days is significant with a significance level of $p < 0.01$ for day 2 and $p < 0.0001$ for all other days. The normalized area of the inner ETs at day 6 and day 7 is significantly larger than the area at day 2 with a significance level of $p < 0.001$ for day 6 and $p < 0.0001$ for day 7.
The area of the outer ETs can be found in **Figure 4.2e**. Here the area increases from 0 μm^2 over 8,112.38 μm^2 at day 2 and 16,586.20 μm^2 at day 4 to its maximum of 21,304.20 μm^2 at day 6. At day 7 the area of the outer ETs was 20,466.00 μm^2. Just like the inner area, the difference between day 0 and the other days of the culture is significant with a significance level of $p < 0.01$ for day 2 and $p < 0.0001$ for the remaining days. Also, the differences in the areas of outer ETs at day 2 and day 6 was significant with a significance level of $p < 0.01$.
The inner and outer ETs' area combined as the area of the total ETs can be seen in **Figure 4.2f**. Here, also the area increased from 0 μm^2 steadily to a final value of 32,171.70 μm^2 at day 7. As before the areas of day 2, 4, 6, and 7 were significantly larger than that of day 0 with a significance level of $p < 0.0001$ for all groups. In the total ETs the areas of day 6 and 7 were significantly larger than that of

day 2 with a level of significance of $p < 0.0001$. Moreover, the area of the total ETs at day 7 was significantly larger than their area at day 4 ($p < 0.05$).

The length of the ETs is shown in **Figure 4.2h-k**. The length of the inner ETs increased from 0 µm at day 0 to 214.88 µm at day 2 and to 258.79 µm at day 4. The longest ETs were observed at day 6 with a length of 416.49 µm. At day 7 the inner ETs were 416.16 µm long. It is noticeable that the increase in length of the was not linear. The increase in length from day 0 to day 2 was rather large with 214.88 µm while the difference between day 2 and day 4 was only 44.91 µm. The increase to day 6 was larger again with 157.7 µm and the ETs at day 7 were almost identical in length to day 6. From day 2 on all ETs are significantly larger than the (non-existent) ETs at day 0 with a significance level of $p < 0.0001$. The ETs at day 6 and 7 were also significantly larger than those at day 2 with a significance level of $p < 0.0001$ for both days. Moreover, the ETs at day 6 and day 7 were significantly longer than the ETs at day 4 ($p < 0.001$ for both).
The normalized inner ETs (compare **Figure 4.2k**) showed a continuous increase in length from 0 to 0.30 at day 7. From day 2 on the increase in length was significant to day 0 with a significance level of $p < 0.001$ for day 2 and $p < 0.0001$ for day 4, 6, and 7. Furthermore, the ETs were significantly longer at day 6 and 7 than at day 2 ($p < 0.05$ for day 6 and $p < 0.01$ for day 7).
The length of outer ETs (compare **Figure 4.2i**) increased over the course of the WHOC form 0 µm at day 0 to a maximum length of 268.49 µm at day 6. At day 7, the outer ETs were 247.67 µm long. From day 2 on, the increase in outer ETs' length was significant to day 0 for all days with a significance level of $p < 0.0001$. While there again was a strong increase from day 0 to day 2 (by 196.99 µm), the "growth spurt" from day 4 to day 6 as with the inner ETs could not be found. Overall, the outer ETs were shorter than the inner ETS.
The length of the total ETs in **Figure 4.2j** showed the same tendencies as inner and outer ETs. From day 2 on the length of the ETs increased significantly compared to day 0 ($p < 0.0001$). Their maximum length of 341.70 µm was reached at day 6. At day 7 the total ETs were 326.11 µm long. The ETs on day 6 and day 7 were significantly longer than the ETs at day 2 ($p < 0.05$ for both).
The top view and microscopic evaluation clearly showed that the wounds heal properly over the course of the WHOC.

a)

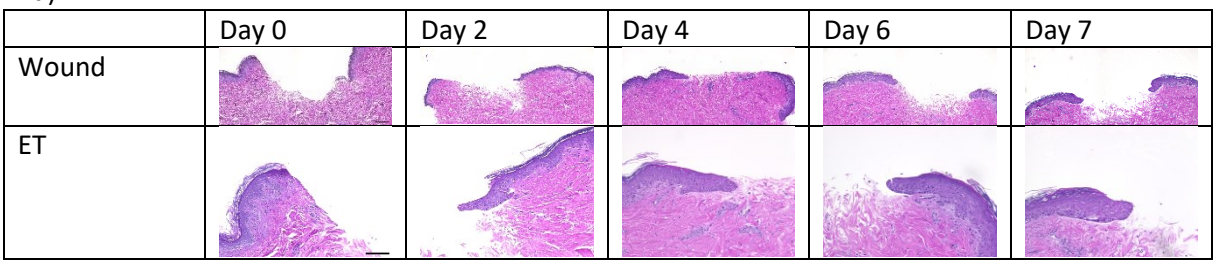

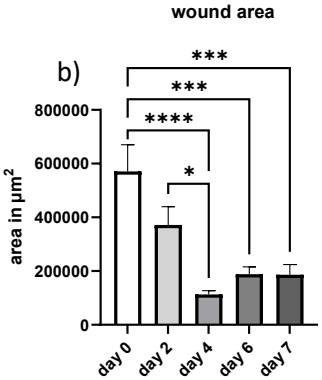

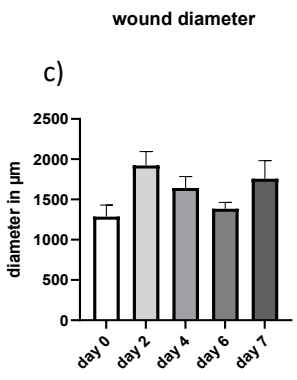

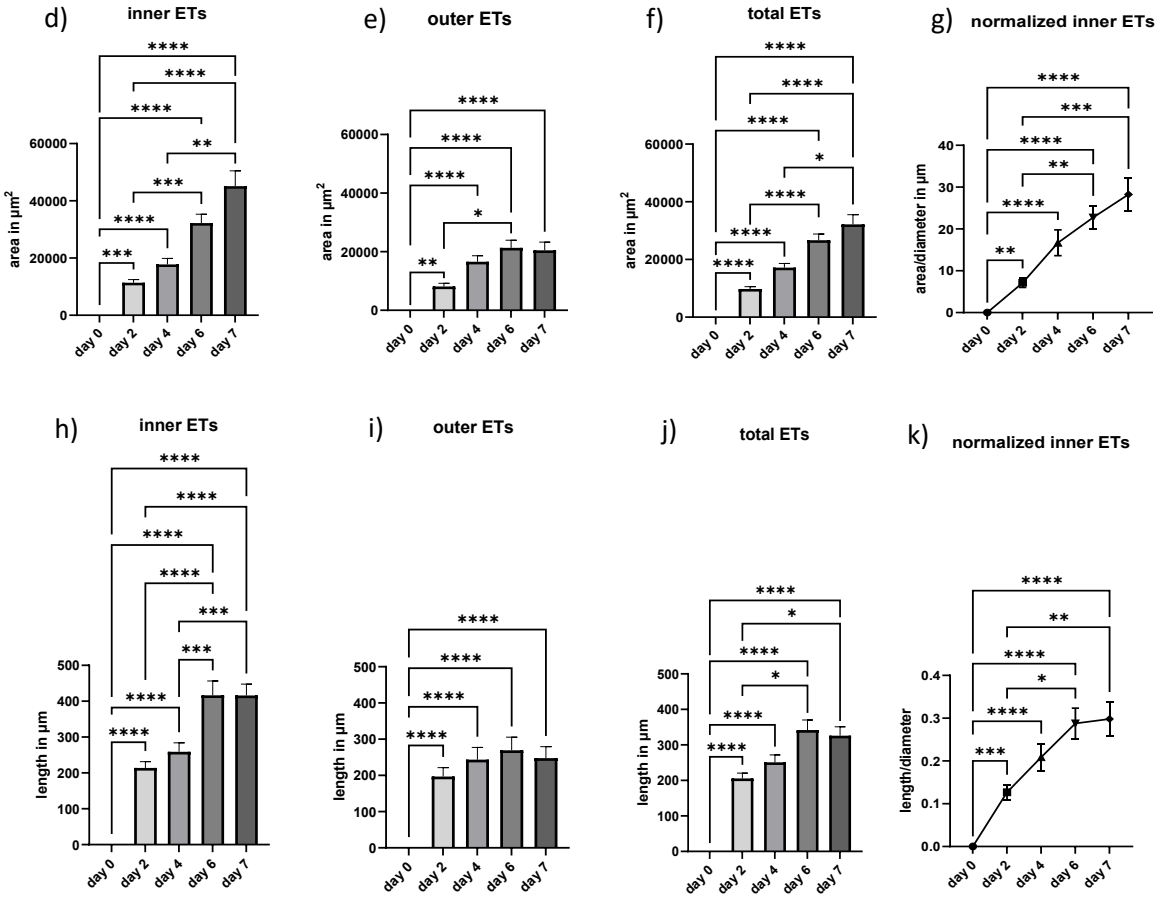

Figure 4.2: Characterization of the microscopic wound healing in the wound healing organ culture model a) Exemplary hematoxylin & eosin microscopy pictures of the wounds (scale bar= 200 µm) and epithelial tongues (ETs, scale bar = 100 µm) during the wound healing organ culture. b) Microscopic wound area, c) microscopic wound diameter, for both n = 4 (1-4 wounds/day), d) area of the inner ETs, e) area of the outer ETs, f) area of the total ETs (inner and outer ETs combined), g) area of the inner ETs normalized on their respective wound diameter, h) length of the inner ETs, i) length of the outer ETs, j) length of the total ETs, k) length of the inner ETs normalized on their respective wound diameter, for all ET measurements n = 4, 8-16 ETs/day. Data is depicted as mean + standard error of the mean. Significances were determined by one-way Annova followed by Turkey's multiple comparisons test (microscopic area and diameter, length of the inner ETs) or Kruskal-Wallis test followed by Dunn's multiple comparisons test (all other ETs evaluation). * $p < 0.05$, ** $p < 0.01$, *** $p < 0.001$, **** $p < 0.0001$

4.1.3 The relative cytokeratin 6 expression increased over the course of the wound healing organ culture

Next, the CK 6 expression in the ETs was investigated. The results can be found in **Figure 4.4**. As CK 6 is not expressed in unwounded skin and the samples from day 0 were embedded for cryo-sectioning and staining directly after wounding, there was no CK 6 expression observable at day 0, as visible in **Figure 4.3a**. The little fluorescence intensity measured on day 0 was auto-fluorescence from the epidermis. To be able to compare the CK 6 expression of different cultures, the values measured at day 0 were set to 100 %.

Figure 4.3b shows the relative CK 6 expression in the inner ETs, which increases strongly from day 0 to 531.4 % at day 2, and 814.66 % at day 4. It reaches it maximum of 861.46 % at day 6. At day 7 the relative CK 6 expression decreases to 710.34 %. At day 4, 6, and 7 the relative expression of CK 6 is significantly higher than it is at day 0 ($p < 0.01$ for day 4 and day 6, $p < 0.05$ at day 7).

The relative CK 6 expression of the outer ETs is depicted in **Figure 4.3c**. Again, a rapid increase in relative CK 6 expression is visible from day 0 to 674.80 % at day 2 but here the maximal CK 6 expression is reached at day 4 with 784.07 %. At day 6 the CK 6 expression is 726.33 % and thus lower at than at day 4. A slight increase in the relative CK 6 expression can be observed from day 6 to day 7, where the expression is 741.07 %. The relative CK 6 expression is significantly higher at day 2, 4, 6, and 7 compared to day 0 ($p < 0.05$).

Just like the outer ETs, the relative CK 6 expression in the total ETs increases from day 0 to 798.87 % at day 4 (compare **Figure 4.3d**). The relative CK 6 expression then decreases to 788.80 % at day 6 and 725.70 % at day 7. From day 2 on the CK 6 expression is significantly higher than it is at day 0 with a significance level of $p < 0.05$ for day 2, $p < 0.0001$ for day 4 and day 6 and $p < 0.001$ for day 7.

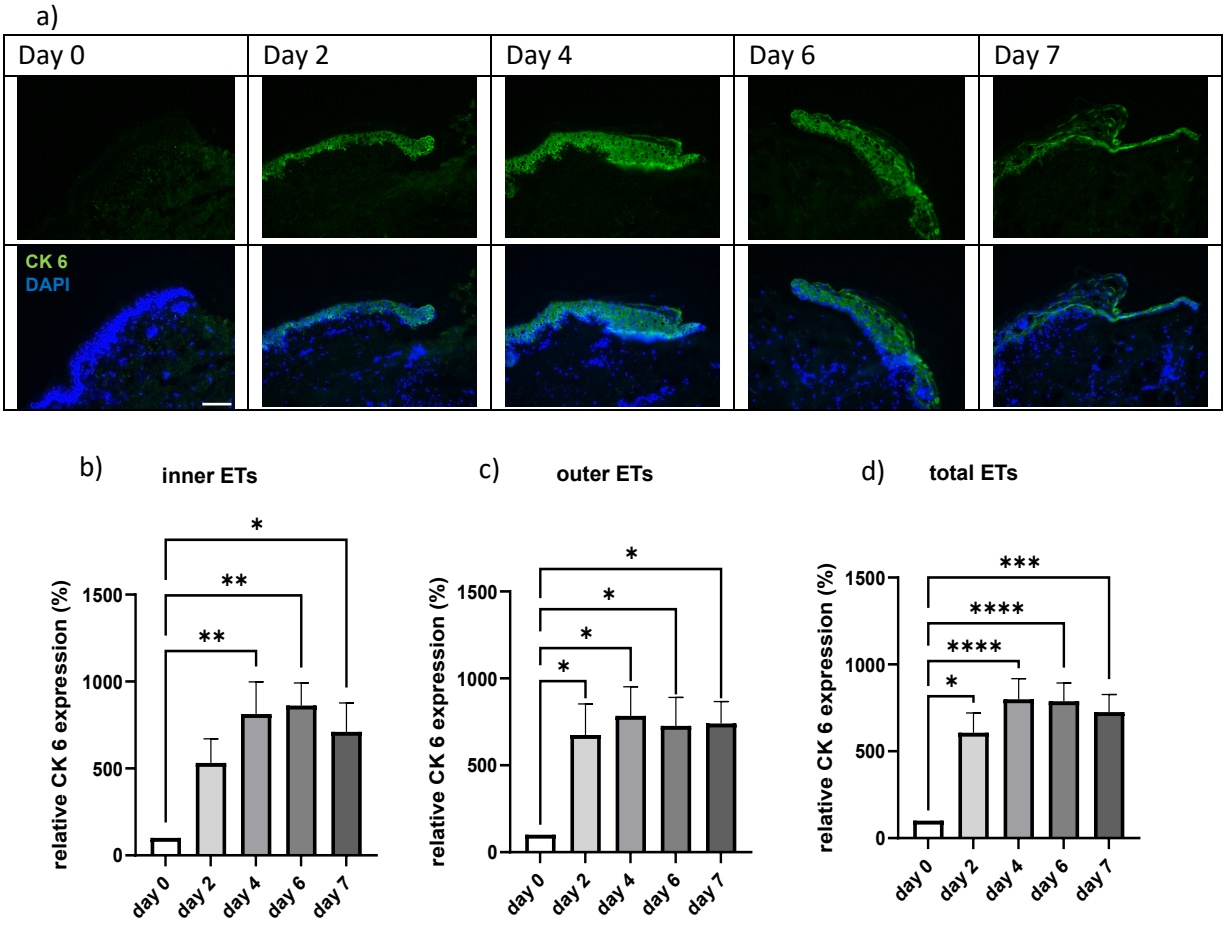

Figure 4.3: Characterization of the cytokeratin 6 expression in the wound healing organ culture model
a) Exemplary microscopy pictures of the cytokeratin (CK) 6 expression during the course of the wound healing organ culture. Scale bar = 100 µm. Relative CK 6 expression of the inner (b), outer (c) and total (d) epithelial tongues (ETs). n = 4 (2-8 wounds/day). Data is depicted as mean + standard error of the mean. Significances were determined by one-way ANOVA followed by Turkey's multiple comparisons test (inner and outer ETs) or Kruskal-Wallis test followed by Dunn's multiple comparisons test (total ETs).
* $p < 0.05$ ** $p < 0.01$, *** $p < 0.001$, **** $p < 0.0001$

4.1.4 Expression of CD31 was significantly higher at day 6 of the wound healing organ culture and the number of CD31 positive cells, cross sections and vessels seemed to be lowest at day 0

CD31 is a marker for endothelial cells. As angiogenesis is an important factor in wound healing (Liao *et al.*, 2019; Xie & Muller, 1996) CD31 expression in the dermis over the course of the WHOC was examined next. The results can be found in **Figure 4.4**. As CD31 is continuously expressed by blood vessels, expression is visible at all measurement days (compare **Figure 4.4a**).

Figure 4.4b depicts the relative CD31 expression normalized on day 0. The expression was lowest on day 2 with 88.35 %. On all other days the relative CD31 expression was higher than it was on day 0. It increased from day 2 over 102.75 % at day 4 until 127.41 % at day 6. The expression at day 6 was significantly higher than at day 2 ($p < 0.05$ %). As with CK6, also for CD31 a decrease in expression was observed from day 6 to 104.93 % day 7.

As **Figure 4.4c** shows, the number of CD31 positive cells increased from 25 positive cells/VF at day 0 up to 37 positive cells/VF at day 6, before it decreases to 32 positive cells/VF at day 7. The changes in numbers of CD31 positive cells are not significant though.

The number of CD31 positive cross sections increases from day 0 (0.2/VF) to day 7 (0.7/VF). The number of cross sections is slightly lower on day 4 than on day 2, otherwise the numbers increase throughout the WHOC. The data is not significant (compare **Figure 4.4d**).

The numbers of CD31 positive vessels increase from day 0 (0.4/VF) to day 2 (0.9/VF) and then decreases slightly again to day 4 (0.6/VF). After an increase to 0.7/VF at day 6the number of positive vessels stagnates there. None of the changes in the CD31 positive vessels are significant (compare **Figure 4.4e**).

a)

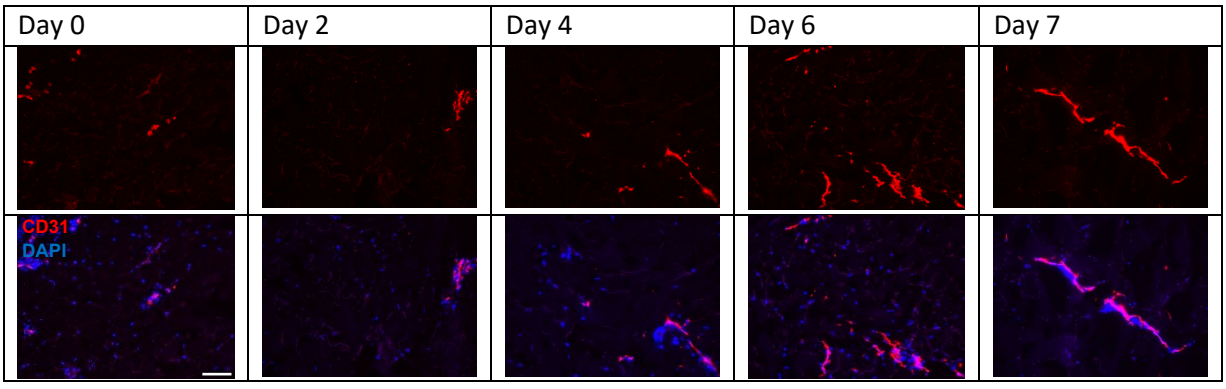

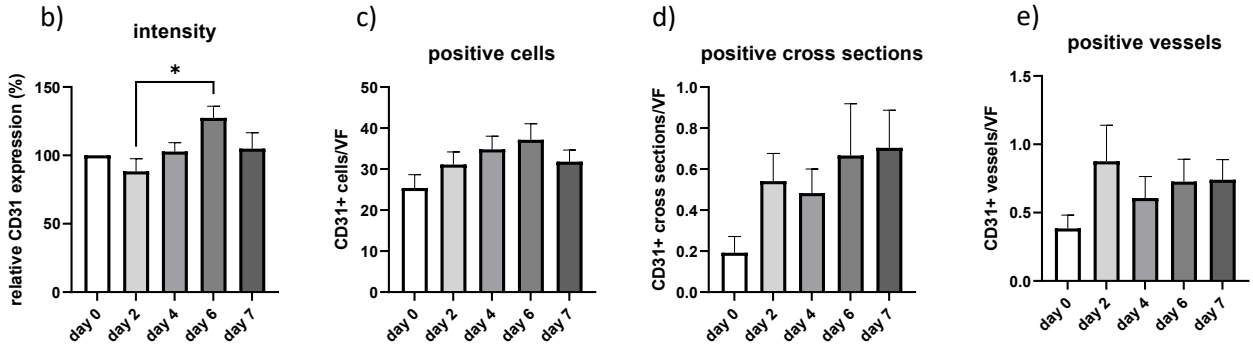

Figure 4.4: Characterization of the CD31 expression in the wound healing organ culture model
a) Exemplary microscopy pictures of the CD31 expression during course of the wound healing organ culture. Scale bar = 100 µm. b) relative CD31 expression, b) number of CD31+ cells/visual field (VF), c) number of CD31+ cross sections/VF, d) number of CD31+ vessels. n = 4 (2-8 sections/day). Data is depicted as mean + standard error of the mean. Significances were determined by one-way ANOVA followed by Turkey's multiple comparisons test (intensity) or Kruskal-Wallis test followed by Dunn's multiple comparisons test (cells, cross sections and vessels). * $p < 0.05$

4.1.5 The percentage of Ki67 positive cells seemed to decrease over the course of the wound healing organ culture, while the percentage of TUNEL positive cells seemed to increase

To assess how the number of proliferating and apoptotic cells changes over the course of the culture, an exemplary Ki67-TUNEL staining was performed. Exemplary pictures and the evaluation of the ETs can be found in **Figure 4.5**. When examining the exemplary pictures in **Figure 4.5a** the low fluorescence intensity of the Ki67 antibody is noticeable. It was found, that the Ki67 expression in abdominal skin was rather low in numbers and intensity compared to for example scalp skin (compare **Chapter 5.2**).

Figure 4.5b shows the percentage of Ki67 positive cells (proliferating cells) and TUNEL positive cells (apoptotic cells) in the inner ETs. At day 0, the highest percentage of Ki67 positive cells was observed (9.08 %), though one must consider the large error bar at this day. At day 2, 4.25 % of the cells are Ki67 positive, at day 4, the percentage of Ki67 positive cells rose to 4.96 % before decreasing to 1.58 % at day 6. At day 7, 2.40 % of the cells in the inner ETs were Ki67 positive. There were no TUNEL positive cells observable at day 0. Their percentage rose to 2.23 % at day 2 and 4.50 % at day 4. On day 6, the percentage of TUNEL positive cells was 6.07 % and therefore higher than the percentage of Ki67 positive cells for the first time during the WHOC. The percentage of TUNEL positive cells increased further to 14.11 % at day 7.

The percentage of Ki67 positive and TUNEL positive cells in the outer ETs can be found in **Figure 4.5c**. At day 0 neither Ki67 positive nor TUNEL positive cells were found in the outer ETs. The highest percentage of Ki67 positive cells was measured on day 2 with 4.53 %. It decreased to 4.37 % on day 4 and to almost 0 on day 6 (0.11 %). At day 7, more cells were positive. Here 1.72 % of the cells of the outer ETs were Ki67 positive. While the percentage of Ki67 positive cells overall decreased from day 2 onwards, the percentage of TUNEL positive cells increased steadily in the outer ETs from 2.07 % on day 2 to 21.36 % on day 7. This increase is especially pronounced from day 6 (8.06 %) to day 7 %.

In the total ETs (**Figure 4.5d**) 4.54 % of the cells were Ki67 positive at the start of the WHOC. Their percentage decreased during the culture to a minimum of 0.85 % of Ki67 positive cells at day 6. At

day 7 the percentage increased to 2.06 %. At day 0 no TUNEL positive cells were detected. Their percentage then rose continuously during the course of the culture to 14.11 % on day 7.
In inner, outer, and total ETs the same trend was observable: The longer the wounded skin was cultivated, the more apoptotic cells could be found in the ETs. This shows that skin cannot be cultivated forever, and the cultivation time should not be much longer than 7 days.

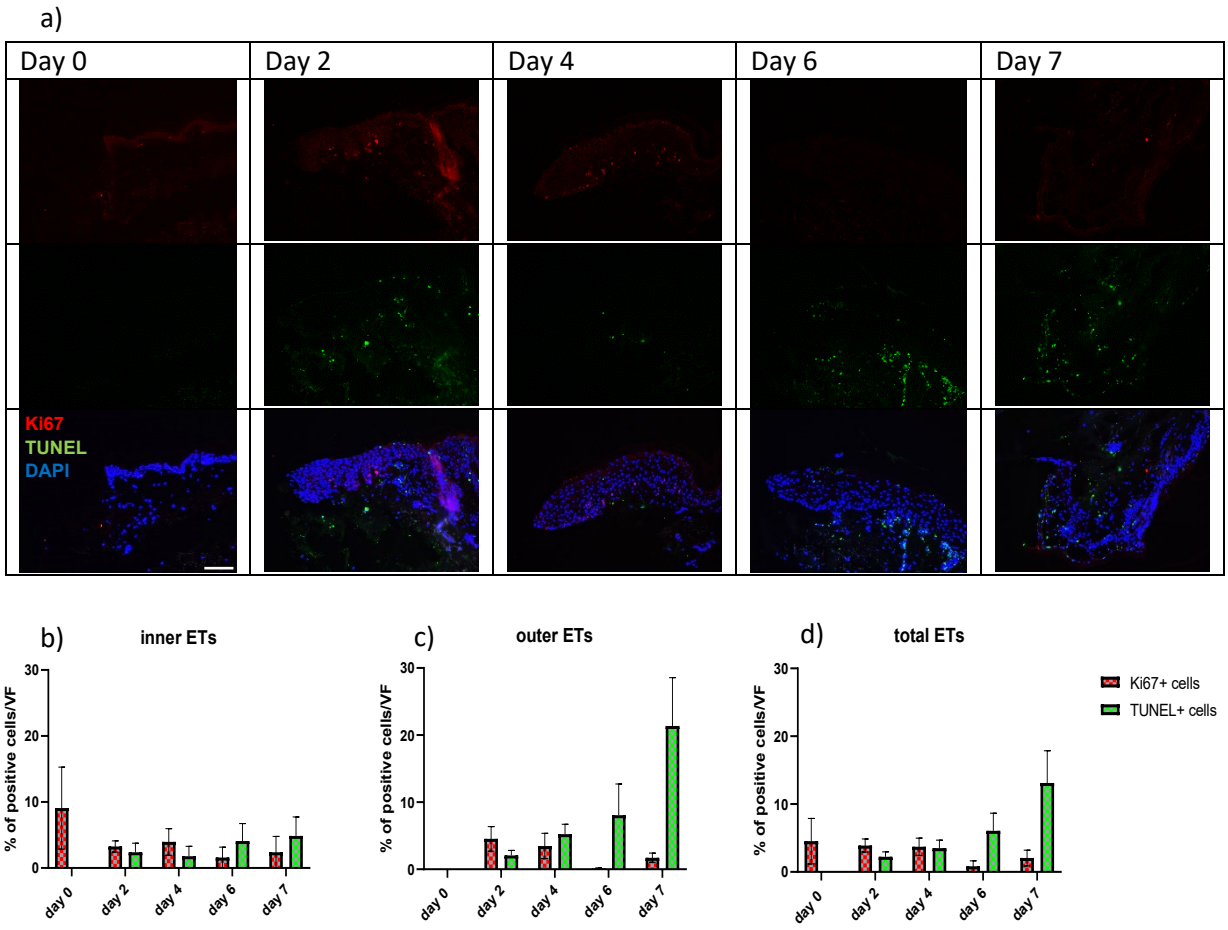

Figure 4.5: Characterization of the KiTUNEL positive cells in the wound healing organ culture model
Ki67 (Ki) is expressed in proliferating cells. TUNEL denotes an enzymatic staining of apoptotic or otherwise damaged cells. a) Exemplary pictures of the KiTUNEL positive cells in the epithelial tongues (ETs) during the wound healing organ culture model. The uppermost panel shows the TUNEL positive cells, the second row shows the Ki67 positive cells and the lowest row shows the overlay of the Ki67 positive cells, TUNEL positive cells and cells counterstained with DAPI. Scale bar = 100 µm. The percentages of Ki67 positive and TUNEL positive cells were calculated in the b) inner, c) outer and d) total ETs. n = 1 (4 – 8 ETs/day). Data is depicted as mean ± Standard error of the mean.

4.1.6 Cortactin is expressed continuously over the course of the wound healing organ culture

Figure 4.6 shows exemplary pictures of the cortactin expression in ETs during the course of the WHOC. Cortactin is an important molecule in actin remodeling and thus important for cell migration, which is a main driver of wound closure in human wound healing (Ammer & Weed, 2008; Eming *et al.*, 2014; Pastar *et al.*, 2014; Zomer & Trentin, 2018). The ETs express cortactin from day 0 on during the entire culture period. At day 6 the cortactin expression seems to be especially pronounced in the tips of the ETs. At day 7, the cortactin expression is especially strong in the lowest layer of the ETs.

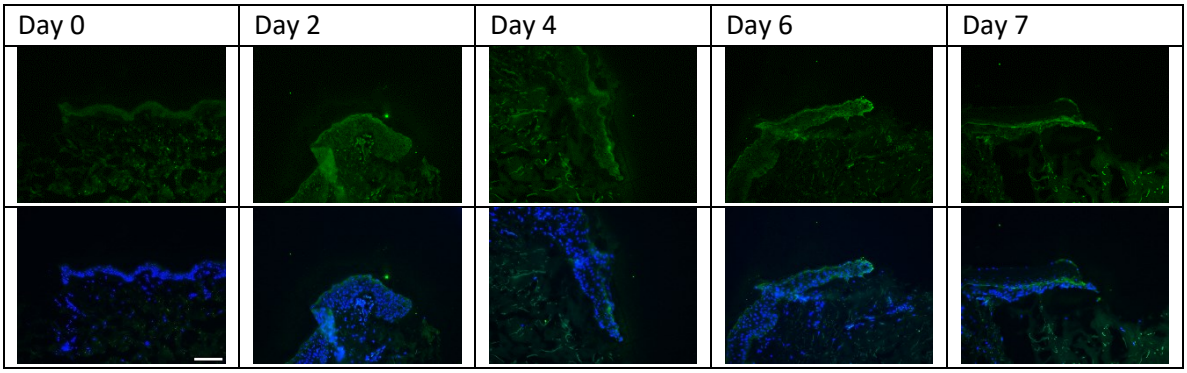

Figure 4.6: Characterization of the cortactin expression in the wound healing organ culture model
Exemplary pictures of the cortactin expression in the epithelial tongues during the wound healing organ culture model. The first row of panels shows the cortactin expression and the second row of panels shows the cortactin expression counterstained with DAPI. Scale bar = 100 µm

This thorough characterization of the *ex vivo* wound healing in the WHOC showed that the untreated wounds heal nicely over the course of the culture. Top-view microscopy allows a characterization of the wound healing during the culture. The other parameters studied (H&E, CK 6, CD31, KiTUNEL, and cortactin) can be used to investigate the wound healing microscopically but for this the studied sample has to be cut and processed. A culturing time much longer than 7 days should be avoided because the skin begins to degrade at that point as shown by the increase in TUNEL positive cells.

4.2 The disinfectant Octenisept® has a detrimental effect on the *ex vivo* wound healing in the wound healing organ culture model

To investigate the *ex vivo* wound healing during the WHOC the 24-well plates with the wounds had to be taken out of the incubator, transported across the campus, and the plates had to be opened for top-view microscopy and OCT in a nonsterile environment. This makes the WHOC prone to infections. To prevent bacterial contamination the culture medium is supplemented with penicillin and streptomycin. Moreover, for the first day of the culture (from day 0 to day 1) the antimycotic amphotericin B was added. To furthermore ensure no infections happened whatsoever, the wound disinfectant Octenisept® was investigated as a possible disinfectant for the WHOC. Octenisept® is not alcohol-based, which is good, as alcohol is known to be cell-toxic (Lachenmeier, 2008; Tapani *et al.*, 1996; Wolf, 1999) As Octenisept® can furthermore be applied as a spray and this is the easiest way to disinfect the *ex vivo* wounds, this disinfectant seemed to be the optimal choice. According to the manufacturer, Octenisept® is a fast-acting wound disinfectant for acute and chronic wounds with a broad spectrum of efficiency against microorganisms (https://www.schuelke.com/de-de/produkte/octenisept-Wund-Desinfektion.php last used on January 7, 2023).
In this chapter the effect of Octenisept® was systematically studied. Therefore, wounds treated with 0.1 % DMSO, which is used in the next chapters as a vehicle control, at day 1 for 24 hours. The Octenisept® group was sprayed with the disinfectant at day 0 before the culture started and then every time after the top-view microscopy (day 2, 4, and 6), the control group was not disinfected at all.

4.2.1 Ex vivo wounds showed significantly less top-view wound closure in the wound healing organ culture when disinfected with Octenisept®

Figure 4.8 shows the results of the top-view microscopy. In the exemplary pictures in **Figure 4.7a** it is clearly visible that the wounds disinfected with Octenisept® heal to a much lesser degree than the control wounds. There is less newly formed epidermal tissue present and black discoloration is visible at the wound edges at day 7 in the Octenisept® group.
The calculation of the relative top-view wound area confirms this finding. As **Figure 4.7b** shows, the relative top-view wound area is distinctly smaller in the control group than in the Octenisept® group. From day 4 on this effect becomes significant with a significance level of $p < 0.05$. It is noticeable, that the wounds disinfected with Octenisept® show a strong decrease in relative top-view wound area from day 0 to 66.83 % at day 2 but thereafter the wound closure seems to stagnate. At day 7, the relative wound area is still at 64.58 %. The control group also shows a strong reduction in top-view area from day 0 to 56.03 % at day 2, but the wound area continues to decrease over the course of the culture to 44.40 % at day 7.

The relative top-view wound perimeter is depicted **Figure 4.7c**. As for the relative top-view wound area, also the relative top-view wound perimeter decreased stronger in the control wounds than in the wound disinfected with Octenisept®. At day 4, 6, and 7 the difference between the two groups is significant ($p < 0.05$ for day 4, $p < 0.01$ for day 6 and 7 respectively). Wounds treated with Octenisept® showed relatively little decrease in relative top-view wound perimeter: the relative top-view wound perimeter is still at 87.77 % at day 7. The perimeter decreases from day 0 over 89.15 % at day 2 to the smallest perimeter of 86.67 % at day 4. Then at day 6, the perimeter increases slightly to 89.72 % before it decreases again at day 7. The relative top-view wound perimeter of the control wounds is continuously lower than the Octenisept® disinfected wounds. At day 2 it is 77.23 % and

decreases further to 74.99 % at day 4. It also shows an increase in perimeter to 75.48 % at day 6 before reaching its minimum of 70.23 % at day 7.
Unfortunately, the OCT system was not available for measurement here.

a)

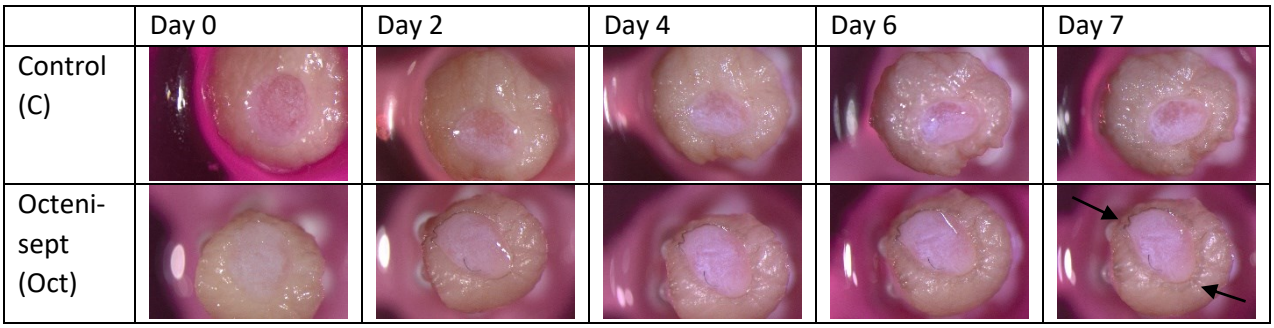

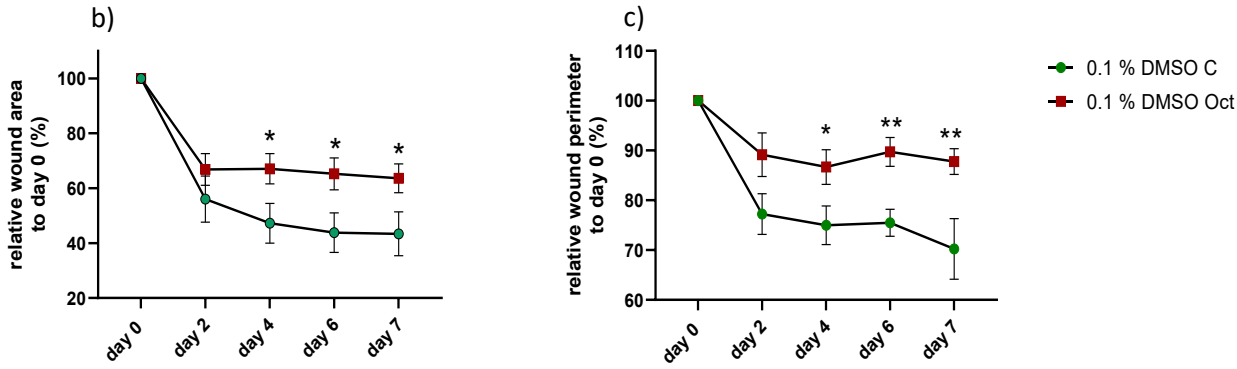

Figure 4.7: Influence of disinfection of the skin in the wound healing organ culture model with Octenisept® on the top-view wound healing
Shown here is the wound healing of skin disinfected with Octenisept® (Oct) before the start of the culture and during the WHOC. To prevent infections after top-view microscopy in a non-sterile environment the wounds were sprayed with Oct after every time pictures were taken. The wounds were treated with 0.1 % dimethyl sulfoxide (DMSO) at day 1 for 24 hours to show the effect of Oct on the negative/treatment controls of the screening of the library. a) Exemplary pictures of wounds disinfected with Oct or not disinfected at all (control = C). Relative top-view wound b) area and c) perimeter throughout the culture (n = 3, 2-4 wounds/condition). Data is depicted as mean ± standard error of the mean. The black arrows at day 7 show the black discoloration observable after disinfection of the wound with Oct. For statistical analysis an unpaired t-test was performed. *$p < 0.05$, ** $p < 0.01$

4.2.2 Wounds disinfected with Octenisept® formed no new epithelial tongues in the wound healing organ culture

Figure 4.8 shows the results of the evaluation of the H&E staining. In the exemplary pictures in **Figure 4.8a** of the microscopic wounds and especially in the close-ups of the ETs it becomes obvious, that Octenisept® has a detrimental effect on *ex vivo* wounds. While without Octenisept® a dense dermis, an intact epidermis. and large growing ETs are visible, in the wounds disinfected with Octenisept® the dermis was partly disrupted, the epidermis often detached from the dermis and almost no ETs present.

The microscopic wound area of the control group is 443,027 µm^2 and thus more than three times the size of the microscopic wound area of the Octenisept® group (137,319 µm) as shown in **Figure 4.8b**. However, the is not significant.
Figure 4.8c shows the microscopic wound diameter. The microscopic wound diameter 1,279.09 µm in the control group and 1,914.99 µm in the Octenisept® group. So, wounds treated with Octenisept® have a larger microscopic wound diameter than the respective wound though not significantly so.

When assessing the ETs in **Figure 4.8a** and **4.8d-k** it is striking how little ETs are detectable in the wounds disinfected with Octenisept®. While the control wounds healed and showed a formation of intact ETs, for the Octenisept® wounds hardly any ETs could be found. The inner (**Figure 4.8d**), outer (**Figure 4.8e**), total (**Figure 4.8f**), and normalized inner (**Figure 4.8g**) ETs were significantly smaller when disinfected with Octenisept® compared to the control group with a significance level of $p < 0.0001$. The area of the inner ETs in the control group was 22,222.90 µm^2, while the Octenisept® group only reaches 727.15 µm^2. After normalization this stark difference is still clearly distinguishable: 25.73 µm for the control and 0.54 µm for the Octenisept® group, as **Figure 4.8g** shows. After disinfection with Octenisept® no outer ETs could be detected while in the control group the outer ETs in **Figure 4.8e** grew 34,324.70 µm^2 large. The total ETs had an area of 28,716.00 µm^2 without disinfection with Octenisept® but only 397.04 µm^2 when the disinfectant was used (compare **Figure 4.8f**).

Just like the area of all ETs the length of the inner, outer, and total ETs as well as the normalized ETs was significantly shorter after disinfecting with Octenisept® than in the control groups ($p < 0.0001$). As **Figure 4.8h** shows, the inner ETs were 230.10 µm in the control groups, but only 22.34 µm in the wounds infected with Octenisept®. Also, the normalized ETs were significantly longer when not disinfected with Octenisept®: 0.22 in the control group and 0.01 in the Octenisept group (compare **Figure 4.8k**). After disinfection no ETs were visible in the outer ETs, while the ETs of the control groups were 476.76 µm long (compare **Figure 4.8i**) and the total ETs were 365.18 µm long after disinfection with Octenisept® and 12.13 µm in the control group (compare **Figure 4.8j**).

Together with the significantly reduced wound closure of the top-view wound area this detrimental effect on the ETs shows that disinfection with Octenisept® clearly harms if not even almost stops the *ex vivo* wound healing in the WHOC model.

a)

	Control (C)	Octenisept (Oct)
Wound	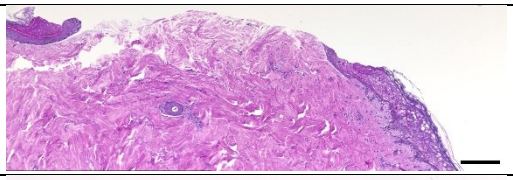	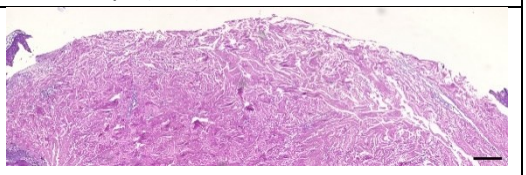
ET	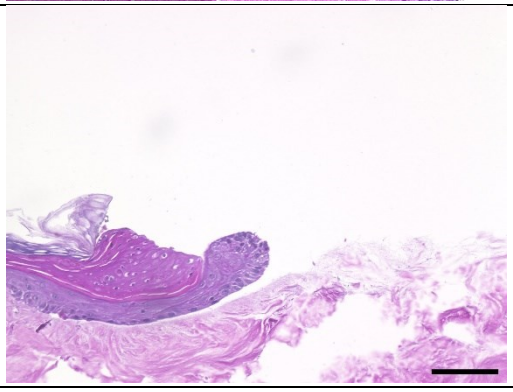	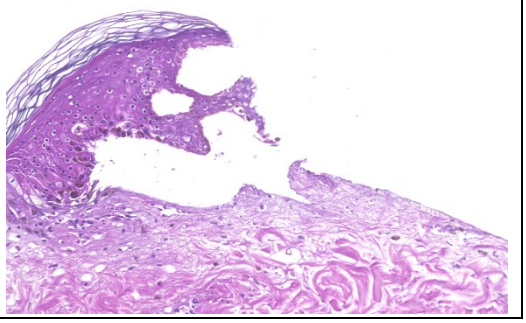

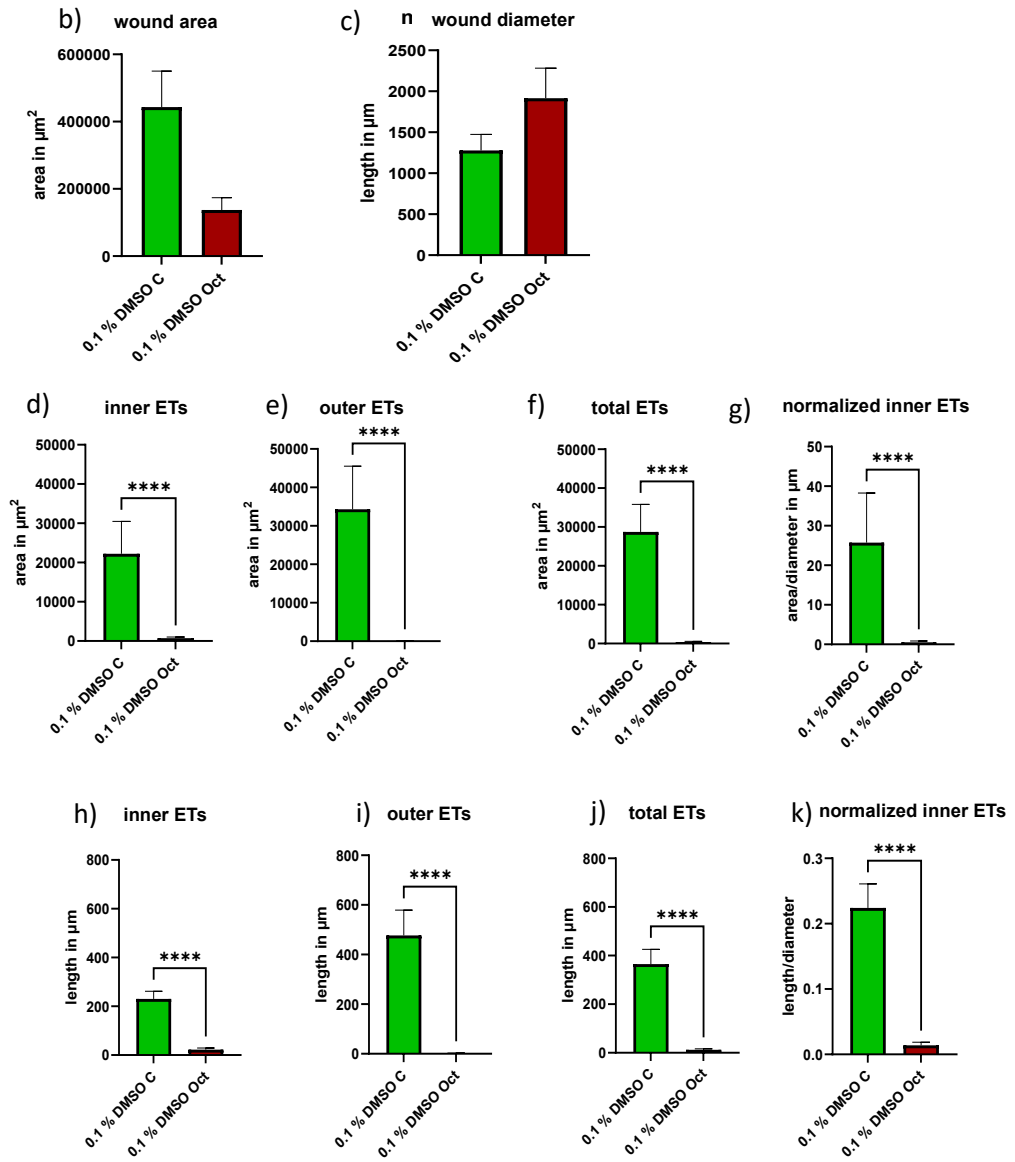

Figure 4.8: Influence of disinfection of the skin in the wound healing organ culture model with Octenisept® on the microscopic wound healing

The wounds were treated with 0.1 % dimethyl sulfoxide (DMSO) at day 1 for 24 hours. One group was disinfected with Octenisept® (Oct) every other day, the other group was not disinfected at all (control group C). Shown here is the evaluation of Hematoxylin & Eosin staining of wounds processed, cut, and stained at day 7 (end of culture). a) Exemplary pictures of microscopic wounds (scale bar = 200 µm) and epithelial tongues (ETs, scale bar = 100 µm) of wounds either treated with Oct or the control grup. b) microscopic wound area, c) microscopic wound diameter (n = 3, 1-4 wounds/condition), area of the d) inner, e) outer and f) total ETs and g) area of the inner ETs normalized on the respective wound diameter, length of the h) inner, i) outer and j) total ETs, k) length of the inner ETs normalized on the respective wound diameter. For all: n = 3, 4-16 ETs/wound for all ET-figures). Data is depicted as mean + standard error of the mean. For statistically analysis a unpaired t-test (microscopic wound diameter) or Mann-Whitney (microscopic wound area and analysis of ETs) was performed. ****p < 0.0001

4.2.3 Disinfection with Octenisept® has no influence on the cytokeratin 6 expression in the wound healing organ culture

The CK 6 expression was not strongly affected by the wound disinfection with Octenisept®, however. Already the exemplary pictures in **Figure 4.9a** prove that CK 6 is expressed in both groups. In the inner ETs the CK 6 expression is even higher in the Octenisept® group (110.99 %) as illustrated in **Figure 4.9b**, while the CK 6 expression in the outer ETs with 80.46 % is lower in the Octenisept® group

(compare **Figure 4.93c**). **Figure 4.9d** depicts the CK 6 expression in the total ETs, so inner and outer ETs combined, which is with 100 % for the control and 95.73 % for the Octenisept® group almost identical.

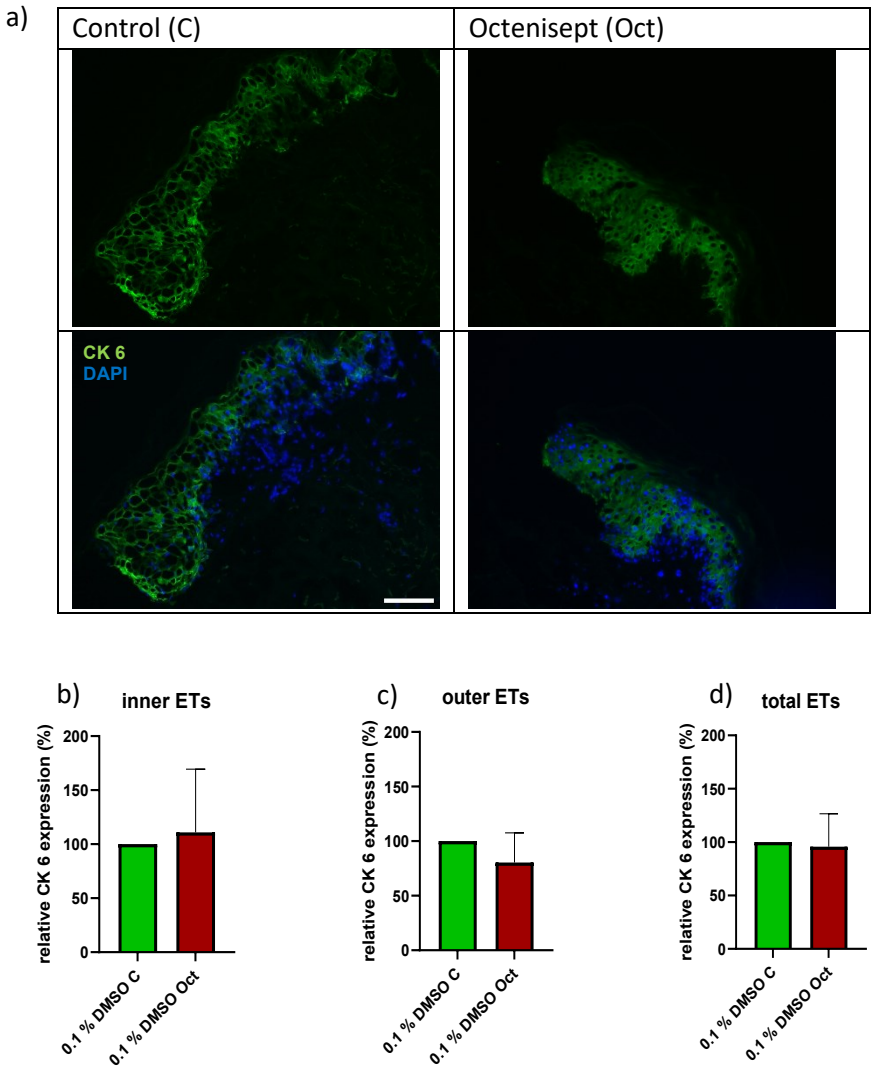

Figure 4.9: Influence of disinfection of the skin in the wound healing organ culture model with Octenisept® on the cytokeratin 6 expression

The wounds were treated with 0.1 % dimethyl sulfoxide (DMSO) at day 1 for 24 hours. One group was disinfected with Octenisept® (Oct) every other day, the other group was not disinfected at all (control group C). Shown here is the evaluation of wounds processed, cut and stained against cytokeratin (CK) 6 at day 7 (end of culture). Scale bar = 100 µm. a) Exemplary pictures of the CK 6 expression in the epithelial tongues (ETs) of wound disinfected with Oct or not disinfected at all (C). CK 6 expression of the b) inner, c) outer and d) total ETs. Expression was normalized on the control condtions. For all: n = 3, 2-8 ETs/wound. Data is depicted as mean + standard error of the mean. For statistical analysis an unpaired t-test (outer ETs) or a Mann-Whitney test (inner and total ETs) was performed. Data not significant.

4.2.4 Disinfection with Octenisept® decreased the number of CD31 positive cells and vessels significantly compared to the control group in the wound healing organ culture model

Figure 4.10 shows the results of the CD31 staining. The exemplary pictures in **Figure 4.10a** already indicate that Octenisept® has an influence on some of the examined paramteres here. There are no significant differences between the relative CD31 expression. The wounds disinfected with Octenisept® showed a relative CD31 expression of 104.40 %, so the expression was slightly higher than in the control groups (**Figure 4.10b**). On the other hand, the number of CD31 positive cells is

significantly higher if the wound were not disinfected with Octenisept® (compare **Figure 4.10c**: 36 cells/VF for the controls and 21 cells/VF for the Octenisept® wounds). As **Figure 4.10d** illustrates the Octenisept® wounds also have less CD31 positive vessels than the control group (0.48/VF for the control and 0.31/VF for Octenisept®), but the difference is not significant. Moreover, control group has approximately 0.86 positive branched vessels per VF, which is significantly more than the 0.31 positive cross sections/VF that wound disinfected with Octenisept®.

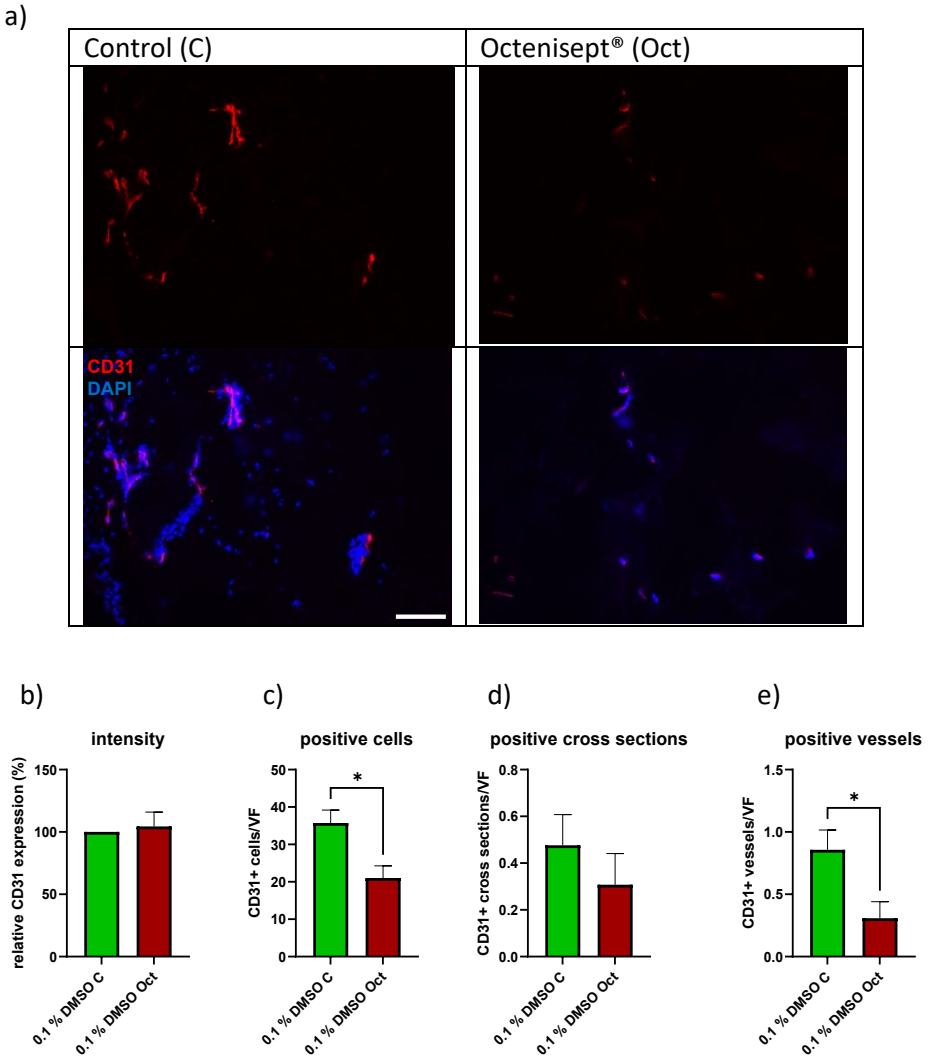

Figure 4.10: Influence of disinfection of the skin in the wound healing organ culture model with Octenisept® on the CD31 expression

The wounds were treated with 0.1 % DMSO at day 1 for 24 hours. One group was disinfected with Octenisept® (Oct) every other day, the other group was not disinfected at all (control group C). Shown here is the evaluation of of wounds processed, cut and stained against cytokeratin (CK) 6 at day 7 (end of culture). a) Exemplary pictures of the CD31 expression in the dermis of wound disinfected with Oct or not disinfected at all (C), the upper panels show only the CD31 expression and in the lower panels the CD31 expression counterstained with DAPI is depcited, scale bar = 100 µm, b) CD31 expression normalized on the control group, c) number of CD31 positive cells/visual field (VF), d) number of CD31 positive cross sections/VF, e) number of CD31 positive branched vessels/VF. For all: n = 3, 4-8 VF/wound. Data is depicted as mean + standard error of the mean. For statistically analysis an unpaired t-test (relative expression) or a Mann-Whitney test (numbers of cells, cross sections and vessels) was performed. * $p < 0.05$

4.2.5 Disinfection with Octenisept® resulted in significantly less Ki67 positive cells and significantly more TUNEL positive cells in the epithelial tongues of the *ex vivo* wounds of the wound healing organ culture model

As disinfection with Octenisept® clearly had a detrimental effect on the *ex vivo* wound healing, a KiTUNEL double staining was performed to investigate if Octenisept® disinfection also influenced cellular proliferation and apoptosis. The results can be found in **Figure 4.11**.
While the expression of Ki67 is generally weak the exemplary pictures in **Figure 4.11a** showed that there is more Ki67 expression in the ETs of the control group than in the Octenisept® group and the percentage of TUNEL positive cells is higher in the Octenisept® group than in the control group. Calculating the number of positive cells for both markers confirmed this visual impression.

As shown in **Figure 4.11b** in the inner ETs 4.93 % of the cells in the control wounds are Ki67 positive, significantly more than the 0.80 % in the Octenisept® disinfected wounds ($p < 0.05$ %). The percentage of TUNEL positive cells on the other hand is significantly higher in the Octenisept® wounds than in the control wounds with a significance level of $p < 0.005$ % (6.64 % in the control group versus 64.66 % in the Octenisept® group). Almost two thirds of the cells in the inner ETs were TUNEL positive when the wounds were disinfected with Octenisept®.

Only 0.23 % of the cells in the outer ETs of the Octenisept® wounds were Ki67 positive, while the percentage was 4.93 % in the control group, a difference that is statistically significant ($p < 0.05$, compare **Figure 4.11c**). Half of the cells in the outer ETs were TUNEL positive after disinfection with Octenisept®, but also the control wounds showed a relatively high number of TUNEL positive cells in the outer ETs (24.93 %). The difference between the 2 groups is not significant here.

The percentage of positive cells in the outer ETs can be found in **Figure 4.11d**. Just like the inner and outer ETs, disinfection with Octenisept® led a to significantly lower percentages of Ki67 positive cells compared to the control wounds with a significance level of $p < 0.01$: 0.51 % Ki67 positive cells in the Octenisept® group and 4.94 % in the control group. 57.33 % of the cells in the total ETs of the Octenisept® wounds were TUNEL positive. In the total ETs of the control wounds only 15.29 % of the cells were TUNEL positive, significantly less than after Octenisept® disinfection ($p < 0.001$)

a)

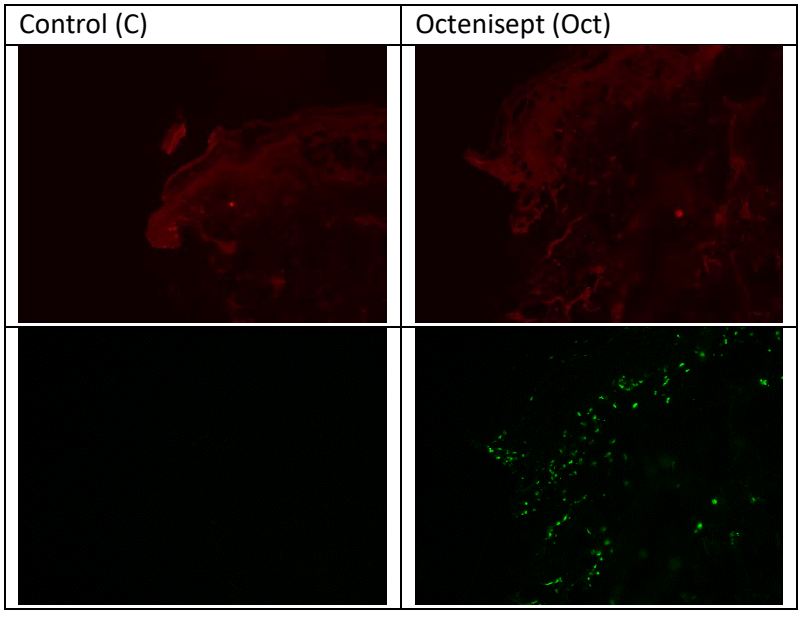

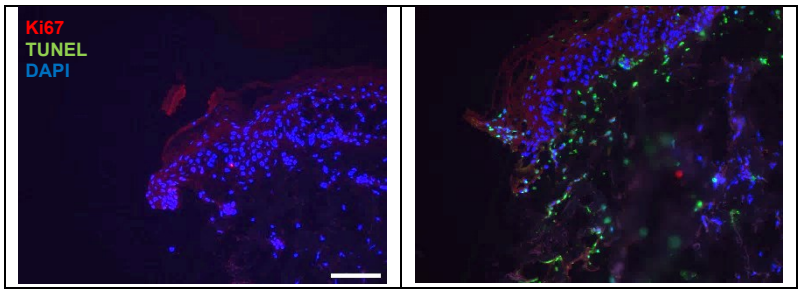

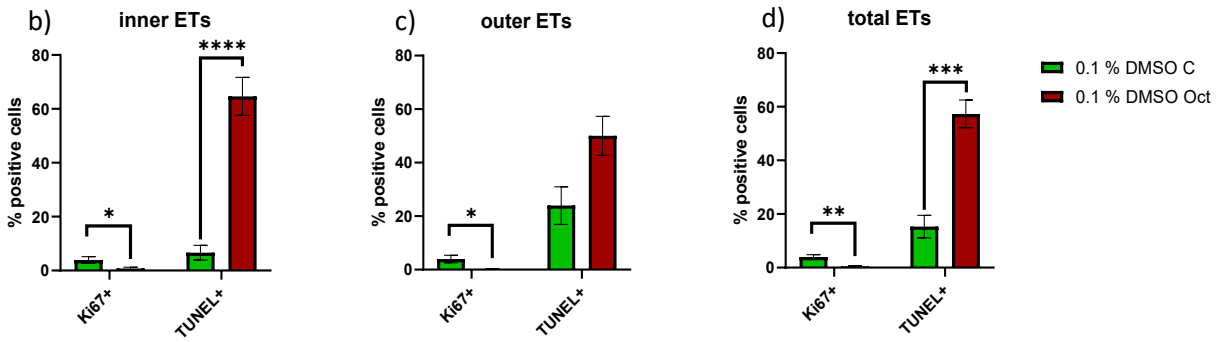

Figure 4.11: Influence of disinfection of the skin in the wound healing organ culture model with Octenisept® on the percentage of KiTUNEL positive cells

Ki67 is expressed in proliferating cells. TUNEL denotes an enzymatic staining of apoptotic or otherwise damaged cells. The wounds were treated with 0.1 % dimethyl sulfoxide (DMSO) at day 1 for 24 hours. One group was disinfected with Octenisept® (Oct) every other day, the other group was not disinfected at all (control group C). a) Exemplary pictures of the KiTUNEL positive cells in the epithelial tongues (ETs) during the wound healing organ culture model. The uppermost panel shows the TUNEL positive cells, the second row shows the Ki67 positive cells and the lowest row shows the overlay of the TUNEL cells, the Ki67 cells, and the DAPI counterstain. Scale bar = 100 µm. The percentages of Ki67 positive and TUNEL positive cells were calculated in the b) inner, c) outer and d) total ETs. n = 3 (2-4 ETs/wound). Data is depicted as mean ± standard error of the mean. For statistical analysis a unpaired t-test (percentage of Ki positive cells in the outer ETs) or a Mann-Whitney test (all other evaluations) was performed. * $p < 0.05$, ** $p < 0.01$, *** $p < 0.001$, **** $p < 0.0001$

4.2.6 Disinfection with Octenisept® seemed to reduce cortactin expression in the epithelial tongues of the *ex vivo* wounds in the wound healing organ culture

That Octenisept® is harmful to the *ex vivo* wound healing is underlined by the cortactin staining, displayed in **Figure 4.12**. In the control wounds an even expression of cortactin in the "old" epidermis and the newly growing ETs is visible, possibly strongest in the tip of the ET, indicating that here the actin remodeling and migration/movement of the epidermal cells is strongest. This is as expected, considering that the ETs have to grow till the tips meet and the wound is thus closed. For the wounds disinfected with Octenisept® cortactin is expressed in the epidermis, but not at the wound edges where ETs should be growing, and a lot of cellular movement and migration would be expected.

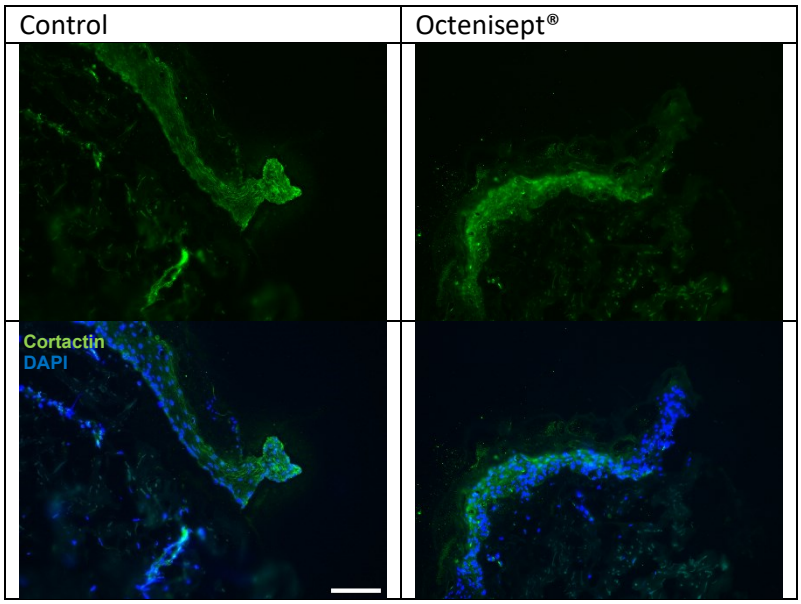

Figure 4.12: Influence of disinfection of the skin in the wound healing organ culture model with Octenisept® on the cortactin expression
The wounds were treated with 0.1 % dimethyl sulfoxide (DMSO) at day 1 for 24 hours. One group was disinfected with Octenisept® every other day, the other group was not disinfected at all (control). Shown here are the exemplary pictures of the cortactin expression in the epithelial tongues. The upper panel shows the cortactin expression and in the lower panel the cortactin expression overlayed with the DAPI counterstain is shown. scale bar = 100 µm

All investigated parameters taken together clearly indicate that for the *ex vivo* wound healing in the WHOC wounds should never be disinfected with Octenisept®. While infections of the WHOC are annoying for the researcher and make a repetition of the culture necessary, this is still preferable to wounds that are not infected but also do not heal.

4.3 The vehicle control for the screening was 0.1 % dimethyl sulfoxide and as a positive control 10 µM sodium gualenate was used

Before the screening could be performed, sufficient vehicle and positive controls had to be found. **Chapter 4.3.1** revealed 0.1 % DMSO as an appropriate vehicle control and **Chapter 4.3.2** showed that 10 µM SG can be used as a positive control.

4.3.1 Influence of different dimethyl sulfoxide concentrations on the wound healing organ culture model: concentrations above 1 % dimethyl sulfoxide were toxic to the skin

Most of the inhibitors provided by Selleck Chemicals are small, organic molecules and as such they do not dissolve well in water or are even insoluble in water. For example SG has a solubility of 60 mg/mL in the organic solvent DMSO but only of 18 mg/mL in water (according to the manufacturer, https://www.selleckchem.com/products/sodium-gualenate.html, last use: December 21, 2022). As DMSO at higher concentrations has a cell-toxic effect (Galvao *et al.*, 2014), before the screening was conducted, the effect of different DMSO concentrations onto the WHOC had to be tested.
Therefore, the wounds were treated with DMSO concentrations between 0 % (ergo untreated) and 100 % for 24 h at day 1. Further, wounds were repetitively treated with 0.1 % DMSO (4 x 0.1 DMSO, corresponding to the four medium changes performed over the course of the WHOC).

Figure 4.13 depicts the influence of the different DMSO concentrations on the top-view *ex vivo* wound healing as well as OCT volume measurements and the results of the LDH assay. In **Figure 4.13a** exemplary pictures of the day of wounding (day 0) and the end of the culture (day 7 or 8) are compared amongst each other. Already by bare eye it is distinguishable, that the wound healing is diminished when adding more than 10 % of DMSO. Almost no opaque, newly formed ETs are detectable in the wounds treated with 50 % DMSO at day 7 and the 100 % DMSO sample even shows some signs of a disintegrating epidermis at the wound edges at day 7. This made the measurement of the top-view wound area and perimeter challenging.

In line with the visible impression the relative top-view wound area (compare **Figure 4.13b**) is noticeably larger in the samples treated with 10 % DMSO or more from day 4 onwards.
At day 2 the relative top-view wound area of the untreated wounds was 79.12 %. Wounds treated with 0.1 % DMSO had the smallest relative top-view wound area with 71.66 %, while the wounds treated with 100 % DMSO had the largest relative top-view wound area with 96.56 %. The rest of the tested DMSO concentrations were within this range. None of the differences was significant on this day.
On day 4, the treatment with 0.1 % DMSO led to the smallest relative top-view wound area of 55.77 %. The untreated wounds had a relative top-view wound area of 61.29 % and were significantly smaller than the wounds treated with 10 % DMSO ($p < 0.05$), which had the largest relative top-view wound area of 87.46 %. This is an increase in wound area compared to day 2 (80.69 %). The wounds treated with 100 % DMSO had a smaller wound area than 10 % and 50 % DMSO at this day.
The relative top-view wound area of all treatment groups decreased further on day 6. Untreated wounds had a relative top-view wound area of 56.51 %. 0.1 % DMSO, 1 % DMSO and 4 x 0.1 % DMSO led to similar relative top-view wound areas, with 0.1 % DMSO treated wounds being slightly smaller (52.43%) and 1 % DMSO and 4 x 0.1 % DMSO treated wounds slightly larger (58.91 % and 61.86 % respectively). Higher DMSO concentrations seemed to reduce the wound healing. Especially wounds

treated with 10 % DMSO showed still the largest area of all treatment conditions at day 6 with 81.48 %. While rather larger in numbers the differences measured here were not significant.
Just like the other days, also on day 7/8 the relative top-view wound area is smallest in wounds treated with 0.1 % DMSO with 46.75 %. In untreated wounds its 49.11 % and thus only slightly larger. Treatment with 1 % led to 55.83 % relative top-view wound area and 4 x 0.1 % DMSO to 59.13 % relative top-view wound area. So repetitive treatment with 0.1 % DMSO seems to reduce wound healing comparably strong as one-time treatment with 1 % DMSO. Treatment with 10 % DMSO led to a relative top-view wound area of 73.86 % at day 7/8. The largest relative top-view wound area was measured in wounds treated with 50 % DMSO. Here the top-view wound area was still 80.87 % of its starting value at day 0. Wounds treated with 100 % DMSO had a relative top-view wound area of 71.49 % at day 7/8. The data at day 7/8 is not significant.

For the relative wound perimeter, shown in **Figure 4.13c**, the damaging influence of high DMSO concentrations is even more pronounced during the later course of the WHOC.
At day 2, however the differences between the different DMSO concentrations are rather small and not significant. The smallest relative top-view wound perimeter is observed in wounds treated with 0.1 % DMSO for 24 h at day 1 with 86.79 %. It is the only DMSO concentration that led to a smaller perimeter than the untreated wounds with 88.80 %. Wounds treated with 100 % DMSO have relative perimeter of 93.90 %, the largest at day 2. Wounds treated with 1 %, 10 %, 50 % and 4 x 0.1 % show a perimeter between these values.
Starting at day 4, there is a distinct difference between DMSO concentrations below 1 % and concentrations of 10 % and higher. Untreated wounds have a relative top-view wound perimeter of 78.46 % at day 4, which is significantly smaller than the relative top-view wound perimeter of wounds treated with 10 % DMSO (97.33 %) and 50 % DMSO (96.38 %) with a significance level of $p < 0.01$ for 10 % DMSO and $p < 0.05$ % DMSO. While treatment with 10 % DMSO resulted in the largest perimeter on day 4, wounds treated with 0.1 % DMSO had a relative perimeter of 76.02 %, which is slightly smaller than even the untreated wounds. The differences in perimeter between 0.1 % DMSO and 10 % and 50 % DMSO are statistically significant ($p < 0.001$ for 10 % and $p < 0.05$ %). Wounds treated with 1 % DMSO had a relative top-view wound perimeter 82.39 %, of wounds treated with 100 % DMSO is 85.71 % and that of wounds treated with 4 x 0.1 % DMSO is 83.07 %.
On day 6, untreated wounds have a relative top-view wound perimeter of 73.14 %, which again is significantly smaller than the perimeter of wounds treated with 10 % DMSO (93.94 %) and 50 % DMSO (96.38 %) with a significance level of $p < 0.01$ for 10 % DMSO and $p < 0.05$ for 50 % DMSO. Wounds treated with 50 % DMSO had the largest relative perimeter. Like the days before, wounds treated with 0.1 % DMSO had the smallest relative perimeter with 72.70 %, though the difference to untreated wounds becomes smaller. The perimeters of wounds treated with 0.1 % DMSO are also significantly smaller than those of wounds treated with 10 % DMSO and 50 % DMSO ($p < 0.01$). The relative wound area of wounds treated with 1 % DMSO is 77.92 %, of wounds treated with 100 % DMSO 87.73 % and of wounds treated with 4 x 0.1 % is 77.87 %.
On day 7/8, the untreated wounds had the smallest relative top-view wound perimeter with 66.35 %. This is significantly smaller than wounds treated with 10 % DMSO (87.96 %, $p < 0.01$), 50 % (95.75 %, $p < 0.001$) and 100 % DMSO (88.93 %, $p < 0.05$). Just like on day 6, treatment with 50 % DMSO led to the largest relative perimeter at the end of the culture. Wounds treated with 0.1 % DMSO had a relative top-view wound perimeter of 72.66 %, which is a bit higher than that of the untreated wounds but significantly lower than the perimeter of wounds treated with 50 % DMSO ($p < 0.05$). Treatment with 1 % DMSO led to a final relative top-view wound perimeter of 74.15 %, which is also significantly lower than that of wound treated with 50 % DMSO ($p < 0.05$). Wounds treated with

4 x 0.1 % DMSO have a relative top-view wound perimeter of 74.87 % at the end of the culture, which is very close to the perimeter of wounds treated with 1 % DMSO.

While 1 % DMSO treatment still shows good healing progression when looking at the top-view relative area and perimeter (compare **Figure 4.13b and c**), the wound volume of wounds treated with 1 % DMSO is 132.14 %, as can be seen in **Figure 4.13d**. Treatment with 0.1 % DMSO did result in a larger relative wound volume than no treatment with DMSO, but unlike the higher DMSO concentrations tested here at least a decrease in wound volume was observable: relative wound volume of 74.414 % for untreated, 83.468 % for 0.1 %, 132.140 % for 1 % and 114.946 % for 10 %. Unfortunately, the OCT was only available for measurements of two cultures, so a statistical analysis was not possible.

Lastly, the LDH-release into the culture medium over the course of the WHOC was investigated, as depicted in **Figure 4.13e**. After day 0, the LDH-levels were high, but decreased at day 2. Untreated wounds had a relative LDH-release of 19.59 % on day 2, wounds treated with 0.1 % DMSO of 23.79 %, wounds treated with 1 % DMSO 19.40 % and wounds treated with 10 % DMSO 8.49 %, the lowest LDH-release on day 2. From day 4 till the end of the WHOC the LDH-levels rose continuously.
At day 4, wounds treated with 0.1 % DMSO had the lowest LDH-release with 17.74 % and wounds treated had the highest LDH-release with 41.73 %. Untreated wounds had a relative LDH-release of 19.21 % and wounds treated with 1 % DMSO 23.92 %.
The lowest amount of LDH with 41.46 % was released by untreated wounds on day 6, the highest amount by wounds treated with 1 % DMSO with 56.84 %. Wounds treated with 10 % DMSO had a relative LDH-release of 42.89 %, which was similar to the untreated wounds.
At day 8 the relative LDH-release of wounds treated with 0.1 % was 73.39 % and the LDH-release of wounds treated with 10 % DMSO (47.28 %) was the lowest. Wounds treated with 0.1 % DMSO had a relative LDH-release of 78.51 % and wounds treated with 1 % DMSO of 81.85 %.

Taken together the results show that treatment with low DMSO concentration (1 % DMSO and lower) is tolerable for the skin in the WHOC. One-time treatment with 0.1 % DMSO seemed to interfere least with the *ex vivo* wound healing in the WHOC compared to the untreated wounds. Therefore, all inhibitors were dissolved to a final concentration of 0.1 % DMSO in each well respectively.

a)

	0 % DMSO	0.1 % DMSO	1 % DMSO
Day 0			
Day 7	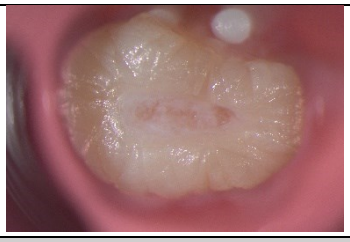	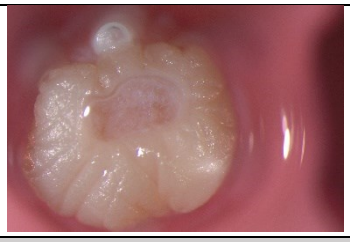	

	10 % DMSO	50 % DMSO	100 % DMSO
Day 0	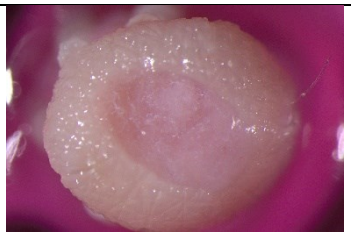		
Day 7	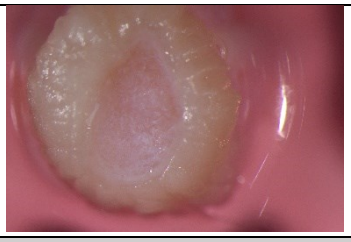		
	4 x 0.1 % DMSO		
Day 0			
Day 7	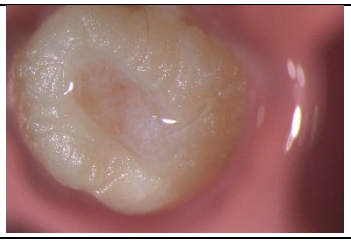		

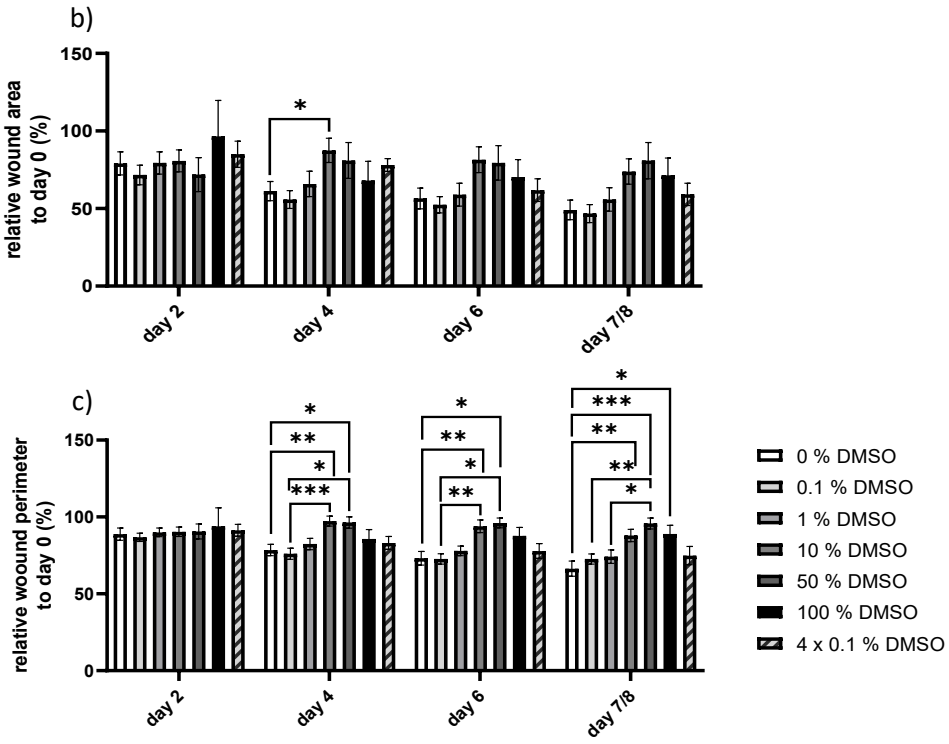

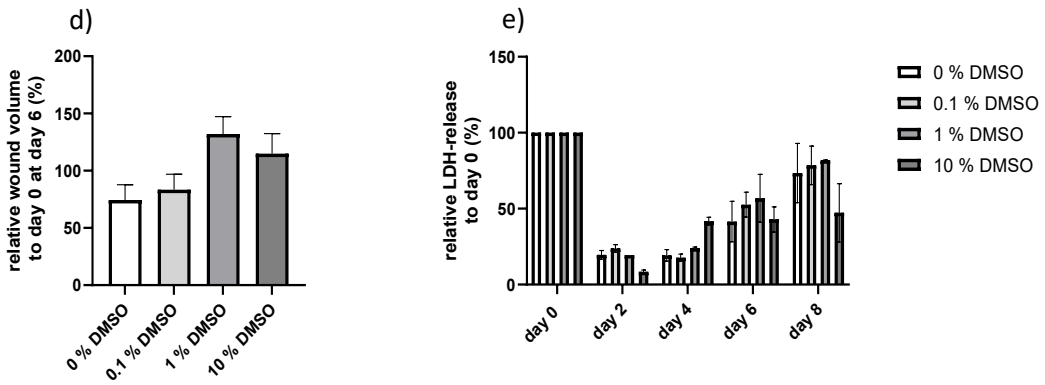

Figure 4.13: Influence of different dimethyl sulfoxide concentrations on the top-view wound healing in the wound healing organ culture model

The wounded skin was treated with different concentrations reining from 0 % (untreated) up to 100 % dimethyl sulfoxide (DMSO) at day 1 for 24 h. 4 x 0.1 % DMSO means treatment starting at day 1 and then repetitively during the culture. a) shows exemplary pictures of the wounds at day 0 (day of wounding) and day 7/8 (end of culture). The relative top-view wound area and wound perimeter can be seen in b) and c) (n = 5 for 0 %, 0.1 %, 1 %, 10 % and 4 x 0.1 %; n = 3 for 50 % and 100 %; 1-4 wounds/condition), c) depicts the relative wound volume at day 6 of the culture obtained by optical coherence tomography (n =2; 2-4 wounds/condition), e) shows the relative lactate dehydrogenase (LDH) release in the culture medium (n = 1, measurements in triplicates). Values are depicted as means plus standard error of the mean (SEM) or as means ± SEM for LDH-release. Significances for the top-view area and perimeter were calculated using the Kruskal-Wallis Test with Dunns' multiple comparisons test at day 2 and one-way ANOVA with Turkeys' multiple comparisons test for day 4, 6 and 7/8. * $p < 0.05$, ** $p < 0.01$, *** $p < 0.001$

4.3.2 The search for a positive control: while L-arginine has no convincing effect on the top-view *ex vivo* wound healing, sodium gualenate seems to be a sufficient positive control for the wound healing organ culture model

After establishing 0.1 % DMSO as a sufficient vehicle control, a positive control was needed for the screening. At the time point of starting the screening Selleck Chemicals offered two substances that should aid wound healing according to the manufacturer: L-Arg and SG. For L-Arg it says on the website: "[…] L-arginine plays an important role in immune regulation by affecting the immune response and inflammation. It is also implicated in cell division [and] wound healing […]" (https://www.selleckchem.com/products/l-arginine.html, *last used December 22, 2022). For SG the website states: "*Sodium gualenate […]has anti-inflammatory and wound-healing effects" (https://www.selleckchem.com/products/sodium-gualenate.html, last used December 22, 2022). **Figure 4.14** shows the structure formula of L-Arg (a) and SG (b). In the following chapter the influence of different concentrations of L-Arg and SG on the WHOC is investigated.

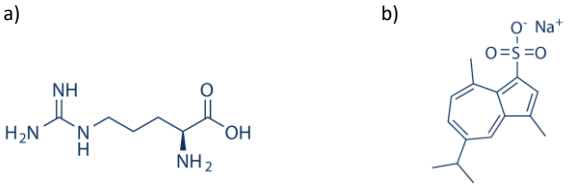

Figure 4.14: Structure formulars of a) L-arginine and b) sodium gualeante.
Images taken from https://www.selleckchem.com/products/l-arginine.html and https://www.selleckchem.com/products/sodium-gualenate.html (both last used on December 22, 2022)

4.3.2.1 L-arginine was not found to aid top-view ex vivo wound healing in the wound healing organ culture model

First the influence of L-Arg on the *ex vivo* wound healing was examined. Therefore, the skin was either treated with 1 µM or 10 µM L-Arg at day 1 for 24 h or starting from day 1 repetitively with 1 µM L-Arg throughout the entire culture. L-Arg is well soluble in water (34 mg/mL according to the manufacturer) but insoluble in DMSO (https://www.selleckchem.com/products/l-arginine.html, last used December 22, 2022). That is why no vehicle control was necessary here. Instead, L-Arg was dissolved directly into the culture medium and the culture medium served as a negative control (0 µM L-Arg).

Figure 4.15 shows the results of the treatment with different L-Arg concentrations. In **Figure 4.15a** exemplary pictures of the wound at day 0 (start of the culture) and day 8 (end of the culture) are shown. Under all conditions the wounds appear smaller on day 8 and newly formed ETs are visible. A distinct positive effect of L-Arg onto the *ex vivo* wound healing is not detectable by bare eye.

The relative top-view wound area over the course of the culture is shown in **Figure 4.15b**. On day 2, the relative top-view wound area of untreated wounds is 65.59 %. The relative top-view wound area of the wounds treated with 1 µM L-Arg is 65.40 %, with 10 µM 66.88 % and with 4 x 1 µM L-Arg 68.29 %.
Until day 4, the wound areas of all conditions tested decrease further, for the untreated wounds to 55.44 %, for the wounds treated with 1 µM L-Arg to 54.04 %, for the wounds treated with 10 µM L-Arg to 53.38 % and for the wounds treated with 4 x 1 µM L-Arg to 57.88 %, which is the largest relative wound area at day 4.
On day 6, the differences between the treatment groups remain small: the smallest relative top-view wound area was found for the untreated wounds with 50.06 %, the highest relative top-view wound area for wounds treated with 4 x 1 µM L-Arg with 57.88 %.

On day 7/8, the untreated wounds had a relative top-view wound area of 45.83 %. With increasing L-Arg concentration also the wound area increased: wounds treated with 1 µM L-Arg had a relative top-view wound area of 48.85 %, treated with 10 µM L-Arg 51.09 % and treatment with 4 x 1 µM L-Arg 54.05 %. None of the found differences in the relative top-view wound area during the course of the WHOC were significant.

The relative top-view wound perimeter is shown in **Figure 4.15c**. On day 2, untreated wounds had a relative top-view wound perimeter of 81.55 %. Just like the relative top-view wound area, the relative top-view wound perimeter of the wound treated with 1 µM L-Arg was very similar to that of the untreated wounds with 82.12 %. Treatment with 10 µM L-Arg led to the lowest relative perimeter at day 2 with 78.49 %, and treatment with 4 x 1 µM to the highest relative perimeter with 83.69 %.
Just like day 2, on day 4 the wounds treated with 10 µM L-Arg showed the smallest relative perimeter with 71.64 % and wounds treated with 4 x 1 µM L-Arg showed the largest relative perimeter with 78.40 %. The relative top-view wound perimeter continues to decrease for all groups.
At day 6, the relative perimeter of untreated wounds was 66.79 %, the smallest value of all concentrations tested on this day. The largest relative perimeter was again observed in wounds treated with 4 x 1 µM L-Arg with 74.12 %. Wounds treated with 1 µM L-Arg had a relative perimeter of 70.92 % and wounds treated with 10 µM L-Arg of 67.94 %. The data was not significant.
On day 7, the untreaded wounds had again the smallest relative top-view wound perimeter with 66.24 %, though the difference to the wounds treated with 10 µM L-Arg is very slight (66.45 %). Wounds treated with 1 µM L-Arg displayed a relative perimeter of 69.55 % and wounds treated with 4 x 1 µM L-Arg of 73.74 %, again the largest value of this day. All data of the relative top-view wound perimeter was not significant.

So, the measurement of the relative top-view wound area and perimeter confirmed what the exemplary pictures already implicate: the wounds heal well *ex vivo*, but the effect of L-Arg on the top-view wound closure is barely noticeable and not significant. However, 1 µM L-Arg seems to have a positive effect on the relative wound volume (compare **Figure 4.15d**). The relative wound volume was 40.38 % on day 6 after treatment with 1 µM L-Arg, the distinctly smallest wound volume measured here. The relative volume of untreated wounds was 70.96 % and of wounds treated with 10 µM L-Arg 80.52 %. Wounds treated with 4 x 1 µM L-Arg barely showed any reduction in wound volume, at day 6 the relative wound volume of wounds treated repetitively with 1 µM L-Arg was 95.76. As the OCT system was only available at 2 of the cultures, no statistics are possible here.

Figure 4.15e shows results of the LDH assay. Just like with DMSO discussed in **Chapter 4.3.1**, here the LDH-release was high on day 0 after the elaborate and time-consuming preparation work. It decreased strongly on day 2, where hardly any differences between the groups were observable. The highest amount of LDH was released by the untreated wounds with 14.06 %, the lowest by the wounds treated with 4 x 1 µM L-Arg with 12.74 %.
For untreated wounds and wounds treated with 4 x 1 µM L-Arg, the relative LDH-release was even lower on day 4 with 11.53 % and 11.68 %. The relative LDH-release of wounds treated with 1 µM L-Arg was 17.35 % and for wounds treated with 10 µM L-Arg 14.70 %.
An increase in LDH-release is visible for all groups at day 6. The untreated wounds released 26.03 % LDH. The highest LDH-release was found in wounds treated with 1 µM L-Arg (36.93 %) and the lowest LDH-release was found in wounds treated with 4 x 1 µM L-Arg (23.44 %). Wounds treated with 10 µM L-Arg had a relative LDH-release of 29.91 %.
On day 8, the untreated wounds had a relative LDH-release of 65.51 %. Only the treatment with 1 µM L-Arg led to a slightly higher LDH-release with 66.84 %. All other L-Arg concentrations reduced LDH-

levels stronger than the untreated wounds. Wounds treated with 10 µM L-Arg released 55.49 % LDH and wounds treated with 4 x 1 µM L-Arg only 46.73 %, the lowest value on this day.

Taken together these results show, that while L-Arg treatment might have some positive effects on the healing process of the WHOC the effect is not strong enough for it to be a useful positive control for the screening.

a)

	0 µM L-Arg	1 µM L-Arg	10 µM L-Arg	4 x 1 µM L-Arg
Day 0		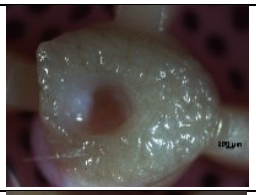		
Day 8				

b)

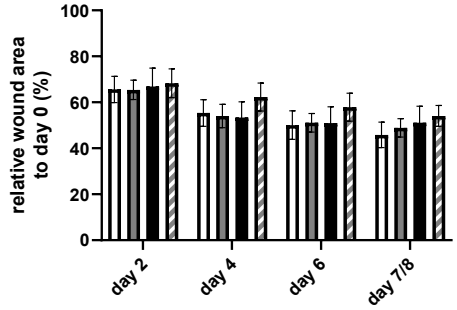

c)

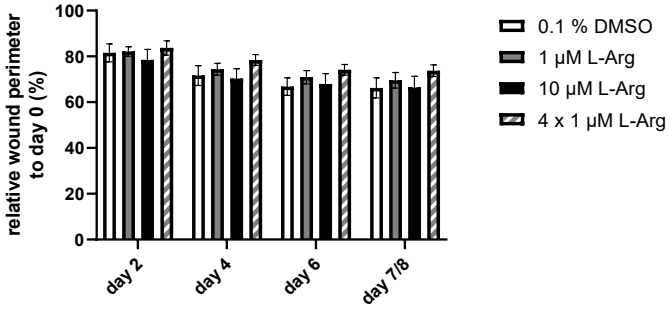

d)

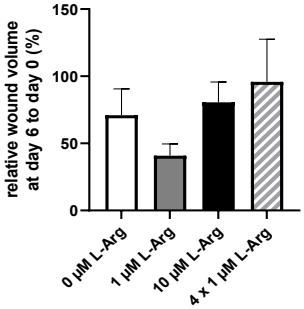

e)

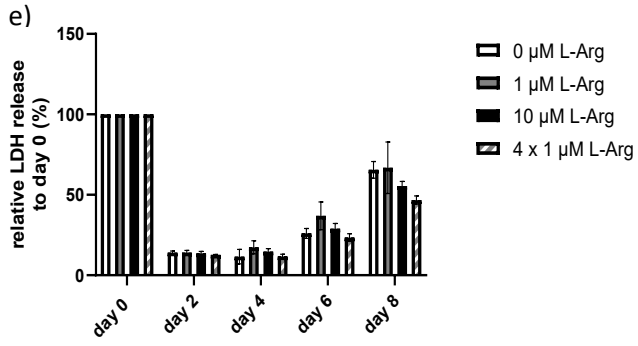

Figure 4.15: Influence of different L-arginine concentrations on the top-view wound healing in the wound healing organ culture model.
Wounds were either untreated (0 µM, negative control) or treated with 1 µM or 10 µM L-arginine (L-Arg) at day 1 for 24 h. Alternatively the wounds were treated with 1 µM L-Arg repetitively during the culture starting at day 1 (4 x 1 µM L-Arg). a) Exemplary pictures of day 0 (day of wounding) and day 8 (end of culture) of the different concentrations tested. b) Relative top-view wound area and c) relative top-view wound perimeter over the course of the culture relative to day 0 (n = 3, 3-4 wounds/condition). d) Wound volume at day 6 obtained by optical coherence tomography relative to day 0 (n = 2, 3-4 wounds/condition). e) Release of Lactate dehydrogenase (LDH) over the course of the culture relative to day 0 (n = 1, measurement in triplicates). Values are depicted as mean ± or + standard error of the mean. One-way ANOVA with Turkey's multiple comparisons test (relative area day all days, relative perimeter day 4, 6 and 7/8) and Kruskal-Wallis' test with Dunn's multiple comparisons test (relative perimeter day 2) was performed for statistical analysis. Data not significant.

4.3.2.1 10 µM sodium gualenate seems to aid top-view ex vivo wound closure in the wound healing organ culture model

Next the influence of SG on the healing process of the WHOC was investigated. The concentrations were chosen as described above for L-Arg. The results of the testing of SG are depicted in **Figure 4.16**.

Figure 4.16a shows exemplary pictures of the wounds at day 0 and day 8. The wounds close well under all conditions. However, a more pronounced closure is visible after one-time treatment with 1 µM and with 10 µM SG.
Determination of the relative top-view area and perimeter confirms this visual impression. The relative top-view wound area during the culture can be found in **Figure 4.16b**. Just as during the entire culture the relative top-view wound area was largest in the wounds of the vehicle control group with 65.14 % on day 2. Wounds treated with 4 x 1 µM SG only had a slightly smaller relative wound area of 62.34 %. The smallest relative area was observed for wounds treated with 10 µM SG: 55.70 %. Treatment with 1 µM led to a relative top-view wound area of 57.98 %.
On day 4, the wounds of the vehicle control had a relative wound area of 54.81 %. Again, the wounds treated with 10 µM SG had the smallest relative area with 40.21 %. The relative top-view wound area of wounds treated with 1 µM SG was 42.43 % and that of wounds treated with 4 x 1 µM was 47.04 %.
The relative wound area decreased to 49.96 % for untreated wounds at day 6, for wounds treated with 4 x 1 µM SG to 43.63 % and for wounds treated with 1 µM to 37.10 %. As before wounds treated with 10 µM SG had the smallest relative area of 36.49 %.
The same was true on day 7/8. Here the relative top-view wound area of wounds treated with 10 µM SG was 29.67 %, the smallest value on this day. Wounds treated with 1 µM SG had a relative area of 38.45 % and wounds treated with 4 x 1 µM SG had a relative area of 42.64 %. Again, untreated wounds showed the highest relative top-view wound area with 48.89 %. Though none of the differences observed in the relative top-view wound area during the WHOC were significant in the overall statistical analysis, a direct comparison between the 0.1 % DMSO group and 10 µM SG treatment showed a significant difference on day 7/8 ($p < 0.05$).

The relative top-view wound perimeter during the culture is displayed in **Figure 4.16c**. On day 2, the relative top-view wound perimeters of all treatment groups are still rather similar. They range from 76.12 % (10 µM SG) to 80.71 % (0.1 % DMSO).
On day 4, the differences in the WHOC became more pronounced. Again, the wounds treated with 0.1 % DMSO as a vehicle control had the largest relative perimeter with a value of 71.58 %. Wounds treated with 1 µM SG showed the smallest relative perimeter of 63.62 % on this day. Treatment with 10 µM SG had a perimeter of 65.25 % and wounds treated with 4 x 1 µM had a relative perimeter of 70.91 %. On this day, the relative top-view wound perimeter of wounds treated with 1 µM SG was 65.95 % and thus slightly larger than on day 2. The relative perimeter of wounds treated with 0.1 %

DMSO decreased to 64.70 % on day 4. Wounds treated with 10 µM SG had the smallest relative perimeter with a value of 56.99 %. The relative perimeter of wounds treated with 4 x 1 µM SG was 65.93 %.
On day 6, the wounds treated with 1 µM SG had the largest relative top-view wound perimeter with 69.95 %. Wounds treated with 4 x 1 µM SG had an almost identical relative perimeter of 65.93 %. The wounds of the vehicle control group had a relative perimeter of 64.70 %. Only wounds treated with 10 µM SG showed a smaller relative perimeter than the vehicle control: 56.99 %.
On day 7/8, again wounds treaded with 10 µM SG had the smallest relative top-view wound perimeter of 55.55 %, followed by wounds treaded with 1 µM SG with a relative perimeter of 60.64 %. The relative perimeter of wounds treated with 0.1 % DMSO was 63.67 % and that of wounds treated with 4 x 1 µM SG was 64.73 %. All measured differences in the relative top-view wound perimeters were not significant.
During the WHOC wounds seem to benefit from one time treatment with SG more than from a repetitive treatment regarding the top-view wound closure.

Figure 4.16d shows the relative wound volume on day 6. Though the wound volume decreased quite a lot in all treatment groups, none of the tested SG concentrations seemed to have a more beneficial effect on the relative wound volume than the vehicle control. The wounds treated with 0.1 % DMSO as vehicle control had a relative volume of 25.94 %, followed by 10 µM SG with 30.36 %, 1 µM SG with 35.58 % and 4 x 1 µM SG with 36.36 %.

The results of the LDH assay are shown in **Figure 4.16e**. As described for the LDH assays in **Chapter 4.3.1** and **Chapter 4.3.2.1** also here the LDH-release is high on day 0 and decreases to day 2 and the differences between the different treatment groups are very slim. They range from 13.42 % (10 µM SG) to 14.21 % (0.1 % DMSO). Over the course of the culture the differences between the groups became more pronounced.
At day 4, the highest LDH-release of 17.82 % was found in the wounds treated with only 0.1 % DMSO. The LDH-release of the wounds treated with 10 µM SG was 14.81 %, which is a slight increase compared to day 2. On the other hand, the LDH-release of wounds treated with 1 µM SG and 4 x 1 µM SG decreased further on day 4 to 12.73 % and 10.92 % respectively.
On day 6, the LDH-release of all samples increased. The highest relative LDH-release was found in the vehicle control group (48.33 %). Treatment with 1 µM SG led to 27.57 % relative LDH-release, treatment with 10 µM SG to 24.48 % and treatment with 4 x 1 µM SG to 18.25 %, the lowest LDH-release on this day.
The increase in LDH-release on day 7/8 in the vehicle control group up to 125.35 % was striking. The wounds treated with different SG concentrations showed a less pronounced increase in LDH-release: 54.88 % for wounds treated with 1 µM SG, 51.52 % for wounds treated with 10 µM SG, and the lowest LDH-release of 44.44 % for wounds treated with 4 x 1 µM SG.

All in all, the treatment with 10 µM SG at day 1 for 24 h shows a positive effect on especially the relative top-view wound area and is thus sufficient as a positive control for the screening.

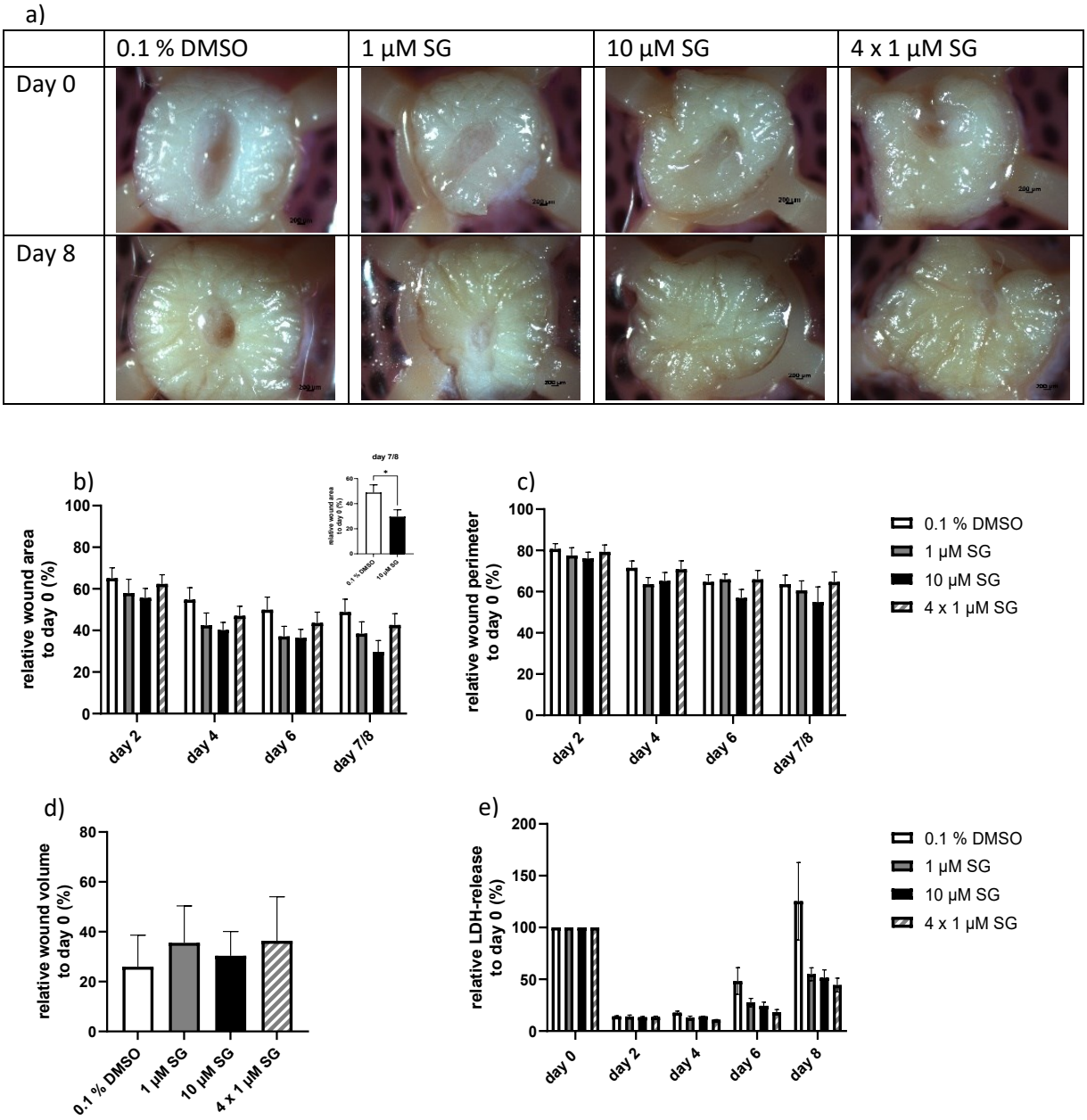

Figure 4.16: Influence of different sodium gualenate concentrations on the top-view wound healing in the wound healing organ culture model

Wounds were either treated with 0.1 % DMSO as a vehicle control or treated with 1 µM or 10 µM sodium gualenate (SG) at day 1 for 24 h. Alternatively the wounds were treated with 1 µM SG repetitively during the culture starting at day 1 (4 x 1 µM SG). a) Exemplary pictures of day 0 (day of wounding) and day 8 (end of culture) of the different concentrations tested, b) relative top-view wound area, and c) relative top-view wound perimeter over the course of the culture relative to day 0 (n = 5, 3-4 wounds/condition), d) wound volume at day 6 obtained by optical coherence tomography relative to day 0 (n = 2, 3-4 wounds/condition), e) release of Lactate dehydrogenase (LDH) over the course of the culture relative to day 0 (n = 1, measurement in triplicates). Values are depicted as mean ± or + standard error of the mean. One-way ANOVA with Turkey's multiple comparisons test (relative area day 2, 4, and 7/8 and relative perimeter all days) and Kruskal-Wallis' test with Dunn's multiple comparisons test (relative area day 6) was performed for statistical analysis. For direct comparison between 0.1 % DMSO and the SG concentrations a t-test was used (except for day 6 where a Mann-Whitney test was used). * $p < 0.05$

4.4 The screening of the Highly Selective Inhibitor Library L3500 revealed 10 promising substances that might aid wound healing

The core piece of this work was the screening of the Highly Selective Inhibitor Library L3500 provided by the company Selleck Chemicals (https://www.selleckchem.com/ last used July 5, 2023) to investigate the influence of those inhibitors on *ex vivo* wound healing. To analyze wound healing in the WHOC 3 parameters were determined: the relative top-view wound area and perimeter over the course of the culture as well as the relative wound volume to day 0 obtained on day 6. For the screening all substances were tested in a concentration of 1 µM and the wounds were treated 24 h with the substance starting at day 1. As it was not feasible to screen all 136 substances in one single screening, the library was divided into inhibitors that were in clinical trials when the screening begun and those that were not (non-clinical trials). Within those groups the inhibitors were screened in smaller sub-screenings with 4 to 22 inhibitors per screening. 0.1 % DMSO and 10 µM SG were always included as vehicle control and positive control respectively. To pass the screening as a potentially promising candidate for further validation, a substance had to perform better than the negative control (preferably also better than the positive control) in at least two of the tree parameters evaluated (area, perimeter, and volume). The histological and immunofluorescence analysis of skin specimen is extremely time-consuming. Therefore, the screening and the validation of the promising candidates was only assessed by macroscopic, non-invasive matters. For better clarity, the following figures of the results of the screening only show the relative top-view area and perimeter at day 7. In **Figure S1** area and perimeter of all days of all inhibitors can be found.

4.4.1 The screening of the clinical trials substances revealed 8 promising candidates which might aid wound healing *ex vivo*

First the 48 clinical-trial substances were screened in 6 sub-screenings.

4.4.1.1 The first sub-screening of the clinical-trials substances showed that treatment with 1 µM S2891 might aid wound healing ex vivo

The results of the first screening are depicted in **Figure 4.17**. Exemplary pictures are shown in **Figure 4.17a**. The relative top-view wound area of day 7 can be found in **Figure 4.17b**. The wounds treated with 0.1 % DMSO as a vehicle control had a relative area of 50.26 %. Treatment with 1 µM S1046 or with 1 µM S8008 led to slightly higher relative top-view wound areas of 51.52 % and 51.03 % respectively. The relative area of wounds treated with 10 µM SG as a positive control was 27.82 %. Only wounds treated with 1 µM S2891 had a smaller relative top-view wound area of 25.24 %. All other inhibitors led to relative top-view wound areas of a size between the vehicle control and the positive control. The positive effect of 1 µM S2891 can be seen during the entire culture, as shown in **Figure S1a**.

The relative top-view wound perimeter of day 7 is shown in **Figure 4.17c**. Wounds of the vehicle control group had a relative perimeter of 64.02 % on day 7. Corresponding to the relative top-view area discussed above, treatment with 1 µM S1046 (68.76 %) and 1 µM S8008 (74.53 %) led to a larger relative perimeter, but the same was true for treatment with 1 µM S1165 (69.82 %) and with 1 µM S2928 (72.55 %). The largest relative top-view wound perimeter was observed in wounds treated with 1 µM S2636. With a value of 95.54 % the perimeter seems to barely have decreased at all during the culture. Treatment with 1 µM S1008 led to a relative perimeter of 61.91 % and treatment with 1 µM S2891 to 56.98 %. Both values are smaller than the vehicle control but larger than the positive control 10 µM SG with a relative perimeter of 54.95 % at day 7, though in the case of 1 µM S2891 the difference is small. On all other days, the relative top-view wound perimeter was smaller if wounds were treated with 1 µM S2891 than after treatment with 10 µM SG (compare **Figure S1a**). Only wounds treated with 1 µM S1574 had a smaller relative perimeter than those of the positive control group on day 7 with a value of 53.62 %.

Figure 4.17d depicts the relative wound volume on day 6. Wounds treated with 0.1 % DMSO as a vehicle control showed an increase in volume to 118.16 % on day 6. Treatment with 1 µM S1574 seems even more harmful for the wound volume, as it is even larger with 168.55 %, though one must keep the large error bar in mind. After treatment with 1 µM S1008 the relative volume was 107.47 %, which is smaller than the vehicle control group but still means an increase in wound volume over the course of the culture. All other treatments led to a reduction in wound volume over the course of the WHOC. Treatment with 10 µM SG led to an especially low relative volume of 42.89 %. Only wounds treated with 1 µM S2929 had a smaller relative wound volume: 31.92 %. All other inhibitors led to wound volumes between 47 % and 75.22 %.

Only treatment with 1 µM S2891 showed a promising effect on two of the three parameters in this first sub-screening, so this is an interesting candidate for further evaluation.

a)

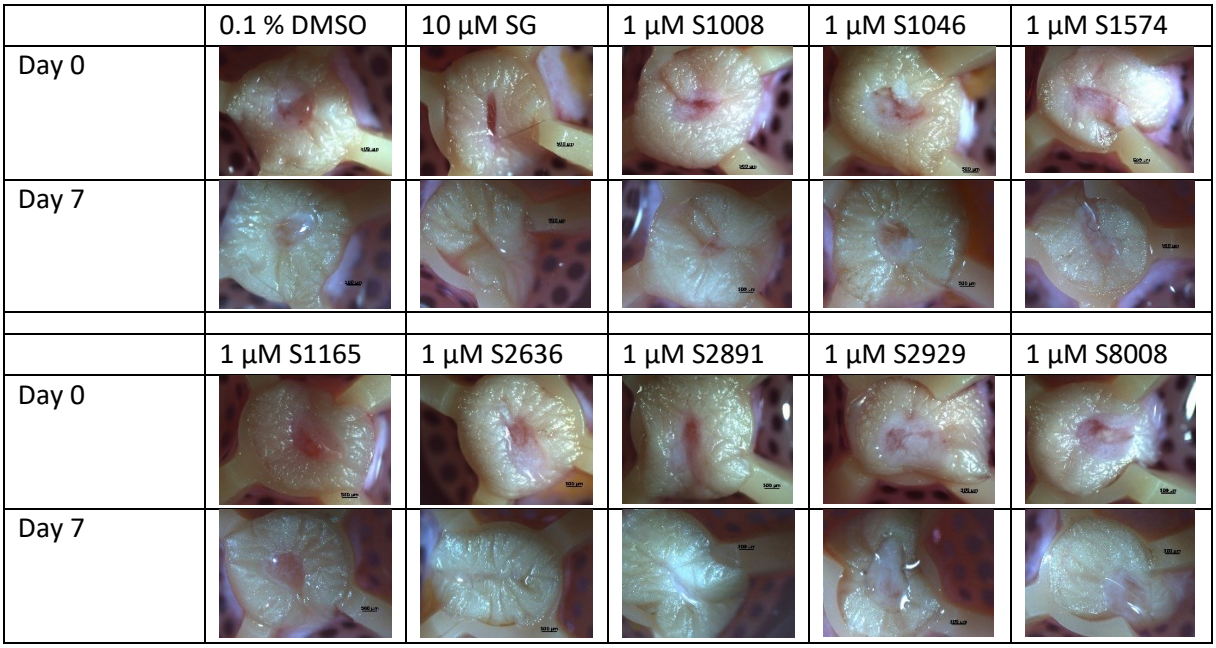

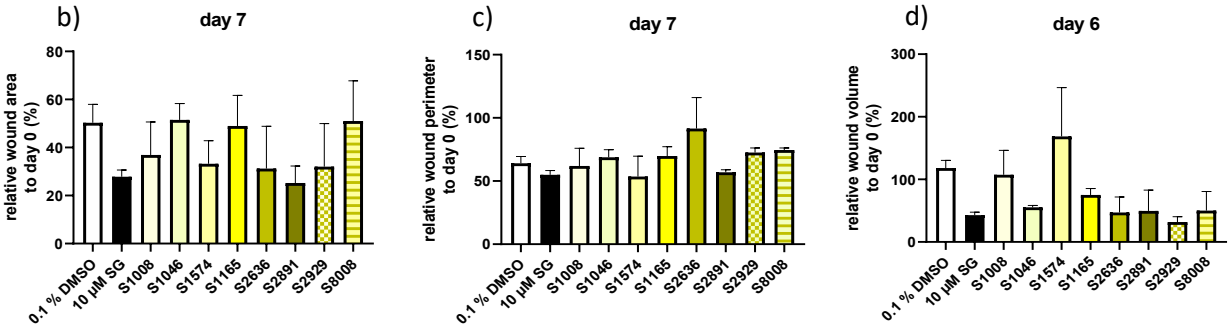

Figure 4.17: Results of the first clinical trials sub-screening in the wound healing organ culture
Shown here are the results of the first sub-screening of the clinical trials substances tested in the wound healing organ culture. Screened here were 8 substances: S1008, S1046, S1574, S1165, S2891, S2929, and S8008. As vehicle control 0.1 % dimethyl sulfoxide (DMSO) was used, as a positive control 10 µM sodium gualenate (SG). All inhibitors were tested in a concentration of 1 µM. The wounds were treated at day 1 for 24 hours. a) Exemplary pictures of day 0 (day of wounding) and day 7 (end of the culture), b) Relative top-view wound area to day 0 at day 7, c) relative top-view wound perimeter to day 0 at day 7, and d) relative wound volume to day 0 at day 6, obtained by optical coherence tomography. n = 1 (2 punches/condition) for all. Values are depicted as mean + standard error of the mean. Statisitcal analysis was not possible because only one biological replicate was performed.

4.4.1.2 The second sub-screening of the clinical-trials substances has to be repeated because the positive control did not work properl

The results of the second clinical sub-screening are shown in **Figure 4.18**. Exemplary pictures comparing the wound healing on day 0 and day 7 can be found in **Figure 4.18a**.
The relative top-view wound area at day 7 is depicted in **Figure 4.18b.** Wounds treated with 0.1 % DMSO as vehicle control had a relative area of 43.77 %, a value slightly lower than that of the positive control: 44.35 % which was unexpected. Treatment with 1 µM S1141 led to a relative area of 54.77 %, the only value higher than those of the controls. All other inhibitors led to relative areas smaller than the vehicle control. The smallest relative area measured was that of wounds treated with 1 µM S2700 with a relative area of 15.04 %.

The relative top-view wound perimeter is shown in **Figure 4.18c**. The wounds of the vehicle control had a relative perimeter of 46.59 %. Like the relative top-view wound area, the relative top-view wound perimeter of the positive control wounds was larger with a value of 64.53 %, though the difference is bigger for the perimeter than for the area. Only treatment with 1 µM S1158 led to smaller relative perimeter than that of wounds treated with 0.1 % DMSO: for wounds treated with 1 µM S1158 a relative perimeter of 45.85 % was measured. All other substances tested here led to a larger perimeter than the vehicle control.

Unlike in the top-view evaluation, for the relative wound volume, the positive control worked, as **Figure 4.18d** shows. The relative wound volume of wounds treated with 0.1 % DMSO had a relative volume of 69.60 %, while wounds treated with 10 µM SG only had a relative volume of 49.01 %. In fact, all substances tested here had a smaller wound volume than the vehicle control. When looking at the graph, the large error bar of the 0.1 % DMSO bar must be kept in mind when judging these results. Treatment with 1 µM S1087 (36.65 %), 1 µM S1110 (40.74 %), 1 µM S1115 (39.23 %), 1 µM S1543 (47.91 %), 1 µM S2149 (28.05 %), 1 µM S2181 (36.80 %), 1 µM S2700 (33.03 %), and 1 µM S2925 (23.03 %) led to smaller relative wound volumes than the positive control 10 µM SG. The smallest wound volume was observed for wounds treated with 1 µM S2925.

As in this sub-screening the positive control did not work properly for the top-view evaluation and some of the wells were infected, all inhibitors that showed a positive effect on the *ex vivo* wound healing in this sub-screening have been tested again in sub-screening 5 and 6 (this means all tested here except S1141 and S1147).

a)

	0.1 % DMSO	10 µM SG	1 µM S1087	1 µM S1110	1 µM S1115
Day 0		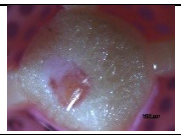			
Day 7	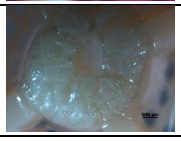	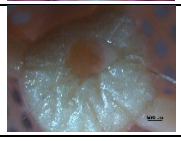	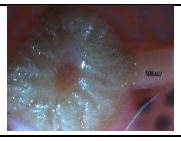		

	1 µM S1141	1 µM S1147	1 µM S1158	1 µM S1453	1 µM S2149
Day 0				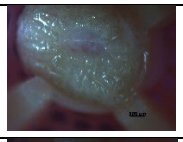	
Day 7	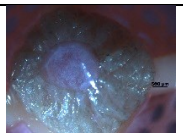			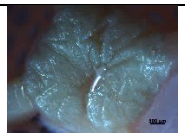	
	1µM S2182	1 µM S2700	1 µM S2925	1 µM S4073	1 µM S6003
Day 0		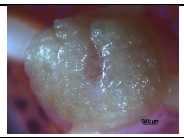	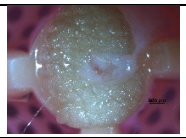		
Day 7	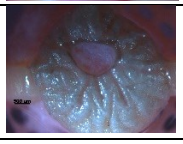	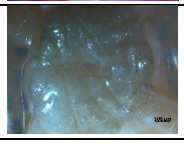		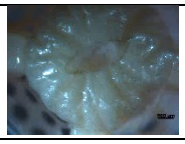	

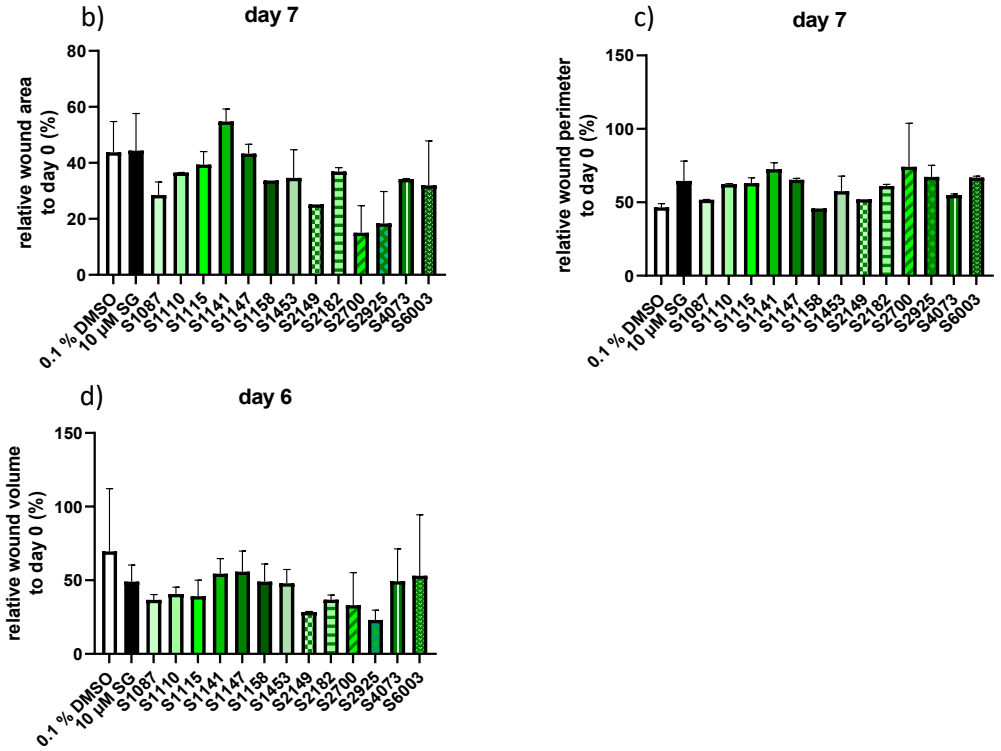

Figure 4.18: Results of the second clinical trials sub-screening in the wound healing organ culture
Shown here are the results of the second sub-screening of the clinical trials substances tested in the wound healing organ culture. Screened here were 13 substances: S1087, S1110; S1115, S1147, S1158; S1453, S2149, S2182, S2700, S2925, S4073, and S6003. As vehicle control 0.1 % dimethyl sulfoxide (DMSO) was used, as a positive control 10 µM sodium gualenate (SG). All inhibitors were tested in a concentration of 1 µM. The wounds were treated at day 1 for 24 hours. a) Exemplary pictures of day 0 (day of wounding) and day 7 (end of the culture), b) relative top-view wound area to day 0 at day 7, c) relative top-view wound perimeter to day 0 at day 7, d) relative wound volume to day 0 at day 6, obtained by optical coherence tomography. n = 1 (2 punches/condition) for all except S1158 and S2149. Values are depicted as mean + standard error of the mean. Statisitcal analysis was not possible because only one biological replicated was performed.

4.4.1.3 The third sub-screening of the clinical-trials substances revealed no promising candidates. Moreover, 1 µM S1130 seems to be the candidate that was most harmful to the wounds in the entire screening

In **Figure 4.19** the results of the third sub-screening are shown. **Figure 4.19a** shows exemplary pictures of the wounds on day 0 and day 7.
In most of the wounds opaque, newly formed epidermis is visible. However, some wounds turned blackish, amongst them wounds treated with 1 µM S1324 and 1 µM S1329. Wounds treated with 1 µM S1130 showed a blackish discoloration. Here, also nearly no newly formed ETs were visible by bare eye. The impression, that S1130 was not beneficial for the top-view wound healing was confirmed by the calculation of the relative top-view wound area, shown in **Figure 4.19b**. Treatment with 1 µM S1130 led to a relative area of 86.61 % at day 7, the largest of all substances tested in this sub-screening. The wounds of the vehicle control group were distinctly smaller with a value of 33.57 % and the wounds of the positive control group had a relative area of 21.37 %. Only two of the tested substances led to a smaller relative area at day 7 than the controls: 1 µM S1055 with 10.20 % and 1 µM S1324 with 15.75 %.

The relative top-view wound perimeter can be found in **Figure 4.19c**. The highest relative perimeter of 100.28 % was found for wounds treated with 1 µM S1324, which means that the perimeter almost stayed the same during the WHOC. Wounds treated with 1 µM S1130 had the second largest relative perimeter with a value of 84.09 %. Wounds of the vehicle control group had a relative perimeter of 47.35 %. The wound treated with 10 µM SG as a positive control showed a larger relative perimeter of 76.50 %. Only two substances led to a smaller perimeter than the wounds treated with 0.1 % DMSO: 1 µM S1055 with a relative perimeter of 39.10 % at day 7 and 1 µM S1139 a perimeter of 32.18 %.

Figure 4.19d shows the relative wound volume at day 6. The largest relative volume was found for wounds treated with 1 µM S1130. Their wound volume was 111.47 %, which means an increase in volume compared to day 0, though the large error bar must be considered. Treatment with 1 µM S1139 also led to a larger wound volume on day 6 than on day 0 (relative volume of 108.65 %). Wounds of the vehicle control group had a relative wound volume of 68.44 % and wounds of the positive control group had a relative wound volume of 60.02 %. Wounds treated with 1 µM S1055 (54.09 %), 1 µM S1091 (35.91 %), 1 µM S1133 (38.44 %), 1 µM S1324 (30.01 %), 1 µM S1456 (46.41 %) had a smaller relative wound volume than the positive controls.

Taking all results together, treatment with 1 µM S1130 did not show a positive effect on any of the studied parameters here. As **Figure S1c** shows this is the case over the entire curse of the culture. In fact, it performed worse than any other substance in the entire screening. The influence of S1130 on the *ex vivo* wound healing in the WHOC will be closer evaluated in **Chapter 4.11**.
Moreover, treatment with S1055 and S1324 had a positive effect on the top-view wound area (and for S1055 also perimeter) on day 7 and on the relative top-view wound volume at day 6. However, treatment with 1 µM of both substances lead to a slower healing in the beginning of the culture (compare **Figure S1c**), the treated wounds only “caught up” with the controls at the end of the culture. As only a limited number of inhibitors could be further validated, I decided against those. For S1324 the fact that skin turned very dark over the course of the culture (compare **Figure 4.19a**) confirmed this decision. The higher relative perimeter of wound treated with 10 µM SG and 1 µM S1324 could be due to a deformation of the wound during healing.

a)

	0.1 % DMSO	10 µM SG	1 µM S1055	1 µM S1078	1 µM S1091
Day 0	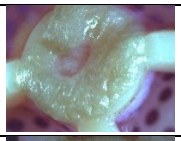			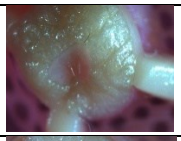	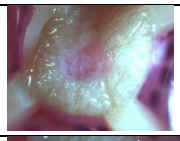
Day 7			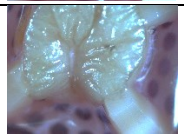	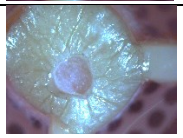	
	1 µM S1130	1 µM S1133	1 µM S1139	1 µM S1208	1 µM S1239
Day 0	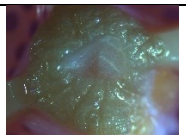	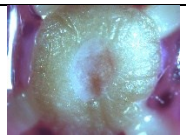	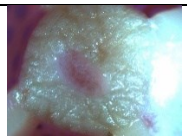	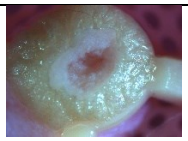	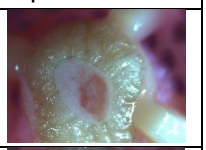
Day 7	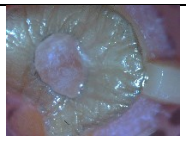			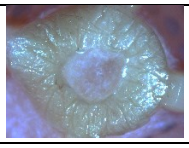	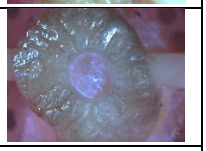
	1µM S1324	1 µM S1329	1 µM S1362	1 µM S1456	1 µM S1525
Day 0				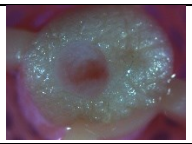	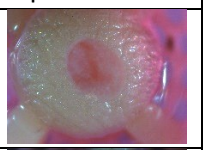
Day 7	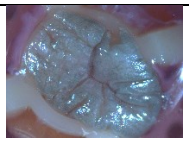		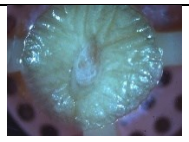	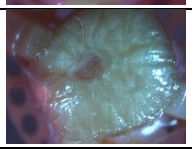	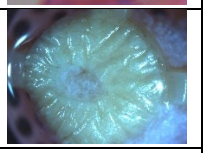
	1 µM S1526				
Day 0					
Day 7	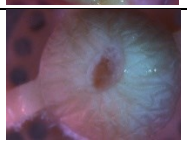				

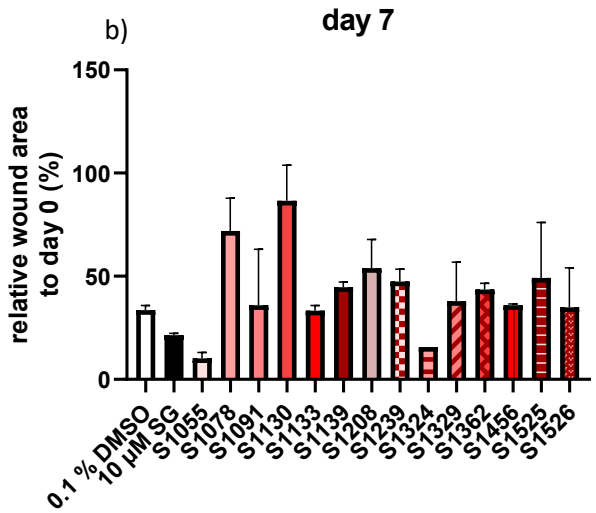

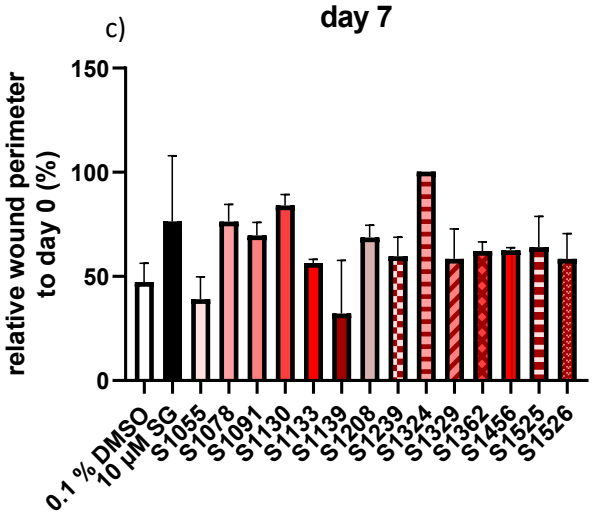

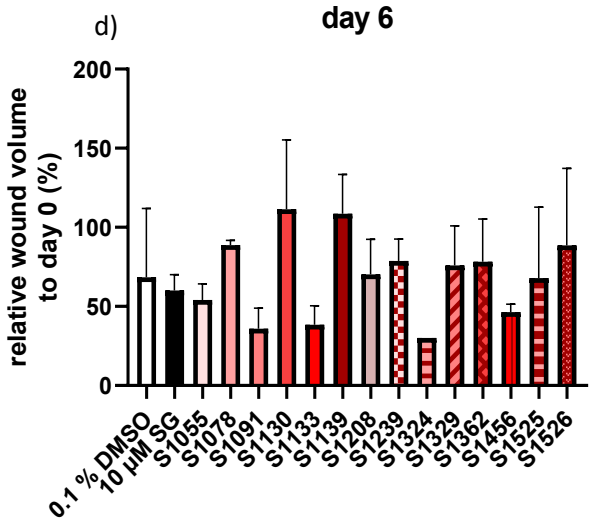

Figure 4.19: Results of the third clinical trials sub-screening in the wound healing organ culture
Shown here are the results of the third sub-screening of the clinical trials substances tested in the wound healing organ culture. Screened here were 14 substances: S1055, S1078; S1091, S1130, S1133, S1139, S1208, S1239, S1324, S1329, S1362, S1456, S1525, and S1526. As vehicle control 0.1 % dimethyl sulfoxide (DMSO) was used, as a positive control 10 µM sodium gualenate (SG). All inhibitors were tested in a concentration of 1 µM. The wounds were treated at day 1 for 24 hours. a) Exemplary pictures of day 0 (day of wounding) and day 7 (end of the culture), b) Relative top-view wound area to day 0 at day 7, c) relative top-view wound perimeter to day 0 at day 7, d) relative wound volume to day 0 at day 6, obtained by optical coherence tomography. n = 1 (2 punches/condition) for all except S1324. Values are depicted as mean + standard error of the mean. Statisitcal analysis was not possible because only one biolgocal replicated was performed.

4.4.1.4 The fourth sub-screening of the clinical-trials substances showed that treatment with 1 µM S2818 might aid wound healing ex vivo

The results of the fourth sub-screening can be found in **Figure 4.20**. **Figure 4.20a** shows the exemplary pictures of wounds on day 0 and day 7. All wounds seem to heal nicely, but the wound area of the control groups and the wounds treated with 1 µM S2818 seems to be especially small at the end of the culture.

The relative top-view wound area at day 7 is depicted in **Figure 4.20b**. Wounds of the vehicle control group had a relative top-view wound area of 27.17 % on day 7 and wounds of the positive control group of 19.20 %. The relative area of wounds treated with 1 µM S2818 was 13.51 %, the smallest area of all inhibitors tested here. S2818 is the only inhibitor that led to a smaller relative area than both controls. The largest relative areas were measured for wounds treated with 1 µM S2232 and 1 µM S2799, with a respective value of 46.99 % and 46.95 %.

Figure 4.20c shows the relative top-view wound perimeter on day 7. Again, only treatment with 1 µM S2818 led to better results than treatment with both controls. The relative area of wounds treated with 1 µM S2818 was 34.39 % on day 7, while that of the vehicle control wounds was 51.15 % and that of the positive control was 42.41 %. All other substances tested in this sub-screening led to larger relative perimeters than the vehicle control. Corresponding to the relative top-view wound area, wounds treated with 1 µM S2232 and 1 µM S2799 had the largest relative perimeter but also large error bars. The relative top-view wound perimeter of wounds treated with 1 µM S2232 was 66.92 % and that of wounds treated with 1 µM S2799 is 67.71 %.

The relative wound volume on day 6 is shown in **Figure 4.20d**. Wounds of the vehicle control group had a relative wound volume of 34.74 %. Only two of the substances tested had a smaller relative

wound volume: 1 µM S2183 with a relative volume of 34.47 % and 1 µM S2549 with a relative volume of 33.35 %, though for both the differences is only small. Surprisingly wounds of the positive control group showed with a value of 42.76 %, a higher relative wound volume than those of the vehicle control. Wounds treated with 1 µM S2818 had the highest relative wound volume of 54.59 %. Treatment with 1 µM S2232 also led to a rather high wound volume of 52.55 %, while treatment 1 µM S2799 led to a comparably low relative wound volume (37.93 %).

Even though treatment with 1 µM S2818 showed no positive effect on the relative wound volume, it was clearly beneficial during the entire WHOC for both relative top-view area and perimeter (compare **Figure S1d**). Its effect on the WHOC will be further validated in **Chapter 4.5**.

a)

	0.1 % DMSO	10 µM SG	1 µM S1541	1 µM S1801	1 µM S2183
Day 0	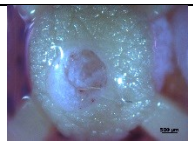				
Day 7	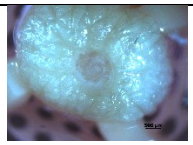	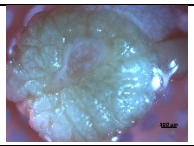	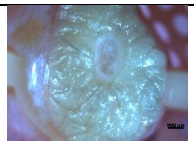	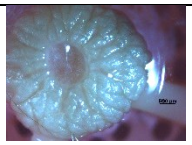	
	1 µM S2216	1 µM S2232	1 µM S2459	1 µM S2507	1 µM S2593
Day 0	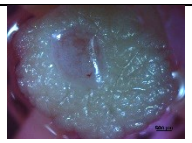		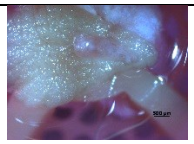		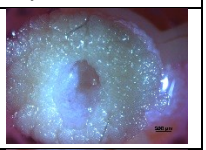
Day 7		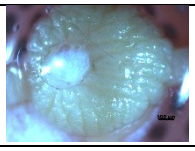			
	1µM S2799	1 µM S2818			
Day 0	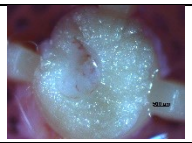	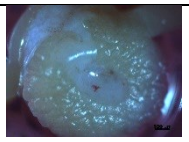			
Day 7		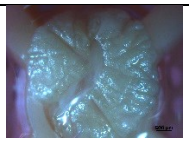			

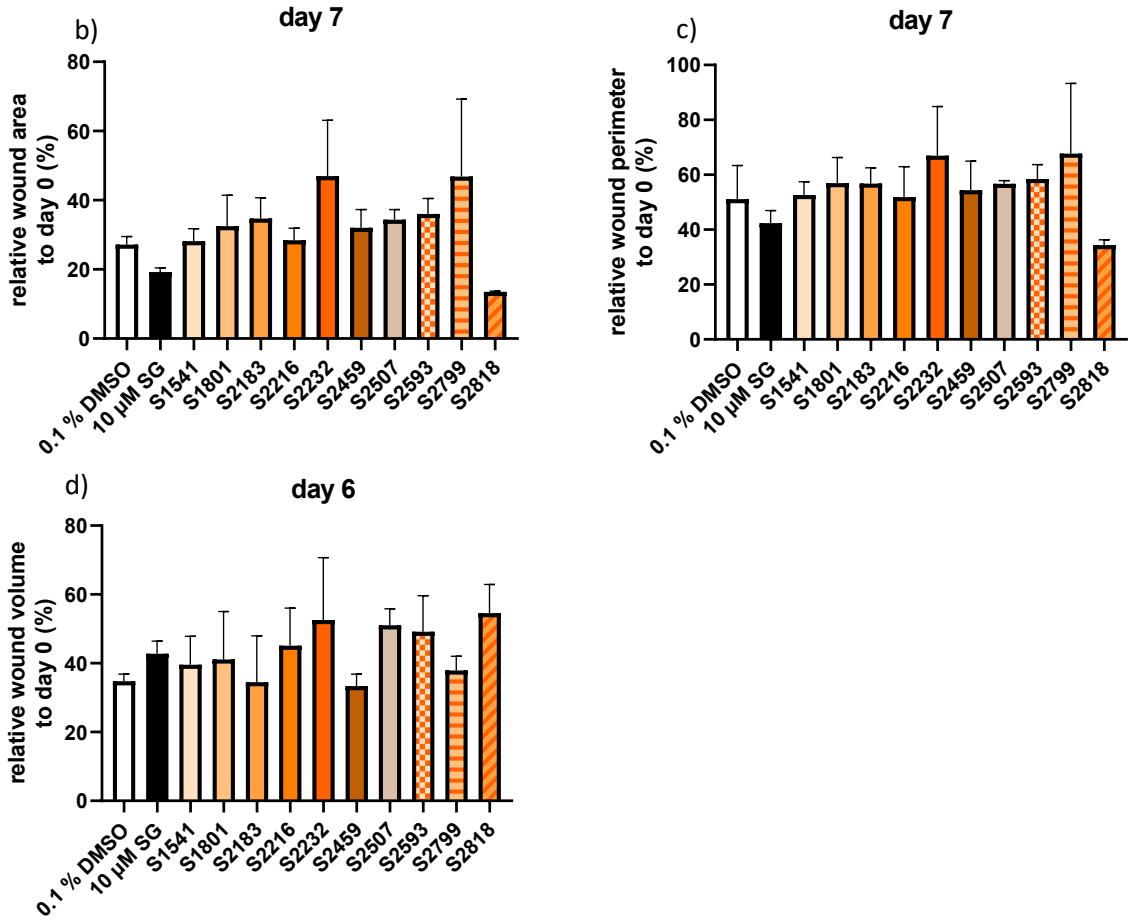

Figure4.20: Results of the fourth clinical trials sub-screening in the wound healing organ culture
Shown here are the results of the fourth sub-screening of the clinical trials substances tested in the wound healing organ culture. Screened here were 10 substances: S1541, S1801, S2183, S2216, S2232, S2459, S2507; S2593, S2799, and S2818 As vehicle control 0.1 % dimethyl sulfoxide (DMSO) was used, as a positive control 10 µM sodium gualenate (SG). All inhibitors were tested in a concentration of 1 µM. The wounds were treated at day 1 for 24 hours. a) Exemplary pictures of day 0 (day of wounding) and day 7 (end of the culture), b) Relative top-view wound area to day 0 at day 7, c) relative top-view wound perimeter to day 0 at day 7, d) relative wound volume to day 0 at day 6, obtained by optical coherence tomography. n = 1 (2 punches/condition) for all. Values are depicted as mean + standard error of the mean. Statisitcal analysis was not possible because only one biolgocal replicated was performed.

4.4.1.5 The fifth sub-screening of the clinical-trials substances showed that treatment with 1 µM S1087, 1 µM S1110, 1 µM S2149, 1 µM S2700 and 1 µM S6003 might aid wound healing ex vivo

Sub-screening five and six are the repetition of sub-screening two. In sub-screening 5 additionally the last remaining clinical trials substances were investigated. For better comprehensibility the inhibitors already tested in sub-screening II are depicted in the same colors and pattern in **Figure 4.21 and 4.22**.

Figure 4.21 shows the results of the fifth sub-screening. **Figure 4.21a** depicts the exemplary pictures of the wounds on day 0 and day 7.
The relative top-view wound area on day 7 can be found in **Figure 4.21b**. Wounds of the vehicle control group had a relative top-view wound area of 33.35 % at day 7 and wounds of the positive control group had a relative top-view wound area of 22.27 %. Treatment with 1 µM S1087 (30.22 %), 1 µM S1110 (24.77 %), 1 µM S1548 (33.89 %), 1 µM S2631 (28.26 %) 1 µM S2700 (32.84 %), 1 µM S2833 (28.14 %), 1 µM S2925 (32.94 %) and 1 µM S6003 (31.24 %) led to relative wound areas between those of the wounds of the vehicle control and the positive control. Only wounds treated with 1 µM S2149 displayed a smaller relative area at day 7 than wounds of the positive control group

with a relative area of 15.66 %. As **Figure S1e** shows, treatment with 1 µM S2149 led to relative top-view wound areas smaller than those of the positive control on all days of the WHOC. Treatment with 1 µM S1087, 1 µM S1110 and 1 µM S6003 had this effect on some of the measurement days.

The relative top-view wound perimeter at day 7 is shown in **Figure 4.21c**. The largest relative perimeter was observed in wounds treated with 1 µM S2149 with a value of 81.21 %. Wounds of the vehicle control group had a relative perimeter of 57.40 % and those of the positive control of 56.55 %. Treatment with 1 µM S1087 (55.8 %), 1 µM S1548 (55.11 %), 1 µM S2631 (51.39 %), 1 µM S2700 (54.35 %), 1 µM S2833 (52.94 %), 1 µM S6003 (43.69 %), 1 µM S7078 (52.86 %), and 1 µM S8046 (54.14 %) led to a smaller relative perimeter on day 7 than the positive control 10 µM S2149. Of those substances, S6003 led to the strongest reduction in relative perimeter at the end of the culture.

Figure 4.21d shows the relative wound volume on day 6. The relative volume of wounds with 1 µM S6003 was 104.15 %, which indicates that the wound volume barely changed during the course of the WHOC and was also the largest relative volume measured in this sub-screening. Wounds of the control group had a relative wound volume of 70.47 % and wounds of positive control group had a relative volume of 51.68 %. Treatment with 1 µM S1110 (41.08 %), 1 µM S2149 (24.51 %), 1 µM S2700 (31.08 %) and 1 µM S8028 (49.85 %) led to a smaller wound volume than that of the positive control wounds. The reduction in relative wound volume was strongest in wounds treated with 1 µM S2149 and 1 µM S2700.

1 µM S2149 seemed to have a positive effect on the relative top-view wound area during the entire WHOC and relative wound volume. For 1 µM S2700 this is true for the relative top-view wound perimeter and the relative wound volume. Both promising candidates will be further validated in **Chapter 4.5**. I also decided to further validate 1 µM S1087, 1 µM S1110 and 1 µM S6003 in **Chapter 4.5**. Their positive effect on the three investigated parameters of wound healing was not as pronounced as for S2149 and S2700 in **Figure 4.21**, but they were convincing over the course of the culture and also performed well in sub-screening 2. For example, in sub-screening 2 the relative wound volume of wounds treated with 1 µM S1087 was distinctly smaller than that of wounds of the positive control group (compare **Figure 4.18d**).

a)

	0.1 % DMSO	10 µM SG	1 µM S1087	1 µM S1110	1 µM S1158
Day 0	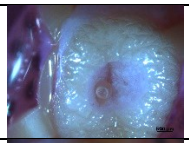	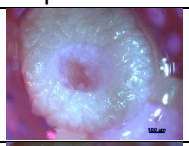			
Day 7			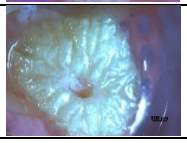		
	1 µM S1548	1 µM S2149	1 µM S2631	1 µM S2700	1 µM S2833
Day 0	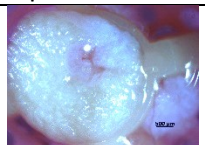		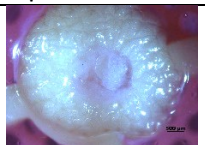	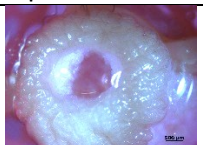	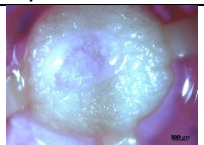
Day 7	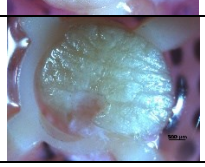	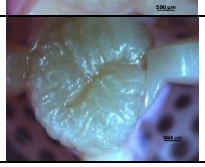		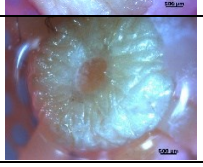	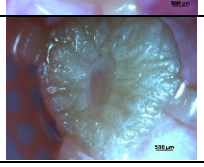
	1µM S2925	1µM S6003/6	1 µM S7018	1 µM S8028	1 µM S8048

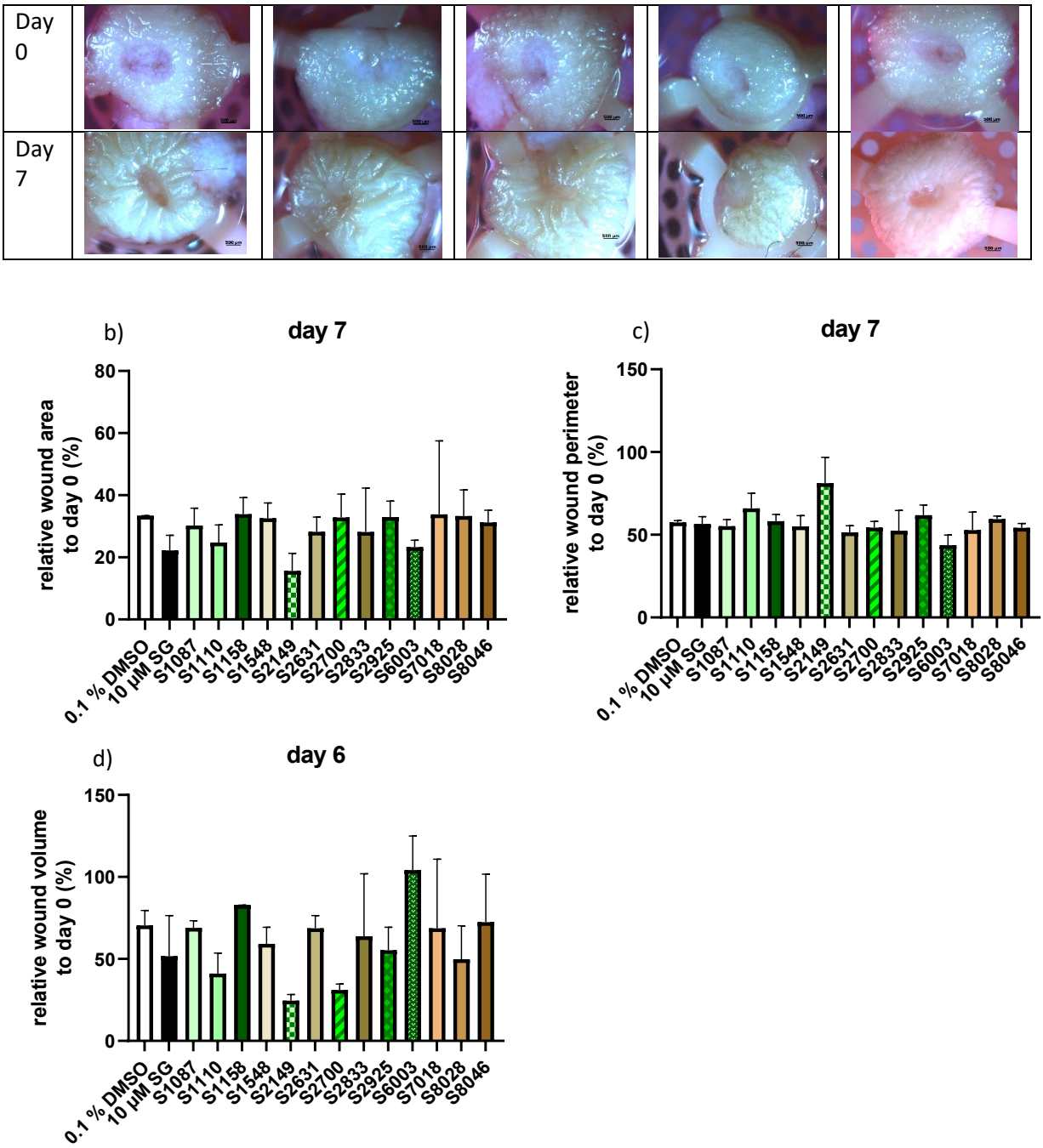

Figure 4.21: Results of the fifth clinical trials sub-screening in the wound healing organ culture
Shown here are the results of the fifth sub-screening of the clinical trials substances tested in the wound healing organ culture. Screened here were 13 substances: S1087, S1110, S1158, S1548, S2149, S2631, S2700, S2833, S2925, S6003, S7018, S8028, and S8046. As vehicle control 0.1 % dimethyl sulfoxide (DMSO) was used, as a positive control 10 µM sodium gualenate (SG). All inhibitors were tested in a concentration of 1 µM. The wounds were treated at day 1 for 24 hours. a) Exemplary pictures of day 0 (day of wounding) and day 7 (end of the culture), b) relative top-view wound area to day 0 at day 7, c) relative top-view wound perimeter to day 0 at day 7, d) relative wound volume to day 0 at day 6, obtained by optical coherence tomography. n = 1 (2 punches/condition) for all. Values are depicted as mean + standard error of the mean. Statisitcal analysis was not possible due to only one biological replicate performed.

4.4.1.6 The sixth sub-screening of the clinical-trials substances showed that treatment with 1 µM S4073 might aid wound healing ex vivo

The results of the last sub-screening of the clinical trials substances can be found in **Figure 4.22**. The 4 substances have all already been tested in sub-screening two. The exemplary pictures area of wounds on day 0 and day 7 are depicted in **Figure 4.22a**.

Figure 4.22b shows the relative top-view wound area at day 7. Wounds of the negative control had a relative area of 47.08 % at day 7. With 57.20 % only treatment with 1 µM S1453 led to a larger relative area. The other substances led to a relative wound area on day 7 between the vehicle control and the positive control (27.53 %). While the relative top-view wound area of wounds treated with 1 µM S4073 with a value of 28.55 % was slightly larger than that of the positive control group on day 7. On day 4 and 6 it was smaller than that of the positive control group (compare **Figure S1f**).

The relative top-view wound perimeter at day 7 is shown in **Figure 4.22c**. Just like the relative wound area, wounds treated with 1 µM S1453 had the largest relative perimeter with a value of 77.17 %. Wounds of the vehicle control group had a relative wound perimeter of 57.95 % and the relative perimeter of the positive control wounds was slightly higher with a value of 58.22 %. Treatment with 1 µM S4073 led to a slightly lower relative perimeter than that of the vehicle control group on day 7: 57.14 %. The smallest relative perimeter at the end of the culture was 54.99 % and was observed for wounds treated with 1 µM S1115.

The relative wound volume on day 6 is shown in F**igure 4.22d**. Again, treatment with 1 µM S1453 led to the largest relative volume of 80.64 %. The wounds of the vehicle control group had a relative volume of 71.61 % and wounds of the positive control group of 40.38 %. Only wounds treated with 1 µM S1115 had an even smaller relative wound volume but only barely (40.34 %). With 67.58 % the relative volume of wounds treated with 1 µM S4073 was larger than that of the positive control but smaller than the vehicle control.
In sub-screening 2 treatment with 1 µM S4073 was beneficial for the relative top-view wound area and for the relative wound volume and in sub-screening 6 it was beneficial for the relative top-view wound area and perimeter and thus will be further validated in **Chapter 4.5**.

a)

	0.1 % DMSO	10 µM SG	1 µM S1115	1 µM S1453	1 µM S2812
Day 0				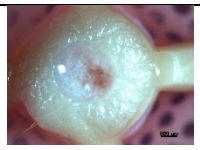	
Day 7	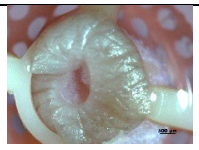		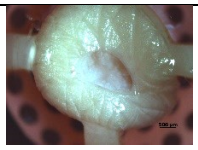	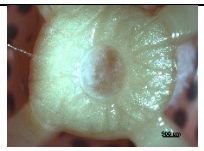	
	1 µM S4073				
Day 0					
Day 7	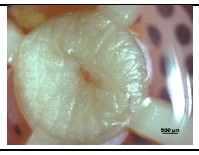				

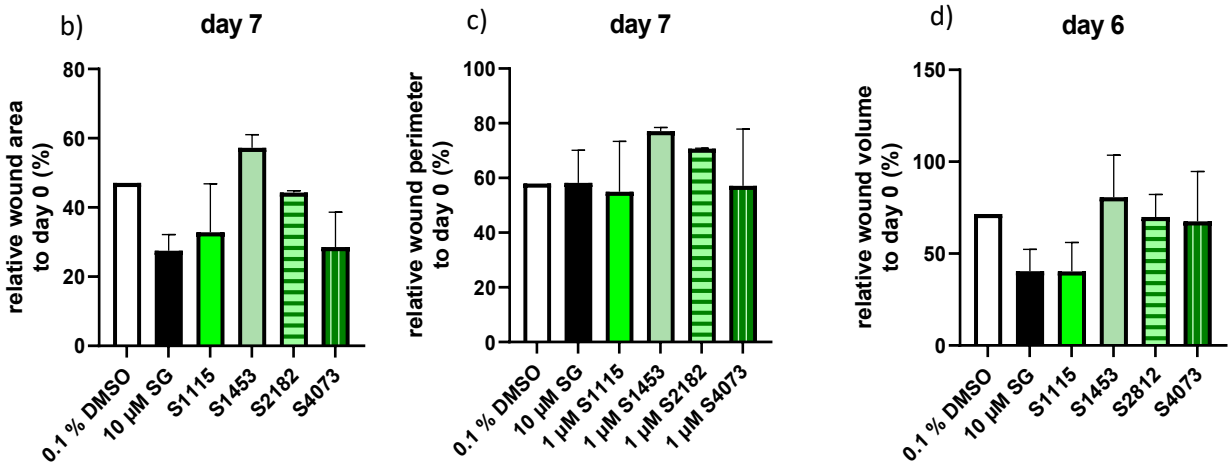

Figure 4.22: Results of the sixth clinical trials sub-screening in the wound healing organ culture
Shown here are the results of the sixth sub-screening of the clinical trials substances tested in the wound healing organ culture. Screened here were 4 substances: S1115, S1453, S2182 and S4007. As vehicle control 0.1 % dimethyl sulfoxide (DMSO) was used, as a positive control 10 µM sodium gualenate (SG). All inhibitors were tested in a concentration of 1 µM. The wounds were treated at day 1 for 24 hours. a) Exemplary pictures of day 0 (day of wounding) and day 7 (end of the culture), b) relative top-view wound area to day 0 at day 7, c) relative top-view wound perimeter to day 0 at day 7, d) relative wound volume to day 0 at day 6, obtained by optical coherence tomography. n = 1 (2 punches/condition) for all except 0.1 % DMSO, where only one punch remained. Values are depicted as mean + standard error of the mean. Statisitcal analysis was not possible because only one biological replicate was performed.

In summary, 8 substances showed a promising effect in the clinical trials screening: S1087, S1110, S2149; S2700, S2818, S2891, S4073 and S6003. **Table 4.1** shows the promising candidates of the clinical trials screening and in which parameters they performed well. As the screening was only performed one time, the effects of these substances were further validated to ensure that they reliably promote wound healing in the WHOC.

Table 4.1: Overview over the 8 promising candidates of the clinical trials screening and the parameters in which they were promising
A substance was defined as promising, when it led to a better wound closure compared to the vehicle control and positive control. Parameters investigated were the relative top-view wound area, relative top-view wound perimeter relative, and wound volume.

Promising in:	S1087	S1110	S2149	S2700	S2818	S2891	S4073	S6006
Top-view area	Yes	Yes	Yes	No	Yes	Yes	Yes	Yes
Top-view perimeter	No	No	No	Yes	Yes	Yes	No	Yes
Volume	Yes	Yes	Yes	Yes	No	No	Yes	No

4.4.2 The screening of the non-clinical trials substances revealed 2 promising candidates

In the second part of the screening, the 88 substances that were not in clinical trials were investigated. This part of the screening was divided into five sub-screenings (non-clinical trials sub-screening one to five).

4.4.2.1 The first sub-screening of the non-clinical trials substances showed that treatment with 1 µM S1169 and 1 µM S1180 might aid wound healing ex vivo

Figure 4.23 shows the results of sub-screening one, the first of the non-clinicals trial screenings. As the exemplary pictures in **Figure 4.23a** show, instead of the EMB-retainers the Freiburg retainers were used.

The relative top-view area on day 7 is shown in **Figure 4.23b**. Wounds of the vehicle control group had a relative top-view wound area of 44.48 % and wounds of the positive control group had one of 39.00 %. Of the tested substances in this screening the following led to smaller relative top-view wound areas than the positive control: 1 µM S1033 (37.52 %), 1 µM S1049 (38.35 %), 1 µM S1079 (16.34 %), 1 µM S1082 (10.61 %), 1 µM S1169 (26.20 %), 1 µM S1180 (16.40 %), and 1 µM S1191 (29.71 %). While for 1 µM S1033 and 1 µM S1049 the difference to the positive control was slight, it was more pronounced for 1 µM S1079, 1 µM S1082, and 1 µM S1180.
The largest relative wound area on day seven was measured for 1 µM S1075 with a relative area of 64.49 %.

Figure 4.23c shows the relative top-view wound perimeter on day 7. Just like the relative wound area, wounds treated with 1 µM S1075 had the largest relative perimeter with a value of 81.00 %. The relative perimeter of wounds treated with 0.1 % DMSO was 71.70 % on day 7 and that of positive controls was 64.02 %. Wounds treated with 1 µM S1078 (63.08 %), 1 µM S1079 (59.18 %), 1 µM S1082 (45.77 %), 1 µM S1169 (57.84 %), 1 µM S1180 (43.78 %), 1 µM S1191 (55.66 %), and 1 µM S1200 (58.55 %) had a smaller top-view wound perimeter than both control groups. Of all those substances, 1 µM S1180 led to the smallest relative perimeter at the end of the WHOC.

The relative wound volume on day 6 can be found in **Figure 4.23d**. The large relative wound volume of 252.42 % of wounds treated with 1 µM S1029 is striking. As here only one biopsy punch was measurable and **Figure 4.23a** shows that the poles of the retainers poke through the wound, this gigantic wound volume might be a measurement error. On the other hand, wounds of both control groups showed a strong decrease in wound volume over the course of the WHOC. The relative volume of the vehicle control wounds was 31.84 % on day 6 and that of the positive control wounds was 24.29 %. 6 of the tested substances in this sub-screening led to a smaller relative volume on day 6 than 10 µM SG as positive control: 1 µM S1079 (21.99 %), 1 µM S1169 (13.21 %), 1 µM S1180 (15.52 %), and 1 µM S1202 (11.38 %).

In the first non-clinical trials sub-screening some highly promising candidates were discovered. For the first time in this screening, inhibitors showed a clear positive effect on all three parameters investigated. Most eye-catching is the positive effect of 1 µM S1180 onto relative top-view area and perimeter as well as relative wound volume. This inhibitor reduces all three parameters distinctly stronger than the controls. The same, though partly to a lesser extent is true for treatment with 1 µM S1169. These two interesting substances were further validated in **Chapter 4.5** regarding their effect on the wound healing in the WHOC.
Treatment with 1 µM S1079 had a positive effect on all parameters at the end of the culture. However, as **Figure S1g** shows, during the WHOC top-view area and perimeter were often higher than that of the vehicle control. That is why this substance was not further validated. Treatment with 1 µM S1082, 1 µM S1191, and 1 µM S1200 also lead to a very visible decrease in relative top-view wound area and perimeter but did not have a beneficial effect on the relative wound volume. As there were now substances found in the non-clinical trials, that had a positive effect on all three investigated parameters, I decided that from the non-clinical trials substances only such would be further validated, that showed a positive effect in all three parameters investigated here.

a)

	0.1 % DMSO	10 µM SG	1 µM S1013	1 µM S1029	1 µM S1033
Day 0					
Day 7			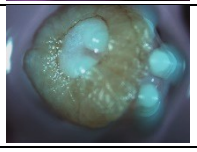	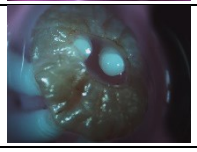	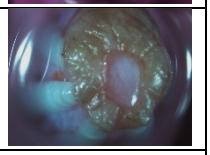
	1 µM S1039	1 µM S1049	1 µM S1061	1 µM S1070	1 µM S1075
Day 0		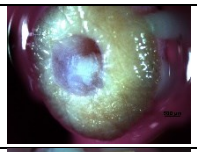		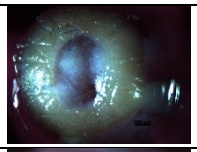	
Day 7	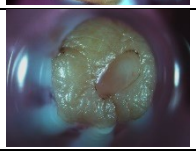	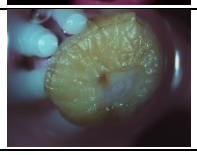	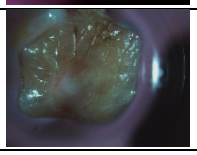	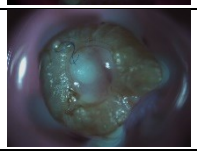	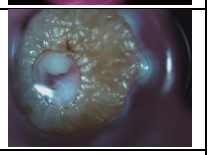
	1µM S1078	1 µM S1079	1 µM S1082	1 µM S1123	1 µM S1169
Day 0		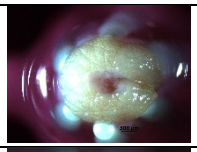	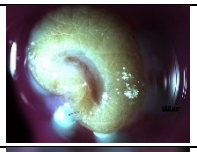		
Day 7	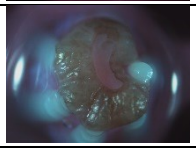	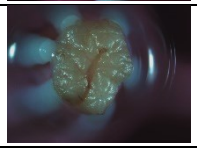	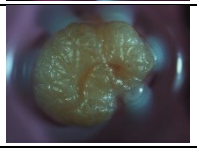	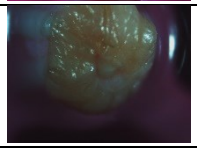	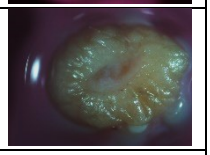
	1 µM S1180	1 µM S1191	1 µM S1200	1 µM S1202	1 µM S1216
Day 0	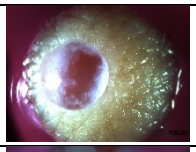	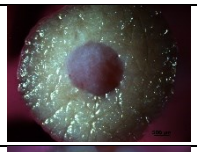			
Day 7			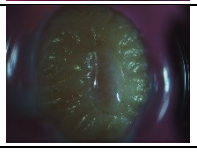	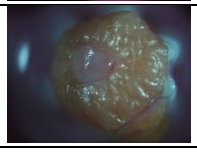	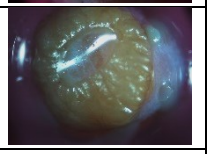
	1 µM S1231				
Day 0					
Day 7					

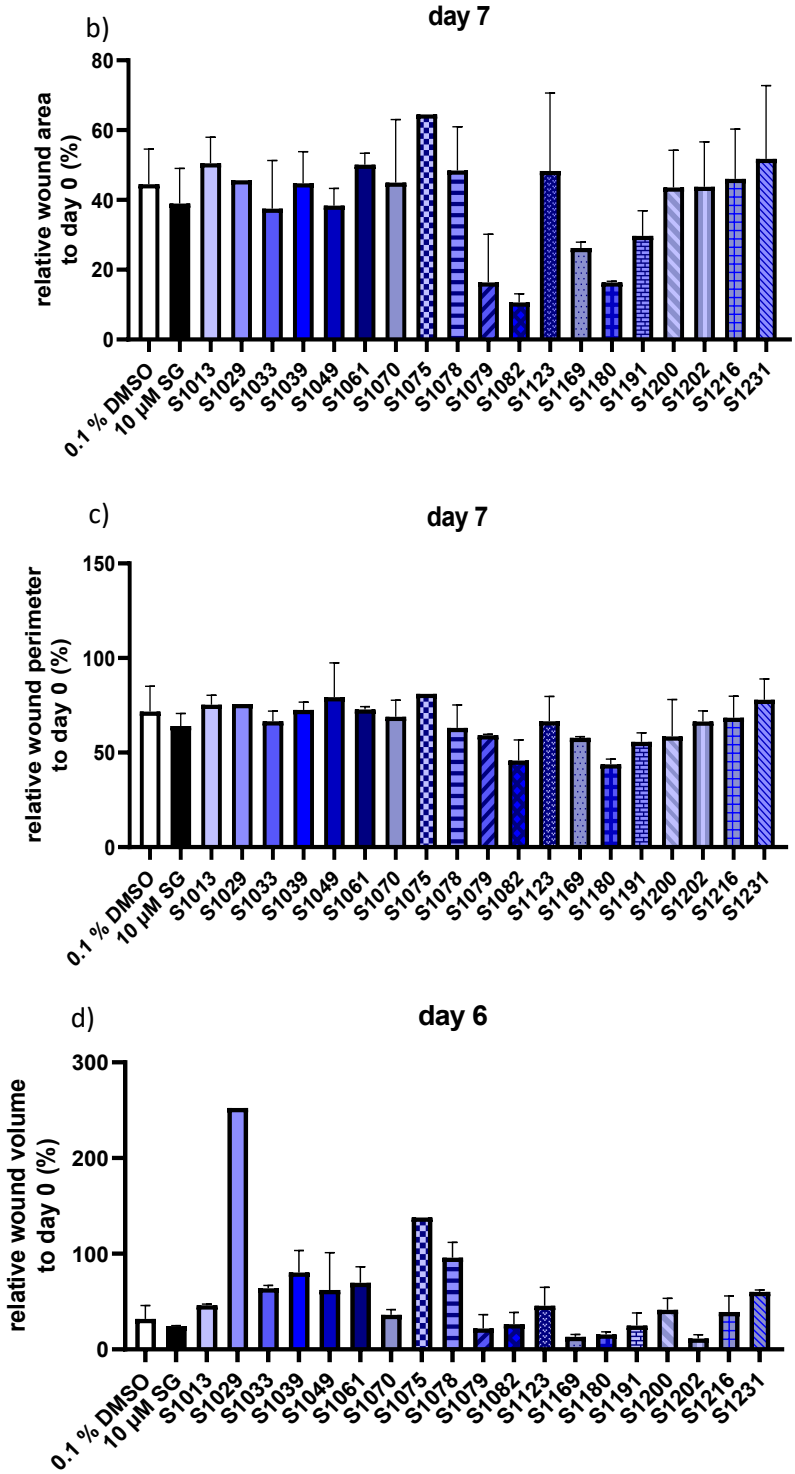

Figure 4.23: Results of the first non-clinical trials sub-screening in the wound healing organ culture
Shown here are the results of the first sub-screening of the non-clinical trials substances tested in the wound healing organ culture. Screened here were 18 substances: S1013, S1029, S1033, S1039, S1049, S1061, S1070, S1075, S1078, S1079, S1082, S1123, S1169, S1180, S1191, S1200, S1216, and S1231. As vehicle control 0.1 % dimethyl sulfoxide (DMSO) was used, as a positive control 10 µM sodium gualenate (SG). All inhibitors were tested in a concentration of 1 µM. The wounds were treated at day 1 for 24 hours. a) Exemplary pictures of day 0 (day of wounding) and day 7 (end of the culture), b) relative top-view wound area to day 0 at day 7, c) relative top-view wound perimeter to day 0 at day 7, d) relative wound volume to day 0 at day 6, obtained by optical coherence tomography. n = 1 (2 punches/condition) for all except S1029 and S1075 where only one punch remained. Values are depicted as mean + standard error of the mean. Statisitcal analysis was not possible because only one biological replicate was performed.

4.4.2.2 The second sub-screening of the non-clinical trials substances showed no promising candidates for further validation

The results of sub-screening eight are depicted in **Figure 4.24**. In the exemplary pictures in **Figure 4.24a** already none of the substances seemed to aid *ex vivo* wound healing more than the positive control.
The relative top-view wound area on day 7 shown in **Figure 4.24b** confirms this finding. Wounds of the vehicle control group had a relative area of 58.66 % on day 7. Treatment with 1 µM S1578 lead to the smallest relative area from all substances tested in this sub-screening with a relative area of 28.29 %, but the area of the positive control group was 27.50 % and thus the smallest relative area on day 7 of all treatment regimes. Treatment with 1 µM S1541 seemed to lead to the largest wound area in this screening with a relative area of 106.83 %. This would mean, that the wound area of wounds treated with 1 µM S1541 did not close at all but instead there was even a slight increase in area during the WHOC. However, the large error bar of these measurements must be kept in mind when assessing the effect of 1 µM S1541.

The relative top-view wound perimeter at day 7 in **Figure 4.24c** showed the same pattern as the relative top-view wound area. The relative top-view wound perimeter of the vehicle control wounds was 81.17 % and that of the positive control wounds was 52.80 %. None of the substances tested in this sub-screening had a smaller relative perimeter than the wounds treated with the positive control 10 µM SG. The largest relative perimeter measured in this sub-screening was 93.60 % in wounds treated with 1 µM S1491. Of all substances tested, treatment with 1 µM S1512 led to the smallest relative perimeter at day 7 of 55.13 %, which was still higher than that of wounds treated with the positive control 10 µM SG.

If you look at the relative wound volume in **Figure 4.24d**, the first thing you notice is the high relative wound volume of the vehicle control group with 172.13 %. This would mean that the wounds of the vehicle control actually increased in volume over the course of the culture. However, this bar has a very high variation between the measured data points and the upper one could be a measurement error. Wounds of the positive control group showed a strong reduction in wound volume over the course of the culture and the relative wound volume at day 6 was 25.19 %. Two of the substances tested here led to a relative volume smaller than the positive control: Wounds treated with 1 µM S1259 had a relative wound volume of 22.35 % and wounds treated with 1 µM S1476 had a relative wound volume of 20.04 %, which is the smallest relative volume measured here.
As none of the substances in non-clinical trials sub screening 2 showed a positive effect on more than one of the parameters studied, they were not further validated.

a)

	0.1 % DMSO	10 µM SG	1 µM S1186	1 µM S1235	1 µM S1250
Day 0		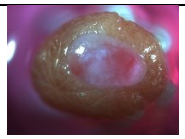	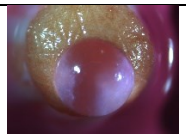	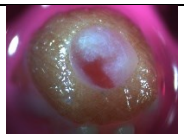	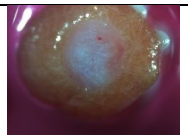
Day 7	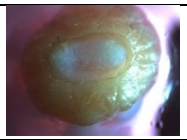	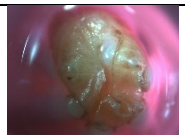	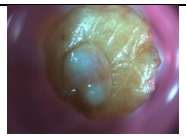		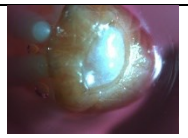

	1 µM S1259	1 µM S1261	1 µM S1289	1 µM S1410	1 µM S1460
Day 0	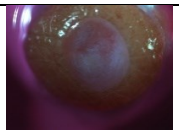		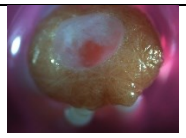	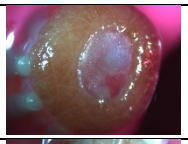	
Day 7	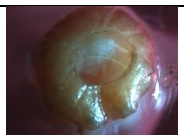		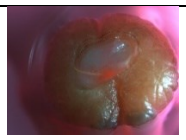	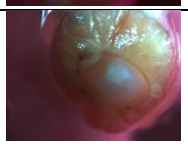	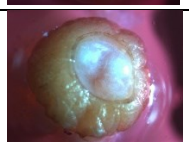
	1 µM S1476	1 µM S1491	1 µM S1498	1 µM S1512	1 µM S1531
Day 0	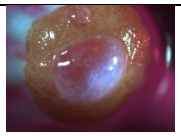	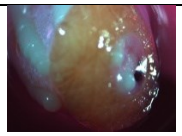	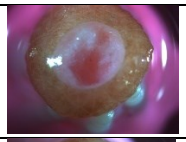	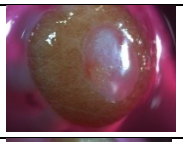	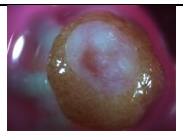
Day 7	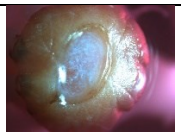	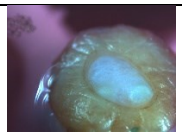	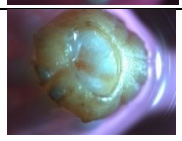	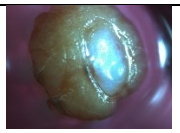	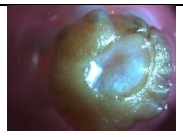
	1 µM S1536	1 µM S1541	1 µM S1544	1 µM S1549	1 µM S1550
Day 0	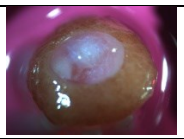	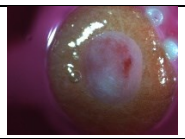		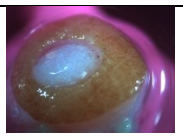	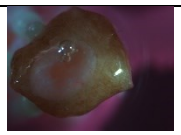
Day 7	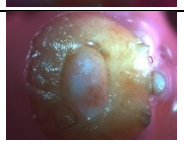	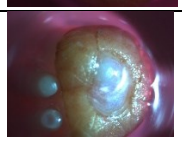		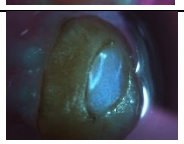	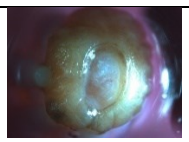
	1 µM S1570	1 µM S1572	1 µM S1577	1 µM S1578	
Day 0	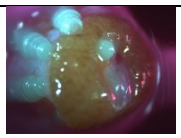	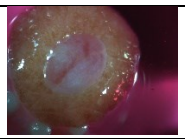	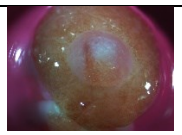	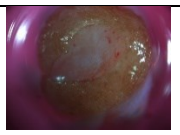	
Day 7	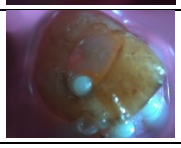	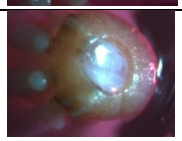	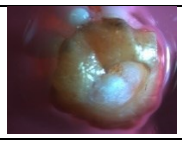	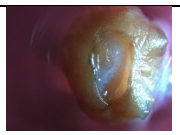	

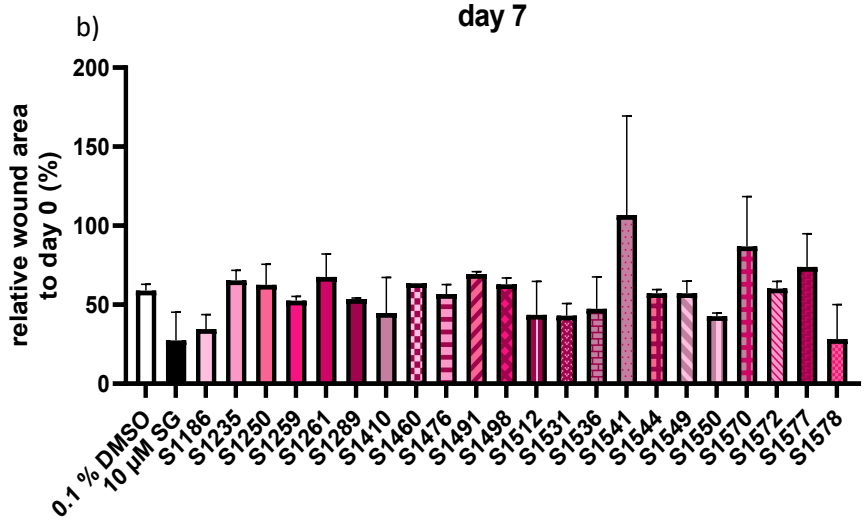

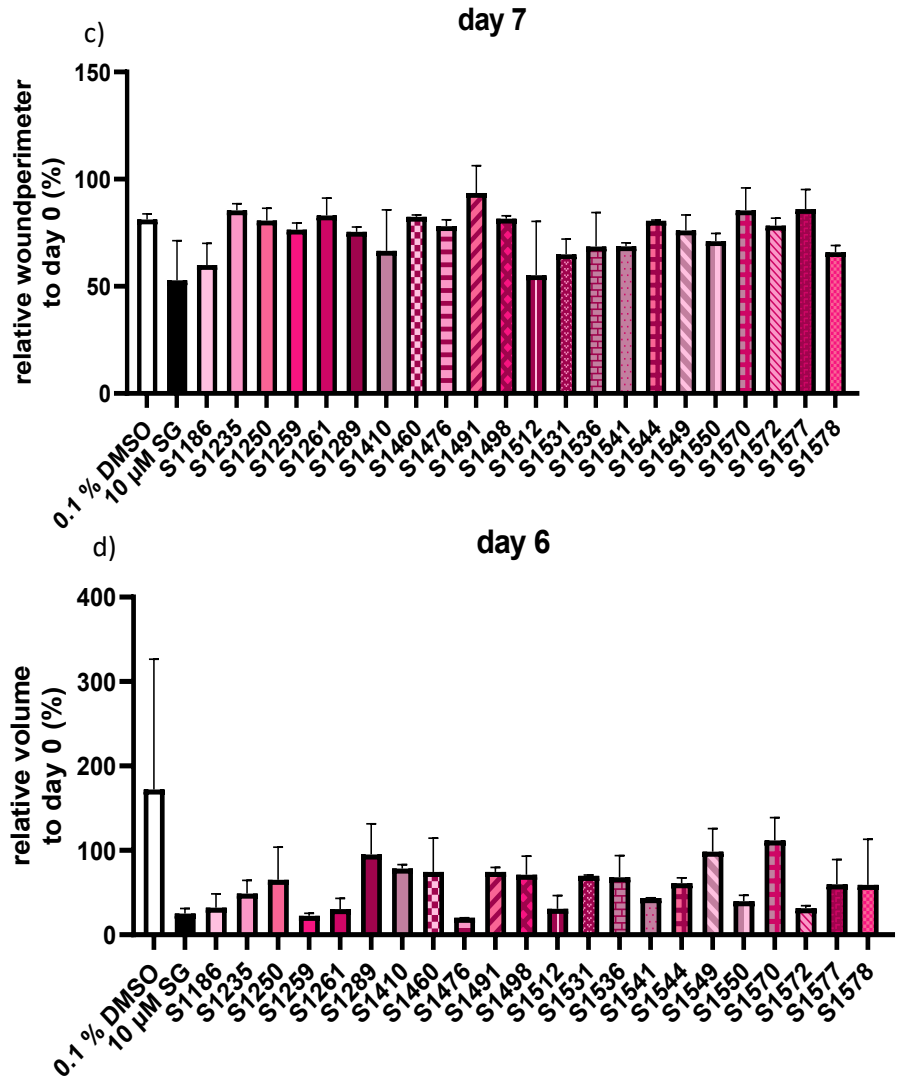

Figure 4.24: Results of the second non-clinical trials sub-screening in the wound healing organ culture
Shown here are the results of the second sub-screening of the non-clinical trials substances tested in the wound healing organ culture, which is the eighth sub-screening in total. Screened here were 22 substances: S1186, S1235, S1250, S1259, S1261, S1289, S1410, S1460, S1476, S1491, S1498, S1512, S1531, S1536, S1541, S1544, S1549, S1550, S1572, S1577; and S1578. As vehicle control 0.1 % dimethyl sulfoxide (DMSO) was used, as a positive control 10 µM sodium gualenate (SG). All inhibitors were tested in a concentration of 1 µM. The wounds were treated at day 1 for 24 hours. a) Exemplary pictures of day 0 (day of wounding) and day 7 (end of the culture), b) relative top-view wound area to day 0 at day 7, c) relative top-view wound perimeter to day 0 at day 7, d) relative wound volume to day 0 at day 6, obtained by optical coherence tomography. n = 1 (2 punches/condition). Values are depicted as mean + standard error of the mean. Statisitcal analysis was not possible because only one biological replicate was performed.

4.4.2.3 The third sub-screening of the non-clinical trials substances showed no promising candidates for further validation

Figure 4.25 shows the results of the third non-clinicals ninth sub-screening. The exemplary pictures can be found in **Figure 4.25a**.

Unlike the second sub screening of the non-clinical trials substances, here wound closure was visible by bare eye in some of the treatment groups, especially wounds treated with 1 µM S1657 or 1 µM S2163 appeared distinctly smaller on day 7 than the wounds of the control groups. The relative top-view wound area on day 7 in **Figure 4.25b** confirms this expression. Wounds treated with 1 µM S1657 had a relative area of 31.27 % and those treated with 1 µM S2163 of 29.76 %, both are distinctly smaller than the wounds of the positive control with a relative area of 47.43 %. Wounds treated with 1 µM S1857 (41.31 %), 1 µM S2199 (36.45 %), and 1 µM S2215 (34.57 %) also had a smaller area than

the positive control 10 µM SG. Treatment with 0.1 % DMSO as a vehicle control led to a relative area of 51.57 % at the end of the WHOC. The relative area was largest for wounds treated with 1 µM S1630 (68.52 %).

The relative top-view wound perimeter at day 7 is shown in **Figure 4.25c**. The relative perimeter of the vehicle control group was 69.74 % and that of the positive control group was slightly higher with a value of 71.39 % (though as **Figure S1i** shows this was not the case on all measurement days). The same 5 substances that were promising in the relative top-view wound area, also led to a smaller relative perimeter than both controls over the course of the culture. At day 7 the relative perimeter of wounds treated with 1 µM S1657 was 49.55 %, that of wounds treated with 1 µM S1857 was 67.68 %, that of wounds treated with 1 µM S2163 was 53.94 %, that of wounds treated with 1 µM S2199 was 62.24 % and that of wounds treated with 1 µM S2215 was 55.40 %. Just like the relative wound area, the largest relative perimeter of 84.15 % was measured for wounds treated with 1 µM S1630.

Treatment with 1 µM S1630 also led to a large relative wound volume on day 6 as **Figure 4.25d** shows. Wounds treated with 1 µM S1630 had a relative volume of 104.77 %, which means the volume of these wounds did not decrease at all during the WHOC. As 1 µM S1630 had a negative effect on all three parameters tested here, one could assume that this substance is harmful for wound healing. Treatment with 1 µM S2012 led to an even larger wound volume of 114.69 %, which indicates an increase over the course of the WHOC. Wounds treated with 0.1 % DMSO had a relative wound volume of 47.48 %. The wound volume of the positive control was 56.53 % and thus higher than that of the vehicle control. The 5 substances that showed a positive effect on the top-view area and perimeter did not lead to a stronger reduction in wound volume than the vehicle control 0.1 % DMSO. Wounds treated with 1 µM S1657 had a relative wound volume of 52.04 %, wounds treated with 1 µM S1857 of 78.86 %, wounds treated with 1 µM S2163 of 59.17 %, wounds treated with 1 µM S2199 of 65.86 %, and wounds treated with 1 µM S2215 of 57.92 %. The only substance tested in this sub-screening that led to a smaller relative wound volume than the positive control was 1 µM S2013 with a relative volume of 34.30 %.
As none of the substances tested in this sub-screening showed a promising effect in all three parameters investigated (unlike the substances out of sub-screening 7), none of the substances tested here was further validated.

a)

	0.1 % DMSO	10 µM SG	1 µM S1630	1 µM S1657	1 µM S1847
Day 0	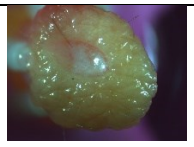	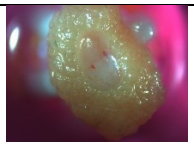	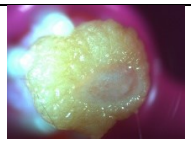	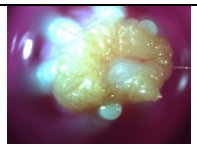	
Day 7		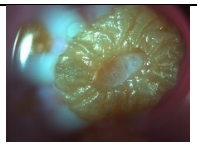	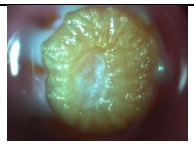	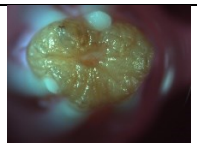	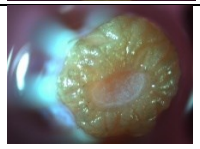

	1 µM S2012	1 µM S2013	1 µM S2131	1 µM S2163	1 µM S2169
Day 0	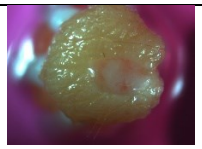	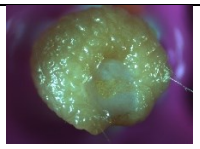	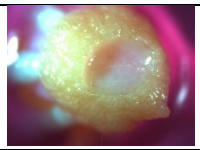		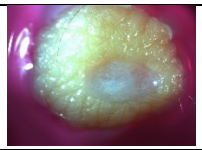
Day 7	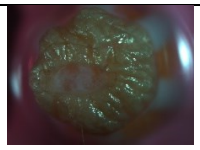	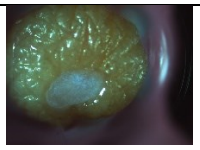	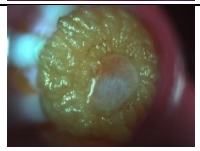	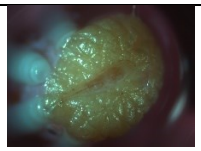	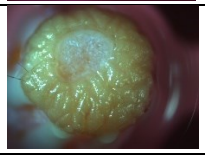
	1 µM S2199	1 µM S2215			
Day 0	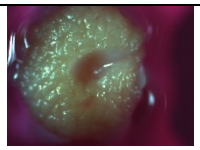	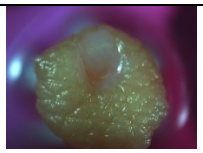			
Day 7	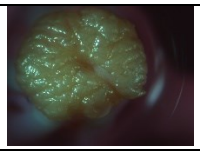	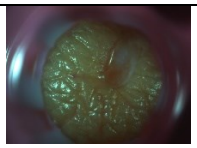			

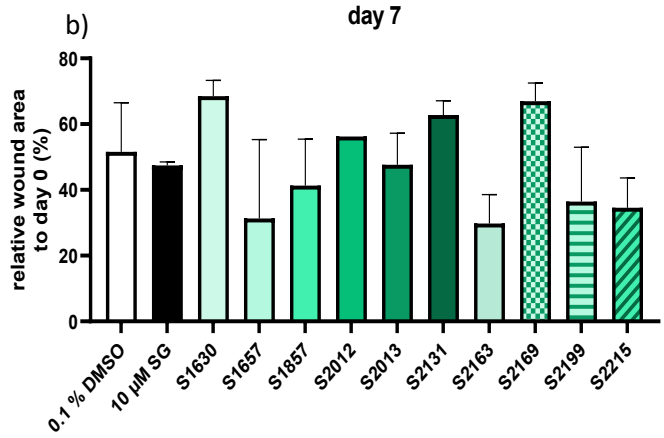

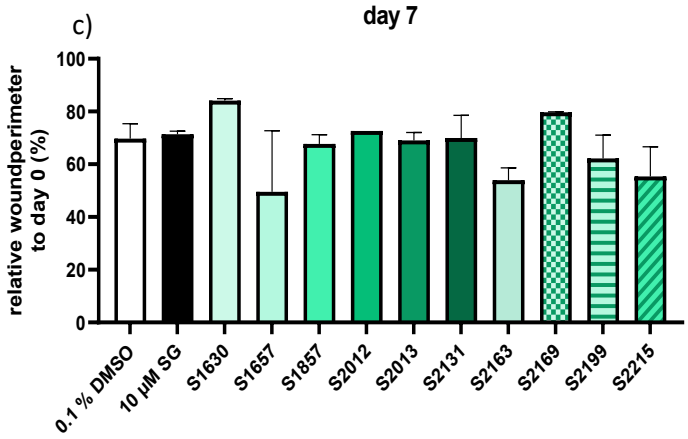

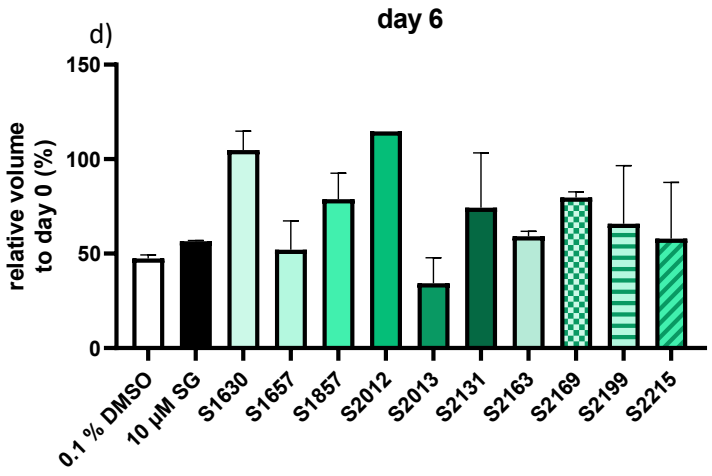

Figure 4.25: Results of the third non-clinical trials sub-screening in the wound healing organ culture
Shown here are the results of the third sub-screening of the non-clinical trials substances tested in the wound healing organ culture. Screened here were 10 substances: S1630, S1657, S1847, S2012, S2013, S2131, S2163, S2169, S2199, and S2215. As vehicle control 0.1 % dimethyl sulfoxide (DMSO) was used, as a positive control 10 µM sodium gualenate (SG). All inhibitors were tested in a concentration of 1 µM. The wounds were treated at day 1 for 24 hours. a) Exemplary pictures of day 0 (day of wounding) and day 7 (end of the culture). b) relative top-view wound area to day 0 at day 7, c) relative top-view wound perimeter to day 0 at day 7, d) relative wound volume to day 0 at day 6, obtained by optical coherence tomography. n = 1 (2 wounds/condition) except S2012 where only one punch remained. Values are depicted as mean + standard error of the mean. Statisitcal analysis was not possible because only one biological replicate was performed.

4.4.2.4 The fourth sub-screening of the non-clinical trials substances showed no promising candidates for further validation

Figure 4.26 shows the results of the fourth non-clinicals trials sub-screening. Exemplary pictures of the wounds on day 0 and day 7 are shown in **Figure 4.26a**. While the wounds of the vehicle control and positive control groups heal well, most of the 16 substances tested here seemed to have no positive effect on the top-view wound healing.

The relative top-view wound area at day 7 in **Figure 4.26b** confirms this impression. Wounds of the vehicle control group had a relative area of 25.96 % on day 7 and wounds of the positive control group had a relative area of 20.00 %. Only treatment with 1 µM S2222 (17.48 %) or 1 µM S4002 (18.85 %) led to a greater reduction in relative top-view wound area than the positive control. **Figure S1j** shows that this is the case for all measurement days for 1 µM S4002 and for 1 µM S2222 except for day 2. At day 7, the largest relative area of 58.25 % was measured for wounds treated with 1 µM S2912.

In accordance with the relative area, treatment with 1 µM S2222 and 1 µM S4002 also led to smaller relative top-view wound perimeters than both controls on all measurement days of the WHOC. **Figure 4.26c** shows the relative top-view wound perimeter on day 7. Here, wounds treated with 1 µM S2222 had a relative perimeter of 37.53 % and wounds treated with 1 µM S4002 had a relative perimeter of 38.19 %. Treatment with 0.1 % DMSO as a vehicle control led to a relative perimeter of 49.31 %. Wounds treated with 10 µM SG as a positive control had a slightly larger area of 50.38 % on day 7. Treatment with 1 µM S2497 (36.07 %) and treatment with 1 µM S3021 (46.70 %) led to a relative perimeter smaller than that of the vehicle control. Wounds treated with 1 µM S2497 had the smallest relative perimeter at the end of this sub-screening and wound treated with 1 µM S3147 (77.07 %) had the largest relative perimeter.

None of the substances that had a positive effect on the top-view wound healing on day 6 shown in **Figure 4.26d**, was beneficial for the relative wound volume. Here only treatment with 1 µM 2915 lead to a greater reduction than treatment with the controls. The wounds of the vehicle control group had a relative volume of 41.91 %, the wounds of the positive control had a relative volume of 35.42 % and the wounds treated with 1 µM S2915 had a relative volume of 23.20 %. The largest relative wound volume of 103.31 % was measured in wounds treated with 1 µM S2683. As none of the substances led to a stronger *ex vivo* wound healing in top-view area, perimeter, and volume, none of the substances were further validated.

a)

	0.1 % DMSO	10 µM SG	1 µM S1247	1 µM S1582	1 µM S2222
Day 0	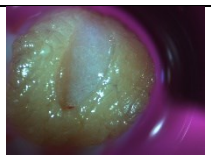	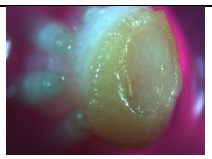	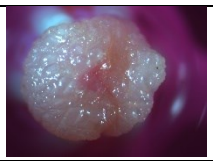		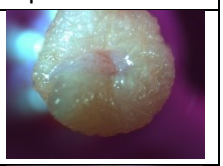
Day 7	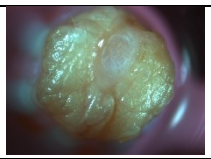	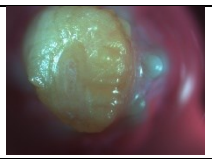	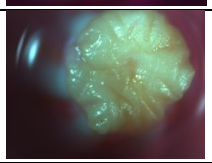	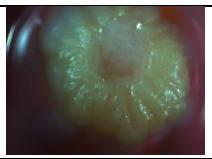	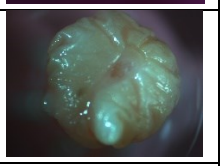
	1 µM S2497	1 µM S2632	1 µM S2638	1 µM S2683	1 µM S2722
Day 0	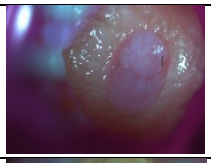	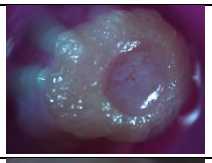	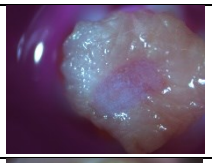	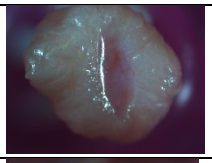	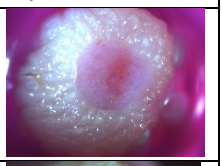
Day 7	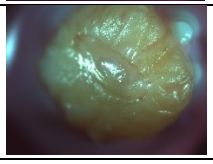	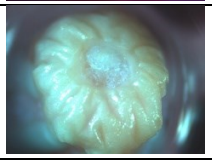	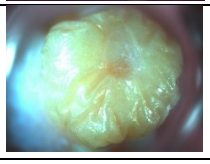		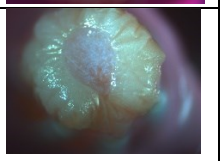
	1 µM S2789	1 µM S2806	1 µM S2824	1 µM S2912	1 µM S2915
Day 0			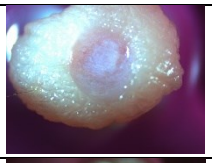		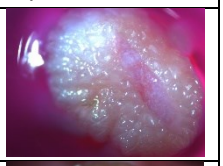
Day 7		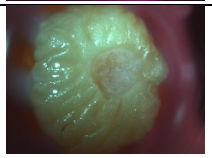			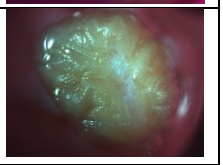
	1 µM S3021	1 µM S3147	1 µM S4002		
Day 0		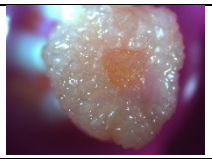			
Day 7		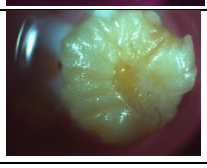	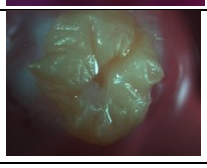		

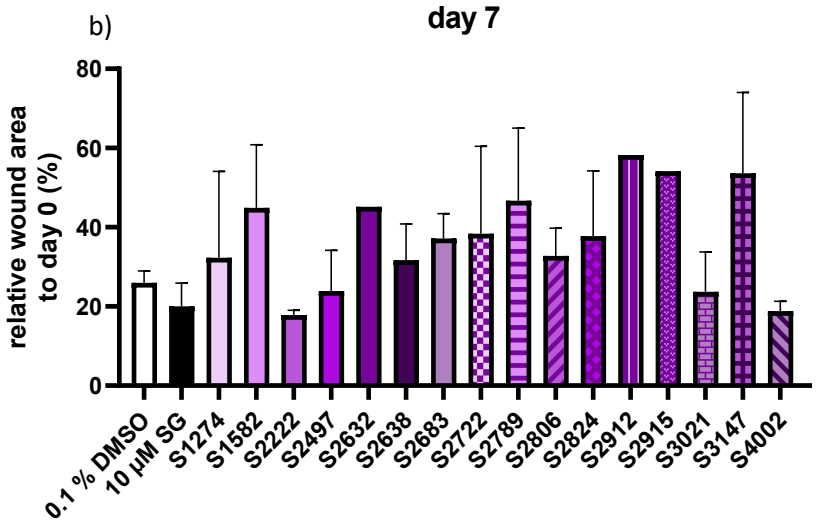
b)
day 7
relative wound area to day 0 (%)
80
60
40
20
0
0.1 % DMSO
10 µM SG
S1274
S1582
S2222
S2497
S2632
S2638
S2683
S2722
S2789
S2806
S2824
S2912
S2915
S3021
S3147
S4002

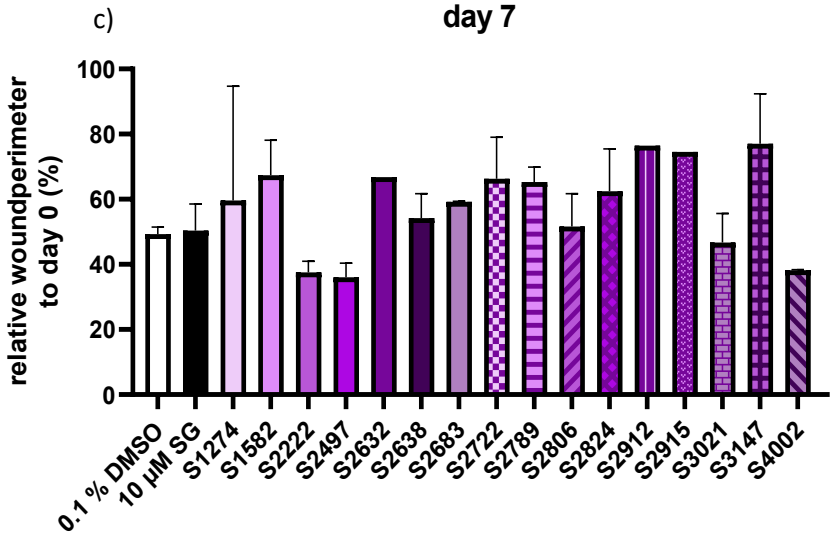
c)
day 7
relative woundperimeter to day 0 (%)
100
80
60
40
20
0
0.1 % DMSO
10 µM SG
S1274
S1582
S2222
S2497
S2632
S2638
S2683
S2722
S2789
S2806
S2824
S2912
S2915
S3021
S3147
S4002

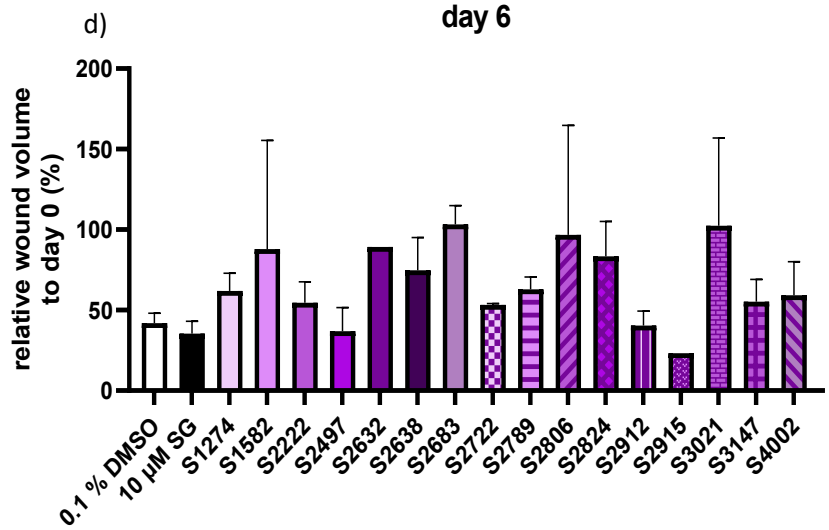
d)
day 6
relative wound volume to day 0 (%)
200
150
100
50
0
0.1 % DMSO
10 µM SG
S1274
S1582
S2222
S2497
S2632
S2638
S2683
S2722
S2789
S2806
S2824
S2912
S2915
S3021
S3147
S4002

Figure 4.26: Results of the fourth non-clinical trials sub-screening in the wound healing organ culture
Shown here are the results of the fourth sub-screening of the non-clinical trials substances tested in the wound healing organ culture, which is the tenth sub-screening in total. Screened here were 16 substances: S1274, S1582, S222, S2497, S2632, S2683, S2722, S2789, S2806, S2824, S2912, S2915, S3021, S3147, and S4002. As vehicle control 0.1 % dimethyl sulfoxide (DMSO) was used, as a positive control 10 µM sodium gualenate (SG). All inhibitors were tested in a concentration of 1 µM. The wounds were treated at day 1 for 24 hours. a) Exemplary pictures of day 0 (day of wounding) and day 7 (end of the culture), b) relative top-view wound area to day 0 at day 7, c) relative top-view wound perimeter to day 0 at day 7, c) relative wound volume to day 0 at day 6, obtained by optical coherence tomography. n = 1 (4 punches/condition for the controls and 2 punches/condition for the substances) except S2632, S2912, and S2915 where only one punch remained. Values are depicted as mean + standard error of the mean. Statisitcal analysis was not possible because only one biological replicate was performed.

4.4.2.5 The fifth sub-screening of the non-clinical trials substances showed no promising candidates for further validation

The results of the final eleventh sub-screening are depicted in **Figure 4.27**. **Figure 4.27a** shows the exemplary pictures of wounds on day 0 and day 7.
The relative top-view wound area at day 7 is shown in **Figure 4.27b**. The relative area of the vehicle control group on day 7 was 48.20 % and that of the positive control was 37.55 %. Wounds treated with 1 µM S2731 had a very slightly smaller relative area of 37.47 % than the positive control at day 7, but the huge error bar must be considered when looking at the effect of this inhibitor. Of all substances of this last sub-screening only 1 µM S2720 and 1 µM S7140 led to a distinctly smaller relative areas than the positive control 10 µM, though especially for 1 µM S2720 the large variation between the measured areas must again be kept in mind when assessing the effect of this inhibitor. Wounds treated with 1 µM S2720 had a relative area of 31.20 % and wounds treated with 1 µM S7140 of 25.45 %, the smallest relative area measured here. The largest relative area of 65.42 % at the end of the WHOC had wounds treated with 1 µM S4009.

Neither 1 µM S2720 (82.55 %), 1 µM S2731 (72.71 %), or 1 µM S7140 (62.70 %) led to a smaller relative top-view perimeter on day 7 than the positive control, as **Figure 4.27c** shows. Instead, the perimeter of 1 µM S2720 and 1 µM S2731 is even larger than the perimeter of the vehicle control group and the relative perimeter of wounds treated with 1 µM S2720 is the largest measured in this culture. Wounds of the vehicle control group had a relative perimeter of 71.07 % and the positive control group had relative perimeter of 61.10 %. The only substance that led to a smaller relative perimeter at the end of the culture was 1 µM S7093 with a value of 44.83 %, the minimum of this WHOC. But also, this measurement has a large error bar.

Figure 4.27c shows the relative wound volume on day 6. The first thing one notices, when looking at this figure is the extremely high relative volume 263.63 % of wounds treated with 1 µM S2893. However, a standard error of the mean this high suggests a measurement error or an outlier. The relative volume of wounds treated with 0.1 % DMSO as a vehicle control group was 96.61 %. The wounds treated with 10 µM SG had a relative volume of 39.91 % at day 6. Treatment with 1 µM S2225 (33.40 %), 1 µM S2550 (29.83 %), 1 µM S7024 (36.77 %), 1 µM S7093 (39.09 %), 1 µM S7111 (32.86 %), and 1 µM S8031 (37.53 %) led to smaller relative volumes than the positive control 10 µM SG.

Just like in sub-screening 2-4 none of the substances tested was better than the controls in all 3 studied parameters and thus none of the substances tested in this sub-screening were further validated.

a)

	0.1 % DMSO	10 µM SG	1 µM S2220	1 µM S2225	1 µM S2516
Day 0		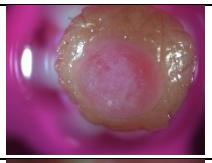		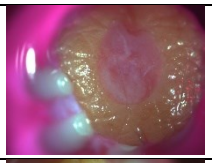	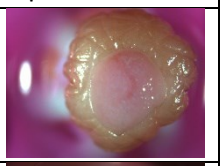
Day 7	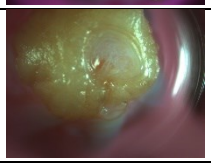	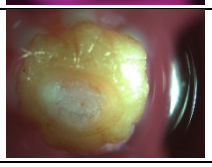	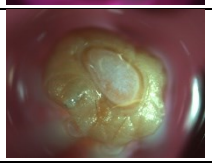	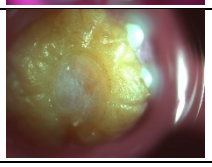	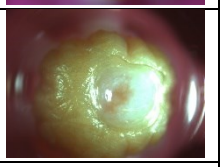
	1 µM S2550	1 µM S2690	1 µM S2720	1 µM S2731	1 µM S2738
Day 0				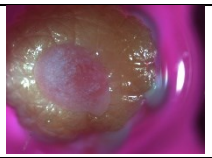	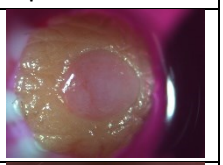
Day 7				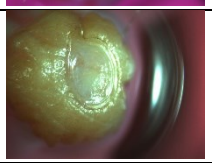	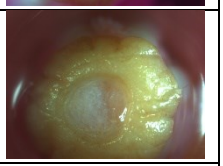
	1 µM S2863	1 µM S4009	1 µM S7024	1 µM S7092	1 µM S7093
Day 0	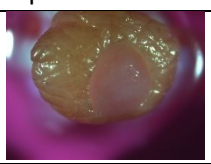	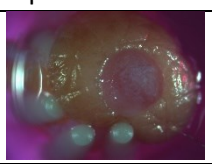	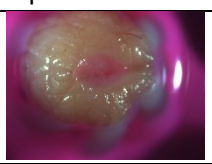	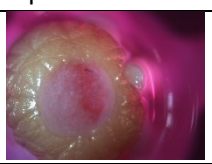	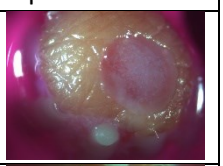
Day 7	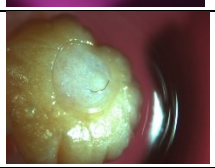	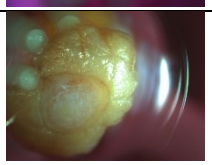	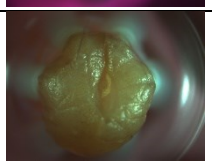	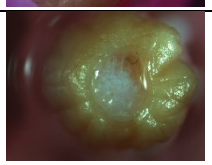	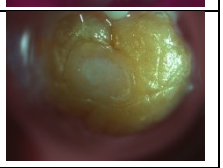
	1 µM S7111	1 µM S7140	1 µM S7153	1 µM S8005	1 µM S8031
Day 0		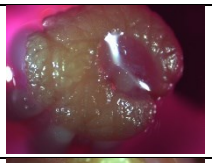			
Day 7	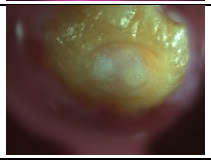	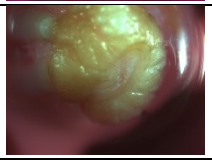	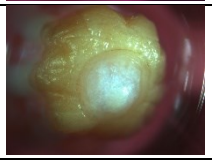	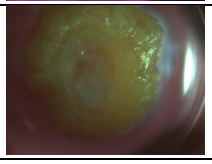	
	1 µM S8032	1 µM S8038	1 µM S8042		
Day 0					
Day 7					

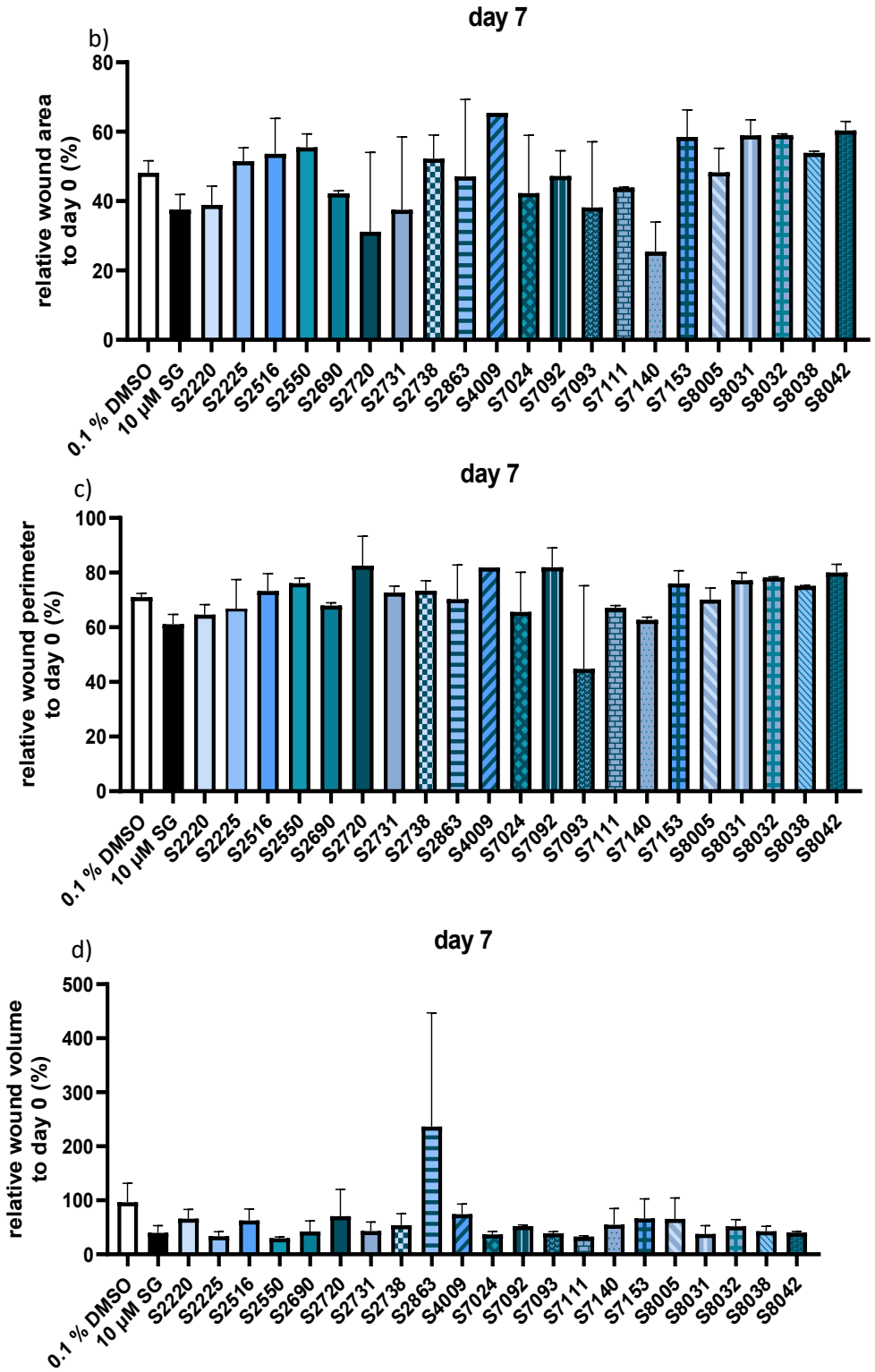

Figure 4.27: Results of the fifth non-clinical trials sub-screening in the wound healing organ culture
Shown here are the results of the fifth sub-screening of the non-clinical trials substances tested in the wound healing organ culture, which is the eleventh sub-screening in total. Screened here were 21 substances: S2220, S2225, S2516, S2535, S2731, S2736, S2690, S2720, S2863, S4009, S7024, S7092, S7093, S7111, S7140, S7153, S8005, S8031, S8032, S8032, S8038, and S8042. As vehicle control 0.1 % dimethyl sulfoxide (DMSO) was used, as a positive control 10 µM sodium gualenate (SG). All inhibitors were tested in a concentration of 1 µM. The wounds were treated at day 1 for 24 hours. a) Exemplary pictures of day 0 (day of wounding) and day 7 (end of the culture), b) relative top-view wound area to day 0 at day 7, c) relative top-view wound perimeter to day 0 at day 7, c) relative wound volume to day 0 at day 6, obtained by optical coherence tomography. n = 1 (4 punches/condition for the controls and 2 punches/condition for the substances) except S4009 where only one punch remained. Values are depicted as mean + standard error of the mean. Statisitcal analysis was not possible due to only one biological replicate performed.

The non-clinical trials screening revealed several substances that would be interesting to further investigate. Only S1169 and S1180 decreased all three parameters greater than the control treatments. These 2 candidates will be further validated. **Table 4.2** shows an overview of the promising candidates that will enter the non-clinical validation.

Table 4.2: Overview over the promising candidates of the non-clinical trials screening and the parameters in which they were promising

An inhibitor was defined as promising, when it led to a better wound closure than the vehicle control and the positive control in all parameters tested. Parameters investigated here were the relative top-view wound area, relative top-view wound perimeter, and wound volume.

Promising in:	S1169	S1180
Top-view area	Yes	Yes
Top-view perimeter	Yes	Yes
volume	Yes	Yes

4.5 The validation revealed 3 successful candidates that aided wound healing and will be further evaluated

The screening of the 136 substances in the library revealed 10 promising candidates, which seemed to have a positive effect on wound healing in the WHOC model. However, as the screening was only performed once, further validation of the promising candidates was necessary to assess the reliability of their effect on wound healing (n = 5). The substances were tested in the same regime as during the screening (1 µM at day 1 for 24 h). Following the organization of the screening this chapter is again divided into the validation of the clinical trials substances and non-clinical trials substances.

4.5.1 The validation of the clinical trials substances showed that S2149 and S2891 were interesting substances to further evaluate

The results of the clinical trials substances can be found in **Figure 4.28**. **Figure 4.28a** shows the exemplary pictures of the wounds treated with the controls or different substances at day 0 (day of wounding) and day 7 (end of culture). Especially in the wounds treated with 1 µM S2891, newly formed ETs are nicely visible.

The relative top-view wound area over the course of the WHOC of all substances tested here is depicted in **Figure 4.28b**. On day 2 the relative area of the vehicle control group was 67.97 %. Only treatment with 1 µM S2700 led to a higher relative area on day 2 than the vehicle control group with a relative area of 71.01 %. Wounds treated with 1 µM S1087 (65.86 %), 1 µM S1110 (63.08 %), 1 µM S2149 (63.43 %), 1 µM 4073 (64.42 %), and 1 µM S6003 (66.15 %) had a relative area between that of the vehicle control wounds and positive control wounds (62.68 %). Treatment with 1 µM S2818 and with 1 µM S2891 led to a relative wound area smaller than that of 10 µM SG as positive control: 59.30 % for 1 µM S2818 and 53.31 % for 1 µM S2891, which is the smallest relative area at day 2.
On day 4, wounds treated with 1 µM S2891 continued to be the smallest with a relative area of 34.17 %. The area was significantly smaller than that of wounds treated with 1 µM S6003 and 0.1 % DMSO as vehicle control (both $p < 0.05$). Wounds treated with 1 µM S6003 had the largest relative area of 54.48 % on day 4, followed by the wounds of the vehicle control with a relative area of 53.80 %. Wounds treated with 1 µM S1110 had a relative area of 49.99 % and wounds treated with 1 µM S2700 one of 52.04 %, both between the relative area of the vehicle control and positive control wounds, which had a relative top-view wound area of 47.65 % on day 4. Next to treatment with 1 µM S2891, also treatment with 1 µM S1087 (44.64 %), 1 µM S2149 (45.64 %), 1 µM S2818 (46.76 %) and 1 µM S4073 (44.00 %) led to a smaller relative wound area than both controls, though these effects were not significant.
On day 6, the relative top-view wound area decreased further for all substances, though to a different degree. For wounds treated with 1 µM S2700 the decrease in wound area was very slight to 51.63 %, which was the largest relative top-view wound area on day 6. On the other hand, wounds treated with 1 µM S2891 showed a strong decrease in relative area and had – just like before – the smallest relative area of 27.43 % on day 6. The difference between wounds treated with 1 µM S2700 and 1 µM S2891 was statistically significant with a significance level of $p < 0.05$. The area of wounds treated with 1 µM S6003 was 44.44 % on day 6, which is slightly larger than the relative area of the vehicle control group of 41.59 %. Treatment with 1 µM S1087 39.27 %, 1 µM S2818 (39.35 %), and 1 µM S4073 (39.42 %) led to wound areas between the vehicle control group and the positive control group, which had a relative wound area of 37.97 % on this day. Wounds treated with 1 µM S1110 (35.16 %) and 1 µM S2149 (37.04 %) had a smaller relative area than the positive control, but for 1 µM S2149 the difference was very slight.

Just like the other days the relative top-view wound area decreased also from day 6 to day 7 for all substances. On day 7, wounds treated with 1 µM S2700 again had the largest relative area with 46.06 % and wounds treated with 1 µM S2891 had the smallest relative area with 23.68 % at the end of the culture. The difference between these two groups was significant ($p < 0.01$). On the last day of the WHOC only 1 µM S2891 led to smaller wounds than those of the positive control group, which had a relative top-view wound area of 32.60 %. Treatment with 1 µM S2149 (34.66 %), 1 µM S2818 (34.15 %), 1 µM S4073 (33.95 %), and 1 µM S6003 (34.08 %) led to a relative wound area between the positive in the vehicle control, which had a relative area of 34.17 %. For all those substances the difference to the vehicle control 0.1 % DMSO is very slight. Wounds treated with 1 µM S1087 (40.08 %) and 1 µM S1110 (37.84 %) had a larger relative top-view wound area than the vehicle control at the end of the WHOC.

Figure 4.28c shows the relative top-view wound perimeter over the course of the WHOC. Similar to the area, the perimeter of wounds treated with 1 µM S2700 was the largest on all measurement days and that of wounds treated with 1 µM S2891 was the smallest. On day 2, wounds treated with 1 µM S2700 had a relative perimeter of 89.39 % and wounds treated with 1 µM S2891 had a significantly smaller relative perimeter of 73.67 %. Treatment with 1 µM S2891 led to a smaller perimeter than the vehicle control 0.1 % DMSO with 83.61 % and the positive control 10 µM SG with 81.59 %, though the differences were not significant. Next to 1 µM S2700, wounds treated with 1 µM S1087 (84.05 %), 1 µM S1110 (85.40 %), and 1 µM S4073 (84.66 %) had a larger perimeter than the vehicle control group on day 2 and next to 1 µM S2891 wounds treated with 1 µM S2149 (81.08 %), and 1 µM S2818 (78.68 %) had a smaller perimeter than the positive control group. The perimeter of wounds treated with 1 µM S6003 (82.58 %) was smaller than that of wounds treated with 0.1 % DMSO but larger than that of wounds treated with 10 µM SG.
Even though the relative top-view wound perimeter decreased in all treatment groups on day 4, 1 µM S2700 still led to the largest relative perimeter with 77.17 %. Next to this inhibitor, also treatment with 1 µM S6003 (73.81 %) led to a relative perimeter large than that of the vehicle control group. On day 4, the relative perimeter of the vehicle control group and the positive control group were very close to each other with a relative perimeter of 72.61 % for the 0.1 % DMSO treated samples and 71.92 % for the 10 µM SG treated samples. Still, wounds treated with 1 µM S1087 (72.36 %) and 1 µM S1110 (72.35 %) had an almost identical, relative perimeter that lay between the control groups on this day. Wounds treated with 1 µM S2149 (69.43 %), 1 µM S2818 (70.91 %), 1 µM S2891 (56.37 %), and 1 µM S4073 (70.28 %) had a smaller relative perimeter than the positive control. The relative perimeter of S2891 was again the smallest measured on day 4. It was in fact significantly smaller than wounds treated with 1 µM S2700 ($p < 0.001$) and 1 µM S6003 ($p < 0.05$).
From day 4 to day 6 the relative top-view wound area of the vehicle control group decreased to 66.87 %. Treatment with 1 µM S2700 (72.98 %) and 1 µM S6003 (67.65 %) led to larger relative perimeter than the vehicle control 0.1 µM DMSO on day 6. Like before, the wounds treated with 1 µM S2700 had the largest relative perimeter. The positive control wounds had a relative perimeter of 61.28 % on day 6. Wounds treated with 1 µM S1087 (66.70 %), 1 µM S1110 (61.37 %), 1 µM S2149 (61.70 %), 1 µM S2818 (64.94 %), and 1 µM S4073 (63.11 %) had a relative perimeter that lay between the control groups. Only treatment with 1 µM S2891 led to a smaller relative perimeter than both controls on day 6. The relative perimeter was 51.63 % and significantly smaller than that of wounds treated with 1 µM S1110 ($p < 0.05$), 1 µM S2700 ($p < 0.001$), and 1 µM S6003 ($p < 0.05$).
At day 7, the end of the culture, the relative top-view wound perimeter had decreased further for all treatment regimes. The relative perimeter of the vehicle control group was 59.04 % and that of the positive control group a slightly lower 57.96 %. The largest relative perimeter was again measured for wounds treated with 1 µM S2700 and was 70.66 % at the end of the WHOC. Next to 1 µM S2700, also

1 µM S1087 (64.59 %) and 1 µM S1110 (62.85 %) led to a larger perimeter than the vehicle control at day 7. Wounds treated with 1 µM S4073 (58.28 %) and 1 µM S6003 (58.95 %) led to a relative perimeter that lay between those of the controls. Finally, treatment with 1 µM S2149 (57.43 %), 1 µM S2818 (57.36 %), and 1 µM S2891 (46.47 %) led to a smaller relative perimeter than the positive control 10 µM SG at the end of the culture. While the difference to the positive control wounds was small for 1 µM S2700 and 1 µM S2818, treatment with 1 µM S2891 led to a clearly visible reduction in relative wound perimeter, resulting in the smallest relative top-view wound perimeter at the end of the WHOC. The difference between wounds treated with 1 µM S2700 and 1 µM S2891 was statistically significant ($p < 0.001$).
The top-view wound healing evaluation clearly showed that treatment with 1 µM S2891 is beneficial for the relative top-view wound area and perimeter. Over the entire course of the culture 1 µM S2891 led to a stronger reduction in area/perimeter than both vehicle and positive control. However, if the whole validation of the non-clinical trials is assessed, these differences are not significant except for the relative top-view area on day 4 (compare **Figure 4.28b**). That is why treatment with 0.1 % DMSO and 1 µM S2891 was compared directly regarding the relative top-view wound area in **Figure 4.28d** and relative top-view wound perimeter in **Figure 4.28e**. In the direct comparison the relative top-view wound area of wounds treated with 1 µM S2891 was significantly smaller than that of the vehicle control over the entire course of the WHOC. On day 2 and day 7 the significance level was $p < 0.05$, on day 4 it was $p < 0.001$, and on day 6 it was $p < 0.01$. The relative top-view wound perimeter was significantly smaller in the direct comparison to 0.1 % DMSO on day 2 ($p < 0.05$), day 4 ($p < 0.01$), and day 6 ($p < 0.01$).

The positive effect of 1 µM S2891 on the top-view wound closure, could not be found on the relative wound volume on day 6, which is shown in **Figure 4.28e**. Unfortunately, the OCT system was only available for two of the cultures, so no statistics were possible here. Here, the smallest relative wound volume of 22.89 % was observed for wounds of the vehicle control group. Wounds treated with 1 µM S2149 had the second smallest relative wound volume of 23,94 %. Treatment with 1 µM S2891 led to a relative volume of 31.93 %. Unlike in the top-view evaluation, here wounds treated with 1 µM S2700 had a smaller relative volume (28.87 %) than those treated with 1 µM S2891, although the difference is rather small. Positive control wounds had a relative volume of 40.93 %. Only wounds treated with 1 µM S1087 had a larger relative wound volume of 45.73 %, the other tested inhibitors had relative volumes between the two control groups.
To summarize, S2891 is the only substance validated here that showed a significance positive effect on the relative top-view area and perimeter. As it has a strong influence on the wound closure and passed the validation successfully, S2891 was further investigated to find the optimal treatment concentration (see **Chapter 4.6**).
The results of the validation of the clinical trials substances can be found in **Table 4.3**. Treatment with 1 µM S2149 did not show a very strong positive effect on the *ex vivo* wound healing, but this substance is currently in clinical trials for type two diabetes (https://www.selleckchem.com/products/GSK1292263.html last used December 25, 2022). A pathological wound model based on Post *et al.* (Post *et al.*, 2021) was planned later in this work (**Chapter 4.12** and **4.13**) and patients with type 2 diabetes often have problems with chronic wounds, so it would be interesting to see if S2149 might have a stronger positive effect on wound healing under pathological conditions. So S2149 was further investigated as well to find the optimal treatment concentration (see **Chapter 4.7**).

a)

	0.1 % DMSO	10 µM SG	1 µM S1087	1 µM S1110
Day 0	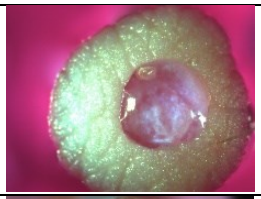			
Day 7			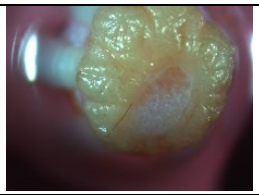	
	1 µM S2149	1 µM S2700	1 µM S2818	1 µM S2891
Day 0		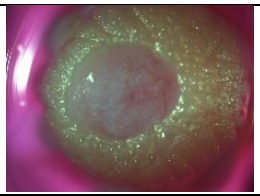	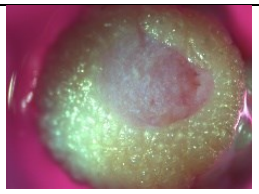	
Day 7		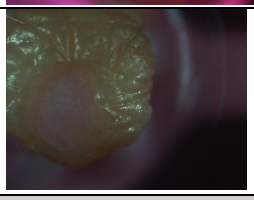	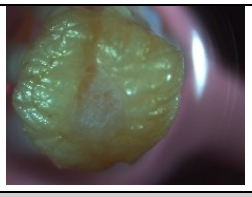	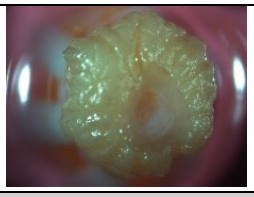
	1 µM S4073	1 µM S6003		
Day 0				
Day 7		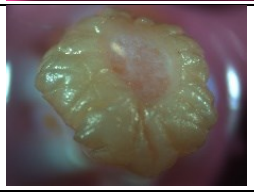		

b)

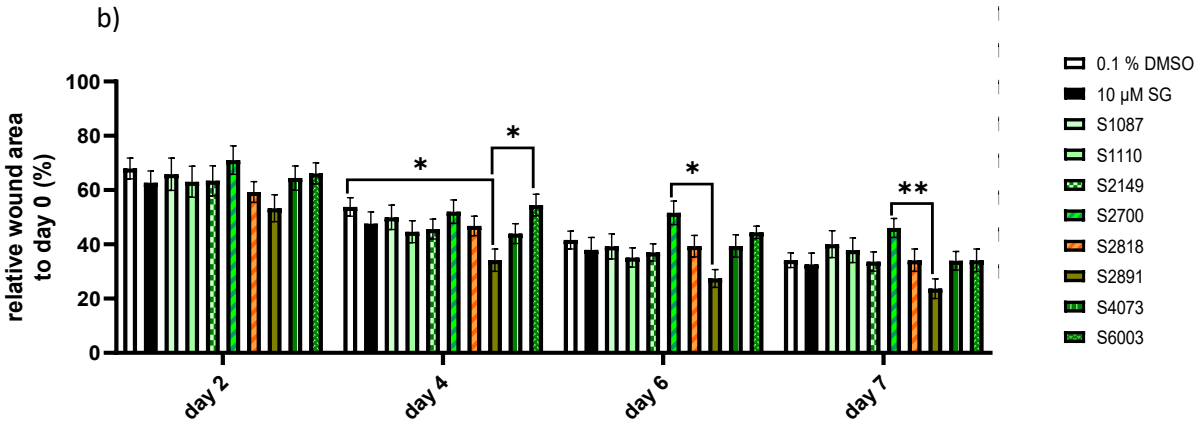

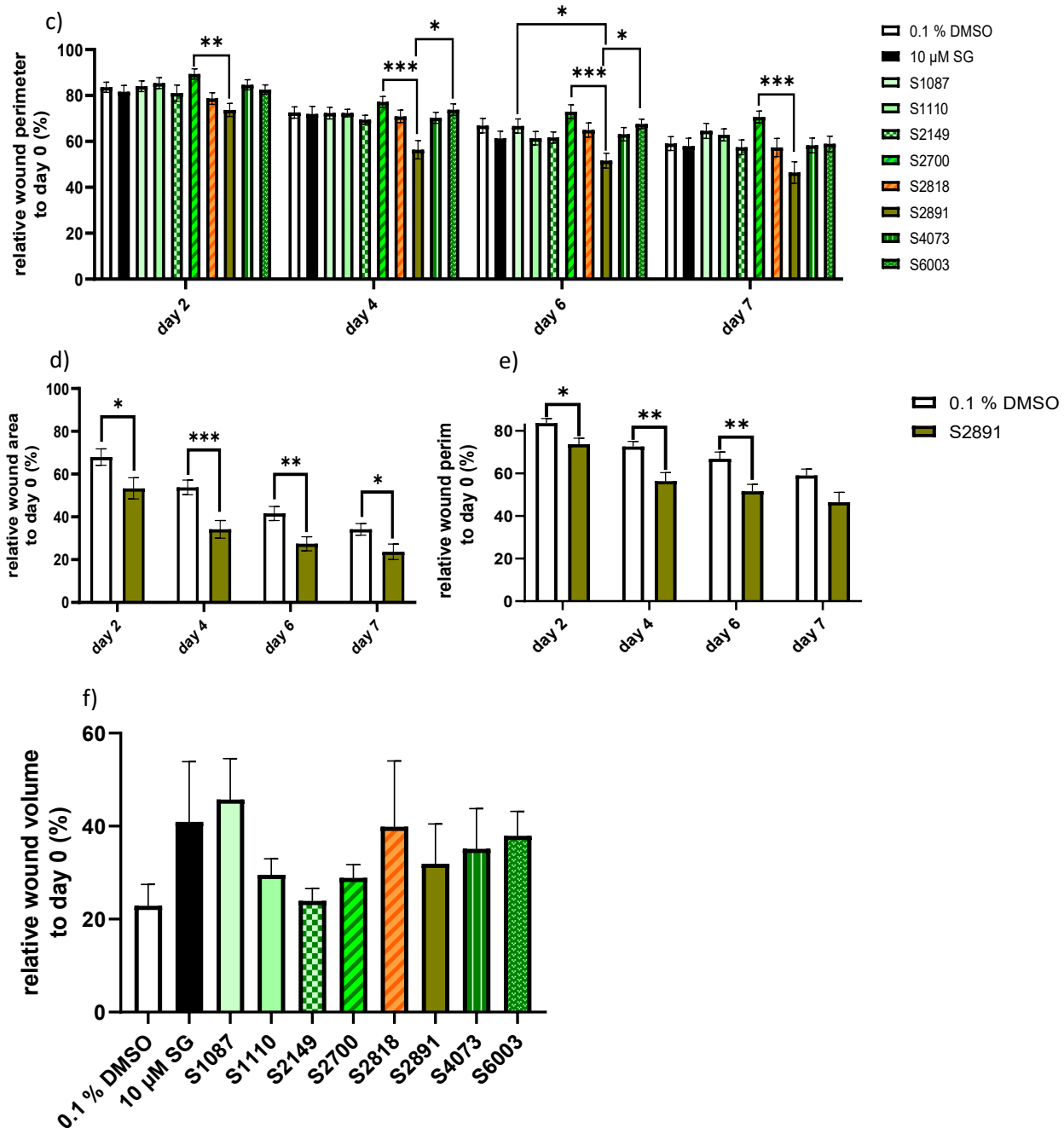

Figure 4.28: Validation of the promising substances of the clinical trials screening in the wound healing organ culture
The 8 promising substances of the clinical trials screening are further validated here: S1087, S1110, S2149, S2700, S2818, S2891, S4073, and S6003. As a vehicle control 0.1 % dimethyl sulfoxice (DMSO) was used, as a positive control 10 µM sodium gualenate (SG). All inhibitors were tested in a concentration of 1 µM . The wounds were treated at day 1 for 24 h hors. a) Exemplary pictures of day 0 (day of wounding) and day 7 (end of the culture), b) relative top-view wound area to day 0 over the course of the wound healing organ culture (WHOC) (n = 5, 2-4 punches/condition), c) relative top-view wound perimter to day 0 over the course of the WHOC (n = 5, 2-4 punches/condition), d) comparison of the relative top-view wound area of just 0.1 % DMSO and S2891 (n = 5, 2-4 punches/condition), e) comparison of the relative top-view wound perimeter of just 0.1 % DMSO and S2891 (n = 5, 2-4 punches/condition), f) relative wound volume to day 0 at day 6, obtained by optical coherence tomography (n = 2, 2-4 punches/condition). Values are depicted as mean + standard error of the mean. Significances were determined by one-way ANOVA with Turkeys' multiple comparisons test (relative top-view wound area), t-test (relative top-view wound area), Kruskal-Wallis test with Dunns' multiple comparison (relative top-view wound perimeter) and Mann-Whitney test (relative top-view wound perimeter). * $p < 0.05$, ** $p < 0.01$, *** $p < 0.001$

Table 4.3: Overview over the 8 candidates of the clinical trials screening and how they performed in the validation
A substance was defined as successful, if it led to a better wound closure compared to the vehicle control and positive control. Parameters investigated were the relative top-view wound area, relative top-view wound perimeter relative, and wound volume.

Successful in:	S1087	S1110	S2149	S2700	S2818	S2891	S4073	S6006
Top-view area	No	No	No	No	No	Yes	No	No
Top-view perimeter	No	No	Yes	No	Yes	Yes	No	No
Volume	No	No	No	No	No	No	No	No

4.5.2 The beneficial effect of treatment with 1 µM S1180 on the top-view wound healing was successfully validated

The results of the non-clinical trials validation are depicted in **Figure 4.29**. **Figure 4.29a** displays the exemplary pictures of wounds on day 0 and day 7. The skin appears more "yellowish" in the pictures at the end of the culture due to some light issues with the stereo microscope. Examination of the exemplary pictures reveals that wounds treated with 1 µM S1180 seem to have more newly formed, opaque ETs than their respective controls.

This impression is confirmed by the relative wound area in **Figure 4.29b**. Treatment with both inhibitors validated here lead to a smaller relative top-view wound area than treatment with the controls throughout the culture.
On day 2, the relative area of the vehicle control wounds was 53.49 % and that of the positive control wounds was 48.19 %. Treatment with 1 µM S1169 led to a relative wound area of 42.47 % and treatment with 1 µM S1180 to a relative wound area of 42.58 %.
Starting on day 4, the reduction in the relative top-view wound area is most pronounced for treatment with 1 µM S1180, which resulted in the smallest relative wound area of 31.91 %. Treatment with 10 µM SG as a positive control led to a relative area of 34.77 % and the wounds treated with the vehicle control had a relative area of 44.92 %. Wounds treated with 1 µM S1169 had a relative area of 37.05 %. In a direct comparison, treatment both with 1 µM S1169 and 1 µM S1180 resulted in a significantly smaller relative top-view wound area on day 4 ($p < 0.05$ for 1 µM S1169 and $p < 0.001$ for 1 µM S1180, data not shown).
From day 4 to day 6, all treatment groups showed a further decrease in the relative top-view wound area. At day 6, the relative area of wounds treated with 0.1 % DMSO as a vehicle control was 33.88 % and that of the positive control wounds was 32.34 %. On this day again the relative top-view wound area of all substances tested here was smaller than both controls. Wounds treated with 1 µM S1169 had a relative area of 29.52 % and wounds treated with 1 µM S1180 had a relative area of 24.93 %. In a direct comparison the relative area of wounds treated with 1 µM S1180 was significantly smaller than the wounds of the vehicle control ($p < 0.05$, data not shown).
At day 7, the relative top-view wound area of wounds treated with 1 µM S1180 was 14.95 %, which is the smallest relative area measured at the end of the WHOC. Moreover, the relative wound area of wounds treated with 1 µM S1180 were significantly smaller than that of the vehicle control wounds, which had a relative area of 30.74 % ($p < 0.01$). Treatment with 1 µM S1180 also led to a significantly smaller relative top-view wound area than the positive control wounds, which had an area of 30.12 %

($p < 0.05$). Treatment with 1 µM S1169 (22.69 %) led to a smaller relative area than both controls, though the effect was not significant for any of them.

The relative top-view perimeter over the course of the WHOC is shown in **Figure 4.29c**. It decreases continuously for all treatment groups during the WHOC. On day 2, the relative perimeter of the vehicle control group was 78.33 %. The perimeter of positive control wounds was slightly higher with 79.05 %. Treatment with 1 µM S1169 led to the smallest relative perimeter of 63.20 % and wounds treated with 1 µM S1180 had a relative perimeter of 69.94 %.
On day 4, the vehicle control wounds and the positive control wounds had almost the same relative perimeter of 72.65 % or 72.64 %. Wounds treated with 1 µM S1169 had a relative perimeter of 60.10 % on this day, which was significantly smaller than the positive control ($p < 0.05$). For wounds treated with 1 µM S1180, the smallest perimeter of 57.58 % was measured on this day, it was significantly smaller than the vehicle control ($p < 0.05$) and the positive control ($p < 0.01$) as well.
On day 6, wounds treated with 0.1 % DMSO as a vehicle control had a relative perimeter of 62.37 % and wounds treated with 10 µM SG as a positive control had a relative perimeter of 64.39 %. Treatment with both 1 µM S1169 (53.69 %) and 1 µM S1180 (52.28 %) led to a smaller relative perimeter than the vehicle control. For treatment with 1 µM S1180 this effect was significant ($p < 0.05$).
On day 7, the positive control wounds had the largest relative perimeter of 61.83 %. Wounds treated with 0.1 % DMSO had a relative perimeter of 59.64 %. Treatment with both 1 µM S1169 (47.74 %) and 1 µM S1180 (39.10 %) led to significantly smaller relative perimeters than both controls ($p < 0.05$ for 1 µM S1169 and $p < 0.001$ for 1 µM S1180).
Assessment of the relative top-view wound area and perimeter showed that 1 µM S1180 had the most promising effect on the top-view wound closure.

Figure 4.29d shows the relative wound volume at day 6. The vehicle control wounds had a relative volume of 41.35 % and the positive control wounds had a relative volume of 34.82 %. Treatment with 1 µM S1169 (36.57 %) led to a relative volume between that of the controls. Treatment with 1 µM S1180 resulted in a relative wound volume of 21.90 %, which was smaller than the volume of both controls. Unfortunately, the OCT system was only available for 2 of the cultures so a statistical analysis was impossible.
Taken together, both substances tested here seemed beneficial for top-view wound closure (compare **Tabel 4.4**). However, the positive effect on all three parameters investigated (relative top-view wound area and perimeter as well as relative wound volume) was much more pronounced for treatment with 1 µM S1180. So, S1180 passed the non-clinical trials, substances validation successfully. It was investigated to find the optimal treatment concentration in **Chapter 4.8**.

a)

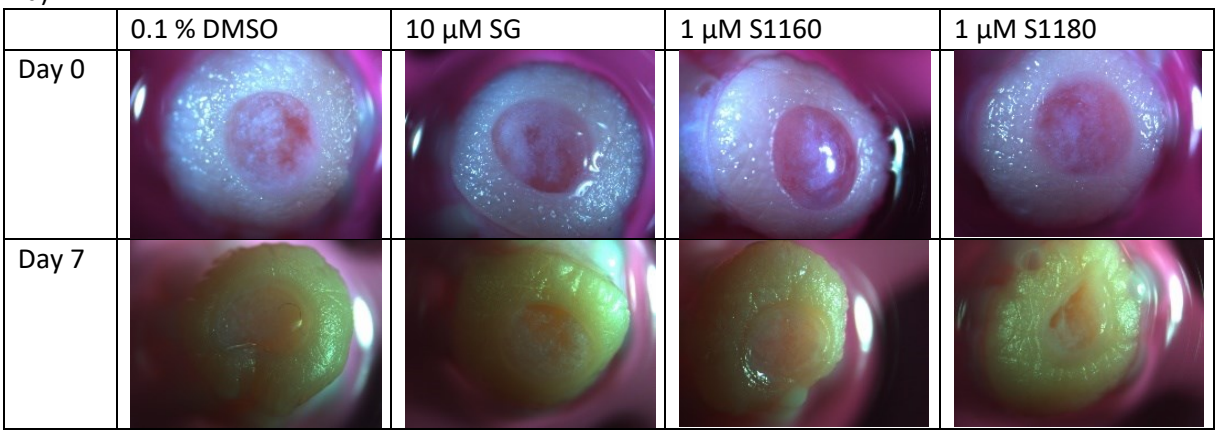
0.1 % DMSO
10 µM SG
1 µM S1160
1 µM S1180
Day 0
Day 7

b)

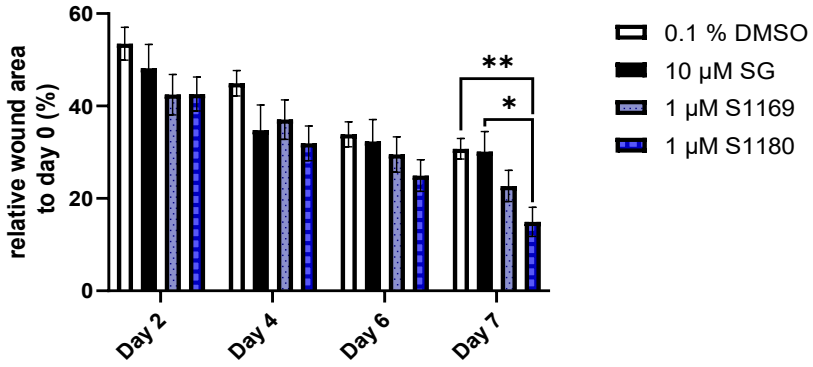
relative wound area to day 0 (%)
60
40
20
0
Day 2
Day 4
Day 6
Day 7
**
*
0.1 % DMSO
10 µM SG
1 µM S1169
1 µM S1180

c)

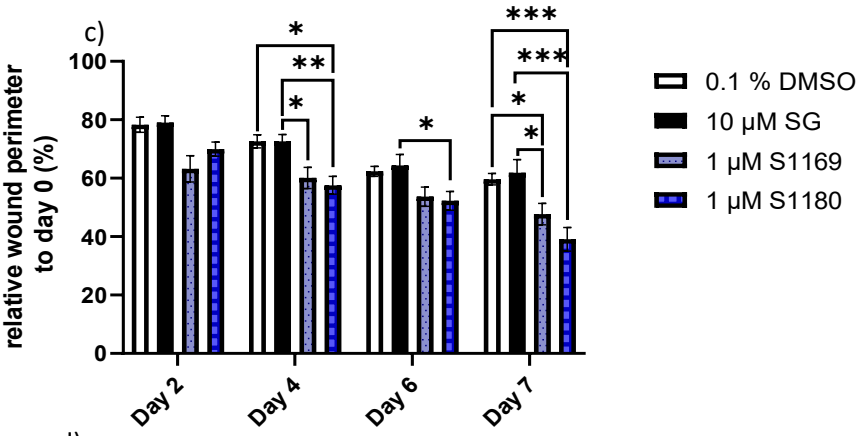
relative wound perimeter to day 0 (%)
100
80
60
40
20
0
Day 2
Day 4
Day 6
Day 7
*
**
*
*
*
***
***
*
*
0.1 % DMSO
10 µM SG
1 µM S1169
1 µM S1180

d)

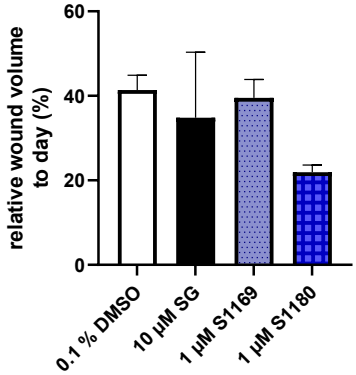
relative wound volume to day (%)
60
40
20
0
0.1 % DMSO
10 µM SG
1 µM S1169
1 µM S1180

Figure 4.29: Validation of the promising inhibitors of the non-clinical trials screening in the wound healing organ culture
The 2 promising inhibitors of the non-clinical trials screening are further validated here: S1169 and S1180. As a vehicle control 0.1 % dimethyl sulfoxice (DMSO) was used, as apositive control 10 µM sodium gualenate (SG). Both inhibitors were tested in a concentration of 1 µM. The wounds were treated at day 1 for 24 h hours. a) Exemplary pictures of day 0 (day of wounding) and day 7 (end of the culture), b) relative top-view wound area to day 0 over the course of the wound healing organ culture (WHOC) (n = 5, 2-4 wounds/condition), c) relative top-view wound perimter to day 0 over the course of the WHOC (n = 5, 2-4 wounds/condition), d) relative wound volume to day 0 at day 6, obtained by optical coherence tomography (n = 2, 2-4 wounds/condition). Values are depicted as mean + standard error of the mean. Significances were determined by one-way ANOVA with Turkeys' multiple comparisons test (relative top-view wound area day 4 and day 6, relative top-view wound perimeter day 6), Kruskal-Wallis test with Dunns' multiple comparison (relative top-view area day 2 and day 7, relative top-view wound perimeter day 2, day 4 and day 7) and Mann-Whitney test (relative top-view wound perimeter). * $p < 0.05$, ** $p < 0.01$, *** $p < 0.001$

Table 4.4: Overview over the 2 candidates of the non-clinical trials screening and how they performed in the validation
A substance was defined as successful, if it led to a better wound closure compared to the vehicle control and positive control. Parameters investigated were the relative top-view wound area, relative top-view wound perimeter relative, and wound volume.

Successful in:	S1169	S1180
Top-view area	Yes	Yes
Top-view perimeter	Yes	Yes
Volume	No	Yes

4.6 S2891 might aid wound healing though the optimal treatment concentration remains unclear

To determine the optimal treatment concentration to aid wound healing, wounds were treated with 0.1 µM, 1 µM, 10 µM S2891 at day 1 for 24 h or repetitively throughout the culture with 1 µM S2891 (4 x 1 µM S2891). 0.1 % DMSO was again used as a vehicle control and 10 µM SG as a positive control.

4.6.1 Treatment with 1 µM S2891, 10 µM S2891 and repetitive treatment with 1 µM S2891 resulted in a smaller relative top-view wound area than the vehicle control

The results of the top-view and OCT evaluation can be found in **Figure 4.30**. **Figure 4.30a** shows the exemplary pictures of the wounds on day 0 and day 7. Compared to the vehicle control wounds, wounds treated with 10 µM SG as a positive control seem larger and wounds treated with 10 µM S2891 appear smaller at day 7.

The relative top-view wound area depicted in **Figure 4.30b** confirms this impression. While all wounds decreased in area over the course of the WHOC, wounds treated with 10 µM SG showed the largest and wounds treated with 10 µM S2891 show the smallest relative area on all measurement days.

On day 2, the relative area of the vehicle control wounds was 55.64 %. Treatment with 0.1 µM S2891 (58.06 %), 1 µM S2891 (62.91 %), and 4 x 1 µM S2891 (61.75 %) led to a larger area than 0.1 % DMSO as vehicle control. Wounds of the positive control group had the largest relative area of 68.02 %. Only wounds treated with 10 µM S2891 had a smaller relative area than the vehicle control group, namely 51.33 %. The difference in relative area between wounds treated with 10 µM SG and 10 µM S2891 was statistically significant ($p < 0.05$.).

On day 4, the same pattern was observed as on day 2: 10 µM SG led to the largest relative area of 56.81 %, followed by wounds treated with 1 µM S2891 (49.55 %), 4 x 1 µM S2891 (48.49 %) and 0.1 µM S2891 (46.53 %). The relative area of the vehicle control wounds was 46.24 %. Treatment with 10 µM S2891 led to a distinctly smaller relative wound area of 41.35 %. As before, the difference between wounds treated with 10 µM SG and 10 µM S2891 was statistically significant ($p < 0.05$). From day 4 to day 6 the other concentrations of S2891 seem to “catch up”.

At day 6, all wounds treated with S2891 displayed a smaller relative top-view wound area than the controls. However, wounds treated with 10 µM SG still had the largest relative area of 50.39 % compared to the relative area of the vehicle control, which was 41.00 %. Wounds treated with 0.1 µM S2891 had a relative area of 37.83 %, those treated with 1 µM S2891 had a relative area of 38.14 % and those treated with 4 x 1 µM S2891 had a relative area of 36.92 %. Treatment with 10 µM S2891 led again to the smallest relative area of 32.61 %, which was significantly smaller than the area of the positive control wounds ($p < 0.05$).

The relative area of the positive control wounds was 50.13 % at day 7, which was again the largest relative area measured. The relative area of the vehicle control group was 38.39 %. While treatment with 0.1 µM S2891 (39.93 %) led to a slightly larger relative area than the vehicle control on this day, treatment with 1 µM S2891 (32.63 %), 10 µM S2891 (27.99 %), and 4 x 1 µM S2891 (34.64 %) resulted in a smaller relative top-view wound area than both controls. Wounds treated with 1 µM S2891 and 4 x 1 µM S2891 were significantly smaller than wounds treated with 10 µM SG with a significance level of $p < 0.05$. The same is true for wounds treated with 10 µM S2891 although the significance level here is $p < 0.001$. Moreover, on day 7, in a direct comparison, wounds treated with

10 µM S2891 are also significantly smaller than the vehicle control wounds ($p < 0.05$, data not shown) and had again the smallest relative area measured.
Throughout all days, treatment with 1 µM S2891 and 4 x 1 µM S2891 led to very similar relative wound areas. Treatment with 0.1 µM S2891 led to larger relative areas and treatment with 10 µM S2891 led to smaller relative areas than 1 µM S2891 as one time or repetitive treatment.

For the relative top-view wound perimeter shown in **Figure 4.30c** a similar pattern is observable. On day 2, the differences between the treatment groups are relatively small. Still, the positive control wounds had the largest relative perimeter of 85.96 %. The perimeter of the vehicle control wounds of this day was 82.08 %. Treatment with 0.1 µM S2891 (84.71 %) and 1 µM S2891 (82.86 %) led to slightly larger relative perimeters and treatment with 10 µM S2891 (78.49 %) and 4 x 1 µM S2891 (81.95 %) to lower relative perimeters, though the difference is very slight in case of 4 x 1 µM S2891.
At day 4, again wounds treated with 10 µM S2891 show the smallest relative perimeter of 69.42 %. The relative perimeter of the vehicle control was 74.93 %, which means that next to 10 µM S2891 also treatment with 1 µM S2891 (71.41 %) and treatment with 4 x 1 µM S2891 (72.19 %) led to smaller relative perimeters than 0.1 % DMSO. Wounds treated with 0.1 µM S2891 had a relative perimeter of 78.09 %. This value lies between the vehicle control and the positive control group, which again had the highest relative perimeter of 79.53 %.
On day 6, the beneficial effect of treatment with S2891 in concentrations above 0.1 µM becomes more pronounced. The perimeter of the vehicle control wounds was 71.38 %. Treatment with 0.1 µM S2891 led to a relative perimeter of 71.31 %, almost the exact same relative perimeter as the vehicle control wounds. On the other hand, treatment with 1 µM S2891 (62.78 %), 10 µM S2891 (60.52 %), and 4 x 1 µM S2891 (63.76 %) resulted in a smaller relative perimeter than 0.1 % DMSO. For 10 µM S2891 this reduction in relative perimeter was strongest. In a direct comparison, the perimeter of wounds treated with 10 µM S2891 or with 4 x 1 µM S2891 were significantly smaller than that of wounds treated with the vehicle control ($p < 0.05$, data not shown). As before, the perimeter of the positive control wounds was largest with 73.17 %.
On day 7, the relative perimeter of wounds treated with 10 µM SG was 73.30 %, which is almost identical to day 6. All other treatment groups showed a decrease in relative perimeter to the end of the WHOC. The perimeter of the vehicle control wounds was 66.74 %. Just like on day 6, the relative perimeter of wounds treated with 0.1 µM S2891 was very similar to the perimeter of the wounds of the vehicle control with a value of 66.37 %. Treatment with 10 µM S2891 led to 55.00 %, the smallest relative perimeter measured in the WHOC and significantly smaller than the relative perimeter of the vehicle control wounds in a direct comparison of only those two groups ($p < 0.05$, data not shown). Also, treatment with 1 µM S2891 and 4 x 1 µM S2891 led to wound perimeter smaller than that of wounds treated with 0.1 % DMSO as vehicle control.

The relative wound volume is shown in **Figure 4.30d**. Unfortunately, the OCT system was only available during 1 of the WHOCs performed, where the 0.1 µM S2891 concentration had not been tested. The relative volume of the vehicle control wounds was 27.18 %. In accordance with the wound area, the treatment with 10 µM SG also led to the largest value, namely a relative volume of 41.17 %. In contrast to the relative wound area, wounds treated with 10 µM S2891 had a relative wound volume of 30.10 % on day 6, which is larger than the negative control wounds. Wounds treated with 4 x 1 µM S2891 had with 27.25 % a relative volume that was very similar to that of the wounds treated with 0.1 % DMSO. Only treatment with 1 µM S2891 resulted in a smaller relative volume than treatment with 0.1 % DMSO as vehicle control, namely a relative wound volume of 23.79 %.

Treatment with 1 µM S2891 (both one time and repetitively) and with 10 µM S2891 appeared beneficial on the top-view wound healing and in the case of 1 µM S2891 also on the wound volume determined by OCT.

a)

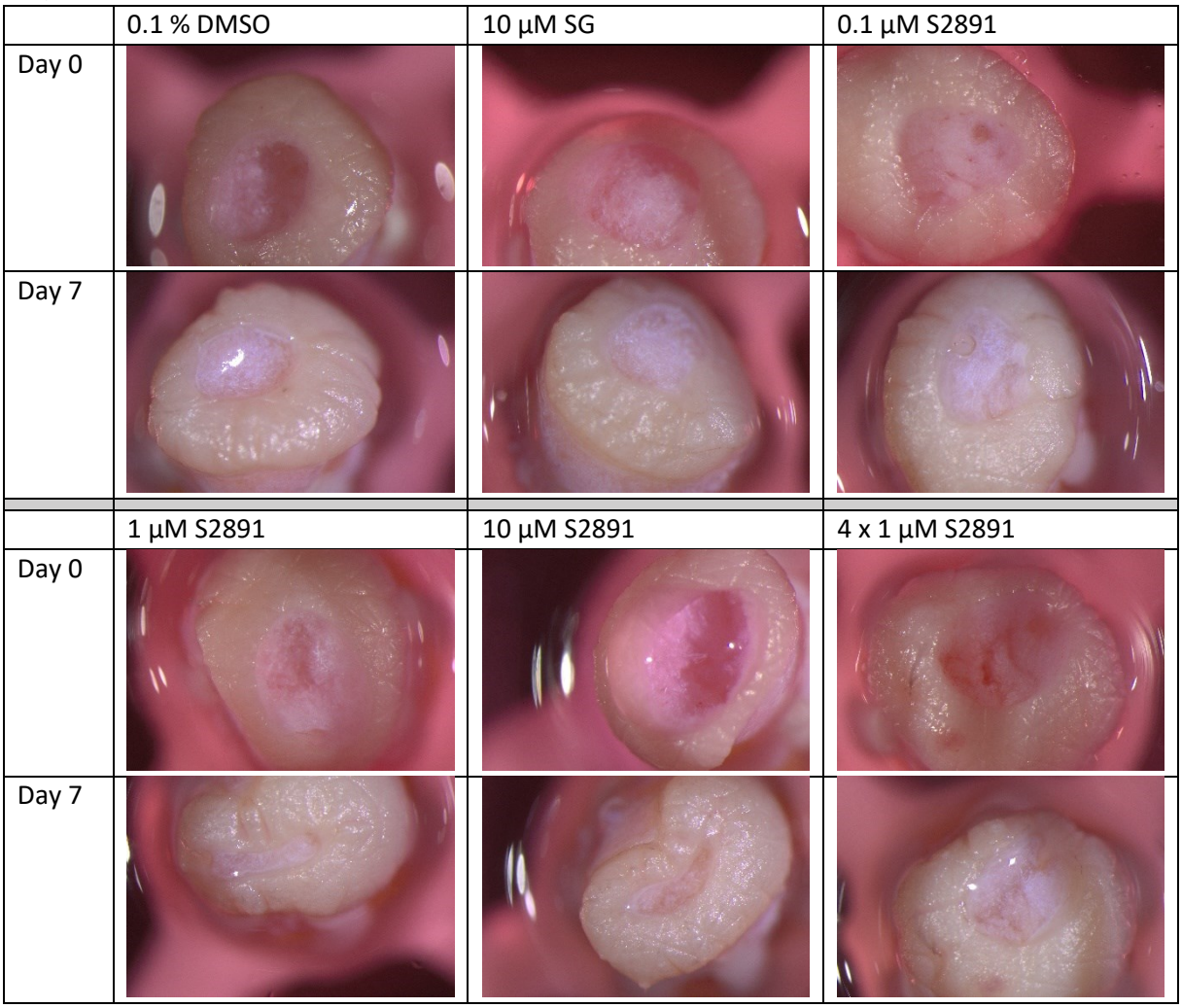

b)

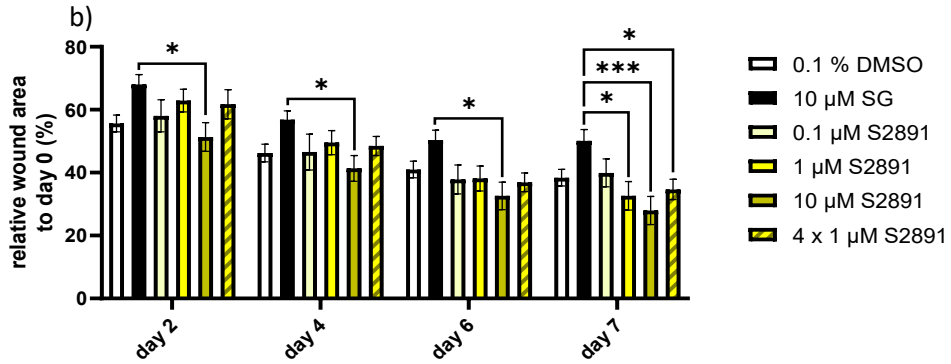

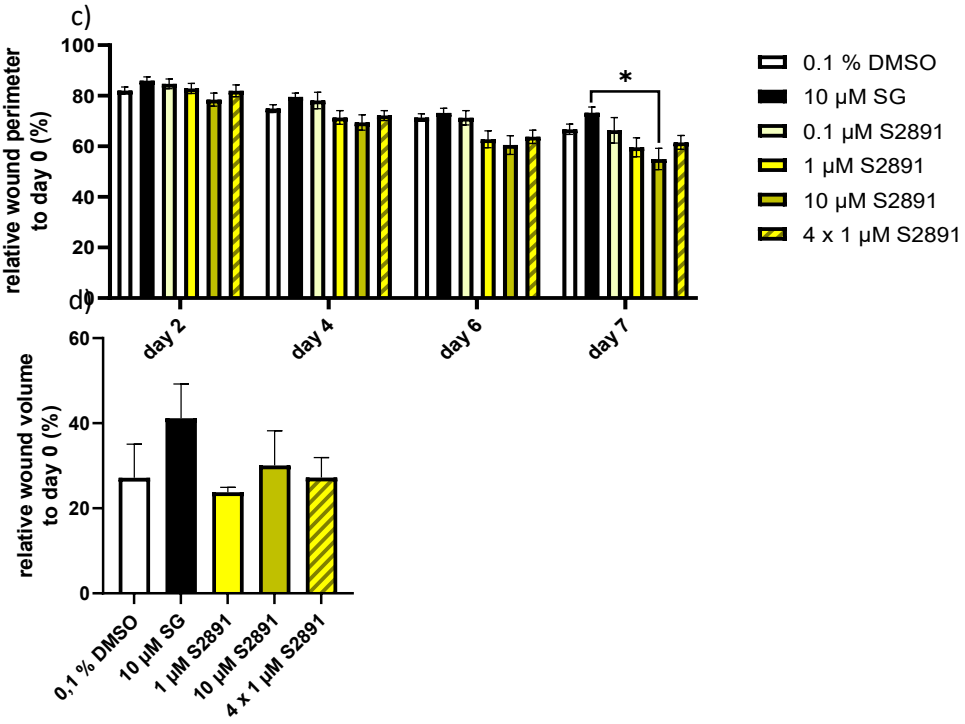

Figure 4.30: Influence of different concentrations of S2891 on the top-view wound healing in the wound healing organ culture model

The wounded skin of the wound healing organ culture was treated with 0.1 µM, 1 µM or 10 µM S2891 at day 1 for 24 h or starting at day 1 repetitively with 1 µM S2891 (4 x 1 µM S2891) throughout the culture. As a vehicle control 0.1 % dimethyl sulfoxide (DMSO) was used, as a positive control 10 µM sodium gualenate (SG) was used. a) Exemplary top-view pictures of day 0 (day of wounding) and day 7 (end of the culture), b) relative top-view wound area to day 0 over the course of the culture (n = 4-10, 1-4 wounds/condition), c) relative top-view wound perimeter to day 0 over the course of the culture (n = 4-10, 1-4 wounds/condition), d) relative wound volume to day 0 at day 6, obtained by optical coherence tomography (n = 1, 4 wounds/condition). Values are depicted as mean ± or + standard error of the mean. Significances were determined by one-way ANOVA with Turky's multiple comparisons test (relative top-view wound area, relative top-view wound perimeter day 2), Kruskal-Wallis test with Dunns' multiple comparison (relative top-view wound perimeter day 4, day 6, day 7). * $p < 0.05$, *** $p < 0.01$

4.6.2 All concentrations of S2891 tested seemed to decrease the microscopic wound size, however only 0.1 µM S2891 and 4 x 1 µM S2891 had a positive effect on the epithelial tongues

Figure 4.31 shows the microscopic evaluation of the wounds treated with S2891. **Figure 4.31a** shows exemplary pictures of the wounds and ETs at day 7. The wounds seem to heal well under all conditions tested and appear smaller after treatment with S2891.

The microscopic wound area is depicted in **Figure 4.31b**. Wounds of the vehicle control group had the largest microscopic wound area of 263,632 µm^2. The area of positive control wounds was 217,684 µm^2. Treatment with all concentrations of S2891 tested here led to a smaller microscopic wound area: 143,236 µm^2 for 0.1 µM S2891, 129,341 µm^2 for 1 µM S2891, 124,003 µm^2 for 10 µM S2891, and 145,980 µm^2 for 4 x 1 µM S2891. Wounds treated with 1 µM S2891 and 4 x 1 µM S2891 were significantly smaller than those treated with 0.1 % DMSO as a vehicle control ($p < 0.05$).

The microscopic diameter is shown in **Figure 4.31c**. Here, the positive control wounds had the largest diameter of 1.770.98 µm, while the vehicle wounds had a diameter of 1,388.01 µm. Wounds treated

with 4 x 1 µM S2891 had the smallest microscopic diameter, namely one of 1,095.95 µm, but the other concentrations of S2891 also led to smaller diameters than both controls: 1,316.87 µm for 0.1 µM S2891, 1,143.54 µm for 1 µM S2891, and 1,280.75 µm for 4 x 1 µM S2891. The difference between 10 µM SG and 1 µM S2891 ($p < 0.01$), 10 µM S2891 ($p < 0.05$) and 4 x 1 µM S2891 ($p < 0.05$) was significant.

Next, the newly formed ETs were assessed regarding their area and length. **Figure 4.31d-g** displays the area of the ETs.
The inner ETs are depicted in **Figure 4.31d.** The area of the inner ETs of the vehicle control wounds was 24,454.70 µm^2. Treatment with 1 µM S2891 (20,763.10 µm^2) and 10 µM S2891 (22,415.10 µm^2) led to smaller inner ETs than those of the vehicle control wounds. The area of the inner ETs of the positive control wounds was 25,370.40 µm^2. Treatment with 0.1 µM S2891 (28,103.10 µm^2) and with 4 x 1 µM S2891 (31,309.30 µm^2) led to larger inner ETs than those of the positive control wounds. So, wounds treated with 4 x 1 µM S2891 had the largest inner ETs. None of the differences detected were significant.
In contrast to the inner ETs, treatment with 4 x µM S2891 resulted in the smallest outer ETs with an area of 19,917.6 µm^2. Treatment with all other concentrations of S2891 led to larger outer ETs: 31,533.60 µm^2 for 0.1 µM S2891, 29,109.60 µm^2 for 1 µM S2891, and 24,020.50 µm^2 for 10 µM S2891. The ETs of wounds treated with 0.1 µM S2891 were significantly larger than wounds treated with 4 x 1 µM S2891. The outer ETs of the vehicle control wounds had an area of 27,837.5 µm^2. Thus, wounds treated with 0.1 µM S2891 and 1 µM S2891 had a larger outer ET area than those treated with 0.1 % DMSO as a vehicle control. However, the largest outer ETs were measured for wounds treated with 10 µM SG as a positive control with an area of 33,009.20 µm^2. The ETs of this group were significantly larger than ETs of the wounds treated with 4 x 1 µM S2891 ($p < 0.05$).
Figure 4.31f shows the area of the total ETs. The total ETs of the vehicle control wounds had an area of 26,089.40 µm^2 and that of the positive control wounds was 29,238.20 µm^2. Only the ETs of wounds treated with 0.1 µM S2891 were larger with an area of 29,788.20 µm^2. Treatment with 1 µM S2891 (24,897.40 µm^2), 10 µM S2891 (23,146.3 µm^2), and 4 x 1 µM S2891 (25847.5 µm^2) led to smaller ETs than the controls.
The normalized area of the inner ETs is depicted in **Figure 4.31g**. The vehicle control wounds had a normalized inner ETs' area of 24.56 µm, which was significantly smaller than the normalized inner ETs' area of wounds treated with 4 x 1 µM S2891 (31.07 µm) with a significance level of $p < 0.05$. The inner ETs of the positive control wounds had the smallest normalized area of 14.83 µm, which was significantly smaller than those of the wounds treated with 4 x 1 µM S2891 ($p < 0.001$). The inner ETs of wounds treated with 0.1 µM S2891 had a normalized area of 32.61 µm, those treated with 1 µM S2891 had a normalized area of 21.47 µm and those treated with 10 µM S2891 had a normalized area of 21.38 µm. Whether normalized or not, treatment with 0.1 µM S2891 and 4 x 1 µM S2891 led to the largest ETs.

The length of the ETs is analyzed in **Figure 4.31h-k**. While the inner ETs of wounds treated with 4 x 1 µM S2891 had the largest area (compare **Figure 4.31d**), they had the shortest length, as **Figure 4.31h** shows. The inner ETS of the vehicle control wounds had a length of 363.07 µm. Treatment with 0.1 µM S2891 (397.14 µm), 1 µM S2891 (426.40 µm) and 10 µM S2891 (393.96 µm) led to larger ETs than those of the vehicle control but to shorter inner ETs than those of the positive control, which had a length of 430.60 µM.
After normalization, however the positive control wounds had the shortest ETs with a value of 0.25 (compare **Figure 4.31i**). Wounds treated with 4 x 1 µM S2891 had normalized inner ETs of the same length. Treatment with 10 µM S2891 resulted in inner ETs with a normalized length of 0.32, which

was the same length of the normalized inner ETs of the vehicle wounds. Treatment with 0.1 µM S2891 (0.40) and with 1 µM S2891 (0.377) led to distinctly longer normalized inner ETs than the vehicle control 0.1 % DMSO, though the differences measured were not significant.
The outer ETs' length is shown in **Figure 4.31j**. The longest outer ETs were measured for wounds treated with 4 x 1µM S2891, namely a length of 547.55 µm. These outer ETs were significantly longer than those of wounds treated with 10 µM SG as positive control (390.00 µm) and those of wounds treated with 10 µM S2891 (379.71 µm). The outer ETs of the vehicle control wounds had a length of 425.45 µm. Just like 10 µM S2891, treatment with 0.1 µM S2891 (400.49 µm) and 1 µM S2891 (420.59 µm) led to shorter outer ETs than the vehicle control.
The length of the total ETs is shown in **Figure 4.31k**. The total ETs of the vehicle controls were the shortest with 395.52 µm and wounds treated with 4 x 1 µM S2891 had the longest total ETs, namely with a length of 437.21 µm. The length of the total ETs of the positive control wounds was 410.56 µm, that of wounds treated with 0.1 µM S2891 was 398.87 µm, that of wounds treated with 1 µM S2891 was 423.41 µm, and that of wounds treated with 10 µM S2891 was 386.20 µm.

Treatment with S2891 seems to be beneficial for the microscopic wound healing and partly also for the formation of the ETs, though which concentration works the best is not entirely clear.

a)

	0.1 % DMSO	10 µM SG	0.1 µM S2891
Wound	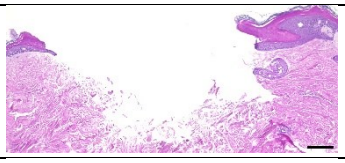	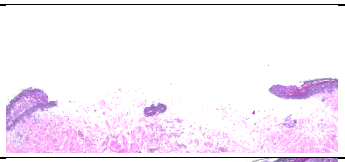	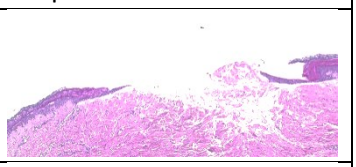
ET	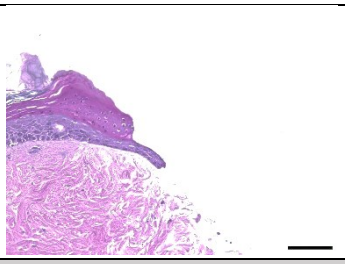	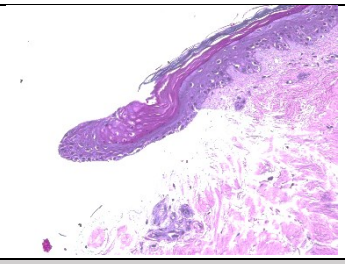	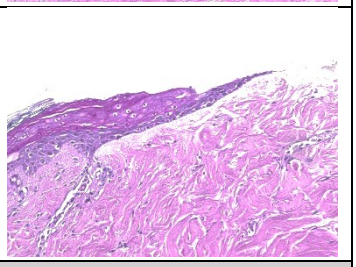
	1 µM S2891	10 µM S2891	4 x 1 µM S2891
Wound	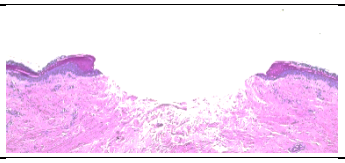	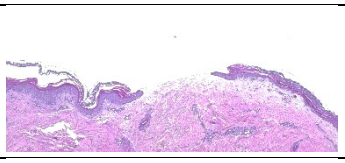	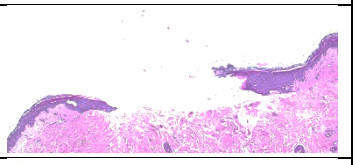
ET	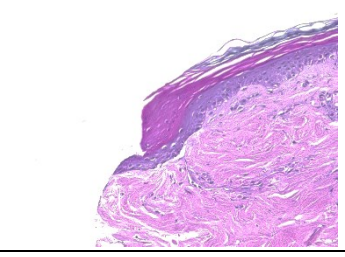	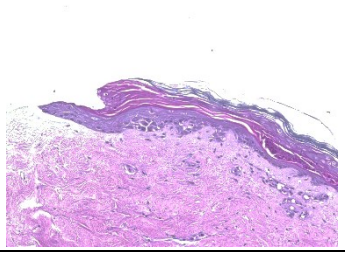	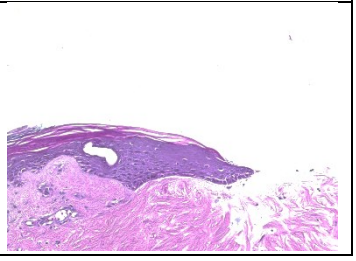

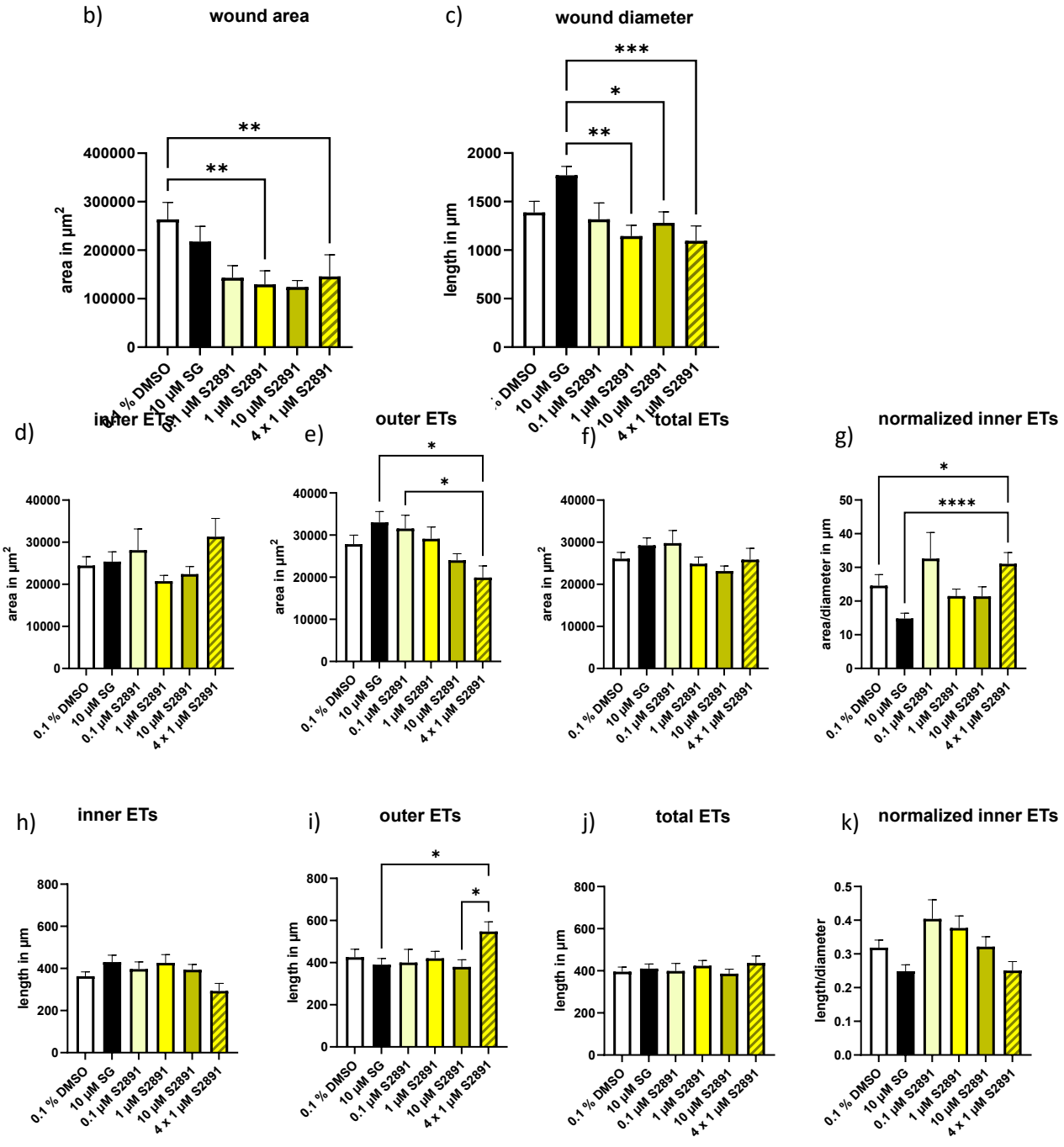

Figure 4.31: Influence of different concentrations of S2891 on the microscopic wound healing in the wound healing organ culture model

The wounded skin of the wound healing organ culture was treated with 0.1 µM, 1 µM, or 10 µM S2891 at day 1 for 24 h or starting at day 1 repetitively with 1 µM. S1180 (4 x 1 µM S1180) over the course of the culture. As a vehicle control 0.1 % dimethyl sulfoxide (DMSO) was used, as a positive control 10 µM sodium gualenate (SG) was used. Shown here are the results of the hematoxylin & eosin (H&E) staining of wounds cut and stained at day 7 (end of the culture). a) Exemplary hematoxylin & eosin stained pictures of the microscopic wounds in 100x magnification (scale bar = 200 µm) and close-up of an exemplary epithelial tongue (ET) in 200x magnification (scale bar = 100 µm), b) microscopic wound area (n = 4-10; 2-4 wounds/condition), c) wound diameter (n = 4-10; 2-4 wounds/condition), d) area of the inner ETs, e) area of the outer ETs, f) area of inner and outer ETs combined, g) normalized area of the ETs on the respective wound diameter, h) length of inner ETs, i) length of outer ETs, j) length of inner and outer ETs combined, k) length of inner ETs normalized on the respective wound diameter. For all ET measurements: n = 4-10; 2-16 ETs/condition. For statistical analysis a Kruskal-Wallis test with Dunns' multiple comparison was performed. * $p < 0.05$, ** $p < 0.01$, *** $p < 0.001$, **** $p < 0.0001$

4.6.3 Treatment with 1 µM S2891 and above seemed to lead to a higher relative cytokeratin 6 expression in the epithelial tongues in the *ex vivo* wound healing organ culture model

The relative CK 6 expression in the ETs is shown in **Figure 4.32**. **Figure 4.32a** shows exemplary pictures of the CK 6 expression at day 7.

The relative CK 6 expression in the inner ETs can be found in **Figure 4.32b**. All treatment groups had a higher relative CK 6 expression than the vehicle control group. For the positive control wounds it was 133.02 %. Treatment with 0.1 µM S2891 (110.74 %) and 4 x 1 µM S2891 (127.58 %) led to a relative CK 6 expression in the inner ETs higher than the vehicle but lower than the positive control. Treatment with 1 µM S2891 (150.06 %) and 10 µM S2891 (165.34 %) led to a distinctly higher relative CK 6 expression than both controls in the inner ETs.

For the outer ETs, as shown in **Figure 4.32c**, only treatment with 10 µM S2891 led to a higher relative CK 6 expression than the vehicle control, namely a relative expression of 107.96 %. Treatment with 10 µM SG as a positive control led to a CK 6 expression of 80.96 % in the outer tongues, treatment with 0.1 µM S2891to 62.71 %, treatment with 1 µM S2891 to 98.29 % and treatment with 4 x 1 µM S2891 to 95.19 % for the outer ETs.

Figure 4.32d shows the relative CK 6 expression in the total ETs. Only treatment with 0.1 µM S2891 resulted in a lower CK 6 expression than the vehicle control, namely 86.72 %. Treatment with the positive control led to a relative CK 6 expression of 103.27 %. The total ETs of wounds treated with 4 x 1 µM S2891 had a relative CK 6 expression of 109.07 % and the total ETs treated with 1 µM S2891 of 121.82 %. Treatment with 10 µM S2891 resulted in the highest relative CK 6 expression in the total ETs, namely 134.04 %. Though not significant, especially treatment with 10 µM S2891 seemed to increase the relative CK 6 expression.

a)

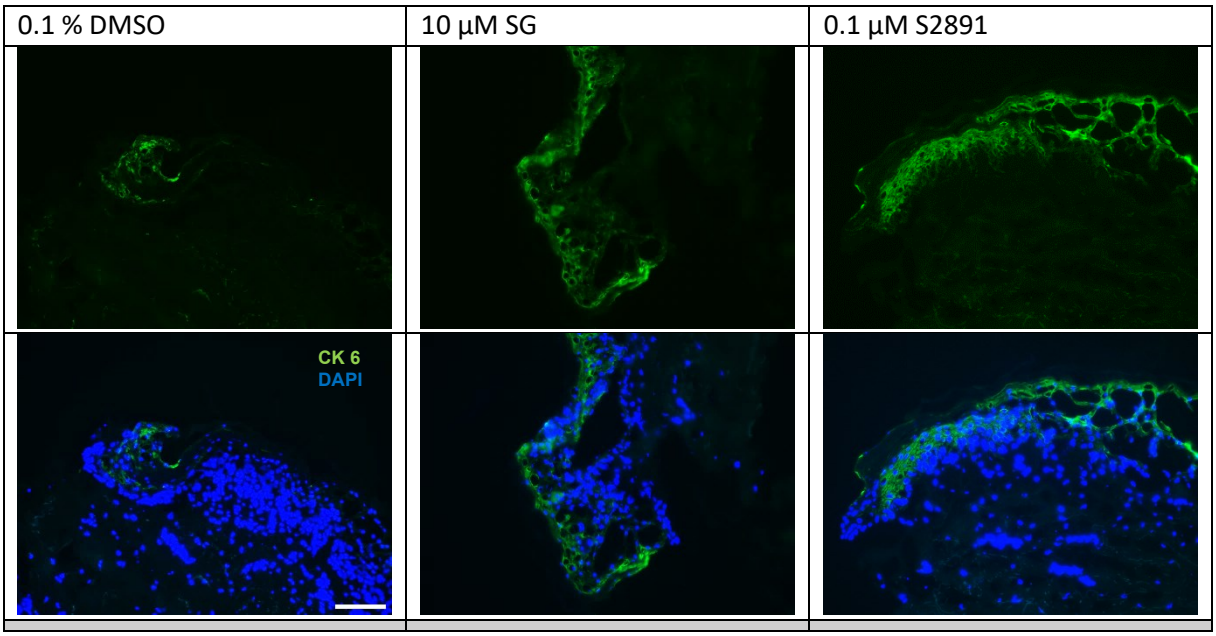

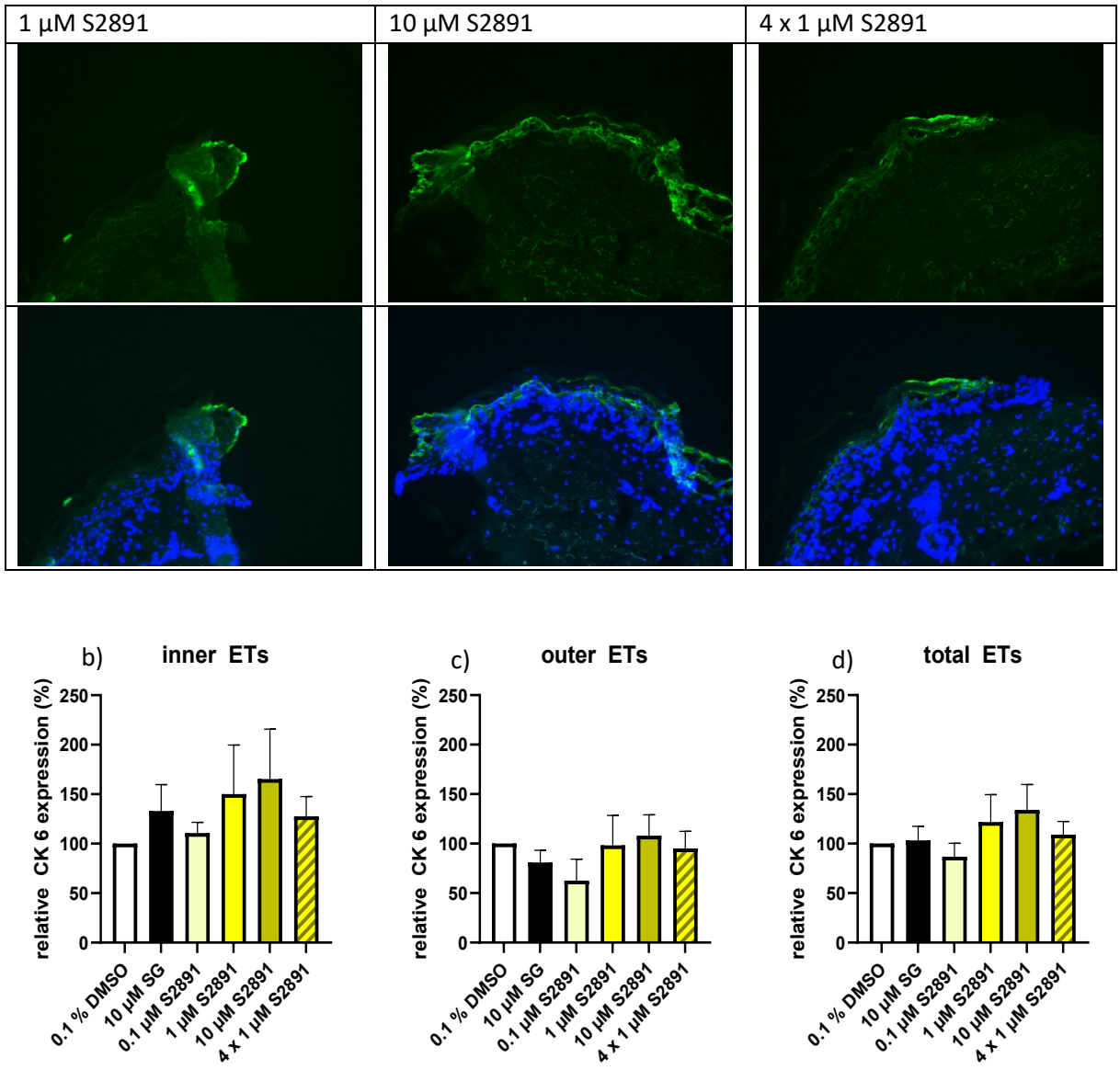

Figure 4.32: Influence of different concentrations of S2891 on the cytokeratin 6 expression in the wound healing organ culture model

The wounds of the wound healing organ culture were treated with 0.1 µM, 1 µM, or 10 µM S2891 at day 1 for 24 hours or starting at day 1 repetitively with 1 µM S2891 (4 x 1 µM S2891) over the course of the culture. As a vehicle control 0.1 % dimethyl sulfoxide (DMSO) was used, as a positive control 10 µM sodium gualenate (SG) was used. Shown here is the cytokeratin (CK 6) expression in the epithelial tongues (ETs) of wounds cut and stained at day 7 (end of culture). a) Exemplary immunofluorescence pictures of the ETs. Scale bar = 100 µm. CK 6 expression in the inner (b), outer (c), and total (d) ETs. For all: n = 3-5, 2-8 ETs/condition. For statistical analysis a Kruskal-Wallis test with Dunn's multiple comparison test (inner and total ETs) or one way ANOVA with Turkeys multiple comparisons test (outer ETs) was performed. Data not significant.

4.6.4 Treatment with S2891 seemed to have no strong effect on the CD31 expression or CD31 positive cells

Figure 4.33 shows the evaluation of the CD31 staining. The exemplary pictures can be found in **Figure 4.33a**.

Figure 4.33b shows the relative CD31 intensity in the dermis. Only treatment with 0.1 µM S2891 resulted in a lower CD31 expression than the vehicle control, namely 91.01 %. After treatment with the positive control the relative CD31 expression was slightly higher than the vehicle control with

101.10 %. Treatment with 1 µM S2891 resulted in a relative CD31 expression of 102.58 %, treatment with 10 µM S2891 in 107.61 %, and treatment with 4 x 1 µM S2891 in 107.07 %.

Figure 4.33c shows the number of CD31 positive cells. Treatment with the vehicle control led to 41.57 cells/VF and with positive control to 38.22 cells/VF. The wounds treated with 0.1 µM S2891 had 41.95 positive cells/VF, those treated with 1 µM S2891 had 36.93 cells/VF, those treated with 10 µM S2891 had 42.00 positive cells/VF, and those treated with 4 x 1 µM S2891 38.32 positive cells/VF.

Figure 4.33d shows the number of CD31 positive cross sections. The highest number of positive cross sections was found in wounds treated with 0.1 µM S2891 (0.50 cross sections/VF), followed by the vehicle control (0.45 cross sections/VF), 4 x 1 µM S2891 (0.43 cross sections/VF), 1 µM S2891 (0.29 cross sections/VF), 10 µM SG (0.24 cross sections/VF), and 10 µM S2891 (0.21 cross sections/VF).

The number of CD31 positive vessels can be found in **Figure 4.33e.** Only treatment with 0.1 µM S2891 led to more positive vessels than the vehicle control (0.84 vessels/VF vs. 0.48 vessels/VF). Wounds treated with 10 µM S2891 and 4 x 1 µM S2891 had the same number of positive vessels: 0.38 vessels/VF. Treatment with 1 µM S2891 resulted in 0.32 positive vessels/VF. Wounds treated with the positive control had the least positive vessels here, namely 0.27.
All found differences were not significant. So, treatment with S2891 seemed to have only little influence on the CD31 expression or cell or vessel count.

a)

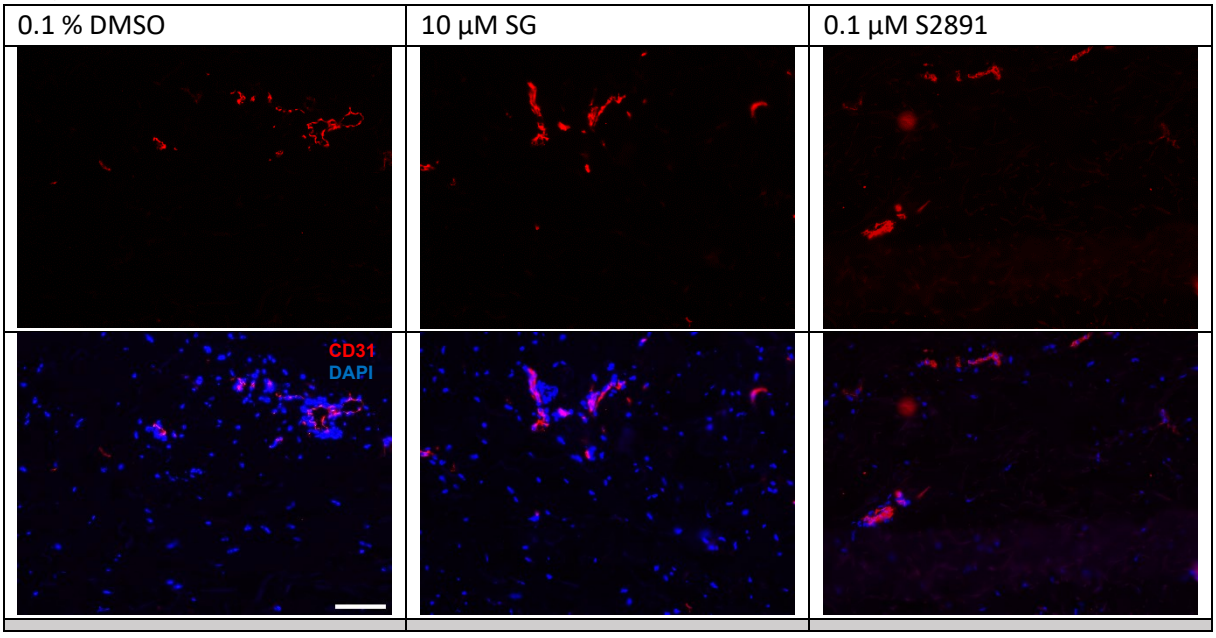

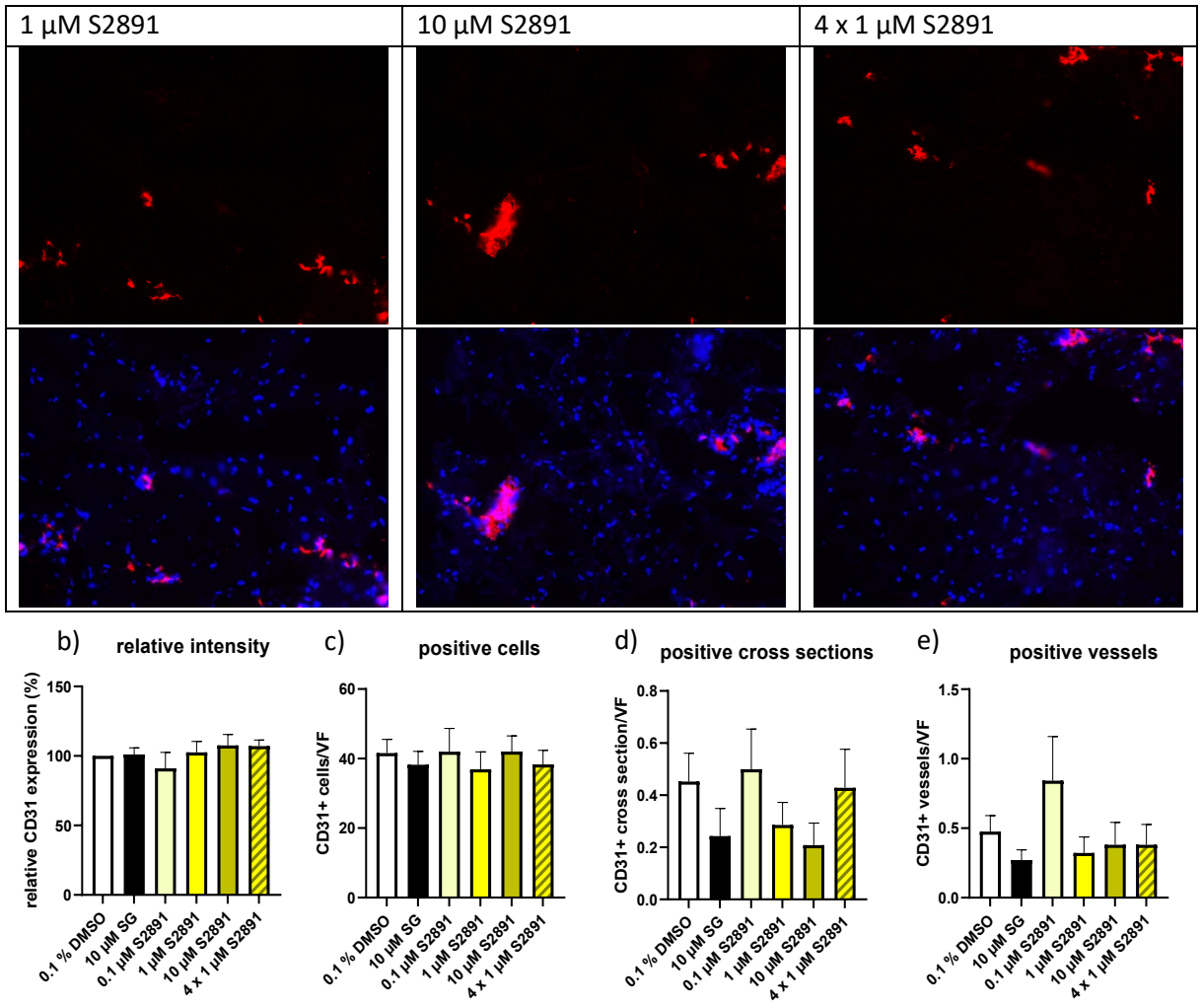

Figure 4.33: Influence of different concentrations of S2891 on the CD31 expression in the wound healing organ culture model

The wounds of the wound healing organ culture were treated with 0.1 µM, 1 µM or 10 µM S2891 at day 1 for 24 hours or starting at day 1 repetitively with 1 µM S2891 (4 x 1 µM S2891) throughout the culture. As a vehicle control 0.1 % dimethyl sulfoxide (DMSO) was used, as a positive control 10 µM sodium gualenate (SG). Shown here is the CD31 expression in the epithelial tongues (ETs) of wounds cut and stained at day 7 (end of culture). a) Exemplary immunofluorescence pictures of the dermis scale bar = 100 µm, b) relative CD31 expression (n = 3-5, 2-4 visual fields (VFs)/wound), c) number of CD31 positive cells/VF (n = 3-5, 2-4 VFs/wound) d) number of CD31 positive vessels/VF (n = 3-5, 2-4 VFs/wound), e) number of CD31 positive cross sections/VF. For all: n = 3-5, 4-7 VFs/wound. For statistical analysis one-way ANOVA with Turkey's multiple comparison and t-test (relative intensity) or Kruskal-Wallis test with Dunn's multiple comparison and Mann-Whitney (for numbers of cells, cross sections and vessels) was performed. Data not significant.

4.6.5 Treatment with S2891 seemed to have no influence on the cortactin expression

Figure 4.34 shows exemplary pictures of cortactin expression in the ETs after treatment with different concentrations of S2891. In all ETs the cortactin expression was strong and evenly distributed, so S28910 seemed to have no influence on the cortactin expression.

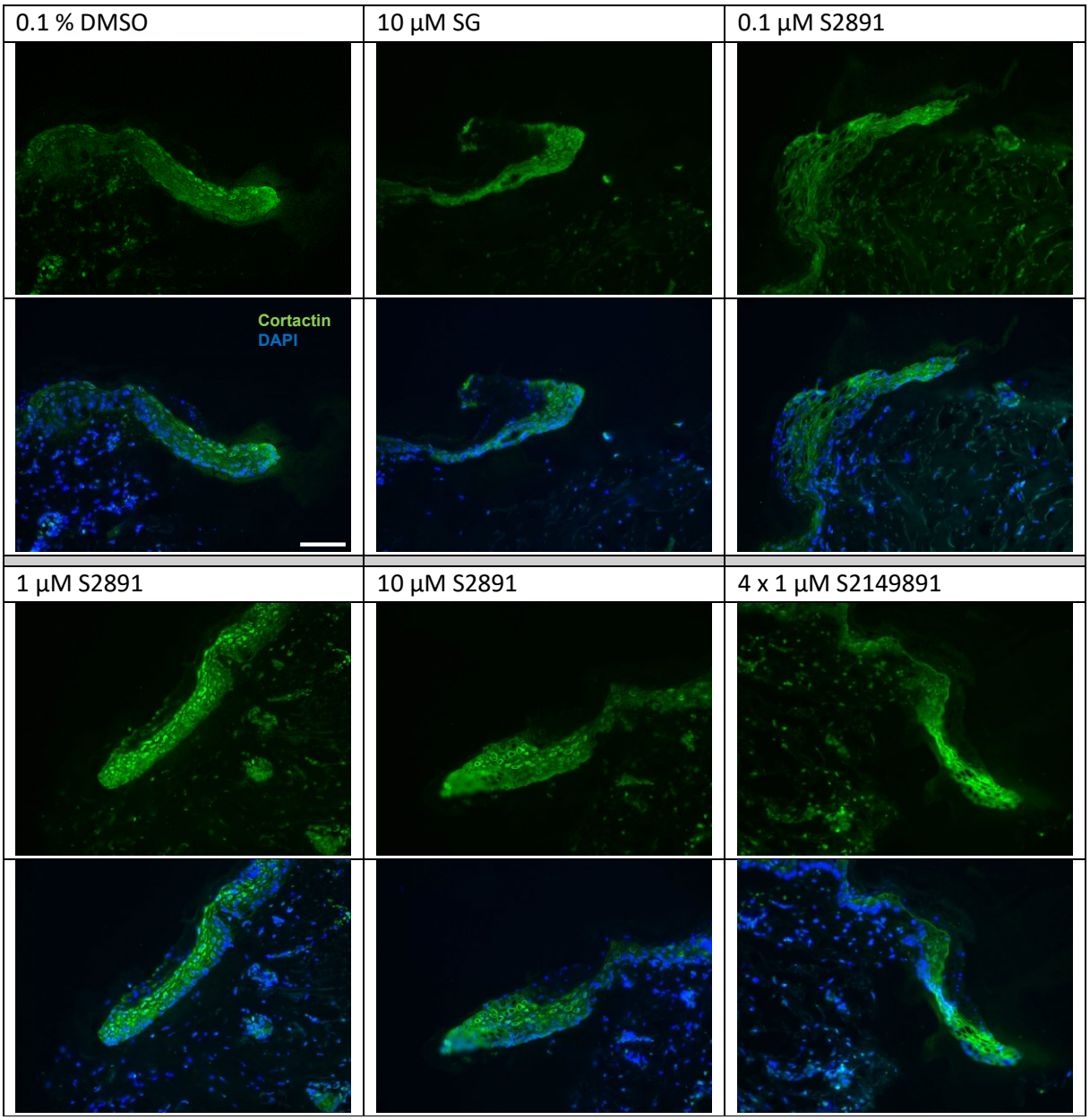

Figure 4.34: Influence of different concentrations of S2891 on the cortactin expression in the wound healing organ culture model

The wounds of the wound healing organ culture were treated with 0.1 µM, 1 µM or 10 µM S2891 at day 1 for 24 hours or starting at day 1 repetitively with 1 µM S2891 (4 x 1 µM S2891) throughout the culture. As a vehicle control 0.1 % dimethyl sulfoxide (DMSO) was used, as a positive control 10 µM sodium gualenate (SG). Shown here are exemplary pictures of the cortactin expression in epithelial tongues of wounds cut and stained at day 7 (end of culture). Scale bar = 100 µm

S2891 showed some promising effects on the WHOC. However, the data is not clear on which concentration is the most beneficial. More research would be needed to find out.

4.7 S2149 did not have a convincing positive effect on the wound healing in the wound healing organ culture model

For further investigating the influence of S2149 on the wound healing in the WHOC model the same concentrations as described for S2891 (**Chapter 4.6**) were tested.

4.7.1 Treatment with 1 µM S2149 (one-time or repetitively) and with 10 µM S2149 seemed to reduce the relative top-view wound area

Figure 4.35 shows the results of the top-view analysis. Over the course of the culture, wound closure is observable in all conditions tested here, as illustrated by the exemplary pictures in **Figure 4.35a**.

As **Figure 4.35b** shows, that the relative top-view area and perimeter are smaller in wounds treated with S2149 than in wounds treated with both controls. On day 2, the relative area of the vehicle control wounds was 73.15 % and that of the positive control wounds was 65.37 %. Treatment with 0.1 µM S2149 (67.83 %) and 10 µM S2149 (66.50 %) led to an area between both controls, while wounds treated with 1 µM S2149 (56.68 %) and 4 x 1 µM S2149 (58.49 %) had a smaller relative area than the positive control wounds. In a direct comparison, the area of wounds treated with 1 µM S2149 (one-time treatment or repetitively) was significantly smaller than that of wounds treated with 0.1 % DMSO as a vehicle control ($p < 0.05$ for 1 µM S2149 and $p < 0.01$ for 4 x 1 µM S2149, data not shown).
On day 4, again the negative control wounds had the largest area, namely 61.82 %. Wounds treated with 10 µM SG as a positive control (58.09 %), wounds treated with 0.1 µM S2149 (58.07 %), and wounds treated with 10 µM S2149 (57.75 %) were very similar in relative area on this day. Like on day 2, treatment with 1 µM S2149 and 4 x 1 µM S2149 led to the smallest relative area, 48.17 % and 48.29 % respectively. Also, the difference to the vehicle control wounds was significant for both groups if compared directly to 0.1 % DMSO ($p < 0.05$ for both).
On day 6, the relative area of the vehicle control wounds was 59.35 % and that of the positive control wounds was 55.74 %. All concentrations of S2149 led to a smaller relative area than both controls here. For 0.1 µM S2149 (53.20 %) and 10 µM S2149 (53.54 %) this difference was smaller than for 1 µM S2149 (49.32 %) and 4 x 1 µM S2149 (46.84 %). On this day, only wounds treated with 4 x 1 µM S2149 were significantly smaller than those treated with 0.1 % DMSO in a direct comparison ($p < 0.05$).
On day 7, the end of the WHOC wounds treated with 0.1 % DMSO had a relative area of 56.14 % and wounds treated with 10 µM SG of 51.29 %. The area of wounds treated with 0.1 % S2149 was 52.62 % and this slightly higher than that of the positive control wounds. Treatment with 1 µM S2149 led to the smallest relative area on this day, namely 43.30 %, but also 10 µM S2149 (45.53 %) and 4 x 1 µM S2149 (44.98 %) led to smaller relative wound areas than both controls.
So, treatment with all concentrations of S2149 tested here resulted in smaller relative areas than the vehicle control. For 1 µM S2149 (one-time treatment or repetitively) this effect was most pronounced, and those wounds were even smaller than wounds treated with the positive control 10 µM SG. Still, the effect was rather small and not significant.

The relative top-view wound perimeter is shown in **Figure 4.35c**. All concentrations tested here (including the positive control 10 µM SG) show a slightly larger relative perimeter than the vehicle control on all days. On day 2, the vehicle control wounds had a relative perimeter of 77.70 % and the positive control wounds of 81.93 %. Treatment with 0.1 µM S2149 (86.85 %) and 10 µM S2149

(87.05 %) led to a relative perimeter larger than that of the positive control wounds and treatment with 1 µM S2149 (80.26 %) and 4 x 1 µM S2149 (78.88 %) resulted in a relative perimeter between both controls.
The same pattern can be observed on day 4: Wounds treated with 0.1 µM S2149 and 10 µM S2149 had a relative perimeter of 80.92 % and 79.82 %, which was higher that of both controls. The wounds treated with 1 µM S2149 (72.27 %) and 4 x 1 µM S2149 (72.77 %) had a relative perimeter that lay between the 78.64 % relative perimeter of the positive control wounds and the 72.17 % relative perimeter of the vehicle control wounds, though the difference between 1 µM S2149 and 0.1 % DMSO was extremely slight.
On day 6, the wounds of the positive control had the largest perimeter of 79.43 %, followed by wounds treated with 0.1 µM S2149 (77.58 %), 10 µM S2149 (77.25 %), 1 µM S2149 (74.60 %), and 4 x 1 µM S2149 (74.34 %). Treatment with 0.1 % DMSO as vehicle control resulted in the smallest relative perimeter of 69.12 %.
The same is true on day 7. Here, the relative perimeter of the vehicle control wounds was 68.01 %. All other treatment groups had a larger relative perimeter: 73.18 % for 10 µM SG, 75.46 % for 0.1 µM S2149, 69.87 % for 1 µM S2149, 74.99 % for 10 µM S2149 and 71.24 % for 4 x 1 µM S2149.
None of conditions tested resulted in a smaller relative top-view perimeter than the vehicle control. All differences in perimeter were rather small and not significant.

The relative wound volume on day 6 can be found in **Figure 4.36d**. The wounds of the vehicle control had a relative volume of 35.97 % and that of the positive control wounds was 34.35 %. Of all concentrations tested only treatment with 1 µM S2149 led to a slightly smaller relative wound volume than treatment with the vehicle control, namely 34.94 %. All other concentrations tested had a higher relative volume than both controls: 40.08 % for 0.1 µM S2149, 47.66 % for 10 µM S2149, and 40.97 & 4 x 1 µM S2149. As the OCT system was only available for two of the cultures, a statistical analysis was unfortunately not feasible.
So far, treatment with 1 µM S2149 seemed the most beneficial, though the difference to the vehicle control is slight.

a)

	0.1 % DMSO	10 µM SG	0.1 µM S2149
Day 0			
Day 7			

	1 µM S2149	10 µM S2149	4 x 1 µM S2149
Day 0		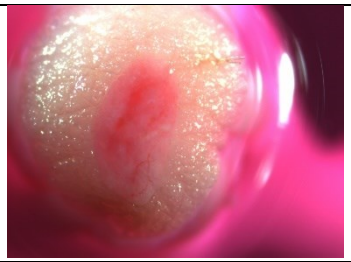	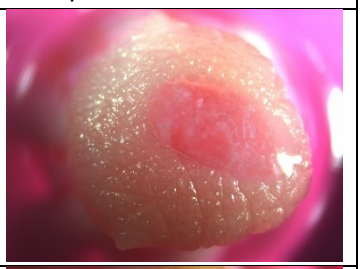
Day 7	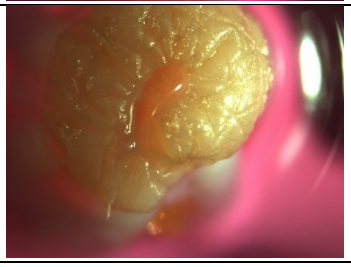		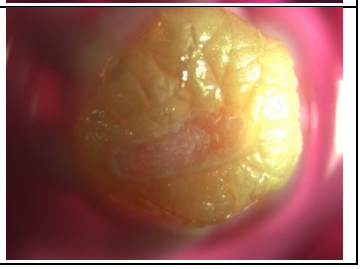

b)

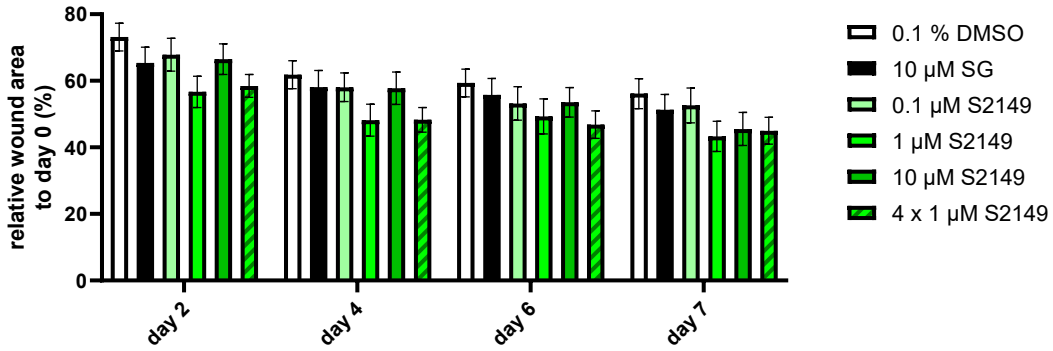

c)

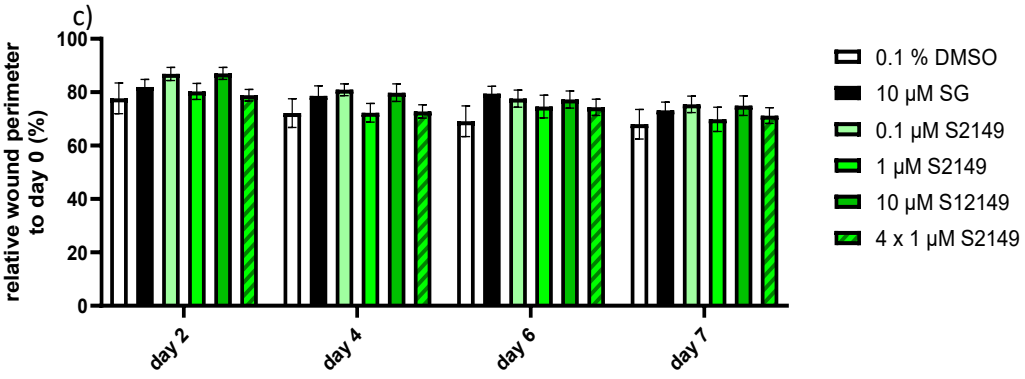

d)

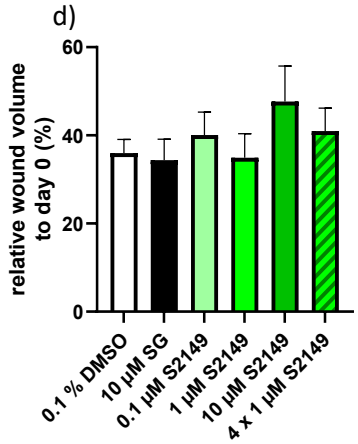

Figure 4.35: Influence of different concentrations of S2149 on the top-view wound healing in the wound healing organ culture model.
The wounded skin of the wound healing organ culture was treated with 0.1 µM, 1 µM or 10 µM S2149 at day 1 for 24 h or starting at day 1 repetitively with 1 µM. S2149 (4 x 1 µM S2149) throughout the culture. As a vehicel control 0.1 % dimethyl sulfoxide (DMSO) was used, as a positive control 10 µM sodium gualenate (SG) was used. a) Exemplary top-view pictures of day 0 (day of wounding) and day 7 (end of the culture), b) relative top-view wound area to day 0 over the course of the culture, c) relative top-view wound perimeter to day 0 over the course of the culture (n = 6, 1-4 wounds/condition), d) relative wound volume to day 0 at day 6, obtained by optical coherence tomography (n = 3, 3-4 wounds/condition). Values are depicted as mean ± or + standard error of the mean. Significances were determined by one-way ANOVA with Turky's multiple comparisons test (relative top-view wound area, relative top-view wound perimeter day), Kruskal-Wallis test with Dunns' multiple comparison (relative top-view wound perimeter day 4, day 6, day 7, relative wound volume). Data not significant.

4.7.2 Treatment with 1 µM S2149 resulted in a reduction of the microscopic wound area and diameter and in larger and longer normalized inner epithelial tongues

Next to the top-view and OCT data, the wound healing was also assessed microscopically on H&E-stained sections, as shown in **Figure 4.36**.
Already the exemplary pictures (**Figure 4.36a**) of the wound cross sections illustrate, that the microscopic wound area is much smaller after treatment with S2149.

The microscopic wound area can be found in **Figure 4.36b**. The vehicle control wounds had the largest area of 374,041 µm^2, followed by the positive control wounds (308,270 µm^2) and the wounds treated with 10 µM S2149 (231,995 µm^2). A striking reduction of the microscopic wound area could be observed for the other S2149 concentrations tested: wounds treated with 0.1 µM S2149 had a microscopic area of 132,046 µm^2, which was significantly smaller than the wounds treated with the vehicle control 0.1 % DMSO ($p < 0.05$). Treatment with 1 µM S2149 resulted in the smallest area, namely 66,836 µm^2, which was significantly smaller than the area of both controls ($p < 0.0001$ for 0.1 % DMSO and $p < 0.001$ for 10 µM SG) and wounds treated with 10 µM S2149 ($p < 0.05$). Wounds treated with 4 x 1 µM S2149 had a microscopic area of 119414 µm^2, which was significantly smaller than both controls as well ($p < 0.05$).

The microscopic wound diameter is shown in **Figure 4.36c**. The microscopic wound diameter of the negative control wounds is 2,201.25 µm, which is the largest perimeter observed. The diameter of all other treatment groups was significantly smaller than that of the vehicle control group ($p < 0.05$ for SG, 0.1 µM S2149 and 10 µM S2149; $p < 0.01$ for 4 x 1 µM S2149 and $p < 0.0001$ for 1 µM S2149. Wounds of the positive control had a perimeter of 1,366.11 µm. Treatment with 0.1 µM S2149 (1,266.81 µm), 10 µM S2149 (1,375.75 µm) and with 4 x 1 µM S2149 (1,196.48 µm) led to perimeters similar in length to the positive control wounds. Like the microscopic area, wounds treated with 1 µM S2149 had the smallest diameter, namely 738.68 µm.

Figure 4.36d shows the area of the inner ETs. Wounds of the vehicle control group had the largest inner ETs of 26,838.80 µm^2. They were even significantly larger than the inner ETs of wounds treated with 0.1 µM S2149 (12,376.70 µm^2) with a significance level of $p < 0.05$. The inner ETs of the positive control group had an area of 17,473.40 µm^2. Treatment with 1 µM S2149 and 10 µM S2149 led to inner ETs of a very similar area, 23,303.40 µm^2 for 1 µM S2149 and 23,150.50 µm^2 for 10 µM S2149 respectively. Both areas were significantly larger than those after treatment with 0.1 µM S2149 ($p < 0.01$ for 1 µM S2149 and $p < 0.05$ for 10 µM S2149). Treatment with 4 x 1 µM S2149 led to an inner ETs' area of 15,924.80 µm^2.

After normalization, the area of the inner ETs of wounds treated with 1 µM S2149 was the largest by far, as shown in **Figure 4.36g**. The normalized inner ETs' area after treatment with 1 µM S2149 was 30.13 µm and significantly larger than the normalized area of the inner ETs after treatment with 0.1 % DMSO (14.16 µm), 10 µM SG (12.54 µm), 0.1 µM S2149 (11.45 µm), 10 µM S2149 (20.26 µm), and 4 x 1 µM S2149 (17.94 µm) with a significance level of $p < 0.05$ for 10 µM S2149 and $p < 0.0001$ for all other groups. Next to 1 µM S2149, also 10 µM S2149 and 4 x 1 µM S2149 led to larger normalized inner ETs than the vehicle control.
The differences between the treatment groups were not as pronounced in the outer ETs. As in **Figure 4.36e** also in **Figure 4.36f**, the area of the ETs of the vehicle control wounds was the largest, namely 30,072.8 μm^2, followed by 0.1 µM S2149 (27,819.00 μm^2), 10 µM S2149 (24,973.8 μm^2), 1 µM S2149 (23,719.8 μm^2), 10 µM SG (23,337.60 μm^2), and 4 x 1 µM S2149 (20,335.40 μm^2). None of the differences measured here were statistically significant.
The area of the total ETs is shown in **Figure 4.36g**. Again, vehicle control wounds had the largest total ETs with an area of 28,455.80 μm^2. Treatment with 1 µM S2149 (23,514.80 μm^2) and 10 µM S2149 (24,877.30 μm^2) led to larger total ETs than those of the positive control (20,368.40 μm^2), while treatment with 0.1 µM S2149 (19,037.8 μm^2) and 10 µM S2149 (18,818.20 μm^2) led to smaller total ETs than those of even the positive control.

The length of the ETs is depicted in **Figure 4.36h-k**. The inner ETs, as shown in **Figure 4.36h,** were longest in the vehicle control group, namely 391.119 µm. The second longest inner ETs have been found in wounds treated with 1 µM S2149 (344.352 µm), followed by 10 µM S2149 (322.338 µm), 10 µM SG (246.186 µm), 4 x 1 µM S2149 (227.357 µm), and 0.1 µM S2149 (206.393 µm). The inner ETs of wounds treated with 1 µM S2149 were significantly longer than those of wounds treated with 0.1 µM S2149 ($p < 0.01$) and 4 x 1 µM S2149 ($p < 0.05$). Moreover, the inner ETs of wounds treated with 10 µM S2149 were significantly longer than those of wounds treated with 0.1 µM S2149 ($p < 0.05$). Just like the area of the inner ETs, normalization of the length of the inner ETs changes the picture strongly, as shown in **Figure 4.36k**. Here, the normalized inner ETs had the longest ETs by far with a value of 0.47. They were significantly longer than the ETs after treatment with 0.1 % DMSO (0.18), 10 µM SG (0.19), 0.1 µM S2149 (0.20), 10 µM S2149 (0.28) and 4 x 1 µM S2149 (0.23) with a significance level of $p < 0.05$ for 10 µM S2149 and $p < 0.0001$ for all other groups. Next to 1 µM S2149 also treatment with 10 µM S2149 and 4 x 1 µM resulted in longer normalized inner ETs than both controls, though the effect is not significant.
Figure 4.36i shows the length of the outer ETs. Here, the ETs of the vehicle control wounds were again the longest, namely 516.72 µm. Treatment with 10 µM S2149 led to an outer ETs' length of 490.38 µm and treatment with 4 x 1 µM S2149 to a length of 389.51 µm. The length of the outer ETs of wounds treated with 10 µM SG (362.92 µm), 0.1 µM S2149 (367.53 µm), and 1 µM S2149 (352.69 µm) was very similar and shorter than that of the vehicle control.
The length of the total ETs is depicted in **Figure 4.36j**. Again, the wounds of the vehicle control had the longest total ETs of 453.23 µm, followed by wounds treated with 10 µM S2149 (410.01 µm), wounds treated with 1 µM S2149 (348.58 µm) and wounds treated with 4 x 1 µM S2149 (312.44 µm). The length of the total ETs of the positive control wounds was 303.81 µm. Treatment with 0.1 µM S2149 led to shorter total ETs of 291.66 µm. None of the differences measured for the outer or total ETs were significant.

The microscopic evaluation showed that the optimal treatment concentration of the those tested here is 1 µM S249. Though its positive effect is not as distinctly visible on the first glance, normalization of the inner ETs revealed, that treatment with 1 µM S2149 could impact wound healing in the WHOC in a positive way.

a)

	0.1 % DMSO	10 µM SG	0.1 µM S2149
Wound	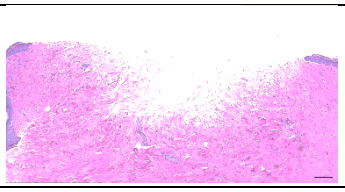	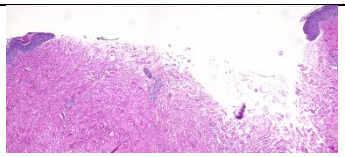	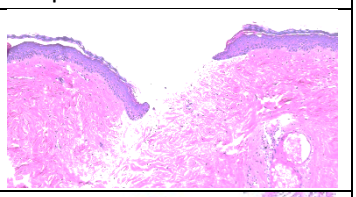
ET	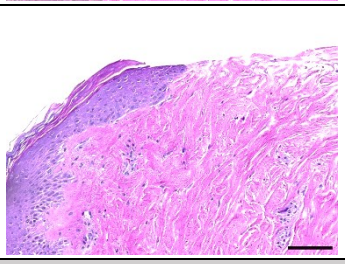	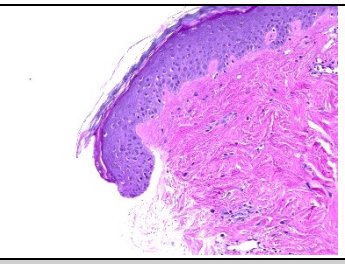	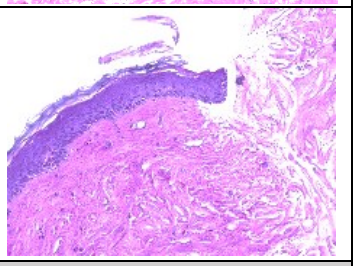
	1 µM S2149	10 µM S2149	4 x 1 µM S2149
Wound	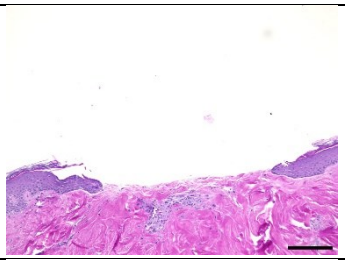	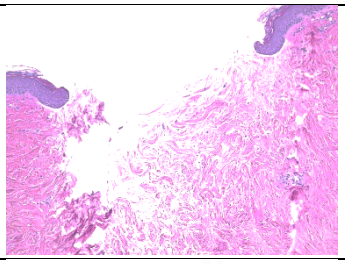	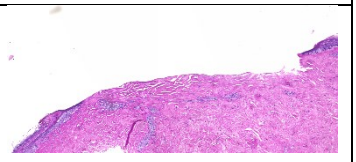
ET	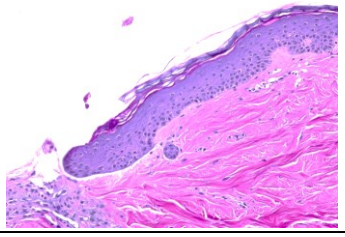	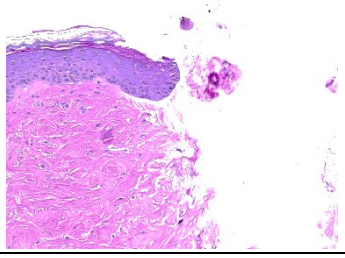	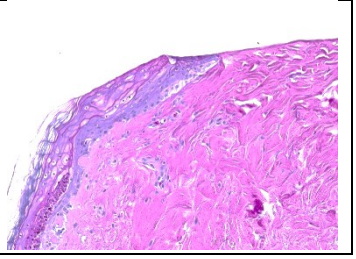

b) **wound area**

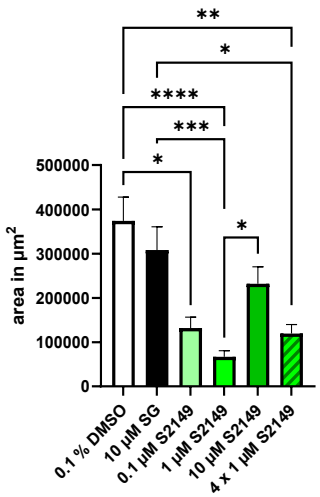

c) **wound diameter**

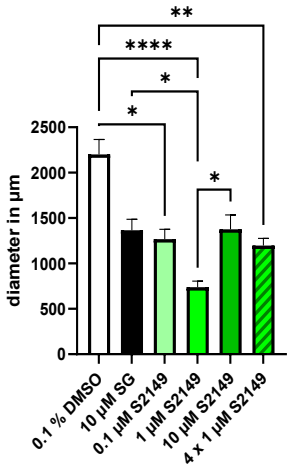

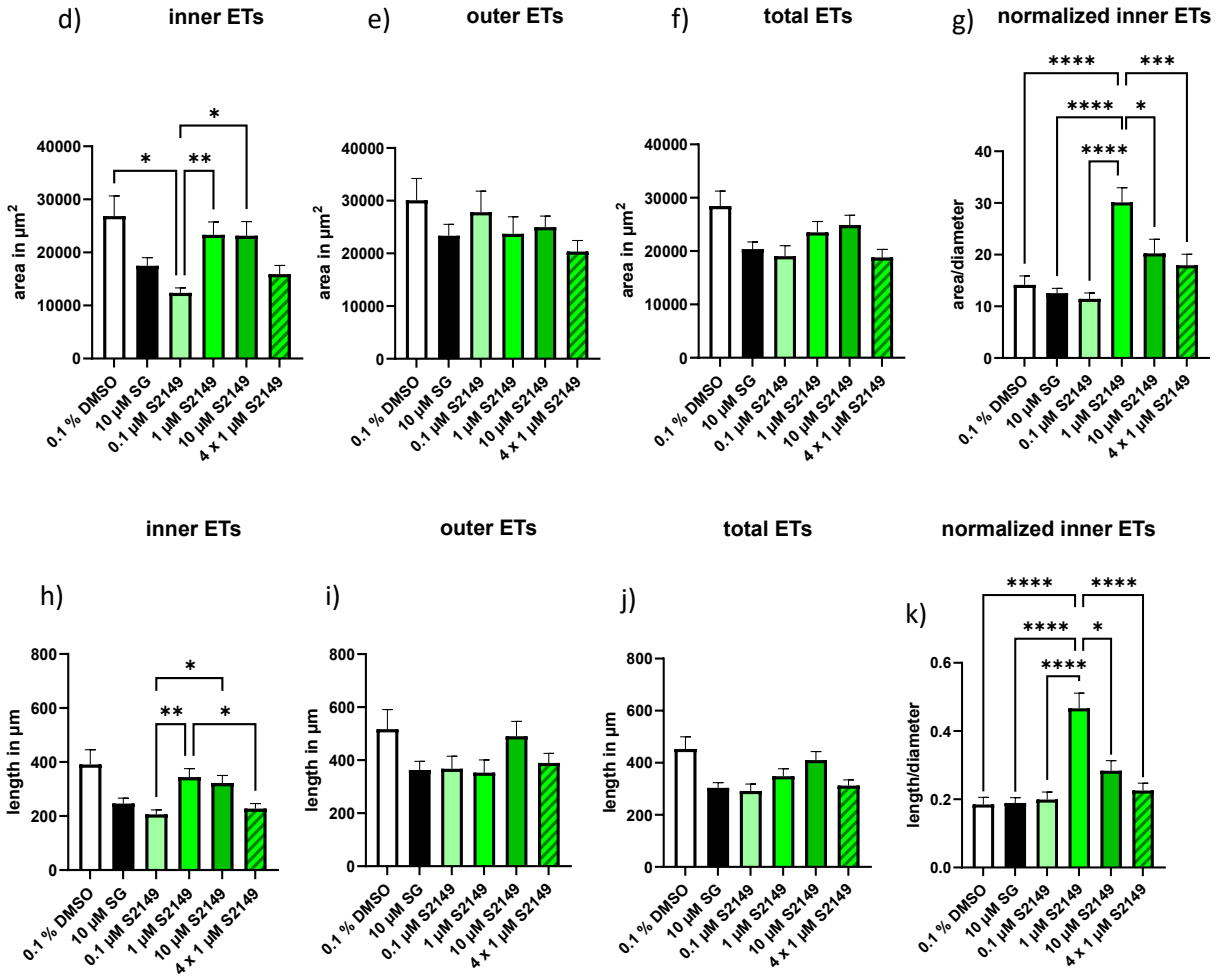

Figure 4.36: Influence of different concentrations of S2149 on the microscopic wound healing in the wound healing organ culture model

The wounded skin of the wound healing organ culture was treated with 0.1 µM, 1 µM or 10 µM S2149 at day 1 for 24 h or starting at day 1 repetitively with 1 µM. S2149 (4 x 1 µM S1180) over the course of the culture. As a vehicle control 0.1 % dimethyl sulfoxide (DMSO) was used, as a positive control 10 µM sodium gualenate (SG) was used. Shown here are the results of the hematoxylin & eosin (H&E) staining of wound cut and stained at day 7 (end of the culture). a) Exemplary hematoxylin and eosin stained pictures of the microscopic wounds (scale bar = 200 µm) and close-up of an exemplary epithelial tongue (ET, scale bar = 100 µm), b) microscopic wound area, c) wound length (n=5-6; 2-4 wounds/condition) d) area of the inner ETs, e) area of the outer ETs, f) area of inner and outer ETs combined, g) normalized area of the ETs on the respective wound diameter, h) length of inner ETs, i) length of outer ETs, j) length of inner and outer ETs combined, k) length of inner ETs normalized on the respective wound diameter. For all ET measurements n = 5-6; 2-16 ETs/condition). For statistical analysis a Kruskal-Wallis test with Dunns' multiple comparison was performed. * $p < 0.05$, ** $p < 0.01$, *** $p < 0.001$, **** $p < 0.0001$

4.7.3 Treatment with S2149 seemed to increase the relative cytokeratin 6 expression

Next, the relative CK6 expression was examined. The results can be found in **Figure 4.37**. The exemplary pictures in **Figure 4.37a** indicate that the CK 6 expression is higher in the ETs of wounds treated with S2149, especially for 4 x 1 µM S2149.

Figure 4.37b shows the relative CK 6 expression of the inner ETs. The CK 6 expression of the inner ETs of the positive control group was 89.58 % and thus lower than the vehicle control. For the CK 6 inner

expression it seemed to make almost no difference whether the wounds were treated with 0.1 µM S2149 (124.15 %), 1 µM S2149 (125.13 %) or 10 µM S2149 (125.64 %), all three concentrations led to a higher CK 6 expression of around 125 %. Treatment with 4 x 1 µM S2149 led to the highest CK 6 expression, namely 141.05 %. In a direct comparison, the CK 6 expression in the inner ETs is significantly higher after treatment with 4 x 1 µM S2149 than 0.1 % DMSO ($p < 0.01$, data not shown).

The CK 6 expression of the outer ETs can be found in **Figure 4.37c**. Here, the CK 6 expression of outer ETs of the vehicle control wounds and the positive control is almost identical (100 % versus 97.72 %). Treatment with all concentrations of S2149 led to a higher CK 6 expression in the outer ETs than both controls: 120.07 % for 0.1 µM S2149, 117.83 % for 1 µM S2149, 113.29 % for 10 µM S2149, and 124.44 % for 4 x 1 µM S2149. In a direct comparison, the CK 6 expression in the outer ETs of wounds treated with 1 µM S2149 and with 4 x 1 µM S2149 were significantly higher than that of the vehicle control wounds ($p < 0.05$ for 1 µM S2149 and $p < 0.01$ for 4 x 1 µM S2149, data not shown).

Figure 4.37d shows the relative CK 6 expression in the total ETs. Again, the controls displayed a very similar CK 6 expression (100 % for 0.1 % DMSO and 101.00 % for 10 µM SG). Treatment with all tested S2149 concentrations led to an increase in the relative CK 6 expression in the total ETs: 121.72 % for 0.1 µM S2149, 115.98 % for 1 µM S2149, 119.72 % for 10 µM S2149, and 133.89 % for 4 x 1 µM S2149. The relative CK 6 expression of the total ETS after treatment with 4 x 1 µM S2149 was significantly higher than that of the vehicle control wounds.

a)

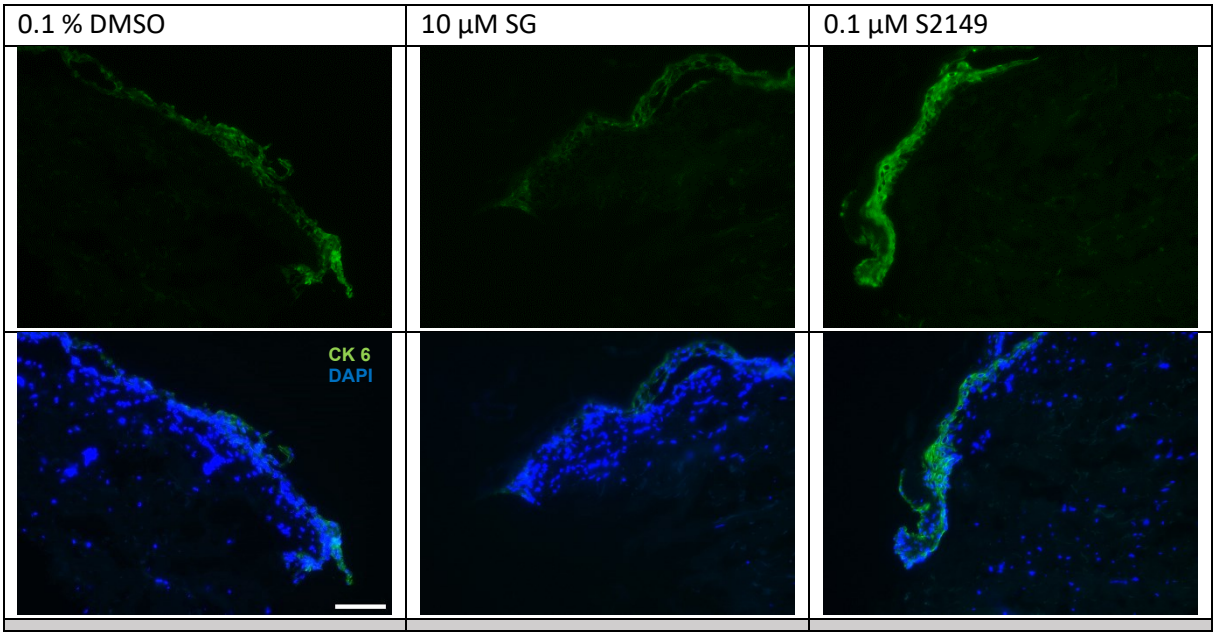

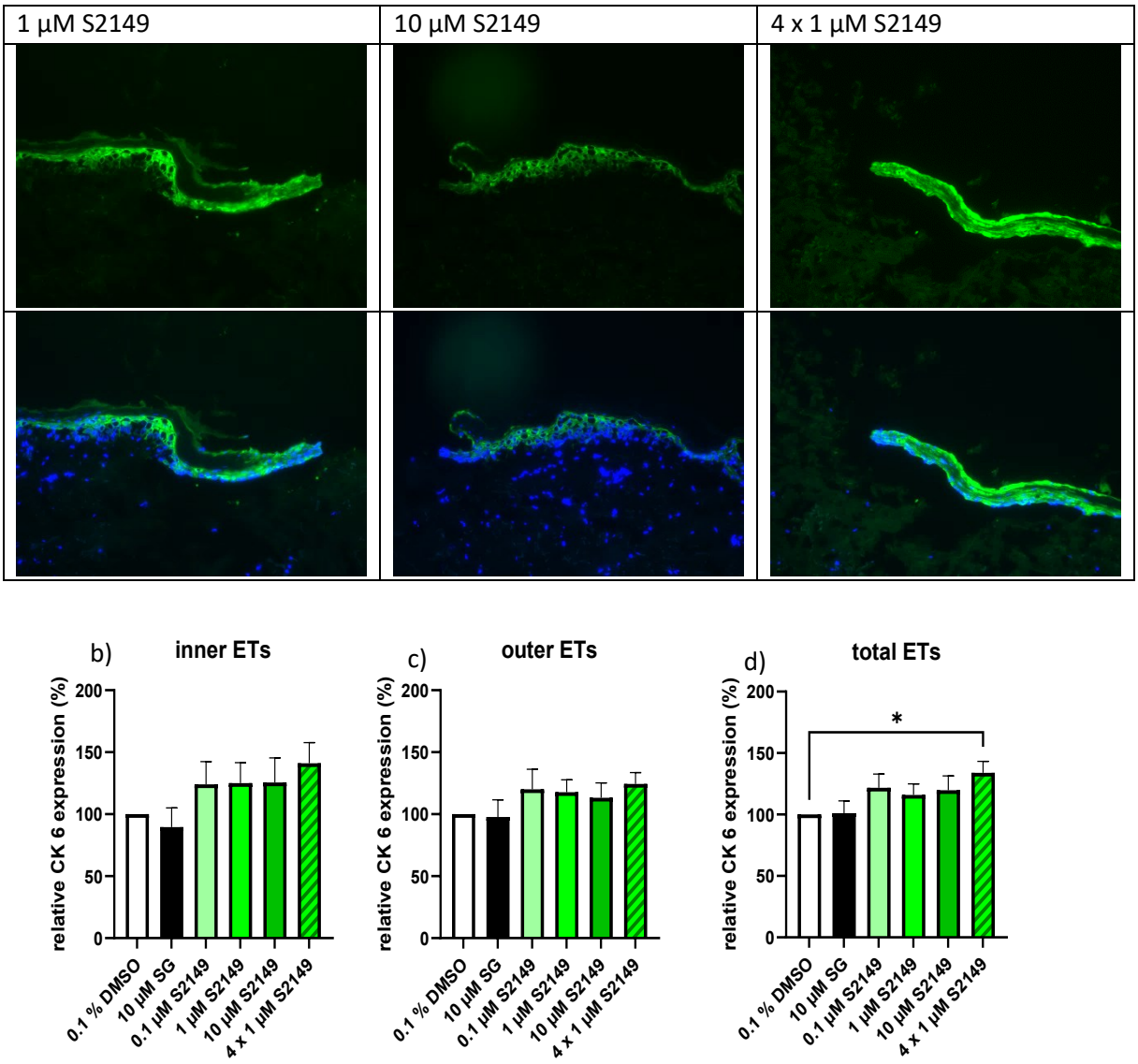

Figure 4.37: Influence of different concentrations of S2149 on the cytokeratin 6 expression in the wound healing organ culture model

The wounds of the wound healing organ culture were treated with 0.1 µM, 1 µM or 10 µM S2149 at day 1 for 24 hours or starting at day 1 repetitively with 1 µM S2891 (4 x 1 µM S2891) over the course of the culture. As a vehicle control 0.1 % dimethyl sulfoxide (DMSO) was used, as a positive control 10 µM sodium gualenate (SG) was used. Shown here is the relative cytokeratin (CK) 6 expression in the epithelial tongues (ETs) of wounds cut and stained at day 7 (end of culture). a) Exemplary immunofluorescence pictures of the ETs in 200x magnification (scale = 100 µm), CK 6 expression in the inner (b), outer (c) and total (d) ETs. For all ETs: n = 6, 2-8 ETs/wounds). For statistical analysis a Kruskal-Wallis test with Dunn's multiple comparison test (inner and total ETs) or one way ANOVA with Turkeys multiple comparisons test (outer ETs) was performed. Data not significant.

4.7.4 Treatment with 1 µM S2149 seemed to increase the relative CD31 expression and number of CD31 positive cells

Next the CD31 staining was evaluated. The results are shown in **Figure 4.38**. The exemplary pictures can be found in **Figure 4.38a**.

As **Figure 4.38b** shows, treatment with 1 µM S2149 resulted in the highest relative CD31 expression (116.97 %). Treatment with 0.1 µM S2149 (103.99 %) and 10 µM S2149 (103.09) also resulted in a higher relative CD31 expression than the vehicle control. Treatment with 10 µM SG (93.11 %) and

4 x 1 µM S2149 (95.54 %) led to less relative CD31 expression than 0.1 % DMSO. The effects were not significant.

Figure 4.38c depicts the number of CD31 positive cells. After treatment with all S2149 conditions an increased number of positive cells could be found in comparison to the 0.1 % DMSO, the highest number of cells (43 cells/VF) was counted in the wounds treated with 1 µM S2149. After treatment with 0.1 µM S2149 34.76 cells/VF were positive, after treatment with 10 µM S2149 35.33 cells/VF, and after treatment with 4 x 1 µM S2149 32.42 cells/VF. The differences were not significant. In a direct comparison of just 1 µM S2149 with 0.1 % DMSO the difference was significant, the same is true for comparison of 10 µM SG (41.04 cells/VF) and 0.1 % DMSO (data not shown).

The number of CD31 positive cross section is shown in **Figure 4.38d**. The highest cross sections count is in wounds treated with 0.1 µM S2149 (0.32/VF), followed by 10 µM SG (0.32/VF), 10 µM S21491 (0.24/VF), 1 µM S2149 (0.23/VF) and then 0.1 % DMSO (0.18/VF). Only treatment with 4 x 1 µM S2149 showed fewer positive vessels than the vehicle control 0.1 % DMSO, namely 0.17/VF. The data is not significant.

All treatment conditions tested show an increase in CD31 positive vessels compared to 0.1 % DMSO (0.19/VF), the increase is strongest in 10 µM SG (0.43/VF), 0.1 µM S2149 (0.43/VF), and 1 µM S2149 (0.44/VF), though the differences are not significant, as shown in **Figure 4.38e**. Treatment with 10 µM S2149 resulted in positive 0.35 vessels/VF and treatment with 4 x 1 µM S2149 in 0.30 positive vessels/VF.

a)

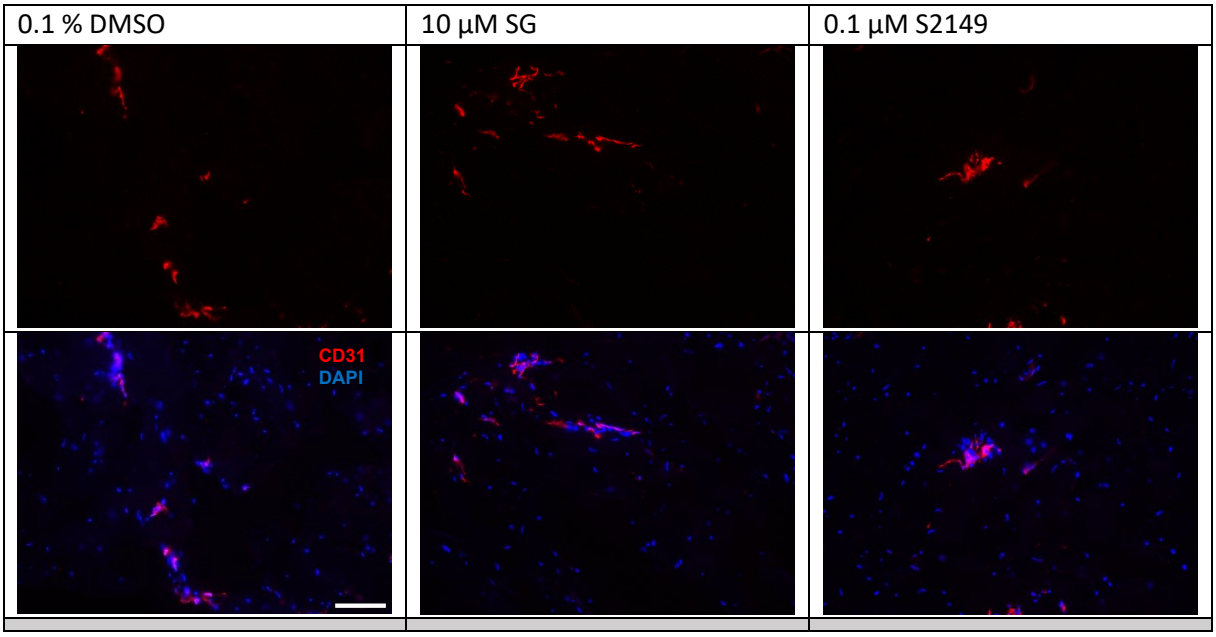

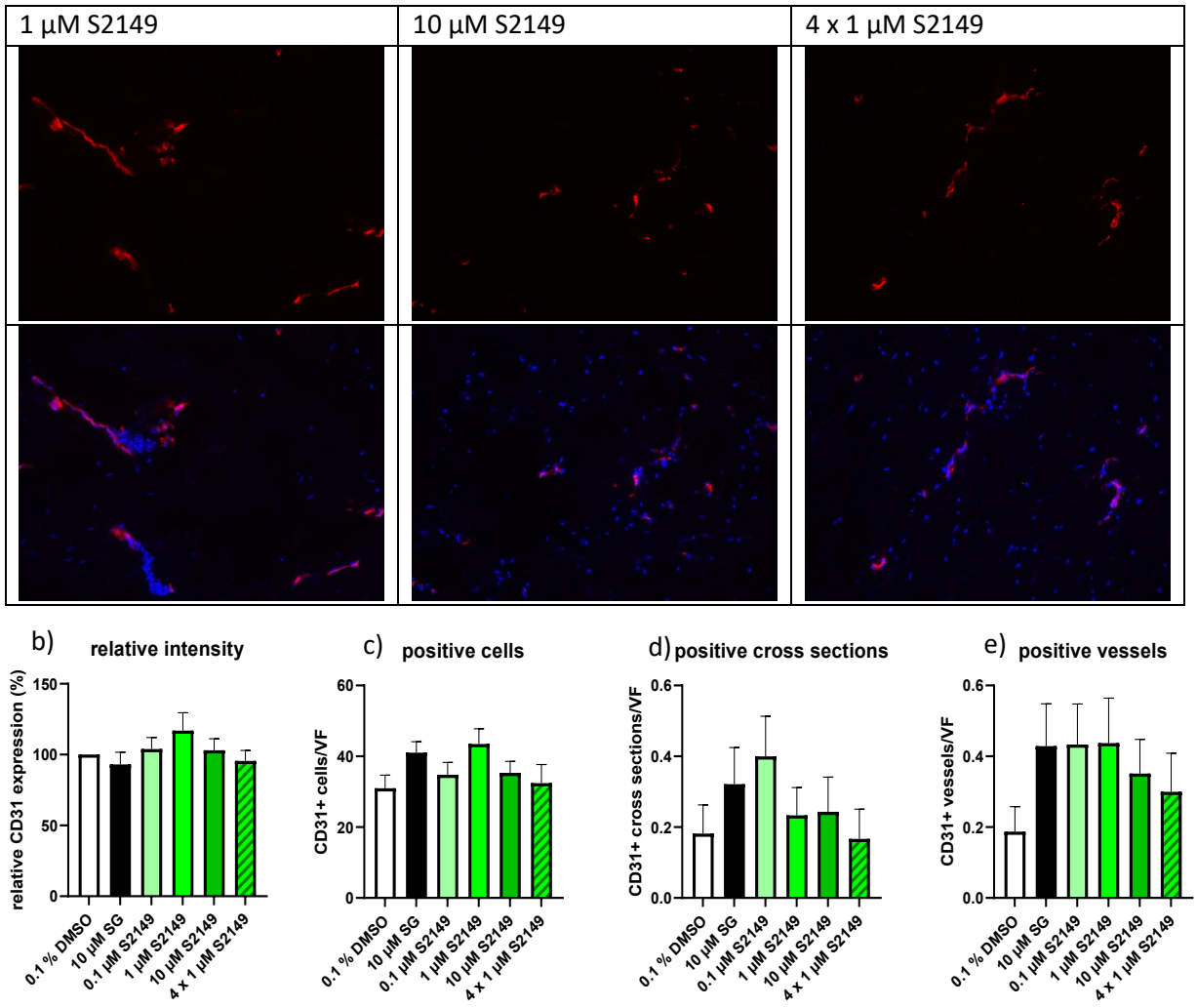

Figure 4.38: Influence of different concentrations of S2149 on the CD31 expression in the wound healing organ culture model

The wounds of the wound healing organ culture were treated with 0.1 µM, 1 µM or 10 µM S2149 at day 1 for 24 hours or starting at day 1 repetitively with 1 µM S2149 (4 x 1 µM S2149) throughout the culture. As a vehicle control 0.1 % dimethyl sulfoxide (DMSO) was used, as a positive control 10 µM sodium gualenate (SG). Shown here is the CD31 expression in the dermis of wounds cut and stained at day 7 (end of culture). a) Exemplary immunofluorescence pictures of the dermis. Scale bar = 100 µm. b) relative CD31 expression, c) number of CD31 positive cells/visual field (VF). d) number of CD31 positive vessels/VF, e) number of CD31 positive cross sections/VF. For all: n = 5, 4-8 VF/wound. For statistical analysis one-way ANOVA with Turkey's multiple comparison and t-test (relative intensity) or Kruskal-Wallis test with Dunn's multiple comparison and Mann-Whitney (for numbers of cells, cross sections and vessels) was performed. Data not significant.

Figure 4.39 shows exemplary pictures of the cortactin expression in ETs after treatment with different concentrations of S2149. Under all conditions a strong cortactin expression can be seen.

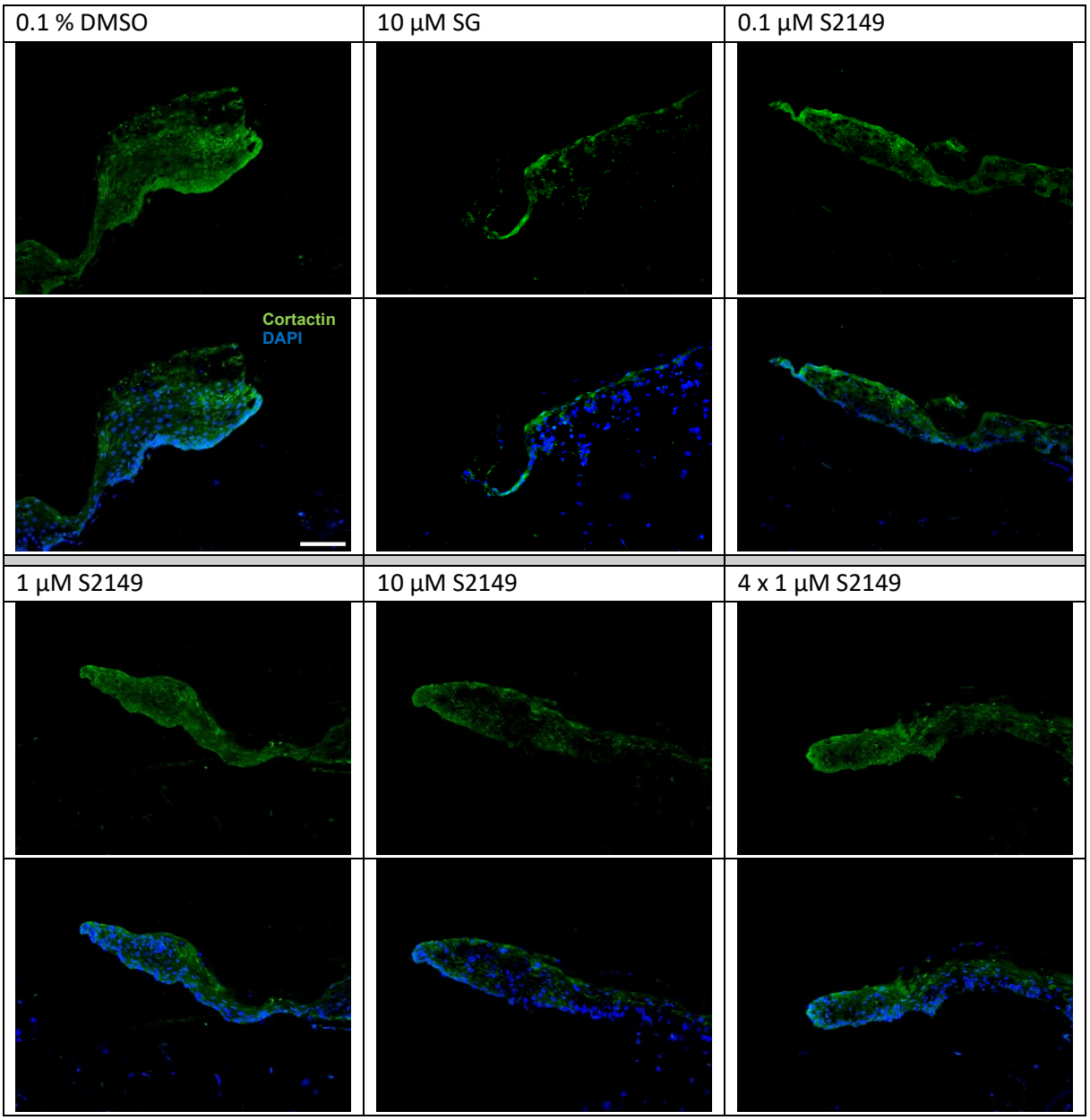

Figure 4.39: Influence of different concentrations of S2149 on the cortactin expression in the wound healing organ culture model

The wounds of the wound healing organ culture were treated with 0.1 µM, 1 µM or 10 µM S2149 at day 1 for 24 hours or starting at day 1 repetitively with 1 µM S2149 (4 x 1 µM S2149) throughout the culture. As a vehicle control 0.1 % dimethyl sulfoxide (DMSO) was used, as a positive control 10 µM sodium gualenate (SG). Shown here are exemplary pictures of the cortactin expression in epithelial tongues of wounds cut and stained at day 7 (end of culture). Scale bar = 100 µm.

All in all, 1 µM S2149 was found to have a small positive effect on *ex vivo* wound healing. A more throughout analysis of different molecular markers might be interesting to see how this effect is conveyed.

4.8 Treatment with 1 µM S1180 and with 10 µM S1180 aids the *ex vivo* wound healing in the wound healing organ culture model

Lastly the most successful inhibitor out of the screening was investigated. Treatment with S1180 was performed as described for S2891 (**Chapter 4.6**).

4.8.1 Treatment with 10 µM S1180 led to a significant reduction in relative top-view wound area and perimeter

Figure 4.40 shows the results of the top-view evaluation. The exemplary pictures in **Figure 4.40a** illustrate that especially treatment with 10 µM S1180 seems beneficial for top-view wound closure.

Figure 4.40b shows the relative top-view wound area over the course of the WHOC. On day 2, the beneficial effect of S1180 on the relative area did not yet show. The relative area of the vehicle control wounds (60.28 %) was smallest and the relative area of the positive control was largest, namely 67.40 %. The higher the concentration of S1180 was on this day, the higher the relative area: 61.50 % for 0.1 µM S1180, 62.75 % for 1 µM S1180 and 64.24 % for 10 µM S1180. Wounds treated with 4 x 1 µM S1180 had a relative area of 65.05 %.

Already on day 4, the reversed picture was observable. While treatment with 10 µM SG still led to the largest relative area of 52.64 %, but with increasing concentration of S1180 the relative area decreased. Wounds treated with 0.1 µM S1180 still had a relative area (50.53 %) larger than that of the negative control, which was 48.22 %. Treatment with 1 µM S1180 (45.93 %), 10 µM S1180 (45.12 %) and 4 x 1 µM S1180 (38.65 %) resulted in smaller relative areas than both controls. Treatment with 4 x 1 µM S1180 seemed especially beneficial on this day.

On day 6, the vehicle control wounds, and the positive control wounds had an almost identical relative area of 47.78 % or 47.26 % respectively. As before, treatment with 0.1 µM S1180 led to the largest relative area of 48.41 % and treatment with 4 x 1 µM S1180 to the smallest relative area of 38.74 %. Also, wounds treated with 1 µM S1180 (43.09 %) and 10 µM S1180 (39.90 %) had a smaller relative area than both controls on this day.

On day 7, the end of the WHOC, wounds treated with 10 µM S1180 had the smallest relative area, namely 29.51 %, which was significantly smaller than the area of wounds treated with the vehicle control 0.1 % DMSO ($p < 0.01$), with the positive control 10 µM SG ($p < 0.05$), and with 0.1 µM S1180 ($p < 0.05$). The relative wound area of the negative control group was 48.86 %. As on the day before the positive control was very similar in relative area with an area of 48.83 %. Next to 10 µM S1180, also treatment with 0.1 µM S1180 (45.57 %), 1 µM S1180 (38.64 %) and 4 x 1 µM S1180 (33.66 %) resulted in a smaller relative area than that of the controls. This effect was more pronounced for 1 µM S1180 and 4 x 1 µM S1180 than for 0.1 µM S1180.

Figure 4.40b shows the relative top-view wound perimeter over the course of the culture. On day 2, the differences in relative perimeter were small. Wounds treated with 1 µM S1180 had the smallest relative perimeter on this day, namely 80.59 %, and the vehicle control wounds had the largest relative perimeter of 85.89 %, which was closely followed by the relative perimeter of wounds treated with 4 x 1 µM S1180, which was 85.88 %. The relative perimeter of the positive control wounds was 84.53 %. Treatment with 0.1 µM S1180 led to a relative perimeter of 84.19 % and treatment with 10 µM S1180 to a perimeter of 84.55 %.

On day 4, the relative perimeter of the vehicle control wounds, the positive control wounds and wounds treated with 0.1 µM S1180 was almost identical with 75.96 %, 75.74 % and 74.27 % respectively. Treatment with 1 µM S1180 (69.17 %), 10 µM S1180 (70.78 %), and 4 x 1 µM S1180 (69.54 %) also resulted in very similar perimeters, that were all smaller than the controls.

On day 6, wounds treated with 0.1 µM S1180 had a slightly larger relative perimeter of 73.42 % than the positive control wounds (71.93 %) and the vehicle control wounds (73.07 %). Wounds treated with 1 µM S1180 (67.32 %), 10 µM S1180 (66.04 %) and 4 x 1 µM S1180 (69.67 %) had a smaller relative perimeter than both controls.
On day 7, the vehicle control wounds had the largest relative perimeter of 74.25 %, followed by the positive control wounds (71.39 %), wounds treated with 0.1 µM S1180 (70.05 %), and wounds treated with 4 x 1 µM S1180 (68.23 %). The relative perimeter of 10 µM S1180, namely 60.90 %, was significantly smaller than that of the vehicle control with a significance level of $p < 0.05$. Treatment with 1 µM S1180 also led to a distinct reduction in relative perimeter, namely 64.45 %. In a direct comparison the difference in the relative perimeter between 0.1 % DMSO and 1 µM S1180 was significant ($p < 0.05$, data not shown).

None of tested concentrations of S1180 could reproduce the positive effect on the relative wound volume on day 6 found in the screening and validation after treatment with 1 µM S1180, as **Figure 4.40d** shows. Treatment with 10 µM S1180 resulted in a relative volume of 33.61 %, which came closest to the relative volume of the vehicle control wounds, namely 31.76 %. Treatment with 4 x 1 µM S1180 led to the largest relative wound volume of 50.40 %. The relative volume of wounds treated with 10 µM SG as a positive control was 38.47 %, that of wounds treated with 0.1 µM S1180 was 38.61 % and that of wounds treated 1 µM S1180 was 36.62 %. None of the measured differences was significant.

The top-view/macroscopic evaluation of treatment with S1180 showed that treatment with 10 µM S1180 led to a significant reduction in relative top-view wound closure, making it so far the most successful concentration. Treatment with 1 µM S1180 for either 24 h at day one or repetitively from day 1 throughout the culture seems to have a positive effect on wound healing in the WHOC as well although not as pronounced as 10 µM S1180. On the other hand, 0.1 µM S1180 seems to have no positive effect on the macroscopic wound closure *ex vivo*. None of the tested S1180 concentrations led to a relative wound volume smaller than the vehicle control 0.1 % DMSO, though wounds treated with 1 µM S1180 and 10 µM S1180 came relatively close.

a)

	0.1 % DMSO	10 µM SG	0.1 µM S1180
Day 0	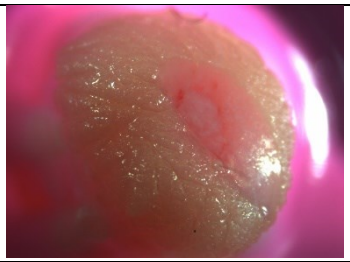		
Day 7			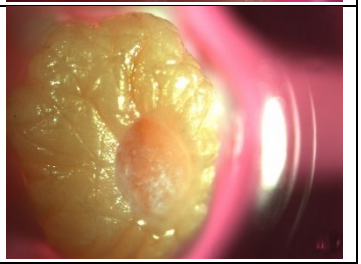

	1 µM S1180	10 µM S1180	4 x 1 µM S1180
Day 0			
Day 7			

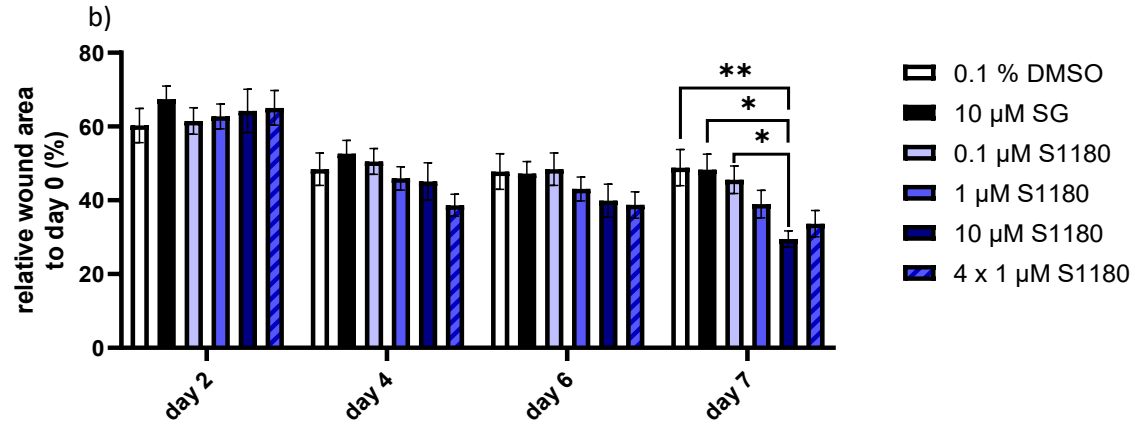

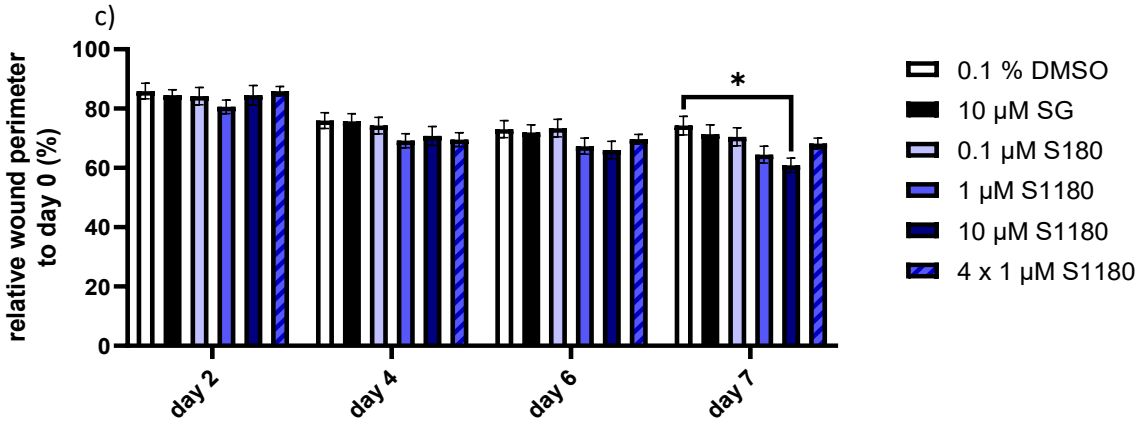

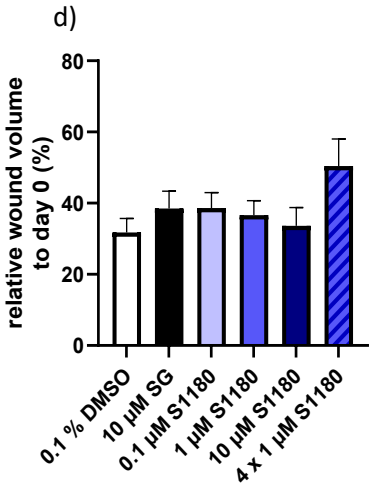

Figure 4.40: Influence of different concentrations of S1180 on the macroscopic wound healing in the wound healing organ culture
The wounded skin of the wound healing organ culture was treated with 0.1 µM, 1 µM or 10 µM S1180 at day 1 for 24 h or starting at day 1 repetitively with 1 µM S1180 (4 x 1 µM S1180) throughout the culture. As a vehicle control 0.1 % dimethyl sulfoxide (DMSO) was used, as a positive control 10 µM sodium gualenate (SG) was used. a) Exemplary top-view pictures of day 0 (day of wounding) and day 7 (end of the culture), b) relative top-view wound area to day 0 over the course of the culture (n = 6, 1-4 wounds/condition), c) relative top-view wound perimeter to day 0 over the course of the culture (n = 6, 1-4 wounds/condition), d) relative wound volume to day 0 at day 6, obtained by optical coherence tomography (n = 3, 4 wounds/condition). Values are depicted as mean ± or + standard error of the mean. Significances were determined by one-way ANOVA with Turky's multiple comparisons test (relative top-view wound area, relative top-view wound perimeter day), Kruskal-Wallis test with Dunns' multiple comparison (relative top-view wound perimeter day 4, day 6, day 7). * $p < 0.05$, ** $p < 0.01$

4.8.2 Treatment with 1 µM S1180 and 10 µM S1180 led to a significant increase in area and length of the epithelial tongues

Next the microscopic wound healing was assessed on H&E-stained sections. The wounds were cut and stained as described for S2891 (**Chapter 4.6.2**). The evaluation of the H&E staining can be found in **Figure 4.41**. **Figure 4.41a** shows exemplary microscopic wounds and ETs. Already here it is visible that treatment with 10 µM S1180 led to noticeably longer ETs. Treatment with 1 µM S1180, 10 µM S1180, and 4 x 1 µM S1180 also seemed to lead to smaller microscopic wound area than the controls.

The microscopic wound area shown in **Figure 4.41b** was distinctly smaller after treatment with 1 µM S1180 (181,094 µm^2), 10 µM S1180 (224,578 µm^2), and 4 x 1 µM S1180 (134,175 µm^2) than after treatment with the vehicle control 0.1 % DMSO (267,564 µm^2) and the positive control 10 µM SG (258,668 µm^2). Treatment with 4 x 1 µM S1180 even led to a significantly stronger decrease in microscopic wound area than treatment with the vehicle control ($p < 0.05$). In a direct comparison wounds treated with 1 µM S1180 had a significantly smaller relative area than the vehicle control wounds. Treatment with 0.1 µM S1180 led to a microscopic area of 249,133 µm^2, which was only slightly lower than both controls.

The wound diameter was larger in wounds treated with 0.1 µM S1180, namely 1,772.65 µm, than that of the vehicle control, which was 2,482.56 µm (compare **Figure 4.41c**). The largest diameter of 1,815.78 µm was measured in the positive control wounds. Wounds treated with 10 µM S1180 (1,418.42 µm) and 4 x 1 µM S1180 (1,423.10 µm) show a smaller diameter than the controls. The smallest diameter was observable after treatment with 1 µM S1180, namely 1,118.28 µm. It was significantly smaller than those of wounds treated with 0.1 µM S1180 or 10 µM SG ($p < 0.05$ for

both). Moreover, in a direct comparison of the diameter of wounds treated with 1 µM S1180 had a significantly smaller diameter than the vehicle control wounds ($p < 0.05$, data not shown).
As with the top-view relative wound area and perimeter treatment with 0.1 µM S1180 does not have a positive effect on microscopic wound area and diameter. Treatment with the other three conditions tested seems to be beneficial for both parameters.

For treatment of the wounds with S1180 the analysis of the ETs is shown in **Figures 4.41d-k**. **Figures 4.41d-g** illustrate the area of the inner ETs. For the inner ETs the large area of wounds treated with 10 µM S1180 (39,553 μm^2, compare **Figure 4.41d**) was striking. These ETs were significantly larger than those treated with 0.1 % DMSO as vehicle control (28,653 μm^2), 10 µM SG as a positive control (26,016 μm^2), and 0.1 µM S1180 (25,265 μm^2) with a significance level of $p < 0.05$. The inner ETs of wounds treated with 4 x 1 µM S1180 had an area of 31,021 μm^2. Treatment with 1 µM S1180 led to an inner ETs' area of 26,876 μm^2, which was smaller than those of the vehicle control wounds.
As **Figure 4.41g** shows, normalization of the area of the inner ETs changes the picture: wounds treated with 1 µM S1180 have the largest ETs by far. Their value of 2,655.20 µm is significantly higher than that of both the vehicle control (745.73 µm) and the positive control (834.68 µm) as well as 0.1 µM S1180 (1,181.52 µm) with a significance level of $p < 0.01$ for 0.1 % DMSO and $p < 0.05$ for 10 µM SG and 0.1 µM S1180. Treatment with 10 µM S1180 still resulted in larger ETs than both controls, namely 1288.04 µm. However, the effect was less pronounced and no longer significant. Also, treatment with 0.1 µM S1180 showed a positive effect on the area of the inner ET when normalized on the diameter but not in absolute numbers. Treatment with 4 x 1 µM S1180 led to a normalized inner ETS' area of 1,520.18 µm. So, 4 x 1 µM S1180 showed a beneficial effect in both cases.
In accordance with the normalized inner ET area, the area of the outer ETs is highest in the wounds treated with 1 µM S1180, as can be seen in **Figure 4.41e**. With an area of 39,471 μm^2 they were significantly larger than that of wounds treated with 10 µM SG as a positive control (23,921 μm^2). Treatment with 4 x 1 µM S1180 led to an outer ETs' area of 34,950 μm^2. Treatment with 10 µM S1180 (31,184 μm^2) and 0.1 µM S1180 (27,182 μm^2) still led to larger ETs than both the positive control and the vehicle control (25,764 μm^2), though the effect was stronger for 10 µM S1180.
Looking at the total ETs area in **Figure 4.41f**, wounds treated with 1 µM S1180 (33,680 μm^2) , 10 µM S1180 (35,460 μm^2), and 4 x 1 µM S1180 (33,050 μm^2) had larger ETs than those treated with 0.1 % DMSO (27,209 μm^2), 10 µM SG (24,968 μm^2), or 0.1 µM S1180 (26,213 μm^2). For 10 µM S1180 the area is significantly larger than those treated with both controls and 0.1 µM S1180 ($p < 0.05$ for 0.1 % DMSO and 0.1 µM S1180; $p < 0.01$ for 10 µM S1180. Wounds treated with 4 x 1 µM S1180 also had a significantly larger total ET area than those treated with 10 µM SG with a significance level of $p < 0.05$. Moreover, in a direct comparison wounds treated with 4 x 1 µM S1180 had significantly larger total ETs than the vehicle control wounds ($p < 0.05$, data not shown).

Figures 4.41h-k show the length of the ETs normalized on the respective wound diameter. The length of the inner ETs in **Figure 4.41h** displayed a similar pattern as their area: Wounds treated with 10 µM S1180 (450.29 µm) had significantly longer ETs than those treated with 0.1 % DMSO (326.89 µm) as a vehicle control or those treated with 0.1 µM S1180 (306.99 µm), but also than wounds treated with 1 µM S1180 (309.57 µm) and 4 x 1 µM S1180 (313.97 µm) with a significance level of $p < 0.01$ for 0.1 % DMSO and $p < 0.05$ for 0.1 µM S1180, 1 µM S1180, and 4 x 1 µM S1180. The length of the inner ETs of the positive control wounds was 337.59 µm.
Just like the area of the inner ETs, the positive effect one-time treatment with 1 µM S1180 has on the inner ETs only became visible when normalizing on the diameter, as **Figure 4.41k** shows. Here, they had a length of 28.39, which was significantly larger than the normalized length of the inner ETs after

treatment with the vehicle control (12.15), positive control (11.41) and 0.1 µM S1180 (13.97) with a level of significance of $p < 0.01$ for 0.1 % DMSO and $p < 0.05$ for 10 µM SG and 0.1 µM S1180. However, just like the area after normalization treatment with 0.1 µM S1180 showed a small positive effect on ETs length. The clearly positive effect of treatment with 10 µM S1180 was no longer as pronounced as it was in absolute numbers. The normalized inner ETs of wounds treated with 10 µM S1180 was 17.13. In a direct comparison of 0.1 % DMSO and 10 µM S1180, the normalized inner ETS were longer when treated with 10 µM S1180 ($p < 0.05$, data not shown). 4 x 1 µM S1180 led to an increase in the length of the inner ETs, namely 15.86.
The length of the outer ETs is shown in **Figure 4.41i**. Just like with the area, treatment with 1 µM S1180 (559.96 µm), 10 µM S1180 (494.85 µm), and 4 x 1 µM S1180 (494.34 µm) led to longer ETs than treatment with the vehicle control 0.1 % DMSO (337.59 µm) or 0.1 µM S1180 (359.78 µm). After treatment with 1 µM S1180 the outer ETs were significantly larger than those treated with the vehicle control or 0.1 µM S1180 ($p < 0.01$ for 0.1 % DMSO and $p < 0.05$ for 0.1 µM S1180). In a direct comparison also the outer ETs of wounds treated with 10 µM S1180 were significantly larger than wounds treated with 0.1 % DMSO ($p < 0.05$, data not shown). The length of outer ETs of the positive control wounds was 375.20 µm.
Figure 4.41j shows the length of the total ETs. Again, treatment with 1 µM S1180 (444.84 µm), 10 µM S1180 (472.10 µm), 4 x 1 µM S1180 (409.11 µm) led to longer ETs than treatment with the vehicle control (332.24 µm) and the positive control (356.20 µm) or 0.1 µM S1180 (333.66 µm). Just like the area, wounds treated with 10 µM S1180 showed significantly larger ETs than those treated with the controls or 0.1 µM S1180 ($p < 0.001$ for 0.1 % DMSO, $p < 0.05$ for 10 µM SG, and $p < 0.01$ for 0.1 µM S1180). In a direct comparison, the total ETs of wounds treated with 1 µM S1180 was significantly longer than those of the vehicle control ($p < 0.0001$, data not shown).
The finding that after normalization also one-time treatment 1 µM S1180 has a positive effect on the ETs fits to the findings of the screening and the validation., where 1 µM S1180 performed extremely well.

Taking the macroscopic and the H&E evaluation together treatment with S1180 supports *ex vivo* wound healing in the WHOC significantly. From the concentrations investigated only 0.1 µM did not show a beneficial effect. All other concentrations had a beneficial influence on some of the parameters studied here. 1 µM S1180 showed the greatest effect in the normalized data, which shows it aids healing in our model. 10 µM showed the greatest effect in absolute number for the ETs and in the top-view data, which allows the conclusion that this concentration has beneficial effects as well. The difference and meaning of normalized and non-normalized data will be further discussed in **Chapter 5**.
Repetitive treatment with 1 µM S1184 shows positive effects on the *ex vivo* wound healing but the effects are not as distinct, so this treatment regime will be further investigated with a more suited vehicle control in **Chapter 4.9**.

a)

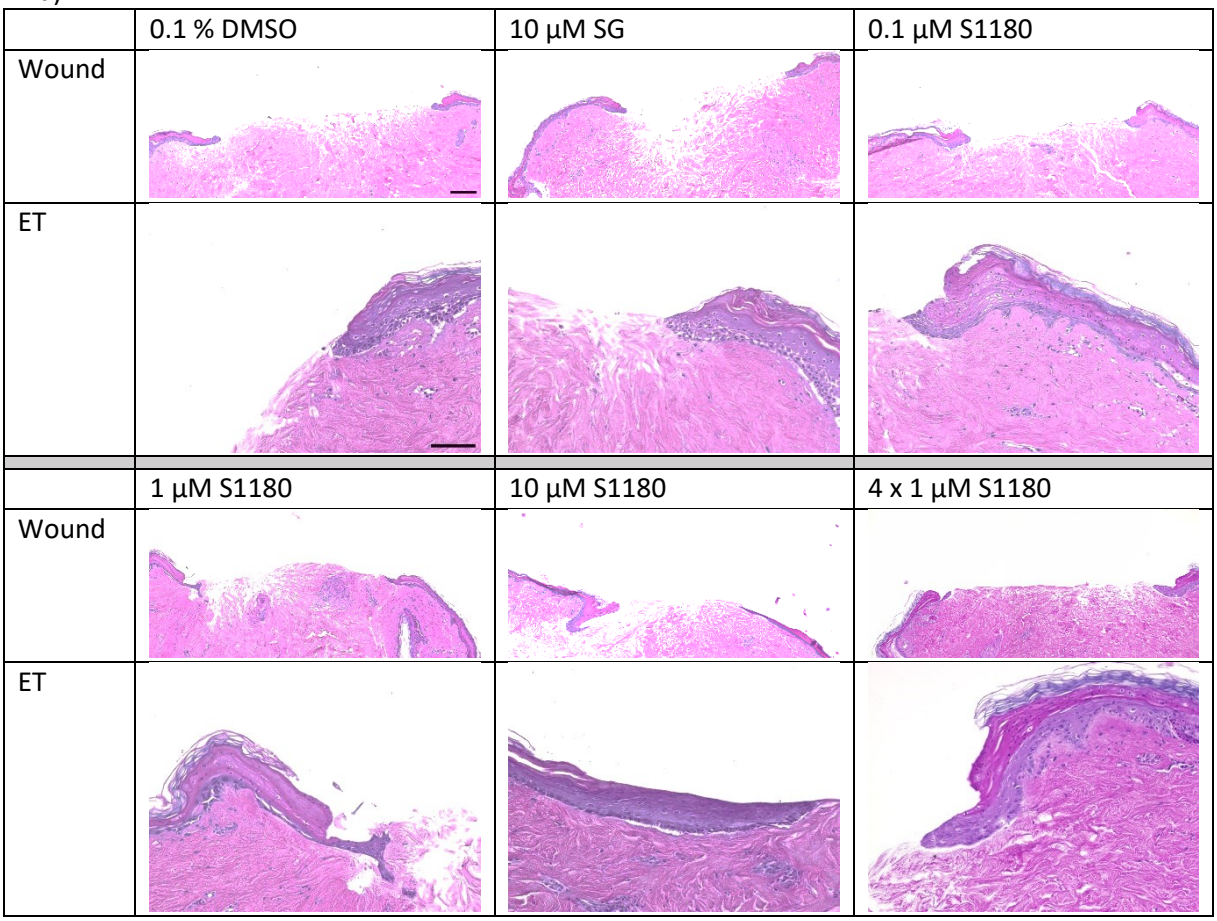

b) wound area

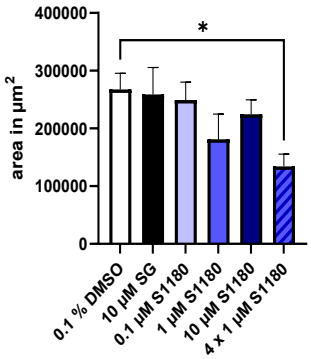

c) wound diameter

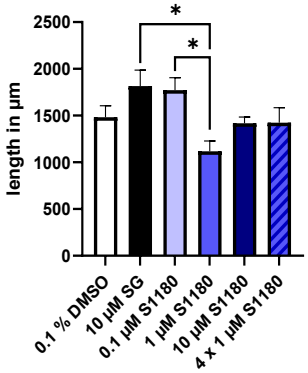

d) inner ETs

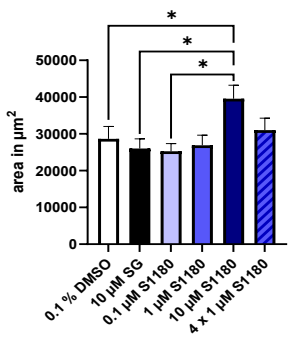

e) outer ETs

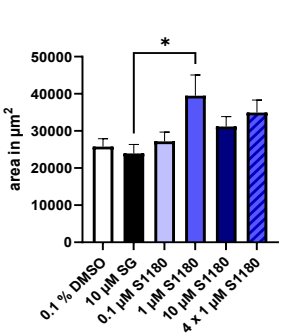

f) total ETs

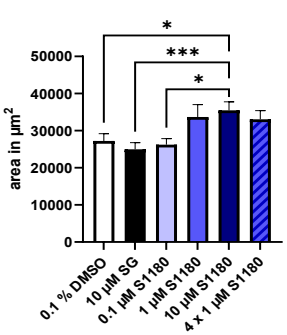

g) normalized inner ETs

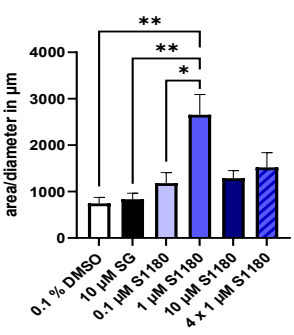

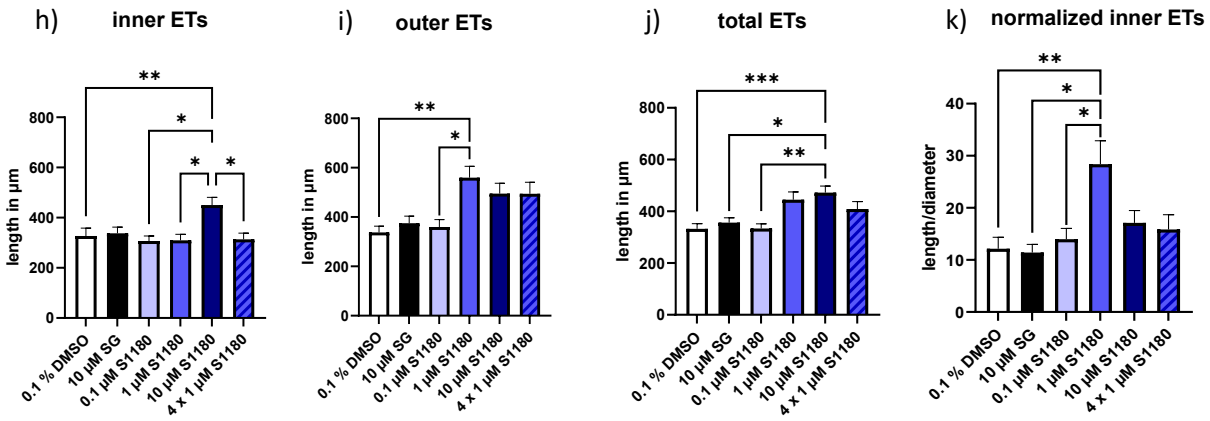

Figure 4.41: Influence of different concentrations of S1180 on the microscopic wound healing in the wound healing organ culture model

The wounded skin of the wound healing organ culture was treated with 0.1 µM, 1 µM or 10 µM S1180 at day 1 for 24 h or starting at day 1 repetitively with 1 µM S1180 (4 x 1 µM S1180) over the course of the culture. As a vehicle control 0.1 % dimethyl sulfoxide (DMSO) was used, as a positive control 10 µM sodium gualenate (SG) was used. Shown here are the results of the hematoxylin & eosin (H&E) staining of wound cut and stained at day 7 (end of the culture). a) Exemplary hematosylin and eosin stained pictures of the microscopic wounds in 100x magnification (scale bar = 200 µm) and close-up of an exemplary epithelial tongue (ET) in 200x magnification (scale bar = 100 µm), b) microscopic wound area, c) wound length (n=5-6; 2-4 wounds/condition) d) area of the inner ETs, e) area of the outer ETs, f) area of inner and outer ETs combined, g) normalized area of the ETs on the respective wound diameter, h) length of inner ETs, i) length of outer ETs, j) length of inner and outer ETs combined, k) length of inner ETs normalized on the respective wound diameter. For all ET measurements n = 5-6; 2-16 ETs/condition). For statistical analysis a Kruskal-Wallis test with Dunns' multiple comparison was performed. * $p < 0.05$, ** $p < 0.01$, *** $p < 0.001$

4.8.3 Treatment with S1180 seemed to increase the relative CK 6 expression

The results of the CK6 staining are shown in **Figure 4.42**. **Figure 4.42a** shows exemplary pictures of CK 6 expression of the ETs after treatment with different S1180 concentrations.

The relative CK 6 expression of the inner ETs can be found in **Figure 4.42b**. Treatment with the vehicle control 0.1 % DMSO led to a relative CK 6 expression of 100 % and the positive control 10 µM SG to 103.26 %. All concentrations of S1180 led to an increase in CK 6 expression: 123.49 % for 0.1 µM S1180, 125.03 % for 1 µM S1180, 108.48 % for 10 µM S1180, and 112.25 % for 4 x 1 µM S1180. Even though 10 µM S1180 led to the smallest increase in relative CK 6 expression, only this concentration led to a significant increase compared to the vehicle control in a direct comparison of both groups ($p < 0.001$, data not shown).

Figure 4.42c shows the relative CK 6 expression of the outer ETs. Again, the relative CK 6 expression after treatment with 0.1 % DMSO was set to 100 %. Treatment with 10 µM SG led to a relative CK 6 expression of 106.71 %. Like the inner ETs, in the outer ETs all S1180 concentrations led to an increase in CK 6 expression: 132.09 % for 0.1 µM S1180, 109.23 % for 1 µM S1180, 115.07 % for 10 µM S1180, and 108.03 % for 4 x 1 µM S1180. In a direct comparison, the relative CK 6 expression after treatment with 0.1 µM S1180 was significantly higher than that of the vehicle control wounds ($p < 0.01$, data not shown).

Figure 4.42d shows the relative CK 6 expression of the total ETs. The relative CK 6 expression in the outer ETs of the vehicle control wounds was 100 % and of the positive control wounds 105.14 %. As before, treatment with S1180 led to an increase in relative CK 6 expression. The highest relative CK 6 expression in the total ETs was observed after treatment with 0.1 µM S1180 (127.98 %), followed by 1 µM S1880 (116.79 %), 10 µM S1180 (111.93 %), and 4 x 1 µM S1180 (110.03 %). In a direct

comparison, the relative CK 6 expression after treatment with 10 µM S1180 was significantly higher than that of the vehicle control wounds ($p < 0.05$, data not shown).

a)

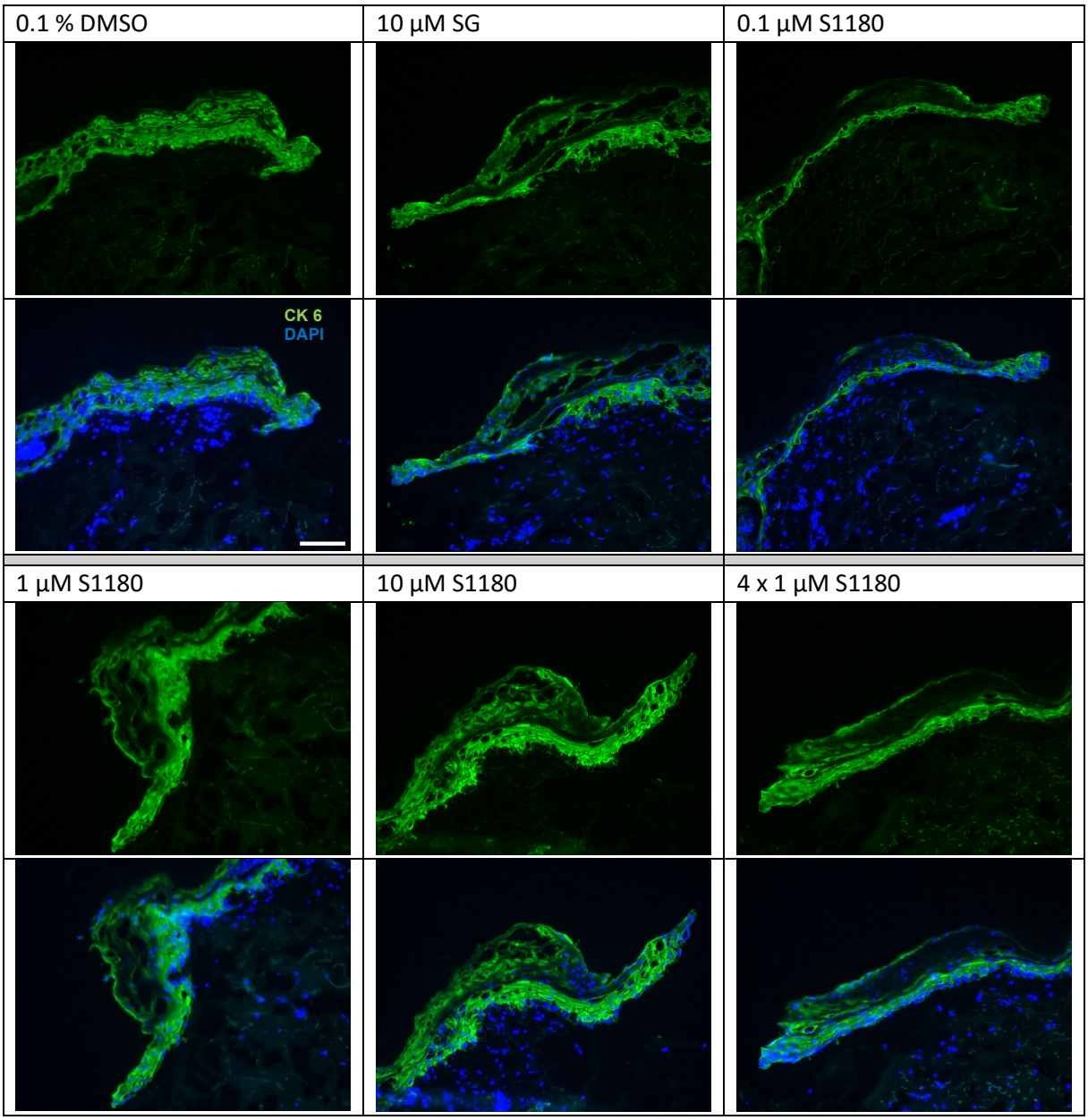

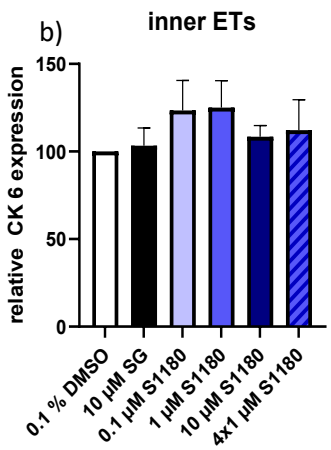

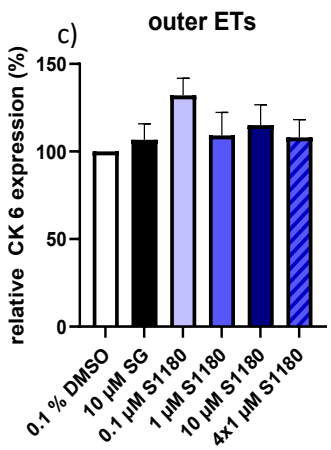

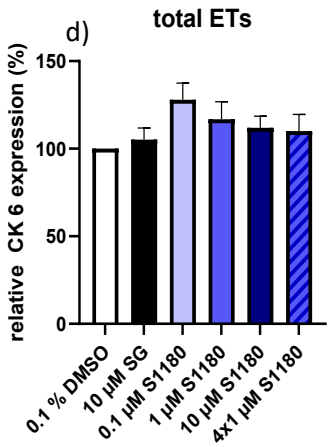

Figure 4.42: Influence of different concentrations of S1180 on the cytokeratin 6 expression in the wound healing organ culture model
The wounds of the wound healing organ culture were treated with 0.1 µM, 1 µM or 10 µM S1180 at day 1 for 24 hours or starting at day 1 repetitively with 1 µM S1180 (4 x 1 µM S1180) over the course of the culture. As a vehicle control 0.1 % dimethyl sulfoxide (DMSO) was used, as a positive control 10 µM sodium gualenate (SG) was used. Shown here is the relative cytokeratin (CK) 6 expression in the epithelial tongues (ETs) of wounds cut and stained at day 7 (end of culture). a) Exemplary immunofluorescence pictures of the ETs. Scale bar = 100 µm. CK 6 expression in the inner (b), outer (c) and total (d) ETs. (n = 6, 2-8 ETs/condition). For statistical analysis a Kruskal-Wallis test with Dunn's multiple comparison test (inner and total ETs) or one way ANOVA with Turkeys multiple comparisons test (outer ETs) was performed. Data not significant.

4.8.4 Treatment with 10 µM S1180 seemed to increase the number of CD31 positive cells

Figure 4.43 shows the results of the CD31 staining. The exemplary pictures of the CD31 expression in the dermis can be found in **Figure 4.43a**.

As **Figure 4.43b** shows, only treatment with 4 x 1 µM S1180 led to an increase in relative CD31 compared to the vehicle control 0.1 % DMSO, namely 102.96 %. The relative CD31 expression of all other groups was lower than that of the vehicle control and very similar to each other: 95.15 % for 10 µM SG, 94.89 % for 0.1 µM S1180, 95.30 % for 1 µM S1180, and 94.18 % for 10 µM S1180.

Figure 4.43c depicts the number of CD31 positive cells. With a value of 41.49 cells/VF, it was highest after treatment with 10 µM S1180, followed by 4 x 1 µM (35.71 cells/VF) and 1 µM S1180 (32.30 cells/VF). The vehicle control wounds had 28.48 CD31 positive cells/VF and the positive control wounds had 31.18 CD31 positive cells/VF. Treatment with 0.1 µM S1180 led to less positive cells than the controls, namely 28.73 cells/VF.

The CD31 positive cross sections are shown in **Figure 4.43d**. The vehicle control wounds had 0.51 % positive cross sections/VF and the positive control wounds 0.56 positive cross sections/VF. Wounds treated with S1180 had less CD31 positive cross sections than both controls: 0.20/VF for 0.1 µM S1180, 0.31/VF for 1 µM S1180, 0.28/VF for 10 µM S1180, and 0.39/VF for 4 x 1 µM S1180.

As **Figure 4.43e** shows, the number of CD31 positive branched vessels was highest in wounds treated with 10 µM S1180 (0.43/VF), followed by 10 µM SG (0.40/VF), 1 µM S1180 (0.34/VF), 4 x 1 µM S1180 (0.33/VF), 0.1 % DMSO (0.28/VF), and 0.1 µM S1180 (0.18/VF).
None of the differences measured in the CD31 evaluation were significant.

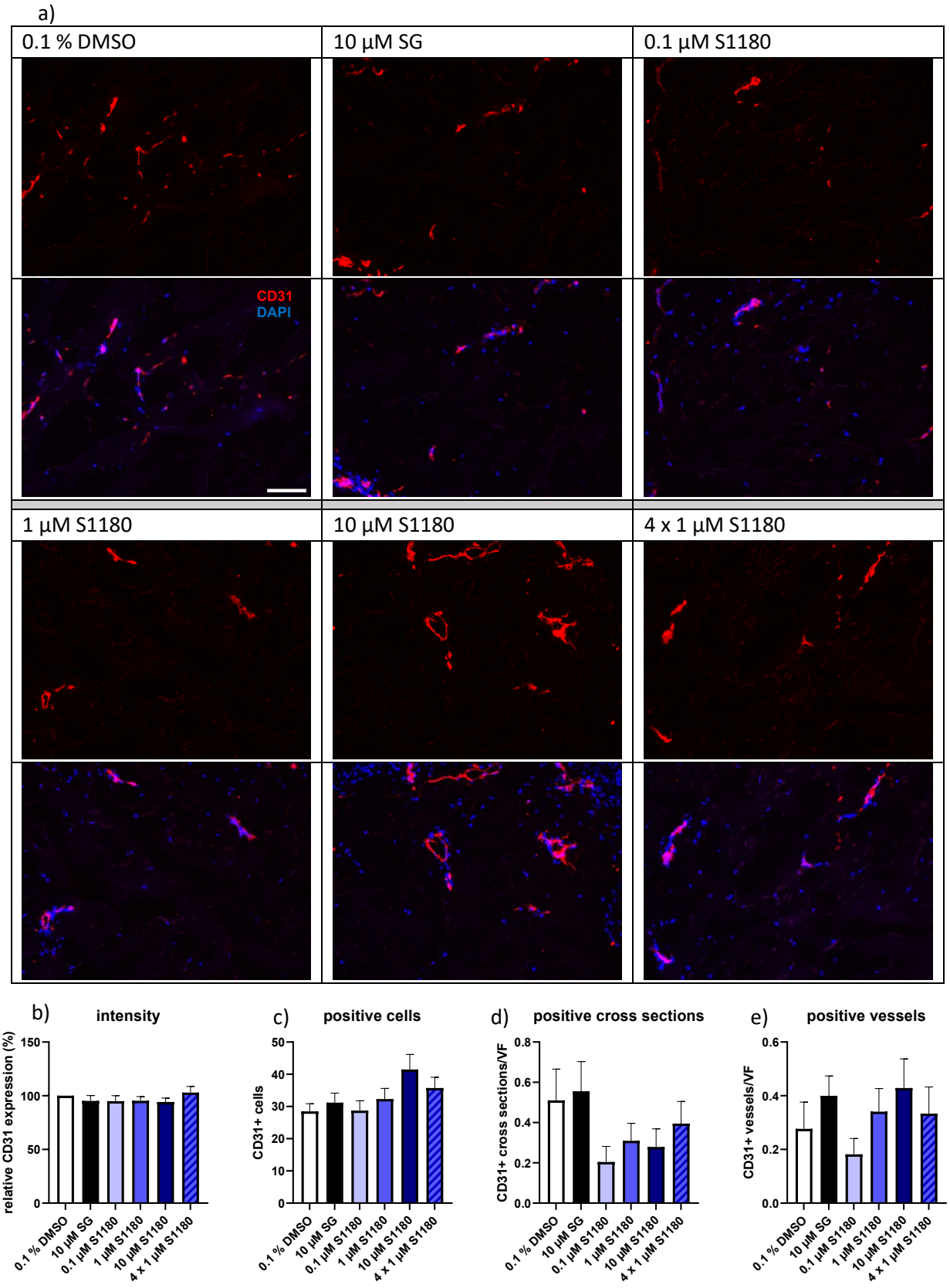
a)
0.1 % DMSO
10 µM SG
0.1 µM S1180
CD31
DAPI
1 µM S1180
10 µM S1180
4 x 1 µM S1180
b)
intensity
relative CD31 expression (%)
150
100
50
0
0.1 % DMSO
10 µM SG
0.1 µM S1180
1 µM S1180
10 µM S1180
4 x 1 µM S1180
c)
positive cells
CD31+ cells
50
40
30
20
10
0
d)
positive cross sections
CD31+ cross sections/VF
0.8
0.6
0.4
0.2
0.0
e)
positive vessels
CD31+ vessels/VF
0.6
0.4
0.2
0.0

Figure 4.43: Influence of different concentrations of S1180 on the CD31 expression in the wound healing organ culture model

The wounds of the wound healing organ culture were treated with 0.1 µM, 1 µM or 10 µM S1180 at day 1 for 24 hours or starting at day 1 repetitively with 1 µM S1180 (4 x 1 µM S1180) throughout the culture. As a vehicle control 0.1 % dimethyl sulfoxide (DMSO) was used, as a positive control 10 µM sodium gualenate (SG). Shown here is the CD31 expression of wounds cut and stained at day 7 (end of culture). a) Exemplary immunofluorescence pictures of the dermis. Scale bar = 100 µm, b) relative CD31 expression (n = 5, 2-4 VF/wound), c) number of CD31 positive cells/visual field (VF) (n = 5, 2-4 VF/wound), d) number of CD31 positive vessels/VF (n = 5, 2-4 VF/wound), e) number of CD31 positive cross sections/VF (n = 5, 2-4 VF/wound). For all: n =5, 2-8 VF For statistical analysis one-way ANOVA with Turkey's multiple comparison and t-test (relative intensity) or Kruskal-Wallis test with Dunn's multiple comparison and Mann-Whitney (for numbers of cells, cross sections and vessels) was performed. Data not significant.

4.8.5 Treatment with S1180 seems to increase the cortactin expression slightly

Figure 4.44 shows exemplary pictures of the cortactin expression after treatment with different concentration of S1180. A clear cortactin expression was observed in all conditions tested here. It seemed especially concentrated in the tip of the ET after treatment with 10 µM SG, 0.1 µM S1180 and 4 x 1 µM S1180.

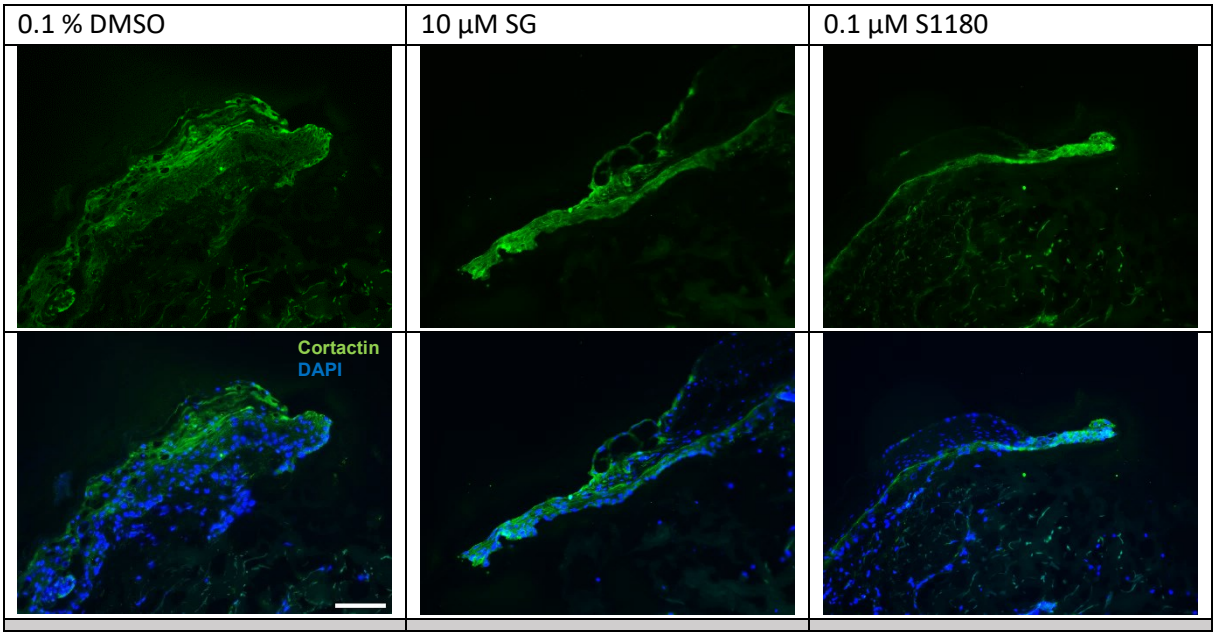

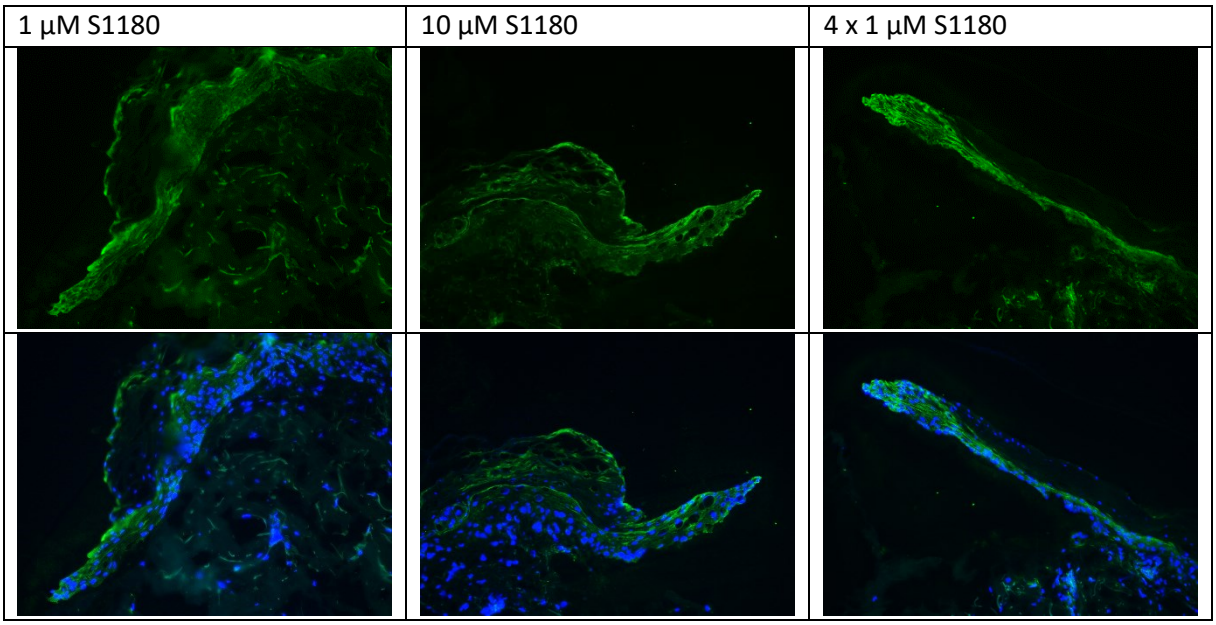

Figure 4.44: Influence of different concentrations of S1180 on the cortactin expression in the wound healing organ culture model

The wounds of the wound healing organ culture were treated with 0.1 µM, 1 µM or 10 µM S1180 at day 1 for 24 hours or starting at day 1 repetitively with 1 µM S1180 (4 x 1 µM S1180) throughout the culture. As a vehicle control 0.1 % dimethyl sulfoxide (DMSO) was used, as a positive control 10 µM sodium gualenate (SG). Shown here are exemplary pictures of the cortactin expression in epithelial tongues of wounds cut and stained at day 7 (end of culture). Scale bar = 100 µm

All in all, S1180 was found to aid wound healing *ex vivo* and is a highly interesting candidate to further investigate regarding how it supports wound healing. Moreover, its effect on the pathological wound healing model will be studied in **Chapter 4.12** and **4.13**.

4.9 Repetitive treatment with S2891, S2149, or S1180 was not more effective in aiding wound healing than one-time treatment with either substance

So far, the 4 x 1 µM concentration of S1180, S2149 or S2891 has only been tested against controls (0.1 % DMSO and 10 µM SG), that had been applied only once at day 0 for 24 h. In this chapter, the 4 x 1 µM concentrations were evaluated and compared with repetitive application of 0.1 % DMSO or 10 µM SG, which is a more sufficient control. As 10 µM S1180 performed very well in **Chapter 4.8**, repetitive treatment with 10 µM S1180 (4 x 10 µM S1180) was also tested here.

4.9.1 Repetitive treatment with 10 µM S1180 or 1 µM S2891 resulted in a smaller relative top-view wound area than the respective controls

Figure 4.45 shows the top-view evaluation. The exemplary pictures in **Figure 4.45a** indicate that wounds treated with 4 x 1 µM S1180 or 4 x 1 µM S2891 were smallest at the end of the culture.

The relative top-view wound area throughout the WHOC can be found in **Figure 4.45b**. Over the course of the culture especially treatment with 4 x 10 µM S1180 and 4 x 1 µM S2891 led to smaller relative areas than the controls.
On day 2, the wounds treated with 4 x 0.1 % DMSO as a vehicle control had a relative area of 78.47 % and the wounds treated with 4 x 10 µM SG as a positive control had a relative area of 70.17 %. Treatment with 4 x 1 µM S1180 and 4 x 1 µM S2149 led to larger relative areas than both controls, namely 86.62 % and 80.87 %. Wounds treated with 4 x 1 µM S2891 (75.20 %) had a relative area smaller than the vehicle control but larger than the positive control. Only treatment with 4 x 10 µM S1180 resulted in a relative area of 67.94 %, which was smaller than both controls.
On day 4, wounds treated with 4 x 1 µM S1180 had the largest relative area of 77.99 %, followed by the vehicle control wounds with 67.01 % and the positive control wounds with 62.64 %. While treatment with 4 x 1 µM S2149 (62.21 %) and 4 x 1 µM S2891 (59.37 %) led to only a slightly smaller relative area than the positive control. Wounds treated with 4 x 10 µM S1180 had a distinctly smaller relative area on this day, namely 48.34 %.
On day 6, again wounds treated with 4 x 1 µM S1180 had the largest relative area of 65.71 %. The relative area of the vehicle control wounds was 58.38 %. Treatment with 4 x 1 µM S2149 led to an almost identical relative area of 58.10 %. The relative area of the positive control wounds was 56.26 %. Wounds treated with 4 x 1 µM S2891 (55.75 %) and especially wounds treated with 4 x 10 µM S1180 (43.95 %) had a smaller relative area than both controls on this day.
The same can be observed on day 7, the last day of the culture. Here, too, treatment with 4 x 1 µM S2891 (45.44 %) and 4 x 10 µM S1180 (41.59 %) resulted in a smaller relative area than both controls. On this day, the positive control 4 x 10 µM SG had a larger relative area than the vehicle control 4 x 0.1 % DMSO (63.61 % versus 55.94 %). Wounds treated with 4 x 1 µM S1180 (60.01 %) and 4 x 1 µM S2149 (57.77 %) also had a larger relative area than the vehicle control. None of the differences measured in relative top-view area were significant.

Figure 4.45c shows the relative top-view wound perimeter over the course of the culture. Here, no convincing effect on the relative perimeter could be found for any concentration of S1180, S2149 nor S2891.
On day 2, the relative perimeter of the positive control wounds was smallest, namely 85.90 %. Wounds treated with 4 x 1 µM S1180 (88.94 %), 4 x 10 µM S1180 (88.26 %), and 4 x 1 µM S2891 (90.77 %) had a perimeter larger than the positive control wounds and smaller than the negative

control wounds, which had a relative perimeter of 92.19 %. Treatment with 4 x 1 µM S2149 resulted in a larger perimeter of 95.43 %.
On day 4, the same pattern was observed: Wounds treated with 4 x 1 µM S2149 had the largest perimeter of 89.72 %, followed by 4 x 0.1 % DMSO (85.54 %), 4 x 1 µM S2891 (83.96 %), 4 x 1 µM S1180 (82.21 %), and 4 x 10 µM S1180 (81.61 %). Only the positive control wounds had a smaller relative perimeter than the vehicle control wounds, namely 79.71 %.
On day 6, wounds treated with 4 x 1 µM S2149 (85.26 %) and 4 x 1 µM S2891 (84.20 %) had a larger relative perimeter than the vehicle control wounds, which had a relative perimeter of 78.86 %. Treatment with 4 x 1 µM S1180 (74.13 %) and 4 x 10 µM S1180 (75.48 %) led to a relative perimeter between both controls. Again, the positive control wounds had the smallest relative perimeter of 72.15 %.
On day 7, wounds treated with 4 x 10 µM SG as a positive control and those treated with 4 x 1 µM S1180 had an almost identical relative perimeter of 74.43 % and 74.17 % respectively. The relative perimeter of the vehicle control wounds was 76.70 %. Treatment with 4 x 10 µM S1180 (77.27 %), 4 x 1 µM S2149 (86.32 %), and 4 x 1 µM S2891 (77.75 %) led to a larger relative perimeter than both controls. None of the differences in perimeter were significant.

Overall, repetitive treatment with the three inhibitors does not seem to be overly beneficial for the top-view wound closure, but 4 x 10 µM S1180 and 4 x 1 µM S2891 seems to have a positive effect on the relative top-view wound area.

a)

	4 x 0.1 % DMSO	4 x 10 µM SG	4 x 1 µM S1180
Day 0			
Day 7			

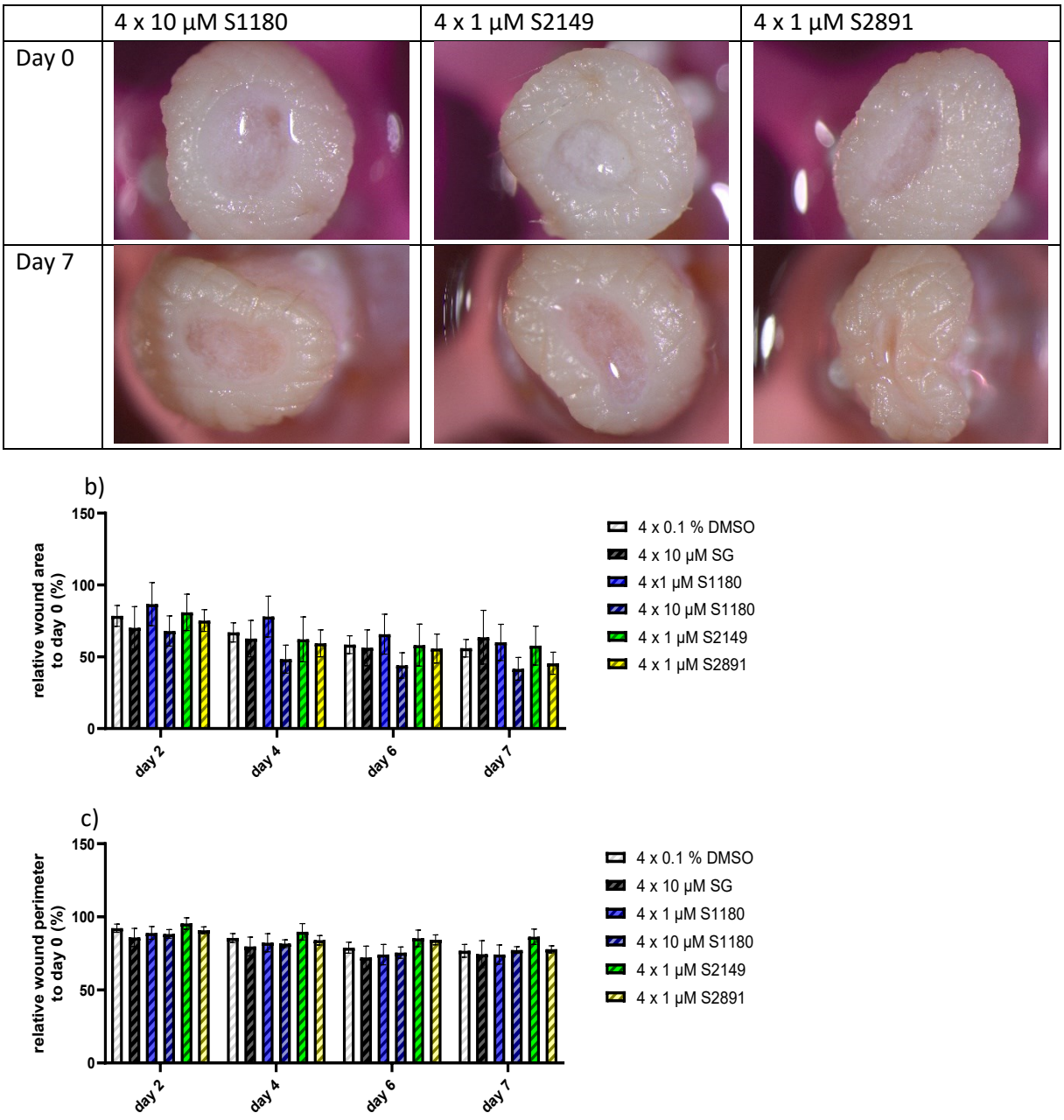

Figure 4.45: Influence of repetitive treatment with S1180, S2149, and S2891 on the top-view wound healing in the wound healing organ culture model

The wounded skin of the wound healing organ culture was from day 1 on repetitively treated with 0.1 % dimethyl sulfoxide (DMSO) as a vehicle control (4 x 0.1 % DMSO), 10 µM sodium gualenate (SG) as a positive control (4 x 10 µM SG), 1 µM S1180 (4 x 1 µM S1180), 10 µM S1180 (4 x 10 µM S1180), 1 µM S2149 (4 x 1 µM S2149), or 1 µM S2891 (4 x 1 µM S2891) throughout the culture. a) Exemplary top-view pictures of day 0 (day of wounding) and day 7 (end of the culture), b) relative top-view wound area to day 0 over the course of the culture, c) relative top-view wound perimeter to day 0 over the course of the culture. n = 3-4, 1-4 wounds/condition. Values are depicted as mean ±. Significances were determined by one-way ANOVA with Turky's multiple comparisons test. Data not significant.

4.9.2 Repetitive treatment with 1 µM S2891 reduced the microscopic wound are and wound diameter and resulted in the formation of larger and longer epithelial tongues

Figure 4.46 shows the microscopic evaluation of the repetitively treated wounds. The exemplary pictures in **Figure 4.46a** indicate, that repetitive treatment with S1180, S2149, and S2891 resulted in

smaller microscopic wound areas and especially treatment with 4 x 1 µM S2891 led to large and long ETs.

The microscopic wound area can be found in **Figure 4.46b**. The area of the vehicle control wounds was largest with a value of 249,980 μm^2. The positive control wounds had a slightly smaller microscopic wound area of 225,289 μm^2. Repetitive treatment with all inhibitors tested here resulted in smaller microscopic areas: 166,697 μm^2 for 4 x 1 µM S1180, 162,814 μm^2 for 4 x 10 µM S1180, 116,827 μm^2 for 4 x 1 µM S2149, and 160,821 μm^2 for 4 x 1 µM S2891. None of the differences measured were significant.

Figure 4.46c shows the microscopic wound diameter. Wounds treated with 4 x 1 µM S1180 had the largest diameter of 1,859.34 µm, followed by the positive control wounds with 1,695.45 µm. The diameter of the vehicle control was 1,648.25 µm. Treatment with the other three conditions led to smaller diameters than the controls: 1,170.87 µm for 4 x 10 µM S1180, 1,174.68 µm for 4 x 1 µM S2149, and 1,542.54 µM for 4 x 1 µM S2891. In a direct comparison the diameter of wounds treated with 4 x 1 µm S2149 was significantly smaller than that of wounds treated with 4 x 0.1 % DMSO as a vehicle control ($p < 0.05$, data not shown).

Figure 4.46d-g shows the area of the ETs. The area of the inner ETs can be found in **Figure 4.46d**. The area of the inner ETs of the vehicle control was 31218 μm^2. Treatment with 4 x 1 µM S1180 (23,021 μm^2) and with 4 x 1 µM S2149 (26,361 μm^2) led to smaller inner ETs than those of the vehicle control. On the other hand, wounds treated with 4 x 10 µM SG as a positive control (51,587 μm^2), 4 x 10 µM S1180 (31,968 μm^2), and 4 x 1 µM S2891 (52,533 μm^2) had larger inner ETs than the vehicle control. After treatment with 4 x 1 µM S2891 the inner ETs had the largest area. Those inner ETs were significantly larger than those treated with 4 x 0.1 % DMSO as vehicle control ($p < 0.01$), with 4 x 1 µM S1180 ($p < 0.0001$), with 4 x 10 µM S1180 ($p < 0.05$), and 4 x 1 µM S2149 ($p < 0.001$).
Figure 4.46g shows the area of the inner ETs normalized on the wound diameter. The normalized area of the inner ETs of the vehicle control wounds was 23.64 µm. While treatment with 4 x 1 µM S1180 (15.49 µm) still resulted in a smaller normalized area than the vehicle control, the wounds treated with 4 x 1 µM S2149 now had a larger inner ETs area than the vehicle control wounds after normalization, namely 26.47 µm. All other conditions tested here had larger inner ETs also after normalization: 4 x 1 µM S2891 had the largest normalized inner ETs with a value of 38.47 µm, followed by 4 x 10 µM S1180 (34.24 µm), 4 x 10 µM SG as a positive control (30.63 µm), and then 4 x 1 µM S2149. The wounds treated with 4 x 1 µM S2891 had a significantly larger normalized inner ETs' area than the vehicle control wounds ($p < 0.05$) and those wounds treated with 4 x 1 µM S1180 ($p < 0.0001$). Moreover, treatment with 4 x 1 µM S1180 resulted in significantly smaller normalized inner ETs than 4 x 10 µM S1180 ($p < 0.001$). While in a direct comparison 4 x 1 µM S1180 led to significantly smaller normalized ETs than 4 x 0.1 % DMSO ($p < 0.05$), 4 x 10 µM S1180 directly compared to 4 x 0.1 DMSO led to significantly larger normalized ETs ($p < 0.01$).
The area of the outer ETs can be found in **Figure 4.46e**. Here the differences in area are much smaller than for the inner ETs and not significant. Moreover, no beneficial effect of the tested inhibitors could be found. The vehicle control had the largest ETs (22,450 μm^2), followed by 4 x 10 µM S1180 (20,364 μm^2), 4 x 1 µM S2891 (20,081 μm^2), 4 x 10 µM SG (19,367 μm^2), 4 x 1 µM S2149 (19,407 μm^2), and finally 4 x 1 µM S1180 (18,920 μm^2).
Figure 4.46f shows the area of the total ETs. When combining the inner and outer ETs' area, only the positive control wounds and those treated with 4 x 1 µM S2891 had larger ETs than the negative control, namely 32,255 μm^2 for 4 x 10 µM SG and 35,602 μm^2 for 4 x 1 µM S2891 compared to 26,938 μm^2 for 4 x 0.1 % DMSO. Treatment with 4 x 1 µM S1180 resulted in the smallest total ETs of

20,677 µm^2, which was significantly smaller than those treated with 4 x 1 µM S2891 ($p < 0.05$). But also, treatment with 4 x 10 µM S1180 (25,638 µm^2) and 4 x 1 µM S2149 (23,116 µm^2) led to smaller total ETs than both controls.

The length of the ETs can be found in **Figure 4.46h-k**. **Figure 4.46h** shows the length of the inner ETs. The length of the inner ETS of the vehicle control was 461.27 µm and that of the positive control wounds was 540.27 µm. Only treatment with 4 x 1 µM S2891 led to longer inner ETs than both controls, namely 660.93 µm. The inner ETs after treatment with 4 x 1 µM S2891 were significantly longer than the inner ETS after treatment with 4 x 1 µM S1180 (293.96 µm), 4 x 10 µM S1180 (319.03 µm), and 4 x 1 µM S2149 (333.06 µm) with a level of significance of $p < 0.0001$ for all. In direct comparison, the inner ETs treated with 4 x 1 µM S2891 were also significantly longer than the inner ETs of the vehicle control wounds ($p < 0.01$, data not shown). The inner ETS after treatment with 4 x 1 µM S1180 were significantly shorter than those of both controls ($p < 0.01$).
Also, after normalization, the inner ETs after treatment with 4 x 1 µM S2891 were the longest with a value of 0.47, as **Figure 4.46k** shows. The normalized length of the inner ETs of the vehicle control was 0.33 and that of the positive control was 0.34. In a direct comparison, the normalized ETs were significantly longer when treated with 4 x 1 µM S2891 compared to the vehicle control wounds ($p < 0.01$, data not shown). Treatment with 4 x 1 µM S1180 resulted in the shortest normalized inner ETS of 0.24, which is significantly shorter than those treated with 4 x 1 µM S2891 ($p < 0.001$). Inner ETs treated with 4 x 10 µM S1180 had a normalized length of 0.34, which was identical to the positive control) and those treated with 4 x 1 µM S2149 of 0.32.
Figure 4.46i shows the length of the outer ETs. Just like the area, the differences in length were smaller than they were for the inner ETs and not significant. The outer ETs were longest after treatment with 4 x 10 µM SG as a positive control, namely 332.33 µm, followed by 4 x 0.1 % DMSO as a vehicle control (319.20 µm), 4 x 1 µM S2891 (309.69 µm), 4 x 10 µM S1180 (289.29 µm), 4 x 1 µM S1180 (286.29 µm), and 4 x 1 µM S2149 (258.32 µm).
The length of the total ETs is depicted in **Figure 4.46j**. The length of the total ETs of the vehicle control was 392.53 µm and that of the positive control was 415.51 µm. Just like the area, only treatment with 4 x 1 µM S2891 led to longer total ETs than both controls, namely 481.41 µm. These total ETs were significantly longer than those treated with 4 x 1 µM S1180 (282.40 µm), 4 x 10 µM S1180 (301.17 µm), and 4 x 1 µM S2149 (298.18 µm) with a level of significance of $p < 0.01$ for all.
In the microscopic evaluation especially the effect of 4 x 1 µM S2891 was convincing. After normalization 4 x 10 µm S1180 too seemed beneficial for the ET formation. These are also the treatment conditions, that seemed to have a positive effect on the relative top-view wound area in **Chapter 4.9.1**.

a)

	4 x 0.1 % DMSO	4 x 10 µM SG	4 x 1 µM S1180
Wound	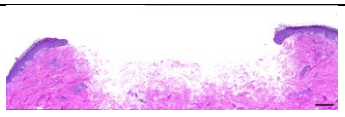	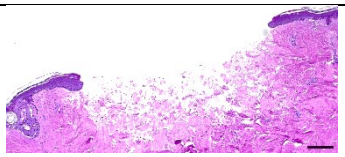	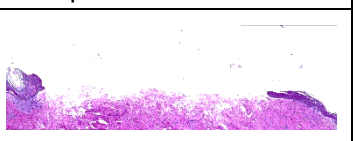
ET	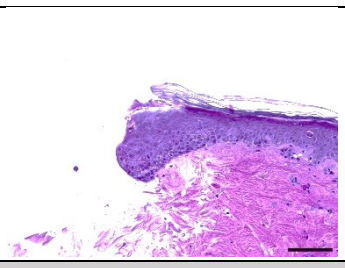	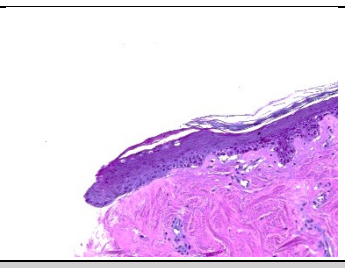	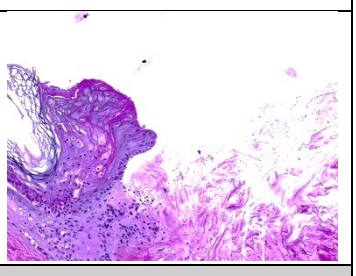

	4 x 10 µM S1180	4 x 1 µM S2149	4 x 1 µM S2891
Wound	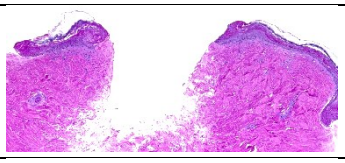	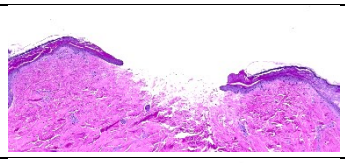	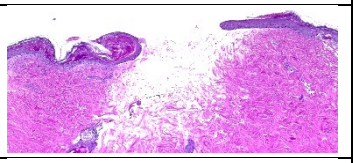
ET	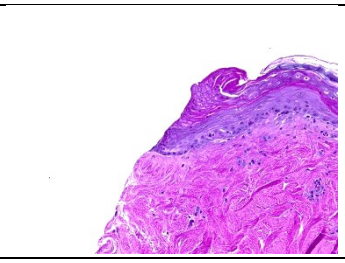	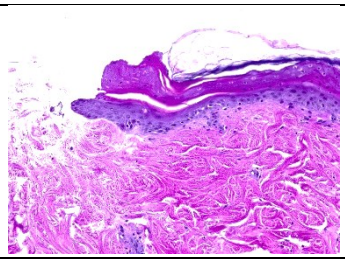	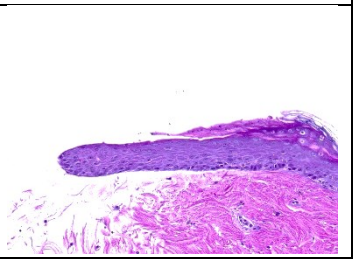

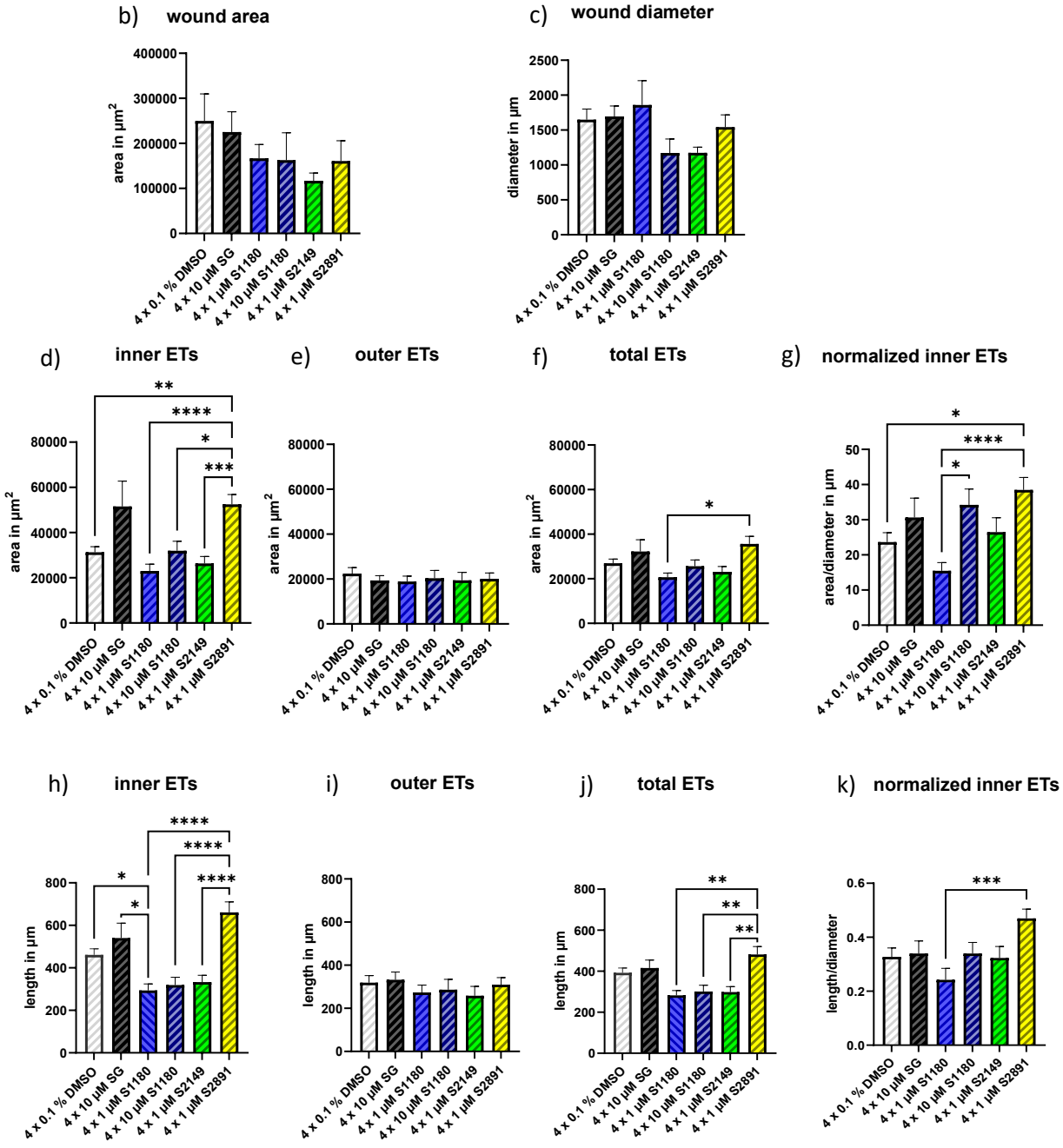

Figure 4.46: Influence of repetitive treatment with S1180, S2149, and S2891 on the microscopic wound healing in the wound healing organ culture model.
The wounded skin of the wound healing organ culture was starting at day 1 repetitively with 0.1 % dimethyl sulfoxide (DMSO) as a negative/treatment control (4 x 0.1 % DMSO), 10 µM sodium gualenate (SG) as a positive control (4 x 10 µM SG), 1 µM S1180 (4 x µM S1180, 10 µM S1180 (4 x 10 µM S1180), 1 µM S2149 (4 x 1 µM S2149) or 1 µM S2891 (4 x 1 µM S2891) throughout the culture. a) Exemplary Hematoxylin & Eosin stained pictures of the microscopic wounds (scale bar = 200 µm) and close-up of an exemplary epithelial tongue (ET) (scale bar = 100 µm), b) microscopic wound area (n=3-4; 1-4 wounds/condition) c) wound length (n = 3-4; 1-4 wounds/condition), d) area of the inner ETs, e) area of the outer ETs, f) area of inner and outer ETs combined, g) normalized area of the ETs on the respective wound diameter, h) length of inner ETs, i) length of outer ETs, j) length of inner and outer ETs combined, k) length of inner ETs normalized on the respective wound diameter. For all ET measurements n = 3-4; 2-16 ETs/wound. For statistical analysis a Kruskal-Wallis test with Dunns' multiple comparison was performed. * $p < 0.05$, ** $p < 0.01$, *** $p < 0.001$, **** $p < 0.0001$

4.9.3 Repetitive treatment with 1 µM S2149 or 1 µM S2891 seems to increase the cytokeratin 6 expression in the wound healing organ culture model

Next, the CK 6 expression after repetitive treatment with the inhibitors was studied. The results can be found in **Figure 4.47**. The exemplary pictures are shown in **Figure 4.47a**.

Figure 4.47b shows the relative CK 6 expression in the inner ETs. Only treatment with 4 x 1 µM S2149 (144.32 %) and 4 x 1 µM S2891 (128.62 %) led to a higher relative CK 6 expression in the inner ETs. Treatment with 4 x 10 µM SG as a positive control (87.79 %), 4 x 1 µM S1180 (97.00 %), and 4 x 10 µM S1180 (82.75 %) resulted in a lower relative CK 6 expression than the vehicle control 4 x 0.1 % DMSO.

Figure 4.47c shows the relative CK 6 expression in the outer ETs. Treatment with 4 x 0.1 % DMSO as a vehicle control (100 %), with 4 x 10 µm SG as a positive control (103.42 %), with 4 x 1 µM S1180 (96.44 %), and 4 x 10 µM S1180 (95.67 %) resulted in very similar relative CK 6 expressions. Only treatment with 4 x 1 µM S2149 and 4 x 1 µM S2891 led to a distinctly higher relative CK 6 expression in the outer ETs of 135.61 % and 109.29 % respectively.

In the total ETs in **Figure 4.47d**, 4 x 10 µM SG (95.60 %), 4 x 1 µM S1180 (96.69 %), and 4 x 10 µM S1180 (89.21 %) led to a lower relative CK 6 expression than the vehicle control 4 x 0.1 % DMSO, though the effect was slight for 4 x 10 µM SG and 4 x 1 µM S1180. Treatment with 4 x 1 µM S2149 (139.09 %) and with 4 x 1 µM S2891 (118.08 %) resulted in a higher relative CK 6 expression in the total ETs.
None of the differences found in the CK 6 evaluation were significant.

a)

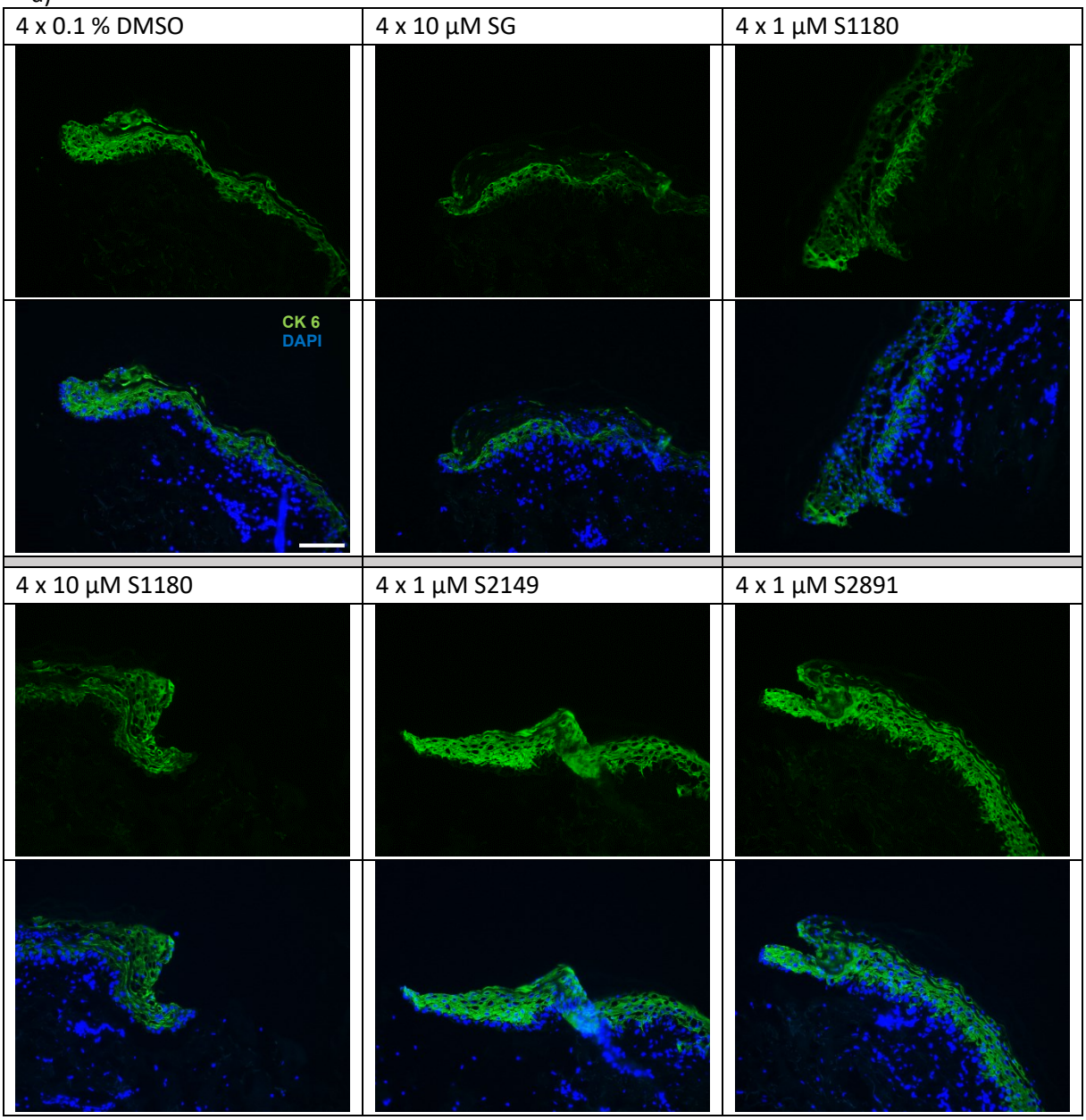
4 x 0.1 % DMSO
4 x 10 µM SG
4 x 1 µM S1180
CK 6
DAPI
4 x 10 µM S1180
4 x 1 µM S2149
4 x 1 µM S2891

b)

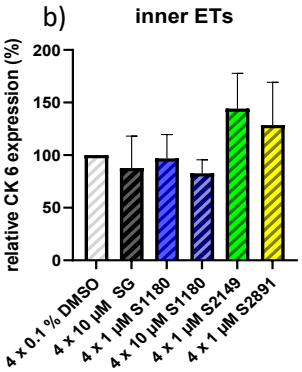
inner ETs
relative CK 6 expression (%)
200
150
100
50
0
4 x 0.1 % DMSO
4 x 10 µM SG
4 x 1 µM S1180
4 x 10 µM S1180
4 x 1 µM S2149
4 x 1 µM S2891

c)

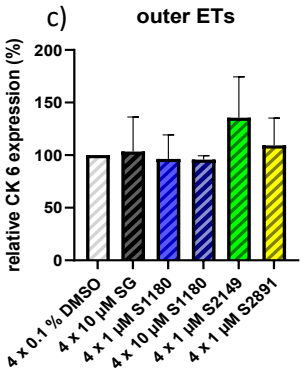
outer ETs
relative CK 6 expression (%)
200
150
100
50
0
4 x 0.1 % DMSO
4 x 10 µM SG
4 x 1 µM S1180
4 x 10 µM S1180
4 x 1 µM S2149
4 x 1 µM S2891

d)

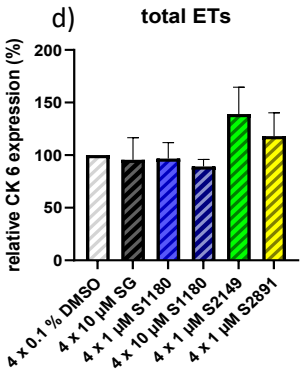
total ETs
relative CK 6 expression (%)
200
150
100
50
0
4 x 0.1 % DMSO
4 x 10 µM SG
4 x 1 µM S1180
4 x 10 µM S1180
4 x 1 µM S2149
4 x 1 µM S2891

Figure 4.47: Influence of repetitively treatment with S1180, S2149, and S2891 on the cytokeratin 6 expression in the wound healing organ culture model
The wounded skin of the wound healing organ culture was starting at day 1 repetitively with 0.1 % dimethyl sulfoxide (DMSO) as a vehicle control (4 x 0.1 % DMSO), 10 µM sodium gualenate (SG) as a positive control (4 x 10 µM SG), 1 µM S1180 (4 x µM S1180, 10 µM S1180 (4 x 10 µM S1180), 1 µM S2149 (4 x 1 µM S2149) or 1 µM S2891 (4 x 1 µM S2891) throughout the culture. Shown here is the cytokeratin (CK) 6 expression in the epithelial tongues (ETs) of wounds cut and stained at day 7 (end of culture). a) Exemplary immunofluorescence pictures of the ETs. Scale bar = 100 µm. CK 6 expression in the inner (b), outer (c) and total (d) ETs. For all: n = 3-4, 2-8 ETs/wound. For statistical analysis a Kruskal-Wallis test with Dunn's multiple comparison test (total ETs) or one way ANOVA with Turkeys multiple comparisons test (inner and outer ETs) was performed. Data not significant.

4.9.4 Repetitive treatment with S1180, S2149, or S2891 did not seem to have a strong influence CD31 expression, cell, cross section, or vessel count

Finally, the CD31 expression was examined, and the results can be found in **Figure 4.48**. **Figure 4.48a** depicts exemplary pictures.

The relative CD31 expression is shown in **Figure 4.48b**. All inhibitors and the positive control 4 x 10 µM SG resulted in a higher relative expression than the vehicle control: 103.81 % for 4 x 10 µM SG, 109.34 % for 4 x 1 µM S1180, 105.87 % for 4 x 10 µM S1180, 121.18 % for 4 x 1 µM S2149, and 114.06 % for 4 x 1 µM S2891.

Figure 4.48c shows the number of CD31 positive cells. The vehicle control wounds had 55.82 positive cells/VF. Treatment with the positive control 4 x 10 µM SG and with 4 x 1 µM S2149 resulted in more CD31 positive cells than the vehicle control, namely 71.47/VF and 61.29/VF. Wounds treated with 4 x 1 µM S1180 (48.57/VF), 4 x 10 µM S1180 (50.24/VF), and 4 x 1 µM S2891 (61.29/VF) had a less CD31 positive cells than the vehicle control.

Figure 4.48d shows the number of CD31 positive cross sections. The vehicle control wounds had positive 0.31 cross sections/VF. Treatment with 4 x 1 µM S1180 (0.39/VF), 4 x 10 µM S1180 (0.50/VF), and 4 x 1 µM S2891 (0.59/VF) resulted in more CD31 positive cross sections than the vehicle control, while wounds treated with 4 x 10 µM SG (0.25/VF) and 4 x 1 µM S1180 (0.29/VF) led to less positive cross sections.

Figure 4.48e shows the number of CD31 positive vessels. Wounds treated with 4 x 10 µM S1180 had the fewest positive vessels, namely 0.20/VF, followed by wounds treated with 4 x 1 µM S1180 (0.59/VF), and the vehicle control wounds (0.31/VF). Treatment with 4 x 10 µM SG (1.24/VF), 4 x 1 µM S2149 (1.07/VF), and 4 x 1 µM S2891 (1.13/VF) led to more positive vessels than the vehicle control.
None of the differences measured in the CD31 evaluation were significant and none of the tested inhibitor concentrations showed a consistent positive effect on the CD31 expression or counts.

a)

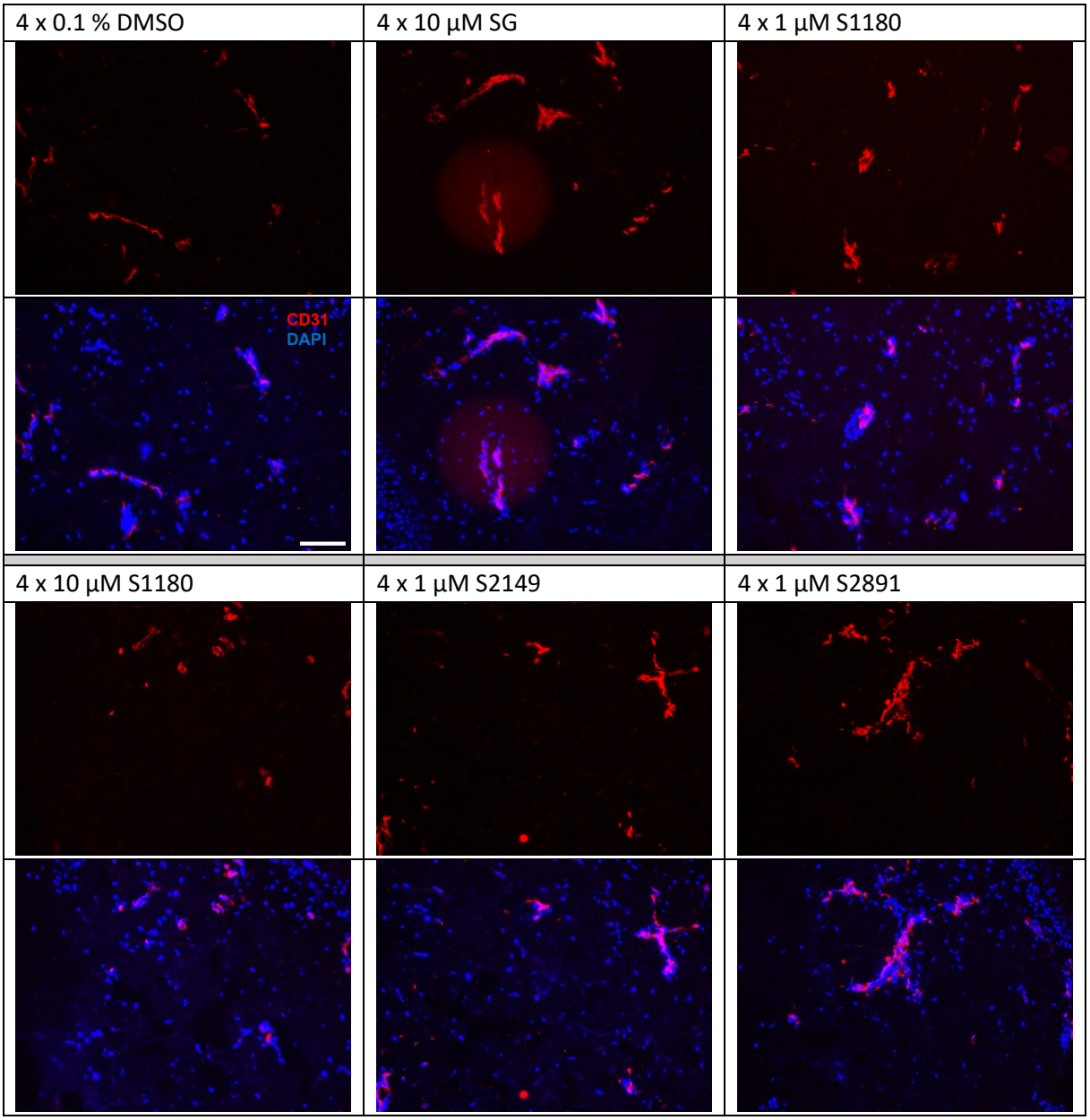
4 x 0.1 % DMSO
4 x 10 µM SG
4 x 1 µM S1180
CD31
DAPI
4 x 10 µM S1180
4 x 1 µM S2149
4 x 1 µM S2891

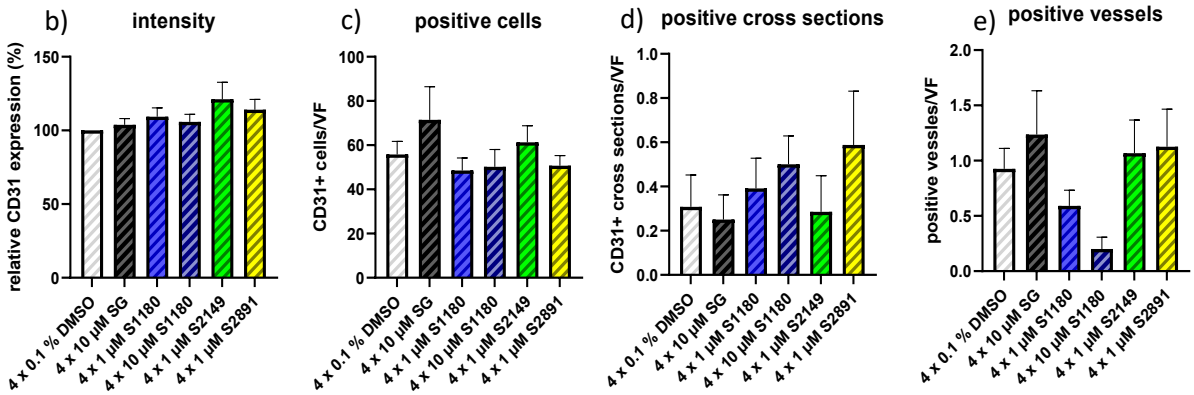
b) intensity
relative CD31 expression (%)
150
100
50
0
c) positive cells
CD31+ cells/VF
100
80
60
40
20
0
d) positive cross sections
CD31+ cross sections/VF
1.0
0.8
0.6
0.4
0.2
0.0
e) positive vessles
positive vessles/VF
2.0
1.5
1.0
0.5
0.0
4 x 0.1 % DMSO
4 x 10 µM SG
4 x 1 µM S1180
4 x 10 µM S1180
4 x 1 µM S2149
4 x 1 µM S2891

Figure 4.48: Influence of repetitive treatment with S1180, S2149, and S2891 on the CD31 expression in the wound healing organ culture model
The wounded skin of the wound healing organ culture was starting at day 1 repetitively with 0.1 % dimethyl sulfoxide (DMSO) as a vehicle control (4 x 0.1 % DMSO), 10 µM sodium gualenate (SG) as a positive control (4 x 10 µM SG), 1 µM S1180 (4 x µM S1180, 10 µM S1180 (4 x 10 µM S1180), 1 µM S2149 (4 x 1 µM S2149) or 1 µM S2891 (4 x 1 µM S2891) throughout the culture. Shown here is the CD31 expression in the epithelial tongues (ETs) of wounds cut and stained at day 7 (end of culture). a) Exemplary immunofluorescence pictures of the dermis. Scale bar = 100 µm. b) relative CD31 expression, c) number of CD31 positive cells/visual field (VF), d) number of CD31 positive vessels/VF, e) number of CD31 positive cross sections/VF. For all: n = 3-4, 4-8 VFs/wound. For statistical analysis one-way ANOVA with Turkey's multiple comparison test (relative expression) or Kruskal-Wallis test with Dunn's multiple comparison test (for numbers of cells, cross sections and vessels) was performed. Data not significant.

All in all, repetitive treatment with 1 µM S2891 shows a positive effect on macroscopic and microscopic wound healing. This treatment regime could be further tested. Treatment with 4 x 10 µM S1180 showed a positive effect on some of the investigated parameters here, but one-time treatment with 10 µM S1180 or 1 µM S1180 seems more promising. 4 x 1 µM S2149 also does not seem more promising than one-time treatment.

4.10 S1180 and S2891 have a positive influence on the *ex vivo* wound healing in the male wound healing organ culture model, while S2149 does not

It is known that the sex[1] of a person has an influence on how they react to certain drugs. While in this study only the skin is investigated, still "every cell has a sex" (Madla *et al.*, 2021). So it is of interest to look at the effect of S1180, S2149 and S2891 on skin of both sexes. Many research questions and drug development are predominantly conducted or tested on male subjects (Madla *et al.*, 2021). The three inhibitors so far have only been tested on female skin. This has the simple reason, that almost all of the donated skin is female. As male skin is so scarce in this field of research, the following experiments could only be performed with an n of 1.
The inhibitor concentrations that showed the best results in *ex vivo* female wound healing, were now tested on a male WHOC: 1 µM S1180, 10 µM S1180, 1 µM S2149 and 1 µM S2891. 0.1 % DMSO again served as a vehicle control and 10 µM SG as a positive control. All substances were administered at day 1 for 24 hours.

4.10.1 Treatment with S1180 and S2891 led to smaller relative top-view wound areas and perimeters than the negative control whereas treatment with S2149 resulted in larger values

Figure 4.49 shows the results of the top-view microscopy. The wounds seemed to heal especially well when treated with 1 µM S2891, as the exemplary pictures in **Figure 4.49a** show.

The relative top-view area over the course of the culture is depicted in **Figure 4.49b**. When looking at it, two substances catch the eye that seemed to have a negative effect on the area: 10 µM SG led to larger relative top-view wound areas than DMSO on all days but the effect is even more striking for 1 µM S2149. This substance performed worst consistently on all days of all substances tested, leading to a wound area of 63.55 % on day 7, while the vehicle control was at 37.407 %.
Treatment with S1180 seems beneficial and led to smaller wound areas than the vehicle control. At day 2 and 4, 10 µM S1180 archived better results than treatment with 1 µM S1180, at day 6 1 µM S1180 seems to have "caught up" and at day 7 the relative top-view wound area is slightly smaller for the wounds treated with 1 µM S1180 than those treated with 10 µM S1180 (23.18 % for 1 µM and 26.14 % for 10 µM).
Wounds treated with 1 µM S2891 had smaller relative top-view wound area than 0.1 % DMSO as vehicle control. Over the course of the culture the positive effect of 1 µM S2891 becomes more and more pronounced. At day 7, the wounds treated with 1 µM S2891 had the smallest relative top-view wound area with 17.71 %.

Figure 4.49c shows the relative top-view wound perimeter. While at day 2 no clear positive or negative effect was detectable for any of the substances tested, this changed over the next days. As for the area, 10 µM SG again led to larger values than 0.1 % DMSO.
Also, treatment with 1 µM S2149 again led to the worst healing outcome, with a relative top-view perimeter of 81.42 % at day 7 compared to 63.60 % for 0.1 % DMSO as vehicle control. Treatment

[1] The term "sex" here refers to the biological difference in reproductive organs and sexual hormones. It explicitly does not refer to the sociological "gender" a person may define as independently from the biological sex.

with 10 µM S1180 did not have positive effect on the relative top-view perimeter leading to a value of 75.91 % at day 7, which is higher than that of 0.1 % DMSO.
Wounds treated with 1 µM S1180 on the other hand showed from day 4 on a smaller relative perimeter than those treated with 0.1 % DMSO. 1 µM S2891 outperformed all other substances, leading to wounds with only a diameter of 36.59 % at day 7, the lowest value of all substances tested here.
Already from the top-view data one could assume that the sex of the skin donor has an important influence on how the skin reacts to treatment with the different substances.

a)

	0.1 % DMSO	10 µM SG	1 µM S1180
Day 0	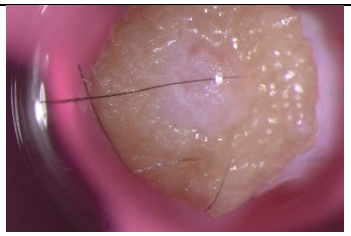		
Day 7		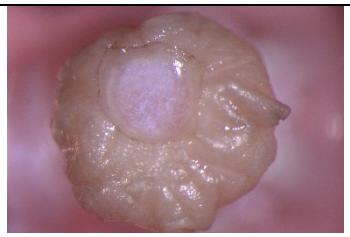	
	10 µM S1180	1 µM S2149	1 µM S2891
Day 0	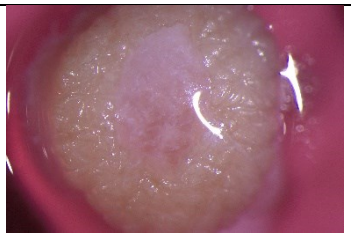	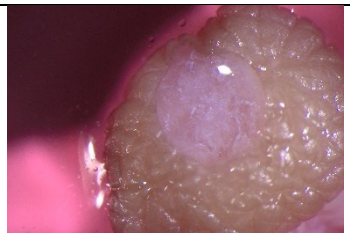	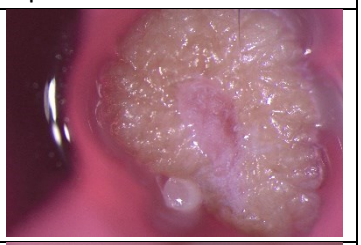
Day 7		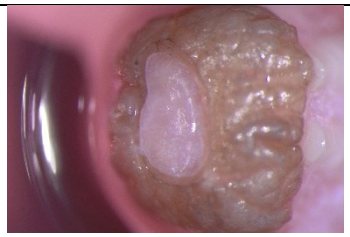	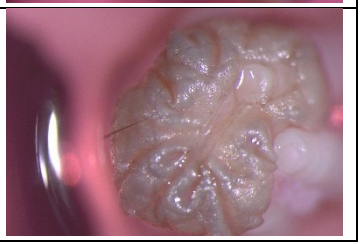

b)

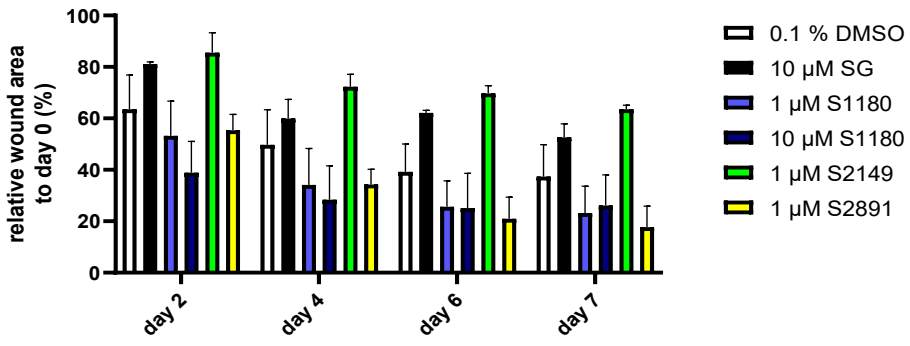

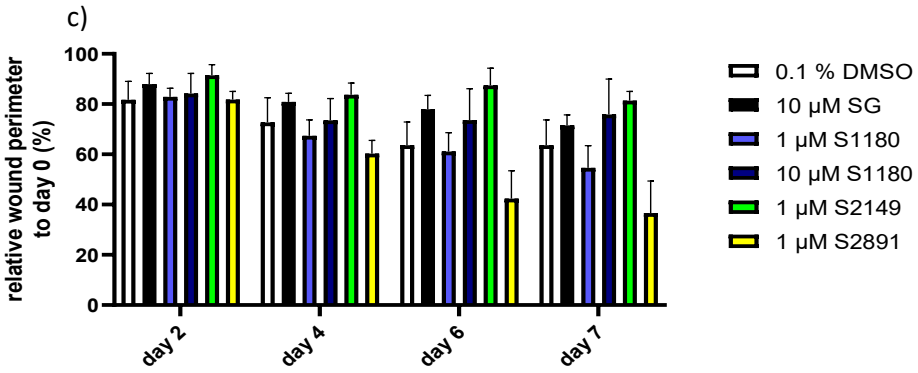

Figure 4.49: Influence of 1 µM S1180, 10 µM S1180, 1 µM S2149, and 1 µM S2891 on the top-view wound healing in the male wound healing organ culture
The wounds of the male wound healing organ culture model were treated with 0.1 % dimethyl sulfoxide (DMSO) as a vehicle control, 10 µM sodium gaulenate (SG) as a positive control, or 1 µM S1180, 10 µM S1180, 1 µM S2149 , at day 1 of the culture for 24 hours. a) Exemplary pictures of the wounds at the start (day 0) and end (day 7) of the culture. Relative top-view wound b) area and c) perimeter throughout the culture (n =1, 3 wounds/condition). Values are depicted as mean+ standard error of the mean. Statisitcal analysis was not possible because only one biological replicate was performed.

4.10.2 Treatment with 1 µM S2891 led to a smaller microscopic wound diameter and treatment with 1 µM S2891 or 1 µM S1180 resulted in larger and longer epithelial tongues than the vehicle control in male skin

The microscopic evaluation can be found in **Figure 4.50**. The exemplary pictures in **Figure 4.50a** indicate that especially treatment with 1 µM S2891 seems beneficial for male *ex vivo* wound healing.

Figure 4.50b shows the microscopic wound area. The huge microscopic area of 601,204 µm^2 after treatment with 1 µM S2149 is striking. But also all the tested substances, including the positive control 10 µM SG had a larger microscopic area than the vehicle control with a value of 164,647 µm^2: 170,091 µm^2 for 1 µM S2891, 212,558 µm^2 for 10 µM SG, 249,745 µm^2 for 1 µM S1180, and 254,249 µm^2 for 10 µM S1180. From all inhibitors tested, 1 µM S2891 led to the smallest microscopic area.

Figure 4.50c shows the microscopic wound diameter. Fitting to the top-view data and the microscopic wound area, treatment with 1 µM S2149 led to more than twice as large wound diameters than treatment with 0.1 % DMSO (2,750.88 µm for S2149 versus 1224.80 µm for 0.1 % DMSO). Wounds treated with 1 µM S1180 also had a larger diameter than the vehicle control wounds, namely 1,699.89 µm. All other substances tested led to a smaller diameter than 0.1 % DMSO: The smallest diameter of 988.72 µm was observed in wounds treated with 1 µM S2891. The difference in diameter between 10 µM SG (1,160.47 µm), 10 µM S1180 (1,163.72 µm) and 0.1 % DMSO is slight.

Next the area and length of the ETs was measured. The respective results are depicted in **Figure 4.50d-k**. As **Figure 4.50d** shows, a larger area of the inner ETs than treatment with the vehicle (32,952.20 µm^2) control was visible for 10 µM SG with 52,701.50 µm^2, 1 µM S1180 with 45,245.50 µm^2 and 1 µM S2891 with 54,238.10 µm^2. Treatment with 10 µM S1180 (24,002 µm^2) and 1 µM S2149 (23,433 µm^2) led to a smaller area of the inner ETs than treatment with the vehicle control.
For the outer ETs the same tendencies are observable, as **Figure 4.50e** shows: Treatment with 10 µM SG (39,626 µm^2), 1 µM S1180 (16,984 µm^2), and 1 µM S2891 (26,284 µm^2) resulted in a larger area for the outer ETs. Strikingly in wounds treated with 1 µM S2149 no outer ETs were observable at all.

Looking at the inner and outer ETs area combined in **Figure 4.50f** shows that treatment with 10 µM SG led to the largest ETs (45,230.00 µm^2), followed by 1 µM S2891 (40,260.9 µm^2), 1 µM S1180 (31,114.90 µm^2), 0.1 % DMSO (20,690.20 µm^2), 10 µM S1180 (11,264.2 µm^2) and lastly 1 µM S2149 (10,042.9 µm^2), so again treatment with 10 µM SG, 1 µM S1180 and 1 µM S2891 seems beneficial for the area of the ETs. Normalization of the area of the inner ETs to the respective wound diameter confirmed the positive influence of treatment with 10 µM SG (57.06 µm) and 1 µM S2891 (62.10 µm) onto the ETs area. Their normalized areas were almost twice the size of the normalized area of 0.1 % DMSO treated wounds (33.33 µm), as **Figure 4.50g** shows.

The length of the inner ETs can be found in **Figure 4.50h**. The inner ETs of wounds treated with 0.1 % DMSO as vehicle control reached a length of 437.95 µm. Only treatment with 1 µM S1180 (555.77 µm) and 1 µM S2891 (460.77 µm) resulted in longer inner ETs. The length of the inner ETs of the other substance treatments was shorter, the shortest ETs are visible after treatment with 10 µM S1180 (197.95 µm).
Figure 4.50h shows the length of the outer ETs. Again, the non-existing outer ETs after treatment with 1 µM S2149 catch the eye. Treatment with all other substances resulted in longer ETs than the vehicle control: 135.95 µm for 0.1 % DMSO, 162.99 µm for 10 µM S1180, 275.26 µm for 1 µM S1180, 480.41 µm for 10 µM SG and 487.34 µm 1 µM S2891. So, wounds treated with 1 µM S2891 showed the longest outer ETs.
The same is true for the outer ETs in **Figure 4.50i**, where treatment with 1 µM S2891 also resulted in the longest ETs, followed by 10 µM SG, 1 µM S1180 and then 0.1 % DMSO. Treatment with 10 µM S1180 and 1 µM S2149 led to shorter total ETs than the vehicle control 0.1 % DMSO (compare **Figure 4.50j**).
The normalized length of the inner ETs is shown in **Figure 4.50k**. After normalization only 1 µM S2891 (0.51) showed longer inner ETs than the vehicle control (0.43).
1 µM S2891 really seems to have a positive effect on top-view and microscopic wound healing. S1180 could have a positive effect, depending on the concentration used, while 1 µM S2149 seemed harmful to the examined parameters here.

a)

	0.1 % DMSO	10 µM SG	1 µM S1180
Wound	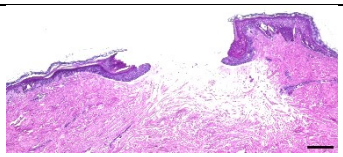	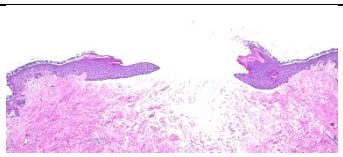	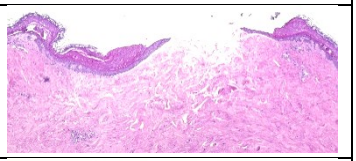
ET	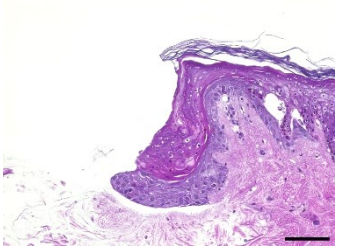	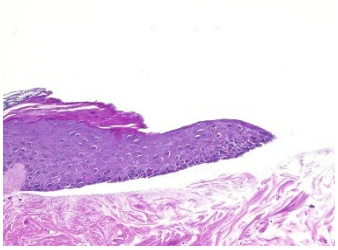	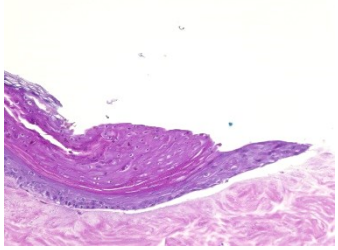

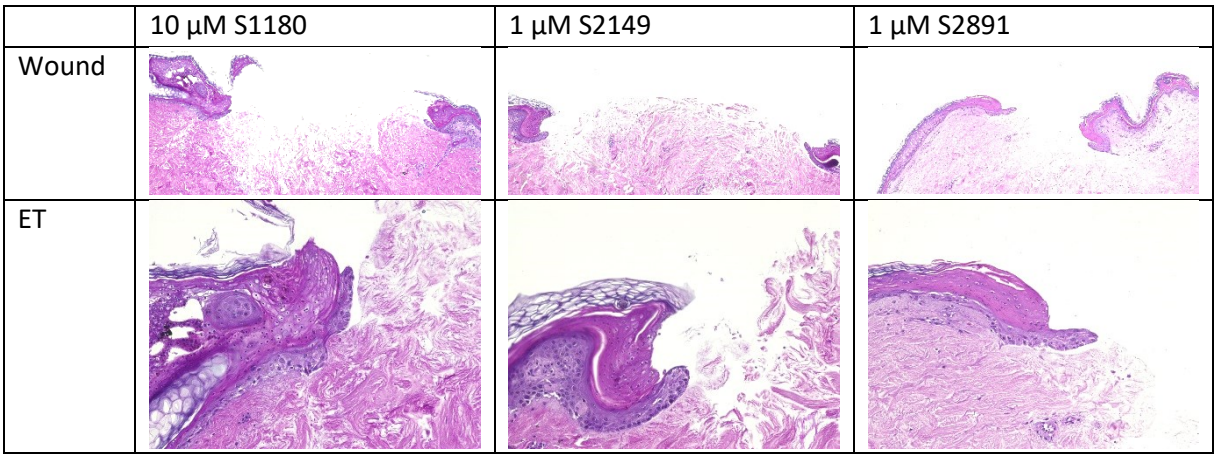
10 µM S1180
1 µM S2149
1 µM S2891
Wound
ET

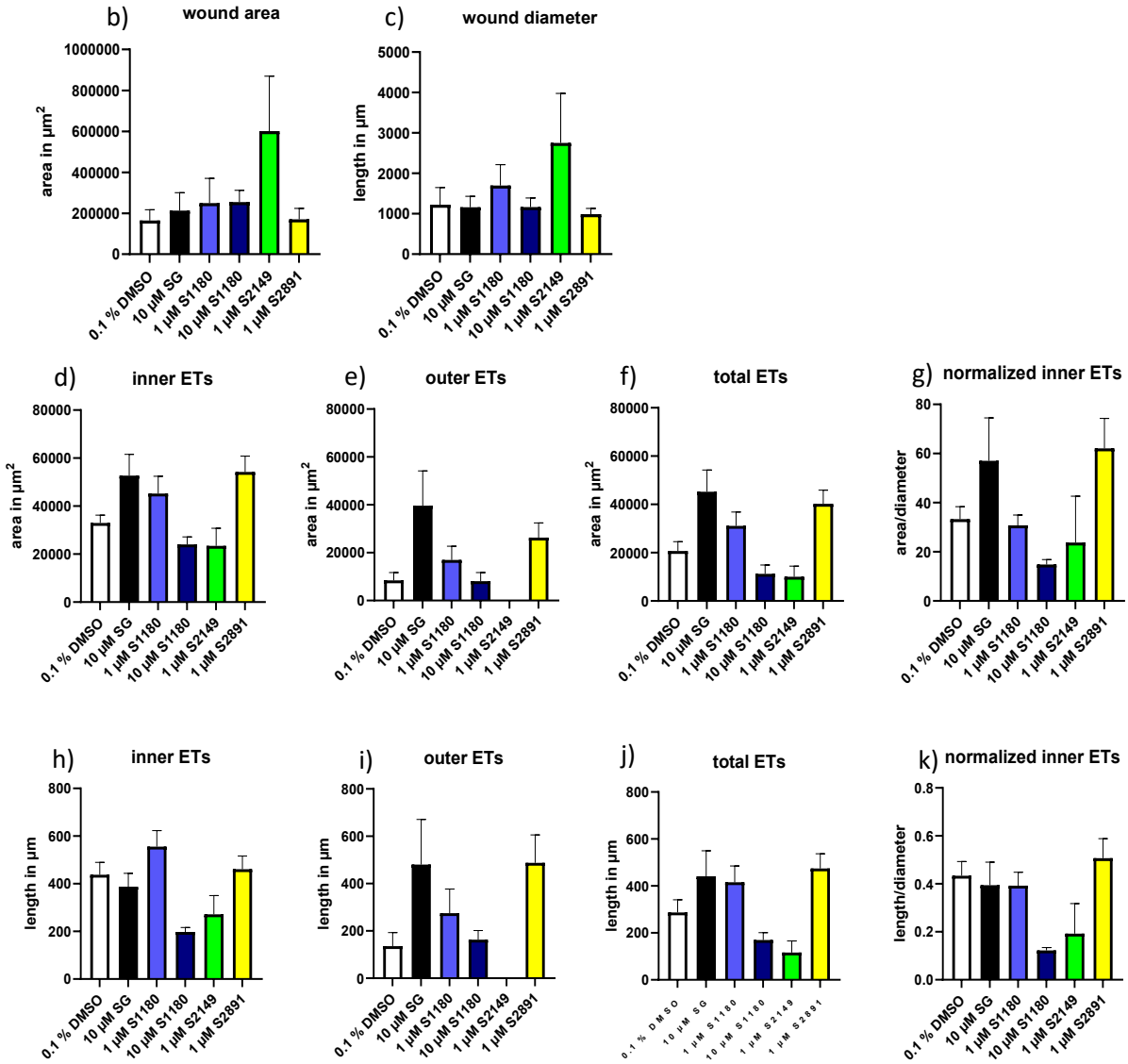
b) wound area
area in µm²
c) wound diameter
length in µm
d) inner ETs
e) outer ETs
f) total ETs
g) normalized inner ETs
area/diameter
h) inner ETs
i) outer ETs
j) total ETs
k) normalized inner ETs
length/diameter
0.1 % DMSO
10 µM SG
1 µM S1180
10 µM S1180
1 µM S2149
1 µM S2891

Figure 4.50: Influence of 1 µM S1180, 10 µM S1180, 1 µM S2149, and 1 µM S2891 on the microscopic wound healing in the male wound healing organ culture
The wounds of the male wound healing organ culture model were treated with 0.1 % dimethyl sulfoxide (DMSO) as a vehicle control, 10 µM sodium gaulenate (SG) as a positive control, or 1 µM S1180, 10 µM S1180, 1 µM S2149 or 1 µM S2891 at day 1 of the culture for 24 hours. a) Exemplary Hematoxylin & Eosin stained pictures of the microscopic wounds (scale bar = 200 µm) and close-up of an exemplary epithelial tongue (ET) (scale bar = 100 µm), b) microscopic wound area, c) microscopic wound length (n = 1, 3-4 wounds/condition), d) area of the inner ETs, e) area of the outer ETs, f) area of inner and outer ETs combined, g) normalized area of the ETs on the respective wound diameter, h) length of inner ETs, i) length of outer ETs, j) length of inner and outer ETs combined, k) length of inner ETs normalized on the respective wound diameter. For all ET measurements n = 1; 2-16 ETs/condition. Data is shown as mean + standard error of the mean. Statisitcal analysis was not possible because only one biological replicate was performed.

4.10.3 Treatment with 1 µM S1180 resulted in an increase in the relative cytokeratin 6 expression in the inner epithelial tongues and 1 µM S2891 in the outer epithelial tongues compared to the negative control

The results of the CK6 immunofluorescence can be found in **Figure 4.51**. The exemplary pictures of the CK 6 expression in the ETs can be found in **Figure 4.51a**.

As **Figure 4.51b** shows, in the inner ETs wounds treated with 1 µM S1180 showed the highest relative CK 6 expression with 149.03 %, followed by 1 µM S2149 with 108.14 % and 10 µM SG with 107.01 %. Treatment with 1 µM S2891 (96.23 %) and 10 µM S1180 (83.54 %) resulted in less relative CK 6 expression than 0.1 % DMSO.

In the outer ETS however treatment with S2891 led to higher relative expression of CK 6 than 0.1 % DMSO (151.99 % for 1 µM S2891, compare **Figure 4.51c**). Of the other substances tested only treatment with 10 µM SG (145.55 %) led to outer ETS with a higher CK6 expression than 0.1 % DMSO. Wounds treated with 1 µM S1180 (72.36 %), 10 µM S1180 (70.32 %), or 1 µM S2149 (92.49 %) had a lower relative CK 6 expression than the vehicle control.

The relative CK 6 expression of the total ETs is shown in **Figure 4.51d**. Here treatment with 10 µM SG (126.28 %), 1 µ S1180 (110.69 %), and 1 µM S2891 (124.11 %) resulted in higher CK 6 levels than 0.1 % DMSO, while 10 µM S1180 (76.92 %) and 1 µM S2149 (97.71 %) did not.

a)

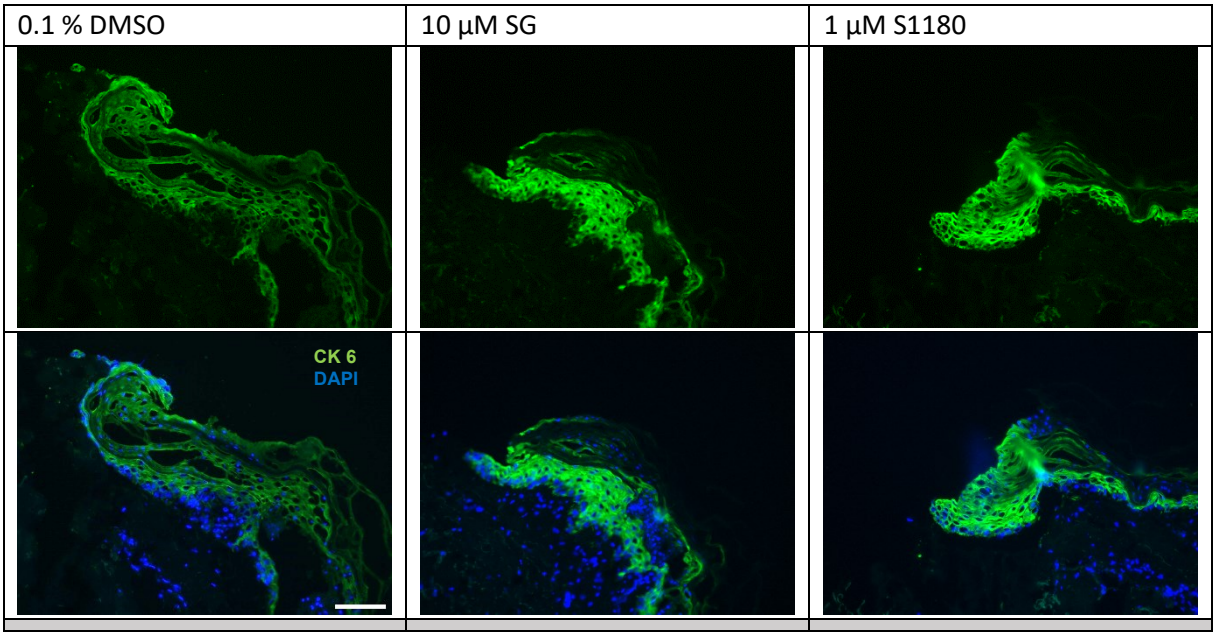

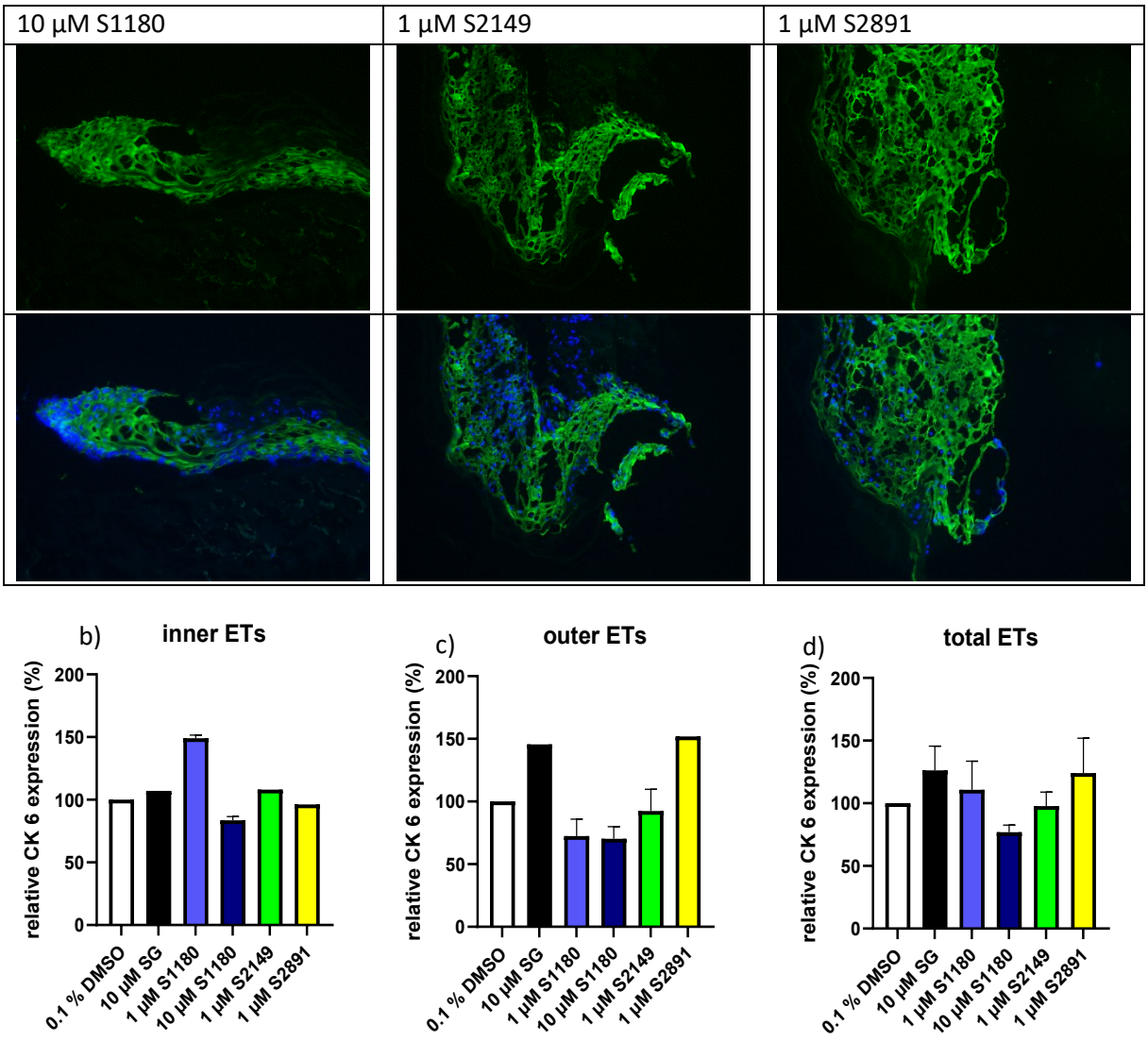

Figure 4.51: Influence of 1 µM S1180, 10 µM S1180, 1 µM S2149, and 1 µM S2891 on the cytokeratin 6 expression in the male wound healing organ culture
The wounds of the male wound healing organ culture model were treated with 0.1 % dimethyl sulfoxide (DMSO) as vehicle control, 10 µM sodium gaulenate (SG) as positive control, or 1 µM S1180, 10 µM S1180, 1 µM S2149 or 1 µM S2891 at day 1 of the culture for 24 hours. Shown here is the cytokeratin (CK) 6 expression in the epithelial tongues (ETs) of wounds cut and stained at day 7 (end of culture). a) Exemplary immunofluorescence pictures of the ETs. Scale bar = 100 µm. CK 6 expression in the inner (b), outer (c) and total (d) ETs. For all: n = 1, 1-8 ETs/wound. Data is shown as mean + standard error of the mean. Statisitcal analysis was not possible because only one biological replicate was performed.

4.10.4 Treatment with 1 µM S2891 or 1 µM S1180 resulted in a higher relative CD31 expression, more CD31 positive cells, more CD31 positive cross sections and more CD31 positive vessels

Figure 4.52 shows the results of the CD31 staining. The exemplary pictures can be found in **Figure 4.52a**.

Only 1 µM S1180 (104.04 %) and 1 µM S2891 (111.06 %) showed a higher relative CD31 expression than the vehicle control 0.1 % DMSO. So, treatment with 1 µM S2891 led to the highest relative CD31 expression, while treatment with 10 µM S1180 to the lowest with 79.86 % (compare **Figure 4.52b**).

As **Figure 4.52c** shows, treatment with 10 µM S1180 also resulted in the least CD31 positive cells (32 cells/VF) and treatment with 1 µM S2891 again in the most CD31 positive cells, with 63 cells/VF almost twice the number of cells counted for 10 µM S1180. In the vehicle control group 54 cells were CD31 per visual field. So, 1 µM S2891 led to an increase in positive cells compared to 0.1 % DMSO. The same is true for 10 µM SG (56 cells/VF) and 1 µM S1180 (61 cells/VF). Treatment with 1 µM S2149 resulted in 60 positive cells/VF, less than the negative control.

The number of positive cross sections is shown in **Figure 4.52d**. All were higher than those counted in wounds treated only with 0.1 % DMSO (0.38 cross sections/VF). The highest count was achieved in wounds treated with 1 µM S2891 (1.25 cross sections /VF), though the high error bars must be kept in mind.
The number of CD31 positive branched vessels is depicted in **Figure 4.52e**. With 2.00 positive cross sections/VF 1 µM S1180 and 1 µM S2149 had the highest value, followed by 1 µM S2149 with 1.80/VF. All three were higher than the 1.25 vessels/VF counted after treatment with 0.1 % DMSO. Wounds treated with 10 µM SG or 10 µM S1180 showed only 0.28 or 0.50 positive vessels /VF respectively.

a)

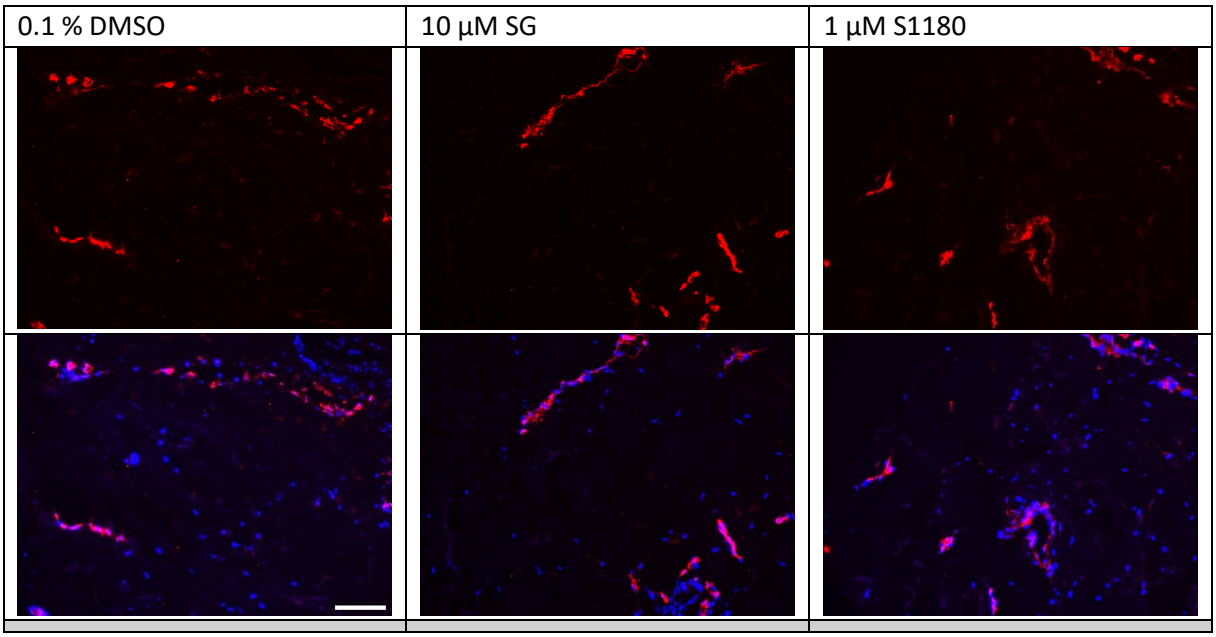

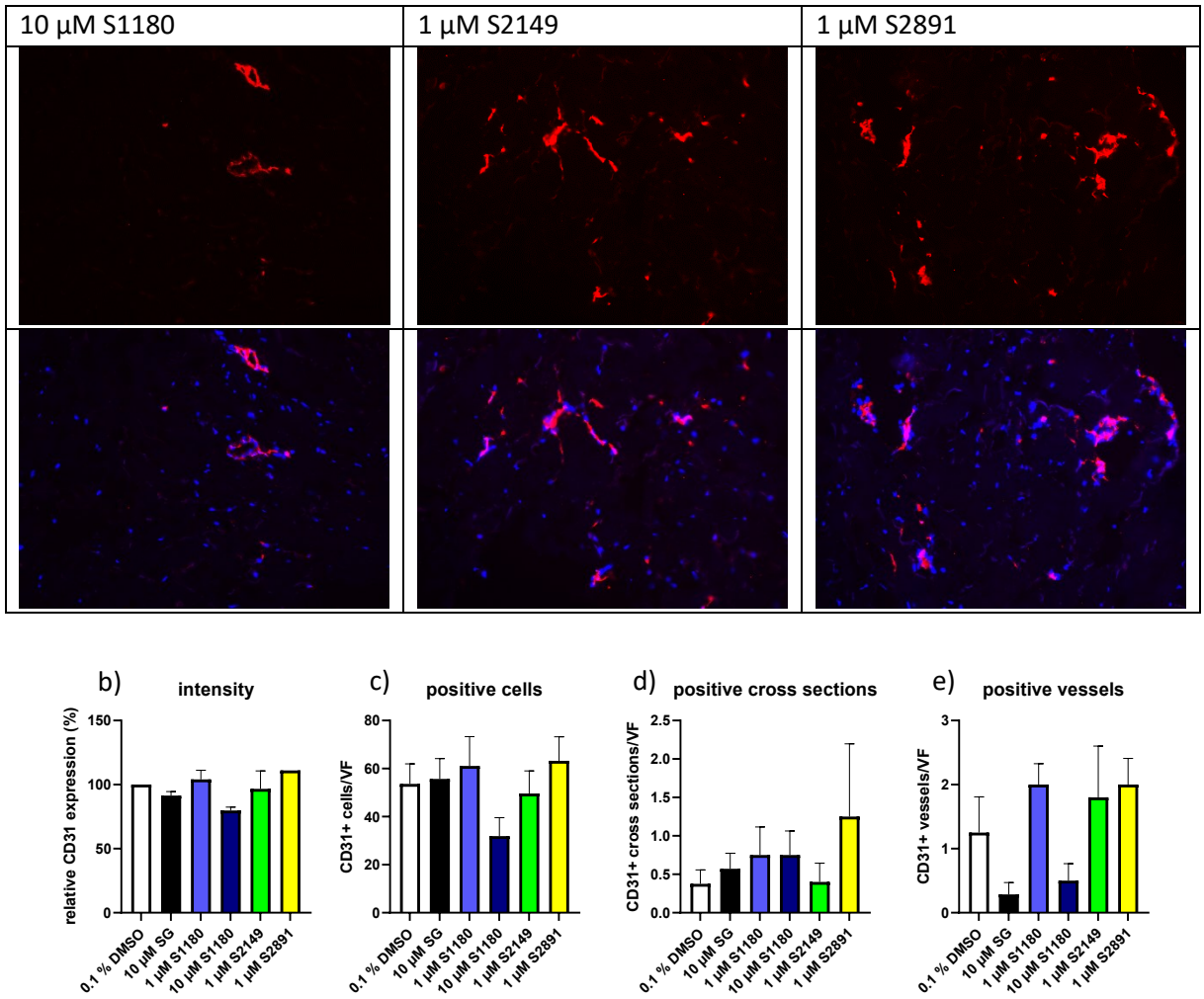

Figure 4.52: Influence of 1 µM S1180, 10 µM S1180, 1 µM S2149, and 1 µM S2891 on the CD31 expression in the male wound healing organ culture

The wounds of the male wound healing organ culture model were treated with 0.1 % dimethyl sulfoxide (DMSO) as vehicle control, 10 µM sodium gaulenate (SG) as positive control, or 1 µM S1180, 10 µM S1180, 1 µM S2149 or 1 µM S2891 at day 1 of the culture for 24 hours. Shown here is the CD31 expression in the dermis of wounds cut and stained at day 7 (end of culture). a) Exemplary immunofluorescence pictures of the dermis. Scale bar = 100 µm, b) relative CD31 expression, c) CD3 positive cells, d) CD31 positive cross sections, e) CD31 positive vessels. For all: n = 1, 4-8 visual fields (VF)/condition. Data is shown as mean + standard error of the mean. Statisitcal analysis was not possible because only one biological replicate was performed.

This study strongly indicates that there is a difference between how male and female wounded skin reacts to the different inhibitors. For *ex vivo* male wound healing studying S2891 would be especially interesting. Though it must be kept in mind, that the results here come from only one donor. Repeating this set up is necessary to achieve sound and secure data.

4.11 The survivin inhibitor S1130 worsens the *ex vivo* wound healing in the wound healing organ culture model

So far, the successful substances out of the screening have been further investigated and especially S1180 was found to have a positive effect on the *ex vivo* wound healing in the WHOC model. As a proof of principle in this chapter an exemplary culture was performed with the inhibitor that performed worst in the entire screening: S1130. S1130 or YM155 (also called sepantronium bromide) is a survivin inhibitor. Here it was tested in a concentration of 1 µM at day 1 for 24 hours and compared to 0.1 % DMSO as a vehicle control and 10 µM SG as a positive control.

4.11.1 Wounds treated with 1 µM S1130 had a larger relative top-view wound area and perimeter than the controls

Figure 4.53 shows the evaluation of the top-view parameters. Already the exemplary pictures show that the wounds treated with 1 µM S1130 did not heal well. Less newly formed, opaque ETs were visible, but rather the distinct edges of the punched wounds are still clearly visible at day 7 (compare **Figure 4.53a**).

Figure 4.53b depicts the relative top-view wound area through the culture. While treatment with 10 µM SG seemed not beneficial for this donors' skin here, the wounds treated with 1 µM S1130 had an even larger area from day 4 throughout the culture.
On day 2, the vehicle control wound had the smallest area of 79.98 %, followed by the wounds treated with 1 µM S1130 (99.69 %) and 10 µM SG (114.16 %) as a positive/treatment control.
On day 4, the wounds treated with 1 µM S1130 had the largest relative area, namely 99.39 %. The relative area of the positive control was 96.57 % and that of the positive control wounds was 71.76 %.
On day 6, the difference between 10 µM SG and 1 µM S1130 became more pronounced. Wounds treated with 1 µM S1130 clearly had the largest relative area of 110.20 % on this day, which was an increase compared to day 4 but also to the starting area (100 %) of the WHOC. The positive control wounds had a relative area of 91.15 % and the negative control wounds of 70.36 %.
On day 7, the wounds treated with 1 µM S1130 once more had the largest relative area, namely 97.95 %, followed by 87.24 µM for the wounds treated with 10 µM S1130 and 66.92 % for the wounds treated with 0.1 % DMSO. While there was a clear decrease in the relative area of the vehicle control, the relative wound area after treatment with 1 µM S1130 hardly changed at all.

The relative top-view wound perimeter over the course of the WHOC is shown in **Figure 4.53c**. Wounds treated with 1 µM S1130 displayed the largest perimeter at all measurement days and seemed to be even slightly larger than on day 0.
On day 2, the relative perimeter of the vehicle control wounds was 91.61 %, followed by the positive control wounds (100.10 %) and wounds treated with 1 µM S1130 (104.09 %).
On day 4, the wounds treated with 1 µM S1130 had the largest relative perimeter of 105.01 %, the positive control wounds had a relative perimeter of 91.55 % and the vehicle control wounds of 86.60 %.
The same pattern was observed on day 6: treatment with 1 µM S1130 led to the largest relative perimeter (108.22 %) followed by 10 µm SG (89.19 %) and 0.1 % DMSO (86.40 %).
On day 7 still, the relative perimeter was slightly larger than it was at day 0 with a value of 105.840 %. The relative perimeter of the negative control wounds was 84.43 % and that of the positive control wounds was 86.55 %.
So, clearly, treatment with 1 µM S1130 is harmful for the top-view wound closure.

The OCT system was unfortunately not available for measurements.

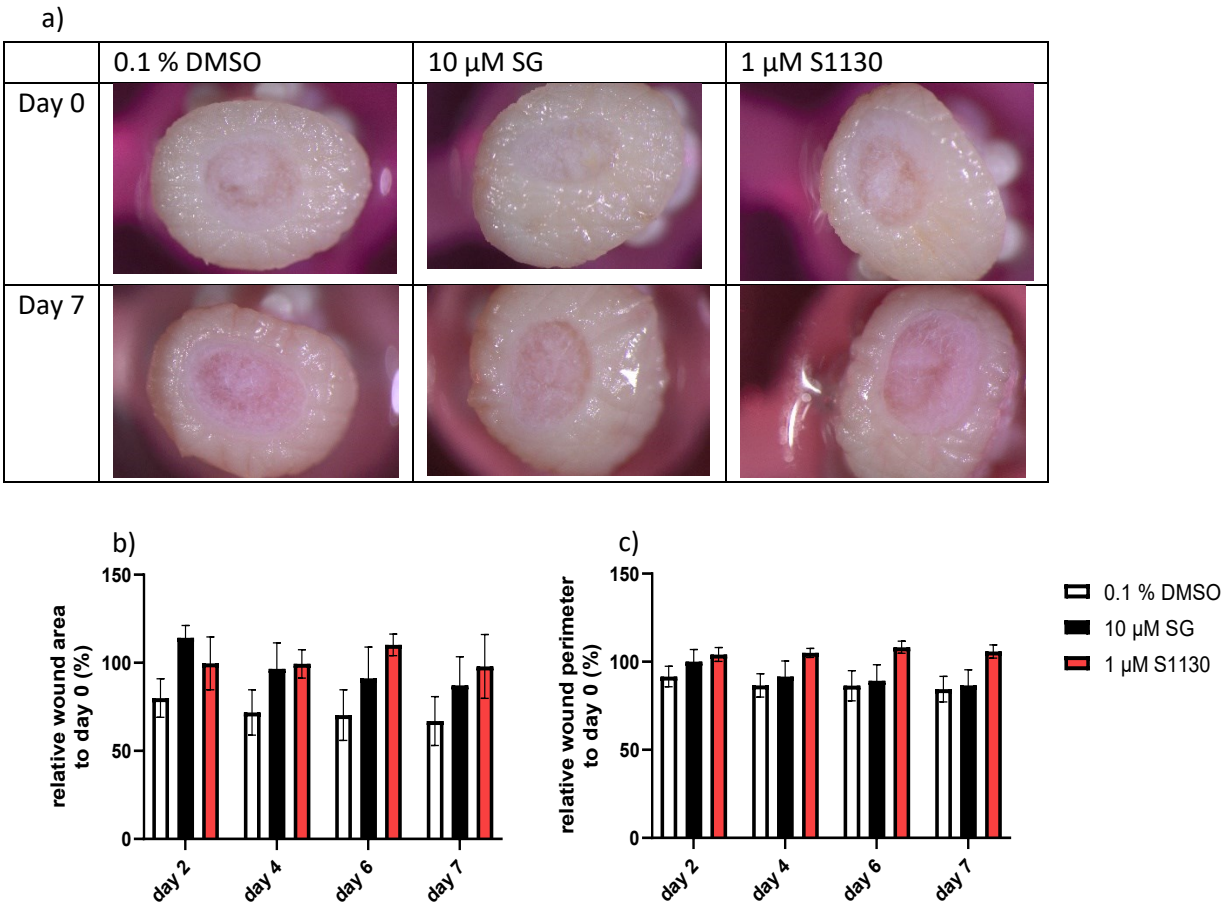

Figure 4.53: Influence of S1130 on the top-view wound healing in the wound healing organ culture model.
The wounds of the wound healing organ culture model were treated with 0.1 % dimethyl sulfoxide (DMSO) as vehicle control, 10 µM sodium gaulenate (SG) as positive control, or 1 µM S1130 at day 1 of the culture for 24 hours. a) Exemplary pictures of the wounds at the start (day 0) and end (day 7) of the culture. Relative top-view wound b) area and c) perimeter throughout the culture (n =1, 3 wounds/condition). Values are depicted as mean ± standard error of the mean. Statisitcal analysis was not possible because only one biological replicate was performed.

4.11.2 Treatment with 1 µM S1130 led to larger microscopic wounds and to less formation of epithelial tongues than the controls

Next the microscopic wound healing was assessed. The evaluation can be found in **Figure 4.54**. Already the exemplary pictures in **Figure 4.54a** of the H&E stained wounds show that the microscopic wound area after treatment with S1130 is distinctly larger than that of the controls. Moreover, the epidermis looked less intact and the ET were much smaller than those of the controls.

The measurement of the microscopic wound area in **Figure 4.54b** confirmed that treatment with 1 µM S1130 led to a larger area than the controls. In fact, the microscopic area of wounds treated with 1 µM S1130 was 375,099 µm^2, which is roughly twice the size than that treated with 0.1% DMSO as vehicle control (184,347 µm^2). Treatment with 10 µM SG led to a slightly larger microscopic wound area than 0.1 % DMSO, namely 204,600 µm^2.
As **Figure 4.54c** shows, the diameter of wounds treated with 1 µM S1130 was 2,903.68 µm, which was more than one third larger than the diameter after treatment with 0.1 % DMSO (1,733.19 µM).

Wounds treated with 10 µM SG show with 1569.76 µm a slightly smaller wound diameter than those treated with 0.1 % DMSO.

The area of the inner ETs is shown in **Figure 4.54d**. The positive control wounds had the largest inner ETs of 36,757 µm^2, followed by the vehicle control wounds with 18,531 µm^2 and the wounds treated with 1 µM S1130 had the smallest inner ETs by far with an area of 3,529 µm^2. After normalization the detrimental effect of S1130 on the formation of ETs became even more clear, as **Figure 4.54g** shows: the normalized area of the positive control wounds was 23.96 µm, that of the vehicle control wounds was 10.62 µm and that of the wounds treated with 1 µM S1130 was only 1.23 µm. **Figure 4.54e** shows the area of the outer ETs. Here, too, treatment with 1 µM S1130 resulted in the smallest ETs (9,704 µm^2), followed by 0.1 µM DMSO (37,473 µm^2), and 10 µM SG (44,415 µm^2). Just like the inner and outer ETs, the area of the total ETs was smallest after treatment with 1 µM S1130 (64,11 µm^2), as depicted in **Figure 4.54f**. The outer ETs' area of the vehicle control wounds was 28,002 µm^2 and that of the positive control wounds was 40,586 µm^2.

Figures 4.54h-k depict the length of the ETs. Matching the areas, the ETs were also shorter after treatment with 1 µM S1130 than after treatment with the controls. The length of the inner ETs is shown in **Figure 4.54h**. Treatment with 1 µM S1130 led to the shortest inner ETs, namely 61.44 µm, followed by 0.1 % DMSO (205.89 µm) and 10 µM SG (351.31 µm). Normalization of the length of the inner ETs again pronounced the positive effect of 10 µM SG and the negative effect of 1 µM S1130 (compare **Figure 4.54k**): The inner ETs had a normalized length of 0.23 after treatment with 10 µM SG, 0.12 after treatment with 0.1 % DMSO and only 0.02 after treatment with 1 µM S1130. As **Figure 4.54i** shows, the outer ETs were longest when treated with 10 µM SG (492.61 µm) and shortest when treated with 1 µM S1130 (80.40 µm). The length of the outer ETs in the vehicle control wounds was 415.99 µm. The same pattern can be found for the length of the total ETs in **Figure 4.54j**: Treatment with 1 µM S1130 resulted in the shortest ETs, namely 70.29 µm, followed by 0.1 % DMSO (310.94 µm) and 10 µM SG (421.96 µm).
The analysis of top-view and microscopic wound healing strongly indicates, that S1130 hampers the *ex vivo* wound healing in the WHOC.

a)

	0.1 % DMSO	10 µM SG	1 µM S1130
Wounds	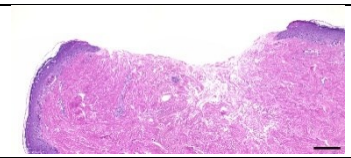	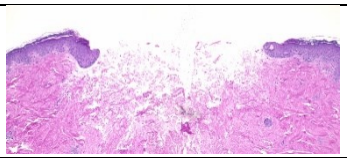	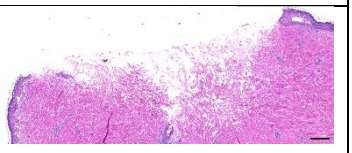
ETs	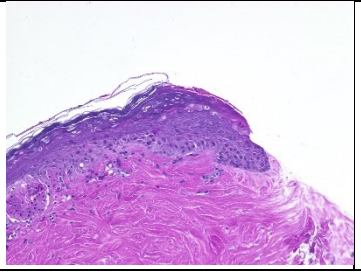	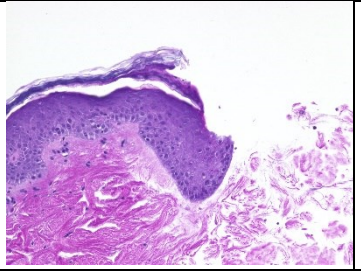	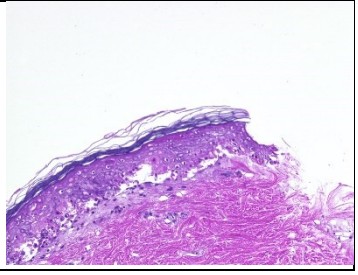

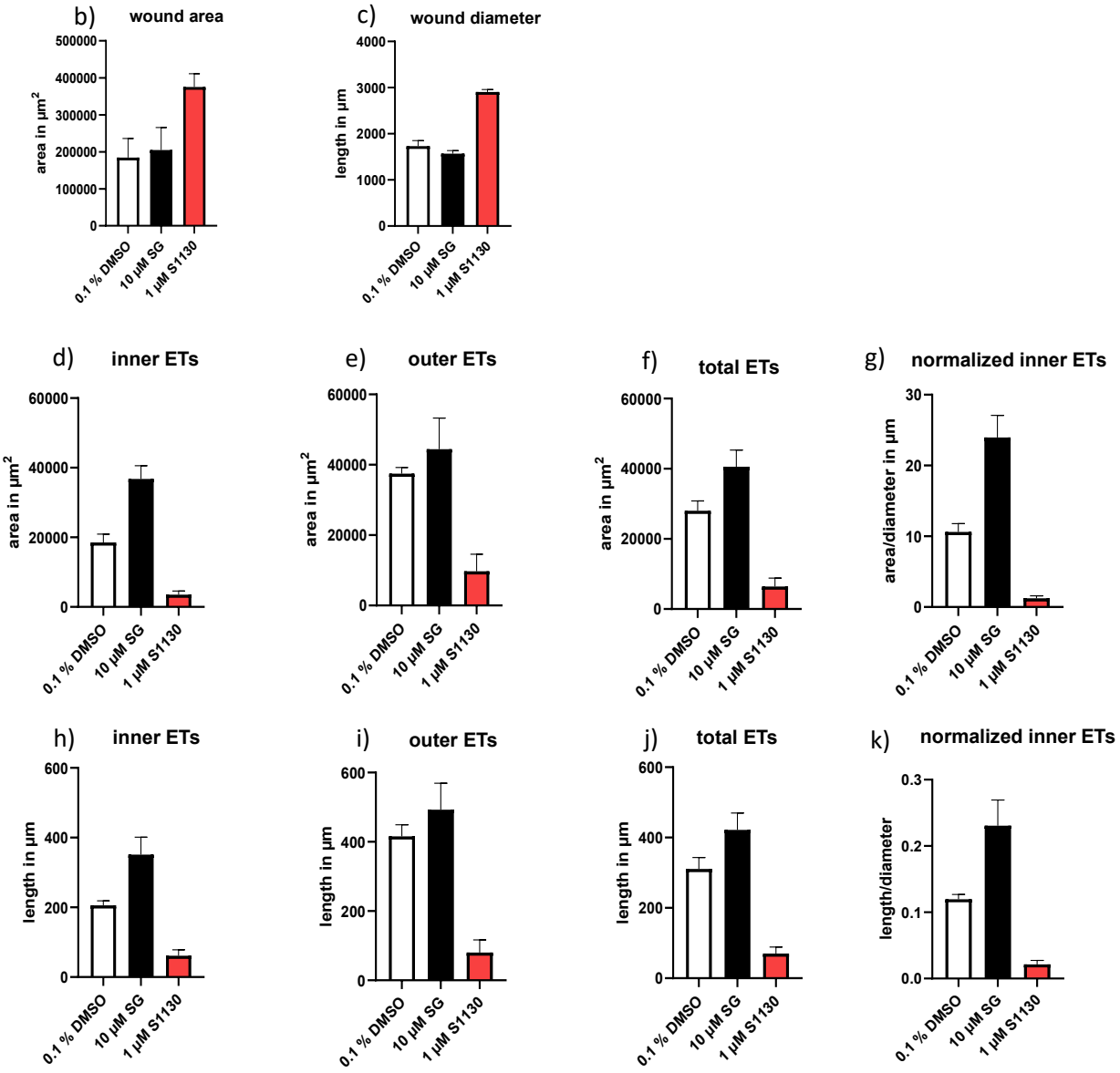

Figure 4.54: Influence of S1130 on the microscopic wound healing in the wound healing organ culture model.
The wounds of the wound healing organ culture model were treated with 0.1 % dimethyl sulfoxide (DMSO) as vehicle control, 10 µM sodium gaulenate (SG) as positive control, or 1 µM S1130 at day 1 of the culture for 24 hours. a) Exemplary hematoxylin & eosin stained pictures of the microscopic wounds in 100x magnification (scale bar = 200 µm) and close-up of an exemplary epithelial tongue (ET) in 200x magnification (scale bar = 100 µm). b) microscopic wound area (n=; 4 wounds/condition) c) wound length n=1; 4 wounds/condition) d) area of the inner ETs, e) area of the outer ETs, f) area of inner and outer ETs combined, g) normalized area of the ETs on the respective wound diameter, h) length of inner ETs, i) length of outer ETs, j) length of inner and outer ETs combined, k) length of inner ETs normalized on the respective wound diameter. For all ET measurements n = 1; 7-16 ETs/condition). Values are depicted as mean + standard error of the mean. Statisitcal analysis was not possible because only one biological replicate was performed.

4.11.3 Treatment with 1 µM S1130 seems to reduce the cytokeratin 6 expression in the wound healing organ culture model

Figure 4.55 shows the CK 6 evaluation. **Figure 4.55a** depicts exemplary pictures of the CK 6 expression in the ETs.

The relative CK 6 expression in the inner ETs is shown in **Figure 4.55b**. The relative CK 6 expression in the inner ETs was highest in the positive control wounds (118.33 %), followed by the vehicle control wounds (100 %), and it was lowest after treatment with 1 µM S1130, namely 86.59 %. The same

pattern can be observed for the relative CK 6 expression in the outer ETs in **Figure 4.55c**: the outer ETs treated with 1 µM S1130 had the lowest relative CK 6 expression with 82.87 %, followed by 0.1 % DMSO (100 %) and 10 µM SG (114.16 %). **Figure 4.55d** shows the relative CK 6 expression in the total ETs. As before, treatment with 1 µM S1130 resulted in the lowest relative CK 6 expression (84.73 %) and 10 µM to the highest relative CK 6 expression (116.24 %).

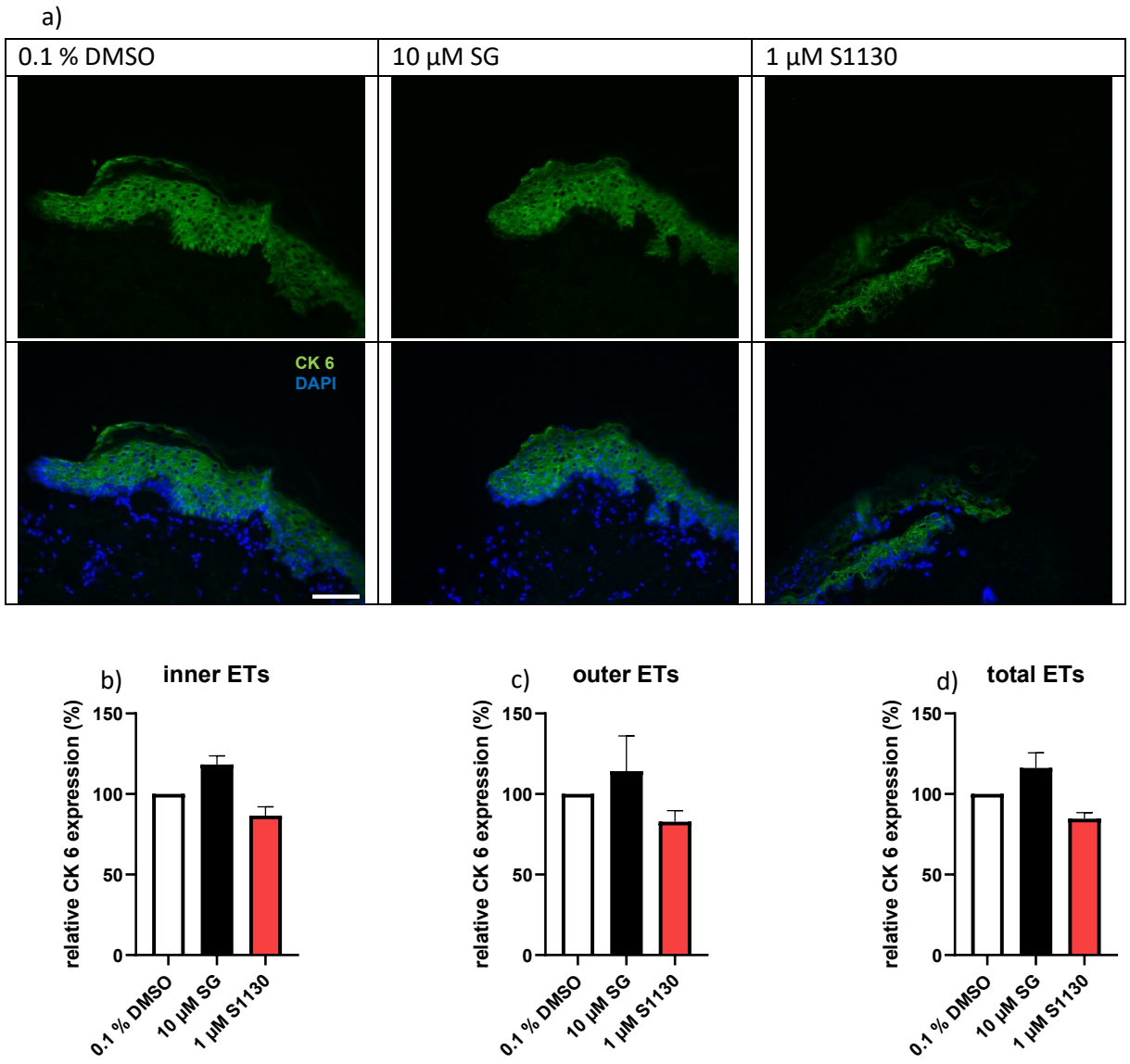

Figure 4.55: Influence of S1130 on the cytokeratin 6 in the wound healing organ culture model
The wounds of the wound healing organ culture model were treated with 0.1 % dimethyl sulfoxide (DMSO) as vehicle control, 10 µM sodium gaulenate (SG) as positive control, or 1 µM S1130 at day 1 of the culture for 24 hours. Shown here is the CK 6 expression in the epithelial tongues (ETs) of wounds cut and stained at day 7 (end of culture). a) Exemplary immunofluorescence pictures of the ETs scale bar = 100 µm. Relative cytokeratin (CK) 6 expression in the inner (b), outer (c) and total (d) ETs. n = 1; 2-8 ETs/wound. Values are depicted as mean + standard error of the mean. Statisitcal analysis was not possible because only one iological replicate was performed.

4.11.4 Treatment with 1 µM S1130 seems to reduce the number of CD 31 positive cells

Figure 4.56 depicts the results of the CD31 immunofluorescence staining. The exemplary pictures are shown in **Figure 4.56a**. Treatment with 1 µM S1130 and 10 µM SG led to a slight decrease in the relative CD31 expression compared to the vehicle control 0.1 % DMSO, of 97.06 % or 93.53 %

respectively (compare **Figure 4.56b**). On the other hand, treatment with 1 µM S1130 had a negative effect on the number of CD31 positive cells (compare **Figure 4.56c**). The highest number of positive cells (49/VF) was observed after treatment with 0.1 % DMSO. Treatment with 10 µM SG led to only slightly less CD31 positive cells (47/VF), while treatment with 1 µM S1130 led to a clear decrease in positive cells (32/VF). As **Figure 4.56d** shows, wounds treated with 10 µM SG showed a higher number of CD31 vessels (0.57/VF), and wounds treated with 1 µM S1130 (0.29/VF) a lower number of CD31 positive vessels compared to DMSO (0.43/VF). The number of CD31 positive cross sections was unaffected by treatment with SG or S1130 (0.57/VF) for all 3 conditions, compare **Figure 4.56d**).

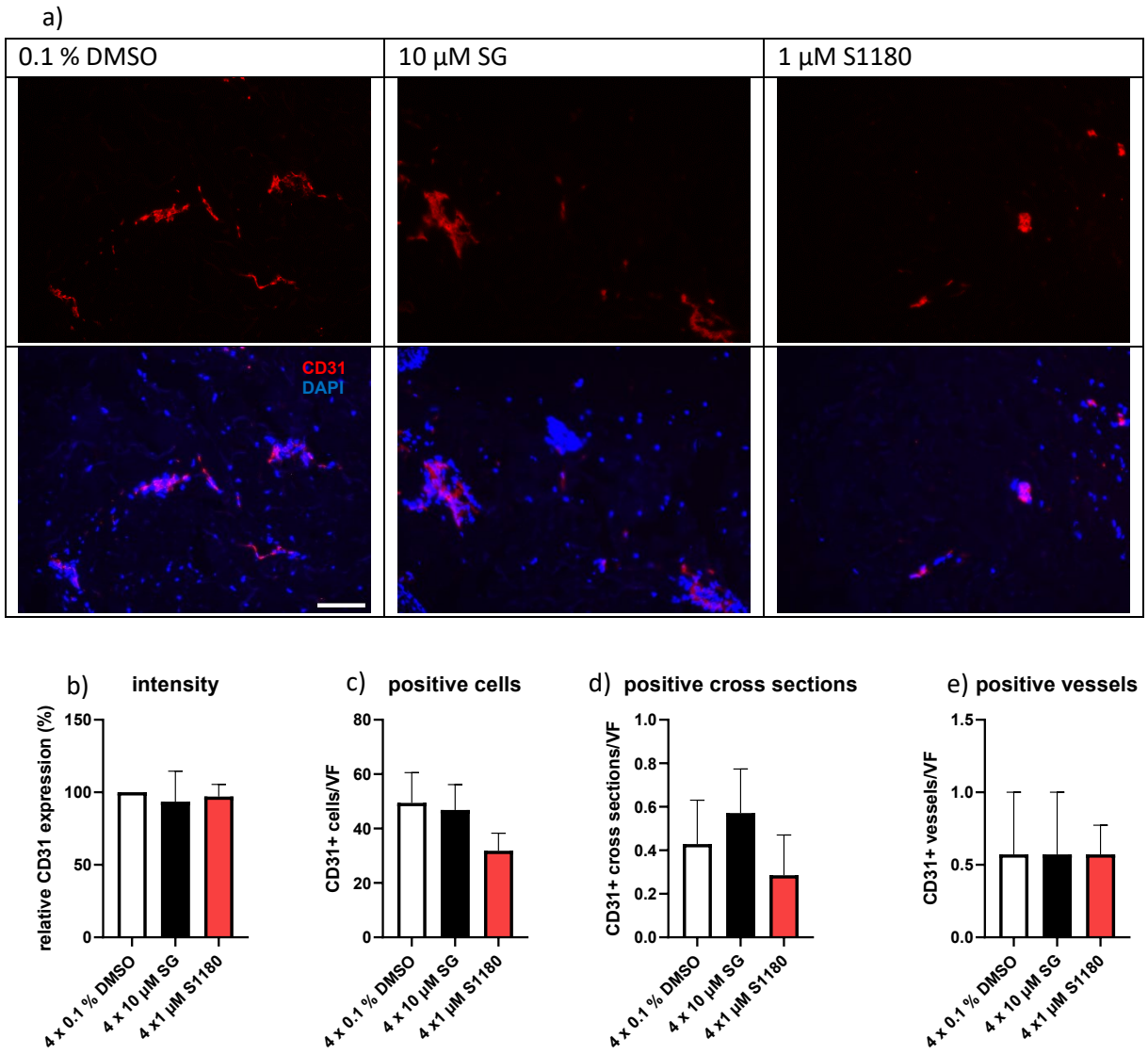

Figure 4.56: Influence of S1130 on the CD31 expression in the wound healing organ culture
The wounds of the wound healing organ culture model were treated with 0.1 % dimethyl sulfoxide (DMSO), 10 µM sodium gaulenate (SG) or 1 µM S1130 at day 1 of the culture for 24 hours. Shown here is the CD31 expression of wounds cut and stained at day 7 (end of culture). a) Exemplary immunofluorescence pictures of the dermis. scale bar = 100 µm, b) relative CD31 expression, c) Number of CD31 positive cells/visual field (VF), d) Number of CD31 positive vessels/VF, e) number of CD31 positive cross sections/VF. n = 1, 2-4 VF/wound for all. Values are depicted as mean + standard error of the mean. Statisitcal analysis was not possible because only one biological replicate was performed.

4.11.5 Treatment with 1 µM S1130 did not change the cortactin expression strongly

Figure 4.57 shows exemplary pictures of the cortactin staining. Here, no strong difference between the different treatment groups was observed. In all groups there was a clearly visible cortactin expression in the ETs, though it was especially pronounced in the tip of the ET, treated with the vehicle control.

a)

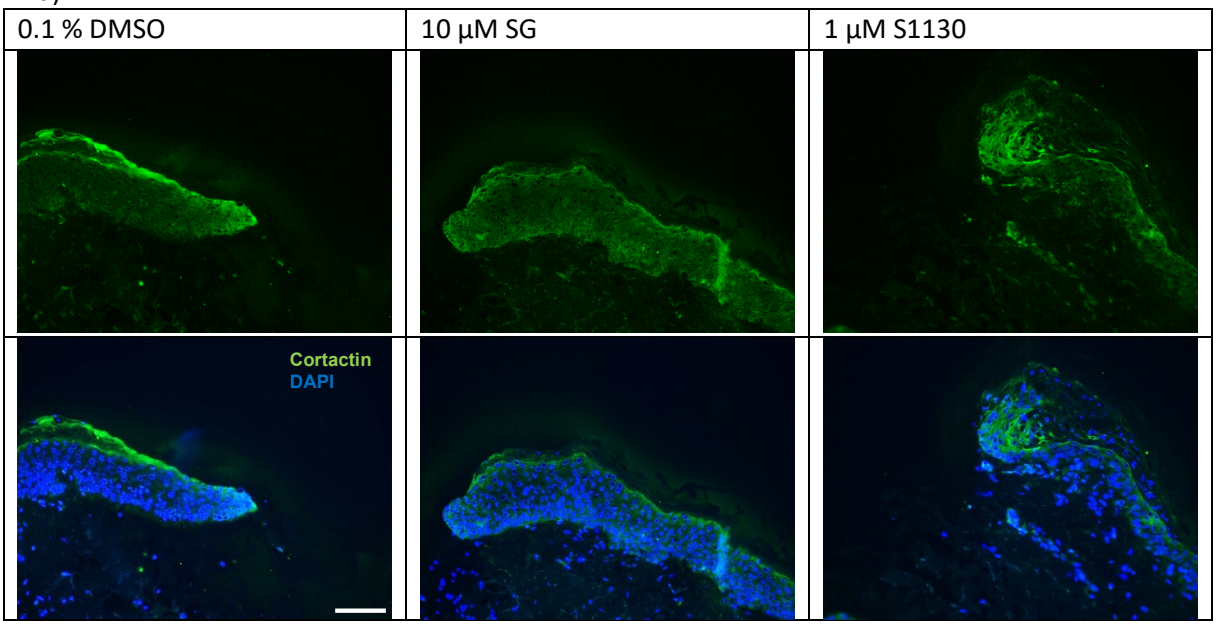

Figure 4.57: influence of S1130 on the cortactin expression in the wound healing organ culture
The wounds of the wound healing organ culture model were treated with 0.1 % dimethyl sulfoxide (DMSO), 10 µM sodium gaulenate (SG) or 1 µM S1130 at day 1 of the culture for 24 hours. Shown here are exemplary pictures of the cortactin staining of wounds cut and stained at day 7 (end of culture). Scale bar = 100 µm. Statisitcal analysis was not possible because only one biological replicte was performed.

This thorough investigation showed, that S1130 had a clearly negative effect on all parameters studied here and thus worsens the *ex vivo* wound healing in the WHOC model.

4.12 Wounds cultured for 6 days under the tested pathological conditions did not heal in the *ex vivo* wound healing organ culture model

The most successful inhibitor of the screening, S1180, was tested in a pathological wound healing model. This model was established by Post *et al*. (Post *et al.*, 2021). In the pathological model the wounds were incubated at 37 C and 5 % CO_2 with only 5 % O_2, no insulin, 138.8 mM D-glucose and 10 mM hydrogen peroxide, to mimic the conditions one might find in a chronic wound. For more information see **Chapter 3**.

As it was shown in **Chapter 4**, the best results in the physiological WHOC were achieved with a one-time treatment of either 1 µM S1180 or 10 µM S1180, so these concentrations were tested here. As an additional positive physiological the thyroid hormone L-thyroxine (T4) was added, as Post *et al.* showed that aids *ex vivo* wound healing under pathological conditions (Post *et al.*, 2021). To optimally compare the pathological and physiological wound healing, a control group was included for all conditions tested here.

4.12.1 Top-view microscopy revealed that the pathological wounds disintegrated and did not show any signs of wound healing

Figure 4.58 shows the results of the top-view evaluation. Already the exemplary pictures in **Figure 4.58a** illustrate clearly the detrimental effect of the pathological conditions on the skin. The skin was discolored, the epidermis partly detached and the wounds were barely visible by eye, while the wounds under physiological conditions looked healthy and healed well.

Figure 4.58b shows the evaluation of the top-view wound area. As the wounds had to be kept under hypoxic conditions throughout the culture, top-view microscopy was only possible on day 0 and day 6. Thus, **Figure 4.58b** only shows the relative top-view wound area at day 6. On day 6, the relative top-view wound area of the pathological wounds was higher in all tested conditions than their respective, physiological wounds. The relative top-view wound area of the physiological wounds treated with 0.1 % DMSO as vehicle control was 58.91 %, that of the pathological wounds 77.48 %. The physiological wounds treated with 10 µM SG had a relative top-view wound area of 44.27 % and the respective pathological wounds 72.61 %. Physiological wounds treated with 100 nM T4 had a relative wound area of 42.99 %, while the respective pathological wounds had a relative area of 58.76 %. The relative top-view wound area of physiological wounds treated with 1 µM S1180 was 42.27 %, which was significantly smaller than the relative area of the respective pathological wound area (65.60 %, $p < 0.01$). Further, for treatment with 10 µM S1180, the pathological wounds had a larger relative area (53.79 %) than their physiological groups (48.55 %), though the difference was comparably small. In the physiological group treatment with 10 µM SG, 100 nM T4, and with both concentrations of S1180 led to smaller relative wounds than treatment with the vehicle control DMSO, though the effect was not significant here. The same tendencies were observed in the pathological model. Here, in a direct comparison, wounds treated with 10 µM S1180 were significantly smaller than the vehicle control ($p < 0.05$, data not shown).

Figure 4.58c shows the relative top-view wound perimeter. Again, the perimeter could only be determined at day 0 and day 6. Just like the area, the pathological wounds had a larger relative top-view wound perimeter in all conditions tested. The pathological wounds treated with 0.1 % DMSO had a significantly larger relative perimeter with a value of 103.12 % than the physiological wounds, which had a value of 81.70 % ($p < 0.05$). The same is true for the wounds treated with 10 µM SG: the

perimeter of the physiological wounds was significantly smaller with a value of 70.75 % than the pathological wounds with a value of 90.76 % ($p < 0.01$). Physiological wounds treated with 100 nM T4 had a relative perimeter of 72.30 %, while the pathological wounds had a relative perimeter of 85.16 %. The relative perimeter of the physiological wounds treated with 1 µM S1180 was 77.21 % and that of the respective pathological wounds was 89.09 %. Treatment with 10 µM S1180 resulted in a relative top-view wound perimeter of 78.51 % in physiological wounds and 89.95 % in pathological wounds.

Again, the vehicle control of both models had the largest relative top-view wound perimeter, though the differences to the other conditions tested was not as pronounced as it was for the area. In a direct comparison, the physiological wounds treated with 10 µM SG were significantly smaller than those treated with 0.1 % DMSO ($p < 0.05$, data not shown). For the pathological wounds the difference between treatment with 0.1 % DMSO and 100 nM T4 was statistically significant in a direct comparison ($p < 0.05$).

a)

Physio-logical	0.1 % DMSO	10 µM SG	100 nM T4	1 µM S1180	10 µM S1180
Day 0					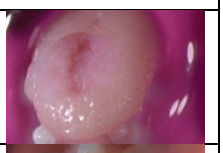
Day 6	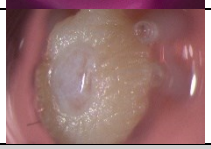				
Patho-logical	0.1 % DMSO	10 µM SG	100 nM T4	1 µM S1180	10 µM S1180
Day 0		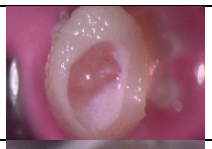			
Day 6		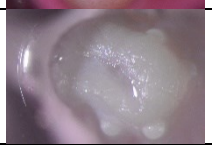			

b)

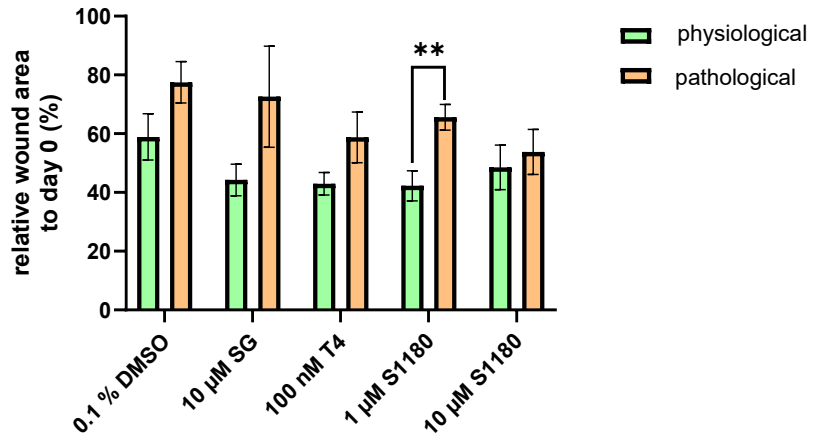

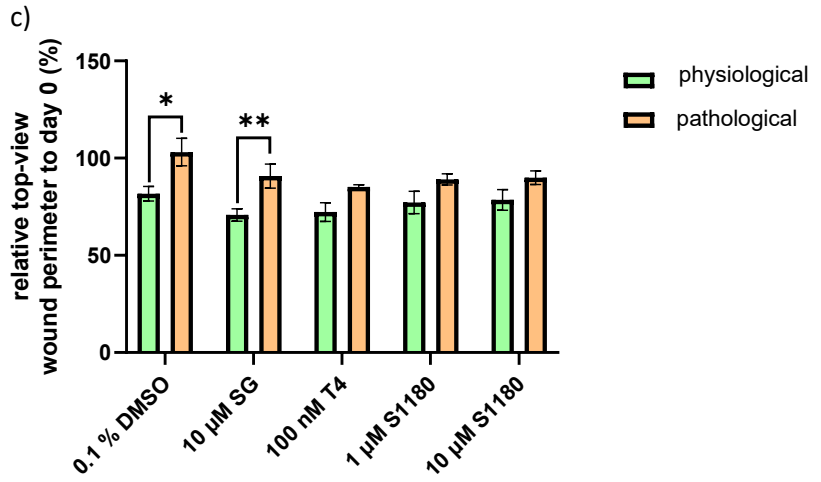

Figure 4.58: Comparison of physiological and pathological conditions on the *ex vivo* top-view wound healing in the wound healing organ culture model
Shown here is the top-view wound closure of skin under physiological and pathological conditions. Pathological conditions include withdrawl of insulin, hypoxia (5 % oxygen), 10 mM hydrogen peoxide and high levels of D-Glucose (138.8 mM). Both, physiological and pathological wounds were treated with 0.1 % dimethyl sulfoxide (DMSO), 10 µM sodium gualenate (SG), 100 nM L-thyroxine (T4), 1 µM S1180, or 10 µM S1180 at day 1 for 24 hours. The total incubation time was 6 days. a) Exemplary pictures of physiological and pathological wounds at day 0 and day 6. Relative top-view wound b) area and c) perimeter at day 6 (n = 3 (2-4 wounds/condition). Data is depicted as mean ± standard error of the mean. For statistical analysis one-way ANOVA and unpaired t-tests were performed, *p < 0.05, ** p < 0.01.

4.12.2 Hematoxylin and eosin evaluation shows that the epidermis of the pathological wounds was partly detached, and no epithelial tongues formed, while the physiological wounds healed nicely

Next the wounds were analyzed microscopically, as can be seen in **Figure 4.59**. Here also the pictures in **Figure 4.59a** show how harmful the incubation under pathological conditions was for the wounds. The epidermis partly detached from the dermis and almost no formation of new ETs was visible.

Figure 4.59b shows the microscopic wound area. Here, no clear differences between the physiological and the pathological groups was observable. For example, physiological wounds and pathological wounds treated with 0.1 % DMSO had a rather similar microscopic area of 167,429 µm^2 and 162,238 µm^2 respectively. The microscopic wound area of physiological wounds treated with 10 µM SG was 122,247 µm^2 and that of pathological wounds was 151,602 µm^2 respectively. Treatment with 100 nM T4 resulted in a microscopic wound area of 165,799 µm^2 in physiological wounds and 203,757 µm^2 in pathological wounds. Treatment with 1 µM S1180 did not led to a smaller microscopic wound area then the vehicle control in both models: the microscopic wound area for the physiological wounds was 218,991 µm^2 and that of the physiological group was 250,958 µm^2. Wounds treated with 10 µM S1180 had a smaller microscopic wound area than the vehicle control in both models, though the effect was not significant (157,813 µm^2 for the physiological wounds and 149,520 µm^2 for the pathological wounds).

The microscopic wound diameter can be found in **Figure 4.59c**. Surprisingly the physiological wounds treated with 0.1 % DMSO had a significantly larger diameter than the pathological wounds (1,967.76 µm vs. 1,228.43 µm, $p < 0.05$). On the other hand, the diameter of physiological wounds treated with 10 µM SG (1,500.76 µm) was smaller than that of the respective pathological wounds (2,215.84 µm). The same is true for treatment with 100 nM T4: here, the diameter of the

physiological wound (1,236.44 µm) was even significantly smaller than that the pathological wounds (1,917.22 µm, $p < 0.05$). Wounds treated with 1 µM S1180 had a relative similar diameter in both models: 1,529.06 µm for the physiological wounds and 1,305.83 µm for the pathological group. Treatment with 10 µM S1180 resulted in significantly wider microscopic wounds in the physiological wounds than in the pathological wounds (1,848.81 µm vs. 747.19 µm, $p < 0.01$). Within the pathological wounds, treatment with 1 µM S1180 resulted in a significantly smaller microscopic wound diameter than treatment with 10 µM SG or 100 nM T4 ($p < 0.001$).

Figures 4.59d-k illustrate the evaluation of the newly formed ETs. The area of the inner ETs can be found in **Figure 4.59d**. The almost complete absence of ETs under pathological conditions was striking. For all conditions tested the physiological wounds had significantly larger inner ETs with a level of significance of $p < 0.0001$. In the physiological wounds treatment with 0.1 % DMSO resulted in inner ETs with an area of 37,846 µm^2. Physiological wounds treated with 10 µM SG had inner ETs with an area of 21,491 µm. Treatment with 100 nM T4 had a significantly smaller inner ETs' area than the vehicle physiological 0.1 % DMSO (16,436 µm^2, $p < 0.05$). Only treatment with 1 µM S1180 resulted in larger inner ETs than the vehicle control in the physiological wounds (44,800 µm^2). These ETs were significantly larger than those of wounds treated with 10 µM SG ($p < 0.05$) and 100 nM T4 ($p < 0.01$). Physiological wounds treated with 10 µM S1180 had an inner ETs area of 34,915 µm^2.
The normalized area of the inner ETs can be found in **Figure 4.59g**. Here also almost no inner ETs were measurable in the pathological wounds. In all conditions tested the normalized inner ETs' area of the physiological wounds was significantly larger than that of the respective pathological wounds ($p < 0.001$). After normalization, treatment with 10 µM SG resulted in the smallest area of the inner ETs in physiological wounds (1.47 µm) and treatment with 1 µM S1180 in the largest (47.83 µm). The other treatment conditions resulted in normalized inner ETs areas between those two values: 18.04 µm for 0.1 % DMSO, 21.34 µm for 100 nM T4, and 20.01 µm for 10 µM S1180.
Figure 4.59e shows the area of the outer ETs. Again, the pathological wounds displayed as good as no ETs. The outer ETs of the physiological wounds were smaller than their inner ETs, but clearly present. Physiological wounds treated with 0.1 % DMSO had the smallest outer ETs area', namely 7,984 µm^2. Treatment with the positive control 10 µM SG resulted in the largest outer ETs' area namely 22,540 µm^2, which was significantly larger than the physiological wounds treated with 0.1 % DMSO and 1 µM S1180 ($p < 0.05$ for both). Physiological wounds treated with 100 µM T4 had an outer ETs' area of 19,441 µm^2, those treated with 1 µM S1180 of 11,449 µm^2 and those treated with 10 µM S1180 of 12,551 µm^2. The outer ETs area of wounds treated with 1 µM S1180 were significantly smaller than those treated with 10 µM SG ($p < 0.05$) and 1 µM S1180 ($p < 0.01$).
The area of the total ETs is shown in **Figure 4.59f**. As described before, pathological wounds barely formed any ETs. The physiological wounds have significantly larger total ETs ($p < 0.0001$ for all conditions tested). For the physiological wounds, the differences in the total ETs' area are relatively small. Treatment with 100 nM T4 resulted in the smallest (19,439 µm) and treatment with 1 µM S1180 in the largest total ETs (28,495 µm). The other conditions tested lay in between: 22,121 µm^2 for 10 µM SG, 22,463 µm^2 for 0.1 % DMSO, and 23,733 µm^2 for 10 µM S1180.

Figure 4.59h-k illustrates the length of the different ETs. **Figure 4.59h** shows the length of the inner ETs. As with the area, pathological wounds had basically no ETs and the physiological wounds displayed significantly longer inner ETs under all conditions tested ($p < 0.0001$). For the physiological wounds, treatment with 10 µm SG resulted in the shortest inner ETs (237.08 µm), followed by 100 nM T4 (288.26 µm), 1 µM S1180 (470.62 µm), and 0.1 % DMSO (476.63 µm). Only physiological wounds treated with 10 µM S1180 had longer inner ETs than the vehicle control 0.1 % DMSO, namely 522.11 µm. The inner ETs of the physiological wounds treated with 10 µM S1180 were significantly

longer than inner ETs of the physiological wounds treated with 10 µM SG and 100 nM T4 ($p < 0.05$ for both). Moreover, treatment with 1 µM S1180 led to significantly longer inner ETs than 10 µM SG.
The normalized inner ETs can be found in **Figure 4.59k**. As before, there were basically no ETs visible in the pathological wounds. For the physiological wounds, again treatment with 10 µM SG resulted in the shortest normalized inner ETs (0.20). However, here the physiological wounds treated with 1 µM S1180 had the longest normalized inner ETs (0.52). Physiological wounds treated with 0.1 % DMSO had a normalized inner ETs' length of 0.27, those treated with 100 nM T4 of 0.27, and those treated with 10 µM S1180 of 0.31.
Figure 4.59i shows the outer ETs length. Here also, the pathological wounds had no ETs at all and in all conditions tested the physiological wounds had significantly longer outer ETs ($p < 0.0001$). Physiological wounds treated with 100 nM T4 had the longest outer ETs, namely 272.07 µm, followed by 10 µM SG (240.40 µm), 1 µM S1180 (191.95 µm), 0.1 % DMSO (164.48 µm), and 10 µM S1180 (136.95 µm).
The length of the total ETs can be found in **Figure 4.59j**. As before, next to no ETs formed in the pathological wounds and the physiological wounds of the respective conditions were significantly longer ($p < 0.0001$). In the physiological wounds, the shortest total ETs were observed after treatment with 10 µM SG (239.07 µm), the longest after treatment with 10 µM S1180 (333.08 µm). The other treatments resulted in ETs' length in between: 280.39 µm for 100 nM T4, 311.38 µm for 0.1 % DMSO, and 328.19 µm for 1 µM S1180.

The microscopic evaluation strongly underlines, how harmful the pathological conditions were on the *ex vivo* wound healing. The physiological wounds healed properly and S1180 appeared to be beneficial for the process, though its effect was not as pronounced as it was found to be in **Chapter 4.8**.

a)

Physio-logical	0.1 % DMSO	10 µM SG	100 nM T4	1 µM S1180	10 µM S1180
Wound	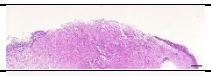	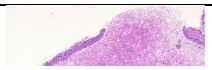	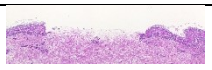	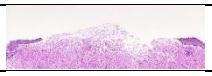	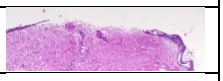
ET	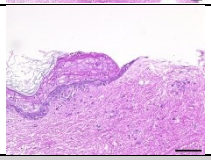	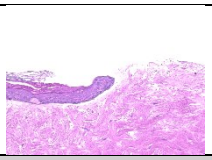	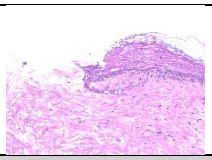	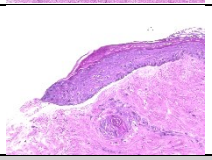	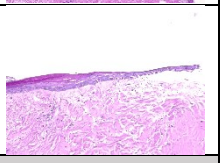
Patho-logical	0.1 % DMSO	10 µM SG	100 nM T4	1 µM S1180	10 µM S1180
Wound	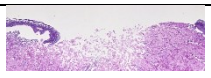	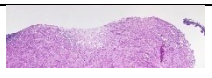	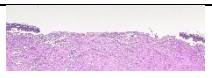	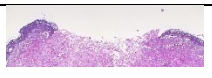	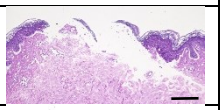
ET	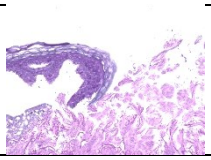	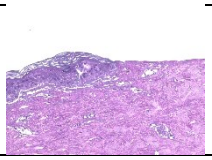	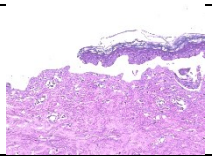	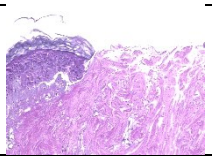	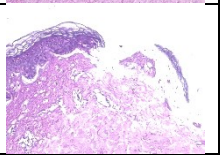

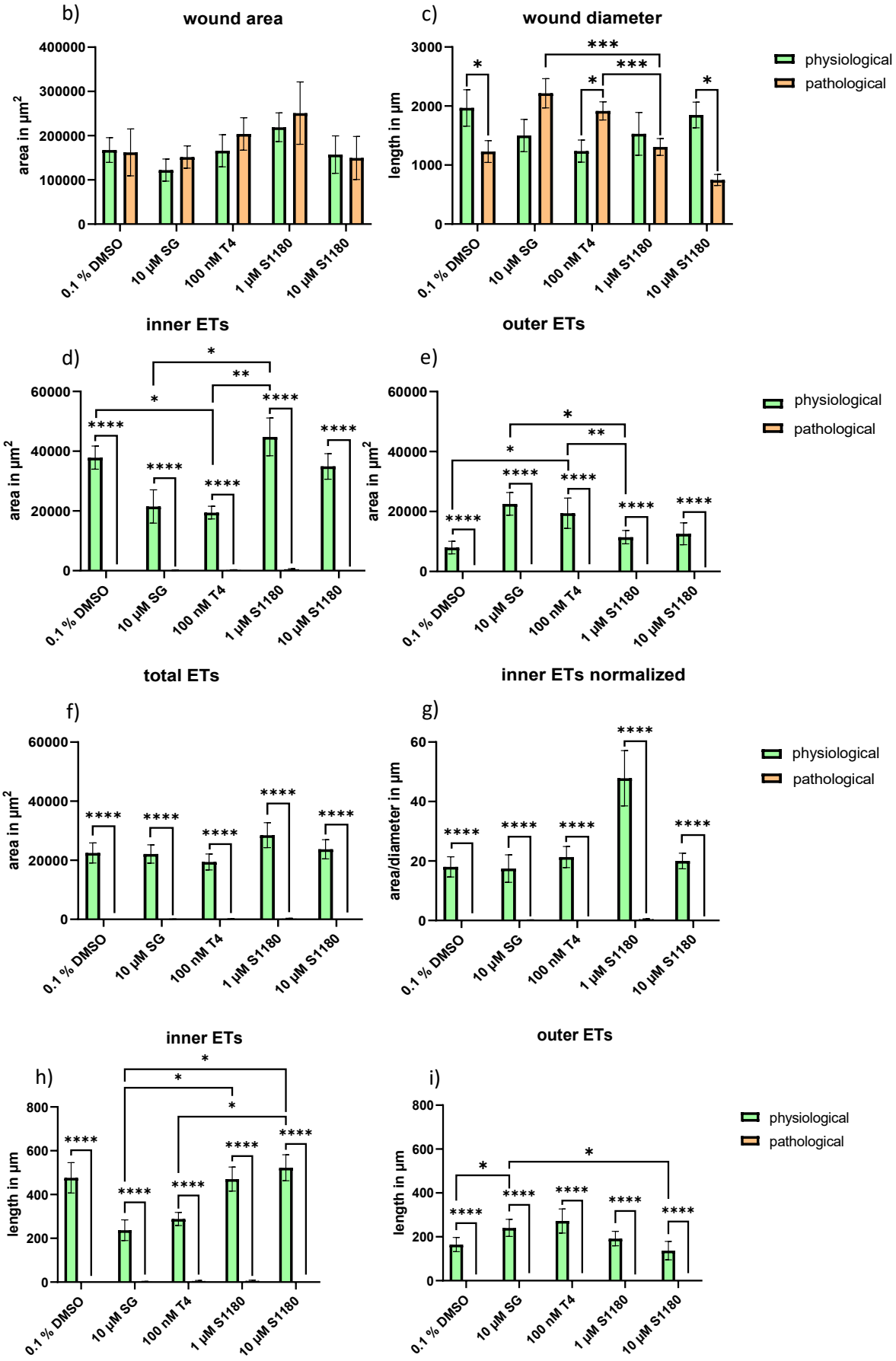
b)
wound area
area in µm²
400000
300000
200000
100000
0
0.1 % DMSO
10 µM SG
100 nM T4
1 µM S1180
10 µM S1180
c)
wound diameter
length in µm
3000
2000
1000
0
***
*
physiological
pathological
inner ETs
d)
area in µm²
60000
40000
20000
0
****
**
outer ETs
e)
total ETs
f)
inner ETs normalized
g)
area/diameter in µm
60
40
20
inner ETs
h)
length in µm
800
600
400
200
outer ETs
i)

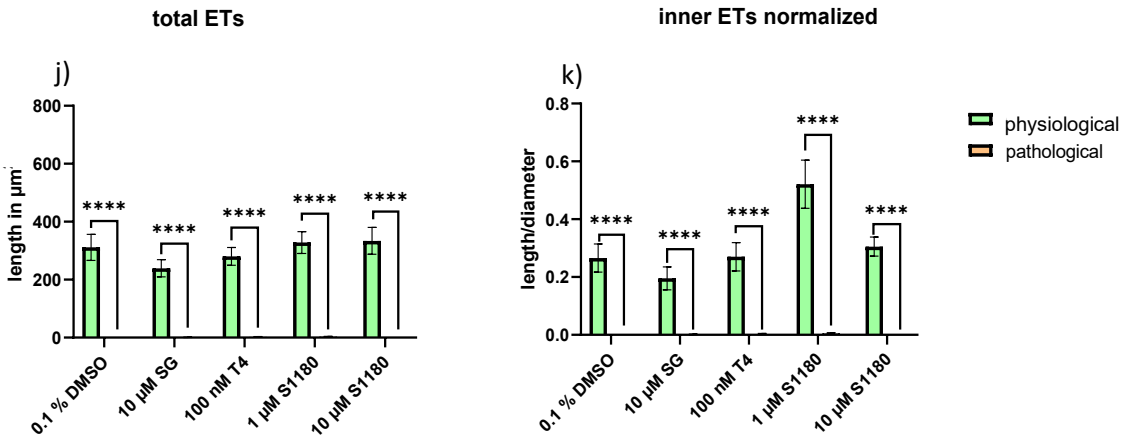

Figure 4.59: Comparison of physiological and pathological conditions on the microscopic wound healing in the wound healing organ culture model.
Shown here is the microscopic wound healing of skin under physiological and pathological conditions in an hematoxylin and eosin staining. Pathological conditions include withdrawl of insulin, hypoxia (5 % oxygen), 10 mMol hydrogen peoxide and high levels of D-Glucose (138.8 mM). Both physiological and pathological wounds were treated with 0.1 % dimethyl sulfoxide (DMSO), 10 µM sodium gualenate (SG), 100 nM L-thyroxine (T4), 1 µM S1180, or 10 µM S1180 at day 1 for 24 hours. The total incubation time was 6 days. a) Exemplary pictures of physiological and pathological wounds: shown are the microscopic wounds (scale bar = 200 µm) and epithelial tongues (ETs, scale bar = 100 µm), b) microscopic wound area, c) microscopic wound diameter (n = 3, 1-4 wounds/condition), area of the d) inner, e) outer and f) total ETs and g) area of the inner ETs normalized on the respective wound diameter, length of the h) inner, i) outer and j) total ETs, k) length of the inner ETs normalized on the respective wound diameter. For all ETs: n = 3, 4-16 ETs/condition for. Data is depicted as mean ± standard error of the mean. For statistically analysis a unpaired t-test (microscopic wound diameter) or Mann-Whitney (microscopic wound area and analysis of ETs) was performed * $p < 0.05$, ** $p < 0.01$, *** $p < 0.001$, ****$p < 0.0001$.

4.12.3 The cytokeratin 6 expression was significantly lower in pathological wounds than in physiological wounds

Next, the relative CK 6 was examined. **Figure 4.60** shows the results. Already the exemplary pictures in **Figure 4.60a** clearly illustrate the CK 6 expression is reduced in pathological wounds. Moreover, the pictures of the pathological wounds show that the skin was not intact here. Instead, the epidermis was often detached and much thinner than in the physiological wounds.

The relative CK 6 expression of the inner ETs can be found in **Figure 4.60b**. The inner ETs of the pathological wounds had a significantly lower relative CK 6 expression then their respective physiological groups. The data was normalized on the physiological wounds treated with 0.1 % DMSO. The inner ETs of the pathological wounds treated with the vehicle control had a significantly lower relative CK 6 expression than the physiological wounds, namely 23.76 % ($p < 0.0001$). Treatment with 10 µM SG resulted in a lower relative CK 6 expression in the physiological wounds than treatment with 0.1 % DMSO, namely 77.93 %. However, this value was still significantly higher than that of the pathological wounds (18.41 %, $p < 0.01$). Treatment with 100 nM T4 resulted in a relative CK 6 expression of 109.83 % in the inner ETs of physiological wounds and 23.24 % in the pathological wounds. This difference was significant with a significance level of 0.0001. The inner ETs of the physiological wounds treated with 1 µM S1180 had the highest relative CK 6 expression of all, namely 124.83 %. This was significantly higher than the respective pathological wounds, which had a relative CK 6 expression of 23.94 % ($p < 0.0001$). Treatment with 10 µM S1180 led to a relative CK 6

expression of 96.23 % in the inner ETs of the physiological wounds and of 18.09 % in the inner ETs of pathological wounds.
The CK 6 expression of the inner ETs of the pathological wounds did barely differ between the conditions tested here. The differences in the physiological wounds were much more pronounced, for example the relative CK 6 expression of the inner ETs after treatment with 1 µM S1180 was significantly larger than after treatment with 10 µM SG ($p < 0.01$).

Figure 4.60c shows the relative CK 6 expression in the outer ETs. Again, the outer ETs of the pathological wounds had a significantly lower relative CK 6 expression than their respective physiological wounds. For example, the pathological wounds had a relative CK 6 expression in the outer ETs of 19.23 %, which was significantly smaller than the respective physiological wounds ($p < 0.01$). Treatment with 10 µM SG led to a relative CK 6 expression of 102.35 % in the outer ETs of physiological wounds and 17.58 % in the pathological wounds. The difference was significant with a level of significance of 0.05. The relative CK 6 expression of the outer ETs of physiological wounds treated with 100 nM T4 was 129.69 %, those of pathological wounds was 21.00 % and significantly lower ($p < 0.01$). Treatment with 1 µM S1180 resulted in a relative CK 6 expression of 112.46 % in the outer ETs of physiological wounds and 18.78 % in pathological wounds, a significant difference. ($p < 0.01$). Outer ETs of the physiological wounds treated with 10 µM S1180 had a relative CK 6 expression of 105.95 % and 15.23 % in pathological wounds.
As with the inner ETs, here also the differences between the different treatment conditions were much more pronounced in the physiological wounds than in the pathological wounds.

Figure 4.60d shows the relative CK 6 expression in the total ETs. The same pattern can be observed as described above. In all conditions tested the CK 6 expression of the total ETs in the pathological wounds was significantly lower than that in the physiological wounds. Here, these differences were all significant with a level of significance of 0.0001. As the data was normalized on the CK 6 expression of the total ETs of the physiological wounds, their value was 100 %, while the that of the pathological wounds was 21.49 %. Treatment with 10 µM SG led to a relative CK 6 expression of 77.93 % in the total ETs of the physiological wounds and 17.93 % in pathological wounds. The outer ETs of physiological wounds treated with 100 nM T4 had relative CK 6 expression of 109.83 % and those of pathological wounds of 22.12 %. The highest CK 6 expression of the total ETs was 124.83 % and observed in the physiological wounds treated with 1 µM S1180, while it was 21.07 % in the respective pathological wounds. Outer ETs treated with 1 µM S1180 had a relative CK 6 expression of 96.23 % in the physiological wounds and 16.66 % in the pathological wounds.

These findings clearly illustrate, that the CK 6 expression is significantly reduced in the pathological wounds.

a)

Physio-logical	0.1 % DMSO	10 µM SG	100 nM T4	1 µM S1180	10 µM S1180
CK 6	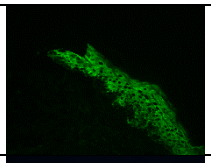	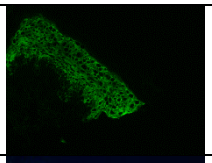	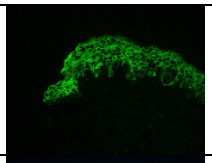	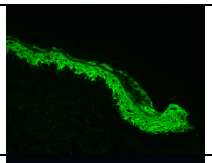	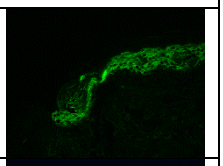
Overlay	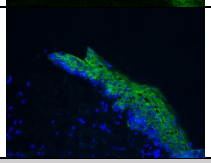	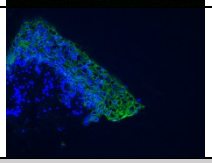	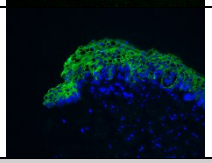	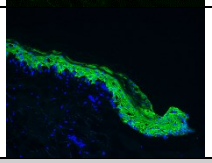	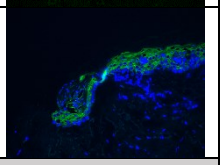
Patho-logical	**0.1 % DMSO**	**10 µM SG**	**100 nM T4**	**1 µM S1180**	**10 µM S1180**
CK 6	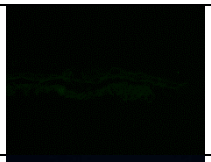	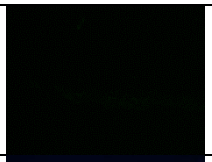	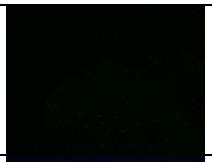	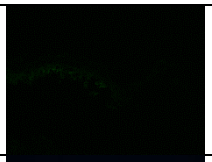	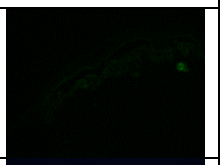
Overlay	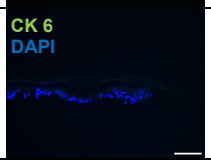	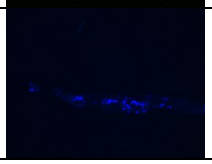	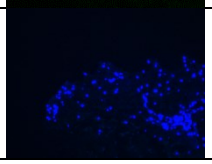	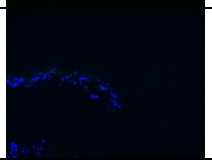	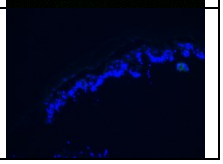

b)

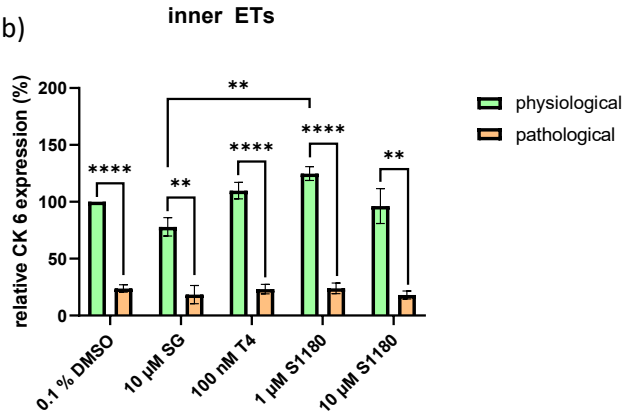

c)

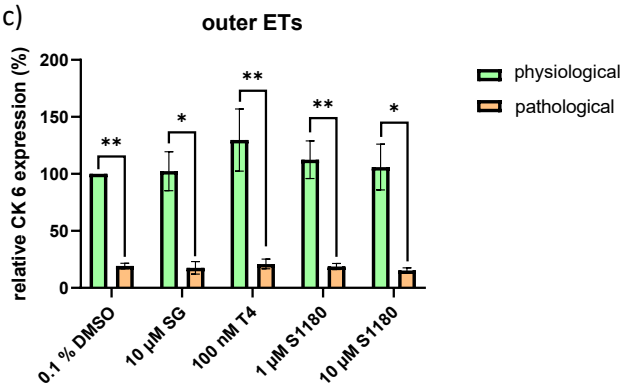

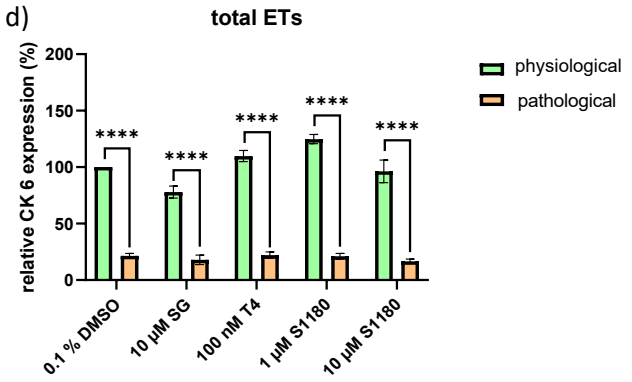

Figure 4.60: Comparison of physiological and pathological conditions on the cytokeratin 6 expression in the wound healing in the wound healing organ culture model
Shown here is the cytokeratin 6 (CK 6) expression of wounds under physiological and pathological conditions. Pathological conditions include withdrawl of insulin, hypoxia (5 % oxygen), 10 mM hydrogen peoxide and high levels of D-Glucose (138.8 mM). Both, physiological and pathological wounds were treated with 0.1 % dimethyl sulfoxide (DMSO), 10 µM sodium gualenate (SG), 100 nM L-thyroxine (T4), 1 µM S1180, or 10 µM S1180 at day 1 for 24 hours. The total incubation time was 6 days. a) Exemplary immunofluorescence pictures of the ETs. Scale bar = 100 µm. CK 6 expression in the inner (b), outer (c) and total (d) ETs. (n = 3-5, 2-8 ETs/condition). Data is depicted as mean ± standard error of the mean. For statistical analysis Kruskal-Wallis test and Mann-Whitney test (pathological wounds, outer ETs), one-way ANOVA and unpaired t-tests (all other conditions) were performed, *p < 0.05, ** p < 0.01, **** p 0.0001.

4.12.4 Not the cell count but the relative CD31 expression was significantly reduced in pathological wounds compared to physiological wounds

Figure 4.61 depicts the results of the CD31 staining. The exemplary pictures in **Figure 4.61a** show, that the CD31 expression was lower in the pathological wounds than in the physiological wounds.

The evaluation of the relative CD31 expression in **Figure 4.61b** underlies this finding. The data was normalized on the physiological wounds treated with 0.1 % DMSO. Pathological wounds treated with 0.1 % DMSO had a relative CD31 expression of 66.05 %, which was significantly lower than the physiological wounds ($p < 0.001$). Treatment with 10 µM SG led to a relative CD31 expression of 97.96 % in physiological wounds and 55.99 % in pathological wounds, a difference that was statistically significant ($p < 0.01$). While not significantly so, also physiological wounds treated with 100 nM T4 had a higher relative CD31 expression than the pathological wounds (94.83 % vs. 76.30 %). Treatment with 1 µM S1180 resulted in a relative CD31 expression of 103.08 % in physiological wounds and 71.91 % in pathological wounds – a significant difference ($p < 0.01$). Physiological wounds treated with 10 µM S1180 had a relative CD31 expression of 90.23 % and pathological wounds of 72.50 %.

As **Figure 4.61c** shows, the number of CD31 positive cells did not differ as strongly between physiological and pathological wounds. The pathological wounds showed a relatively similar increase or decline in numbers to the different conditions. Treatment with 0.1 % DMSO resulted in 50.95 % positive cells/VF in physiological wounds and 43.9 % positive cells/VF. Physiological wounds treated with 10 µM SG had 55 positive cells/VF and pathological wounds 43.5 positive cells/VF. Only wounds treated with 100 nM T4 had more positive cells under pathological conditions than under physiological conditions (60.47 cells/VF compared

to 54.83 cells/VF). Treatment with 1 µM S1180 resulted in the most positive cells in both kind of wounds: 64.84 cells/VF for the physiological wounds and 61.45 cells/VF for pathological wounds. Physiological wounds treated with 10 µM S1180 had 58.17 cells/VF and pathological wounds 52.70 cells/VF.

Figure 4.61d shows the number of CD31 positive cross sections. Physiological wounds treated with 0.1 % DMSO had 1.11 cross sections/VF and pathological wounds 0.40 cross sections/VF. Treatment with 10 µM SG resulted in 0.79 positive cross sections/VF in physiological wounds and 0.13 positive cross sections/VF in pathological wounds. This difference was significant ($p < 0.05$). Treatment with the other conditions resulted in more positive CD31 cross sections in the pathological wounds than in the physiological wounds. 100 nM T4 led to 0.28 cross sections/VF in physiological wounds but 0.76 cross sections/VF in pathological wounds. The increase in positive cross sections was especially striking after treatment with 1 µM S1180. Here, the pathological wounds had 2.05 cross sections/VF, which was significantly more than the 0.65 cross sections/VF in physiological wounds ($p < 0.05$). Moreover, the pathological wounds treated with 1 µM S1180 had significantly more positive cross sections than the pathological wounds treated with 10 µM SG ($p < 0.01$). Treatment with 10 µM S1180 resulted in 0.65 positive cross sections/VF in physiological wounds and 1.15 positive cross sections/VF in pathological wounds.

Figure 4.61e shows the number of CD31 positive cross sections. Physiological wounds treated with 0.1 % DMSO had 1.17 positive vessels/VF, which was significantly more than their respective pathological wounds (0.60 vessels/VF, $p < 0.05$). Treatment with 10 µM SG also resulted in significantly more positive vessels in the physiological wounds than in the pathological wounds (1.35 vessels/VF vs. 0.53 vessels/VF, $p < 0.05$). Physiological wounds treated with 100 nM T4 had 1.12 vessels/VF and pathological wounds 0.80 vessels/VF. Only after treatment with 1 µM S1180 the number of positive vessels was higher in pathological wounds than in physiological wounds, though the difference was slight (0.90 vessels/VF vs. 0.84 vessels/VF). Physiological wounds treated with 10 µM S1180 had 0.94 vessels/VF and pathological wounds 0.80 vessels/VF.

All in all, the relative CD31 expression was decreased in pathological wounds, but S1180 seemed to increase the number of CD31 positive cells in both models. The increase in positive cross sections in pathological wounds treated 1 µM S1180 is noteworthy.

a)

Physio-logical	0.1 % DMSO	10 µM SG	100 nM T4	1 µM S1180	10 µM S1180
CD31	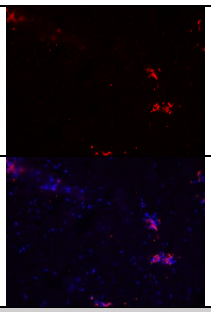	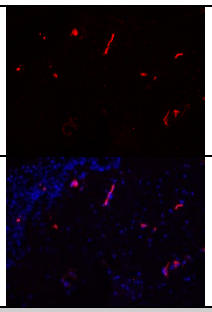	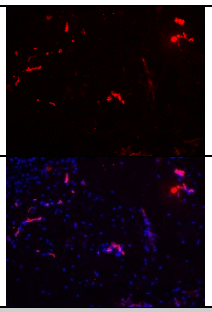	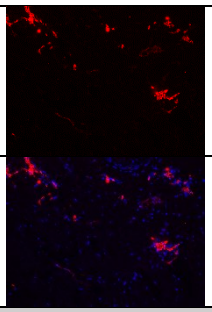	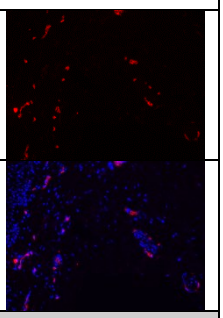
Overlay					
Patho-logical	0.1 % DMSO	10 µM SG	100 nM T4	1 µM S1180	10 µM S1180
CD31	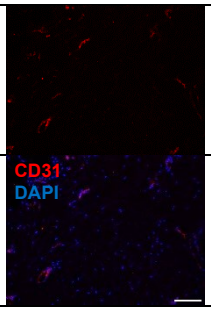	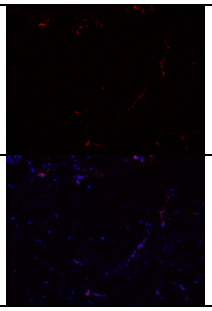	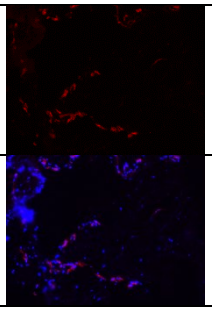	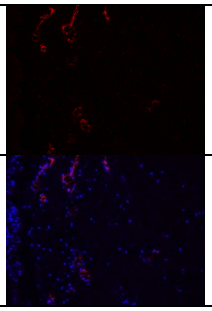	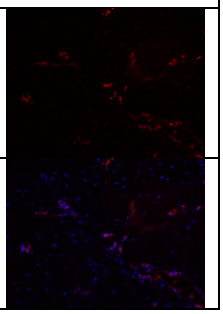
Overlay					

b)

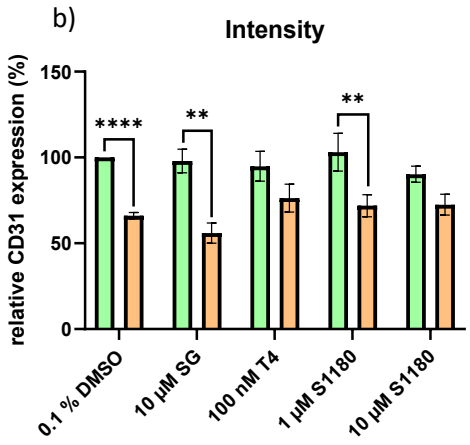

c)

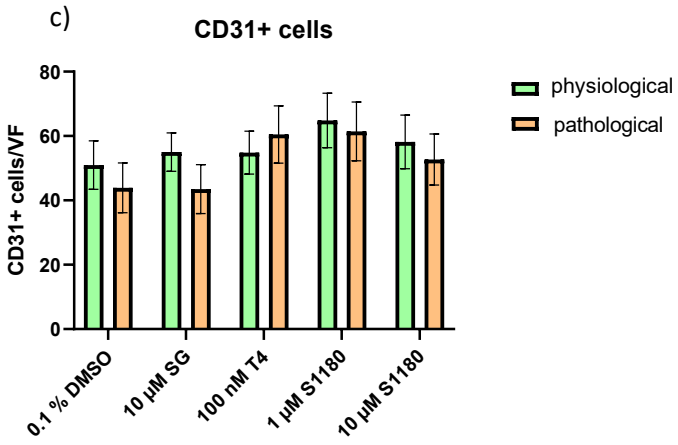

d) CD31+ cross sections

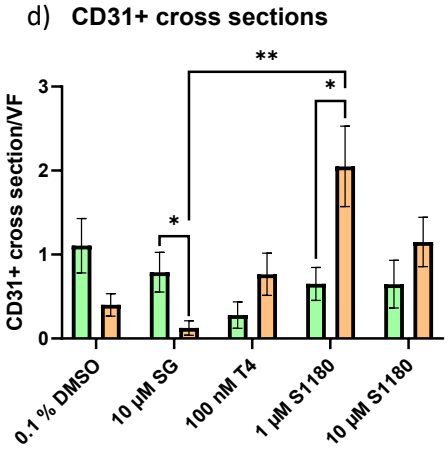

e)

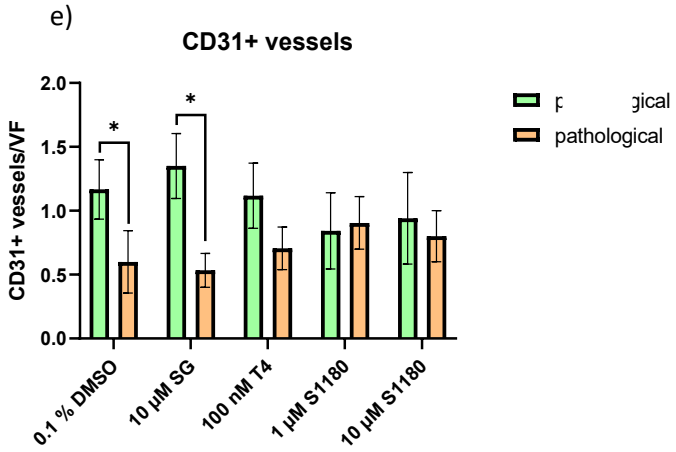

Figure 4.61: Comparison of physiological and pathological conditions on the CD31 expression in the wound healing organ culture model

Shown here is the CD31 expression of wounds under physiologial and pathological conditions. Pathological conditions include withdrawl of insulin, hypoxia (5 % oxygen), 10 µM hydrogen peoxide and high levels of D-Glucose (138.8 mM). Both control and pathological wounds were treated with 0.1 % dimethyl sulfoxide (DMSO), 10 µM sodium gualenate (SG), 100 nM L-thyroxine (T4), 1 µM S1180, or 10 µM S1180 at day 1 for 24 hours. The total incubation time was 6 days. a) Exemplary immunofluorescence pictures of the dermis. Scale bar = 100 µm, b) relative CD31 expression (n = 3, 4-8 visual fields (VFs)/wound), c) number of CD31 positive cells/VF (n = 3, 4-8 VF/wound), d) number of CD31 positive vessels/VF (n = 3, 4-8 VF/wound), e) number of CD31 positive cross sections/VF (n = 3, 2-4 VF/wound). For statistical analysis one-way ANOVA with Turkey's multiple comparison and t-test (intensity and number of cells) or Kruskal-Wallis test with Dunn's multiple comparison and Mann-Whitney (for numbers of cross sections and vessels) was performed, * $p < 0.05$, ** $p < 0.01$, **** $p < 0.0001$.

4.12.5 The epithelial tongues of pathological wounds had significantly less Ki67 positive cells but significantly more TUNEL positive cells than the physiological wounds

As the pathological wounds healed so badly, a KiTUNEL staining was performed lastly to assess the proliferation and apoptosis in pathological and physiological wounds. The staining was only performed on wounds treated with 0.1 % DMSO, as none of the other conditions seemed to really aid wound healing more than this vehicle control in the pathological model.

Figure 4.62 shows the results of the KiTUNEL staining. The exemplary pictures in **Figure 4.62a** illustrate, that there are more TUNEL positive cells in the pathological wounds than in the physiological wounds. In the physiological wounds some Ki67 positive cells could be found, while they were absent in the pathological wounds.

The percentage of Ki67 positive and TUNEL positive cells can be found in **Figure 4.62b**. While there are no positive Ki67 in the pathological wounds, 6.48 % of the cells in the inner ETs of the physiological wounds were Ki67 positive, a difference that was significant ($p < 0.01$). In contrast to this, there were significantly more TUNEL positive cells in the inner ETs of pathological wounds than of physiological wounds (73.71 % vs. 10.77 %, $p < 0.05$).

Figure 4.62c shows the percentage of Ki67 positive and TUNEL positive cells in the outer ETs. Again, no Ki67 positive cells could be found in the outer ETs of pathological wounds. In the outer ETs of the physiological wounds significantly more cells were Ki67 positive, namely 3.30 % ($p < 0.05$). In the outer ETs of pathological wounds 72.26 % cells were TUNEL positive, significantly more than in physiological wounds, were only 20.97 % were TUNEL positive ($p < 0.01$).

The percentage of Ki67 positive and TUNEL positive cells in the total ETs can be found in **Figure 4.62d**. As before, no Ki67 positive cells were found in the pathological wounds. In the total ETs of the physiological wounds 4.89 % of cells were Ki67 positive. The difference between the 2 groups was statistically significant ($p < 0.001$). Again, significantly more cells were TUNEL positive in the pathological wounds than in the physiological wounds (73.02 % vs. 16.43 %, $p < 0.0001$).

The KiTUNEL staining clearly proofed, that the pathological conditions are detrimental for the human skin. There were so many TUNEL positive cells in the epidermis of pathological wounds, that one can ask if the skin was even still alive.

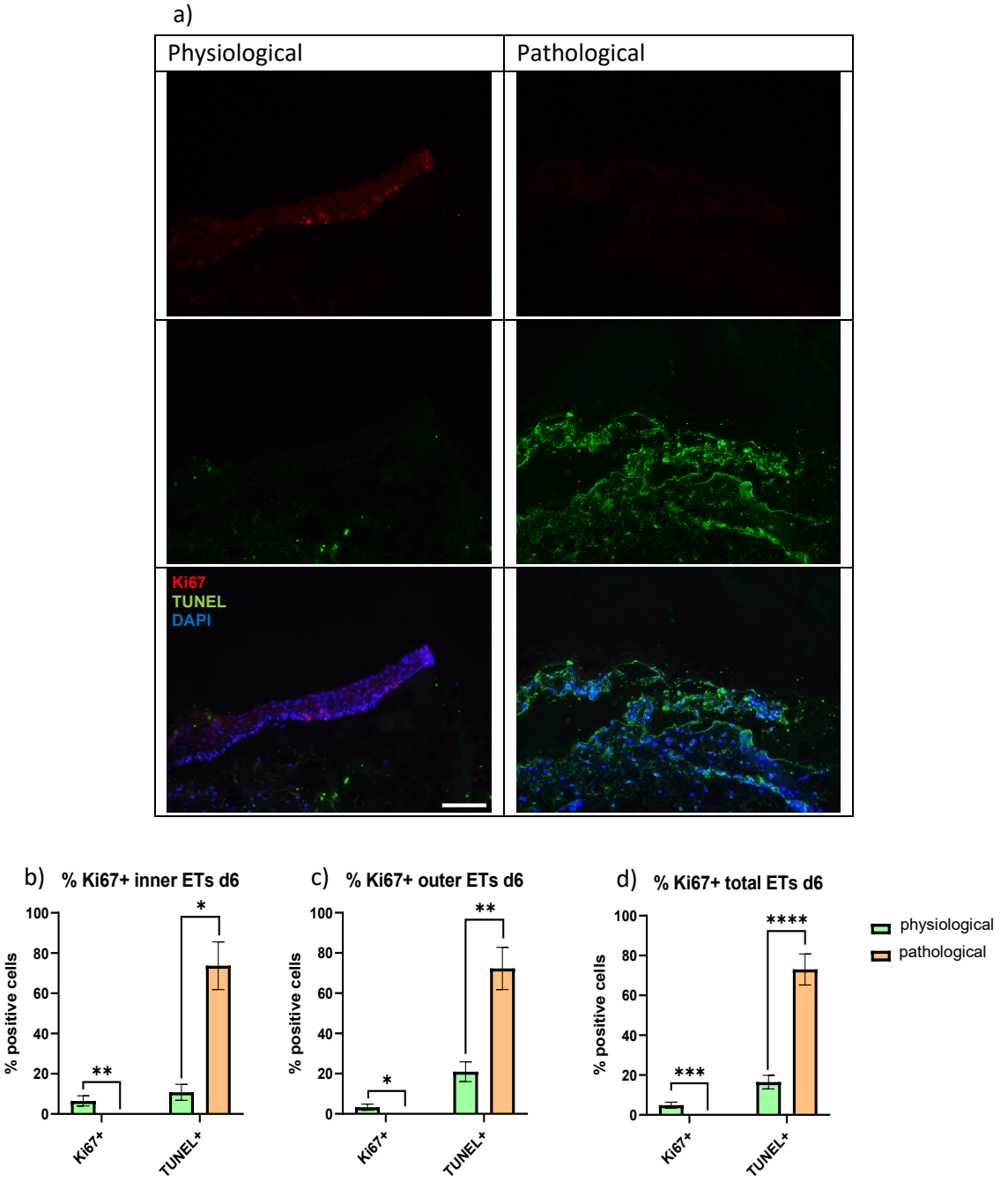

Figure 4.62: Comparison of physiological and pathological conditions on the KiTUNEL expression in the wound healing organ culture model

Shown here is the KiTUNEL staining of wounds under physiological and pathological conditions. Pathological conditions include withdrawl of insulin, hypoxia (5 % oxygen), 10 µM hydrogen peoxide and high levels of D-Glucose (138.8 mM). Both, physiological and pathological wounds were treated with 0.1 % dimethyl sulfoxide (DMSO). Proliferating cells express Ki67 (Ki67+). TUNEL denotes apoptotic cells. a) Exemplary immunofluorescence pictures of the epithelial tongues. Scale bar = 100 µm. b) Percentage of positive cells in the inner ETs (n = 3, 2-4 ETs/wound), c) percentage of positive cells in the outer ETs (n = 3, 2-4 ETs /wound), d) percentage of positive cells in the total ETs (n = 3,2-4 ETs /wound). Data is shown as mean ± standard error of the mean. For statistical analysis one-way ANOVA with Turkey's multiple comparison and t-test (Ki67+ cells of the inner and total ETs) or Kruskal-Wallis test with Dunn's multiple comparison and Mann-Whitney (Ki67+ cells of the outer ETs, all TUNEL evaluation) was performed. * $p < 0.05$, ** $p < 0.01$, *** $p < 0.001$, **** $p < 0.0001$.

4.12.6 The cortactin expression is decreased in epithelial tongues under pathological conditions

Figure 4.63 shows exemplary pictures of ETs treated with 0.1 % DMSO under physiological and pathological conditions. In the physiological wounds a clear cortactin expression is visible in the entire ETs, while the epidermis in the pathological wounds only shows some cortactin expression in the basal layer. This finding further underlies that migration of keratinocytes was severely impaired under pathological conditions.

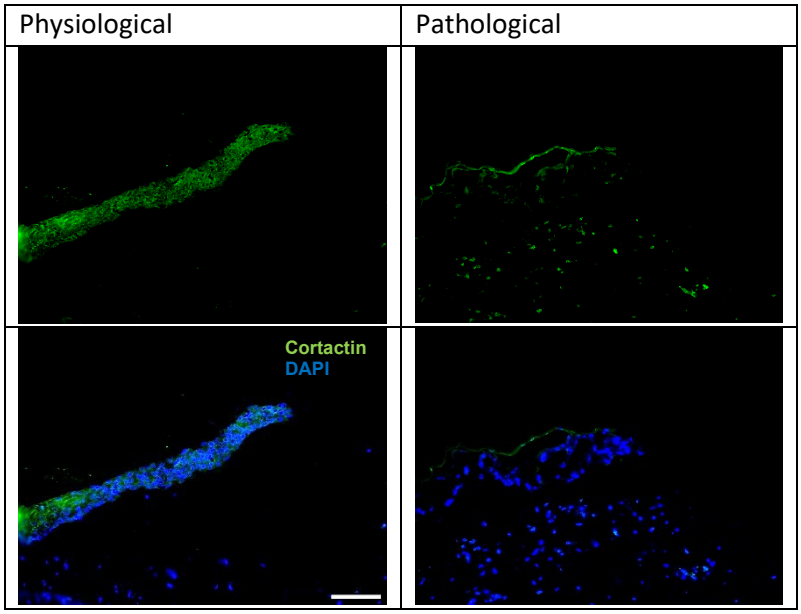

Figure 4.63: Comparison of physiological and pathological conditions on the cortactin expression in the wound healing organ culture model

Shown here is the cortactin staining of wounds under physiological and pathological conditions. Pathological conditions include withdrawl of insulin, hypoxia (5 % oxygen), 10 µM hydrogen peoxide and high levels of D-Glucose (138.8 mM). Both, physiological and pathological wounds were treated with 0.1 % dimethyl sulfoxide (DMSO). Depicted are exemplary immunofluorescence pictures of the epithelial tongues. Scale bar = 100 µm

Looking at all the results, clearly the pathological conditions were too harsh to assess if any of the tested substances had a positive effect on the pathological wounds.

4.13 Wounds cultured for 3 days under the tested pathological conditions did not heal in the *ex vivo* wound healing organ culture model

As the previous chapter clearly showed, the pathological conditions were too harsh to assess whether S1180 might aid wound healing in this setup. As Post *et. al* only incubated the skin for 3 days (Post *et al.*, 2021), in this chapter an exemplary culture of 3 instead of 6 days length was performed using the same conditions as described in **Chapter 4.12**.

4.13.1 Top-view microscopy revealed that the pathological wounds did not show any signs of wound healing

First the top-view microscopy was evaluated (**Figure 4.64)**. While not as pronounced as with the 6 days culture, 3 days under pathological conditions seemed to be enough for the wounds to show signs of degradation, though the discoloration was less pronounced than after 6 days (compare **Figure 4.59** from **Chapter 4.12** and **Figure 4.64a**). On the other hand, the physiological wounds showed clear signs of healing, such as newly formed, opaque epidermis. The healing was observable to a lesser extent than at day 6, which was to be expected.

Figure 4.64b shows the relative top-view wound area of physiological and pathological after 3 days of incubation. For most, but not all conditions, the pathological wounds had a larger relative area here. Pathological wounds treated with the vehicle control had a relative area of 66.85 %, while the respective physiological wounds only had a relative area of 45.14 %. Treatment with 10 µM SG however resulted in a relative area of 53.77 % in pathological wound but 67.08 % in physiological wounds. Physiological wounds treated with 100 nM T4 had the largest relative area of all wounds here, namely 101.92 %. The respective pathological wounds were smaller, but with a value of 73.23 % still had the largest relative area of all pathological wounds. For both concentrations of S1180 tested here, physiological wounds were smaller than pathological wounds: physiological wounds treated with 1 µM S1180 had a relative area of 50.46 %, pathological wounds of 65.66 %, and treatment with 10 µM S1180 led to a relative area of 36.66 % in physiological wounds and 59.95 % in pathological wounds.
For the physiological wounds only treatment with 10 µM S1180 resulted in a smaller relative top-view wound area than the vehicle control. For the pathological wounds, all conditions resulted in a smaller relative top-view area than the vehicle control except for 100 nM T4.

Figure 4.64c shows the relative top-view wound perimeter. The relative wound perimeter after treatment with the vehicle control 0.1 % DMSO was 72.01 % in physiological wounds and 83.87 % in pathological wounds. Only treatment with 10 µM SG led to a larger relative perimeter in physiological wounds than in pathological wounds, though the difference was slight (85.97 % vs. 82.28 %). The difference in relative perimeter also was comparably small after treatment with 100 nM T4: 81.62 % for physiological wounds and 85.96 % for pathological wounds. Treatment with both concentrations of S1180 resulted in a smaller perimeter in physiological wounds than in pathological wounds. The relative perimeter of wounds treated with 1 µM S1180 was 72.14 % in physiological wounds and 87.02 % in pathological wounds. Physiological wounds treated with 10 µM S1180 had the smallest perimeter of all, namely 67.48 %, while the respective pathological wounds have a perimeter of 81.04 %.

As with the area, in physiological wounds only treatment with 10 µM S1180 resulted in a smaller relative top-view wound perimeter than the vehicle control. The differences between the different treatments were rather slight in the pathological wounds (differed by about 6 % maximum).

Unfortunately, the OCT was not available for this culture. As only one culture was performed, no statistical analysis was possible.

a)

Physiological	0.1 % DMSO	10 µM SG	100 nM T4	1 µM S1180	10 µM S1180
Day 0	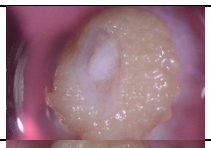	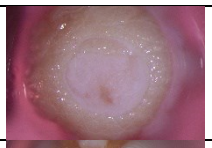			
Day 3					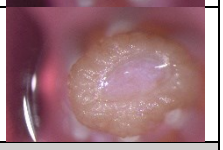
Patho-logical	0.1 % DMSO	10 µM SG	100 nM T4	1 µM S1180	10 µM S1180
Day 0	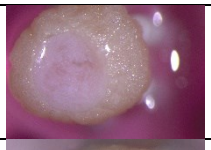	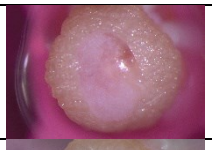	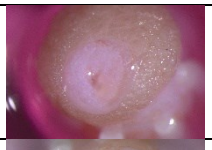	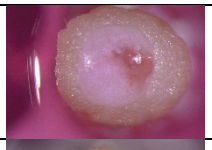	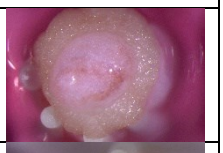
Day 3	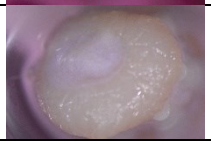	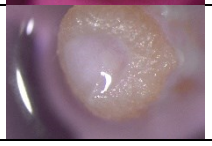	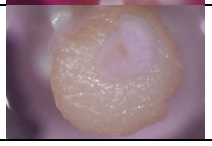	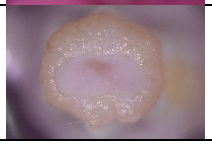	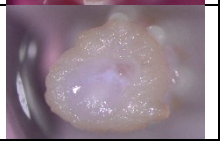

b)

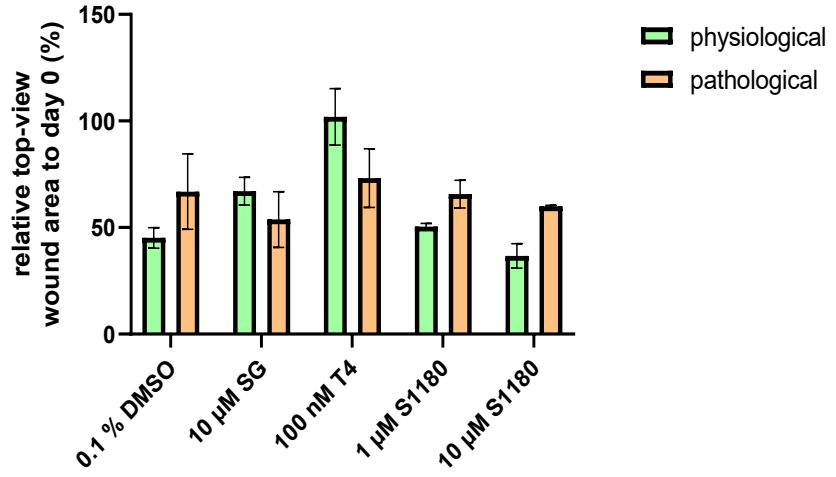

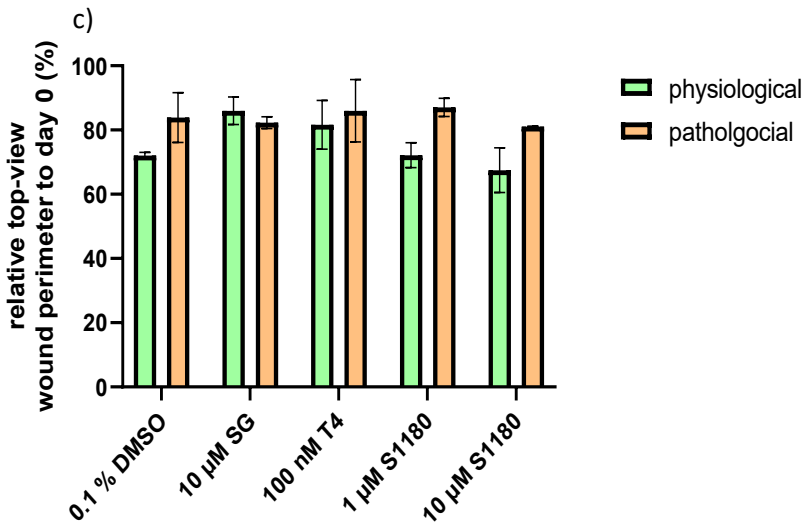

Figure 4.64: Comparison of physiological and pathological conditions on the *ex vivo* top-view wound healing in the 3-day wound healing organ culture model.
Shown here is the top-view wound healing of skin under physiological and pathological conditions. Pathological conditions include withdrawl of insulin, hypoxia (5 % oxygen), 10 mM hydrogen peoxide and high levels of D-Glucose (138.8 mM). Both physiological and pathological wounds were treated with 0.1 % dimethyl sulfoxide (DMSO), 10 µM sodium gualenate (SG), 100 nM L-thyroxine (T4), 1 µM S1180, or 10 µM S1180 at day 1 for 24 hours. The total incubation time was 3 days. a) Exemplary pictures of physiological and pathological wounds at day 0 and day 3. Relative top-view wound b) area and c) perimeter at day 3 (n = 1, 2-4 wounds/condition). Data is depicted as mean ± standard error of the mean. Statisitcal analysis was not possible because only one biological replicate was performed.

4.13.2 Hematoxylin and eosin evaluation shows that the epidermis of the pathological wounds formed no epithelial tongues, while the physiological wounds showed clear signs of healing

Figure 4.65 shows the evaluation of the H&E staining. The exemplary pictures in **Figure 4.65a** illustrate that the pathological wounds barely healed and that no new ETs were formed, while the physiological wounds healed nicely.

Figure 4.65b shows the microscopic wound area. Under most treatments the pathological wounds were larger than the physiological wounds. Treatment with 0.1 % DMSO led to a microscopic area of 75,661 µm^2 in physiological wounds and 136,741 µm^2 in pathological wounds. The microscopic wound area after treatment with 10 µM SG was 103.547 µm^2 in physiological wounds and 219,723 µm^2 in pathological wounds. The extremely large wound area of 927,038 µm^2 of pathological wounds treated with 100 nM T4 was striking, their respective physiological wounds had a microscopic area of 146,516 µm^2. Physiological wounds treated with 1 µM S1180 were smaller than the pathological wounds (191,196 µm^2 compared to 142,724 µm^2). After treatment with 10 µM S1180 on the other hand the physiological wounds (131,961 µm^2) were smaller than the pathological wounds (291,929µm^2).
The physiological wounds treated with the vehicle control were smaller than all other physiological wounds.

Figure 4.65c shows the microscopic wound diameter. Treatment with 0.1 % DMSO resulted in a diameter of 1,684.38 µm in physiological wounds and of 2,121.95 µm in pathological wounds. After treatment with 10 µM SG however, the physiological wounds had a larger diameter than the

pathological wounds (1,562.11 µm vs. 971.57 µm). The same is true after treatment with 100 nM T4: here, the physiological wounds had a diameter of 2,382.13 µm and the pathological wounds of 1,443.58 µm. The wound diameter of physiological wounds treated with 1 µM S1180 was 1,260.38 µm and that of pathological wounds was 1,972.81 µm. Physiological wounds treated with 10 µM S1180 had a wound diameter of 1,303.60 µm and the respective pathological wounds had a diameter of 2854.67 µm.
Only physiological wounds treated with 100 nM T4 had a larger perimeter than those treated with the vehicle control. For the pathological wounds this is true for 10 µM S1180.

Figures 4.65d-g show the area of the ETs. In **Figure 4.65d** the inner ETs' area is depicted. It is striking, that none of the pathological conditions showed any inner ETs at all, while the physiological wounds had clearly measurable inner ETs. After treatment with the vehicle control their area was 33,237 µm^2, after treatment with the positive control 25,257 µm^2. Physiological wounds treated with 100 nM T4 had an inner ETs' area of 30,681 µm^2. Treatment with 1 µM S1180 led to an inner ETs area of 18,774 µm^2 and with 10 µM S1180 to an area of 22,688 µm^2.
After normalization (**Figure 4.65g**) still treatment with the vehicle control resulted in the largest inner ETs (21.71 µm). The area of the inner ETs of the physiological wounds treated with 10 µM SG was 16.93 µm, in those treated with 100 nM T4 12.90 µm. Inner ETs treated with 1 µM S1180 had a normalized area of 17.28 µm and those treated with 10 µM S1180 17.38 µm.
Figure 4.65e shows the area of the outer ETs. Here also, barely any ETs were present in the pathological wounds. In the physiological wounds 100 nM T4 resulted in the smallest outer ETs (12,241 µm^2), followed by 0.1 % DMSO (20,446 µm^2), 10 µM SG (22,349 µm^2), 1 µM S1180 (33,673 µm^2), and 10 µM S1180 (43413 µm^2).
The area of the total ETs can be found in **Figure 4.65f**. As before, the pathological wound basically had no ETs. Treatment with 100 nM T4 resulted in the smallest total ETs in the physiological wounds, namely 21,461 µm^2. Physiological wounds treated with the vehicle control 0.1 % DMSO had a total ETs area of 25,928 µm^2 and those treated with the positive control 10 µM SG 23,803 µm^2. Total ETs of the physiological wounds treated with 1 µM S1180 had an area of 26,223 µm^2. Treatment with 10 µM S1180 resulted in the largest total ETs in the physiological wounds, namely 32,360 µm^2.

Figures 4.65h-k show the length of the ETs. The length of the inner ETs can be found in **Figure 4.65h**. Corresponding to the inner ETs' area, the pathological wounds did barely show any inner ETs length, unlike the physiological wounds. The physiological wounds treated with the vehicle control had the longest inner ETs (538.96 µm), followed by 100 nM T4 (487.71 µm), and 10 µM SG (390.24 µm). Treatment with 1 µM S1180 and 10 µM S1180 resulted in almost the same inner ETs length in physiological wounds, namely 334.52 µm for 1 µM S1180 and 337.42 µm for 10 µM S1180.
Figure 4.65k shows the normalized length of the inner ETs. Still treatment with 0.1 % DMSO resulted in the largest normalized length in physiological wounds, namely 0.34, but now treatment with 100 nM T4 had the shortest normalized inner ETs (0.21). Treatment with 1 µM S1180 resulted in a normalized inner ETs length in physiological wounds of 0.32, treatment with 10 µM SG in a normalized length of 0.27 and treatment with 10 µM S1180 in a normalized length of 0.26.
The outer ETs were again basically absent in pathological wounds as described before. Treatment with 10 µM S1180 resulted in the longest outer ETs in the physiological wounds, namely 588.48 µm, followed by those treated with 1 µM S1180, namely 556.29 µm (compare **Figure 4.65i**). Physiological wounds treated with 0.1 % DMSO had an outer ETs' length of 318.19 µm, those treated with 10 µM SG had a length of 273.02 µm, and those treated with 100 nM T4 of 277.03 µm.
Figure 4.65j shows the total ETs' length. Again, the pathological wounds showed barely any ETs. Those physiological wounds treated with 1 µM S1180 and 10 µM S1180had the longest ETs

(445.40 µm for 1 µM S1180 and 445.02 µm for 10 µM S1180), followed by 0.1 % DMSSO (412.80 µm). Treatment with 10 µM SG resulted in an outer ETs' length of 335.53 µm in physiological wounds and treatment with 100 nM T4 to a length of 382.37 µm.

The H&E staining and evaluation clearly showed how strongly the pathological conditions inhibit the growth of new ETs and thus the wound healing.
The positive effect of S1180 was not as pronounced as in **Chapter 4.8**, but did show e.g. in the longer ETs. However, a statistical analysis was not possible as this experiment was only performed once.

a)

Physio-logical	0.1 % DMSO	10 µM SG	100 nM T4	1 µM S1180	10 µM S1180
Wound	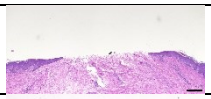	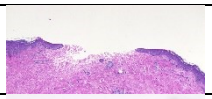	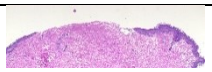	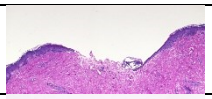	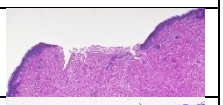
ET	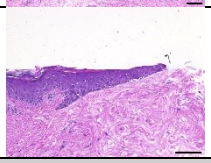	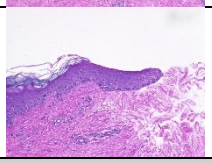	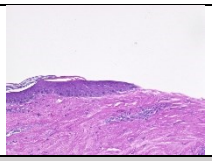	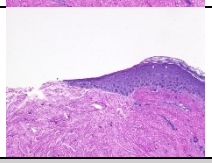	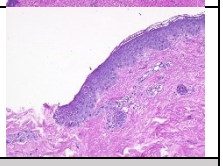
Patho-logical	**0.1 % DMSO**	**10 µM SG**	**100 nM T4**	**1 µM S1180**	**10 µM S1180**
Wound	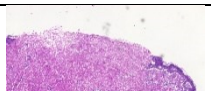	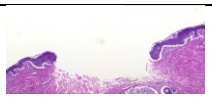	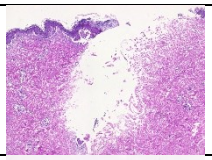	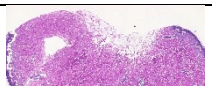	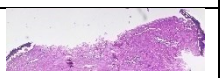
ET	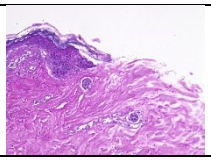	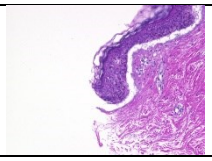	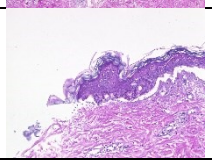	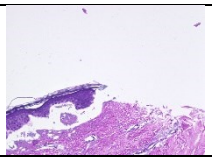	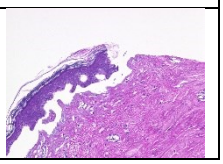

b)

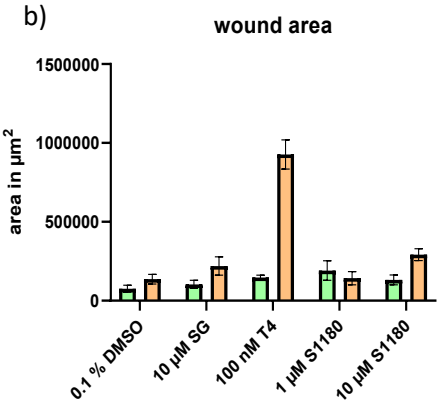

c)

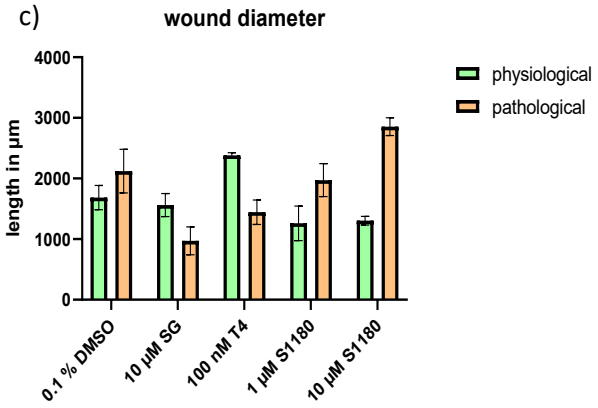

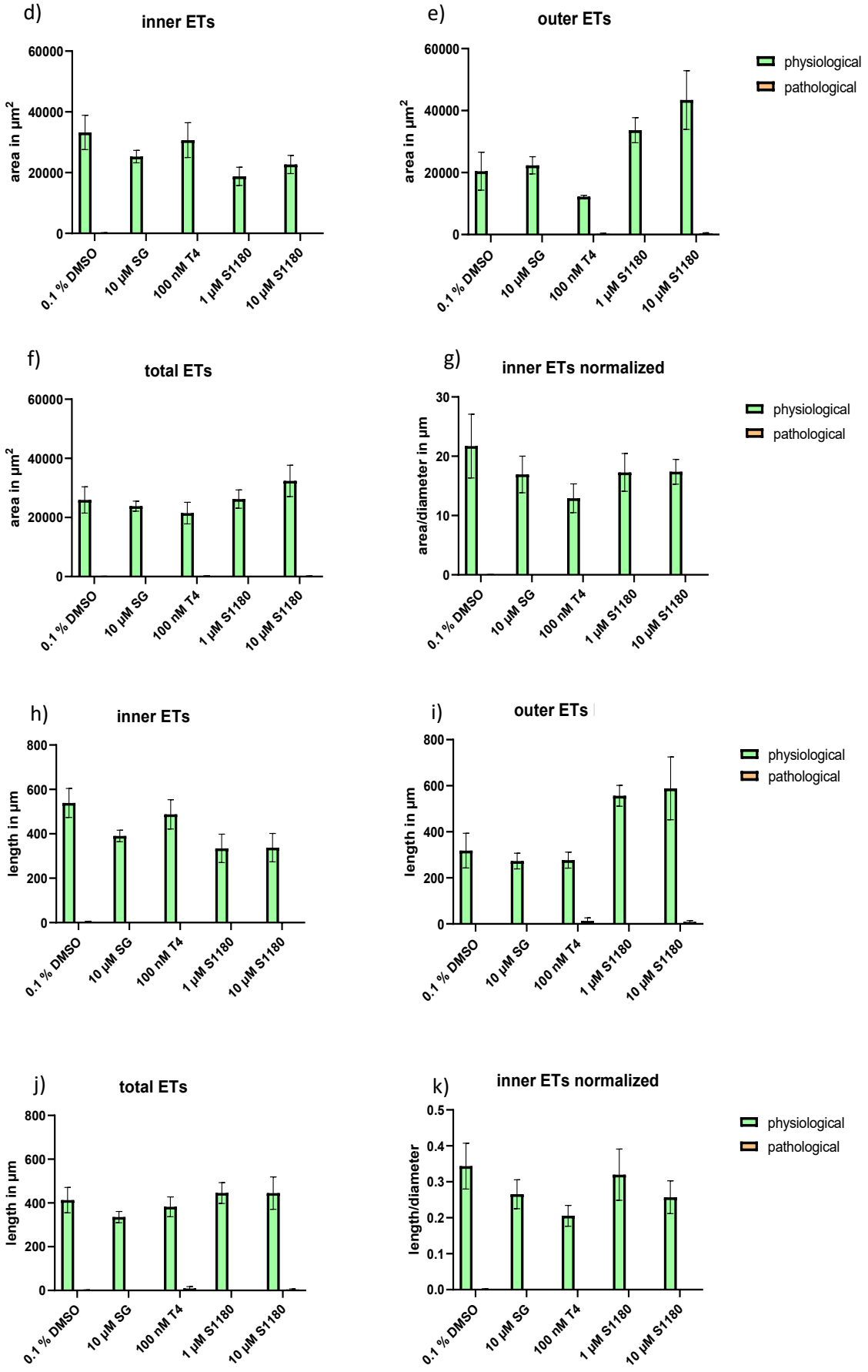
d)
inner ETs
area in µm²
60000
40000
20000
0
0.1 % DMSO
10 µM SG
100 nM T4
1 µM S1180
10 µM S1180
e)
outer ETs
area in µm²
physiological
pathological
f)
total ETs
area in µm²
g)
inner ETs normalized
area/diameter in µm
30
20
10
h)
inner ETs
length in µm
800
600
400
200
i)
outer ETs
j)
total ETs
k)
inner ETs normalized
length/diameter
0.5
0.4
0.3
0.2
0.1
0.0

Figure 4.65: Comparison of physiological and pathological conditions on the *ex vivo* microscopic wound healing in the 3-day wound healing organ culture model.
Shown here is the microscopic wound healing of skin under physiological and pathological conditions in an hematoxylin & eosin staining. Pathological conditions include withdrawl of insulin, hypoxia (5 % oxygen), 10 mM hydrogen peoxide and high levels of D-Glucose (138.8 mM). Both physiological and pathological wounds were treated with 0.1 % dimethyl sulfoxide (DMSO), 10 µM sodium gualenate (SG), 100 nM L-thyroxine (T4), 1 µM S1180, or 10 µM S1180 at day 1 for 24 hours. The total incubation time was 3 days. a) Exemplary pictures of physiological and pathological wounds: shown are the microscopic wounds (scale bar = 200 µm) and epithelial tongues (ETs, scale bar = 100 µm). b) microscopic wound area (n = 1, 1-4 wounds/condition), c) microscopic wound diameter (n = 1, 1-4 wounds/condition), area of the d) inner, e) outer and f) total ETs and g) area of the inner ETs normalized on the respective wound diameter, length of the h) inner, i) outer and j) total ETs, k) length of the inner ETs normalized on the respective wound diameter (n = 1, 4-16 ETs /condition for all ET-figures). Data is depicted as mean + standard error of the mean. Statisitcal analysis was not possible because only one biological replicate was performed.

4.13.3 The cytokeratin 6 expression was lower in pathological wounds than in physiological wounds

Figure 4.66 shows the results of the CK 6 staining. Already the exemplary pictures in **Figure 4.66a** illustrate, that the CK 6 expression is diminished in the pathological wounds.

Figure 4.66b shows the relative CK 6 expression in the inner ETs. The data was normalized on the physiological wounds treated with 0.1 % DMSO. Pathological wounds treated with 0.1 % DMSO had a relative CK 6 expression of 26.61 %. Physiological wounds treated with 10 µM SG had a relative CK 6 expression of 92.22 %, but pathological wounds had a relative CK 6 expression from 121.99 %, though the error bar was very large. Treatment with 100 nM T4 resulted in a relative CK 6 expression of 76.38 % in physiological wounds and 24.46 % pathological wounds. Only after treatment with 1 µM S1180 was the CK 6 expression in physiological wounds higher than after treatment with the vehicle control, namely 115.68 %, while the respective physiological wounds had a much lower relative CK 6 expression (19.90 %). Inner ETs of physiological wounds treated with 10 µM S1180 had a relative CK 6 expression of 86.48 % and their respective pathological wounds 19.00 %.

Figure 4.66c shows the relative CK 6 expression in the outer ETs. Under all treatment conditions, the CK 6 expression was much higher in physiological wounds than in pathological wounds. Again, the data was normalized on the physiological wounds treated with 0.1 % DMSO. The respective pathological wounds had a relative CK 6 expression of 24.20 %. All physiological wounds had a higher relative CK 6 expression than those treated with 0.1 % DMSO. The relative CK 6 expression of the physiological wounds treated with 10 µM SG was 137.02 %, that of the pathological wounds was 79.24 %, the highest relative CK 6 expression in pathological wounds. Treatment with 100 nM T4 resulted in a relative CK 6 expression of 127.14 % in the outer ETs physiological wounds and 19.59 % in pathological wounds. The outer ETs treated with 1 µM S1180 had a relative CK 6 expression of 171.00 % in physiological wounds and of 27.49 % in pathological wounds. Treatment with 10 µM S1180 led to a relative CK 6 expression of 156.06 % in physiological wounds and 24.20 % in pathological wounds.

Figure 4.66d shows the relative CK 6 expression in the total ETs. The data was again normalized on the physiological wounds treated with 0.1 % DMSO. The total ETs of the pathological wounds treated with 0.1 % DMSO had a relative CK 6 expression of 25.40 %. The total ETs of the pathological wound treated with 10 µM SG had a relative CK 6 expression of 100.61 %. This was close to the physiological wounds treated with 0.1 % DMSO and the highest CK 6 expression in all pathological wounds, though

the high error bar must be kept in mind. Physiological wounds treated with 10 µM SG had a relative CK 6 expression of 114.62 %. Treatment with 100 nM T4 resulted in a relative CK 6 expression of 101.76 % in physiological wounds and 21.21 % in pathological wounds. The total ETs of physiological wounds treated with 1 µM S1180 had the highest relative CK 6 expression of all, namely 143.34 %, while their respective pathological total ETs had a relative CK 6 expression of 23.70 %. Treatment with 10 µM S1180 resulted in a relative CK 6 expression of 121.27 % in physiological wounds and 21.60 % in pathological wounds.

This all clearly demonstrated, that the CK 6 expression was lower in pathological wounds than in physiological wounds.

b)

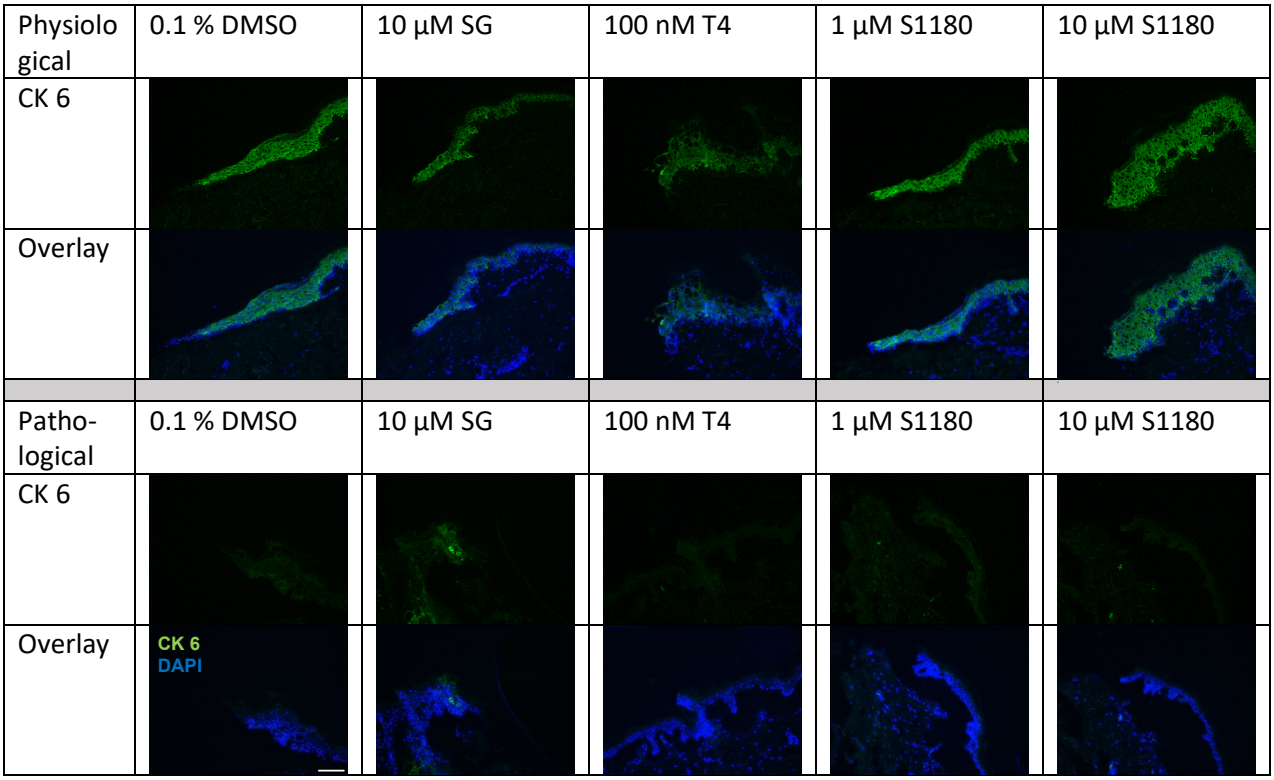

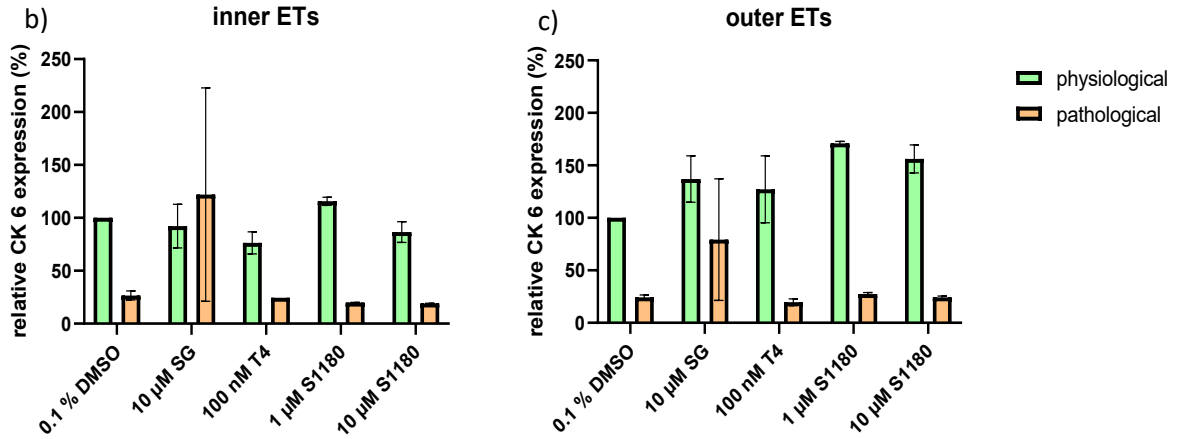

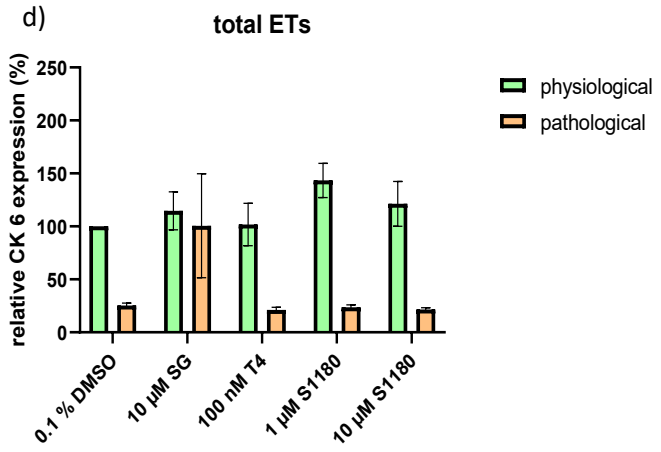

Figure 4.66: Comparison of physiological and pathological conditions on the cytokeratin 6 expression in the 3-day wound healing in the wound healing organ culture model.
Shown here is the cytokeratin 6 (CK 6) expression of wounds under pathological and physiological conditions. Pathological conditions include withdrawl of insulin, hypoxia (5 % oxygen), 10 mM hydrogen peoxide and high levels of D-Glucose (138.8 mM). Both physiological and pathological wounds were treated with 0.1 % dimethyl sulfoxide (DMSO), 10 µM sodium gualenate (SG), 100 nM L-thyroxine (T4), 1 µM S1180, or 10 µM S1180 at day 1 for 24 hours. The total incubation time was 3 days. a) Exemplary immunofluorescence pictures of the ETs, scale bar = 100 µm. CK 6 expression in the inner (b), outer (c) and total (d) ETs. (n = 1, 1-8 ETs/condition). Data is depicted as mean ± standard error of the mean. Statisitcal analysis was not possible because only one biological replicate was performed.

4.68 Not the cell count but the relative CD31 expression was reduced in pathological wounds compared to physiological wounds

Figure 4.67 shows the results of the CD31 staining. Just like the 6 days culture, the intensity of the CD 31 expression was diminished in the pathological wounds after 3 days, as can be seen in **Figure 4.67a**.

The relative CD31 expression in **Figure 4.67b** underlies this finding. The data was normalized on the physiological wounds treated with 0.1 % DMSO and the respective pathological wounds had a relative CD31 expression of 78.49 %. Physiological wounds treated with 10 µM SG had a relative CD31 expression of 86.03 % and the pathological wounds of 77.06 %. Only after treatment with 100 nM T4 was the CD31 expression in pathological wounds higher than in physiological wounds (91.34 % for the pathological and 85.51 % for the physiological wounds). Treatment with 1 µM S1180 had a relative CD31 expression of 92.08 % in physiological wounds and 84.06 % in pathological wounds. Physiological wounds treated with 10 µM S1180 had a relative CD31 expression of 81.81 %, while their respective pathological wounds only had an expression of 64.18 %.

Figure 4.67c shows the number of CD31 positive cells. In all conditions except 10 µM S1180 there were more positive cells found in the pathological wounds than in the physiological wounds. Physiological wounds treated with 0.1 % DMSO had 61.13 positive cells/VF in physiological wounds and 68.86 positive cells/VF in pathological wounds. After treatment with 10 µM SG the difference was more pronounced: 62.00 positive cells/VF in physiological wounds and 110 positive cells/VF in pathological wounds. Treatment with 100 nM T4 led to 47.43 positive cells/VF in physiological wounds and 84.86 positive cells/VF in pathological wounds. Physiological wounds treated with 1 µM S1180 had 71.40 positive cells/VF and pathological wounds 75.67 positive cells/VF. Finally, treatment with 10 µM S1180 resulted in 65.00 positive cells/VF in physiological wounds and 36.83 positive cells/VF in pathological wounds.

Figure 4.67d shows the number of CD31 positive cross sections. Treatment with 0.1 % DMSO resulted in 1.63 positive cross sections/VF in physiological wounds and 0.29 positive cross sections/VF in pathological wounds. Physiological wounds treated with 10 µM SG had 1.67 positive cross sections/VF and pathological wounds 2.43 positive cross sections/VF. Also, after treatment with 100 nM T4 there were more positive cross sections in the pathological wounds than in the physiological wounds (2.00 positive cross sections/VF for pathological wounds and 0.57 positive cross sections/VF for physiological wounds). While there were no positive cross sections in the pathological wounds treated with 1 µM S1180 and few in the physiological wounds (0.20 positive cross sections/VF), after treatment with 10 µM S1180 there were no positive cross sections in the physiological wounds and few in the pathological wounds (0.14 positive cross sections/VF).

The number of CD31 positive vessels can be found in **Figure 4.67e**. Physiological wounds treated with 0.1 % DMSO had 0.75 positive vessels/VF and pathological wounds 0.57 positive vessels/VF. After treatment with 10 µM SG the highest number of vessels of the entire culture could be found in the physiological wounds (2.00 positive vessels/VF) but one of the lowest pathological wounds (0.14 positive vessels/VF). The number of CD31 positive vessels after treatment with 100 nM T4 was 0.71/VF in physiological wounds and 0.29 in pathological wounds. Treatment with 1 µM S1180 led to 0.60 positive vessels/VF in physiological wounds and 0.50 positive vessels/VF in pathological wounds. The number of positive vessels in physiological wounds treated with 10 µM SG was 1.00 and the number of positive vessels in pathological wounds was 0.14.

As the with the CK 6 expression, also the CD31 expression was reduced in pathological wounds. On the other hand, the number of cells and the number of cross sections was higher under some treatment conditions.

a)

Physiological	0.1 % DMSO	10 µM SG	100 nM T4	1 µM S1180	10 µM S1180
CD31	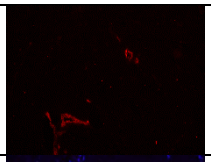	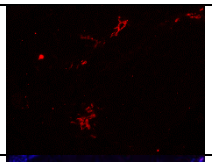	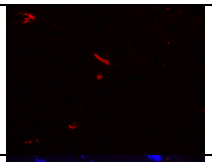	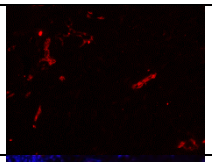	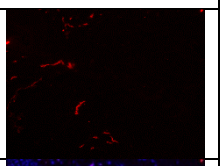
Overlay	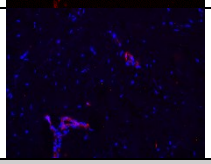	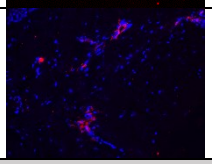	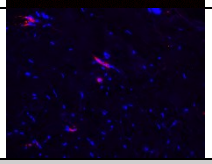	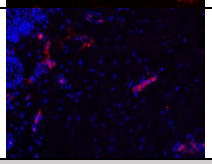	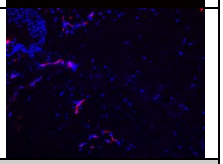
Patho-logical	0.1 % DMSO	10 µM SG	100 nM T4	1 µM S1180	10 µM S1180
CD31	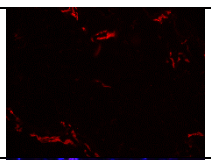	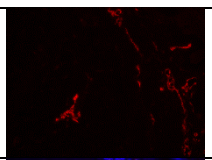	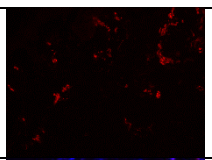	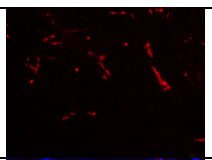	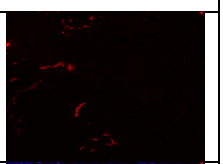
Overlay	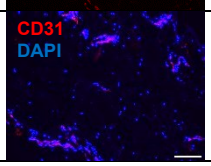	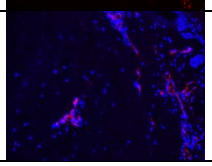	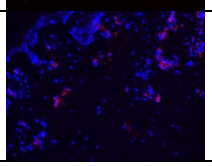	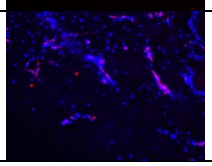	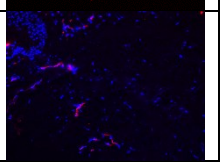

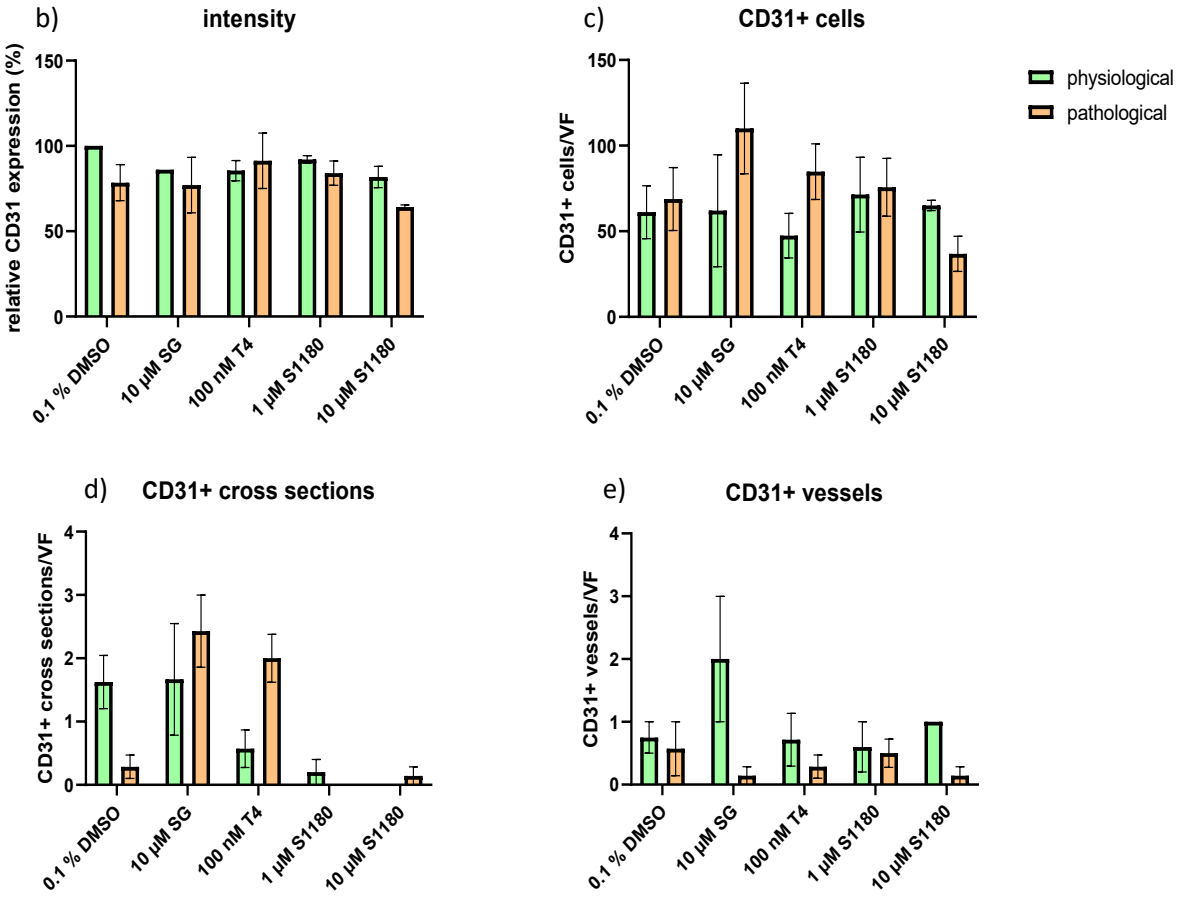

Figure 4.67: Comparison of physiological and pathological conditions on the CD31 expression in the 3-day wound healing organ culture model

Shown here is the CD31 expression of wounds under physiological and pathological conditions. Pathological conditions include withdrawl of insulin, hypoxia (5 % oxygen), 10 mM hydrogen peoxide and high levels of D-Glucose (138.8 mM). Both physiological and pathological wounds were treated with 0.1 % dimethyl sulfoxide (DMSO), 10 µM sodium gualenate (SG), 100 nM L-thyroxine (T4), 1 µM S1180, or 10 µM S1180 at day 1 for 24 hours. The total incubation time was 3 days. a) Exemplary immunofluorescence pictures of the dermis. Scale bar = 100 µm, b) relative CD31 expression, c) number of CD31 positive cells/visual field (VF), d) number of CD31 positive vessels/VF, e) number of CD31 positive cross sections/VF (for all: n = 1, 2-4 VFs/wound). Values are expressed mean + standard error of the mean. Statisitcal analysis was not possible because only one biological replicate was performed.

4.13.5 The epithelial tongues of pathological wounds had less Ki67 positive cells but more TUNEL positive cells than the physiological wounds

Figure 4.68 shows the results of the KiTUNEL staining. Already the exemplary pictures in **Figure 4.68a** illustrate, that just like in the 6 days culture, there were some Ki67 positive cells in the ETs of physiological wounds but none in the ETs of pathological wounds. However, many TUNEL positive cells were found in the pathological wounds.

Figure 4.68b shows the percentage of Ki67 positive and TUNEL positive cells in the inner ETs. While few cells are Ki67 positive in the inner ETs of the physiological wounds (1.06 %), none were positive in the ETs of the pathological wounds. 12.62 % of the cells in the inner ETs of the physiological wounds were TUNEL positive. Under pathological conditions this number increased to 66.07 %.

Figure 4.68c shows the percentage of Ki67 positive and TUNEL positive cells in the outer ETs. 1.77 % of the cells in the outer ETs of physiological wounds were Ki67 positive, while none were positive in

the pathological wounds. In the outer ETs of the physiological wounds 13.76 % of the cells were TUNEL positive, in pathological wounds this percentage increased to 42.86 %.

Figure 4.68d shows the percentage of Ki67 positive and TUNEL positive cells in the total ETs. Again, there were no Ki67 positive cells in the ETs of pathological wounds, but 1.42 % of the cells were Ki67 positive in the physiological wounds. 13.19 % of the cells in the total ETs of the physiological wounds were TUNEL positive and 58.33 % in the ETs of pathological wounds.
So, after 3 days there were some Ki67 positive cells in the ETs of physiological wounds but none in the pathological wounds, while there cleary were more TUNEL positive cells in the pathological wounds compared to the physiological wounds.

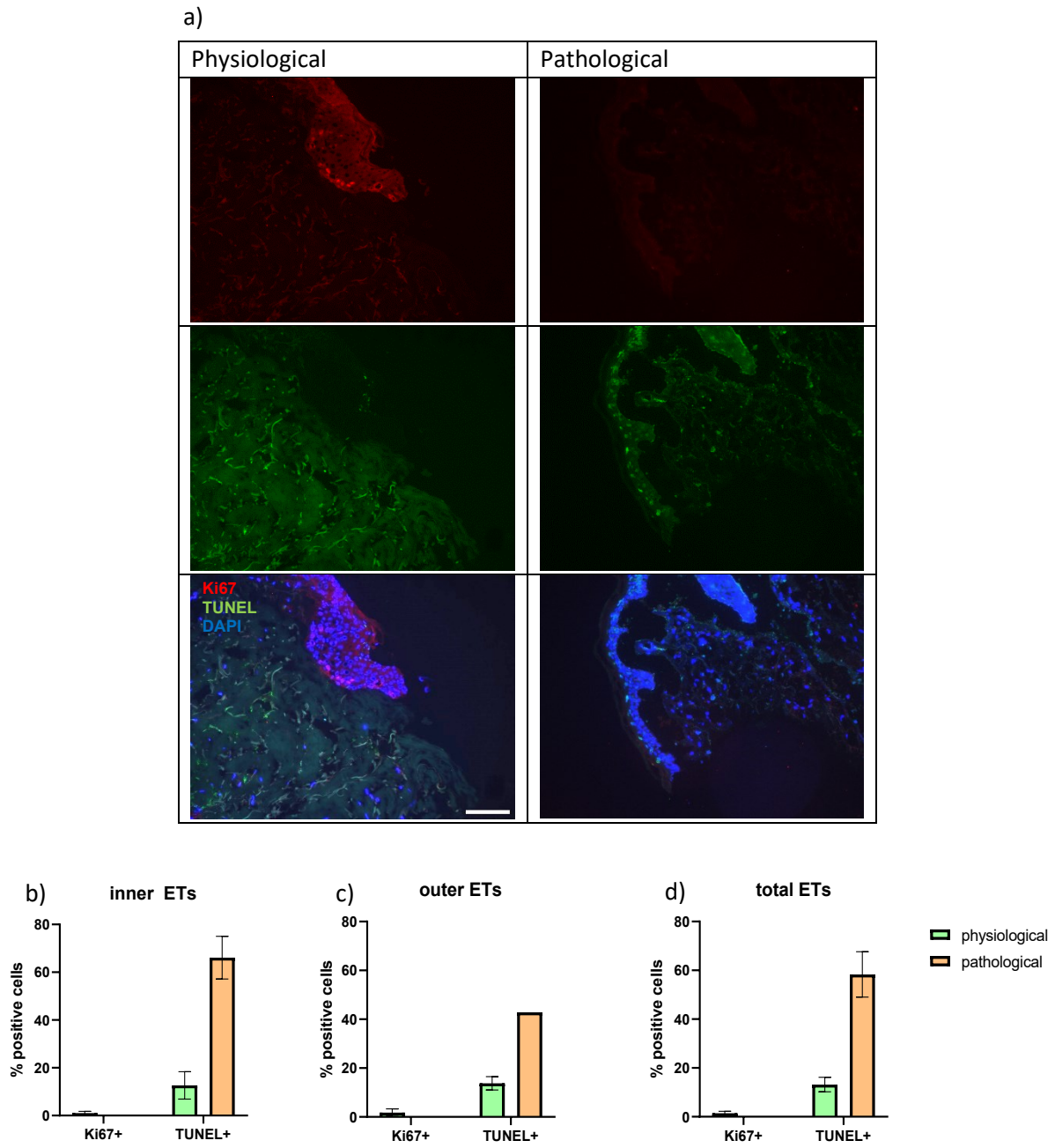

Figure 4.68: Comparison of physiological and pathological conditions on the KiTUNEL expression in the 3-day wound healing organ culture model

Shown here is the KiTUNEL staining of wounds under physiological and pathological conditions. Pathological conditions include withdrawl of insulin, hypoxia (5 % oxygen), 10 µM hydrogen peoxide and high levels of D-Glucose (138.8 mM). Both, physiological and pathological wounds were treated with 0.1 % dimethyl sulfoxide (DMSO). The cultivation time was 3 days. Proliferating cells express Ki67 (Ki67+). TUNEL denotes apoptotic cells. a) Exemplary immunofluorescence pictures of the epithelial tongues (ETs). Scale bar = 100 µm. b) Percentage of positive cells in the inner ETs, c) percentage of positive cells in the outer ETs, d) percentage of positive cells in the total ETs (n = 1, 1-4 ETs/wound). Data is depicted as mean ± standard error of the mean. Statisitcal analysis was not possible because only one biological replicate was performed.

4.13.6 The cortactin expression seems slightly diminished after cultivation for 3 days under pathological conditions

Figure 4.69 shows exemplary ETs of wounds treated with 0.1 % DMSO and incubates for 3 days in physiological or pathological conditions. Both wounds express cortactin, though the expression seems a little less intense and not as evenly distributed under pathological conditions. Moreover, the epidermis was detached and much smaller under pathological conditions.

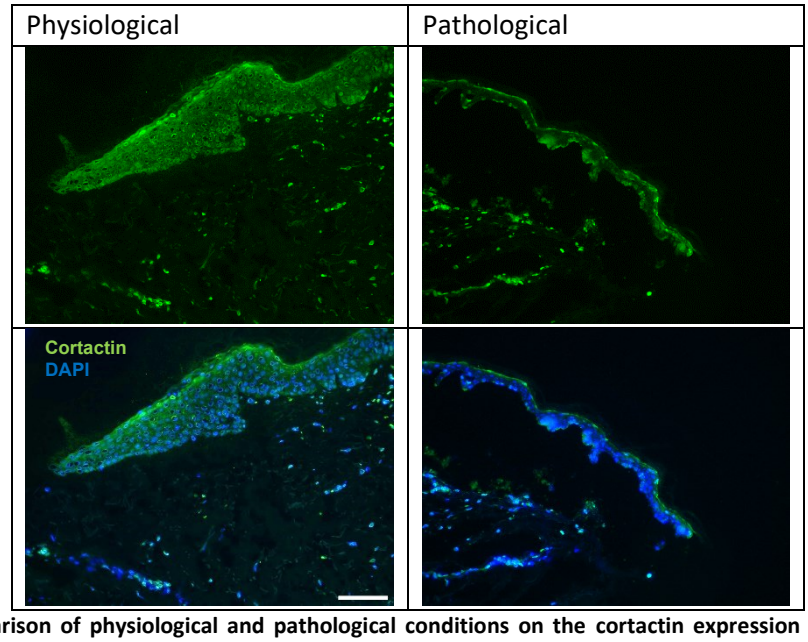

Figure 4.69: Comparison of physiological and pathological conditions on the cortactin expression in the 3-day wound healing organ culture model

Shown here is the cortactin staining of wounds cultivated for 3 days under physiological and pathological conditions. Pathological conditions include withdrawl of insulin, hypoxia (5 % oxygen), 10 mM hydrogen peoxide and high levels of D-Glucose (138.8 mM). Both, physiological and pathological wounds were treated with 0.1 % dimethyl sulfoxide (DMSO). Exemplary immunofluorescence pictures of the epithelial tongues. Scale bar = 100 µm

While the effects were slightly less pronounced, already 3 days under pathological conditions were sufficient to harm the wounds so much that no healing was observable. On the other hand the physiological wounds showed clear signs of wound healing in the *ex vivo* WHOC.

5 Discussion

5.1 General remarks on the wound healing organ culture model

The WHOC is a very powerful tool to study human wound healing. It allows insights into the human skin healing process, which are difficult to achieve by other methods. Furthermore, it is a valuable tool to investigate different treatment methods or drug candidates. The main drawbacks of the WHOC are the limited culturing time – the remodeling phase cannot be studied in its entirety in this model – and its missing blood flow. This also means that there is no clot formation in the WHOC. Still the wounds clearly heal over the course of the culture. The healing cascade is probably started by the remaining blood cells. Moreover, it is possible to study the role of resident immune cells in a WHOC model (Gherardini *et al.*, 2020; Sturmheit *et al.*, n.d.).
Advantages and limitations of the WHOC models in more details as well as advantages and drawbacks of all its evaluation parameters can be found in **Table 5.1**. Just like many models, the evaluation parameters of the WHOC model have specific limitations that need to be considered when assessing them. In evaluating as many parameters as possible, a good and reliable picture of the wound healing process of the respective WHOC can be gained.

When conducting a Pubmed search for "wound healing organ culture" one notices that organ cultures for corneal wound healing are very commonly used. There are fewer publications available on WHOCs for human skin healing, but it still an often-used tool (https://pubmed.ncbi.nlm.nih.gov/?term=wound+healing+organ+culture, last used July 21, 2023).
The idea of studying wound healing in an *ex vivo* fashion is not new. Bhora *et al.* published a paper using *ex vivo* human skin to study the effects of specific growth factors on epithelialization in 1995 (Bhora *et al.*, 1995). Moll *et al.* and Kratz both introduced versions of the punch-in-a-punch approach or "donut model" used in this work as well in 1998 or 1999 respectively (Kratz, 1998; Moll *et al.*, 1999). These models have been used and refined over the next decades. Still, there is no standardized model regarding punch and wound size, medium used, cultivation period and other parameters. A majority of papers seems to be based on the model of Moll *et al.*, thus using a 6 mm outer punch and a 3 mm inner punch as a wound (Moll, 2003; Moll *et al.*, 1999). The WHOC of this work is in line with those of Meier *et al.,* Liao *et al.*, and Sturmheit *et al.* (Liao *et al.*, 2019; Meier *et al.*, 2013; Sturmheit *et al.*, n.d.). Thus, here a 2 mm wound was set into a 4 mm biopsy. While more challenging in the making, the smaller size of the punches has two advantages: As the amount of skin available can be very limited, smaller punches allow to produce more wounds. This makes a higher number of technical replicates or more different experiments at the same time possible. The second benefit we assume is that complete diffusion of the culture medium and all the vital nutrients in it is easier achieved in a smaller punch. As the WHOC model has no blood flow, the nourishment of the skin cells can only be achieved by this diffusion of the culture medium.
Concerning the culture medium: a lot of the WHOC models were conducted in Dulbeccos Modified Eagle Medium (DMEM) with up to 10 % fetal bovine serum (FBS) (Chan *et al.*, 2008; Kratz, 1998; Moll, 2003). Mendoza-Garcia *et al.* compared different culture media and found DMEM with FBS to promote *ex vivo* wound healing best, with WEM with FBS also performing very well (Mendoza-Garcia *et al.*, 2015). While FBS is a very important and often crucial component to keep cells and tissue viable in culture, its exact composition is not yet known and may also differ from batch to batch. This makes standardization of a model using FBS difficult. Also, for most cells and organs serum is no physiological fluid and it can contain substances that act inhibitory or even cytotoxic on cells and tissues. Even though the serum is produced sterile, it can still introduce microorganism into the culture. FBS prices and availability differ strongly on the global market. All this can be prevented

when a switch to a serum-free medium is possible (Barosova *et al.*, 2021; Gstraunthaler & Lindl, 2021; Liu *et al.*, 2023).

Serum-free culture medium allows work under chemically defined conditions, which are exactly reproducible. If cellular products or secretions are of interest, here no FBS interferes with their isolation or measurement. Moreover, the WHOC model can at least for some questions serve as an alternative to animal models. In these cases, it would be good to perform it without FBS, to be completely animal free, to prevent animal suffering (Gstraunthaler & Lindl, 2021; Liu *et al.*, 2023).

Kleszczynski and Fischer established a serum-free human skin organ culture. By using WEM supplemented with L-Glutamin, hydrocortisone, human insulin and antibiotics they cultured human skin successfully for up to 5 days (Kleszcyński & Fischer, 2012). Gherandini *et al.* described in their instruction of how to perform a WHOC, that a culturing period up to 10 days is feasible when using WEM with the supplements described above. However, they recommend a culturing period of no more than 7 days to avoid a falsification of results due to skin decay (Gherardini *et al.*, 2020). This finding is in line with the culturing period used by Meier *et al.,* Liao and Lehmann *et al.,* and Sturmheit *et al* and in this work (Liao *et al.*, 2019; Meier *et al.*, 2013; Sturmheit *et al.*, n.d.). A shorter culturing period is of course also feasible. A literature search showed that many authors found a 6- to 7-days culture suited their research question best (Brandner *et al.*, 2004; Chan *et al.*, 2008; Gherardini *et al.*, 2020; Moll, 2003; Tomic-Canic *et al.*, 2007).

The WHOCs also differ regarding the anatomical region the donated skin originated from. The earlier publications used skin that was relatively close (about 2 cm away) from a cyst or something similar, when this skin structure was surgically removed (Moll, 2003; Moll *et al.*, 1999). Later publications, as did this work, utilized skin donations after elective surgery (Liao *et al.*, 2019; Meier *et al.*, 2013; Mendoza-Garcia *et al.*, 2015; Sturmheit *et al.*, n.d.; Y. Wang *et al.*, 2016). This skin was mostly abdominal and breast skin (Kratz, 1998; Langan *et al.*, 2018; Liao *et al.*, 2019; Nasir *et al.*, 2018; Y. Wang *et al.*, 2016), though also facelift was often used for example by Sturmheit *et al.* (Sturmheit *et al.*, n.d.). The skin used in these studies was mainly from female donors and often derived from plastic surgeries (Glinos *et al.*, 2017; Liao *et al.*, 2019; Meier *et al.*, 2013; Mendoza-Garcia *et al.*, 2015; Sturmheit *et al.*, n.d.).

Most of the wounds were set by a punch biopsy of different sizes, though some paper also used a scalpel to cut the wound. The wound depth was often only roughly defined as punching into the papillary dermis (Gherardini *et al.*, 2020; Liao *et al.*, 2019; Mendoza-Garcia *et al.*, 2015). Some authors, like Meier *et al*. made full thickness wounds (Meier *et al.*, 2013). Sturmheit *et al.* defined the wound depth by using an argon fluoride laser, which ablated the skin to a defined depth of 600 µm (Sturmheit *et al.*, n.d.). This is a very elegant approach to standardize the WHOC. However, I found that lasering a wound takes at least 9 minutes. For a large-scale screening as done in this work, this is much too long. It would have also been difficult to keep the freshly lasered wounds viable, while lasering the rest as there was no incubator available in close proximity to the laser. That is why the spacer was developed together with Dr. Thomsen in this work. It is not as precise as lasering but placing it onto a 2 mm biopsy punch results in a more standardized wound depth.

Throughout most of the papers and also in this work, the skin was incubated at 37 °C and 5 % CO_2 with medium changes done daily or every other day (Balaji *et al.*, 2015; Gherardini *et al.*, 2020; Ojeh *et al.*, 2016; Sturmheit *et al.*, n.d.; Y. Wang *et al.*, 2016).

To bring the WHOC closer to the *in vivo* situation it is important to culture the epidermis of the human skin at the air-liquid interface. In the human body, the epidermis of the skin is in constant contact with air. This contact is an important stimulant for correct differentiation of the epidermal layers and for cornification (Bernstam *et al.*, 1986; Glinos *et al.*, 2017). Many authors cultivate their skin punches at air-liquid interface. To ensure the epidermis stays at this interface and that the punches do not topple over, different techniques were introduced, e.g. placing the skin on sterile

gauze, placing the skin into a trans-well insert, or embedding part of the dermis in rats tail collagen (Balaji *et al.*, 2015; Gherardini *et al.*, 2020; Mendoza-Garcia *et al.*, 2015; Moll, 2003). Sturmheit *et al.* introduced an especially elegant idea: they designed retainers, which would hold the skin in place and ensure it is cultivated at the air-liquid interface (Sturmheit *et al.*, n.d.). In this work, in cooperation with Dr. Thomsen we developed a new set of retainers, which are autoclavable and thus easily reusable.
Another crucial question when designing an *ex vivo* wound healing study on human skin is whether to keep the subcutaneous fat or remove this tissue and only cultivate dermis and epidermis. In last years more and more was learned about the importance of adipose tissue also in wound healing (Ahmadi *et al.*, 2020; Eming *et al.*, 2014; Glinos *et al.*, 2017; Hassan *et al.*, 2014). For example, Guo et al. found that stem cells derived from adipose tissue can aid wound healing in a WHOC model (Guo & DiPietro, 2010). Thus, it is probably advisable to keep all three layers of the skin when setting up a WHOC model. In these full thickness skin models, it might still be necessary to trim some of the excess fat, which can easily take up multiple centimeters.
The different WHOC systems were used to address a multitude of different scientific questions regarding human wound healing. Different treatment regimes – such as cellular therapies or addition of chemicals into the culturing medium and/or directly into the wounds – were studied often (Gherardini *et al.*, 2020; Glinos *et al.*, 2017; Liao *et al.*, 2019; Meier *et al.*, 2013; Tomic-Canic *et al.*, 2007). WHOCs can also be used to study wound infections by adding e.g. bacteria (Yoon et al., 2019) or pathological wound healing (Post *et al.*, 2021).
The WHOC model of this work consists out of 2 mm wide and ca. 500 μm^2 deep circular wounds in a 4 mm wide punch biopsy. They are cultivated in specifically designed retainers in WEM with the above-mentioned supplements for up to 8 days at 37 C and 5 % CO_2. Human skin – predominantly female abdominal and breast – from plastic surgeries was used.

There are many different parameters that can be studied while and after performing a WHOC. This broad variety of information out of one experiment makes the WHOC a very valuable tool. During the culture, the top-view wound area and perimeter can be assessed by top-view microscopy. OCT allows non-invasive wound volume measurement at multiple time points of the culture. The culture supernatant can be used for different assays, for example the LDH assay. After the culture is performed, the wounds can be embedded in different ways or snap-frozen for molecular analysis. In this work, I focused on the evaluation of during the culture and different stainings at the end of the culture. To get a concise impression of the wounds, I decided to take slides at different wound depths and averaging e.g. the microscopic wound area instead of just looking at one wound depth.

From the WHOCs performed in this study, 7 days proved to be a satisfactory culturing period. Though the changes from day 6 to day 7 were relatively small, a progression of healing was still visible. A much longer culturing period is not recommended, due to the rising LDH-levels and the deceleration of the healing process. On the other hand, a shorter culturing period could be of interest, if specifically the very early stages of wound healing should be studied.

On the following pages the findings of **Chapter 4** will be further discussed.

Table 5.1: Advantages and limitations of the wound healing organ culture (WHOC) model and different evaluation parameters of the WHOC

WHOC = wound healing organ culture, OCT = optical coherence tomography, LDH = lactate dehydrogenase, H&E = hematoxylin and eosin, ETs = epithelial tongues, CK = cytokeratin

	Advantages	Limitations
Ex vivo WHOC model in general	The WHOC uses **human material**, which makes the data more easily transferable and comparable to clinical findings.	
	The **high donor-to-donor variation** (humans are not genetically identical) reflects the reality and ensures that findings are later relevant in e.g. the clinics.	**High donor-to-donor variation,** not only regarding the reaction to a certain treatment but also regarding the general wound healing rate. This makes it more difficult to make a scientific sound and reliable statement.
	In the WHOC an **entire organ**, namely the skin consisting out of epidermis, dermis, and subcutis, is studied. This allows unique insights on the complex cellular network being active in wound healing. Moreover, the WHOC is well suited for studies of resident macrophages and other resident immune cells (Sturmheit *et al.*, n.d.).	In the WHOC **no circulating blood and immune cells** are present, which of course differs strongly from the situation *in vivo.* Circulating blood and immune cells are especially important in the inflammation phase of wound healing, which cannot be studied in full extent in the WHOC. On the other hand, already in 1996 Lukas *et al.* could show that dendritic cells travel through lymphatic vessels in an *ex vivo* human skin organ culture (Lukas *et al.*, 1996), so studying of the vasculature is possible, but limited.
	For **finding a treatment that aids "troubled" wound healing**, possible underlying diseases or former obesity of skin donors can be a chance to get closer to the situation in future patients.	The skin donors are declared healthy, but we cannot rule out they might have an **underlying (maybe undiagnosed) disease** that interferes with the wound healing. Many of the skin donors were severely **obese** at one point of their life, before losing weight. That than might make an abdominoplasty necessary. Obesity is known to interfere with wound healing (Guo & DiPietro, 2010).
	After the donors' approval, there are **no ethical problems** with this model, as it uses basically "waste products" and is animal-free.	

	The WHOC is a relatively **easy to perform, standardized model**.	Despite the spacer to define the wound depth, there are still **variations in wound depth**. The **culturing time is finite**, so the last phase of the wound healing (remodeling) cannot be studied completely.
Relative top-view wound area and perimeter	Relative top-view wound area and perimeter are easy and relatively **fast to measure** and to calculate. They give a **good first impression** on whether the wound healed or not. **Repeated measurements** at different time points of the same sample are possible.	The skin becomes softer as the culture progresses, making the wounds more prone to **collapse**. This in turn falsifies the relative top-view wound area and perimeter. By excluding completely collapsed wounds, it is possible to correct for this. The **relative top-view wound perimeter** is **not always meaningful**, because wounds do not always heal in a circular shape. Instead dents/protrusions can grow, which lead to a larger perimeter than the start value while the wound is actually healing.
Wound volume determination by OCT	Wound volume determination by OCT is **non-invasive, fast**, and allows **repeated measurements** at different time points of the same sample. This data gives a **good first impression** on whether the wound healed or not.	OCT measurements are prone to **segmentation errors** due to water reflexes. The resolution becomes worse with increasing wound depth This means, that this measurement is not extremely precise.

		The OCT might not always be available if you do not have your own machine.
LDH assay	The LDH assay is a **fast** assay that is easy to perform and gives a good impression on the **skin viability**.	The LDH release does **not** really make a prediction **about** the *ex vivo* **wound healing**.
H&E evaluation, including microscopic wound area, microscopic wound diameter, and area and length of the ETs	The H&E staining is **comparatively easy and fast** to perform and gives a good tissue overview. The microscopic evaluation gives an **in-depth evaluation** of wound healing. H&E staining allows the evaluation of the **ETs**, meaning the amount of new epidermis grown during the WHOC becomes measurable. To correct for differences in wound diameter, the inner ETs can be **normalized** on the wound diameter, adding another layer of depth to this evaluation. The H&E staining allows an assessment of the **granulation tissue formation**. (If wounds do not heal, the dermis still shows the clear edges of the punched wounds. If the dermis heals well, the loose tissue associated with dermal regeneration is visible)	The microscopy and **analysis** of the H&E staining is very **time-consuming**. Evaluation is only possible at **one time-point** per sample. Deformation of the wounds during embedding in paraffin can **distort the wounds** and thus falsify the microscopic wound area and diameter. Another potential source of errors is present if the wounds do not heal evenly (i.e. oval instead of round), because the direction of cutting then also influences the area and perimeter. In the latter case this also affects the ETs as their maximal archivable length differs strongly between wounds that healed evenly and those that did not
CK 6 evaluation	CK 6 is a **wound healing marker**. An increase in CK 6 expression is associated with well healing wounds (Freedberg *et al.*, 2001; Groh & Magin, 2023).	The **changes** in relative CK 6 expression observed in the WHOC were **relatively small** and seldomly significant. Evaluation is **time consuming** and only possible at **one time-point** per sample.
CD31 evaluation	The CD31 staining allows the assessment of blood and lymph vessel development during the WHOC. Especially **angiogenesis** is a crucial factor in wound healing (Grambow *et al.*, 2021).	

	This staining gives an impression about healing in the **dermis**, while the other markers studied concentrate on the epidermis.	Microscopy and evaluation must be **performed with care**. Large, well perfused structures such as hair follicles or sweat glands should not be included as they distort the picture. The number of CD31 positive cross sections and vessels often show **large error bars**, indicating that this data needs to be considered with care. The deviation in data can be explained by the simple fact that the numbers of sections and vessels vary greatly between different visual fields (either there is a vessel present or not). Evaluation is **time consuming** and only possible at **one time-point** per sample.
KiTUNEL	Ki67 allows the assessment of **proliferating** cells. TUNEL allows the assessment of **dying** cells. The double staining allows the assessment of the skins **vitality**.	Especially abdominal skin showed **little expression of Ki67**. TUNEL positive cells have damaged DNA. How this happened, or which sort of cell death is happening, cannot be said (Dmitrieva & Burg, 2007). Evaluation is **time consuming** and only possible at **one time-point** per sample.
Cortactin	Cortactin allows the assessment of rearrangement of the cytoskeleton and thus **migration**, a crucial part of human wound healing (Ammer & Weed, 2008; Eming *et al.*, 2014).	The **changes** in cortactin expression observed in the WHOC were **relatively small**. Evaluation is **time consuming** and only possible at **one time-point** per sample.
Conclusion	The WHOC model is an **interesting** and **valuable** tool to study human wound healing. The most limiting factor is probably the missing blood circulation. Still, the WHOC model gives the unique possibility to study an entire human an organ *ex vivo.* It is well suited for testing of new treatment strategies as shown in this work. As all the studied parameters have a drawback, it is important to take as many parameters into account as possible so that a complete picture emerges.	

5.2 The time course experiment revealed that the wounds in the wound healing organ culture heal nicely

The first chapter of this work was a characterization of the course of the WHOC. This experiment helped to understand *ex vivo* wound healing in the WHOC better.
Already by bare eye formation of new epithelium and dermal tissue is visible. The wounds become smaller over the course of the culture. Correspondingly, the evaluation of relative top-view wound area and diameter showed, that both decreased significantly during the culture. This was the first proof that the untreated wounds healed properly in the WHOC. The decrease in wound closure was especially strong from day 0 to day 2 and from day 2 to day 4. From day 0 till day 4 the relative top-view wound area was reduced by about 50 %. During the rest of the culture, the decrease in relative top-view wound area and perimeter is less pronounced. On day 7, the relative top-view wound area and perimeter are even slightly larger than they were on day 6. The strong wound closure rate especially from day 0 to day 2 is seen in all top-view evaluations of this work. While ETs are already clearly visible at day 2, this strong decrease could also be due to softening of the skin in culture. This then can lead to a partial collapse and contraction. Mendoza-Garcia *et al*. found maceration of skin punches which could explain the collapse of some of the punches (Mendoza-Garcia *et al.*, 2015).
The slight increase in relative top-view wound area and perimeter from day 6 to day 7 (in both cases only about 2 %) lies within measurement uncertainty of this evaluation method and can thus probably be disregarded. However, this finding does indicate that the top-view wound closure slows down over the course of the culture. This might be because the skin viability in culture is finite. Liao *et al.* and Sturmheit *et al.* showed that the culturing period of *ex vivo* WHOCs should not exceed 9 days (Liao *et al.*, 2019; Sturmheit *et al.*, n.d.). As the viability of the skin *ex vivo* decreases this might slow the wound healing process down.

The microscopic evaluation of the H&E sections mostly confirmed what the top-view evaluation showed. The wounds become smaller over the course of the WHOC, and the ETs increase significantly in area and length. So, while some wounds might collapse, wound healing is definitely observable in the WHOC. Over the course of the WHOC, formation of granulation tissue (as loose, somewhat disordered dermal connective tissue) and ETs (missing the stratum corneum) were clearly visible.
While the microscopic wound area decreased over the course of the WHOC, it is curious that the smallest microscopic wound area was measured at day 4. In the same way it was unexpected to find that the wounds at day 0 have the smallest wound diameter of all days. The fact that the microscopic wound area and diameter showed values, which did not fit to the other parameters was observed in some of the other experiments as well. These unexpected findings are probably embedding artifacts. As stated above, the skin becomes soft over the course of the WHOC. When it is taken out of the retainer and placed into the paraffin embedding cassette for fixation in Roti-Histofix®, deformation of the wounds is inevitable. Depending on how strong this deformation is, it can falsify the measurement data of area and diameter. Still, this data is not without meaning, simply prone to outliers. Hence it must be considered with care. The measurement of the ETs is barely affected by this kind of deformation, as the new epidermis is not raised or even destroyed by the embedding process.
Another issue that one needs to consider during the microscopic evaluation of the wounds is the following: while in theory wounds keep their circular shape during the healing process, in practice they often assume an oval shape sometimes with dents during wound healing. **Figure 5.1** shows exemplary illustrations of those shapes. Depending on these shapes, the wound diameter can differ quite a lot.

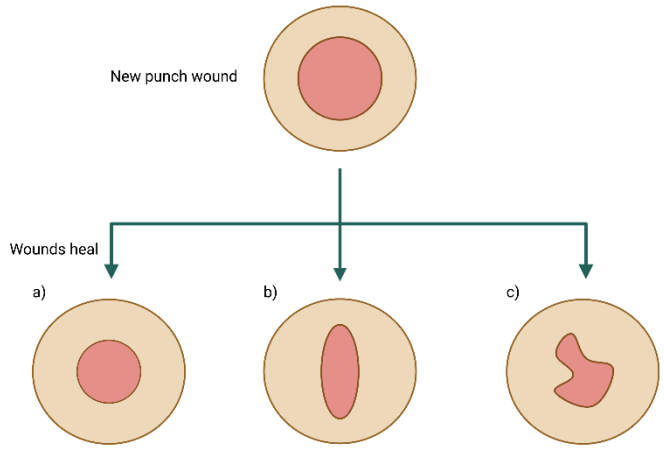

Figure 5.15: Schematic drawing of the different shapes a partially healed *ex vivo* wound can have
The new punch wound is round. In the healing process wounds can heal roundly (a), assume an oval shape (b), or heal in a more deformed way (c). Created with BioRender.

Liao *et al.*, Meyer *et al.*, and Sturmheit *et al.* did not report these issues. However, they used human scalp skin which is a lot coarser and more stable than abdominal skin, which was mainly used in this work (Liao *et al.*, 2019; Meier *et al.*, 2013; Sturmheit *et al.*, n.d.). The usage of scalp skin was not feasible for this work, as most of the experiments required more skin than a face lift can provide.
The difference in diameter can also have an influence on the length and with that also the area of the ETs, because the distances they have to overcome to completely close the wound can differ. If the diameter is small, wounds might be completely re-epithelialized but still have smaller and shorter ETs than those wounds with a large diameter. To adjust for this the area and length of the inner ETs was considered in absolute numbers and normalized on the respective diameter. As the analysis of the time-course experiment shows, in a robustly, well healing wound the area and length of the inner ETs increases over the course of the culture in absolute numbers and in normalized ones.
While the ETs did not increase much in length from day 6 to day 7, a distinct increase in area was observable here.

CK 6 is an important wound healing marker. As expected, it was not expressed at the start of the WHOC (day 0), but from day 2 on the relative CK 6 expression increased significantly over the course of the culture. As CK 6 is an important marker for activated keratinocytes and thus re-epithelialization (Freedberg *et al.*, 2001), this shows that the re-epithelialization process is already beginning at day 2.
The relative CK 6 expression increased until day 4 for the outer ETs and day 6 for the inner ETs. The following slight decrease in CK 6 expression might be because CK 6 is only expressed in actively healing wounds (Freedberg *et al.*, 2001). Thus, as the healing progresses, the CK 6 expression will decrease until healing is complete and no CK 6 is expressed anymore at that side. Fittingly one can see in the exemplary pictures in **Chapter 4.1.3**, that on day 2-6 the CK 6 expression seems to be evenly distributed in the entire ET while it seems to recede in the upper layers of the ET at day 7 and only the lower layers show a bright fluorescence.

The relative CD31 expression was significantly higher at day 6 of the WHOC compared to day 0. In addition, also the number of CD31 positive cells, cross sections, and vessels seemed to be lowest at day 0.
CD31 as a marker for endothelial cells is also expressed in non-healing skin (Xie & Muller, 1996) and can thus be already detected at day 0. On day 2 the relative CD31 expression is even slightly lower than at day 0, but it then increases over the course of the culture, though the changes from

measurement point to measurement point are relatively small. The highest CD31 expression was found on day 6. The number of CD31 positive cells also increases until day 6. Taking this together, one could speculate that angiogenesis and formation of new lymphatic vessels as part of the proliferation phase of wound healing reach their maximum around day 6 in the WHOC. The slight reduction observed from day 6 to day 7 does not necessarily contradict a good wound healing. Remodeling and removing of excess endothelial cells once the newly formed tissue is sufficiently perfused is part of wound healing (Greenhalgh, 1998).
The number of CD31 positive cross sections and vessels both increase during the culturing period, indicating an increase in angiogenesis.

The percentage of Ki67 positive cells seemed to decrease over the course of the wound healing organ culture, while the percentage of TUNEL positive cells seemed to increase.
When assessing the KiTUNEL analysis, the low fluorescence intensity of the Ki67 staining catches the eye. This made evaluation of the Ki67 staining challenging. As **Figure 5.2** shows the staining worked well in a hair follicle as positive control. So, the issue here clearly was not the antibody against Ki67 cells or the staining protocol itself.

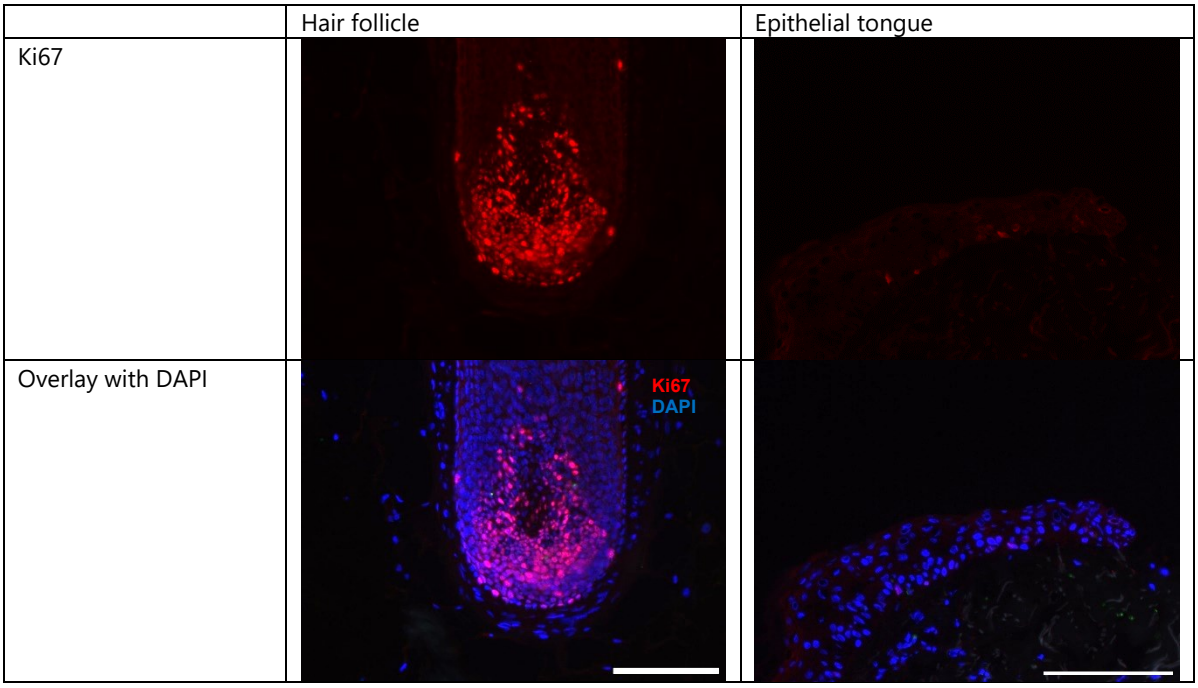

Figure 5.2: Exemplary Ki67 staining of a hair follicle and an epithelial tongue of a wound incubated for 4 days in the wound healing organ culture model
The hair follicle stems from skalp skin, the wound from abdominal skin. Scale bar = 100 µm

Kleszczyński and Fischer, Meier *et al.*, Liao *et al.*, and Topouzi *et al.* all performed Ki67 staining on their human skin organ models or WHOC models, but none of them reported the same issues. However, all these experiments were performed on scalp skin (Kleszczyński & Fischer, 2012; Liao *et al.*, 2019; Meier *et al.*, 2013; Topouzi *et al.*, 2020). The Ki67 stainings in this work were performed on abdominal skin. So, a possible explanation for this finding could be, that abdominal skin might not express Ki67 strongly or abundantly.

As far as evaluation was possible, most Ki67 positive cells were found at the beginning of the culture. As Ki67 is a marker for proliferation, it is to be expected that always few cells in the basal layer are positive.
TUNEL positive cells indicate cell death. On day 0 no TUNEL positive cells were found. This shows that the skin arrives viable at the laboratory and survives the preparation process well. The number of TUNEL positive cells increases over the course, which was expected. On the one hand, because also apoptosis is a part of wound healing (Greenhalgh, 1998) and on the other hand also because the viability of the skin *ex vivo* is finite. The increase in TUNEL positive cells in the outer ETs from day 6 to day 7 was strikingly high, however. It fits to the fact, that the outer ETs were found shorter and smaller than the inner ETs, indicating that they might not have been as viable as the inner ETs.
The decrease of Ki67 positive cells together with the increase of TUNEL positive cells means, that over the course of the WHOC less proliferating basal layer keratinocytes and more dying keratinocytes are present. This shows that – as stated before – the culturing period of the WHOC is limited. Lu *et al.* and Kleszczyński and Fischer also found that the balance between Ki67 positive and TUNEL positive cells in a serum-free human skin organ culture changes in a similar pattern as found here over the course of the culture. After cultivating the skin for five days, Kleszczyński and Fischer were not even able to detect any Ki67 positive cells in the epidermis any longer (Kleszcyński & Fischer, 2012; Lu *et al.*, 2007).

Cortactin is expressed continuously over the course of the wound healing organ culture. The cortactin expression is especially pronounced in the ETs, indicating that the rearrangement of the cytoskeleton, necessary for migration takes place.
Cortactin plays an important role in the remodeling of the cytoskeleton and is thus crucial for migration of cells during wound healing (Ammer & Weed, 2008). In the time course it can be seen that there is almost no expression at day 0, but a strong expression in the ETs on all other days. On day 6, the cortactin expression in the tip of the ETs is especially pronounced and shows nicely the expected rearrangement of cytoskeleton during migration into the wound. This is a clear sign that the wounds heal properly *ex vivo*.

The time course experiment showed, that the WHOC is a sufficient tool to study wound healing and many different wound healing parameters *ex vivo*. Especially the proliferation phase of wound healing can be examined well utilizing this model. We observe the formation of granulation tissue and re-epithelialization. The phases of homeostasis and inflammation can in principle be observed in the WHOC. However, there is no blood flow in this model, so the influx of immune cells will be limited to those cells already in the vessels and tissue resident cells. The last phase of the wound healing, the remodeling phase, can take up to months as described earlier. As the culturing period of skin *ex vivo* is limited, it cannot be studied to its full extend in this model.

5.3 Disinfection of wounds with Octenisept® inhibited *ex vivo* wound healing

The preparation of the wounds was done in the laboratory under non-sterile conditions. To reduce the risk of infection, the skin was incubated with an antimycotic for the first 24 hours. Together with the development of new, autoclavable retainers (Freiburg-retainers), this minimized mold infections to almost zero. However, infections with different candida species throughout the culture still occurred sometimes. This is not surprising, as the top-view microscopy and the OCT-measurements could only be performed in a non-sterile environment. For the OCT-measurements, the skin specimens even had to be transported to a different building. That is why the effect Octenisept® as a disinfectant that is not ethanol based and should be skin compatible was tested in the WHOC.

Moreover, Octenisept® is commonly used to disinfect mucosa, skin, and wounds (Hübner *et al.*, 2010; Schupp & Holland-Cunz, 2009; Stahl *et al.*, 2011).
Surprisingly, I found that Octenisept® had a detrimental effect on the *ex vivo* wound healing in the WHOC. After repetitive disinfection with Octenisept® black discolorations were visible at the wound edges. This could be a sign of wound edge necrosis, as necrosis is often associated with a dark discoloration in skin (Peetermans *et al.*, 2020; Qiu *et al.*, 2019). Moreover, there was barely any opaque, newly formed epidermal tissue visible in the Octenisept® group, in contrast to the control group. Accordingly, the top-view wound closure was significantly decreased in wounds disinfected with Octenisept® compared to the control group.
As in the time course experiment, here also the strongest reduction in relative top-view wound area and perimeter occurred from day 0 to day 2 in both groups, which reinforces the theory that part of the strong decrease seen at the very beginning of the culture might be due to collapsing/contraction of the wounds. However, the control group decreases more than the non-healing Octenisept® group. This proves that the decrease in area and perimeter observed in most experiments from day 2 to day 4 is only partly due to collapsing/contraction, but also due to the beginning of the wound healing. From day 2 on the wounds treated with Octenisept® showed an almost constant wound area and even an increase in wound perimeter. The decrease in relative top-view wound area is not very large from day 2 in the control group either, but it is at least discernable, and the relative top-view wound perimeter clearly decreases over the course of the culture. From day 4 on the relative top-view wound area and perimeter of wounds disinfected with Octenisept® were significantly larger than those of the control group. This already strongly indicates that Octenisept® impairs the *ex vivo* wound healing.

The devastating effect of Octenisept® on wound healing became really clear during microscopic evaluation. Wounds disinfected with Octenisept® formed no new epithelial tongues in the wound healing organ culture. Interestingly sometimes there seemed to be a little epithelial growth in Octenisept® wounds. However, this growth was never visible on the wound surface. Rather it grew backwards, beneath the existing epidermis or deep inside the dermis, an “underground” ETs so to speak **Figure 5.3** showed an exemplary picture hereof.
Seemingly epithelial growth was possible under Octenisept® conditions, but only in regions that the disinfectant could not reach.

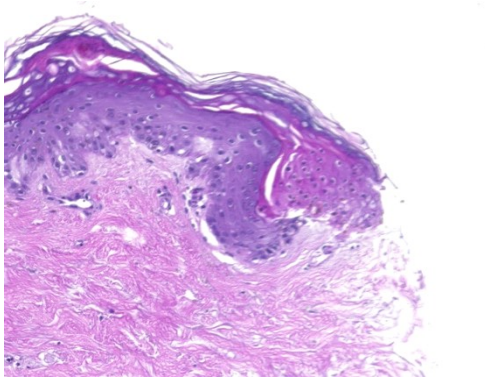

Figure 5.3: Exemplary hematoxylin & eosin picture of an “underground“ epithelial tongue that formed after disinfection of *ex vivo* wounds with Octenisept®

The microscopic wound area was smaller in the Octenisept® wounds than in the control wounds, though not significantly. This different could either be an indicator that Octenisept® has a positive influence on wound healing in the dermis or this difference could be due to differences in the wound

size due to embedding artifacts. One could also assume that Octenisept® harms the skin integrity so that wounds collapse more easily. Though, a collapsed wound likely would also have a smaller diameter, which is not the case here. So, this is likely an embedding artifact. Increasing the number of replicates could be a way to verify this.

Interestingly, disinfection with Octenisept® did not influence the CK 6 expression in the ETs. This could indicate that Octenisept® has no harmful or beneficial effect on the hyperproliferation associated with wound healing.

Disinfection with Octenisept® had no influence on the relative CD31 expression, but it decreased the number of CD31 positive cells and vessels significantly compared to the control group in the WHOC. This could indicate that disinfection with Octenisept® is harmful to angiogenesis and thus also impairs dermal *ex vivo* wound healing.

The KiTUNEL staining highlighted the damaging effect of Octenisept® on the WHOC. It resulted in significantly less Ki67 positive cells and significantly more TUNEL positive cells in the ETs. There actually were no Ki67 positive, proliferating cells in the Octenisept® group, but more than half of the cells were TUNEL positive and thus undergoing cell death. TUNEL is not as specific for apoptosis as often stated. The TdT-enzyme detects free 3‘-OH DNA ends, which happen in different sort of cell deaths (Dmitrieva & Burg, 2007). So, it cannot be said, what kind of cell death occurs here. What this staining certainly can show is that Octenisept® disinfection reduces the percentage of proliferating cells while inducing cell death in the WHOC – both facts contradict a smooth wound healing.
The increased number of TUNEL cells underlies that the black discolorations could be due to cell death like necrosis.

Disinfection with Octenisept® seemed to reduce cortactin expression in the ETs. This strongly hints that migration is impaired by disinfection with Octenisept®. While in the control group cortactin assembles in the tip of the ET, the ET of the Octenisept® wounds is almost void of it, showing that no migration can happen and thus no formation of ETs.
If Octenisept® would impair cellular migration this could also be true for the endothelial cells in the dermis. This would explain, why the number of CD31 positive cells and vessels were lower after disinfection with Octenisept®.

All findings clearly show that Octenisept® should not be used as a disinfectant in *ex vivo* skin studies. It is especially detrimental for wound healing studies as it seems to prevent the formation of ETs *ex vivo*.

Octenisept® contains two active substances: 0.1 % octenidinhydrochloride and 2 % phenoxyethanol. Both are antiseptics, that make Octenisept® a very powerful, fast-acting and effective disinfectant against bacteria, fungi, and enveloped viruses. It was even found to be effective against some multi-resistant bacteria. Next to its high efficiency, Octenisept® is also commonly used because its application is less painful for the patient compared to ethanol-based antiseptics, it has a low cytotoxicity, and octenidinhydrochloride has a remnant effect.
So, Octenisept® should not interfere with wound healing at all. Fittingly, Stahl *et al.* found that Octenisept® does not interfere with porcine wound healing *in vivo*. On the other hand, they found that phenoxyethanol could penetrate the skin of different animals, which could have toxic implications (Stahl *et al.*, 2011).

Obviously, there is little research done on human wounds *in vivo*, but there are several case reports of severe adverse effects if Octenisept® is applied to disinfect abscesses or wounds where a proper drainage is not possible. In one case even fatty tissue necrosis was observed. The manufacturer issued a warning to ensure proper drainage of disinfectant and not to apply it with too much pressure to ensure these severe effects do not occur (Bauer *et al.*, 2012; Hübner *et al.*, 2010; Kim *et al.*, 2017; Schupp & Holland-Cunz, 2009). Still, this could already indicate a potentially harmful effect of Octenisept® onto skin cells.
In accordance with this hypothesis, Hirsch *et al.* found that while Octenisept® is extremely effective in killing different bacteria, it can also be cell toxic to keratinocytes and fibroblasts *in vitro*. In their dose dependency experiments, already a 10 % Octenisept® solution was sufficient to strongly decrease viability and proliferation of *in vitro* cultivated keratinocytes and fibroblasts (Hirsch *et al.*, 2010). Kim *et al.* published that Octenisept® has a detrimental effect on adipose tissue derived stem cells, which can play an important role in human wound healing. Upon treatment with a low dose of Octenisept®, adipose tissue derived stem cells proliferated significantly less, were less viable and the number of dying cells increased. Moreover, specific stem cell markers were reduced. The authors assume that the adipose tissue derived stem cells actually undergo necrosis after treatment with Octenisept® (Kim *et al.*, 2017). This would fit to the black discoloration I observed at the wound edges after disinfecting the WHOC with Octenisept® and which I assumed could be necrosis. Induction of necrosis is clearly the opposite of wound healing, so this finding was rather shocking.

What is important to note here is that the findings in this work are *ex vivo* findings. According to the manufacturer, the drainage of Octenisept® out of the wound must always be ensured and it should not be administered systemically (Hübner et al., 2010, https://www.schuelke.com/de-de/produkte/octenisept-Wund-Desinfektion.php, July 21, 2023). In the WHOC however, Octenisept® stayed in the wells after spraying the wounds. Further *in vivo* studies would be interesting to see if Octenisept® is harmful to *in vivo* wound healing when it cannot drain the wound or even enters the blood flow.
Moreover, more studies are needed to investigate the molecular mechanisms of how Octenisept® impairs *ex vivo* wound healing.

5.4 0.1 % DMSO does not interfere with *ex vivo* wound healing

The inhibitors that were tested in the screening were all dissolved in DMSO, but DMSO is known to be cell-toxic in higher concentrations by forming pores in the plasma membrane of cells (Galvao *et al.*, 2014; Rubin, 1975). Thus, a tolerable concentration for the WHOC had to be found, which ideally does not influence the *ex vivo* healing at all.

For the DMSO testing and the testing for a positive control some of the cultures were performed for 7 days and some for 8 days. I switched from the original 8 days of culture (based on Sturmheit *et al.* (Sturmheit *et al.*, n.d.)) to 7 days of culture out of methodical reasons: The skin deliveries usually happened once a week. A culture of 7 days allowed me to use every skin, as the culture would be finished on the day the new skin arrived. If I had stuck to 8 days of culturing even with the increased number of Freiburg retainers, I could have performed a lot less of experiments. As the wound healing slows down at the end of the week of culturing, I deemed a day less of culture but more experiments possible a good compromise. Moreover, a 7-days-culture was recommended by some of the other authors (Bhora *et al.*, 1995; Moll, 2003; Moll *et al.*, 1999). For treatment regimes and evaluation, I chose the same process as later on for the screening.

This experiment is the first one in this work, where OCT was applied to determine the wound volume in a non-invasive way. Advantages and limitations of this method can be found in **Table 5.1**. Application of OCT in the WHOC model to monitor *ex vivo* wound healing was found by Sturmheit *et al*. and Glinos *et al.* to be a very elegant way to rapidly measure the wound volume of the same wound at multiple timepoints, which allows a quantification of the wound healing (Glinos *et al.*, 2017; Sturmheit *et al.*, n.d.).
The OCT measurements were done by Madita Göb, M. Sc., in the Institute of Biomedical optics. There, scientists built a stage which allowed the automated scanning of wounds within the 24 well plates by moving the measurement arm of the OCT over the different samples automatically. This sped up the measurement process immensely. Within 10 minutes the wound volume of an entire 24 well plate could be measured, saved, and calculated.
OCT could revolutionize wound healing research. Glinos *et al.* even managed to visualize re-epithelialization of *ex vivo* wounds by OCT. Their *en face* (meaning top-view) OCT data was equal or even better than their microscopic evaluation. The authors hypothesize that OCT measurements could replace the extremely time-consuming and elaborate histomorphometric analysis, which is the current standard to assess wound healing (Glinos *et al.*, 2017).

When assessing the effect of DMSO, concentrations of 10 % DMSO and higher were found to be toxic to the skin and to worsen the *ex vivo* wound healing. Already the top-view microscopic pictures show that concentrations above 50 % DMSO were toxic for the skin. No new ETs formed and after incubating the skin for 24 hours in pure DMSO the epidermis showed signs of disintegration. Determination of the relative top-view wound area and perimeter confirmed this and further showed, that 10 % DMSO also impairs wound healing. Incubation with 1 % DMSO and with 0.1 % DMSO for 24 hours were well tolerated by the skin. Repetitive treatment with 0.1 % DMSO seemed to stress the skin a little more than one time treatment, which was unsurprising as the toxic substance was added more frequently here. Still, the wounds displayed a proper wound closure over the course of the culture.
For determination of the relative wound volume and LDH-release only DMSO concentrations up to 10 % were tested, as 50 % DMSO and 100 % DMSO resulted in a significantly worse wound closure and were thus ruled out as treatment options.

No concentration of DMSO showed a smaller wound volume than untreated wounds. Treatment with 0.1 % DMSO still resulted in a reduction of the relative wound volume. Treatment with 1 % and 10 % did not. Both volumes at day 6 were larger than at day 0. For 10 % DMSO this is in accordance with its harmful influence on the relative top-view wound area and perimeter, but for 1 % DMSO this finding was unexpected. It could indicate that 1 % DMSO might not reduce the formation of new ETs but led to less formation of granulation tissue in the dermis or even some decay there. In any case, this finding made 0.1 % DMSO the most suited treatment concentration.

The LDH-release pattern observed here is like the one observed by Sturmheit *et al.* (Sturmheit *et al.*, n.d.). A high LDH-release is associated with cellular stress. As the skin had to be transported, wounded, and taken into culture, the relatively high LDH levels at day 0 were unsurprising. The decrease of LDH-release at day 2 of the culture shows that the skin is still viable and can regenerate during the culturing process. The increase during the culturing period was expected, as the life span of the skin *ex vivo* is limited. Wounds treated with 0.1 % and 1 % DMSO showed about the same pattern as untreated wounds. Surprising is the low LDH-release of wounds treated with 10 % DMSO

at day 8. These wounds did not heal well, so it would be expected that the LDH release is highest here. As there is no biological sound explanation as to why this could be and the error bar is quite large, this is probably a measurement error.

0.1 % DMSO was well tolerated by the skin and did not interfere significantly with wound healing. This is in accordance with literature, where low DMSO concentrations were found to be tolerated by cells or could even aid wound healing (Guo & DiPietro, 2010; Rubin, 1975). The tested substances were all dissolved in DMSO to a concentration of 0.1 % of DMSO in the well. To ensure that measured effects were not due to DMSO, a vehicle control of 0.1 % DMSO was carried along.
The findings of Galvao *et al.* that even lowest concentrations of DMSO can be cell toxic (in their case retinal cells) underlies how important it is to test for an appropriate DMSO concentration before beginning an experiment (Galvao *et al*., 2014).

5.5 The search for a sufficient positive control revealed that L-arginine does not influence *ex vivo* wound healing while treatment with 10 µM sodium gualenate resulted in a better top-view wound closure

Ideally, the effect of a substance on wound healing is not only tested against the vehicle control but also against a positive control, that aids wound healing. This would help to define the effect of the screened substances more clearly. Therefore, I tested L-Arg and SG to see if one of them is suited as a positive control.
As treatment concentrations 1 µM and 10 µM for 24 hours at day 1, or 1 µM at every medium change were chosen. These concentrations were chosen based on other trials conducted in our lab (Burmester et al., 2020) with *ex vivo* skin. Day 1 as treatment day was chosen based on the planned layout for the screening (more on this **Chapter 5.6**), repetitive treatment was performed to see if continuous exposure to L-Arg or SG increased their efficiency.
Of the two possible candidates the company Selleck Chemicals offered in 2019 to aid wound healing, L-Arg had no convincing effect on the top-view *ex vivo* wound healing, but SG seems to be a sufficient positive control for the WHOC model.

L-Arg was the first substance to be tested. The top-view evaluation showed that L-Arg has no positive influence on the *ex vivo* wound closure. Especially the relative top-view wound area was slightly larger after treatment with L-Arg at day 7, but the difference was not significant, and the wounds still healed well. So, L-Arg seems to have no influence on the *ex vivo* wound closure.

The wound volume was lowest after treatment with 1 µM L-Arg, which could mean that L-Arg supports the formation of granulation tissue. Interestingly, L-Arg is known to increase the collagen synthesis after wounding, which fits to this finding (Arribas-López *et al.*, 2021; Wittmann *et al*., 2005). Further studies on this point could be interesting but were not the focus of this work.

Whether L-Arg has a beneficial effect onto human wound healing next to the increase of collagen synthesis is still discussed. While some studies find further positive effects upon wound healings other do not. For example, Debats *et al.* found that intravenous administration of L-Arg had no effect on wound healing rates in humans. Which is in line with our *ex vivo* findings. (Arribas-López *et al.*, 2021; Debats *et al.*, 2011).

10 µM L-Arg and especially 4 x 1 µM L-Arg resulted in a noticeably lower relative LDH-release than untreated skin at the end of the culture. This is interesting, because it might be possible to extend the cultivation period of the WHOC by supplementing the medium with the amino acid L-Arg. This is another intriguing finding, that could be further studied in another work. As this is not per se aiding wound healing, this question was not further investigated here. All in all, L-Arg has no positive effect on *ex vivo* wound healing and is thus not a suitable positive control.

SG as a positive control was tested in the same way as L-Arg was. Unlike L-Arg, SG aids top-view wound closure *ex vivo*. Especially treatment with 10 µM SG clearly reduced the relative top-view wound area and perimeter. A positive effect on the wound volume could not be found, though if one keeps the rather large standard deviation in mind SG probably does not negatively impact the relative wound volume either.
All SG concentrations tested here led to a lower LDH-release than the vehicle control starting at day 4. This difference becomes really noticeable at day 6 and is striking at day 8. However, the vehicle control wounds display a very high error bar here, probably due to an outlier.
One time treatment with 10 µM SG led to a better wound closure than the vehicle control and was thus deemed a sufficient positive control for the screening.

While there are papers, that state that SG is anti-inflammatory and aids wound healing, the authors do not explain why this is the case (Nakamichi *et al.*, 2003; Seki *et al.*, 1985). So, clearly more research is needed to examine the mode of action of SG.

5.6 The screening of the Highly Selective Inhibitor Library L3500 revealed 10 promising candidates, that might aid *ex vivo* wound healing.

The core piece of this work was the screening of the Highly Selective Inhibitor Library L3500 library in the WHOC. Not all chemicals out of the 136 inhibitor library actually had an inhibitory effect (for example S2149 is an agonist of the GPR119, https://www.selleckchem.com/products/GSK1292263.html, July 30, 2023). That is why they are referred to as substances in this work.

As the results of the screening are crucial for the further scope of this work, the evaluation of the screening was done by one blinded person. This ensured maximal neutrality in evaluation and minimized the risk of unintentionally falsifying data.

Wounds were treated with a concentration of 1 µM at day 1 for 24 hours. This concentration was chosen based on the screening of an inhibitor library in a human skin organ culture model for the autoimmune blistering disease pemphigus vulgaris (Burmester *et al.*, 2020).
As transport, wounding, and culturing are very stressful for the skin (as indicated by the high LDH-release measured before), treatment with the substances was not done at day 0 but at day 1, after the skin had time to recover.
Day 1 as default treatment day for a one-time treatment was chosen, because we hypothesized that adding the wounds early on is most crucial for a successful healing process. For example, Lánden

et al. state, that the switch from inflammation to proliferation is crucial for proper wound healing (Lánden *et al.*, 2016). While this approach might not allow substances that aid later stages of wound healing to show their full potential, testing a repetitive treatment of the most promising candidates later showed no benefit of a later treatment.

Ideally all substances would have been tested in a single run with just one skin donor. However, due to skin availability and number of retainers this was not feasible. So, the library was divided into multiple sub screenings. The clinical trials substances were tested first, as they are especially interesting because safety and toxicity studies would not necessarily need to be repeated in case of finding a successful candidate.

Simultaneously to the clinical trials substances screening, a new type of retainers was developed. The testing and production of the Freiburg retainers were performed simultaneously to the clinical-trials screening, and they were found to work equally well as the EMB retainers did (data not shown). The FB retainers were available in larger numbers, which allowed larger experiments. They were furthermore autoclavable, which made cleaning and the reuse of these retainers much easier.

In the different screenings a high donor-to-donor variation already between the vehicle controls was visible. Wounds treated with 0.1 % DMSO had a relative top-view wound area at day 7 between about 26 % (fourth sub-screening of the non-clinical trials substances) and about 50 % (first sub-screening of the non-clinical trials substances). These differences were expected, as skin of different donors was used. These donors were all female but differed in age. Moreover, skin of anatomically different sites was used, mainly abdominal and breast skin. As discussed for the KiTUNEL staining before, the anatomical region of the skin can have an influence on the experiment. For example, thickness of the skin, expression of cytokeratins, elasticity and frictional properties of the skin can depend on the age, sex, and anatomical region of the skin (Cua *et al.*, 1990b, 1990a; Johansson & Headon, 2014; Kleesz *et al.*, 2012; Yay *et al.*, 2018). Song *et al.* even found that properties of the skin, such as sebum secretion, differ with the anatomical region of the face (Song *et al.*, 2019).
Moreover, wounds do not heal equally well and fast in all humans, depending for example on age, oxygenation, or venous sufficiency of the respective skin donor (Guo & DiPietro, 2010). Plus, while only skin from healthy donors was used, we do not know if some of the patients might still have an undiagnosed, underlying disease that impairs wound healing (see **Table 5.1** for more information). A workaround for the high donor-to-donor variation would be to increase the number of biological replicates. However, this was not feasible for such a huge experiment as this screening.
The high donor-to-donor variation makes it more challenging to find a substance that reliably aids wound healing. On the other hand, this depicts the reality in the clinics very well, as humans are not identical in their wound healing processes. Even though personalized medicine is a promising tool for treating complex cases of chronic wounds, in this work the goal was to find a substance that could be a new treatment for many if not all wounds. The aim is also to find a substance to learn more about important pathways in wound healing. So, in the end I want the effect of treatment to be stronger than the donor-to-donor variation.

The WHOC proved to be a suitable tool to screen for possible new drug candidates and targets. If enough skin and retainers are available, about 20 substances can be tested in one run. Testing of more substances is in principle possible if more manpower is present. Otherwise, the preparation and wounding process takes too long for the skin to remain viable.
By evaluating “only” the top-view microscopic data and the wound volume via OCT, a sound first impression whether a candidate can aid wound healing or not can be obtained, without the need of

the immensely time-consuming microscopic evaluation. This was proven by finding S1180 to be the most promising candidate of the screening and later validating its positive effect in different concentrations microscopically. The same is true for the harmful effect of S1130 on wound healing. Still, the screening was performed with only one biological replicate. Interesting candidates have to be validated with more biological replicates to ensure that they indeed aid wound healing reliably and were not just on outlier.

When looking at the top-view evaluation in detail, one notices that while mostly relative top-view wound area and perimeter go hand in hand, this is not always the case. For example, in the first sub-screening of the clinical trials substances, the relative wound perimeter after treatment with 1 µM S2636 barely decreased over the course of the culture, while the relative wound area was comparably small. This can probably be explained by a deformation of the wound in the healing process. Ideally wound area and perimeter should be proportional to each other, meaning that wounds with a smaller wound area also show a smaller perimeter. However, the wounds do not always heal ideally in a circular shape but dents and dips do occur. This is partly because the skin becomes softer while cultivating it for a week, making it more prone to small deformations (compare **Figure 5.1** above).

When assessing the OCT data, the sometimes quite large error bars stand out, as they show that the measurement points vary quite a lot. This is mainly because water reflexes on the surface of the culturing medium can lead to measurement errors. In experiments with more technical replicates these errors can be more easily recognized as outliers and thus excluded.

The second clinical trials substances sub-screening revealed another issue that could be seen in some of the experiments throughout this work: Treatment with 10 µM SG did not lead to a smaller relative top-view wound area and perimeter than the vehicle control. This is contrary to the previous findings were 10 µM SG resulted in a better wound closure than the vehicle control. Considerations about why SG did not always aid wound healing, can be found in **Chapter 5.13**.
I decided to repeat screenings where SG led to worse results than 2 out of the 3 parameters examined and promising candidates (in comparison to the vehicle control) were found.

In the screening of the Highly Selective Inhibitor Library L3500 10 promising substances were found that could aid wound healing in the WHOC. The screening of the clinical trials substances revealed 8 promising substances, that were further validated: S1087, S1110, S2149, S2700, S2818, S2891, S4073, and S6003. All these substances performed better in 2 of the 3 investigated parameters (top-view wound area, top-view wound perimeter, and wound volume determined by OCT). In the non-clinical trials substances screening 2 substances were found that led to a better macroscopic wound healing in all the 3 parameters than the vehicle control: S1169 and S1180. These will also be further validated. Several other substances resulted in better values in 2 of the 3 parameters, but I decided to only validate the most promising ones, as the validation is a very time and resources consuming process.

In the screening 10 (8+2) promising substances were found, which might have a positive effect on wound healing in the WHOC model. While less substances out of the non-clinical trials screening qualified for further validation, these candidates are of special interest. Further validation was necessary for all substances to test whether these substances indeed promote wound healing or the observed effect in the screening was just by chance.

5.7 After validating the results of the screening 3 substances were found to be further investigated: S2891, S2149, and S1180

In total 3 of the 10 promising candidates out of the screening passed the validation successfully. In the validation of the clinical trials substances, S2891 and S2149 were interesting substances to be further evaluated. In the validation of the non-clinical trials substances, the beneficial effect of treatment with 1 µM S1180 on the top-view wound healing was successfully validated.

The validation of the clinical trials substances proved how important the validation process was. Of the 8 promising clinical trials substances, only treatment with S2891 again resulted in smaller values in 2 out of the 3 tested perimeters. Wounds treated with 1 µM S2891 had a smaller relative area and perimeter than both controls. In a direct comparison treatment with 1 µM S2891 led to a significantly better top-view wound closure in the WHOC than the vehicle control. This confirms the finding of the screening and qualifies S2891 for further studies.
None of the other substances showed a convincing effect on 2 of the 3 parameters evaluated. This probably means that for these 7 substances the findings in the screening were just by chance or they do not help wound healing in all patients. In either case they were not interesting for further studies. An exception was made for S2149, because this substance is in clinical trials against type 2 diabetes. As patients suffering from type 2 diabetes are prone to develop chronic wounds (Dallas *et al*., 2019), a drug that helps with the underlying disease and with wound healing itself would be ideal. As S2149 performed well in the screening and was the best of all clinical trials substances validated regarding the wound volume, it too was further tested to see if it could promote wound healing at a different concentration.

In the validation of the non-clinical trials substances, treatment with S1180 resulted in a smaller relative top-view wound area, perimeter, and relative wound volume than both controls, just as it did in the screening. At the end of the culture the top-view wound closure was even significantly better than that of both controls. S1169 led to a better top-view wound closure than both controls, but not to a stronger reduction in wound volume. While S1169 is not an uninteresting target, S1180 passed the validation so successfully, that only this substance was further tested in different concentrations. If none of the 3 chosen substances (S2891, S2149, and S1180) had not worked, S1169 would have been a good backup option.

5.8 Especially treatment with 1 µM and 10 µM S1180 was found to aid wound healing *ex vivo*

S2891, S2149, and S1180 were now tested in different concentrations to find the optimal treatment concentration. The concentrations were again based on work previously done in our lab on an *ex vivo* blistering skin model (Burmester *et al*., 2020). Each substance was tested in a concentration of 1 µM (as in the screening and the validation), 10 µM and as the saying “the more the better” is not necessarily true in pharmacology, in 0.1 µM (https://www.msdmanuals.com/professional/clinical-pharmacology/pharmacodynamics/dose-response-relationships, last used July 28, 2023). Moreover, it was investigated whether repetitive treatment with 1 µM will increase the wound healing promoting effect of the 3 substances.

As these substances and their influence on the *ex vivo* wound healing in the WHOC model were especially interesting, a more thorough analysis was performed here. These wounds were assessed

macroscopically as before but also microscopically and important markers for wound healing were studied as well.

5.8.1 S2891 seemed to aid wound healing in some parameters but an optimal working concentration could not be determined

Previously 1 µM S2891 was found to have a positive effect on the relative top-view wound closure – this finding could be reproduced here. Moreover, also treatment with 4 x 1 µM S2891 seemed beneficial. Interestingly repetitive treatment with 1 µM S2891 resulted in very similar results than one time treatment. This confirms once again our hypothesis, that helping the wound healing cascade to start smoothly is probably the most crucial point to promote *ex vivo* wound healing. The highest top-view wound closure was found after treatment with 10 µM S2891. Treatment with 0.1 µM S2891 on the other hand did not result in a noticeably better top-view wound closure than the vehicle control.

When assessing the top-view wound closure of wounds treated with S2891, one notices that again SG did not result in smaller relative top-view wound area and perimeter than the vehicle control. Considerations regarding this finding can be found in **Chapter 5.13**.

Wounds treated with 1 µM S2891 had a slightly smaller relative wound volume than the vehicle control, but all in all again S2891 once more had no convincing beneficial effect on the wound volume.

All concentrations of S2891 tested seemed to decrease the microscopic wound size, however only 0.1 µM S2891 and 4 x 1 µM S2891 had a positive effect on the ETs.
After treatment with all concentrations of S2891 the microscopic wound area was smaller than the controls. For the microscopic diameter the beneficial effect of S2891 was less pronounced. While treatment with 10 µM SG resulted in a smaller microscopic area than the vehicle control, its diameter was larger. This might be because the wounds diverged over the course of the culture or during the embedding process.

The evaluation of the ETs after treatment with different concentrations of S2891 did not show a consistent picture. For example, wounds treated with 4 x 1 µM S2891 had the largest inner ETs, but the smallest outer ETs. For the length of the inner ETs the exact opposite was observed: the inner ETs were shortest after treatment with 4 x 1 µM S2891, but the outer ETs were longest under the same treatment. This shows how important it is to assess both area and length of the ETs. Repetitive treatment with 1 µM S2891 seemed beneficial on the ETs in any case, although why it behaved differently in inner and outer ETs is unclear.
Especially in the normalized data also treatment with 0.1 µM S2891 seemed beneficial for formation of ETs – an effect not observed in the top-view evaluation. This is surprising especially for the normalized length of the ETs, as longer ETs should go hand in and with a smaller wound area. As none of the measurements were significant, the effect might just be too small to see in the rougher top-view evaluation.
Treatment with 1 µM S2891 or 10 µM S2891 did not show a convincingly positive effect on formation of ETs. This was unexpected as especially treatment with 10 µM S2891 was beneficial for the top-view wound closure.
As with the top-view evaluation, the H&E staining did not reveal a positive effect of treatment with SG. So here top-view and macroscopic evaluation go hand in hand.

All in all, the microscopic evaluation gave hints that S2891 might promote wound healing, but none of the tested concentrations could convince in all parameters.

Treatment with 1 µM S2891 and above seemed to lead to a higher relative CK 6 expression in the ETs in the *ex vivo* WHOC model. In the inner ETs, the relative CK 6 expression was higher after treatment with S2891 than the vehicle control, especially for 1 µM S2891 and 10 µM S2891. In the outer ETs, only treatment with 10 µM S2891 resulted in a slightly higher relative CK 6 expression.
For this experiment skin from different anatomical regions (abdomen and breast). Expression of markers such as CK 6 can differ depending on the anatomical location of the skin (Yay *et al.*, 2018), which could explain the relatively larger error bars detect here.

Treatment with S2891 seemed to have no strong effect on the CD31 expression or CD31 positive cells. Caporali and Emanueli state that neurotrophin signaling via TrkA is important in angiogenesis (Caporali & Emanueli, 2009). This could explain why an inhibition of TrkA is not beneficial for endothelial cells. However, the tested concentrations of S2891 did not harm the endothelial cells either. They just seemed to have no effect on the endothelial cells at all.

S2891 showed a positive effect on some of the investigated parameters, but not on all. A more in-depth evaluation would be necessary to find out exactly to what extent S2891 aids wound healing. S2891 was tested partly on breast and partly on abdominal skin. The donors of the breast skin where 12 years older than the donors of the abdominal skin. Both factors (age and anatomical region) could influence the effect of S2891 on wound healing.

S2891 is an inhibitor of TrkA (https://www.selleckchem.com/products/gw-441756.html, last used July 21). Especially its ligand NGF is associated with good wound healing. So even finding a slightly positive effect of S2891 on the WHOC was surprising. However, this could be explained by considering that NGF does not only bind the high-affinity receptor TrkA, but also the low affinity receptor CD271 (Iwata *et al.*, 2017; M. Zhang *et al.*, 2017, 2018). Zhang *et al.* reported, that CD271 positive epidermal stem cells promoted wound healing especially well in a burn wound mouse model (M. Zhang *et al.*, 2017, 2018). Moreover, Iwata *et al.* found that CD271 positive dermal cells aid dermal wound healing in an ear punch model in mice (Iwata *et al.*, 2017). Since TrkA and CD271 are in equilibrium, inhibition of TrkA could shift the ratio more towards CD271. This could then promote wound healing. More research is needed here, to investigate this theory. It would be highly interesting to study CD271+ cells in the WHOC and see whether they increase after treatment with different concentrations of S28891.

5.8.2 1 µM S2149 might have a positive effect on some of the parameters investigated in the wound healing organ culture model

S2149 did not show a strong positive effect on the wound healing in the WHOC model. This already showed in the macroscopic evaluation of treatment with S2149. Here, it did not have a strong effect on the top-view wound closure or wound volume. Still wounds treated with 1 µM, 10 µM, and 4 x 1 µM S2149 had a smaller relative wound area than both controls. As observed for S2891 wounds treated with 1 µM S2149 and 4 x 1 µM S2149 were very similar in relative wound area.

In the microscopic evaluation, a strong reduction of wound area and diameter was observed, especially after treatment with 1 µM S2149. This could indicate that S2149 indeed promotes wound

healing – maybe by increasing the formation of granulation tissue. On the first glance S2149 had no beneficial effect on ETs' area or length, but after normalization on the diameter, ETs treated with 1 µM S2149 were significantly larger and longer compared to all other groups. This is an example of why normalization is important and can give a new view on data. Wounds treated with 1 µM S2149 were smaller than those of the vehicle control group. This means, that the maximal length ETs treated with 1 µM S2149 could achieve was smaller than that of ETs of the vehicle control wounds. To correct for this, the data was normalized on the diameter. However, the diameter is prone to distortions during the embedding process, so this striking finding must be considered with care.

Treatment with all concentrations of S2149 tested here, but especially with repetitive treatment with 1 µM S2149, resulted in an increase in relative CK 6 expression compared to the controls. This finding indicates that S2149 might indeed aid wound healing. That 4 x 1 µM S2149 increased the CK 6 expression strongest here, shows that repetitive treatment can have its merits and is worth further investigation against a more suited positive and vehicle control – as done later in this work.

Treatment with S2149 also seemed beneficial for endothelial cells in the WHOC. The most promising concentrations here were 0.1 µM S2149 and 1 µM S2149.

Though the effect was only moderate, 1 µM S2149 was found to promote some parameters of *ex vivo* wound healing. S2149 is an agonist of GPR119 (https://www.selleckchem.com/products/GSK1292263.html, last used July 21, 2023). There is little research on GPR119 on skin cells. However, cells of the sebaceous glands and melanocytes were found to express the receptor. So, it is present in the skin and an activation of it could have some effect on the skin and maybe promote wound healing (Markovics *et al.*, 2020; Scott *et al.*, 2006). Here, more research would be needed to investigate whether GPR119 is also expressed on cells more involved in wound healing such as keratinocytes or fibroblasts.

5.8.3 1 µM S1180 and 10 µM S1180 aided wound healing in the wound healing organ culture

Treatment with 1 µM S1180 and with 10 µM S1180 aids the *ex vivo* wound healing in the WHOC. As in the screening and in the validation, treatment with S1180 showed the most promising results in the top-view evaluation. Of the three closer investigated substances only after treatment with 10 µM S1180 a significant decrease in relative top-view wound area and perimeter at the end of the culture was observed in a multiple-group comparison test. Treatment with 1 µM S1180 also resulted in a decrease in area and perimeter, though not as strikingly. In a direct comparison between 1 µM S1180 and the vehicle controls still a significant decrease was seen, so this experiment confirms the findings of the validation. It just seems that treatment with 10 µM S1180 is even more beneficial for top-view wound closure. However, the positive effect of S1180 on the wound volume in the screening and validation could not be reproduced.

In the microscopic evaluation, treatment with S1180 also resulted in a smaller microscopic wound area and diameter, though here 1 µM S1180 or 4 x 1 µM S1180 seemed more efficient than 10 µM S1180. Considerations why macroscopic (i.e. top-view and OCT) and microscopic data do not always match can be found in **Chapter 5.14**.

The fact that 4 x 1 µM S1180 had the smallest wound area but not the smallest perimeter, hints that these wounds were flat but wide. The rather large diameter could be due to the wounds diverging over the course of the WHOC or during the paraffin embedding process.
Clearly, S1180 also resulted in longer and larger ETs. Treatment with 10 µM S1180 showed a promising effect in both inner and outer ETs, though it was more pronounced in the inner ETs. Treatment with 1 µM S1180 resulted in the longest and largest outer ETs. Looking at the small wound diameter and the normalized area and length of the inner ETs, it becomes apparent that 1 µM S1180 also strongly promotes formation of the inner ETs.

Treatment with S1180 also resulted in an increase of the relative CK 6 expression. However, here the wound healing promoting effect was less pronounced as in the top-view or microscopic evaluation (no significances). Interestingly, treatment with 0.1 µM S1180 resulted in the highest relative CK 6 expression, though it did not show especially beneficial for top-view or microscopic wound healing in the WHOC. CK 6 is only expressed in actively healing wounds, not in normal, healthy skin (Freedberg *et al.*, 2001; Groh & Magin, 2023). So, maybe the CK 6 expression is higher after treatment with 0.1 µM S1180 than after treatment with the other concentrations because these wounds have not yet healed as strongly.

The relative CD31 expression was not influenced by treatment with S1180, a slight increase was only observed after treatment with 4 x 1 µM S1180. Especially 10 µM S1180 and 4 x 1 µM S1180 resulted in more CD31 positive cells and vessels than the vehicle control, though not cross sections. None of the effects were statistically significant.

The cortactin expression seems unchanged by treatment with S1180, indicating that this inhibitor has no influence on cortactin levels.

This experiment showed that treatment with 1 µM S1180 and 10 µM S1180 promotes wound healing in the WHOC model. 0.1 µM S1180 did not prove especially beneficial, while repetitive treatment also seems to have its merits. That is why repetitive treatment of 1 µM S1180 and 10 µM S1180 were further investigated.

S1180 inhibits tankyrase and stabilizes axin. Thereby the death complex of β-catenin remains stable. Correspondingly β-catenin is degraded and the Wnt/β-catenin pathway remains inactive. The activity of S1180 is highly specific, so no other pathways should be inhibited by treatment with S1180 (Wang *et al.*, 2014, https://www.selleckchem.com/products/XAV-939.html, last used 21st July 2023). Wang *et al.* also stated that by stabilizing specifically axin 2, treatment with S1180 stops abnormal activation of the Wnt/β-catenin pathway but does not interfere with normal cellular functions. They found that this helps in a lung fibrosis mouse model. Lung fibrosis is characterized by access fibroblast and myofibroblast activation and proliferation. Inhibition of the Wnt/β-catenin pathway helped to restore a physiological state of the mice lungs (C. Wang *et al.*, 2014).
This is interesting in wound healing, as wound healing in mammals is sort of a fibrotic process, characterized in the dermis by fibroblast activation, proliferation and scar tissue formation. Bastakoty *et al.* found that transient inhibition of the Wnt/β-catenin pathway significantly aided dermal wound healing in a mouse model. After treatment with Wnt/β-catenin inhibitors, amongst them S1180, the wounds showed a more regenerative type of wound healing in the dermis. This means that less fibrotic processes were observed, and skin appendages even could regenerate in the healing process. The positive effect was mainly observed in the dermis of the mice. The authors found very high Wnt/β-catenin levels in the dermis early in murine wound healing, which sunk back to baseline within

10 days. (Bastakoty *et al.*, 2015) An early, transient inhibition of the Wnt/β-catenin pathway might inhibit this peak and result in a more regenerative wound healing without disrupting the crucial function Wnt has in cells.
This publication combined with the results of this study could indicate that these findings could be transferable to human wound healing. It would for example explain why one-time treatment with S1180 at day 1 of the WHOC showed such promising results, but a repetitive treatment was not found more successful.
However, Bastakoty *et al.* reported a positive effect on dermal wound healing (Bastakoty *et al.*, 2015), while I found that treatment with S1180 mainly aided epidermal processes, i.e. resulted in better top-view wound closure and longer and larger ETs than the vehicle control.
Regarding the epidermis the literature is conflicting, because Wnt is thought to be crucial for epidermal homeostasis and growth as studies in mice showed. So here more research is needed to understand how S1180 aided epidermal wound healing in the human WHOC model. Though Bastakoty *et al.* only found the peak in Wnt/β-catenin levels in the dermal tissue, maybe in humans this also happens in the epidermis. Or the seen effect could be due to the epidermal stem cells of the hair follicle bulge. Wnt/β-catenin was shown to be important for epidermal stem cells in the hair follicle bulge to differentiate into follicle cells (Bastakoty *et al.*, 2015; Ito *et al.*, 2005, 2007). Hair follicles are known to be an important source of stem cells in wound healing (Ashcroft & Ashworth, 2003; Ito & Cotsarelis, 2008). Maybe a transient inhibition of Wnt/β-catenin stops the differentiation process, leaving more epidermal stem cells "free" to aid epidermal wound healing.
If this is true, the effect of Wt/β-catenin inhibition on hair follicles needs to be carefully studied, to make sure that the transient inhibition does not harm the hair follicle or the hair growth. Bastakoty *et al.* did not find abnormalities in murine hair follicles, which is encouraging (Bastakoty *et al.*, 2015).
Stojadinovic *et al.* found that the β-catenin was upregulated in the wound edges of chronic ulcers of 10 patients. Moreover, they showed that β-catenin stabilization impaired wound healing and keratinocyte migration in a WHOC model (Stojadinovic *et al.*, 2005). While the primary finding was in chronic wounds, this could mean that also normal wound healing could benefit from transient β-catenin inhibition – which would fit to the findings of this thesis.

All in all, the literature on wound healing and Wnt/β-catenin inhibition is sparse, but what little can be found in literature and my findings in this study show that this is an extremely interesting and promising field of research. More in depth studies should be conducted to examine how S1180 and transient inhibition of the Wnt/β-catenin pathway aid wound healing.

5.9 Repetitive treatment with S2891, S2149, and S1180 was not more beneficial than one-time treatment in the wound healing organ culture

The repetitive treatment has been so far not tested against a sufficient vehicle and positive control (repetitive treatment of 0.1 % DMSO or 10 µM SG). Because 10 µM S1180 promoted wound healing in the WHOC, repetitive treatment with 10 µM S1180 was tested here as well.

The results of the top-view evaluation were rather sobering. Treatment with 4 x 10 µM S1180 and 4 x 1 µM S2891 led to a smaller relative wound area than the vehicle control at the end of the WHOC.

However these findings were not significant and none of the other tested substances performed better than the vehicle control.

Repetitive treatment with S1180, S2149, and S2891 decreased the microscopic wound area, though the effects were not significant. Interestingly, wounds treated with 4 x 1 µM S2149 were the smallest microscopically, even though the top-view wound closure did not profit from this treatment.
Treatment with 4 x 10 µM S1180, 4 x 1 µM S2149, and 4 x 1 µM S2891 seemed to decrease the microscopic perimeter. Repetitive treatment with 1 µM S2891 resulted in larger and longer inner ETs (both before and after normalization), which fit to the earlier experiments and the reduction in top-view wound area after treatment with 4 x 1 µM S2891. This indicates that repetitive treatment with 4 x 1 µM S2891 is beneficial for wound healing in the WHOC.
Interestingly, in this set up repetitive treatment with 1 µM S1180 did not prove beneficial for top-view wound closure, wound diameter, and ETs. Treatment with 4 x 10 µM S1180 seemed more promising and at least resulted in larger inner ETs after normalization than the vehicle control. Still, repetitive treatment with S1180 could not be found to be more promising than one-time treatment at day 1.
Itawa *et al.* found that in mice the Wnt/β-catenin pathway is only shortly up-regulated after wounding before returning to "normal" levels (Iwata *et al.*, 2017). Inhibiting this pathway when it is up-regulated, meaning from day 1 to day 2 was found to be helpful. Here, it seems that further inhibition was not of any benefit – corresponding to the findings of Iwata *et al.*
Also, repetitive treatment with 1 µM S2149 was not beneficial for the formation of ETs. Even after normalization 4 x 1 µM S2149 did not result in a strong increase in ETs area or length.
Moreover 4 x 10 µM SG did not promote *ex vivo* wound healing, quite on the contrary. Again, this strongly indicates that for many substances one-time treatment early in *ex vivo* wound healing is the optimal treatment regime.

The most surprising finding when evaluating the ETs was probably that none of the substances influenced the outer ETs.

Only treatment with 4 x 1 µM S2149 and 4 x 1 µM S2891 led to an increase in relative CK 6 expression. In the case of S2891 this fits to the results so far, which indicate that repetitive treatment with 1 µM S2891 has a wound healing promoting effect. On the other hand, repetitive treatment with 4 x 1 µM S2149 did not show a promising effect in most of the other parameters. So, the increase in relative CK 6 expression is not as easily explained. Maybe 4 x 1 µM S2149 was enough to increase the relative CK 6 expression but just not for more.

None of the tested substances had a strong or even significant positive effect on the endothelial cells. Although the number of positive cross sections vessels is higher under repeatitive treatment of S2891, the large error bars make a reliable statement difficult here. The same is true for 4 x 1 µM S2149 and the number of positive vessels.

To summarize, only repetitive treatment with 1 µM S2891 seemed beneficial in most of the evaluated parameters here. While treatment with 4 x 10 µM S1180 also showed a positive influence on some of the parameters, the effect was much less pronounced than after one-time treatment. Treatment with 4 x 1 µM S1180 did not seem to help at all in this experiment, neither did treatment with 4 x 1 µM S2149.
Still, the one-time treatment with 1 µM S1180 and 10 µM S1180 promoted wound healing in the WHOC much stronger than any of the repetitive treatments. Hence, these concentrations will be tested in the pathological model.

This experiment showed that more treatment (meaning in this case repetitive application) does not always guarantee more effect, quite the contrary. Granted, this is partly also due to the nature of the screening, as here only one-time treatment was tested. However, one could still assume, that repetitive treatment increases the effect of substances tested. That this is not the case, can have different reasons. For once, we assume that the beginning of the wound healing is the most crucial step for a sufficient and satisfactory wound healing. At day 1, when the wounds were treated, homeostasis should be completed. The inflammation phase (somewhat attenuated in our WHOC model as no blood flow was present) should be in full swing, but also the proliferation phase already begins here. This is clearly shown by the small ETs visible already on day 2. So, treatment at this crucial time point, where inflammation slowly decreases and proliferation increases, could promote an orderly transition and maybe a faster progression through the phases of wound healing.
One could also hypothesize, that treatment beneficial to the early stages of wound healing is not necessary beneficial to later stages of wound healing.

Lastly, a comment on the controls: the size of wounds (macroscopically and microscopically as well as the ETs) did not differ strongly between wounds treated for one time with 0.1 % DMSO or repetitively with 0.1 % DMSO. This was already observed when testing the toxicity of DMSO on the human skin *ex vivo* but could be shown here again. This confirms that treatment with 0.1 % DMSO was harmless for the skin.
On the other hand, repetitive treatment with 10 µM SG did not promote *ex vivo* wound healing at all and is thus not suited as a positive control under these treatment conditions.

5.10 There seems to be sex-specific differences in response to S2891, S2149, and S1180 in the wound healing organ culture

There can be striking differences in the reaction to and the effect of a drug depending on the sex (Franconi & Campesi, 2014). Moreover, there are differences in wound healing depending on the sex of the patient, especially in elderly. Among other things, this is because estrogen can support cutaneous wound healing (Gilliver & Ashcroft, 2007). Another factor to consider is that male abdominal skin is in average much more hairy than female abdominal skin and hair follicles play an important role in skin repair. For example, they serve as epithelial stem cell reservoir (Ansell *et al.*, 2011; Ito *et al.*, 2005; Ito & Cotsarelis, 2008).
Due to the female beauty ideal and its importance in our society, the vast majority of skin donors available are female. That is why so far, the substances were only tested on female skin. As a male donation was available during the scope of this work, the 3 inhibitors were tested on male wound healing. As repetitive treatment was not found too successful, one-time treatment was chosen. S2149 and S2891 were tested in a concentration of 1 µM. S1180 as the most successful was tested in 1 µM and 10 µM.

When evaluating the relative top-view wound area and perimeter two things caught the eye: 10 µM SG and 1 µM S2149 did not aid the wound closure at all, while 1 µM S2891 reduced both area and perimeter strongest. S1180 seemed beneficial in both concentrations on the relative area, but only 1 µM S1180 could influence the relative perimeter positively. Here already, a difference to the female skin becomes noticeable, where S1180 clearly was the most promising of the candidates regarding the top-view wound closure and SG was chosen as a positive control because it displayed a positive effect on the top-view parameter. Also, in female skin the relative top-view wound area was smaller than the vehicle control, while the contrary is true in this male skin.

In the microscopic area and diameter, the harmful effect of S2149 is again striking – the microscopic area and diameter of wounds treated with 1 µM S2149 were the largest by far. None of the other substances tested led to a smaller area than the vehicle control, but the difference was not as striking. Only treatment with 1 µM S2891 resulted in a smaller wound diameter than the vehicle control. The positive influence of 1 µM S2891 really becomes clear when evaluating the ETs. In all parameters measured here the S2891 performed better than the vehicle control. 1 µM S1180 also seemed beneficial for formation of ETs (but not in the normalized ETs). 1 µM S1180 also resulted in larger and longer ETs than the vehicle control, one can assume a positive effect on the wound healing anyhow.
As before, 10 µM S1180 and 1 µM S2149 had a negative effect on wound healing.
Surprisingly, huge and long ETs were also observed after treatment with 10 µM SG – contrary to the other evaluations. Possible explanations for differences in top-view and microscopic parameters are discussed in **Chapter 5.14**.

The CK 6 expression is not consistent between the inner and outer ETs. In the inner ETs only treatment with 1 µM S1180 resulted in an increased CK 6 expression, while in the outer ETs treatment with 10 µM SG and 1 µM S2891 was especially successful. The differences are relatively small and the standard deviation relatively large though. So, this might be just by chance. Further repetitions are needed to determine if this is the case, or if e.g., the missing wound bed for the outer ETs plays a role.

The differences in intensity of the CD31 expression are relatively small, but 1 µM S2891 showed the highest relative CD31 intensity. Overall, treatment with 1 µM S2891 seems beneficial for endothelial cells in the male WHOC – as did treatment with 1 µM S1180, but not 10 µM S1180.

It is noteworthy, that in the female WHOC 10 µM S1180 was found at least as effective in aiding wound healing as 1 µM S1180 if not more so. In the male WHOC 10 µM S1180 did not show a convincing effect on the *ex vivo* wound healing, while 1 µM S1180 did. This could be another example of the fact, that male and female patients might need different doses of medication for optimal treatment results (Franconi & Campesi, 2014).

To summarize, a distinct difference in the reaction to treatment could be observed between male and female skin. This was a first trial study with only one biological replicate. Repetition of this experiment is necessary, before a definitive statement can be made. A point that underlies this finding is the fact that skin 20-003 was also from a male donor and here SG aided the top-view wound closure at least to some extent (data not shown). Nonetheless this experiment still hints, that there is a striking difference in male and female wound healing.
For wound healing studies the same is true as for so many other fields of medical research: it is crucial to look at both sexes, to ensure that the experimental findings can later successfully be transferred into the clinics.
Inhibition of TrkA by S2891 appeared to be much more beneficial for male than for female wound healing while the GPR119 agonist S2149 did not aid wound healing in the male skin at all. Also, SG did not function as a proper positive control here. If these findings can be reproduced, further research is needed to explain these differences.
One could speculate that the increased amount of hair follicles or the different hormone levels play a role here. Indeed, sex steroids are known to influence wound healing *in vivo.* For skin wounds, estrogen was found to accelerate the wound healing rate, while androgen slowed cutaneous wound

healing down. It would be interesting to investigate, whether these systemic influences also effect the skin in the WHOC (Ashcroft *et al.*, 2003; Ashcroft & Ashworth, 2003; Ashcroft & Mills, 2002; Tripathi *et al.*, 2019). If this is the case, one could then examine whether and in which way sex steroids interact with the signaling pathways S2891, S2149, and S1180 influence.

5.11 Treatment with S1130 inhibits *ex vivo* wound healing

The focus of this work was on finding candidates that aid wound healing, but it is also possible to learn more about wound healing by studying candidates that interfere with wound healing. Moreover, I wanted to test how reliable the results of the screening were. That is why the candidate that performed worst in the screening – the surviving inhibitor S1130 – was more closely evaluated in a proof of principle study.

Just like in the screening, S1130 worsens the *ex vivo* wound healing in the WHOC. Already in the top-view microscopic pictures it becomes apparent that no new epithelium is formed after treatment with 1 µM S1130. This also reflects in the top-view evaluation. Relative top-view wound area and perimeter do not decrease over the course of the culture, as they do for the vehicle control wounds. Hence, wounds treated with S1130 showed less top-view wound closure than both controls. Here again treatment with 10 µM SG resulted in a larger wound area and perimeter than the vehicle control, but at least a decrease in both perimeters was observed.

The harmful effect of S1130 on the *ex vivo* wound healing really shows in the H&E staining and its evaluation. Wounds treated with 1 µM S1130 showed only very small ETs, a large microscopic wound area and diameter, and in the microscopic pictures a slight detachment of the epidermis from the dermis is visible. Both controls on the other hand, display clear signs of wound healing: large and long ETs, a smaller microscopic wound area and diameter and the skin remained intact after treatment.
Microscopically 10 µM SG led to well healing wounds. This is surprising as no beneficial effect could be detected in the top-view evaluation. For more on why top-view and microscopic data do not always match, see **Chapter 5.14**.

The relative CK 6 expression was also reduced in wounds treated with 1 µM S1130, though the effect was not as striking as the findings before. The immunofluorescence pictures show, that the CK 6 expression after treatment with S1130 seems to be restricted to the lower layers of the epidermis only, while the entire epidermis expressed CK 6 in the control groups. Maybe the lower layers of the epidermis could still express CK 6 as they were not as directly exposed to S1130 as the upper layers of the epidermis.

While the relative CD31 expression and the number of CD31 positive vessels seems unaffected by treatment with S1130, a clear decrease in number of CD31 positive cells and cross section was observed. This indicates that S1130 also impairs angiogenesis in the WHOC.

The cortactin expression was comparably strong in wounds treated with 1 µM S1130 and the control wounds, so S1130 probably did not interfere with the remodeling of the cytoskeleton but inhibits wound healing in another way.

S1130 is a survivin inhibitor (https://www.selleckchem.com/products/YM155.html, last used July 21, 2023). Survivin belongs to the inhibitor of apoptosis protein family. As their name suggests, these

proteins play an important role in cell survival by inhibition of apoptotic processes. Unlike its family members, Survivin also is crucial in regulating cell proliferation. Survivin is only expressed in few adult, non-tumor human tissues, but skin is one of them. Here, survivin was found exclusively in epidermal stem cells, where it is probably involved in preservation of their "stem-cellness". Thus, survivin would be essential for remaining the proliferative potential and homeostasis of the epidermis (Dallaglio *et al.*, 2012).
While survivin overexpression is associated with cancerous growth and poor therapy prognosis (Dallaglio *et al.*, 2012), the findings of this work strongly indicate that normal survivin expression is necessary for normal wound healing.
Fittingly, Shojaei-Gharizjani *et al.* reported that in mice treatment of wounds with survivin-overxpressing fibroblasts resulted in better wound healing than control groups (Shojaei-Ghahrizjani *et al.*, 2020). Survivin could be an interesting target for treatment of wounds, but its role in cancer progression must always be kept in mind.

5.12 The pathological conditions tested here were too harsh to study treatment effects in the wound healing organ culture model, regardless of whether the skin was cultivated for 6 or 3 days

So far, all inhibitors were tested on (relatively) healthy female skin. Especially S1180 showed very promising effects here. Wounds had progressed further along the wound healing process when treated with S1180 than the vehicle control wounds. It would be highly interesting to know, if S1180 could also aid healing of chronic wounds, which are "stuck" in one of the phases of wound healing and might not heal at all without treatment.
The pathological model used in this work was based on that of Post *et al.* who established culturing conditions, that mimic a chronic wound by adding 138.8 mM glucose and 100 mM hydrogen peroxide but no insulin to the culture medium and culturing the skin punches in this medium at 5 % O_2 (Post *et al.*, 2021). The idea behind this was that in diabetic foot ulcers, elevated blood glucose levels but decreased insulin levels were found. Moreover, diabetic patients often suffer from poor blood circulation in the extremities and in chronic ulcers elevated levels of oxidative stress were found (Berlanga-Acosta *et al.*, 2013; Eming *et al.*, 2009; Gould *et al.*, 2015; Mekkes *et al.*, 2003; Post *et al.*, 2021).
Post *et al*. also found that 100 nM T4 could aid wound healing under pathological conditions (Post *et al.*, 2021). Hence, in this experiment 100 nM T4 was added as an additional positive control.
Deviating from Post *et al.* the skin was wounded and placed in the retainers as described before. Moreover, the wounds were incubated for 6 days to study wound healing for a longer time period (Post *et al.* incubated the skin biopsies for 3 days (Post *et al.*, 2021)). A culturing period of 7 days was not possible due to availability of the hypoxic incubator. As the wounds should remain under hypoxic conditions for the entire culturing period, top-view microscopy was only possible on day 0 and day 6.

The effect of the pathological medium and hypoxia on the human skin was astonishing. The skin lost its color and became greyish. No formation of new ETs was observable and when taking the skin punches out of the retainers, often the epidermis would detach completely from the dermis. The physiological wounds on the other hand looked healthy and formation of new ETs was seen. Accordingly, the relative top-view wound area and perimeter were larger in pathological wounds than in the respective physiological wounds. The difference between the two groups was not as large as expected after the obviously disastrous state the pathological wounds. An explanation for this could

be, that the evaluation of the discolored wounds was very challenging, as the difference between epidermis and dermis was hard to determine.
A color change was observable in the pathological model. Under pathological conditions the skin seemed almost drained from color and maybe a bit blueish. Hypoxia is known to turn skin blue (Baernstein *et al.*, 2008), so this might be the reason.

A strong effect of treatment with the different substances could not be found in the pathological wounds – probably because they are in such a bad condition.
In the physiological wounds, the relative top-view wound area of the vehicle control wounds was largest. Treatment with 10 µM SG, 100 nM T4, and 1 µM S1180 resulted in very similar, smaller relative areas, though the effect was not significant. Treatment with 10 µM S1180 seemed not quite as promising, which is probably because one of the skins used in this experiment was male. As discussed above, 10 µM S1180 did not seem to aid wound healing as much in male skin as it did in female skin.

The pictures of the H&E stained slides reveal the extent of damage the pathological conditions inflict on the skin. The epidermis seemed thinner and was almost always detached from the dermis. No ETs at all were observable. The fact that the epidermis was detached made the determination of the microscopic wound area and diameter challenging and not very precise. So, this data must be considered with care.
The differences in wound area between in physiological and pathological groups were small, but the differences in diameter were more pronounced. Here, sometimes the controls even had a significantly larger diameter than the pathological wounds. Due to the inaccuracy of the diameter in the pathological group, these findings alone possess little significance.
Within the physiological group, no significant difference could be found in the microscopic wound area and diameter. Treatment with 1 µM S1180 seemed beneficial for formation of ETs, which fits to the previous findings. While resulting in a better top-view closure, treatment with 10 µM SG did not result in formation of longer or larger ETs than the vehicle control. Considerations why top-view and microscopic evaluation do not always go hand in hand in hand can be found in **Chapter 5.14**.
10 µM S1180 did not show a convincing influence on the formation of ETs or top-view wound healing which probably is due to the one male skin included here. In **Figure 5.4** the relative top-view wound area at day 6 of the physiological wounds are shown – this time separated between the one male and the two female skin donors.

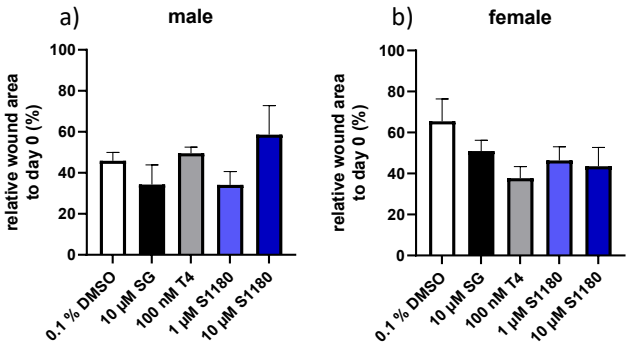

Figure 5.4: The relative top-view wound area of the physiological wounds at day 7 seperated between the male and female donors
a) The relative top-view wound area of the male donor (n = 1, 2-4 wounds/condition), b) the relative top-view wound area of the female donors (n = 2, 1-3 wounds/condition). DMSO = dimethyl sulfoxide, SG = sodium gualenate, T4 = L-thyroxine

The difference, especially regarding the effect of treatment with 10 µM S1180 becomes apparent here. In the male patient, wounds treated with 0.1 % DMSO healed better than in the females, while the beneficial effect of wounds treated with 10 µM S1180 only becomes apparent in female patients. This interesting finding has to be validated to make sure it is not just by chance, as only few repetitions were performed so far.

Pathological wounds expressed no CK 6 at all, while the physiological wounds did so. Within the physiological group 1 µM S1180 seemed most promising in the inner and 100 nM T4 in the outer ETs. The CK 6 evaluation again shows that the pathological conditions tested here were too harsh to study whether S1180, SG, or T4 can aid pathological wound healing.

The relative CD31 intensity was lower in the pathological wounds than in the physiological wounds – in some groups even significantly so. Interestingly, the number of CD31 positive cells is similar under both conditions and shows the same patterns. Both, under physiological and under pathological conditions wounds treated with 1 µM S1180 had the highest number of CD31 positive cells. This could indicate, that within the dermis, which is not as exposed to the harsh pathological conditions, angiogenesis also occurs to a certain degree in the pathological model. Moreover, S1180 might be beneficial for this process in the pathological wounds also.
The significantly increased number of CD31 positive cells after treatment with 1 µM S1180 in the pathological wounds compared to the physiological wounds could support this finding further.
The number of CD31 vessels is significantly lower in pathological wounds than in physiological wounds, but similar in pathological and physiological wounds treated with S1180. Angiogenesis is especially crucial under hypoxic conditions, and it seems that S1180 aids this process also under hypoxia. As the Wnt/β-catenin pathway is often associated with angiogenesis (Han *et al.*, 2016; Jiang *et al.*, 2015), further research is needed to understand how S1180 can have a positive effect on endothelial cells in the WHOC.

As previously described, the pathological conditions were so harsh that ETs could not form. Therefore, further comparison of the different treatment groups did not appear useful. Accordingly, KiTUNEL staining was performed only on the vehicle controls. This staining proved, what was already assumed before: Under pathological conditions the epidermis shows significantly more TUNEL positive, i.e., dying cells than the physiological wounds and less Ki67 positive, i.e. proliferating cells than the physiological wounds. The fact that more than 70 % of the keratinocytes showed signs of cell death under pathological conditions, while proliferating cells are absent is striking.
Fittingly to the high number of dying cells and absence of proliferating cells, the wounds under pathological conditions scarcely expressed cortactin, indicating that cytoskeleton rearrangement and migration of keratinocytes were also hindered. Just like the H&E staining, the cortactin staining and the CK 6 staining showed that the epidermis had detached under pathological conditions and was very thin.

As the 6 days long pathological model clearly is too harmful to the skin to study the effect of any sort of treatment, in the next step the wounds were only cultured for 3 days under pathological conditions. Post *et al.* also cultured the skin for 3 days and did not observe the clear signs of degradation found here (Post *et al.*, 2021). So, I hypothesized that maybe with a shorter cultivation period, skin damage would be manageable.

The top-view evaluation of the 3 days culture shows that the discoloration of the skin is much less apparent than it was after 6 days. The wounds look “healthier”, and the epidermis did not detach as easily as in the 6 days culture. For wounds treated with 10 mM SG and 100 nM T4 the relative top-view wound area was even smaller in pathological wounds than in physiological wounds. Though the effect was not as strong as in longer cultures, S1180 seemed beneficial for top-view wound closure under physiological conditions.

However, the H&E staining revealed skin damage already after 3 days. A detachment of the epidermis was visible and absolutely no ETs could be found. As for the 6 days model, evaluation of the area and diameter was difficult here due to the detachment.
When assessing the microscopic data, the extremely large microscopic wound area of pathological wounds treated with 100 nM T4 catches the eye. As T4 did not perform as badly in any other parameters this is likely an outlier or an experimental mistake.
Especially in the outer ETs, treatment with both concentrations of S1180 seemed beneficial for ET formation.

Just like the 6 days model, almost no CK6 expression was measured for the pathological wounds, that were incubated for 3 days. The only exception was found in pathological wounds treated with 10 µM SG, where in some ETs the measured CK 6 expression was very high. As the wounds otherwise looked rather poor and the CK 6 expression was not high in all sections of this wound, likely some sort of mistake occurred during the staining process. A repetition of this staining wound make sense to confirm this.
Treatment with S1180 seemed to increase the relative CK 6 expression in the outer ETs of physiological wounds at least.

In the 3 days model the relative CD31 intensity was similar between pathological and physiological wounds. The number of cells and cross sections was noticeably higher in pathological wounds treated with 10 µM SG and 100 nM T4. This could indicate, that in the shorter cultures the positive controls were able to increase angiogenesis in the pathological wounds. However, the high error bars must be kept in mind here.
It is surprising, that there were almost no positive cross sections in wounds treated with S1180. This experiment was only performed once and in the other experiments treatment with S1180 always resulted in several CD31 positive cross sections. So, this finding here is likely an outlier or it could indicate that the positive effect on the CD31 positive cells manifests later in the culture.
The number of CD31 vessels was higher in all physiological wounds compared to the pathological ones.
The CD31 staining did not show a cohesive picture whether treatments increased angiogenesis. So, further repetition would be needed here.

The KiTUNEL staining again visualizes how harmful the pathological conditions were. Even in the wounds which were only cultivated for 3 days more than 70 % of keratinocytes at the wound edges were TUNEL positive, while no Ki67 positive cells were found in the pathological wounds.

Interestingly, there was a distinct cortactin expression visible if wounds were incubated for only 3 days under pathological conditions. This indicates that the skin might be a bit more “alive” in the short pathological model compared to the 6 days culture – though the epidermis was still detached from the dermis.

Clearly the pathological model did not work in the way it was intended to. The model was developed by Post *et al.* to study pathological wound healing (Post *et al.*, 2021). So, skin damage and delay in wound healing to some extend was expected. However, in this work the conditions were too harsh. They impaired wound healing in the WHOC completely. Especially after 6 days of cultivation the epidermis formed no new ETs but instead detached from the epidermis. This detachment could be due to the skin degrading under pathological conditions and thus losing the interactions between epidermis and dermis.
These findings are in contrast with what Post *et al.* demonstrated. While they also observed epidermal detachment, skin damage, and signs of cell death, still ETs formed, and a healing process could be evaluated. A possible explanation could be that in this work the medium was preincubated under hypoxic conditions to ensure a continuous hypoxia. Post *et al*. do not explicitly state that they also did this (Post *et al.*, 2021). If the medium is prepared directly before adding it to the skin samples, it will bring fresh oxygen into the model, probably making it less harsh. Also, the pH value of the medium will stay constant. If the medium is pre-incubated under hypoxic conditions it switches color from red to pink/transparent. This could indicate a harmful pH switch. Both factors – continuous hypoxia and a strong pH switch could explain why the pathological model here was so much more harmful that that of Post *et al* (Post *et al.*, 2021).
Post *et al*. did not perform a punch-in-a-punch approach, instead they took 4 mm skin punches and evaluated wound healing of the outer ETs. The 2 mm wound in the 4 mm skin punches of this work might have facilitated epidermal detachment to a degree, where formation of ETs was no longer possible. Furthermore, Post *et al.* used facelift and head skin, which is more coarse and more hairy than the abdominal skin used in this work (Post *et al.*, 2021). Maybe abdominal skin is more sensitive to the pathological conditions than head skin.
Moreover, the wound healing aiding effect of 100 nM T4 published by Post *et al.* (Post *et al.*, 2021) could not be reproduced in this study – not even under physiological conditions. It was observed that T4 dissolved poorly in the culture medium. I wanted to stick to the protocol given to us by Post *et al.* but maybe another solvent would have been better.

Whitin the physiological group, treatment with S1180 overall again showed a promising effect on wound healing. That 10 µM S1180 was not as successful as in previous experiments is probably due to the fact that one of skin donors for the 6 day model was the same male used for the evaluation of the 3 substances on male skin.

5.13 Sodium gualenate – an unreliable positive control at best

Throughout this work, 10 µM SG was shown to be an unreliable positive control. While it showed a beneficial effect on the top-view wound closure in the initial search for a suitable positive control, this finding was not always reproducible. Moreover, even if SG showed a positive effect on the top-view wound area, it did not always do so in the H&E evaluation. As the literature regarding the effect of SG on skin and wound healing is rather sparse, I took a closer look onto the cultures performed and how those where SG worked and where it did not might differ. **Table 5.2** shows the results of this investigation.

Table 5.2: Differences in skin donations from wound healing organ cultures where sodium gualenate (SG) aided wound healing or did not aid wound healing
Same day delivery means that the skin reached our lab on the day of the surgery.

Parameter	SG aided *ex vivo* wound healing	SG did not aid *ex vivo* wound healing
Mean year of birth	1976	1978
Anatomical location	80 % abdomen, 12 % breast, 4 % thigh, 4 % upper arm	76 % abdomen, 24 % breast
Same day delivery	60 %	29 %

As can be seen in **Table 5.2** skin donors were of similar age in both groups and most of the skin used was abdominal skin. These two findings cannot explain why SG did not always work. But it shows that our WHOC model is rather robust regarding age and anatomical skin location if enough repetitions are performed. However, there is a large difference regarding the amount of same day delivery. In the experiments were SG worked, the skin was of the same day in 60 % of all deliveries, while this was only the case for 29 % of the skin donations where SG did not aid wound healing. Same day delivery does not necessarily mean that the experiment was performed on that day. Sometimes, the skin was still cooled overnight. Nevertheless, in the cases where the skin arrived at the day of surgery instead of overnight transport, a proper cooling of the samples is without doubt. Although we take precaution that the skin is cooled on transportation, long transportation ways, delays in pick-up and other difficulties might arise on the way and interfere with proper cooling of the skin samples. If the skin is not transported at 4 °C this might damage the skin and change its responses to treatment. As the effect of 10 µM SG was not extremely strong from the beginning, this could be one reason why SG did not aid wound healing in all WHOCs.

Another thing to keep in mind is that we only use skin from healthy donors, but it cannot be ruled out that they might have an underlying, undiagnosed disease or take some kind of medication. As little is known about how SG interacts with different diseases or medications, this could also influence the results. For a substance with a strong influence on wound healing, such as S1180, this will probably not play an important role, but if the effect on the WHOC is not as pronounced, little factors might make the difference.

Lastly, SG is instable as a solid according to the manufacturer (https://www.selleckchem.com/products/sodium-gualenate.html, last used December 22, 2022). While the manufacturer does not state something about its stability when dissolved, it is conceivable that multiple thaw-and-freeze-cycles of aliquots are especially harmful for the effect of SG.

All in all, more in depth research is needed to really understand this finding. One would have to look at the signaling pathways SG influences and how those relate to aiding wound healing in some patients while slightly worsening the wounds in other patients.

5.14 The struggle with conflicting top-view and microscopic results

Ideally, top-view, OCT, and microscopic data (i.e., H&E evaluation) would match, meaning that a good top-view wound closure and a small wound volume resulted in a small microscopic wound with long ETs. Often this is the case. However, there were experiments where macroscopic and microscopic data did not fit together. To name a few examples: in **Chapter 4.8** treatment with 4 x 1 µM S1180 resulted in the smallest microscopic area, but not in the smallest relative top-view wound area, perimeter, or wound volume. Another example is the experiment in **Chapter 4.11**, where treatment with 10 µM SG did not result in a good top-view wound closure but still large and long inner ETs formed. The opposite was observed in **Chapter 4.12**: Here, physiological wounds treated with 10 µM SG resulted in a reasonably well top-view wound closure, but the ETs formed were smaller and shorter than those of the vehicle control wound.

There are some explanations why macroscopic and microscopic data do not always fit together. One issue is the before mentioned fact, that the wounds do not always heal in a circular fashion (compare **Figure 5.1**). If a wound heals into more of an oval shape, depending on the direction the wound is later cut, the diameter and thus the area can vary immensely. If the wound is cut at the short site, this could result in a much smaller microscopic area and perimeter than excepted when looking at the top-view wound closure and vice versa.
As stated before, during the culturing period, the skin becomes softer, which can lead to two opposite phenomena: the wounds can either collapse or diverge. Both can happen during the culture or at the end of the it when the wounds are placed into the paraffin cassettes. If a wound does not heal well, but collapses during the embedding process, the top-view wound area and perimeter would be rather large, while the microscopic wound area and diameter would be small. The opposite would be true for a well healing wound, that diverges during the embedding process. That is why it is crucial to always also assess the inner ETs. If a wound heals, clearly visible, large ETs will form. Normalization of the inner ETs on the diameter can help with the assessment. As the time course experiment **Chapter 4.1** showed, in healing wounds an increase in normalized and non-normalized inner ETs' area and length should be measurable.
For the physiological wounds treated with 10 µM SG in **Chapter 4.12**, a collapse of the wounds during the culture is probable. For the wounds treated with 10 µM SG in **Chapter 4.11**, the wounds might have diverged during the culture. This could result in a larger wound, that even the quite long and large ETs could not span sufficiently to make an impact in the evaluation. As this experiment was only performed once it is especially likely that this contradiction can be explained by experimental challenges.
The example of wounds treated repetitively with 1 µM S1180 in **Chapter 4.8** possesses another layer of complexity as here also OCT-measurements were available. In general, a relatively large top-view wound area and perimeter but a very small microscopic one could be explained by a shallow wound at the end of the culture. This could be either due to not punching the wounds deep enough or by formation of a lot of granulation tissue, i.e., a well healing wound. However, in this case the wound volume of wounds treated with 4 x 1 µM S1180 was higher than all other conditions tested in this experiment. OCT measurements were performed at day 6 and the final evaluation at day 7. So, the wounds had a bit more time to heal but this likely does not explain the differences entirely. Probably the wounds collapsed a bit, leading to a smaller microscopic wound area.
These considerations show that the microscopic wound area and diameter are prone to deformations when using abdominal or breast skin. Here, further improvement of the embedding process seems sensible. It would be helpful to develop a sort of cassette that can stabilize the wounds so that the soft tissue does not distort so easily.
To summarize: Most of the time macroscopic and microscopic evaluation go hand in hand. Smaller differences between different evaluation methods can be explained by measuring inaccuracy. Larger differences are most likely due to either not circularly healing wounds or distortion of wounds during the culture or during the embedding process.

Summary and Outlook

My work established the WHOC as a screening platform for discovering new wound healing targets. Though there are some challenges with this model, as the high donor-to-donor variations and the tendency of the wounds to collapse, the WHOC was found to be an efficient and successful model. Determination of top-view wound closure in combination with wound volume determination with OCT were found to be a comparatively fast, non-invasive, and sufficient way of testing large numbers of different substances. The findings of this macroscopic wound healing need further evaluation and

assessment of more parameters, such as microscopic parameters, but macroscopic evaluation can serve as a mean to filter out non-successful treatment strategies.
With the tankyrase inhibitor S1180 a promising and highly interesting target to aid wound healing was discovered.
In the next steps, it would make sense to test more different concentrations of S1180 in the WHOC, as 1 µM S1180 and 10 µM S1180 both aided wound healing. Higher concentrations could be tested to see if the maximum effect has already been reached. 0.1 µM S1180 did not prove as promising as 1 µM S1180. That is why lower concentrations probably do not need to be tested further. On the other hand, concentrations between 1 µM and 10 µM S1180 would be worth investigating. Once the optimal concentration range of S1180 in the WHOC is found, further investigations regarding the exact mode of action of S1180 would be of interest. For example, the exact genes and signaling pathways activated after inhibition of the Wnt/β-catenin pathway should be studied.
Moreover, the development of a less harsh pathological model would be beneficial to investigate the effect of S1180 under these conditions. It might also be interesting to test S1180 in an animal model – preferably in a porcine model – to see if application of S1180 has side effects on a whole organism and how it aids wound healing in an *in vivo* situation.

Appendix

Ethics votes

UNIVERSITÄT ZU LÜBECK

Universität zu Lübeck · Ratzeburger Allee 160 · 23538 Lübeck

Herrn
PD Dr. med. Tobias Fischer
Klinik für Dermatologie und Venerologie

im Hause

Ethik-Kommission
Vorsitzender:
Herr Prof. Dr. med. Dr. phil. H. Raspe
Stellv. Vorsitzender:
Herr Prof. Dr. med. F. Gieseler
Universität zu Lübeck
Ratzeburger Allee 160
23538 Lübeck

Sachbearbeitung: Frau Janine Erdmann
Tel.: +49 451 500 4639
Fax: +49 451 500 3026
janine.erdmann@medizin.uni-luebeck.de

Aktenzeichen: 06-109
Datum: 15. März 2012

In-vitro-Untersuchung der Biologie des humanen Haarfollikels in bezug auf Wachstumseigenschaften, Apoptose, Wachstumsregulation, Pigmentierung und Immunprivileg im Haarorgankulturmodell
Hier: Amendment 2 –Ihr Schreiben vom 13. März 2012

Sehr geehrter Herr Dr. Fischer,

das Amendment bezüglich der Nutzung von Haut aus anderen behaarten Arealen mit den folgenden Unterlagen habe ich zustimmend zur Kenntnis genommen:

- Aufklärung und Einwilligung sowie
- Studienprotokoll.

Es bedarf keiner weiteren Begutachtung durch die Kommission.

Bitte beachten Sie folgenden Hinweis: Die Haarproben können nur vernichtet werden, wenn diese in pseudonymisierter Form vorliegen.

Die ärztliche und juristische Verantwortung des Leiters der klinischen Prüfung und der an der Prüfung teilnehmenden Ärzte bleibt entsprechend der Beratungsfunktion der Ethikkommission durch unsere Stellungnahme unberührt.

Mit freundlichem Gruß und besten Wünschen
für den weiteren Verlauf Ihrer Forschung bin ich
Ihr

Prof. Dr. med. Dr. phil. H. Raspe
Vorsitzender

UNIVERSITÄT ZU LÜBECK

Universität zu Lübeck · Ratzeburger Allee 160 · 23562 Lübeck

Frau
Prof. Dr. Hundt, Lübecker Institut für experimentelle Dermatologie (LIED)
im Hause

jennifer.hundt@uni-luebeck.de.de
Ralf.Ludwig@uksh.de

Ethik-Kommission

Vorsitzender:
Herr Prof. Dr. med. Alexander Katalinic
Stellv. Vorsitzender:
Herr Prof. Dr. med. Frank Gieseler

Geschäftsstelle:
Dr. phil. Angelika Hüppe
Dr. rer. nat. Inga Kaufhold
Janine Kurzaj-Erdmann
Doris Seuthe

E-Mail: ethikkommission@uni-luebeck.de

Website: www.uni-luebeck.de/forschung/kommissionen/ethikkommission

Aktenzeichen: 21-191
Datum: 12. November 2021 DS/IK

Sitzung der Ethik-Kommission am 03. Juni 2021, Nachreichung vom 30. September 2021 und 08. November 2021
Antragsteller: Frau Prof. Dr. Hundt
Titel: In vitro Untersuchungen der Biologie von Haut und Schleimhaut samt Anhangsgebilden

Sehr geehrte Frau Prof. Hundt,

vielen Dank für Ihre o.g. Schreiben, in denen Sie unserem Wunsch nach weiteren Informationen zum Studienvorhaben nachkommen.

Folgende Unterlagen lagen vor:

- Ihr Anschreiben vom 30. September 2021
- Ihre E-Mail vom 08. November 2021
- Ethikantrag (Basisformular) vom 22. April 2021
- Studienprotokoll Version 1 vom 30. September 2021
- Geänderte Patienteninformationen
- Geänderte Einwilligungserklärung
- Erklärung zur Körperspende

Die Kommission hat gegen die Durchführung der Studie **keine Bedenken**.

Bei Änderung des Studiendesigns sollte der Antrag erneut vorgelegt werden.
Über alle schwerwiegenden oder unerwarteten und unerwünschten Ereignisse, die während der Studie auftreten, ist die Kommission umgehend zu benachrichtigen.
Die Deklaration von Helsinki in der aktuellen Fassung fordert in § 35 dazu auf, jedes medizinische Forschungsvorhaben mit Menschen zu registrieren. Daher empfiehlt die Kommission grundsätzlich die Studienregistrierung in einem öffentlichen Register (z.B. unter www.drks.de).
Die ärztliche und juristische Verantwortung des Studienleiters und der an der Studie teilnehmenden Ärzte bleibt entsprechend der Beratungsfunktion der Ethikkommission durch unsere Stellungnahme unberührt.
Datenschutzrechtliche Aspekte von Forschungsvorhaben werden durch die Ethikkommission grundsätzlich nur kursorisch geprüft. Dieses Votum / diese Bewertung ersetzt mithin nicht die Konsultation des zuständigen Datenschutzbeauftragten.

Mit freundlichem Gruß

Prof. Dr. med. Alexander Katalinic
Vorsitzender

Information sheet for the patient

UNIVERSITÄTSKLINIKUM Schleswig-Holstein –Campus Lübeck
Lübecker Institut für Experimentelle Dermatologie Ratzeburger Allee 160 23538 Lübeck

Entnahmestelle:.....

Geschlecht:.....

Alter:.....

Lübecker Institut für Experimentelle Dermatologie

LIED – Lübecker Institut für Experimentelle Dermatologie
Direktorium: Prof. Dr. Hauke Busch
Prof. Dr. Saleh Ibrahim
Prof. Dr. Ralf Ludwig
Prof. Dr. Dr. Enno Schmidt

Prof. Dr. med. vet. Jennifer Hundt
Tel: 0451 / 500-80810
Fax: 0451 / 500-50888
E-Mail: jennifer.hundt@uni-luebeck.de

„*In vitro*-Untersuchung der Biologie des humanen Haarfollikels in Bezug auf Wachstumseigenschaften, Apoptose, Wachstumsregulation, Pigmentierung und Immunprivileg im Haarorgankulturmodell“

Patienteninformation

Sehr geehrte Patientin,
sehr geehrter Patient,

wir wollen eine medizinische Versorgung auf hohem Niveau bieten und diese auch konsequent verbessern. Daher ist zusätzlich zur Patientenversorgung die Forschung eine wichtige Aufgabe in unseren Kliniken. Hierzu bitten wir Sie nachfolgend um Ihre Unterstützung.

Bitte lesen Sie sich diese Patienteninformation sorgfältig durch und fragen Sie Ihren Arzt, wenn Sie etwas nicht verstehen oder zusätzlich etwas wissen wollen.

In Kooperation mit anderen Institutionen sowie Forschungslaboren der Industrie werden von uns wissenschaftliche **Projekte zur Erforschung der Funktion sowie der Erkrankungen der Haut und ihrer Anhangsgebilde (Haare, Nägel, Talgdrüsen, Schweißdrüsen)** durchgeführt. Ferner werden neue Behandlungsmöglichkeiten sowie die Entstehung, der Verlauf und die Behandlung von Hautalterung, Wundheilung und Haarwuchsstörungen untersucht. Für derartige wissenschaftliche Untersuchungen werden Gewebeproben von menschlicher Haut und ihren Anhangsgebilden benötigt.

Ihre Haut- bzw. Haarprobe verwenden wir v.a. für sogenannte Haut- bzw. Haarfollikel-Organkulturen, die in unserem Labor an der Universität zu Lübeck angelegt werden und an denen wir verschiedene wissenschaftliche Fragestellungen untersuchen (einige davon in enger Zusammenarbeit mit wissenschaftlichen Kooperationspartnern im In- und Ausland). Ferner versuchen wir anhand dieser Proben, bestimmte Hautzellen gezielt zu isolieren und zu kultivieren, die Expression von bestimmten Proteinen und Genen zu analysieren oder zu verändern und/oder die Gewebereaktion auf verschiedene Testsubstanzen zu untersuchen.

Ihr Gewebe fällt im Rahmen einer medizinisch notwendigen Maßnahme an. Für unsere Untersuchungen wird ausschließlich solches Gewebe verwendet, das aus medizinischen Gründen entnommen werden musste und das andernfalls entsorgt und ungenutzt verworfen werden würde (**es wird kein zusätzliches Gewebe entnommen,** und alle evtl. notwendigen diagnostischen Maßnahmen sind vor der Weitergabe des Gewebes an uns abgeschlossen).

Zwar können von den geplanten wissenschaftlichen Untersuchungen kein direkter Einfluss auf den gewünschten OP-Verlauf bzw. auf Ihren Krankheitsverlauf oder die Behandlung Ihrer Krankheit erwartet werden, aber Sie leisten durch Ihre Bereitschaft, Hautgewebe zu wissenschaftlichen Zwecken zur Verfügung zu stellen, einen sehr wichtigen Beitrag zum besseren Verständnis und zur besseren Behandlung der Haut und ihrer Anhangsgebilde. Die Ergebnisse dieser Untersuchungen können in Zukunft für andere Patienten oder Patientinnen von großer Bedeutung sein.

Ihre Teilnahme an diesem Vorhaben ist freiwillig. Sie haben jederzeit und ohne Angabe von Gründen das Recht, von diesem Vorhaben zurückzutreten. In diesem Fall würden wir Ihre bereits verwendeten Haut- und Hautanhangsgebilde im oben genannten Vorhaben nicht weiter einsetzen und die daraus resultierenden Daten nicht veröffentlichen. Die Nichtteilnahme bzw. der Widerruf Ihrer Einwilligung sind für Sie ohne Nachteile für Ihre ärztliche Weiterbehandlung. Ihre anonymisierte Gewebeprobe kann auch zu wissenschaftlichen Zwecken anderen, mit uns kooperierenden Forschergruppen (auch außerhalb der Universität zu Lübeck) zur Unterstützung und zum Fortschritt der Forschung weitergegeben werden (anonymisiert). Sollte das Gewebe bereits an andere Zentren weitergegeben worden sein, so können Sie auch dann Ihre Einwilligung jederzeit zurücknehmen. In diesem Fall werden die Gewebeproben zurückgefordert und Ihrem Wunsch entsprechend vernichtet und die dazugehörigen Daten gelöscht.

Die Untersuchungen, zu denen Ihre Haut und Ihre Hautanhangsgebilde verwendet werden sollen, sind von der Ethikkommission der Medizinischen Fakultät der Universität zu Lübeck für unbedenklich erachtet worden. Ihr Gewebe, welches während der experimentellen Studie vollständig verwendet werden wird, wird für keine anderen als den hier dargestellten Untersuchungen verwendet werden. Nach Abschluss der Untersuchung, spätestens aber 10 Jahre nach der Gewebeentnahme, werden alle aus den Untersuchungen resultierenden Daten und Materialien vernichtet werden.

Datenschutzrechtliche Informationen

Die einzigen Angaben, die wir von Ihrem behandelnden Arzt zu Ihrer Gewebeprobe erhalten, sind: Entnahmestelle der Hautgewebeprobe, Ihr Alter und Geschlecht. Dies bedeutet, dass Wissenschaftler oder Personen, die mit Ihren Proben und Daten in weiterführenden wissenschaftlichen Untersuchungen arbeiten werden, nicht wissen werden, von wem diese Proben oder Daten stammen. Sie werden keine Möglichkeit erhalten, diese Proben oder Daten bis zu Ihrer Person zurückzuverfolgen (Anonymisierung der Daten). Dies kann ausschließlich Ihr behandelnder Arzt. Eine zusätzliche Zustimmung für durchgeführte Untersuchungen wird daher von Ihnen nicht nochmals eingeholt. Diese Einverständniserklärung verbleibt bei Ihrem behandelnden Arzt.

Verantwortliche Kontaktperson:
Prof. Dr. med. vet. Jennifer Hundt, Lübecker Institut für Experimentelle Dermatologie

erreichbar unter:
0451 500-80810

Patient consent form

UNIVERSITÄTSKLINIKUM Schleswig-Holstein –Campus Lübeck
Lübecker Institut für Experimentelle Dermatologie Ratzeburger Allee 160 23538 Lübeck

Lübecker Institut für Experimentelle Dermatologie

LIED – Lübecker Institut für Experimentelle Dermatologie
Direktorium: Prof. Dr. Hauke Busch (Geschäftsführ.)
Prof. Dr. Saleh Ibrahim
Prof. Dr. Ralf Ludwig
Prof. Dr. Dr. Enno Schmidt

Prof. Dr. med. vet. Jennifer Hundt
Tel: 0451 / 500-80810
Fax: 0451 / 500-50888
E-Mail: jennifer.hundt@uni-luebeck.de

Patient:.....

Geburtsdatum:.....

2. November 2021

„*In vitro*-Untersuchung der Biologie des humanen Haarfollikels in Bezug auf Wachstumseigenschaften, Apoptose, Wachstumsregulation, Pigmentierung und Immunprivileg im Haarorgankulturmodell“

Einwilligungserklärung

Ich erkläre mich bereit, an dem Forschungsvorhaben „*In vitro*-Untersuchung der Biologie des humanen Haarfollikels in Bezug auf Wachstumseigenschaften, Apoptose, Wachstumsregulation, Pigmentierung und Immunprivileg im Haarorgankulturmodell“ teilzunehmen.

Während meiner Behandlung im/in_____(Praxis/Klinik) am _____(Datum) ist ein ärztlicher Eingriff geplant, der dazu führen wird, das überschüssiges Hautmaterial anfällt. Das dabei anfallende sogenannte Restgewebe (Haut und ihre Anhangsgebilde) stelle ich für wissenschaftliche Untersuchungen im dermatologischen Forschungslabor der Universität zu Lübeck zur Verfügung.

Ich bin von meinem Arzt ausführlich und verständlich über die Teilnahme sowie über Wesen, Bedeutung und Tragweite der Untersuchung und die sich für mich daraus ergebenden Anforderungen aufgeklärt worden. Aufgetretene Fragen wurden mir vom Arzt verständlich und vollständig beantwortet. Außerdem habe ich eine schriftliche Aufklärung über die Studie erhalten

und gelesen. Ich hatte ausreichend Zeit, um die Zustimmung zu meiner Teilnahme an der Untersuchung frei zu treffen. Ich habe zurzeit keine weiteren Fragen mehr.

Ich wurde über datenschutzrechtliche Aspekte dieses Vorgehens informiert, insbesondere darüber, dass die durch meine Teilnahme entstehenden Daten nur anonym weiterverarbeitet und weitergegeben werden. Eine Rückverfolgung der anonymisierten Daten durch Wissenschaftler oder Personen, die mit meinen Proben und Daten arbeiten werden, ist nicht möglich.

Ich behalte mir jedoch das Recht vor, meine freiwillige Mitwirkung jederzeit zu beenden, ohne dass mir daraus Nachteile für meine weitere medizinische Betreuung entstehen. Ich wurde darüber informiert, dass dies ausdrücklich einschließt, dass ich jederzeit eine Löschung meiner Daten verlangen kann.

Mit meiner Unterschrift stimme ich der freiwilligen Teilnahme an der oben genannten Untersuchung zu.

Lübeck, den .....

_____

Name des Patienten in Druckschrift

....

Unterschrift des Patienten Unterschrift des Arztes

Results of the screening Highly Selective Inhibitor Library L3500

a) Relative top-view wound area and perimeter of sub-screening 1 of the clinical trials substances

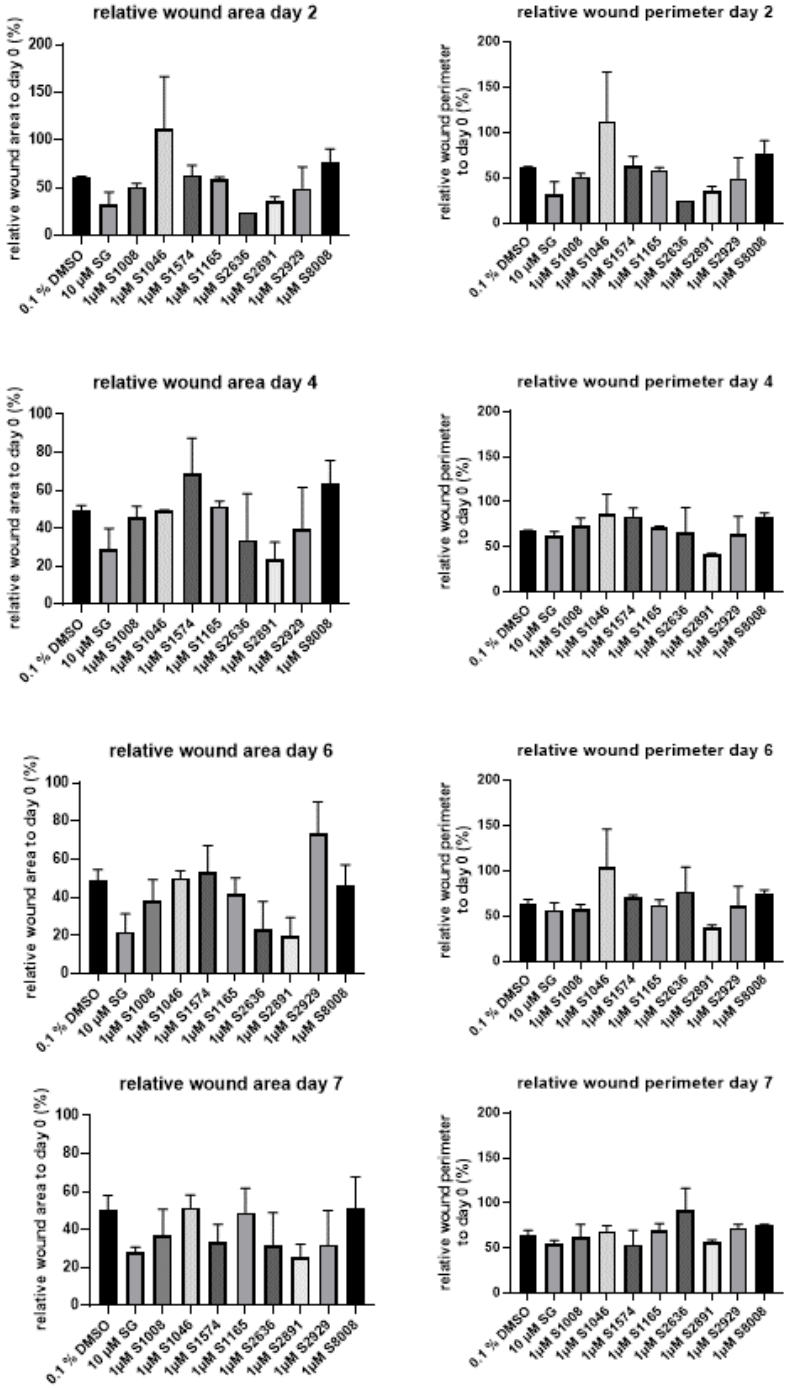

b) Relative top-view wound area and perimeter of sub-screening 2 of the clinical trials substances

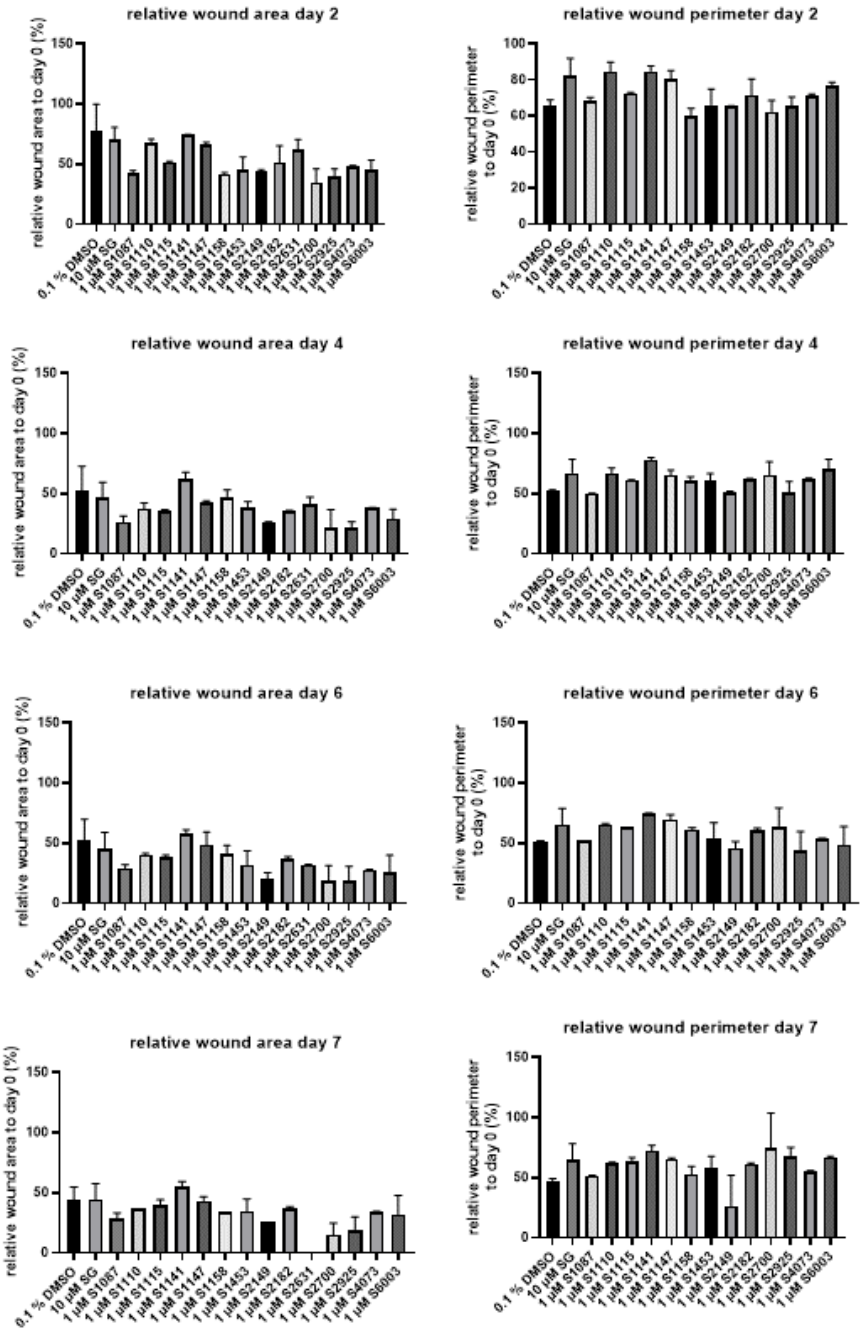

c) Relative top-view wound area and perimeter of sub-screening 3 of the clinical trials substances

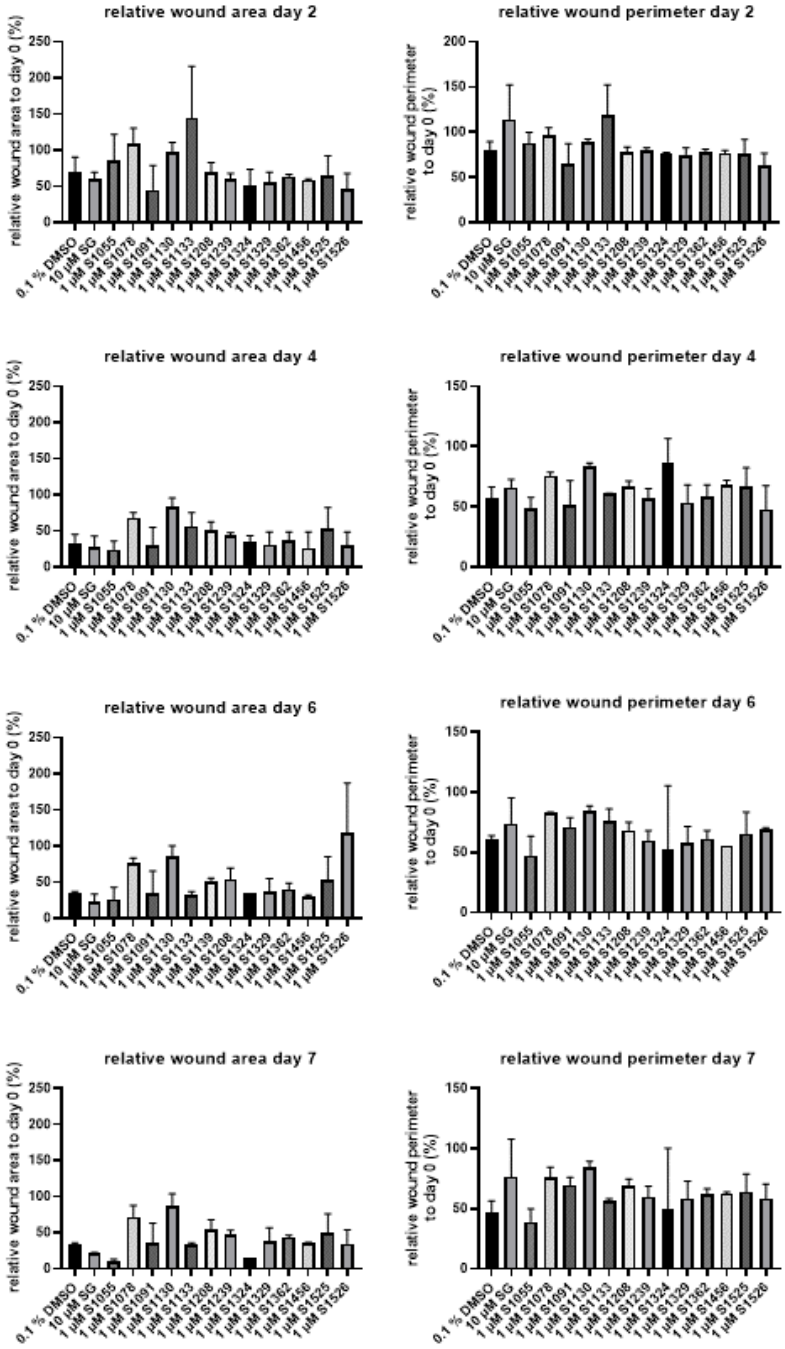

d) Relative top-view wound area and perimeter of sub-screening 4 of the clinical trials substances

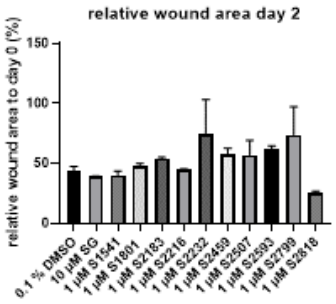

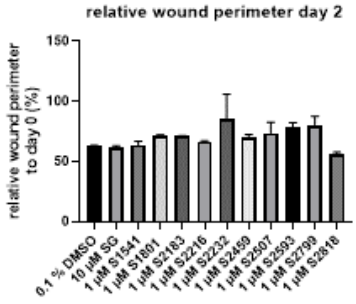

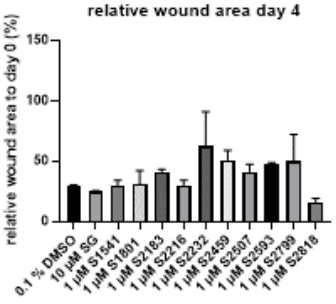

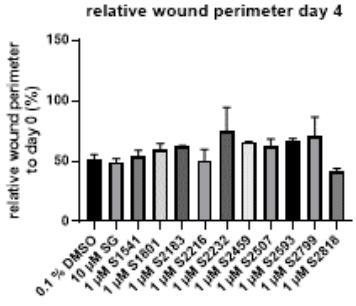

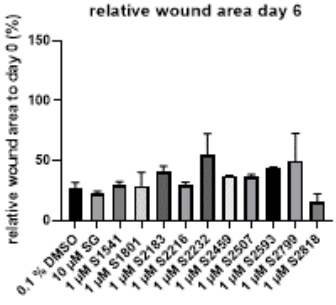

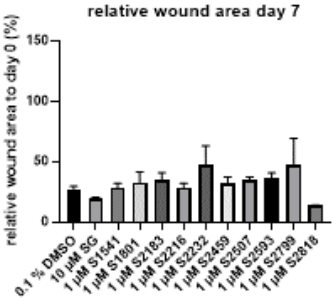

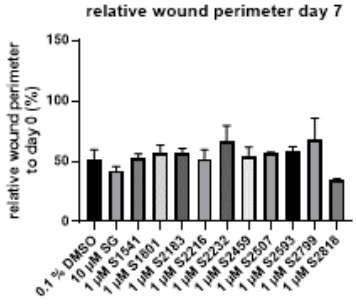

e) Relative top-view wound area and perimeter of sub-screening 5 of the clinical trials substances

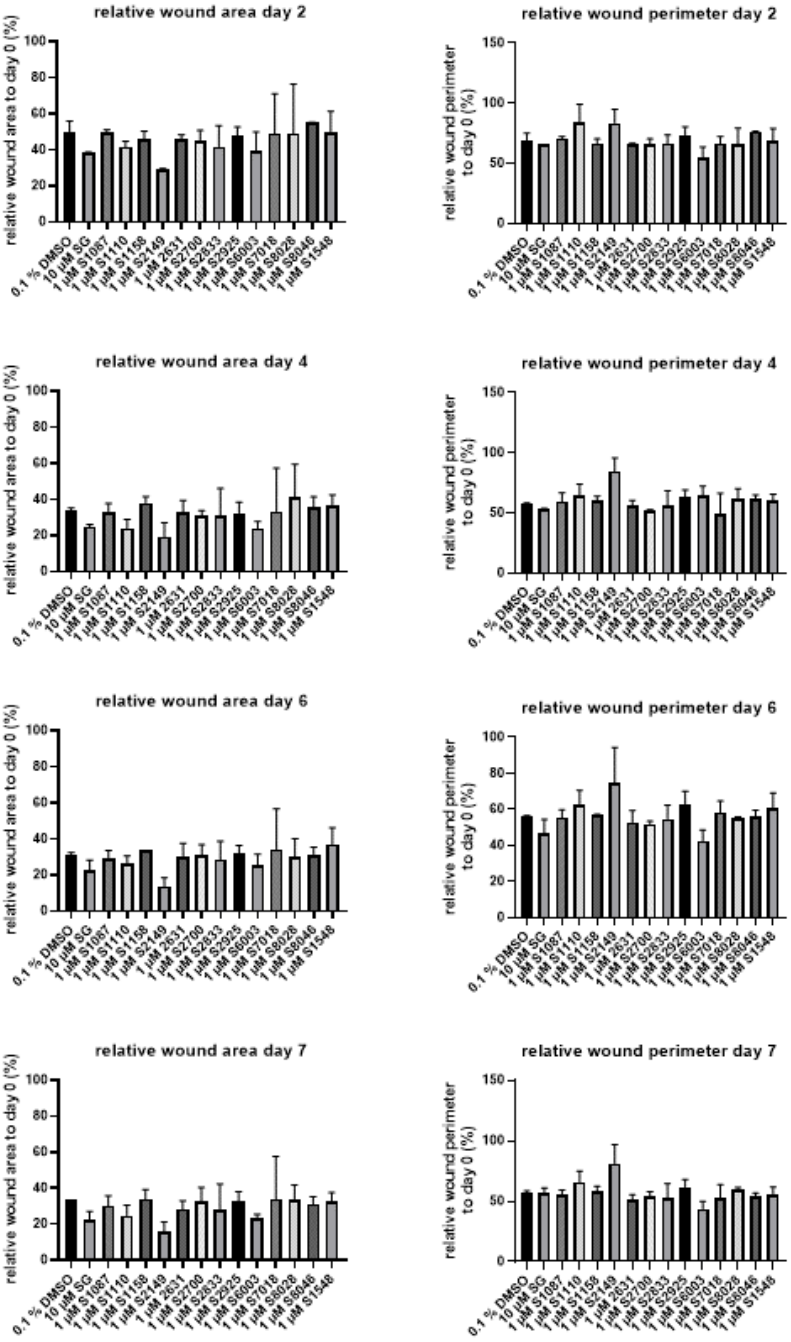

f) Relative top-view wound area and perimeter of sub-screening 6 of the clinical trials substances

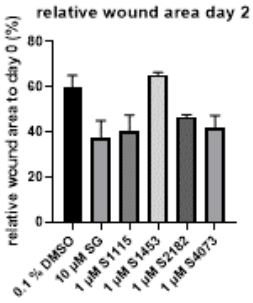

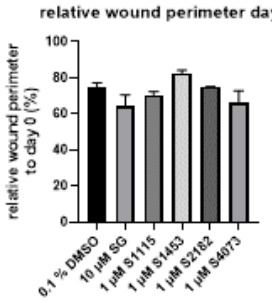

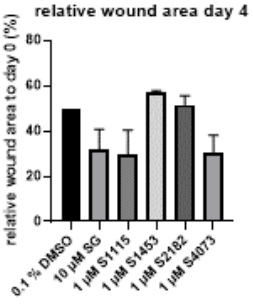

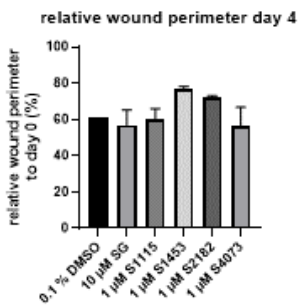

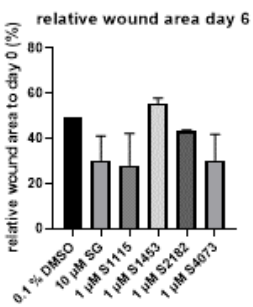

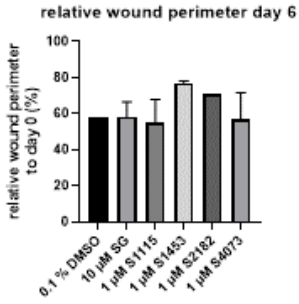

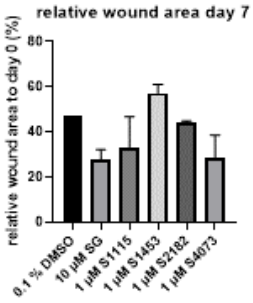

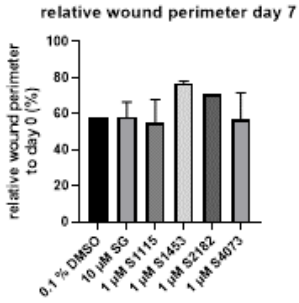

g) Relative top-view wound area and perimeter of sub-screening 1 of the non-clinical trials substances

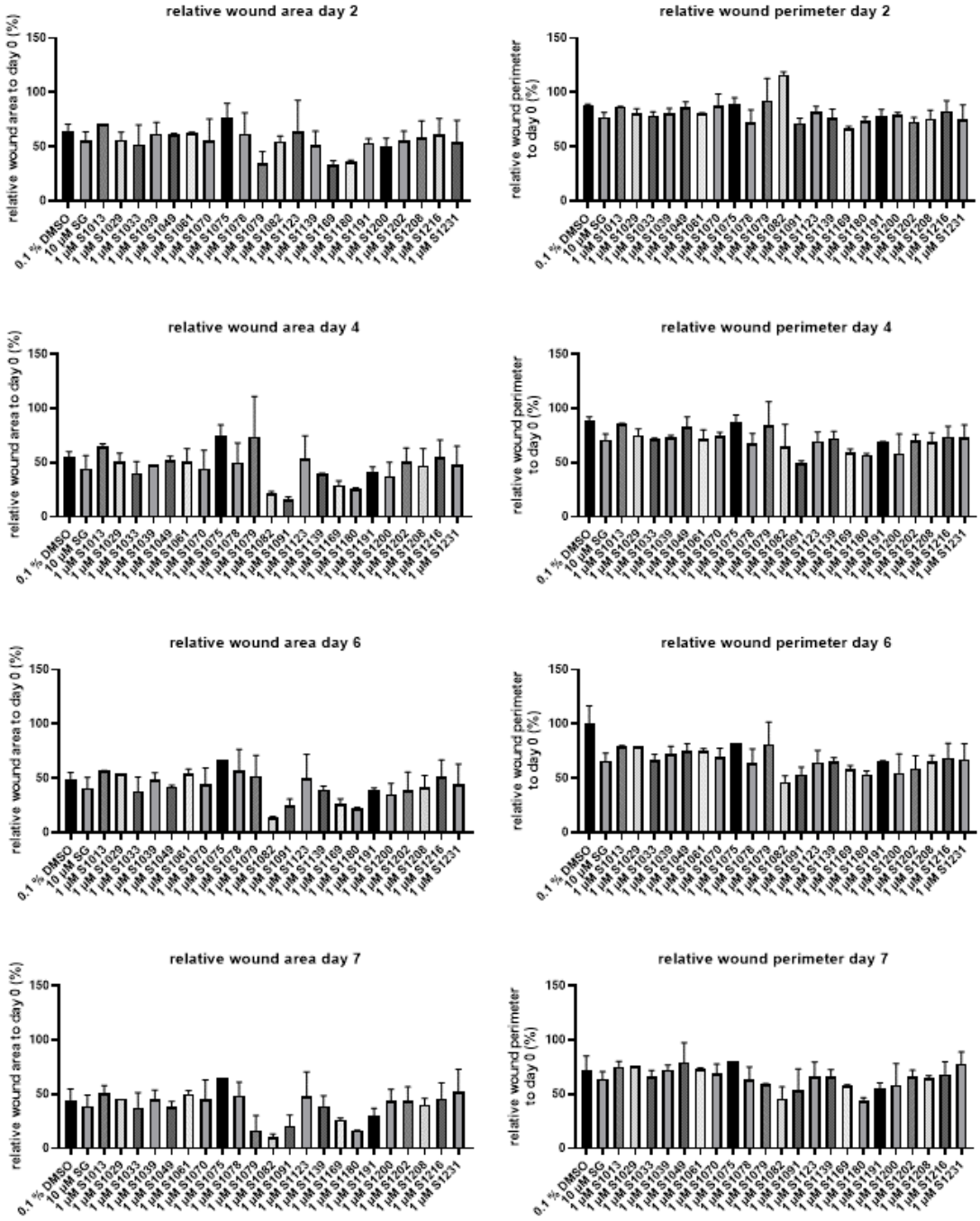

h) Relative top-view wound area and perimeter of sub-screening 2 of the non-clinical trials substances

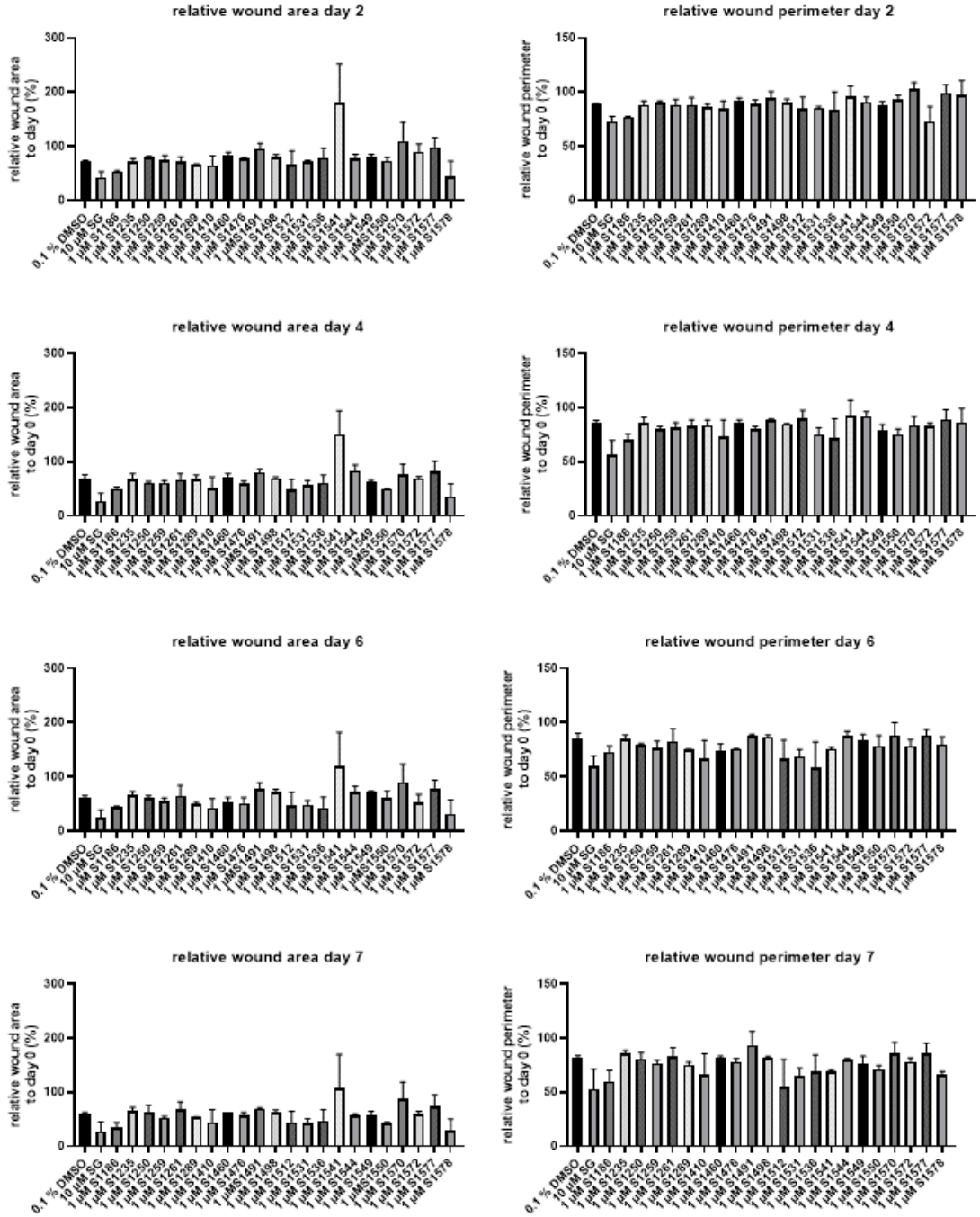

i) Relative top-view wound area and perimeter of sub-screening 3 of the non-clinical trials substances

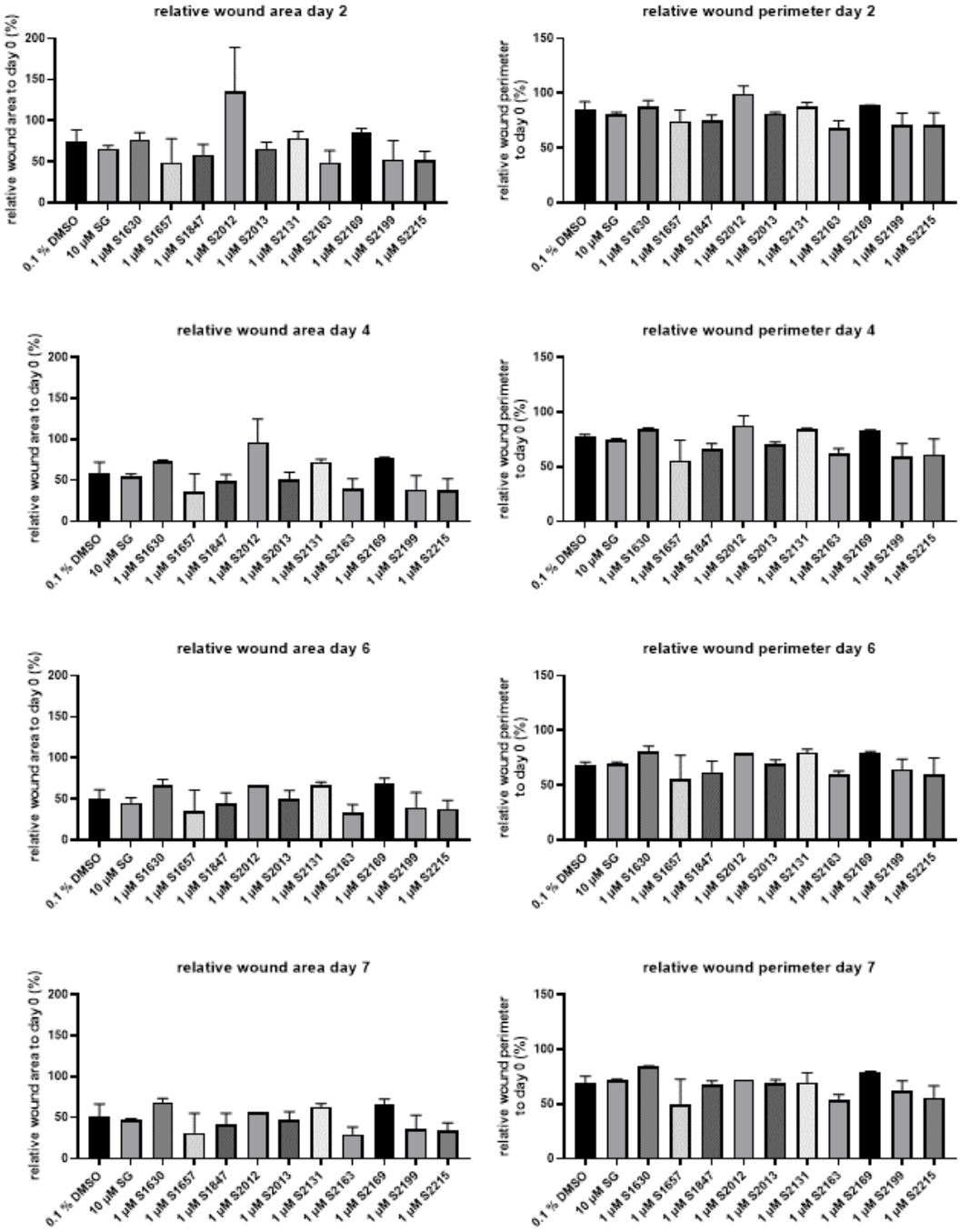

j) Relative top-view wound area and perimeter of sub-screening 4 of the non-clinical trials substances

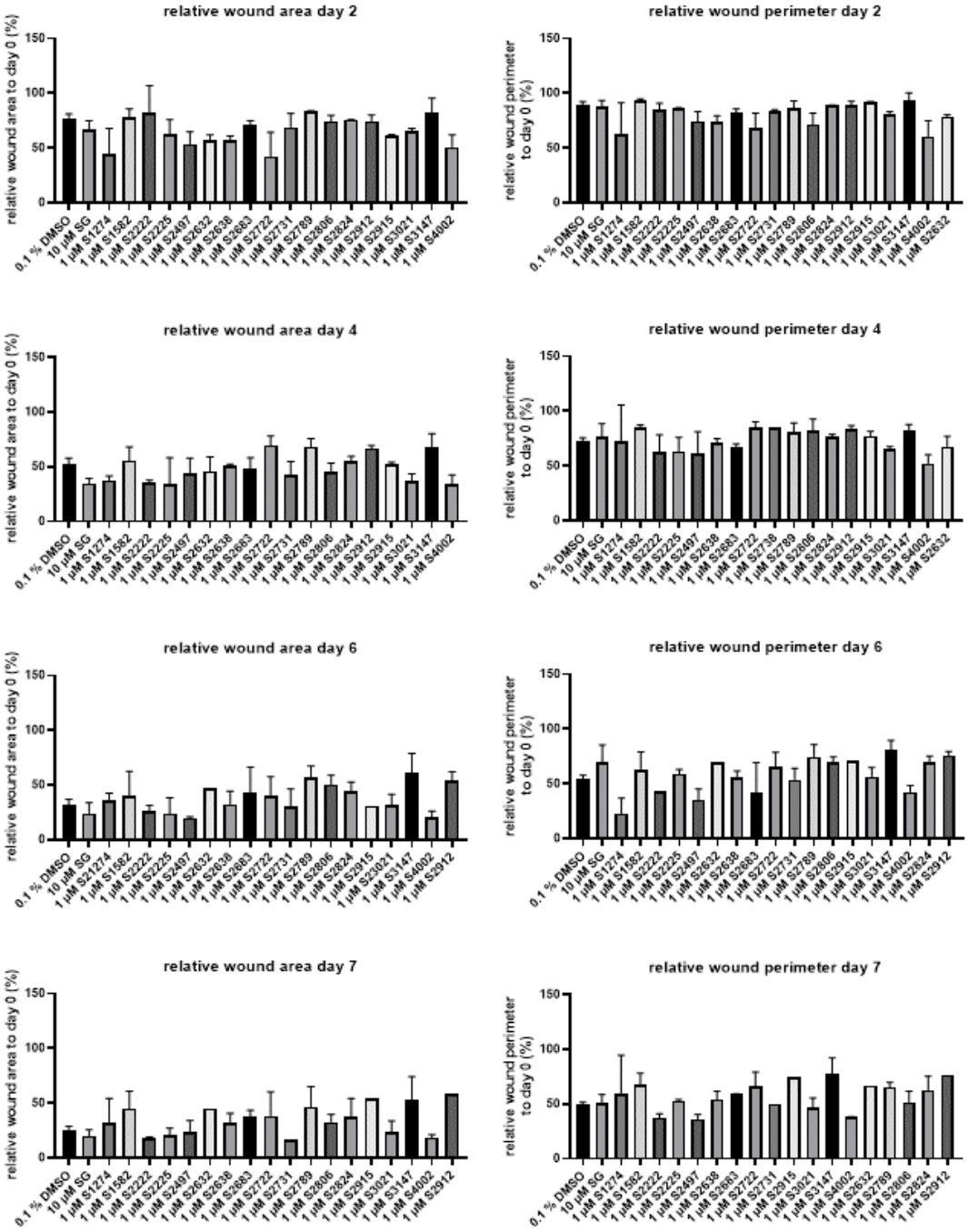

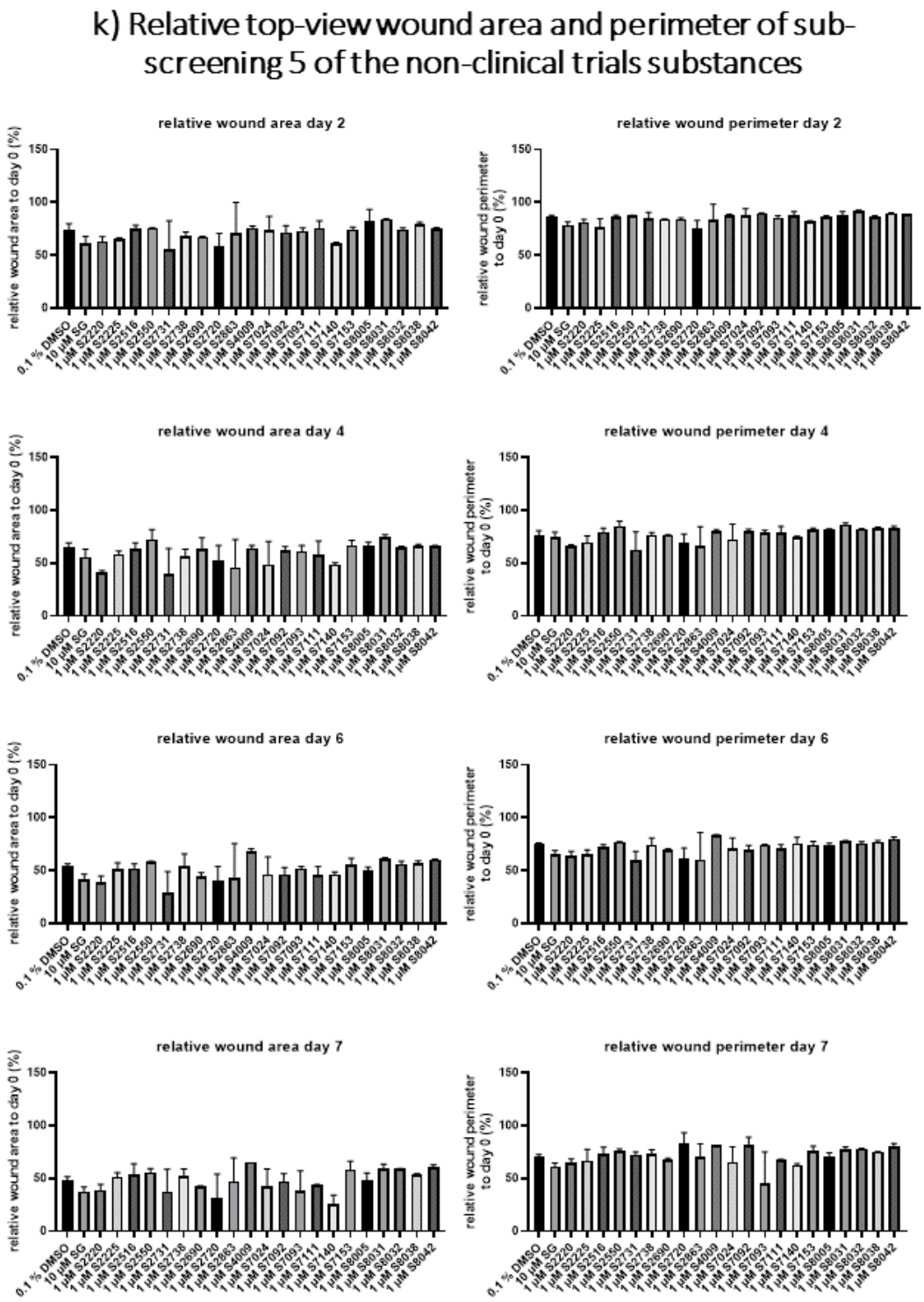

Figure S1: relative top-view wound area and perimeter to day 0 throughout the culture of all substances tested, shown are the sub-screenings of the clinical trials substances (a-f) and of the non-clinical trials substances (g-k). n = 1, 1-2 replicates/substance. Data is shown as mean + standard error of the mean. Statisitcal analysis was not possible because only one biological replicate was performed.

List of abbreviations

Abbreviation	Meaning
ANOVA	Analysis of variance
APC	adenomatous polyposis colo protein
BCA	Bicinchoninic acid
BSA	Bovine serum albumin
CD	Cluster of Differentiation
CK	Cytokeratin
CKIα	Casein kinase Iα
CO_2	Carbon dioxide
DNA	Deoxyribonucleic acid
DAPI	4‘, 6-Diamidin-2-phenylindol
DMEM	Dulbeccos Modified Eagle Medium
DMSO	Dimethyl sulfoxide
EMB	*Einrichtung für marine Biotechnologie*
ECM	Extracellular matrix
ET	Epithelial tongue
FBS	Fetal bovine serum
FDA	Food and drug administration
FGF	Fibroblast growth factor
GPCR	G-protein coupled receptor
GSK-3β	Glycogen synthase kinase 3β
H&E	Hematoxylin and eosin
HIF-1α	Hypoxia inducible factor 1α
IF	Immunofluorescence
IL	interleukin
KGF	Keratinocyte growth factor
L-Arg	L-arginine
LDH	Lactate dehydrogenase
LRP	Low density lipoprotein receptor-related *protein*
MAPK	Mitogen activated protein kinase
MMP	Matrix metalloprotease
NGF	Nerve growth factor
NGS	Normal goat serum
O_2	Oxygen
OCT	Optical coherence tomography
PBS	Phosphate buffered saline
PDGF	Platelet derived growth factor
PECAM	Platelet endothelial cell adhesion molecule
RNA	Ribonucleic acid
ROS	Reactive oxygen species
RT	Room temperature
SG	Sodium gualenate
T4	thyroxine
TBS	Tris-buffered saline
TCF/LEF	T cell factor/lymphoid enhancer factor family
TdT	Terminal deoxynuclotidyl transferase
TGF	Tumor necrosis factor
TIMP	Tissue inhibitor of MMPs

TRIS	Tris(hydroxymethyl)aminomethan
TrkA	Tropomyosin receptor kinase A
TUNEL	Terminal deoxynucleotidyl transferase deoxyuridine triphosphate nick end labeling
VEGF	Vascular endothelial growth factor
VF	Visual field
WEM	Williams Medium E
WHOC	Wound healing organ culture
WHOK	*Wundheilungshautorgankultur*

List of figures

List of tables

References

Ahmadi, H., Amini, A., Fadaei Fathabady, F., Mostafavinia, A., Zare, F., Ebrahimpour-Malekshah, R., Ghalibaf, M. N., Abrisham, M., Rezaei, F., Albright, R., Ghoreishi, S. K., Chien, S., & Bayat, M. (2020). Transplantation of photobiomodulation-preconditioned diabetic stem cells accelerates ischemic wound healing in diabetic rats. *Stem Cell Research and Therapy*, *11(1)*,494 https://doi.org/10.1186/s13287-020-01967-2

Albertin, G., Astolfi, L., Fede, C., Simoni, E., Contran, M., Petrelli, L., Tiengo, C., Guidolin, D., De Caro, R., & Stecco, C. (2023). Detection of Lymphatic Vessels in the Superficial Fascia of the Abdomen. *Life*, *13(3)*, 836. https://doi.org/10.3390/life13030836

Ammer, A. G., & Weed, S. A. (2008). Cortactin branches out: Roles in regulating protrusive actin dynamics. *Cell Motility and the Cytoskeleton*, 65*(9)*, 687-707. https://doi.org/10.1002/cm.20296

Ansell, D. M., Kloepper, J. E., Thomason, H. A., Paus, R., & Hardman, M. J. (2011). Exploring the hair growth-wound healing connection: Anagen phase promotes wound re-Epithelialization. *Journal of Investigative Dermatology*, *131(2)*, 518–528. https://doi.org/10.1038/jid.2010.291

Arribas-López, E., Zand, N., Ojo, O., Snowden, M. J., & Kochhar, T. (2021). The effect of amino acids on wound healing: A systematic review and meta-analysis on arginine and glutamine. *Nutrients 13(8)*, 2498. https://doi.org/10.3390/nu13082498

Ashcroft, G. S., & Ashworth, J. J. (2003). Potential Role of Estrogens in Wound Healing. *Am J Clin Dermatol*, *4(11)*, 737–743. https://doi.org/10.2165/00128071-200304110-00002

Ashcroft, G. S., & Mills, S. J. (2002). Androgen receptor–mediated inhibition of cutaneous wound healing. *Journal of Clinical Investigation*, *110(5)*, 615–624. https://doi.org/10.1172/jci200215704

Ashcroft, G. S., Mills, S. J., Lei, K., Gibbons, L., Jeong, M.-J., Taniguchi, M., Burow, M., Horan, M. A., Wahl, S. M., & Nakayama, T. (2003). Estrogen modulates cutaneous wound healing by downregulating macrophage migration inhibitory factor. *Journal of Clinical Investigation*, *111(9)*, 1309–1318. https://doi.org/10.1172/jci200316288

Augustin, I. (2014). Wnt signaling in skin homeostasis and pathology. *Journal of the German Society of Dermatology*, *13(4)*, 302–306. https://doi.org/10.1111/ddg.12620

Baernstein, A., Smith, K. M., & Elmore, J. G. (2008). Singing the Blues: Is It Really Cyanosis? *Respiratory Care*, *53*(8), 1081–1084.

Balaji, S., Moles, C. M., Bhattacharya, S. S., Lesaint, M., Dhamija, Y., Le, L. D., King, A., Kidd, M., Muhammad, F., Shaaban, A., Crombleholme, T. M., Bollyky, P., Keswani, S. G., Colorado, H., & Alto, P. (2015). *Comparison of interleukin 10 homologs on dermal wound healing using a novel human skin ex vivo organ culture model*. *190(1)*, 358–366. https://doi.org/10.1016/j.jss.2014.02.027.Comparison

Baron, J. M., Glatz, M., & Proksch, E. (2020). Optimal Support of Wound Healing: New Insights. In *Dermatology, 236(6)*, 593-600. S. Karger AG. https://doi.org/10.1159/000505291

Baroni, A., Buommino, E., De Gregorio, V., Ruocco, E., Ruocco, V., & Wolf, R. (2012). Structure and function of the epidermis related to barrier properties. *Clinics in Dermatology*, *30(3)*, 257–262. https://doi.org/10.1016/j.clindermatol.2011.08.007

Barosova, H., Meldrum, K., Karakocak, B. B., Balog, S., Doak, S. H., Petri-Fink, A., Clift, M. J. D., & Rothen-Rutishauser, B. (2021). Inter-laboratory variability of A549 epithelial cells grown under submerged and air-liquid interface conditions. *Toxicology in Vitro*,75, 105178. https://doi.org/10.1016/j.tiv.2021.105178

Bastakoty, D., Saraswati, S., Cates, J., Lee, E., Nanney, L. B., & Young, P. P. (2015). Inhibition of Wnt/β-catenin pathway promotes regenerative repair of cutaneous and cartilage injury. *FASEB Journal*, *29*(12), 4881–4892. https://doi.org/10.1096/fj.15-275941

Bauer, B., Majic, M., Rauthe, S., Bröcker, E. B., & Kerstan, A. (2012). Persistent swelling after flushing of an abscess with Octenisept®. *Unfallchirurg*, *115(12)*, 1116–1119. https://doi.org/10.1007/s00113-011-2116-5

Berdigaliyev, N., & Aljofan, M. (2020). An overview of drug discovery and development. *Future Med. Chem*, *12(10)*, 939–947. https://doi.org/10.4155/fmc-2019-0307

Berlanga-Acosta, J., Schultz, G. S., López-Mola, E., Guillen-Nieto, G., García-Siverio, M., & Herrera-Martínez, L. (2013). Glucose toxic effects on granulation tissue productive cells: The diabetics' impaired healing. *BioMed Research International*, 2013, 256043. https://doi.org/10.1155/2013/256043

Bernstam, L. I., Vaughan, F. L., & Bernstein, I. A. (1986). Keratinocytes grown at the air-liquid interface. *In Vitro Cellular & Developmental Biology*, *22(12)*, 695–705. https://doi.org/10.1007/BF02621086

Bhora, F. Y., Dunkin, B. J., Batzri, S., Ain, M. H., Bass, B. I., Sidawy, A. N., & Harmon, M. D. (1995). Effect of Growth Factors on Cell Proliferation and Epithelialization in Human Skin. *Journal of Surgical Research*, *59(2),* 236–244. https://doi.org/10.1006/jsre.1995.1160

Brandner, J. M., Houdek, P., Hüsing, B., Kaiser, C., & Moll, I. (2004). Connexins 26, 30, and 43: Differences among spontaneous, Chronic, and Accelerated Human Wound Healing. *Journal of Investigative Dermatology*, *122(5)*, 1310–1320. https://doi.org/10.1111/j.0022-202X.2004.22529.x

Buffoli, B., Rinaldi, F., Labanca, M., Sorbellini, E., Trink, A., Guanziroli, E., Rezzani, R., Rodella, L. F., Rinaldi, S., & Correspondence Luigi Rodella, I. F. (2013). The human hair: from anatomy to physiology. *International Journal of Dermatology*, *53(3)*, 331–341. https://doi.org/10.1111/ijd.12362

Burmester, I. A. K., Emtenani, S., Johns, J. G., Ludwig, R. J., Hammers, C. M., & Hundt, J. E. (2019). Translational Use of a Standardized Full Human Skin Organ Culture Model in Autoimmune Blistering Diseases. *Current Protocols in Pharmacology*, *85(1)*, e56. https://doi.org/10.1002/cpph.56

Burmester, I. A. K., Flaswinkel, S., Thies, C. S., Kasprick, A., Kamaguchi, M., Bumiller-Bini, V., Emtenani, S., Feldmann, N., Kridin, K., Schmidt, E., van Beek, N., Zillikens, D., Hammers, C. M., Hundt, J. E., & Ludwig, R. J. (2020). Identification of novel therapeutic targets for blocking acantholysis in pemphigus. *British Journal of Pharmacology*, *177(22)*, 5114–5130. https://doi.org/10.1111/bph.15233

Cadigan, K. M., & Nusse, R. (1992). Wnt signaling: a common theme in animal development. *Genes and Development, 11(24), 3286-3305.* https://doi.org/10.1101/gad.11.24.3286

Caporali, A., & Emanueli, C. (2009). Cardiovascular Actions of Neurotrophins. *Physiol. Rev*, *89(1)*, 279–309. https://doi.org/10.1152/physrev.00007.2008.-Neurotrophins

Chambers, E. S., & Vukmanovic-Stejic, M. (2020). Skin barrier immunity and ageing. *Immunology, 160(2), 116-125*. Blackwell Publishing Ltd. https://doi.org/10.1111/imm.13152

Chan, K. L. A., Zhang, G., Tomic-Canic, M., Stojadinovic, O., Lee, B., Flach, C. R., & Mendelsohn, R. (2008). A coordinated approach to cutaneous wound healing: Vibrational microscopy and molecular biology. *Journal of Cellular and Molecular Medicine*, *12*(5B), 2145–2154. https://doi.org/10.1111/j.1582-4934.2008.00459.x

Clayton, K., Vallejo, A. F., Davies, J., Sirvent, S., & Polak, M. E. (2017). Langerhans cells-programmed by the epidermis. *Frontiers in Immunology*, *29(8)*, 1676. https://doi.org/10.3389/fimmu.2017.01676

Cua, A. B., Wilhelm, K.-P., & Maibach, H. I. (1990a). Elastic properties of human skin: relation to age, sex, and anatomical region. *Archives of Dermatological Research*, *282(5)*, 283–288. https://doi.org/10.1007/BF00375720

Cua, A. B., Wilhelm, K.-P., & Maibach, H. I. (1990b). Frictional properties of human skin: relation to age, sex and anatomical region, stratum corneum hydration and transepidermal water loss. *British Journal of Dermatology*, *123(4)*, 473–479. https://doi.org/ 10.1111/j.1365-2133.1990.tb01452.x

Dallaglio, K., Marconi, A., & Pincelli, C. (2012). Survivin: A dual player in healthy and diseased skin. *Journal of Investigative Dermatology, 132(1), 18-27.* https://doi.org/10.1038/jid.2011.279

Dallas, A., Trotsyuk, A., Ilves, H., Bonham, C. A., Rodrigues, M., Engel, K., Barrera, J. A., Kosaric, N., Stern-Buchbinder, Z. A., White, A., Mandell, K. J., Hammond, P. T., Mansbridge, J., Jayasena, S., Gurtner, G. C., & Johnston, B. H. (2019). Acceleration of Diabetic Wound Healing with PHD2- and miR-210-Targeting Oligonucleotides. *Tissue Engineering - Part A*, *25*(1–2), 44–54. https://doi.org/10.1089/ten.tea.2017.0484

Danner, S., & Ciba, P. (2009). Neue Haut - Perspektiven der zellbasierten Wundtherapie. *Labor&more*, *5*, 42–44. https://doi.org/10.1007/978-3-642-02824-3

Debats, I. B. J. G., Koeneman, M. M., Booi, D. I., Bekers, O., & van der Hulst, R. R. W. J. (2011). Intravenous arginine and human skin graft donor site healing: A randomized controlled trial. *Burns*, *37(3)*, 420–426. https://doi.org/10.1016/j.burns.2010.06.003

Debeer, S., Le Luduec, J. B., Kaiserlian, D., Laurent, P., Nicolas, J. F., Dubois, B., & Kanitakis, J. (2013). Comparative histology and immunohistochemistry of porcine versus human skin. *European Journal of Dermatology*, *23*(4), 456–466. https://doi.org/10.1684/ejd.2013.2060

Diegelmann, R. F., & Evans, M. C. (2004). Wound healing an overview of acute, fibrotic and delayed healing. *Frontiers in Bioscience*, *9*, 283–289. https://doi.org/ 10.2741/1184

Dissemond, J. (2006). Wann ist eine wunde chronisch? *Hautarzt, 57(1), 55*, https://doi.org/10.1007/s00105-005-1048-9

Dmitrieva, N. I., & Burg, M. B. (2007). Osmotic Stress and DNA Damage. *Methods in Enzymology, 428,* 241-252, Academic Press Inc. https://doi.org/10.1016/S0076-6879(07)28013-9

Eming, S. A., Hammerschmidt, M., Krieg, T., & Roers, A. (2009). Interrelation of immunity and tissue repair or regeneration. In *Seminars in Cell and Developmental Biology, 20(5),*517-527. Elsevier Ltd. https://doi.org/10.1016/j.semcdb.2009.04.009

Eming, S. A., Kaufmann, J., Löhrer, R., & Krieg, T. (2007). Chronische wunde: Neue Wege in Forschung und Therapie. *Hautarzt 58(11)* 939-944, https://doi.org/10.1007/s00105-007-1402-1

Eming, S. A., Martin, P., & Tomic-Canic, M. (2014). Wound repair and regeneration: Mechanisms, signaling, and translation. In *Science Translational Medicine*. 6(265), 265sr6, American Association for the Advancement of Science. https://doi.org/10.1126/scitranslmed.3009337

Enoch, S., & Leaper, D. J. (2005). Basic science of wound healing. *Surgery (Oxford)*, *23*(1), 37–42. https://doi.org/10.1383/surg.23.2.37.60352

Fathke, C., Wilson, L., Hutter, J., Kapoor, V., Smith, A., Hocking, A., & Isik, F. (2004). Contribution of Bone Marrow-Derived Cells to Skin: Collagen Deposition and Wound Repair. *Stem Cells.*, *22*(5), 812–822. https://doi.org/10.1634/stemcells.22-5-812

Franconi, F., & Campesi, I. (2014). Sex and gender influences on pharmacological response: An overview. *Expert Review of Clinical Pharmacology*, 7(4), 469-485, Expert Reviews Ltd. https://doi.org/10.1586/17512433.2014.922866

Freedberg, I. M., Tomic-Canic, M., Komine, M., Blumenberg, M., & Ronald Perelman, T. O. (2001). Keratins and the Keratinocyte Activation Cycle. *Journal of Investigative Dermatology*, *116*(5), 633–640. https://doi.org/10.1046/j.1523-1747.2001.01327.x

Fritsch, P., & Schwarz, T. (2018). *Dermatologie Verologie*. 3

Frykberg, R. G., & Banks, J. (2015). Challenges in the Treatment of Chronic Wounds. *Advances in Wound Care*, *4*(9), 560–582. https://doi.org/10.1089/wound.2015.0635

Gallucci, R. M., Sloan, D. K., Heck, J. M., Murray, A. R., & O'dell, S. J. (2004). Interleukin 6 Indirectly Induces Keratinocyte Migration. *Journal of Investigative Dermatology*, *122(3)*, 764–772. https://doi.org/10.1111/j.0022-202X.2004.22323.x

Galvao, J., Davis, B., Tilley, M., Normando, E., Duchen, M. R., & Cordeiro, M. F. (2014). Unexpected low-dose toxicity of the universal solvent DMSO. *FASEB Journal*, *28*(3), 1317–1330. https://doi.org/10.1096/fj.13-235440

Gamelli, R. L., & He, L.-K. (2003). Incisional wound healing Model and Analysis of Wound Breaking Strength. *Methods in Molecular Medicine*, *78*, 37–54. https://doi.org/10.1385/1-59259-332-1:037

Gantwerker, E. A., & Hom, D. B. (2011). Skin: Histology and Physiology of Wound Healing. *Facial Plastic Surgery Clinics of North America* , *19*, 441–453. https://doi.org/10.1016/j.fsc.2011.06.009

Gherardini, J., van Lessen, M., Piccini, I., Edelkamp, J., & Bertolini, M. (2020). Human wound healing ex vivo model with focus on molecular markers. N. V. Botchkareva & G. E. Westgate (Eds.), *Molecular Dermatology Methods and Protocols.* 2154, 249–254,vye https://doi.org/10.1007/978-1-0716-0648-3_21

Gilliver, S. C., & Ashcroft, G. S. (2007). Sex steroids and cutaneous wound healing: The contrasting influences of estrogens and androgens. *Climacteric, 10(4),* 276–288. https://doi.org/10.1080/13697130701456630

Glinos, G. D., Verne, S. H., Aldahan, A. S., Liang, L., Nouri, K., Elliot, S., Glassberg, M., Cabrera DeBuc, D., Koru-Sengul, T., Tomic-Canic, M., & Pastar, I. (2017). Optical coherence tomography for assessment of epithelialization in a human ex vivo wound model. *Wound Repair and Regeneration*, *25*(6), 1017–1026. https://doi.org/10.1111/wrr.12600

Goldberg, S. R., & Diegelmann, R. F. (2017). *Basic Science of Wound Healing* (R. Dieter, J. R. Dieter, I. R. Dieter, & A. Nanjundappa, Eds.; Crit. Limb Ischemia). Springer. https://doi.org/10.1007/978-3-319-31991-9_14

Gontcharova, V., Youn, E., Sun, Y., Wolcott, R. D., & Dowd, S. E. (2010). A Comparison of Bacterial Composition in Diabetic Ulcers and Contralateral Intact Skin.*The Open Microbiology Journa, 17(4)*, 8-19. https://doi.org/10.2174/1874285801004010008

Gonzales, K. A. U., & Fuchs, E. (2017). Skin and Its Regenerative Powers: An Alliance between Stem Cells and Their Niche. *Developmental Cell, 43(4),* 387–401. Cell Press. https://doi.org/10.1016/j.devcel.2017.10.001

Gould, L., Abadir, P., Brem, H., Carter, M., Conner-Kerr, T., Davidson, J., DiPietro, L., Falanga, V., Fife, C., Gardner, S., Grice, E., Harmon, J., Hazzard, W. R., High, K. P., Houghton, P., Jacobson, N., Horne, F. M., Reed, M. J., Sullivan, D. H., … Schmader, K. (2015). Chronic Wound Repair and Healing in Older Adults: Current Status and Future Research. *Wound Repair and Regeneration*, *63*(3), 427–438. https://doi.org/10.1111/wrr.12245

Grambow, E., Sorg, H., Sorg, C. G. G., & Strüder, D. (2021). Experimental Models to Study Skin Wound Healing with a Focus on Angiogenesis. *Medical Sciences*, *9*(3), 55. https://doi.org/10.3390/medsci9030055

Greenhalgh, D. G. (1998). The role of apoptosis in wound healing. *The International Journal of Biochemistry and Cell Biology*, *30*, 1019–1030. 10.1016/s1357-2725(98)00058-2

Groh, N., & Magin, T. M. (2023). Pseudomonas-Derived Pyocyanin Links Oxidative Stress and Keratin 6 Expression to Wound Healing. *Journal of Investigative Dermatology*. Online ahead of print. https://doi.org/10.1016/j.jid.2023.04.003

Groscurth, P. (2002). Anatomy of Sweat Glands. *Current Problems in Dermatology*, *30*, 1–9. https://doi.org/10.1159/000060678

Gstraunthaler, G., & Lindl, T. (2021). *Zell- und Gewebekultur Allgemeine Grundlagen und spezielle Anwendungen* (Vol. 8). Springer Spektrum.

Guan, J., Wu, C., He, Y., & Lu, F. (2023). Skin-associated adipocytes in skin barrier immunity: A mini-review. In *Frontiers in Immunology*, *14*. https://doi.org/10.3389/fimmu.2023.1116548

Gunin, A. G., Petrov, V. V., Golubtzova, N. N., Vasilieva, O. V., & Kornilova, N. K. (2014). Age-related changes in angiogenesis in human dermis. *Experimental Gerontology*, *55*, 143–151. https://doi.org/10.1016/j.exger.2014.04.010

Guo, S., & DiPietro, L. A. (2010). Critical review in oral biology & medicine: Factors affecting wound healing. *Journal of Dental Research*, *89*(3), 219–229. https://doi.org/10.1177/0022034509359125

Ha, L., & Hundt, J. E. (2019). Optical coherence tomography for fast bedside imaging, assessment and monitoring of autoimmune inflammatory skin diseases? *Focus Dermatological Research, 18(9),* 937-942. https://doi.org/10.1111/ddg.14266

Hachem, R., Parikh, U. M., Reitzel, R., Rosenblatt, J., Kaul, A., Vargas-Cruz, N., Hill, L., Moore, L., Meyer, J., Chaftari, Anne-Marie, Gagea, M., Balaji, S., & Raad, I. I. (2021). Novel antimicrobial ointment for infected wound healing in an in vitro and in vivo porcine model. *Wound Repair and Regeneration*, *29(5),* 830.842.https://doi.org/10.1111/wrr.12922

Han, D., Cao, C., Su, Y., Wang, J., Sun, J., Chen, H., & Xu, A. (2016). Ginkgo biloba exocarp extracts inhibits angiogenesis and its effects on Wnt/ß-catenin-VEGF signaling pathway in Lewis lung cancer. *Journal of Ethnopharmacology. 192,* 406-412. https://doi.org/10.1016/j.jep.2016.09.018

Hassan, W. U., Greiser, U., & Wang, W. (2014). Role of adipose-derived stem cells in wound healing. *Wound Repair and Regeneration, 22(3),* 313–325, Blackwell Publishing. https://doi.org/10.1111/wrr.12173

Hauser, A. S., Chavali, S., Masuho, I., Jahn, L. J., Martemyanov, K. A., Gloriam, D. E., & Babu, M. M. (2018). Pharmacogenomics of GPCR Drug Targets. *Cell*, *172(1-2)*, 41-54.e19. https://doi.org/10.1016/j.cell.2017.11.033

Hema Sree, G., Saraswathy, G., Murahari, M., & Krishnamurthy, M. (2019). An update on Drug Repurposing: Re-written saga of the drug's fate. *Biomedicine and Pharmacotherapy. 110*, 700-716. Elsevier Masson SAS. https://doi.org/10.1016/j.biopha.2018.11.127

Hirsch, T., Koerber, A., Jacobsen, F., Dissemond, J., Steinau, H. U., Gatermann, S., Al-Benna, S., Kesting, M., Seipp, H. M., & Steinstraesser, L. (2010). Evaluation of toxic side effects of clinically used skin antiseptics in vitro. *Journal of Surgical Research*, *164*(2), 344–350. https://doi.org/10.1016/j.jss.2009.04.029

Huber, R., Wojtkowski, M., & Fujimoto, J. G. (2006). Fourier Domain Mode Locking (FDML): A new laser operating regime and applications for optical coherence tomography. *OPTICS EXPRESS*, *14*(8), 3225–3237. https://doi.org/10.1364/oe.14.003225

Hübner, N. O., Siebert, J., & Kramer, A. (2010). Octenidine dihydrochloride, a modern antiseptic for skin, mucous membranes and wounds. *Skin Pharmacology and Physiology, 23(5),* 244-258. https://doi.org/10.1159/000314699

Ito, M., & Cotsarelis, G. (2008). Is the hair follicle necessary for normal wound healing? *Journal of Investigative Dermatology, 128(5),* 1059–1061. https://doi.org/10.1038/jid.2008.86

Ito, M., Liu, Y., Yang, Z., Nguyen, J., Liang, F., Morris, R. J., & Cotsarelis, G. (2005). Stem cells in the hair follicle bulge contribute to wound repair but not to homeostasis of the epidermis. *Nature Medicine*, *11(12)*, 1351–1354. https://doi.org/10.1038/nm1328

Ito, M., Yang, Z., Andl, T., Cui, C., Kim, N., Millar, S. E., & Cotserelis, G. (2007). Wnt-dependent de novo hair follicle regeneration in adult mouse skin after wound healing. *Nature*, *447 (7142)*, 316–321. https://doi.org/10.1038/nature05766

Iwata, Y., Hasebe, Y., Hasegawa, S., Nakata, S., Yagami, A., Matsunaga, K., Sugiura, K., & Akamatsu, H. (2017). Dermal CD271+ cells are closely associated with regeneration of the dermis in the wound healing process. *Acta Dermato-Venereologica*, *97(5)*, 593–600. https://doi.org/10.2340/00015555-2624

Jiang, L., Yin, M., Wei, X., Liu, J., Wang, X., Niu, C., Kang, X., Xu, J., Zhou, Z., Sun, S., Wang, X., Zheng, X., Duan, S., Yao, K., Qian, R., Sun, N., Chen, A., Wang, R., Zhang, J., Chen, S., & Meng, D. (2015). Bach1 Represses Wnt/β-Catenin Signaling and Angiogenesis HHS Public Access. *Circ Res*, *117*(4), 364–375. https://doi.org/10.1161/CIRCRESAHA.115.306829

Johansson, J. A., & Headon, D. J. (2014). Regionalisation of the skin. *Seminars in Cell & Developmental Biology*, *25*(26), 3–10. https://doi.org/10.1016/j.semcdb.2013.12.007

Kabakov, A. E., & Gabai, V. L. (2018). Cell death and survival assays. *Methods in Molecular Biology, 1709,* 107–127, Humana Press Inc. https://doi.org/10.1007/978-1-4939-7477-1_9

Kim, B. S., Ott, V., Boecker, A. H., Stromps, J. P., Paul, N. E., Alharbi, Z., Cakmak, E., Bernhagen, J., Bucala, R., & Pallua, N. (2017). The Effect of Antiseptics on Adipose-Derived Stem Cells. *Plastic and Reconstructive Surgery*, *139(3)*, 625–637. https://doi.org/10.1097/PRS.0000000000003125

Kleesz, P., Darlenski, R., & Fluhr, J. W. (2012). Full-Body Skin Mapping for Six Biophysical Parameters: Baseline Values at 16 Anatomical Sites in 125 Human Subjects. *Skin Pharmacology and Physiology*, *25(1)*, 25–33. https://doi.org/10.1159/000330721

Kleszcyński, K., & Fischer, T. W. (2012). Development of a short-term human full-thickness skin organ culture model in vitro under serum-free conditions. *Archives of Dermatological Research*, *304(7)*, 579–587. https://doi.org/10.1007/s00403-012-1239-z

Kratz, G. (1998). Modeling of Wound Healing Processes in Human skin Using Tissue Culture. *Microscopy Research and Technique*, *42(5)*, 345–350. https://doi.org/10.1002/(SICI)1097-0029(19980901)42:5<345::AID-JEMT5>3.0.CO;2-O

Krisp, C., Jacobsen, F., McKay, M. J., Molloy, M. P., Steinstraesser, L., & Wolters, D. A. (2013). Proteome analysis reveals antiangiogenic environments in chronic wounds of diabetes mellitus type 2 patients. *Proteomics, 13(17)*, 2670-2681. https://doi.org/ 10.1002/pmic.201200502

Lachenmeier, D. W. (2008). Safety evaluation of topical applications of ethanol on the skin and inside the oral cavity. In *Journal of Occupational Medicine and Toxicology, 13(3),* 26. https://doi.org/10.1186/1745-6673-3-26

Lánden, N. X., Li, D., & Stahle, M. (2016). Transition from inflammation to proliferation: a critical step during wound healing. *Cellular and Molecular Life Sciences*, *73(20)*, 3861–3885. https://doi.org/10.1007/s00018-016-2268-0.

Langan, E. A., Fink, T., & Paus, R. (2018). Is prolactin a negarive neuroendocrine regulator of human skin re-epithelisation after wounding? *Archives of Dermatological Research*, *310(10)*, 833–841. https://doi.org/10.1007/s00403-018-1864-2.

Lazarus, G. S., Cooper, D. M., Knighton, D. R., Margolis, D. J., Pecoraro, R. E., Rodeheaver, G., & Robson, M. C. (1994). Definitions and Guidelines for Assessment of Wounds and Evaluation of Healing. *Archives of Dermatology*, *130(4),* 489–493. https://doi.org/10.1001/archderm.1994.01690040093015

Lee, J.-W., Bae, S.-H., Jeong, J.-W., Kim, S.-H., & Kim, K.-W. (2004). Hypoxia-inducible factor (HIF-1)α: its protein stability and biological functions. *Experimental and Molecular Medicine*, *36(1)*, 1–12. Htpps://doi.org/ 10.1038/emm.2004.1

Liao, T., Lehmann, J., Sternstein, S., Yay, A., Zhang, G., Matthießen, A. E., Schumann, S., Siemers, F., Kruse, C., Hundt, J. E., Langan, E. A., Tiede, S., & Paus, R. (2019). Nestin + progenitor cells isolated from adult human sweat gland stroma promote reepithelialisation and may stimulate angiogenesis in wounded human skin ex vivo. *Archives of Dermatological Research*, *311(4)*, 325–330. https://doi.org/10.1007/s00403-019-01889-x

Lin, J. Y., & Fisher, D. E. (2007). Melanocyte biology and skin pigmentation. *Nature, 445(7130),* 843–850. Nature Publishing Group. https://doi.org/10.1038/nature05660

Liu, S., Yang, W., Li, Y., & Sun, C. (2023). Fetal bovine serum, an important factor affecting the reproducibility of cell experiments. *Scientific Reports*, *13(1),* 1942. https://doi.org/10.1038/s41598-023-29060-7

Lu, Z., Hasse, S., Bodo, E., Rose, C., Funk, W., & Paus, R. (2007). Towards the development of a simplified long-term organ culture method for human scalp skin and its appendages under serum-free conditions. *Experimental Dermatology*, *16(1)*, 37–44. https://doi.org/10.1111/j.1600-0625.2006.00510.x

Lukas, M., Stössel, H., Hefel, L., Imamura, S., Fritsch, P., Sepp, N. T., Schuler, G., & Romani, N. (1996). Human Cutaneous Dendritic Cells Migrate Through Dermal Lymphatic Vessels in a Skin Organ Culture Model. *The Journal of Investigative Dermatology*, *106(6)*, 1293–1299. https://doi.org/10.1111/1523-1747.ep12349010

Madla, C. M., Gavins, F. K. H., Merchant, H. A., Orlu, M., Murdan, S., & Basit, A. W. (2021). Let's talk about sex: Differences in drug therapy in males and females. *Advanced Drug Delivery Reviews 175,* 11380. https://doi.org/10.1016/j.addr.2021.05.014

Mamilos, A., Winter, L., Schmitt, V. H., Barsch, F., Grevenstein, D., Wagner, W., Babel, M., Keller, K., Schmitt, C., Gürtler, F., Schreml, S., Niedermair, T., Rupp, M., Alt, V., & Brochhausen, C. (2023). Macrophages: From Simple Phagocyte to an Integrative Regulatory Cell for Inflammation and Tissue Regeneration—A Review of the Literature. *Cells, 12(2),* 726 https://doi.org/10.3390/cells12020276

Manaithiya, A., Alam, O., Sharma, V., Naim, Mohd. J., Mittal, S., & Khan, I. A. (2021). GPR119 agonists: Novel therapeutic agents for type 2 diabetes mellitus. *Bioorganic Chemistry*, *113,* 104998. https://doi.org/10.1016/j.bioorg.2021.104998

Markovics, A., Angyal, Á., Tóth, K. F., Ádám, D., Pénzes, Z., Magi, J., Pór, Á., Kovács, I., Törőcsik, D., Zouboulis, C. C., Bíró, T., & Oláh, A. (2020). GPR119 Is a Potent Regulator of Human Sebocyte Biology. *Journal of Investigative Dermatology*, *140(10),* 1909-1918.e8. https://doi.org/10.1016/j.jid.2020.02.011

Marlin, M. C., & Li, G. (2015). Biogenesis and Function of the NGF/TrkA Signaling Endosome. *International Review of Cell and Molecular Biology, 314,* 239–257. https://doi.org/10.1016/bs.ircmb.2014.10.002

Martinotti, S., & Ranzato, E. (2020). Scratch wound healing assay. *Methods in Molecular Biology*, *2109*,225–229). https://doi.org/10.1007/7651_2019_259

Meier, N. T., Haslam, I. S., Pattwell, D. M., Zhang, G. Y., Emelianov, V., Paredes, R., Debus, S., Augustin, M., Funk, W., Amaya, E., Kloepper, J. E., Hardman, M. J., & Paus, R. (2013). Thyrotropin-releasing hormone (TRH) promotes wound re-epithelialisation in frog and human skin. *PloS One*, *8(9)*. e73596. https://doi.org/10.1371/journal.pone.0073596

Mekkes, J. R., Loots, M. A. M., Van der Wal, A. C., & Bos, J. D. (2003). Causes, investigation and treatment of leg ulceration. *British Journal of Dermatology*, *148(3)*, 388–401. https://doi.org/10.1046/j.1365-2133.2003.05222.x

Mendoza-Garcia, J., Sebastian, A., Alonso-Rasgado, T., & Bayat, A. (2015). Optimization of an ex vivo wound healing model in the adult human skin: Functional evaluation using photodynamic therapy. *Wound Repair and Regeneration*, *23(5)*, 685–702. https://doi.org/10.1111/wrr.12325

Menon, G. K., Cleary, G. W., & Lane, M. E. (2012). The structure and function of the stratum corneum. *International Journal of Pharmaceutics, 435(1),* 3–9. https://doi.org/10.1016/j.ijpharm.2012.06.005

Moll, I. (2003). Human Skin Organ Culture. In *Methods in Molecular Medicine, 78,* 305–310. https://doi.org/10.1385/1-59259-332-1:305

Moll, I., Houdek, P., Schäfer, S., Nuber, U., & Moll, R. (1999). Diversity of desmosomal proteins in regenerating epidermis: immunohistochemical study using a human skin organ culture model. *Archives of Dermatological Research*, *291 (7-8)*, 437–446. https://doi.org/10.1007/s004030050435

Monavarian, M., Kader, S., Moeinzadeh, S., & Jabbari, E. (2019). Regenerative Scar-Free Skin Wound Healing. *Tissue Engineering - Part B: Reviews, 25(4),* 294–311. https://doi.org/10.1089/ten.teb.2018.0350

Nakamichi, K., Nakano, T., Yasuura, H., Izumi, S., & Kawashima, Y. (2003). Stabilization of sodium guaiazulene sulfonate in granules for tableting prepared using a twin-screw extruder. *European Journal of Pharmaceutics and Biopharmaceutics*, *56(3)*, 347–354. https://doi.org/10.1016/s0939-6411(03)00100-0

Nasir, N. A. M., Paus, R., & Ansell, D. M. (2018). Fluorescent cell tracer dye permits real-time assessment of re-epithelialization in a serum-free ex vivo human skin wound assay. *Wound Repair and Regeneration*, *27(1),* 126-133. https://doi.org/10.1111/wrr.12688

Niemann, C., & Horsley, V. (2012). Development and homeostasis of the sebaceous gland. *Seminars in Cell and Developmental Biology, 23(8),* 928–936. https://doi.org/10.1016/j.semcdb.2012.08.010

Nosbaum, A., Prevel, N., Truong, H.-A., Mehta, P., Ettinger, M., Scharschmidt, T. C., Ali, N. H., Pauli, M. L., Abbas, A. K., & Rosenblum, M. D. (2016). Cutting Edge: Regulatory T Cells Facilitate Cutaneous Wound Healing. *The Journal of Immunology*, *196(5)*, 2010–2014. https://doi.org/10.4049/jimmunol.1502139

Nusse, R., & Varmust, H. E. (1992). Wnt Genes. *Cell, 69(7),* 1073-1087. Htpps://doi.org/10.1016/0092-8674(92)90630-u

Oikarinen, A. (1994). Aging of the skin connective tissue: how to measure the biochemical and mechanical properties of aging dermis. *Photodermatol Photoimmunol Photomed*, *10(2),* 47–52.

Ojeh, N., Stojadinovic, O., Pastar, I., Sawaya, A., Yin, N., & Tomic-Canic, M. (2016). The effects of caffeine on wound healing. *International Wound Journal*, *13(5)*, 605–613. https://doi.org/10.1111/iwj.12327

Overton, H. A., Babbs, A. J., Doel, S. M., Fyfe, M. C. T., Gardner, L. S., Griffin, G., Jackson, H. C., Procter, M. J., Rasamison, C. M., Tang-Christensen, M., Widdowson, P. S., Williams, G. M., & Reynet, C. (2006). Deorphanization of a G protein-coupled receptor for oleoylethanolamide and its use in the discovery of small-molecule hypophagic agents. *Cell Metabolism*, *3(3)*, 167–175. https://doi.org/10.1016/j.cmet.2006.02.004

Pascalau, R., & Kuruvilla, R. (2020). A Hairy End to a Chilling Event. *Cell, 182(3),* 539–541. Cell Press. https://doi.org/10.1016/j.cell.2020.07.004

Pastar, I., Stojadinovic, O., Yin, N. C., Ramirez, H., Nusbaum, A. G., Sawaya, A., Patel, S. B., Khalid, L., Isseroff, R. R., & Tomic-Canic, M. (2014). Epithelialization in Wound Healing: A Comprehensive Review. *Advances in Wound Care*, *3(7),* 445–464. https://doi.org/10.1089/wound.2013.0473

Peetermans, M., de Prost, N., Eckmann, C., Norrby-Teglund, A., Skrede, S., & De Waele, J. J. (2020). Necrotizing skin and soft-tissue infections in the intensive care unit. *Clinical Microbiology and Infection, 26(1),* 8–17. https://doi.org/10.1016/j.cmi.2019.06.031

Pfeiffer, T., Göb, M., Draxinger, W., Karpf, S., Kolb, J. P., & Huber, R. (2020). Flexible A-scan rate MHz-OCT: efficient computational downscaling by coherent averaging. *Biomedical Optics Express*, *11(11)*, 6799. https://doi.org/10.1364/boe.402477

Poblet, E., Jiménez, F., & Ortega, F. (2005). The contribution of the arrector pili muscle and sebaceous glands to the follicular unit structure. *Journal of the American Academy of Dermatology*, *51(2)*, 217–222. https://doi.org/10.1016/j.jaad.2004.01.054

Podoleanu, A. G. (2012). Optical coherence tomography. *Journal of Microscopy*, *247(3)*, 209–219. https://doi.org/10.1111/j.1365-2818.2012.03619.x

Post, H., Hundt, J. E., Zhang, G., Depping, R., Rose, C., Langan, E. A., & Paus, R. (2021). Thyroxine restores severely impaired cutaneous re-epithelialisation and angiogenesis in a novel preclinical assay for studying human skin wound healing under “pathological” conditions ex vivo. *Archives of Dermatological Research*, *313(3)*, 181–192. https://doi.org/10.1007/s00403-020-02092-z

Powers, J. G., Higham, C., Broussard, K., & Phillips, T. J. (2016). Wound healing and treating wounds Chronic wound care and management. *Journal of the American Academy of Dermatology*, *74(4)*, 607–625. https://doi.org/10.1016/j.jaad.2015.08.070

Pyter, L. M., Yang, L., da Rocha, J. M., & Engeland, C. G. (2014). The effects of social isolation on wound healing mechanisms in female mice. *Physiology and Behavior*, *127*, 64–70. https://doi.org/10.1016/j.physbeh.2014.01.008

Qiu, C. C., Browin, A. E., Lobitz, G. R., Shanker, A., & Hsu, S. (2019). The color of skin: black diseases of the skin, nails, and mucosa. *Clinics in Dermatology*, *37(5)*, 447–467. https://doi.org/10.1016/j.clindermatol.2019.08.003

Rao, T. P., & Kühl, M. (2010). An updated overview on wnt signaling pathways: A prelude for more. *Circulation Research, 106(12),* 1798–1806. https://doi.org/10.1161/CIRCRESAHA.110.219840

Rittié, L., Sachs, D. L., Orringer, J. S., Voorhees, J. J., & Fisher, G. J. (2013). Eccrine sweat glands are major contributors to reepithelialization of human wounds. *American Journal of Pathology*, *182(1)*, 163–171. https://doi.org/10.1016/j.ajpath.2012.09.019

Röcken, M., Martin, S., Elke, S., & Walter, B. (2010). Taschenatlas Dermatologie Grundlagen Diagnostik Klinik. *Georg Thieme Verlag*. https://doi.org/10.1055/b-002-40826

Rubin, L. F. (1975). Toxicity of dimethyl sulfoxide, alone and in combination. *Annals of the New York Academy of Sciences*, *243*, 98–103. https://doi.org/10.1111/j.1749-6632.1975.tb25348.x

Scholzen, T., & Gerdes, J. (2000). The Ki-67 Protein: From the Known and the Unknown. *Journal of cellular physiology, 182(3),* 311-322. https://doi.org/10.1002/(SICI)1097-4652(200003)182:3<311::AID-JCP1>3.0.CO;2-9

Schupp, C. J., & Holland-Cunz, S. (2009). Persistent subcutaneous oedema and aseptic fatty tissue necrosis after using Octenisept®. *European Journal of Pediatric Surgery*, *19(3)*, 179–183. https://doi.org/10.1055/s-0029-1216379

Scott, G. A., Jacobs, S. E., & Pentland, A. P. (2006). sPLA2-X stimulates cutaneous melanocyte dendricity and pigmentation through a lysophosphatidylcholine-dependent mechanism. *Journal of Investigative Dermatology*, *126(4)*, 855–861. https://doi.org/10.1038/sj.jid.5700180

Seki, J., Mukai, H., & Sugiyama, M. (1985). Studies on the absorption of sudium guaiazulene-3-sulfonate. II. Absorption mechanism from nasal and intestinal membrane. *Journal of Pharmacobio-Dynamics*, *8(5)*, 337–343. https://doi.org/10.1248/bpb1978.8.337

Shojaei-Ghahrizjani, F., Rahmati, S., Mirzaei, S. A., & Banitalebi-Dehkordi, M. (2020). Does survivin overexpression enhance the efficiency of fibroblast cell-based wound therapy? *Molecular Biology Reports*, *47(8)*, 5851–5864. https://doi.org/10.1007/s11033-020-05656-4

Sim, S. L., Kumari, S., Kaur, S., & Khosrotehrani, K. (2022). Macrophages in Skin Wounds: Functions and Therapeutic Potential. *Biomolecules*, *12(11)*,1569. https://doi.org/10.3390/biom12111659

Song, Y., Pan, Y., Wang, H., Liu, Q., & Zhao, H. (2019). Mapping the face of young population in China: Influence of anatomical sites and gender on biophysical properties of facial skin. *Skin Research and Technology*, *25(3)*, 325–332. https://doi.org/10.1111/srt.12652. Epub 2019 Jan 10

Stahl, J., Braun, M., Siebert, J., & Kietzmann, M. (2011). The percutaneous permeation of a combination of 0.1% octenidine dihydrochloride and 2% 2-phenoxyethanol (octenisept®) through skin of different species in vitro. *BMC Veterinary Research*, *11(7),* 44. https://doi.org/10.1186/1746-6148-7-44

Stephens, P., Caley, M., & Peake, M. (2013). Alternatives for animal wound model systems. *Methods in Molecular Biology*, *1037*, 177–201. https://doi.org/10.1007/978-1-62703-505-7_10

Sterry, W., Czaika, V. A., Drecoll, U., Hadshiew, I., Kiecker, F., Papakostas, D., Philipp, S., Stefaniak, R., Stieler, K., & Terhorst, D. (2011). Kurzlehrbuch Dermatologie. *Georg Thieme Verlag*, 1. https://doi.org/10.1055/b-002-43882

Stojadinovic, O., Brem, H., Vouthounis, C., Lee, B., Fallon, J., Stallcup, M., Merchant, A., Galiano, R. D., & Tomic-Canic, M. (2005). The Role of β-Catenin and c-myc in the Inhibition of Epithelialization and Wound Healing. *Cell Injury, Repair, Aging and Apoptosis*, *167*, 59–69. https://doi.org/10.1016/s0002-9440(10)62953-7

Sturmheit, T. M., Nissen, N., Jacobi, C., Göb, M., Pfündl, R., Landt, S. K., Pfeiffer, T., Kren, C., Wendt, D., Ludwig, R. J., Koop, N., Huber, R., Paus, R., Kruse, C., & Hundt, J. E. (n.d.). Sweat gland derived stem cells promote re-epithelialization in a newly standardized human skin wound healing assay. *Publication in Progress*.

Tapani, E., Taavitsainen, M., Lindros, K., Vehmas, T., Lehtonen, E., & Tapani, E. (1996). Toxicity of ethanol in low concentrations experimental evaluation in cell culture. *Acta Radiológica*, *37(6)*, 923–926. https://doi.org/10.1177/02841851960373P296

Tay, S. S., Roediger, B., Tong, P. L., Tikoo, S., & Weninger, W. (2013). The Skin-Resident Immune Network. *Current Dermatology Reports*, *3(1)*, 13–22. https://doi.org/10.1007/s13671-013-0063-9

Tiede, S., Kloepper, J. E., Bodò, E., Tiwari, S., Kruse, C., & Paus, R. (2007). Hair follicle stem cells: Walking the maze. *European Journal of Cell Biology*, *86(7)*, 355–376. https://doi.org/10.1016/j.ejcb.2007.03.006

Tomic-Canic, M., Mamber, S. W., Stojadinovic, O., Lee, B., Radoja, N., & McMichael, J. (2007). Streptolysin O enhances keratinocyte migration and proliferation and promotes skin organ culture wound healing in vitro. *Wound Repair and Regeneration*, *15(1)*, 71–79. https://doi.org/10.1111/j.1524-475X.2006.00187.x

Topouzi, H., Boyle, C. J., Williams, G., & Higgins, C. A. (2020). Harnessing the Secretome of Hair Follicle Fibroblasts to Accelerate Ex Vivo Healing of Human Skin Wounds. *Journal of Investigative Dermatology*, *140(5)*, 1075-1084.e11. https://doi.org/10.1016/j.jid.2019.09.019

Tripathi, R., Giuliano, E. A., Gafen, H. B., Gupta, S., Martin, L. M., Sinha, P. R., Rodier, J. T., Fink, M. K., Hesemann, N. P., Chaurasia, S. S., & Mohan, R. R. (2019). Is sex a biological variable in corneal wound healing? *Experimental Eye Research*, *187*, 107705. https://doi.org/10.1016/j.exer.2019.107705

Trzaskowski, B., Latek, D., Yuan, S., Ghoshdastider, U., Debinski, A., & Filipek, S. (2012). Action of Molecular Switches in GPCRs-Theoretical and Experimental Studies. *Current Medicinal Chemistry, 19(8),* 1090-1109. https://doi.org/10.2174/092986712799320556

Tsuruta, D., Green, K. J., Getsios, S., & Jones, J. C. R. (2002). The barrier function of skin: how to keep a thight lid on water loss. *TRENDS in Cell Biology*, *12(8)*, 355–357. https://doi.org/10.1016/s0962-8924(02)02316-4

Wall, I. B., Moseley, R., Baird, D. M., Kipling, D., Giles, P., Laffafian, I., Price, P. E., Thomas, D. W., & Stephens, P. (2008). Fibroblast dysfunction is a key factor in the non-healing of chronic venous leg ulcers. *Journal of Investigative Dermatology*, *128(10)*, 2526–2540. https://doi.org/10.1038/jid.2008.114

Wang, C., Zhu, H., Sun, Z., Xiang, Z., Ge, Y., Ni, C., Luo, Z., Qian, W., & Han, X. (2014). Inhibition of Wnt/-catenin signaling promotes epithelial differentiation of mesenchymal stem cells and repairs bleomycin-induced lung injury. *Am J Physiol Cell Physiol*, *307(3)*, 234–244. https://doi.org/10.1152/ajpcell.00366.2013.-Idio

Wang, F., Liu, B., Yu, Z., Wang, T., Song, Y., Zhuang, R., Wu, Y., Su, Y., & Guo, S. (2018). Effects of CD100 promote wound healing in diabetic mice. *Journal of Molecular Histology*, *49*(3), 277–287. https://doi.org/10.1007/s10735-018-9767-2

Wang, W., Liu, P., Lavrijsen, M., Li, S., Zhang, R., Li, S., van de Geer, W. S., van de Werken, H. J. G., Peppelenbosch, M. P., & Smits, R. (2021). Evaluation of AXIN1 and AXIN2 as targets of tankyrase inhibition in hepatocellular carcinoma cell lines. *Scientific Reports*, *11(1),* 7470. https://doi.org/10.1038/s41598-021-87091-4

Wang, Y., Gutierrez-Herrera, E., Ortega-Martinez, A., Anderson, R. R., & Franco, W. (2016). UV fluorescence excitation imaging of healing of wounds in skin: Evaluation of wound closure in organ culture model. *Lasers in Surgery and Medicine*, *48(7)*, 678–685. https://doi.org/10.1002/lsm.22523

Weis, W. I., & Kobilka, B. K. (2018). The Molecular Basis of G Protein-Coupled Receptor Activation. *Annual Review of Biochemistry, 87,* 897-919. https://doi.org/10.1146/annurev-biochem-060614-033910

Wettschureck, N., & Offermanns, S. (2005). Mammalian G Proteins and Their Cell Type Specific Functions. *Physiol. Rev.*, *85(4)*, 1159–1204. https://doi.org/10.1152/physrev.00003.2005.-Heterotrimeric

Williams, C. T. (2016). Food and Drug Administration Drug Approval Process A History and Overview. *Nursing Clinics of North America*, *51(1)*, 1–11. https://doi.org/10.1016/j.cnur.2015.10.007

Wittmann, F., Prix, N., Mayr, S., Angele, P., Wichmann, M. W., van den Engel, N. K., Hernandez-Richter, T., Chaudry, I. H., Jauch, K. W., & Angele, M. K. (2005). L-Arginine Improves Wound Healing after Trauma-Hemorrhage by Increasing Collagen Synthesis. *The Journal of TRAUMA® Injury, Infection, and Critical Care*, *59*(*1*), 162–168. https://doi.org/10.1097/01.ta.0000171529.06625.a8.

Wolf, R. (1999). Alcohol and the Skin. *Clinical Dermatology*, *17*(4), 351–352.

Woodley, D. T. (2017). Distinct Fibroblasts in the Papillary and Reticular Dermis: Implications for Wound Healing. *Dermatologic Clinics 35(1)*, 95–100. https://doi.org/10.1016/j.det.2016.07.004

Xie, Y., & Muller, W. A. (1996). Fluorescence in Situ Hybridization Mapping of the Mouse Platelet Endothelial Cell Adhesion Molecule-1 (PECAM1) to Mouse Chromosome 6, Region F3-G1. *Genetics*, *37*(2), 226–228. https://doi.org/10.1006/geno.1996.0546

Yay, A., Goktepe, O., Bahadir, A., Ozdamar, S., Oktem, I. S., Coruh, A., & Baran, M. (2018). Assessment of markers expressed in human hair follicles according to different skin regions. *Advances in Clinical and Experimental Medicine*, *27*(7), 929–939. https://doi.org/10.17219/acem/74429

Yoon, D. J., Fregoso, D. R., Nguyen, D., Chen, V., Strbo, N., Fuentes, J. J., Tomic-Canic, M., Crawford, R., Pastar, I., & Isseroff, R. R. (2019). A tractable, simplified ex vivo human skin model of wound infection. *Wound Repair and Regeneration*, *27*(4), 421–425. https://doi.org/10.1111/wrr.12712

Zaiss, D. M., Minutti, C. M., & Knipper, J. A. (2019). Immune- and non-immune-mediated roles of regulatory T-cells during wound healing. *Immunology, 157(3),* 190–197. https://doi.org/10.1111/imm.13057

Zhan, T., Rindtorff, N., & Boutros, M. (2017). Wnt signaling in cancer. In *Oncogene, 36(11), 1461-1473*. https://doi.org/10.1038/onc.2016.304

Zhang, M., Cao, Y., Li, X., Hu, L., Taieb, S. K., Zhu, X., Zhang, J., Feng, Y., Zhao, R., Wang, M., Xue, W., Yang, Z., & Wang, Y. (2017). Cd271 mediates proliferation and differentiation of epidermal stem cells to support cutaneous burn wound healing. *Cell and Tissue Research*, *371(2)*, 273–282. https://doi.org/10.1007/s00441-017-2723-8

Zhang, M., Zhang, Y., Ding, J., Li, X., Zang, C., Yin, S., Ma, J., Wang, Y., & Cao, Y. (2018). The role of TrkA in the promoting wounding–healing effect of CD271 on epidermal stem cells. *Archives of Dermatological Research*, *310(9)*, 737–750. https://doi.org/10.1007/s00403-018-1863-3

Zhang, Y., Liu, S., Mickanin, C., Feng, Y., Charlat, O., Michaud, G. A., Schirle, M., Shi, X., Hild, M., Bauer, A., Myer, V. E., Finan, P. M., Porter, J. A., Huang, S.-M. A., & Cong, F. (2010). RNF146 is a poly(ADP-ribose)-directed E3 ligase that regulates axin degradation and Wnt signalling. *Nature Cell Biology*, *13(5)*, 623–629. https://doi.org/10.1038/ncb2222

Zomer, H. D., & Trentin, A. G. (2018). Skin wound healing in humans and mice: Challenges in translational research. *Journal of Dermatological Science*, *90(1)*, 3–12. https://doi.org/10.1016/j.jdermsci.2017.12.009

Acknowledgements

Just as the African proverb says: “It takes a village to raise a child”, a lot of people helped with this thesis, and I could have never written it on my own. I want to take this opportunity to thank everyone involved.

My first and foremost thank you goes to Prof. Dr. med. vet. Jennifer Hundt, my Phd-supervisor, and the best “Doktormutter” anyone could hope for. Thank you for everything Jenny. From the moment I met you in the interview for my master’s thesis, working with you has been a pleasure. You taught me so much, not only about science but about how to manage all the smaller and bigger problems of life. I really could not have done this without you, and I will miss our weekly meetings. The last four years have not been the easiest of my life. Thank you also for creating a safe haven with your working group that carried us all through the pandemic and everything else life dished out.

Next, I want to thank the examination committee, Prof. Dr. rer. nat Norbert Tautz and Prof. Dr. Las Redecke for assuming the role of head of examination committee and second referee.

I also want to thank the LIED managing director, Prof. Dr. med. Ralf Ludwig, for the valuable input, support and interesting meetings.

My PhD thesis relied on skin donations. I am forever grateful to all donors and the surgeons that made this work possible.

Then a gigantic thank you goes out to the Hundt-lab. I am going to miss you all so much. Thanks for all the support, laughs, and shoulders to cry on.

Nadine, I do not even know where to begin… so I’ll try to keep this short and simple: Thank you for all your help, for always being there, for everything.

Marieke, thank you for all your support, and for always lending an ear and offering advice, when I was wondering on how exactly one does a PhD at the University of Lübeck. We still need to sacrifice the “Cocktail-Sparschwein” together!

Sylva, thank you so much for all your support, especially cutting what felt like millions of cryostat samples. I would have been lost without your patience and expertise.

Sina, a big thank you for all your help in organizational matters – from refunding to the mini-job. All that would not have been possible without you.

Skadi (or Skoda?), thank you for our nice lunches, your advice and your humor.

Linh, thank you for the PMI-meetings visited together and showing me the commercial OCT-system.

Sarah, Vero, and Tasja, you three have been the best “Doktor-Schwestern”, that I could have asked for. Thank you for your support – scientific and emotional. For all the coffee-talks, lunches, laughs and helpful discussions. I will really miss sharing an office with you.

The good thing about working in academia is that you get to know a lot of fascinating and brilliant people, the bad thing is, that some of them only stay with you for a short time. In the following I want to thank all visiting scientists, Bachelor students, Master students and medical students, who filled the Hundt lab with life:

Uta, Julia, Paul, Christi, Friedi, Birte, Inka and Valeria: you welcomed me with open arms, when I started my PhD and taught me everything I needed to know to start my work – thank you so much for that. Thanks also for making me leave my comfortable couch and go celebrating with you. I was so sad to see you all finish and leave. It seems crazy that I will now do the same thing.

Trixi, Anna, and Emelie – three Bachelor students at once is quite a lot in a small lab, but with you it has been a lot of fun. Thank you for the good times in the lab together.

Felix, thank you for making me laugh – even during Corona times, and for teaching me the PamGene lysis protocol.

Baria, thank you for your support in the lab. Working with you has been a pleasure.

Johannes, even though your future was not in lab work, I enjoyed having you with us – and I still use the owl-mug almost daily.
Bety, thanks for your help. I hope you are doing well.
Laura and Chiara, thank you for bringing so many laughs and good mood into the lab!
Lilly and Luise, the same is true for you. Lilly, thank you so much for working together on the porcine models. I'm looking forward to finishing that paper together. Luise, thank you for making me on time for Mondays lab meetings. I miss our commune together to the lab.
Luca, thank you for your serenity and optimism. Max, thank you for your sometimes challenging but always important questions – and for finding the H&E resolution issue.
Julia, Jade, and Bara, you were the last students I got to meet while being somewhat active in the lab. It has been a pleasure working with you!
Last, but not least from the Hundt lab people I want to thank "my" students for all your help and work, your questions that made my thesis better, and for just being great. When I started my PhD, I asked Jenny whether I could supervise some students as their primary supervisor, in the end I was lucky to have the six of you. Annika, you were the first student I ever supervised, and you set the bar incredibly high for everyone following you. Thank you for your patience with me, while I figured out how to best supervise students – you made supervision very easy. Lenny, thank you for all the valuable input and challenging some of my ideas – you made this thesis better with it. Jack, thank you for bringing American cheeriness to our lab and your unwavering support. Linus, thank you for your help with everything – I really enjoyed developing the evaluation of our wound healing organ culture together. Luna and Mareike, thank you two with your help with the immune fluorescence staining– I would have never managed to do all that by myself. Luna, you made the lab a happier place with your bubbly personality and wise insights. Mareike, thank you for your support even after you finished and your help with the pathological model – I felt a lot less lost with you when the gas bottles were empty again.

I want to also thank the Ludwig lab as well as Dr. med. Dr. rer. nat. Christoph Hammers and his working group for the good collaborations. A special thank you to Dr. Nancy Ernst and Collin Osterloh for their help with the PamGene experiments, that did not make it into this thesis but I am looking forward to writing that paper.
Thank you to Prof. Dr. rer. Hauke Busch and his working group for the great joint summer events.

To the routine lab of the dermatology in house B9: Thank you so very much for all your help and for making working at the embedding station so much fun.
The wound volume determination by optical coherence tomography was a big part of the screening of this work, so I want to thank the working group of Prof. Dr. rer. nat. Robert Huber of the Institute for Biomedical Optics of the University of Lübeck, who developed the system used in this work. Thank you, Robert, for making this collaboration possible and Madita, thank you so much for making it so pleasurable. I always enjoyed our measurement dates. Also, thank you for all the work you put into this project. I did not take this for granted.

I want to thank Dr. Reinhard Depping and his working group for providing the hypoxic incubator and all the help while working with it.
I also want to thank the former Fraunhofer "*Einrichtung für marine Biotechnologie"* for their support and access to the stereomicroscope.

A big thank you to Dr. med. Andreas Thomsen for designing the new retainers and the spacers, which made this work definitely better. It has been a pleasure working with you.

I also want to thank Prof. Dr. med. Thomas Walther for all the stimulating conversations and discussions that led to the chapter about the influence of Octenisept® in this work.

Lastly, I want to thank my friends and family for all their support during my PhD. Yara, Hanna, Anna-Clara, and Marco thank you for all the years of friendship and just being a phone call away. Valerie, Linnea, Fabienne, Laura, Sarah, and Fabi thank you for the years of studies together that led to this PhD. Studying without you would not have been half as fun. Lea, Andrea, and Nora thank you for all the great brunches, board game afternoons, and everything else. Lenny, Danielle, Tom, Thore, Piet, and Andrea (again) thank you for the evenings fighting dragons together.
And of course, an extra thank you to Thore, who stayed by my side no matter how chaotic life chose to be and made me laugh even when I was feeling down. Thank you for keeping me calm and making me happy.
Thank you to my fantastic family. I could not ask for more loving and supporting people in my life.
Jens, thank you so much for all your support from high school on, through my studies and now my PhD.
This work began with a dedication to my parents, and I want to close it by saying thank you, mum, for all that you have done. For all your support throughout the years, the help you always gave, sometimes even before I could ask for it, and your uncanny knack for always knowing when something is not right and then doing your best to fix it.
Dad, though you are no longer here, you at least saw me start this project and you still helped me push through it. I hope that wherever you are now, you are a bit proud of your daughter, who no longer has a matriculation-background now.

Curriculum vitae Caren Jacobi

University education

November 2019 – 2023 (estimated)		**PhD degree** at the Lübeck for Experimental Dermatology (LIED), University of Lübeck, Germany Topic: "Screening for wound healing promotors using a human wound healing organ culture model"
February 22nd – 25th 2023		Participation in the 49th annual meeting of the "*Arbeitsgemeinschaft Dermatologische Forschung"* (ADF) in Innsbruck, Austria Poster presentation: Searching for new drug candidates that aid wound healing by screening an inhibitor library
September 28th – October 1st 2022		Participation in the 51st annual meeting of the European Society for Dermatological Research (ESDR) in Amsterdam, the Netherlands Poster presentation: Searching an inhibitor library for new drug candidates to promote wound healing
February 23rd – 26th 2022		Participation in the 48th annual meeting of the ADF (virtually due to the Corona pandemic) Poster Presentation: Screening for novel drug candidates to aid wound healing
October 2016 – October 2019		**Master of Science** in **Molecular Life Science** at the University of Lübeck, Germany Topic of the Master thesis: Plasma-induced wound healing of human skin
March 2018 – September 2018		Internship in the filed of Fungal infections at the University Utrecht, the Netherlands Topic: Persistence of fungal spores in lung epithelial cells
March 23rd – 24th		Participation in the International Workshop on Magnetic Particle Imaging Poster presentation of my Bachelor thesis
October 2013 – September 2016		**Bachelor of Science** in **Molecular Life Science** at the University of Lübeck, Germany

School education

2005 – 2013		Heinrich-Heine High school in Hamburg, Germany (A-levels)
2001 – 2005		Primary school Lemsahl-Mellingstedt in Hamburg, Germany

Study-related activities

2014 – 2017		Student assistant in the Institute for Chemistry and Metabolomics, University of Lübeck (supervision of practical and theoretical courses)
October 2014 – October 2015		Part of the organization committee of welcoming new students to the University of Lübeck